Acetylenic phosphanes and carbo-mers for coordination chemistry

Dan Chen

RÉPUBLIQUE FRANÇAISE
Liberté Égalité Fraternité

Université de Toulouse

Doctorat de l'Université de Toulouse

préparé à l'Université Toulouse III - Paul Sabatier

Phosphanes acétyléniques et carbo-mères pour la chimie de coordination

Thèse présentée et soutenue, le 16 juillet 2024 par

Dan CHEN

École doctorale
SDM - SCIENCES DE LA MATIERE - Toulouse

Spécialité
Chimie Moléculaire

Unité de recherche
LCC - Laboratoire de Chimie de Coordination

Thèse dirigée par
Rémi CHAUVIN et Xiuling Cui

Composition du jury
M. Didier BOURISSOU, Président, CNRS Occitanie Ouest
Mme Muriel HISSLER, Rapporteure, Université de Rennes
M. Jean-francois NIERENGARTEN, Rapporteur, CNRS Alsace
M. Rémi CHAUVIN, Directeur de thèse, Université Toulouse III - Paul Sabatier

Membres invités
Mme Xiuling CUI, HUAQIAO UNIVERSITY

Acknowledgement

Until this day, I still vividly remember the night of October 13, 2021, when I first set foot in France. With a mix of nervousness, excitement, and anticipation, I officially embarked on my journey pursuing a Ph.D. at LCC. Time has raced by, and here I am, sitting in front of my computer, with countless memories flooding my mind. I'm at a loss for where to begin, but I want to take this opportunity to engage in a dialogue with myself and reflect on this incredible journey. There are so many people I want to express gratitude to—my mentors, family, friends, and the companions in my laboratory. Without your presence, there wouldn't be the person I am today, nor would there be this thesis presented before you.

Firstly, I want to thank the version of myself from four years ago. It was your determination and passion that secured this precious opportunity for education. Many couldn't understand why, with a decent job and stable position, you would invest so much time and energy, even temporarily leaving behind your family and young daughter to study in a foreign land at this age. You are a daughter, a wife, a mother. But beyond these roles, you are still you. When others were watching how far you ran, you started asking yourself, "What landscapes have I encountered? What kind of life have I seen on this journey of running?" Compared to the time right after graduation,

you now truly understand what you want and what you love. Therefore, your gaze is firmer, and your love for chemistry is purer. Thank you, brave self, for daring to dream and pursue those dreams, thus marking the beginning of this story.

Thank you to my mentors. With your help and support, this incredible journey of life found a pause in France. Thank you, Professor Xiuling CUI. Although I didn't officially register in Huaqiao University as a Ph.D. student, you always treated me as your own student, teaching me, encouraging me, supporting me. It's because of your recommendation that I had the opportunity to start my Ph.D.in France.

Thank you, Professor Remi CHAUVIN, for introducing me to LCC for my Ph.D. and your guidance on my thesis; As an outstanding chemistry scientist, your profound knowledge and passion for the field of chemistry have earned my admiration. Every discussion with you about chemistry brought me immense joy.

Thank you, Dr. Valerie Maraval. I will always remember your smile, full of vitality and energy. It always lifted me up from failures and made me more confident on the road to becoming a competent researcher. I will never forget your excited expression when I succeeded in synthesizing my first important compound here, it was the greatest affirmation of my work. Without you, I will not be able to finish this thesis and my phD here. You have

been of tremendous help to me, being both a mentor and a friend, caring for me in every detail, even comforting me in the situations which was difficult for both of us. I am truly fortunate to have met you. You are always with me, you share my joy and empathize with my pain. You have given France a different meaning for me.

Thank you, my husband, for the immense effort you put into fulfilling my dreams. Our love isn't like a sigma covalent bond, which is always head to head. It's more like a pi covalent bond, where we're shoulder to shoulder, working towards a common goal in life. Thank you for loving me, understanding me, and supporting me. Taking care of our home and educating our daughter while I was away, encouraging me in times of difficulty, cheering me up on unhappy days—though you sometimes felt anxious and frustrated, you always took care of my emotions, allowing me to feel at ease.

Thank you, my obedient daughter. Mom feels most guilty for not being able to be with you every moment while you were so young. When I heard your childish voice supporting me to pursue my Ph.D. in France at the age of five, I gained the greatest strength and courage. I especially hope to be a mother you can be proud of, and more importantly, to let you know that everyone has the right to pursue their dreams, whether you're ten, twenty, thirty, or even sixty or eighty years old. It's something to be proud of, daring to dream and

striving for ideals.

Thank you to my parents and family. You are my strongest support. It's your support that gives me the courage to move forward, and without you, I wouldn't have this peaceful present.

Thank you to my friends—Chengna WANG, Xingyan LIN, Jun ZENG, Xuening LI, Nina HUANG, Cecile BARTHES. You are the gifts angels brought to me. In my most difficult days, your comfort and companionship gave me the motivation and courage to start again.

I will never forget my laboratory companions who have been with me all the way: Charlotte APARICI, Jaspreet KOUR, Juliette MICHAUT, Corentin BOUVIER, Jon BOUVET, Zhengyu YAO, Yu Zou, Dyhia AMRANE, Mohcen CHAHID, Sebastian MESA... Though our time together may not have been long, our stories are numerous. We've laughed and joked happily together, and we've shed tears together. I feel extremely lucky to work and study with you, and I hope we'll have the opportunity to continue our stories in the future.

My thank also goes to Xiamen Medical College, that permit my absence and support my PhD study funding and all my colleagues in at the Marine Pharmacology Research office: Professor Lianzhong LUO, Gang ZHANG, Yung Husun CHEN, Jingna WU, zhen ZENG, Bingye YANG, Li XU and Zixu WU. Especially Xuli, you've shouldered a significant amount of work for me without complaint, and always putting my worries at ease and

allowing me to focus solely on my studies.

In closing, my gratitude extends beyond words to encompass the depth of emotion and sincerity that each person mentioned here has brought into my life. As I embark on the next chapter of my journey, I carry with me not just the knowledge gained from research but also the profound impact of your support, guidance, and unwavering belief in me. Together, you have illuminated my path with kindness, resilience, and boundless generosity. As I step forward, I do so with a heart full of appreciation and a commitment to honor your contributions by working and living conscientiously, maintaining a deep reverence for science. Thank you for being the guiding stars in my academic voyage; your presence in my life is a cherished blessing beyond measure.

Table of Contents

Acknowledgement 1

Table of Contents 7

Compounds synthesized in this thesis 11

General Introduction 15

Chapter 1. Synthesis and properties of carbo-mer molecules 21

1. *Carbo*-mers: definition and synthetic approach 23

2. [n]Pericyclynes derivatives 25

2.1. Fully hydrocarbon [n]pericyclynes derivatives 26

2.1.1. Synthesis of hydrocarbon pericyclynes 26

2.1.2. Synthesis of expanded hydrocarbon pericyclynes 26

2.2. Hetero [n]Pericyclynes derivatives 28

2.2.1. Hetero [n]pericyclynes with alternation of carbon and heteroatom vertices. 29

2.2.2. [n]Pericyclynes with heteroatoms at each vertex. 31

2.2.3. Expanded [n]pericyclynes with heteroatoms at each vertex. 34

2.2.4. Poly[n]pericyclynes cages with heteroatoms at each vertex 35

2.3. Oxy[n]pericyclynes derivatives 36

2.3.1. Synthesis of oxy[n]pericyclynes derivatives without heteroatom. 37

2.3.2. Synthesis of oxy[n]pericyclynes derivatives with one hetero atom in or on the ring. 45

2.3.3. Synthesis of expanded oxy[n]pericyclynes derivatives 47

2.3.4. Poly macrocyclic oxy[n]pericyclynes derivatives 51

3. Reduction of n-oxy[n]pericyclyne derivatives 54

3.1. *Carbo*-benzene derivatives 54

3.2. Synthesis of *carbo*-barrelenes 58

3.3. Synthesis of a *carbo*-naphthalene 59

3.4. Synthesis of *carbo*-biphenyl and *carbo*-terphenyl derivatives 60

3.5. Synthesis of expanded *carbo*-benzene derivatives 61

3.6. Synthesis of a *carbo*-phospholene 62

4. The properties of *carbo*-benzenes 63

4.1. Electrical: single molecule conductance 63

4.2. Two-photon absorption 64

4.3. Mesogenic properties: liquid crystal (LC) properties 65

4.4. Photosensitizers for hydrogen production 66

5. Conclusion 68

References 68

Chapter 2. Synthesis of carbo-diphosphacyclohexane and carbo-diphosphinine derivatives 80

1. Introduction 82

2. Results and discussion 84

2.1. Preparation of the triyne C_8 precursor of $C_{16}P_2$ macrocycles 84

2.2. Synthesis of diphospha-[6]pericyclyne derivatives 84

2.3. Synthesis of the diphospha-[6]pericyclyne oxide and sulfide derivatives 90

2.4. Hexaphenyl-*carbo*-1,4-dithio-1,4-dihydro-1,4-diphosphinine and hexaphenyl-di(thiophosphinylethynyl)butatriene model thereof 92

2.4.1. *Synthesis of a carbo*-1,4-dithio-1,4-dihydro-1,4-diphosphinine and an acyclic model thereof 92

2.4.2. Evolution of hexaphenyl-*carbo*-1,4-dithio-1,4-dihydro-1,4-phosphinine **13** in DCM without protection from light 94

2.4.3. NMR characterization of **13** and **3b** 95

2.4.5. Electrochemical behavior of **13** and **3b** 97

2.4.6. X-ray diffraction of hexaphenyl-carbo-1,4-dihydro-1,4-dithiodiphosphinine 99

2.4.7. Exploratory DFT calculations 100

3. Conclusion 107

4. Experimental Section 108

References 120

Chapter 3. Synthesis and properties of Carbo-diphosphabarrelene derivatives 124

1. Introduction 126

1.1. Barrelene 126

1.2. Mono- and di-phospha-barrelene derivatives 126

1.3. *Carbo*-barrelene 127

2. Results and discussion 129

2.1. Synthesis of a *carbo*-diphosphabarrelane dioxide 129

2.2. Attempt at synthesis of *carbo*-dithiophosphabarrelane 130
2.3. Alternative access to *carbo*-dithiodiphosphabarrelanes 132
2.4. Synthesis and partial characterization of a *carbo*-dithiodiphospha-barrelene 137
2.4.1. Synthesis of a *carbo*-dithiodiphospha-barrelene 137
2.4.2. NMR characterization 138
2.4.3. UV-visible spectroscopy 139
2.4.4. Theoretical calculation 140
3. Conclusion 146
4. Experimental section 146
References 154
Chapter 4. Reactivity and coordination chemistry of ring carbo-mers of P-heterocyles and acyclic model thereof 158
1. Introduction 160
2. Reduction of dialkynylthiophosphines to corresponding phosphines 163
3. Explorations in coordination chemistry 167
4. Perspectives of alkynylphosphine complexes in catalysis 171
5. Conclusion 173
6. Experimental section 173
References 178
General Conclusion 186
Résumé en Français 192
Annexes 214
Crystallographic Data and Structural Refinement Parameters for Compounds 216
Crystal Data **3b** 217
Crystal Data **13** 222
Crystal Data **24** 227
Crystal Data **39** 244
Crystal Data **41** 252
Crystal Data **43** 260
Electrochemistry Data of **3b** 294
Electrochemistry Data of **13** 298
Electrochemistry Data of **39** 302
Electrochemistry Data of **43** 306

Electrochemistry Data of **46** 310

DFT calculations 314

Abstract 326

Résumé 327

Compounds synthesized in this thesis

Chapter 2

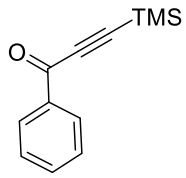

1

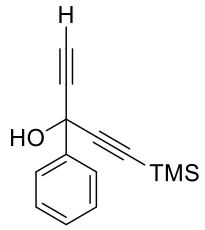

2

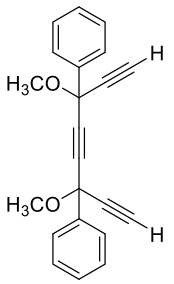

3

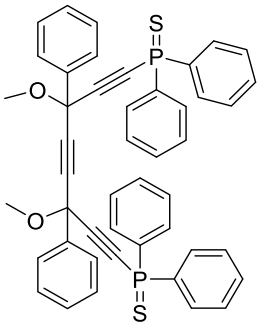

3a

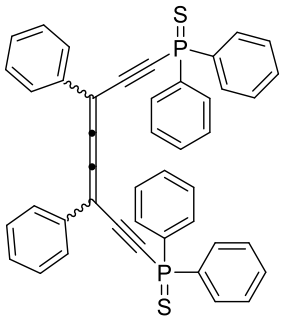

3b

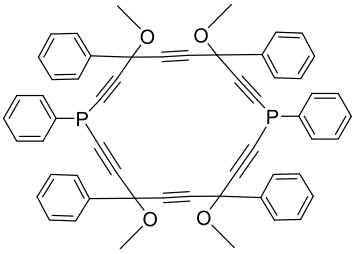

4

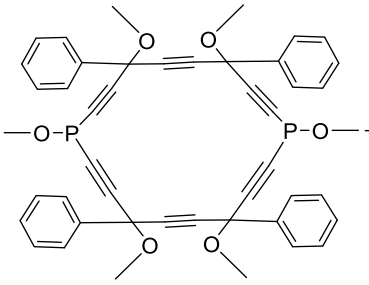

5

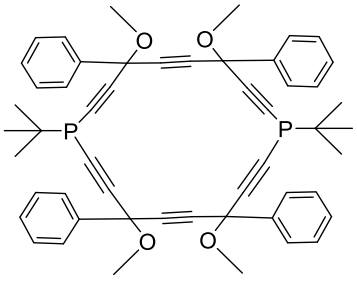

6

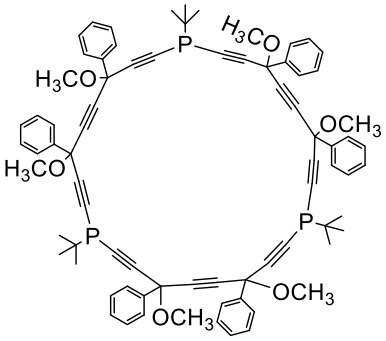

7

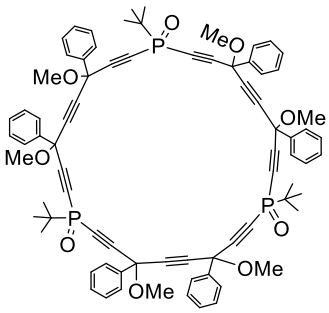

8

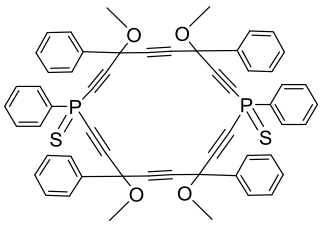

9

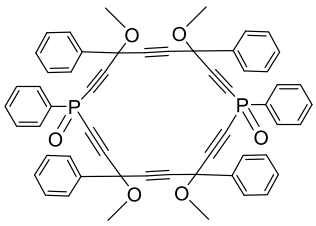

10

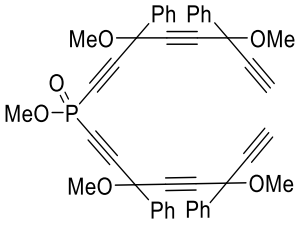

11

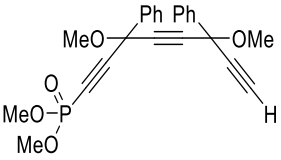

12

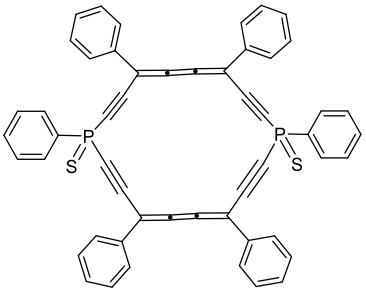

13

Chapter 3

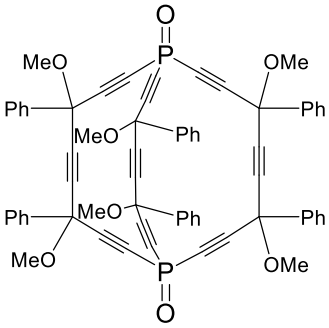

16

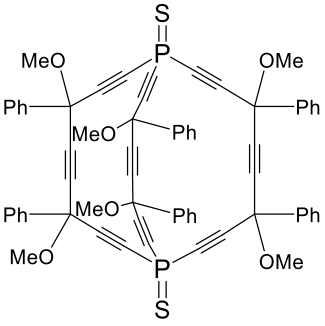

17

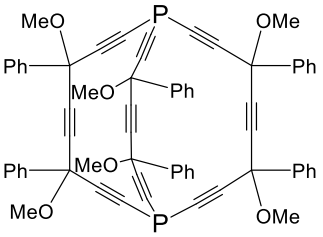

18

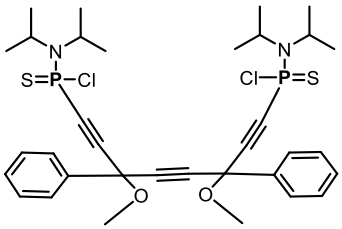

19

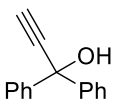

20

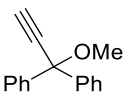

21

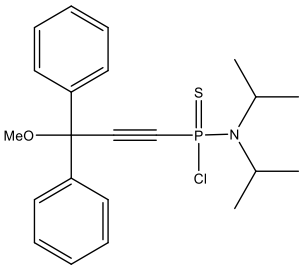

22

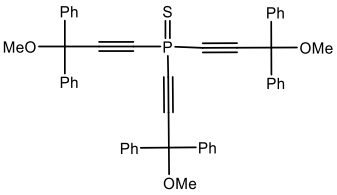

23

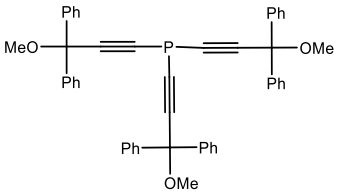

24

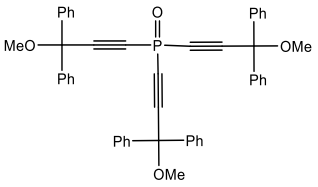

25

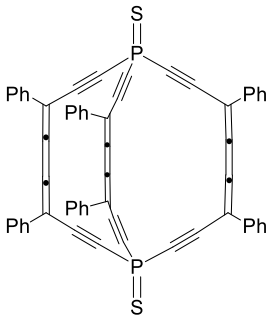

26

Chapter 4

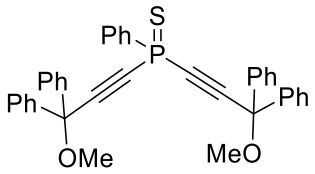

39

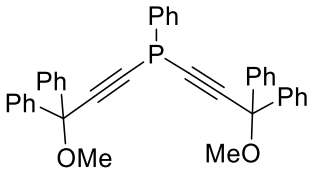

40

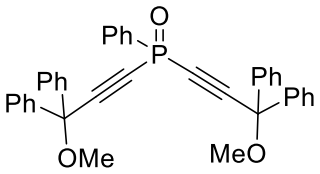

41

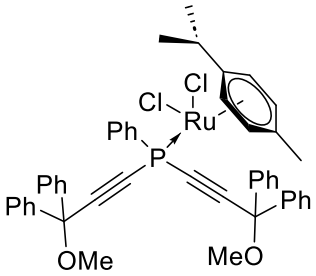

43

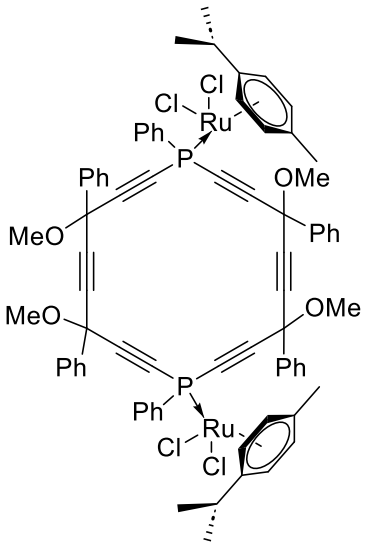

46

General Introduction

General Introduction

The thesis is made of four chapters relying on the interplay between *carbo*-mer chemistry and phosphorus chemistry, the main objective of the work being the introduction of phosphorus atoms inside the ring of *carbo*-mer derivatives.

The term "*carbo*-mer " refers to a chemical concept where a C_2 unit (a two-carbon fragment) is inserted into each (or a selected part of) covalent bond of a representative Lewis structure of any parent molecule. The *carbo*-merization process induces the increase of the carbon content as compared to the parent molecule and leads to about three times larger molecules, which can exhibit various properties. The fundamental characteristics of the parent molecule, crucial for controlling their physical properties, are preserved in its *carbo*-mer at a preliminary level of approximation. This includes the connectivity, shape, symmetry, π-resonance, and configurations of chirality elements.

Organophosphines and their metal complexes are intensively used in catalysis because of the possibility to finely tune their electronic and steric properties. Such catalysts can be applied in some reactions performed in aqueous or biphasic media provided that ionic or polar groups are attached to these phosphines. In 1966, a first example of 2,4,6-triphenylphosphinine was reported by Märkl. From then, a remarkable expansion of phosphorus-containing heterocyclic chemistry has started. For the first time, the unsubstituted phosphinine (along with arsenine) was synthesized by Ashe in 1971.

By integrating phosphorus atoms into *carbo*-mer chemistry, one can ambition to access a broader range of new phosphorus-containing compounds with diverse properties and applications. This approach can lead to innovative solutions and new avenues for exploration in synthetic chemistry and materials science.

Although phospha-[n]pericyclynes, having either a phosphorus atom at each sp^3

vertex of a pericyclyne framework or only one phosphorus atom in the case of the *carbo*-phospholane derivatives, were reported in the literature, the investigation of *carbo*-heterocycles and *carbo*-heterobarrelene containing two heteroatoms in their structure has never been envisaged up to now. The synthesis, characterization and properties of *carbo*-phosphaheterocycles are thus the aim of the following thesis work (**Scheme 1**).

The first chapter comprises a literature review, divided into two main parts. The first part focuses on various synthetic approaches to *carbo*-benzene precursors, namely [n]pericyclynes derivatives, including hetero-[n]pericyclynes derivatives. The second part describes the reduction of n-oxy[n]pericyclyne derivatives into the corresponding *carbo*-benzenes, as well as the properties and applications of these molecules.

In Chapter 2, the ring *carbo*-mers, i.e. C_2-expanded, of phosphinines (or phosphorines, or phosphabenzenes) are envisaged. *Carbo*-phosphinines are still unknown experimentally. Their soft electrophilic character should allow evidence of original coordination chemistry (in particular regarding possible competition between P- and C_2- coordination), with related prospects for catalytic properties of the corresponding metal complexes. In this chapter, an efficient a [8+1+8+1] strategy for synthesizing macrocyclic *carbo*-diphosphacyclohexane derivatives is described, followed by the presentation of a first case of *carbo*-1,4-dihydro-dithiophosphinine which has been fully characterized.

Chapter 3 describes an efficient deprotonation method for constructing *carbo*-diphosphabarrelane derivatives. Barrelene is a fascinating bicyclic organic compound, characterized by its chemical formula C_8H_8 and systematic name bicyclo[2.2.2]octa-2,5,7-triene. It was first synthesized and described by H. E. Zimmerman in 1960. The emerging family of *carbo*-barrelenes in 2021 by Zhu *et al*. unveils numerous possible applications, including their anticipated ability to encapsulate cations and to exhibit high single molecule conductance (SMC) efficiency. The insertion of phosphorus atoms in a *carbo*-meric ring, a new element with a different electronegativity and atomic size, is thus susceptible to affect the distribution of electron density within the molecule.

Indeed, phosphorus is typically less electronegative than carbon, leading to changes in the electron distribution and potentially altering the molecule's overall electronic structure, including changes in bond lengths, bond angles, molecular orbitals and polarizability. Additionally, the presence of phosphorus can introduce new electronic effects, such as lone pair interactions, that are absent in barrelene. Therefore, the electronic properties of phospha-barrelene can differ significantly from those of barrelene.

In Chapter 4 is described a preliminary study regarding the reactivity and possible use as ligands towards metal centers of *carbo*-diphosphacyclohexanes and *carbo*-dihydrodiphosphinines developed in Chapter 2 and Chapter 3. While the phosphabarrelene and diphosphacyclohexane derivatives were investigated for their coordination chemistry and application in catalysis, the properties of the ring *carbo*-mers of such molecules have never been considered. It is challenging to study the coordination chemistry of such compounds because they contain P(III) atoms and triple bonds that can both play the role of ligands towards metals. The study of the coordination chemistry of *carbo*-diphosphacyclohexanes, and *carbo*-dihydrodiphosphinines, whose syntheses are described in the previous chapters, is a challenging endeavor that was envisaged in this chapter. The ruthenium (II) moiety Ru(*p*-cymene) Cl_2, occurring in efficient pre-catalysts for transfer hydrogenation of acetophenones, was envisaged as a first example of coordination center for P-containing *carbo*-mer derivative.

This thesis manuscript ends with a general conclusion summarizing the main results issued from this work and presenting possible perspectives.

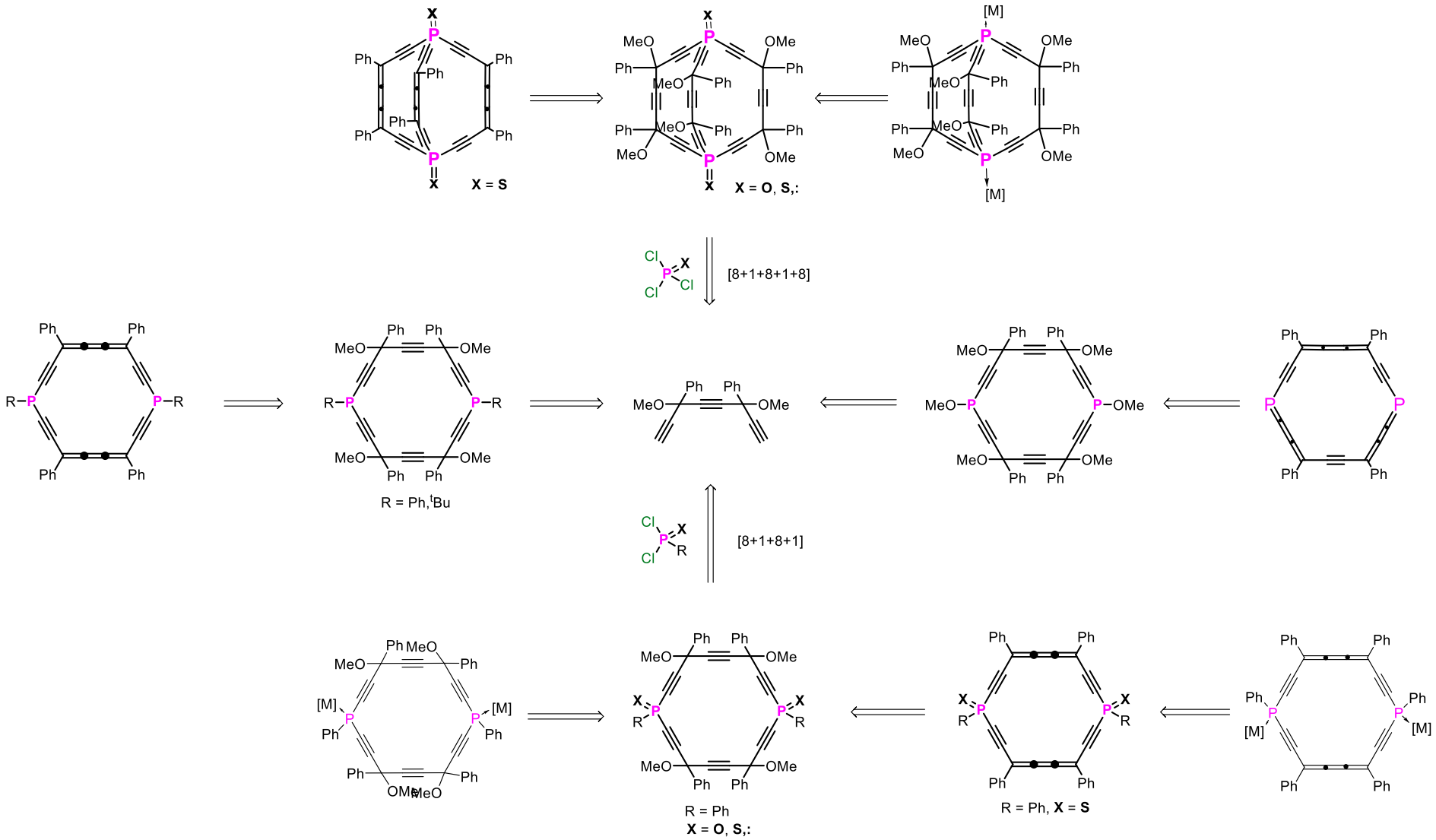

Scheme 1 The objectives of the thesis

Chapter 1. Synthesis and properties of carbo-mer molecules

The acetylene unit, historically employed as a utilitarian entity within synthetic organic chemistry, has undergone a paradigm shift in the past decades. Along with the fast growing set of tools goes an ever increasing number of publications concerning impressive arrays - cyclic, two-dimensional and even three dimensional - of acetylenic and diacetylenic units linked by aliphatic, aromatic or organometallic connectors.[1] It has transcended its conventional role and ascended to the status of a distinctive structural motif within the realm of physical organic chemistry. This transformation has notably delineated polyacetylene chemistry as a discernible and specialized field of scholarly research.

1. *Carbo*-mers: definition and synthetic approach

"*Carbo*-mer " refers to a formal process where a C_2 unit (a two-carbon sp-hybridized fragment) is inserted into each bond of the set of covalent bonds (or selected part thereof) of a representative Lewis structure of any parent molecule[2]. The *carbo*-merization process involves the increase of the carbon content of a specific molecule and lead to larger molecules, potentially exhibiting different properties. Meanwhile, a significantly robust relationship is observed in *carbo*-k-mers, where C_{2k} units are inserted the parent molecule corresponding to $k = 0$[3]. The fundamental characteristics of the parent molecule, crucial for controlling their physical properties, are preserved in its *carbo*-mer at a preliminary level approximation. This includes the connectivity, shape, symmetry, π -resonance, and configurations of chirality elements.

The suffix "mer" is often used in polymer chemistry to refer to repeating structural units within a polymer chain, and more generally to design “alternative forms” of a given molecular type(“isomers”, “conformers”, “isotopomers”, “mesomers”….) . In the context of "*carbo*-mer chemistry," it seems to imply the insertion of a C_2 unit within the bonds of a molecular structure. This process can result in diverse carbon-rich compounds with varied possible properties, across various domains of chemistry, ranging from fundamental organic chemistry, coordination chemistry to materials science. Additionally, *carbo*-mers offer opportunities for the design and development of advanced materials with enhanced functionalities, such as conducting molecule and catalysis.

In a rigorous context, a *carbo*-mer is devised through the systematic insertion of C_2 units into every covalent bond of a designated parent lewis structure [2]. Alternatively, partial *carbo*-

mers can be delineated, when the C_2 connector is selectively introduced within specific regions of the Lewis structure. For example, the " total *carbo*-mer" is achieved by C_2 insertion into all bonds, while a "ring *carbo*-mer" results from C_2 insertion into all bonds of a ring[4] (including all potential annelated rings). Similarly, "peripheral *carbo*-mers" are generated by C_2 insertion into all non-endocyclic bonds connected to a ring（see **Figure 1.1**).[3]

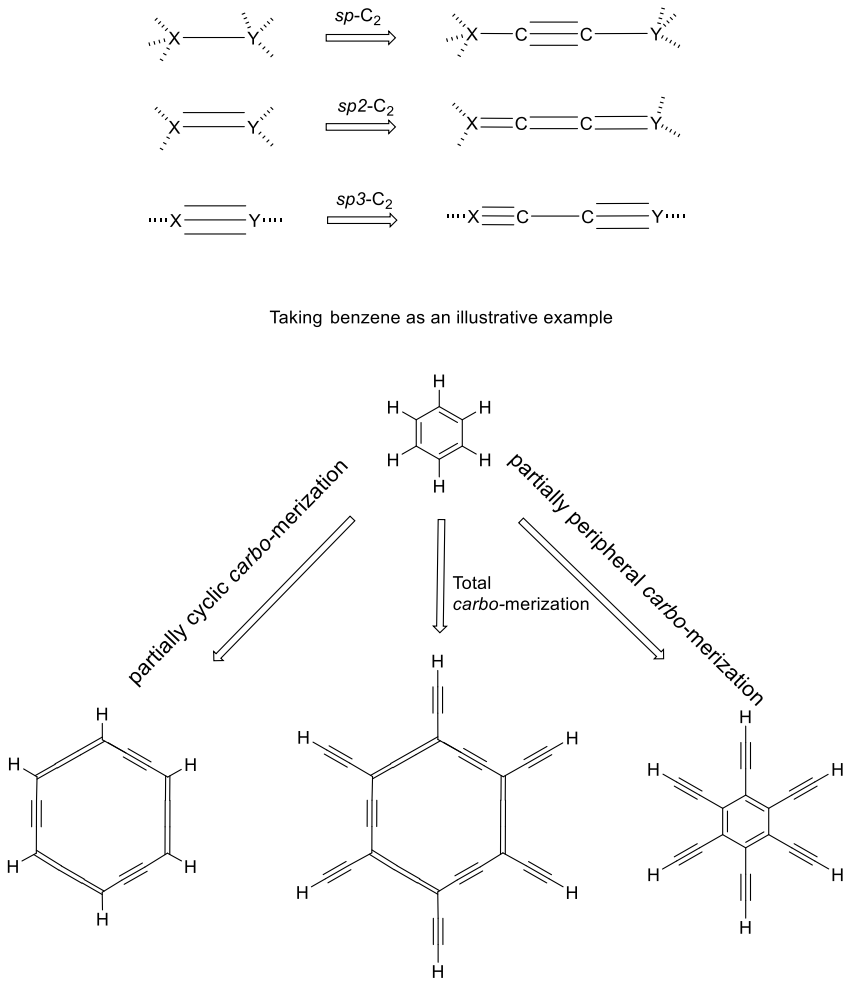

Figure 1.1.. Basic *carbo*-merization process.

The carbo-merization process leads to larger molecules with altered properties. This process allows for the expansion of molecular frameworks, enabling the exploration of diverse carbon-based compounds since it can be applied to any kind of molecule. It thus provides a formal method for systematically increasing the carbon content of molecules while retaining some of their initial characteristics

One notable example is *carbo*-benzene, an unsubstituted ring *carbo*-mer of benzene consisting of 18 carbon atoms bearing 6 hydrogen atoms, being formally obtained through symmetry-preserving C2-expansion of the benzene molecule[2]. It is a putative example of Hückel-aromatic *carbo*-benzene[5] which represents a significant synthetic challenge but holds promise for novel aromatic compounds with tailored properties.

The preparation of *carbo*-benzene derivatives involves a final reductive elimination step performed from hexaoxy[6]pericyclyne precursors. In this last step, all the methoxy or hydroxy groups are removed and the three butatriene edges of *carbo*-benzenes are formed (**Scheme 1.1**).

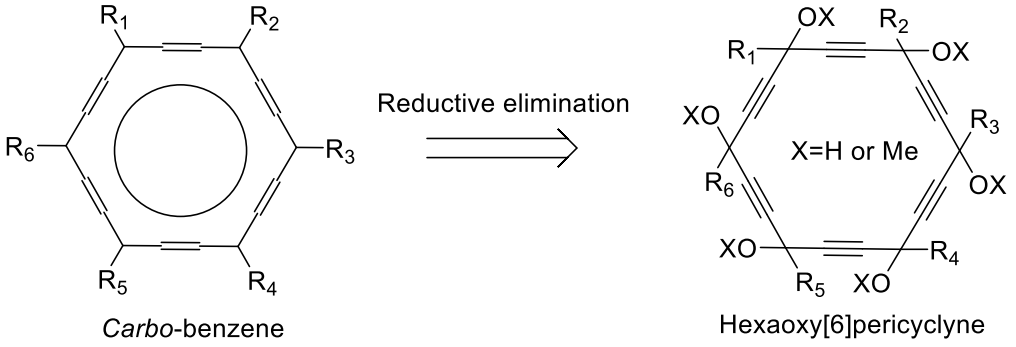

Scheme 1.1. *Retrosynthetic analysis of carbo-benzene*

2. [n]Pericyclynes derivatives

The term "[n]pericyclyne" was advanced in the pioneering work of L.T. Scott *et al*. in 1983 [6] to describe molecules containing n -C≡C- units distributed symmetrically on every edge of a cycle with n vertices, i.e. a cycloalkane with an ethynediyl moiety inserted into each single C-C bond (**Figure. 1.2**). They can thus be regarded as ring *carbo*-mers of saturated cycloalkanes in which Csp-Csp units were inserted. Those rings thus exhibit an alternation of -C≡C- units (on the edges) and Csp^3 atoms (at the vertices). [n]Pericyclynes derivatives offer a unique platform for the advancement of organic chemistry research.

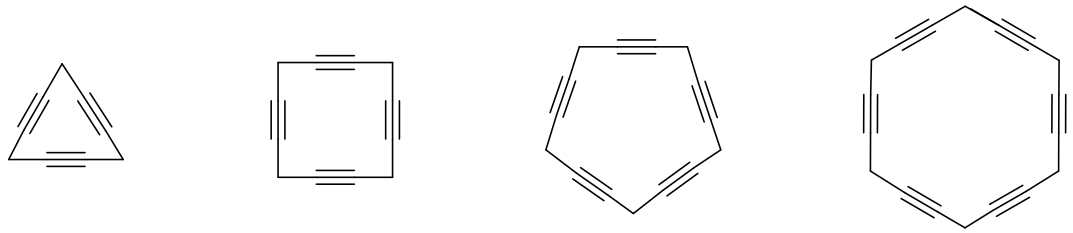

Figure. 1.2. The structure of [n] pericyclynes

2.1. Fully hydrocarbon [n]pericyclynes derivatives

2.1.1. Synthesis of hydrocarbon pericyclynes

The first example of pericyclyne was reported by L.T. Scott *et al*. in 1983 by proposing the synthesis of the decamethyl[5]pericyclyne representative[6]. Other permethylated derivatives of [5]-, [6]-, [7]-, and [8]pericyclynes were synthesized by the same authors using sequential alkynyl-propargyl coupling reactions.[7] These compounds were obtained by an original cyclization step and isolated as white crystalline solids **(Scheme 1.2**).

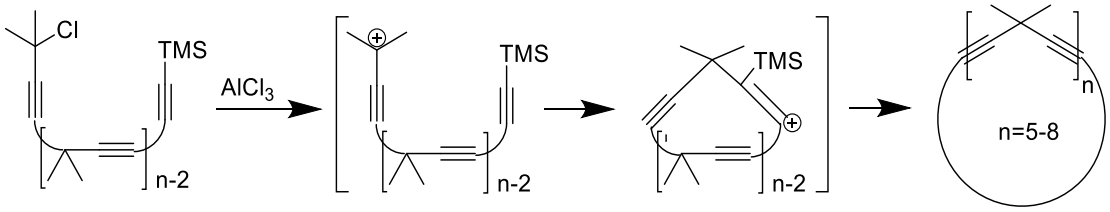

Scheme 1.2. Strategy applied for the preparation of the first examples of permethylated [n]pericyclyne.

The initial members of this family, specifically cyclonona-1,4,7-triyne and cyclododeca-1,4,7,10-tetrayne (with n=3 and 4, respectively), along with their substituted counterparts, have remained elusive. Due to challenges in their preparation related to labile hydrogens on doubly propargylic carbon atoms, the higher [n]pericyclynes (3–6) were exclusively synthesized in the form of fully or nearly fully alkylated derivatives to overcome these preparative difficulties[8].

2.1.2. Synthesis of expanded hydrocarbon pericyclynes

[n]Pericyclynes can be thought of as “expanded” cycloalkanes with acetylene spacers inserted between their corners [6], while the family obtained by insertion of 1,3-diyne spacers can be thought of as “expanded” [n]pericyclynes.

Expanded [n]pericyclynes are thus achieved through the incorporation of 1,4-butadiyndiyl C4 units into the edges of the original parent cycloalkane rings. The chemistry pertaining to expanded pericyclynes benefits from a plethora of efficient methods for oxidative (such as Glaser, Eglinton, Hay, etc.) or isohypsic (like Cadiot-Chodkiewicz) Csp-Csp coupling reactions. These reactions facilitate the synthesis of expanded [n]pericyclynes while in the synthesis of simple [n]pericyclynes, the pivotal step involves a propargylic Csp3-Csp cross-coupling process that is generally less effective.

The exploration of expanded [n]pericyclynes was initiated by Scott, particularly focusing on those with dimethyl substituents (where n ranges from 3 to 6)[9]. A notable characteristic highlighted among these strained π -electron-rich macrocycles is their significant explosive shock sensitivity, which emerged as a common feature. Since then, new variants have been described, including the spirocyclopropanated [12]pericyclyne, which features a C_{60} macrocyclic core. The permethylated spirocyclopropanated [6]pericyclyne **1** was synthesized through the dehydrodimerization and dehydrocyclization of corresponding precursors with either terminal (≡C-H) or silylated ends (≡C-$SiMe_3$) in the presence of CuCl and $Cu(OAc)_2$ **(Scheme 1.3)**. Through rapid scan FT-IR spectroscopy monitoring, it was observed during the thermal decomposition of the expanded[6]rotane **1** that the only gaseous product evolved is tetramethylethylene.

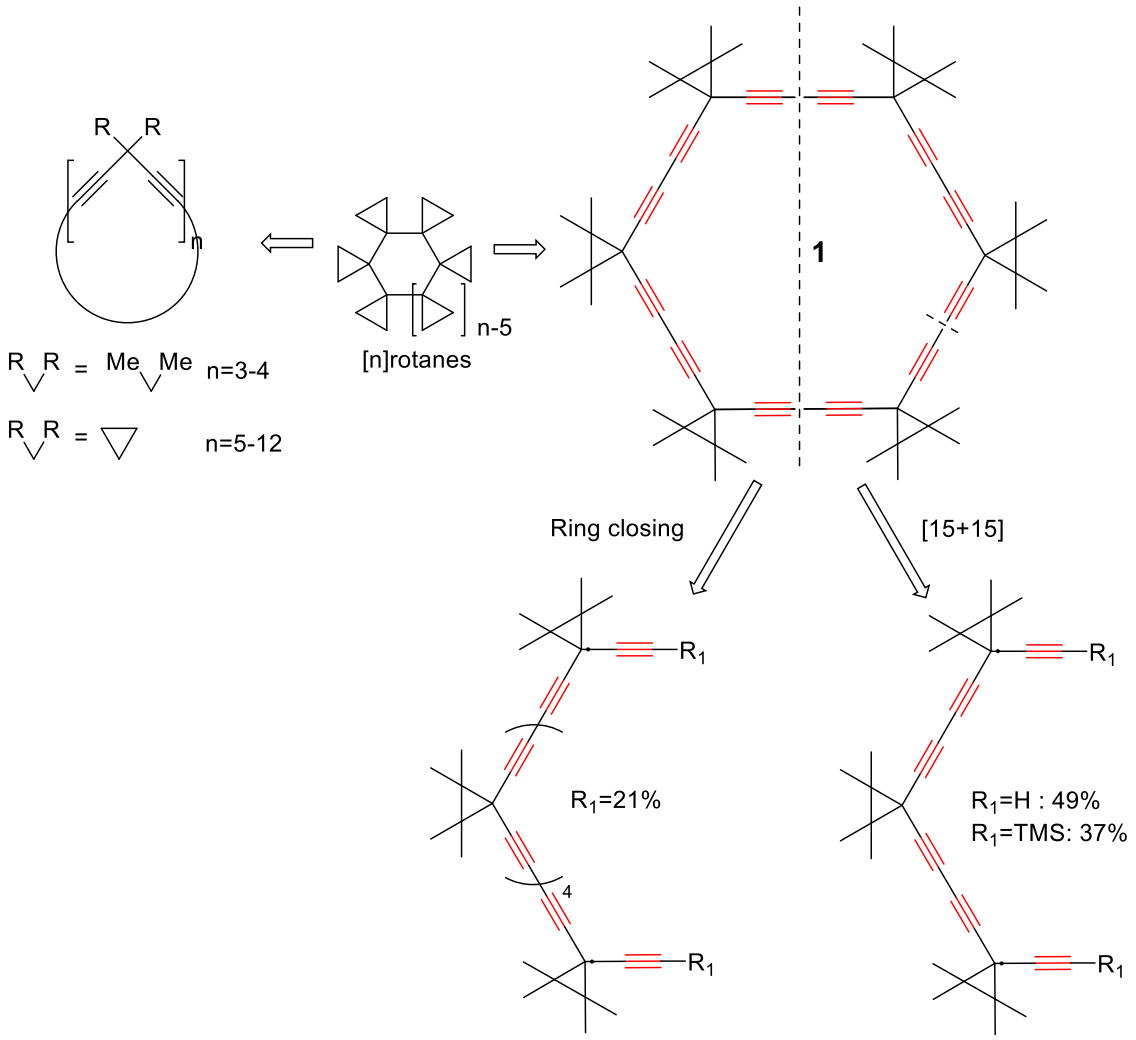

Scheme 1.3. "Expanding" permethylcycloalkanes and [n]rotanes[10].

2.2. Hetero [n]Pericyclynes derivatives

Transitioning from fully hydrocarbon [n]pericyclynes derivatives to hetero [n]pericyclynes derivatives marks a shift from purely carbon-based cyclic structures to those incorporating heteroatoms such as nitrogen, oxygen, or sulfur. While fully hydrocarbon [n]pericyclynes derivatives offer insights into the unique properties of more or less strained cyclic hydrocarbons, the introduction of heteroatoms in heterocyclic [n]pericyclines derivatives expands their chemical diversity and potential applications, resulting in compounds with varied reactivity. Additionally, these derivatives find applications in materials science, where their unique functionalities contribute to the design and fabrication of advanced materials with tailored properties.

2.2.1. Hetero [n]pericyclynes with alternation of carbon and heteroatom vertices.

Hetero[n]pericyclynes with alterations of carbon and heteroatom vertices exhibit diverse reactivity and properties due to the presence of both carbon and heteroatoms.

In [n]pericyclynes, the orientations of accessible frontier orbitals (such as n, π, σ, σ*, etc.) associated with heteroatomic vertices X (S, PR, SiR_2, etc.) are constrained. The heteroatoms from the third or fourth periods at one or more vertices within a pericyclyne ring play a significant role in minimizing ring strain. These heteroatoms, compared to carbon, have larger covalent radii, allowing for smaller bond angles at a lower energetic expense. Additionally, their increased softness, characterized by a reduced HOMO-LUMO gap, is expected to enhance homoconjugation between adjacent triple bonds, potentially leading to homoaromaticity[11], as illustrated in **Figure 1.3**.

Scott *et al*. have described mixed hetero-[n]pericyclynes characterized by diverse combinations of heteroatoms (including SiRR', PR, S) and dimethylmethylene (CMe_2) vertexes, as depicted in **Figure 1.3.**

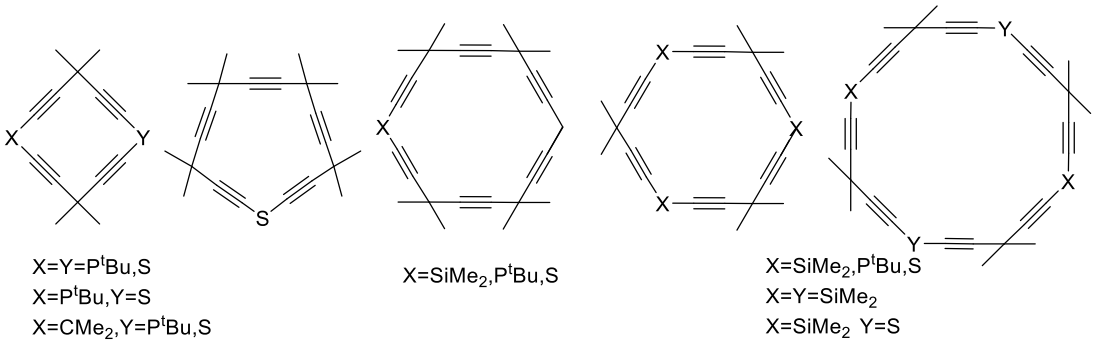

Figure 1.3. Representative mixed H/C-[n]pericyclynes with one, two, or three heteroatom vertexes.[12]

From the dianion of 3,3-dimethylpenta-1,4-diyne, researchers obtained [4]pericyclynes **2** and [6]pericyclynes **3** bearing heteroatoms at one out of two vertices, both with sulfur and with phosphorus, as illustrated in **Scheme 1.4**. However, when silicon was utilized, it resulted in the formation of the [6]pericyclyne,**6**, and [8]pericyclyne, **7**, with none of the [4]pericyclyne observed. This change in behavior observed when replacing sulfur or phosphorus by silicon remains unexplained.

Unlike carbon and silicon, phosphorus and sulfur have preferred bond angles in the 90-100° range, and this should relieve significant angle strain in the smallest pericyclynes. In fact,

Scott and his colleagues found that the tetraphospha[4]pericyclyne ring system is formed with relatively little difficulty (**Scheme 1. 4**) [13]. The corresponding [3]pericyclyne with phosphorus at every vertex can also be prepared. Upon closer examination of these compounds, distinct properties of the phosphorus heterocycles become apparent. Due to the substantial energy barrier for pyramidal inversion at phosphorus atoms, the di-t-butyl-diphospha[4]pericyclyne, **4** exists as two non-interconverting epimers. These isomers were successfully separated through meticulous preparative thin-layer chromatography. Similarly, the tri-t-butyl-triphospha[6]pericyclyne **5** also exists as two non-interconverting diastereoisomers, which were separated both from the [4]pericyclynes and from each other. It is presumed that the previously mentioned tetraphospha[8]pericyclyne was also obtained as a mixture of diastereoisomers, although no attempt was made to separate them. It's worth noting that all of these phospha[n]pericyclynes undergo rapid oxidation to the corresponding phosphine oxides when exposed to air.

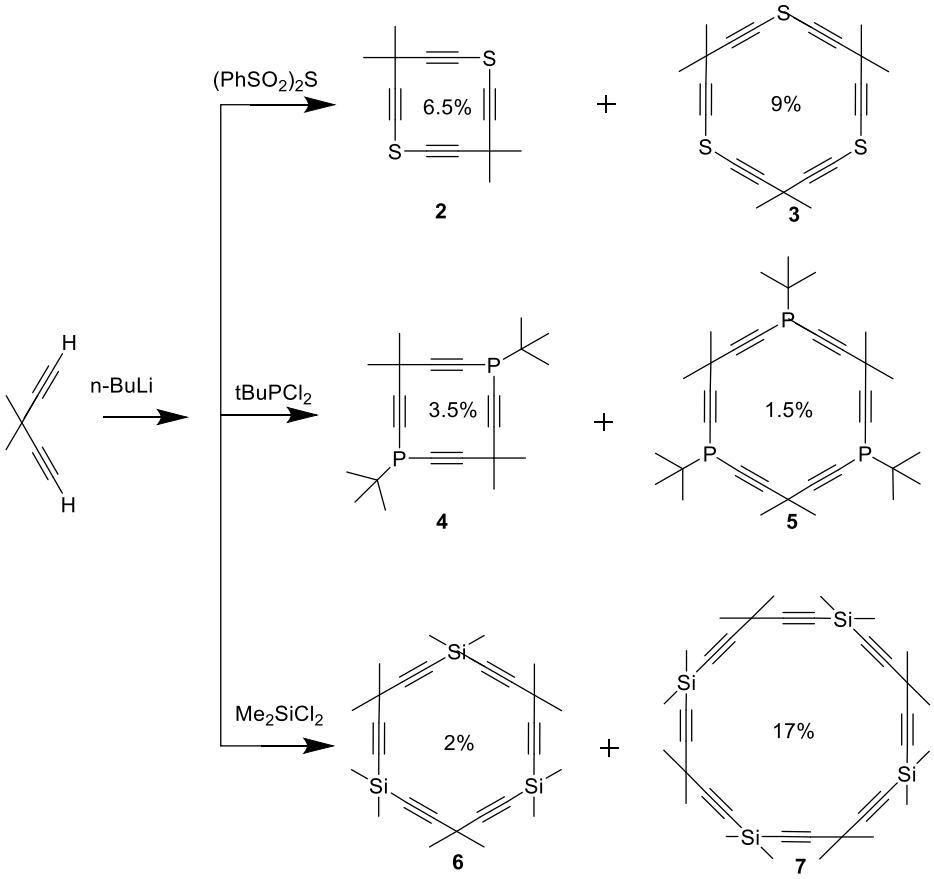

Scheme1. 4. Hetero[n]pericyclynes n=4,6,8 with heteroatoms at one out of two vertices

The syntheses of a mono-thia[5]pericyclyne[14] was achieved employing n-butylithium base. the termini of hexayne **8** were capable of being linked to the same sulfur atom with sulfurization agent $(PhSO_2)_2S$, leading to the formation of a mono-thia[5]pericyclyne **9**, (as depicted in **scheme 1.5**).

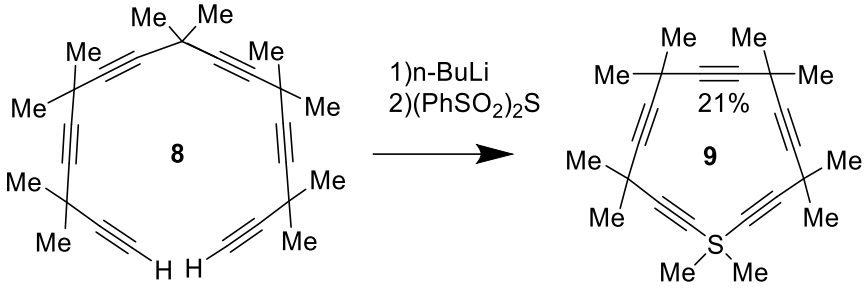

Scheme 1.5. syntheses of a mono-thia[5]pericyclyne[14]

2.2.2. [n]Pericyclynes with heteroatoms at each vertex.

[n]Pericyclynes with heteroatoms at each vertex exhibit exceptional properties due to the presence of heteroatoms positioned at every vertex within the cyclic structure, imparting distinct chemical functionalities and electronic characteristics to the molecule as a whole.

Cyclic silicon-based molecules known as cyclosilanes, with the formula $(SiR_2)_n$ (where R can represent various groups such as *t*Bu, Me, etc., and n is equal to or greater than 3), have been studied for some time. While isolating fully hydrocarbon [3]pericyclyne ring has proven challenging[8](see **section 2.2.1**), hexamethyltrisila[3]pericyclyne **10** (**Figure 1.4**) was successfully synthesized by removing dimethylsilylene from the precursor 12-membered hexasilacyclotriyne **10a**, which can be considered as a *carbo*-mer of cyclohexasilane. The involvement of silicon atoms in homoconjugation was investigated using photoelectron spectra. Additionally, the tetrasila[4]pericyclynes **11** has been reported, and a range of persila[n]pericyclynes, such as **12** and **13**, have been described for n greater than 5. More recently, persila[n]pericyclynes with methyl and isopropyl substituents (where n equals 6, 8, 10) have been characterized using X-ray crystallography[15–22].

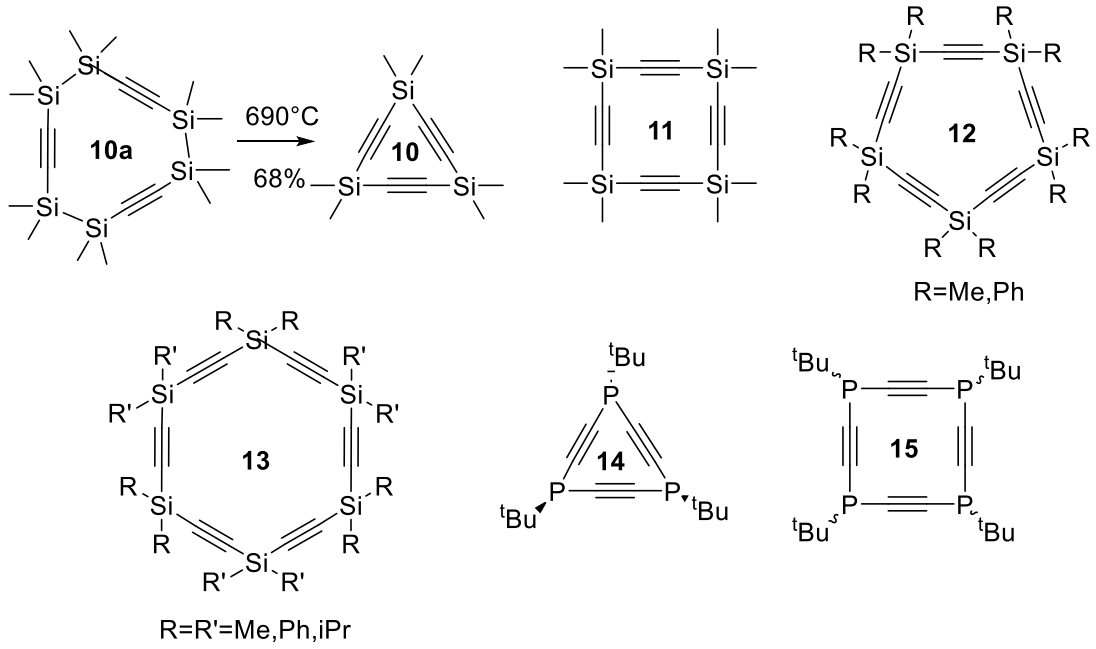

Figure 1.4. Persila- and perphospha[n]pericyclynes.[15–22]

Triphospha[3]- and tetraphospha[4]-pericyclynes **14** and **15**, as depicted in **Figure 1.4,** have also been documented. UV spectroscopy revealed robust cyclic electronic interactions within these molecules[13]. Despite the stereogenic nature of the vertexes, X-ray crystallography allowed characterization of one stereoisomer of each compound.

Acetylenic scaffolds have been heavily pursued for a long time, mainly because of their optoelectronic properties.[23,24,25] From the perspective of carbon networks, beautifully designed one-, two-, and three-dimensional scaffolds have been prepared.[26,27] However, the heteroatoms have rarely been embedded in these rigid wires, rings, boxes, and cages of acetylenic scaffolds. Especially in the context of the special P/C relationship,[28] it is surprising that very few attention has been paid to the incorporation of phosphorus atoms into acetylenic scaffolds until recent decades. Examples of their attractivity are the thiophene- and pyridine-conjugated phospholes that possess remarkable optical and electrochemical properties.[29–31]

The first phospha[n]pericyclynes were reported in 1990 by Scott and Unno [13]. By condensing t-BuPCl$_2$ with doubly deprotonated diethynylphosphinos **16** and **18**, both formed from t-BuPCl$_2$ and HC ≡ CMgBr, they were able to generate small quantities of tetraphospha[4]pericyclyne **15** (11%) and triphospha[3]pericyclyne **14** (16%), respectively (**Scheme. 1.6**). Four isomers were observed in the product mixture of **15** and one for **14**. The

most abundant *cis,trans*-**15** isomer shows three resonances in the ^{31}P NMR spectrum, while each of the other isomers show a single signal. X-ray crystal structures were reported for all-*trans*-**15** and *cis,trans*-**14**. Both compounds display a broad UV-vis. absorption band around 225 nm, which is indicative of (cyclic) electronic delocalization, either over the phosphorus centers or by means of through-space interaction of the in-plane acetylenic π -orbitals.

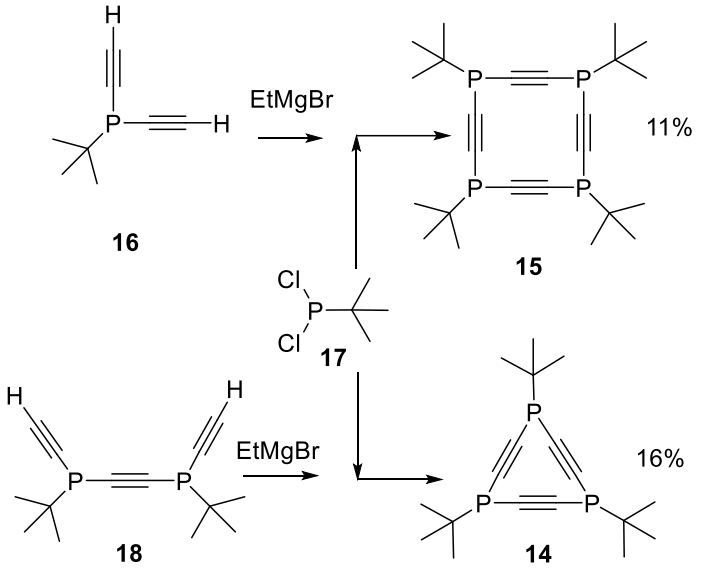

Scheme 1.6. Synthesis of tetraphospha[4]pericyclyne **15** and triphospha[3]pericyclyne **14**

The synthesis of sila- and germa[n]pericyclynes, where n ranges from 3 to 12, incorporating various substituents such as H, aryls, and C_1-C_{15} alkyls were also described[32] (**Scheme 1.7**). Specifically, germa[4]- and -[6]pericyclynes, designated as compounds **20** and **21** respectively, were produced using a method involving random lithium-mediated dehydrochlorination between diethynylgermanes and the corresponding dichlorogermanes. Moreover, it is mentioned that dodecaphenylgerma[6]pericyclyne **21** has the ability to form inclusion compounds with $AgBF_4$ and can generate ceramic powders upon heating.

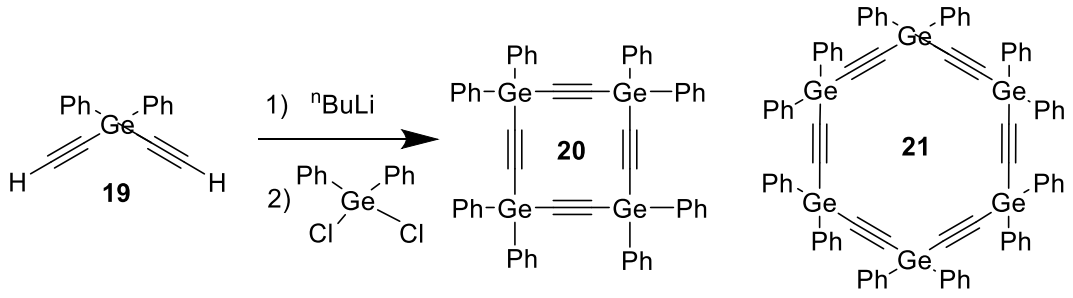

Scheme 1.7. Direct random synthesis of germa[n]pericyclynes.[32]

Perchalcogena[n]pericyclynes, denoted as $C_{2n}X_n$ (with X = O, S, Se, or Te), have not been reported so far, even the octathia[8]pericyclyne **22**, which is the *carbo*-mer of the S_8 allotrope of sulfur, as shown in Figure **1.5**. However, recent theoretical investigations utilizing Density Functional Theory (DFT) have suggested that perchalcogena[n]pericyclynes (where n = 3-6,8) are plausible molecules, exhibiting high (uncorrected) heats of formation, such as 1506 $kJ \cdot mol^{-1}$ with zero strain energy for $C_{16}S_8$[33].

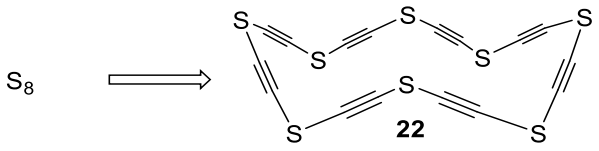

Figure 1.5. The *carbo*-mer of the S_8 molecular allotrope investigated through DFT calculations

2.2.3. Expanded [n]pericyclynes with heteroatoms at each vertex.

Märkl *et al*. have synthesized expanded phospha[n]pericyclynes (**24**, n = 3–6) containing butadiyndiyl edges using both a one-pot approach and stepwise couplings of open-chain precursors[34] (**Scheme 1.8**). In the one-pot oxidative Eglinton coupling of building block $MesP(C{\equiv}CH)_2$ (where Mes = 2,4,6-tri-tert-butylphenyl) with $Cu(OAc)_2$, a mixture of four macrocycles (**24a–d**) was obtained. Triangular **24a** and pentagonal **24c** could be isolated in very small amounts, while square **24b** and hexagonal **24d** were inseparable. The stepwise (de)protection approach showed better results. For instance, Eglinton coupling of **25a** predominantly produced dimer **24b** (86%) with some trimer and tetramer. Although the product mixture was not separated, all products could be obtained in pure form by different methods. Coupling of **25b** yielded mainly triangle **24a** by intramolecular coupling (70%) with some dimer (hexagonal **24d**), and coupling of **25c** mainly produced the monomer (**24b**) by intramolecular coupling. Additionally, coupling of **25f** resulted in the formation of octagonal product **24e** (9%), which was not obtained in the one-pot procedure, while pentagonal species **24c** was exclusively obtained through this procedure[35].

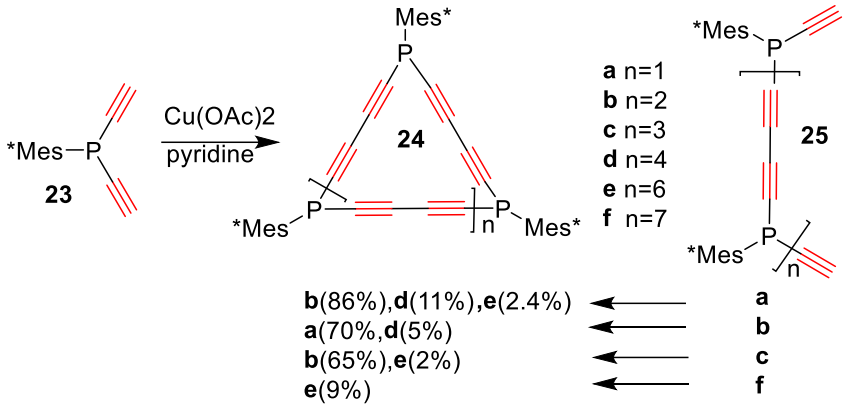

Scheme 1.8. Expanded phospha[n]pericyclynes **24** *via* a one-pot approach from **23** and from linear precursors **25**

2.2.4. Poly[n]pericyclynes cages with heteroatoms at each vertex

Though it is difficult to say how much electronic interaction among the acetylenic units occurs via orbitals on the phosphorus atoms and how much occurs via through-space overlap of the in-plane p-orbitals, there is little doubt that these N-phospha[n]pericyclynes exhibit a substantial degree of cyclic electron delocalization. One of the interests of using phosphorus in phospha[n]pericyclynes derivatives is their potential for building into the third dimension.

Scott and his colleagues embarked on the synthesis of three-dimensional structures wherein phospha[n]pericyclyne units are extended into the third dimension [6,14,36]. In their pursuit of phospha[n]pericyclyne-based cage **26**, they treated precursor triethynylphosphine **27**, derived from t-BuP(C≡CH)$_2$ and PCl$_3$, with EtMgBr followed by POCl$_3$ trapping. Unexpectedly, instead of **26**, they obtained the remarkable phosphine acetylenic cage **29**, likely formed through the dimerization of intermediate **28** (**Scheme 1.9**). Molecular cage **29**, for which an X-ray structure was reported, stands as the first known compound with a 3D phosphine-acetylenic architecture, devoid of transition metal complexes.

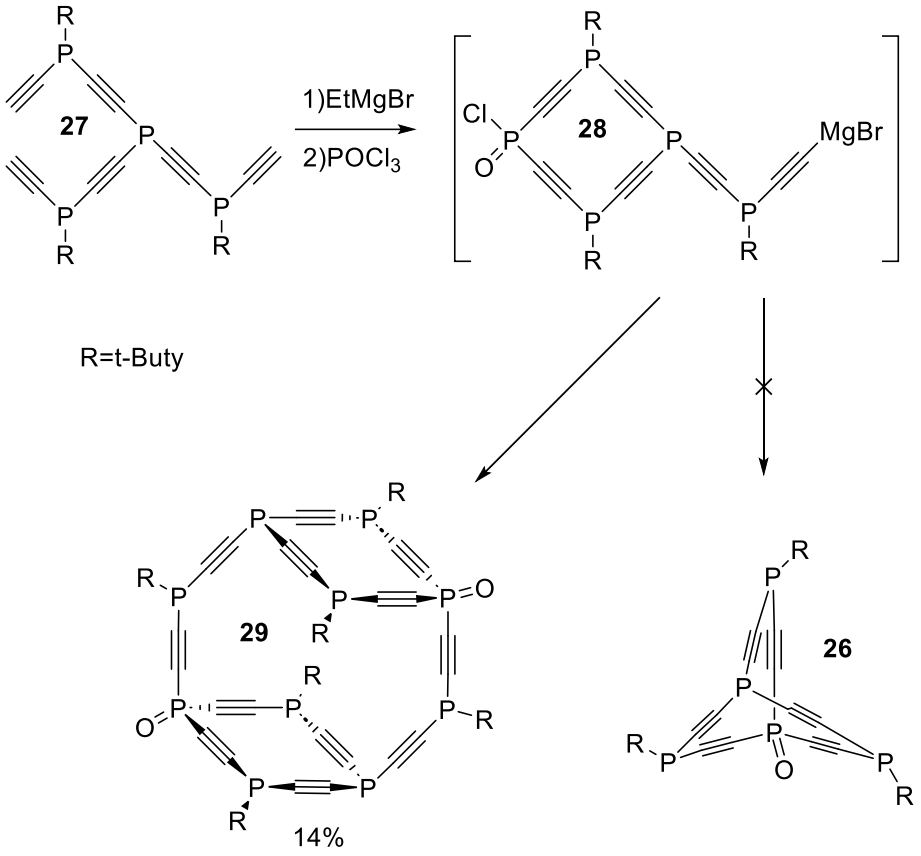

Scheme 1.9. Construction of a phosphine-acetylenic cage

2.3. Oxy[n]pericyclynes derivatives

Oxy[n]pericyclines serve as important precursors in the synthesis of *carbo*-benzene derivatives. Indeed, *carbo*-benzenes have been mainly prepared from hexaoxy[n]pericyclynes through a reductive aromatization involving the elimination of all hydroxyl or methoxy by reductive and acidic treatments. The stereochemical resolution of oxy[n]pericyclynes has been infrequently pursued, as the stereochemical ambiguity is expected to be resolved during the final aromatization step. Many substituents (alkyl, aryl, alkynyl) can be introduced on these hexaoxy[n]pericyclynes and can thus give access to many *carbo*-benzenes, with various substituents that allow providing them various properties. Thus, oxy[n]pericyclynes play a crucial role as intermediates in the synthesis of *carbo*-benzene derivatives, offering a versatile platform for the design and preparation of novel aromatic compounds with tailored properties and functionalities.

2.3.1. Synthesis of oxy[n]pericyclynes derivatives without heteroatom.

Oxy[n]pericyclynes or [n]pericyclynols exhibit carbinols and carbinol ether functions as their predominant functional vertices, and are formed through the nucleophilic addition of terminal alkynes to carbonyl compounds (**Scheme 1.10**). The initial instances reported involved [4]- and [5]pericyclynes, where a single secondary carbinol vertex was produced through the cyclization of bisterminal skipped oligoynes onto ethyl formiate[38]. Simultaneously, [8] and [10]pericyclynes, featuring two secondary carbinol vertices, were isolated, albeit as mixtures of stereoisomers. In a broader context, carbinoxy vertices become stereogenic when multiple heterodisubstituted vertices are present, the corresponding [n]pericyclynes being obtained as stereoisomeric mixtures. When all the vertices in [n]pericyclynes are of the carbinol type, these molecules can be viewed as ring *carbo*-mer derivatives of cyclitols, which are nonbranched cyclic isomers of carbohydrates referred to as "*carbo*-[n]cyclitols."[37]

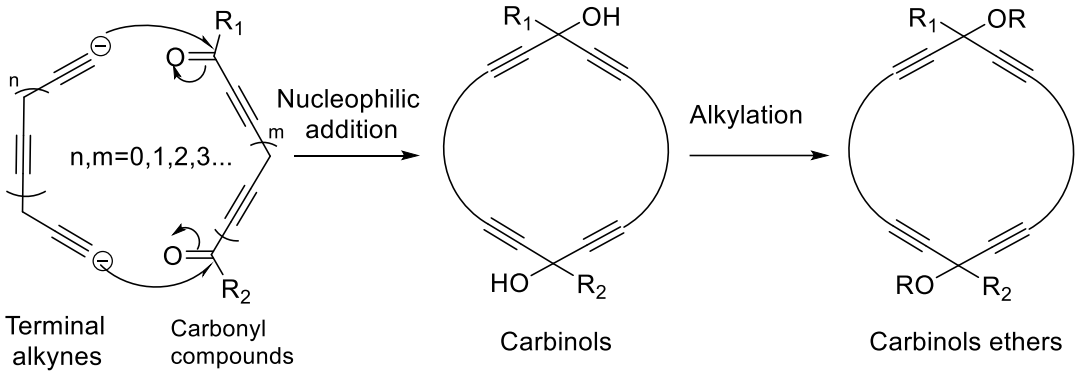

Scheme 1.10. Synthesis of predominant functional vertices carbinols and carbinol ethers

Scott's syntheses of [n]pericyclynes hydrocarbons relied on a straightforward ring-closing process. In contrast, the syntheses of *carbo*-[n]cyclitol derivatives required cyclization strategies of the [m + (3n - m)] type[38]. The ring formation process involves the double nucleophilic attack of a ω-bisterminal m-carbon oligoyne onto a ω-dioxo (3n - m)-carbon oligoyne.

2.3.1.1. Hexaoxy [6] -pericyclynes

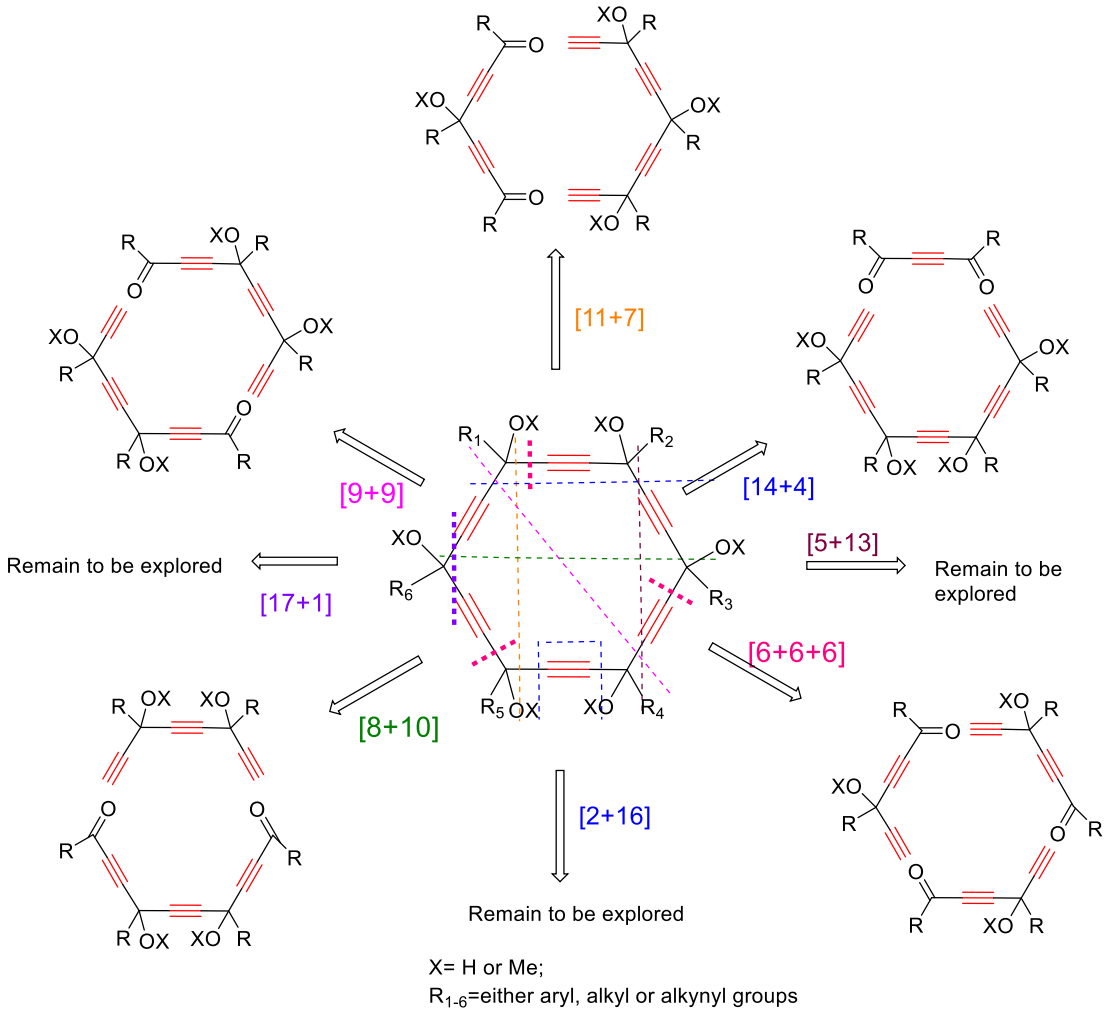

Figure 1.6. Possible [m + (18 - m)] strategies for ring formation of hexaoxy[6]pericyclynes by double alkynyl-propargyl coupling reactions.

From a general standpoint, homologous [(18 - m) + m] strategies for synthesizing hexaoxy[6]pericyclynes were explored. Among the nine possible strategies, attempts have been made previously for the odd strategies where m equals 7 and 9, and the even strategies, where m equals 4 and 10. Additionally, the [13 + 5], [16 + 2], and [17 + 1] strategies remain avenues for investigation (**Figure 1.6**). These strategies offer further possibilities for synthesizing hexaoxy[6]pericyclynes and warrant exploration in future research endeavors.

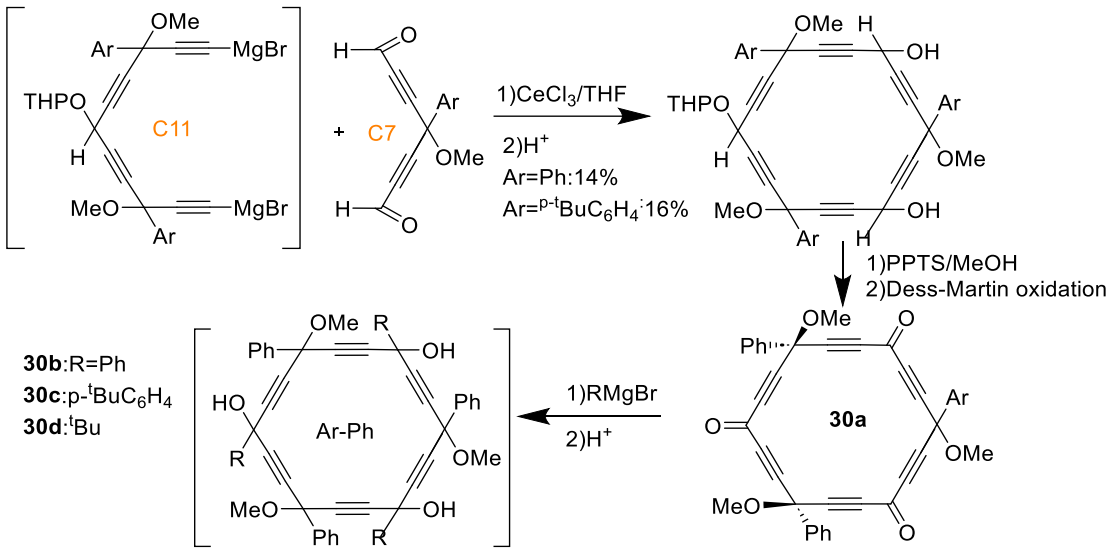

Scheme 1.11. Ueda-Kuwatani's [11 + 7] route to *carbo*-[6]cyclitol derivatives.

In 1995, while our group was attempting to synthesize unsubstituted *carbo*-[6]cyclitol ($C_{18}(H_2O)_6$), Ueda, Kuwatani, *et al*. simultaneously disclosed the first examples of substituted *carbo*-[6]cyclitol derivatives[39]. These derivatives were further investigated and described in 1998[40]. The *carbo*-[6]cyclitol ethers **30a-d** were prepared through a [11 + 7] ring formation process using the bis-Grignard reagent of a C11 tetrayne and a C7 diyne dicarbaldehyde (**Scheme 1.11**). The chemo-selectivity of the reaction was relatively low (6% in the presence of cerium trichloride additive). Both the C11 dinucleophile and C7 dielectrophiles were present as mixtures of stereoisomers, and the overall stereoselectivity of the process, considering over 20 possible diastereoisomers, was not determined.

The [14 + 4] strategy was initially employed using dibenzoylacetylene as the C4 dielectrophile and various C14 pentadiynes (**Scheme 1.12**). This approach yielded two hexaphenyl *carbo*-[6]cyclitol derivatives, **31a** and **31b**, featuring either two or four free OH groups in high yield (approximately 40%). NMR spectroscopy clearly indicated that these compounds were obtained as mixtures of stereoisomers. This same synthetic route also led to another hexaaryl *carbo*-[6]cyclitol diether, **31c**, with 4-anisyl and 4-pyridyl substituents. The ring formation followed by double desilylation proceeded in acceptable yield (14%) and resulted in **31c** as a mixture of stereoisomers, all lacking any symmetry. The [14 + 4] strategy was also applied starting from a C14 heptayne, resulting in a stereoisomeric mixture of dialkynyl *carbo*-[6]cyclitol tetraether **31d** in good yield (43%). All these results indicate that

[14 + 4] ring formation processes (14-43%) are more efficient than [11 + 7] processes (14-16%).[39]

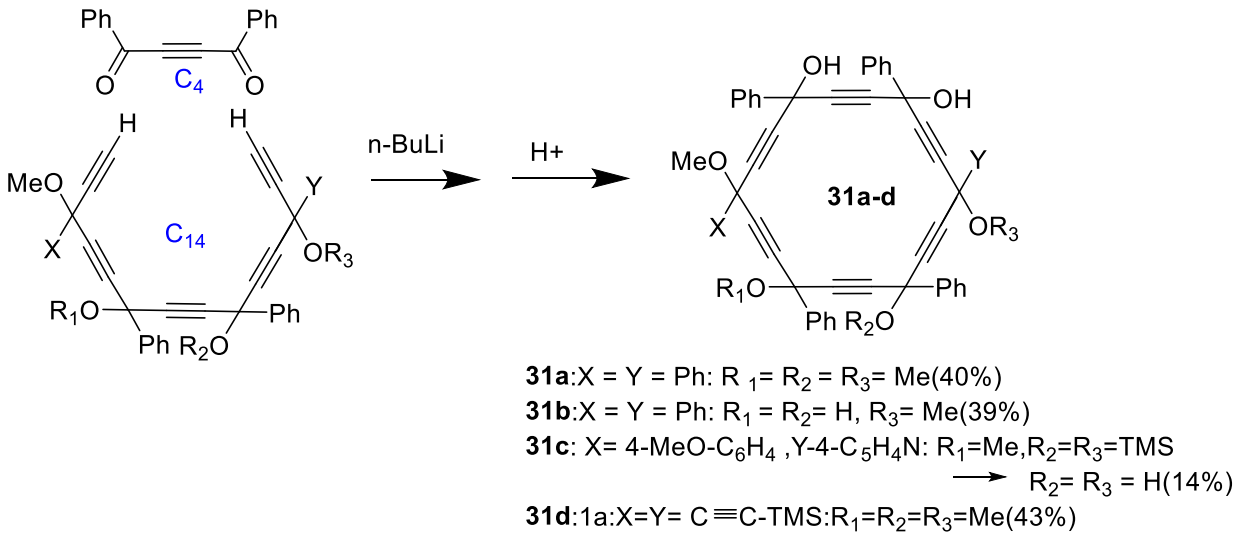

Scheme 1.12. [14 + 4] Strategy for the synthesis of *carbo*-[6]cyclitol ethers.

The [8 + 10] route was first investigated in view of preparing an isomeric derivative of **31b** with nonadjacent CH(OH) vertices. The dilithium salt of a C8 triyne (**Scheme 1.13**) was reacted with a C10 dialdehyde,[41] to give the *carbo*-[6]cyclitol tetraether **32** in 12% yield as a mixture of diastereoisomers (14 in theory). Oxidation of both the carbinol vertices afforded [6]pericyclynedione **33**, the five steroisomers of which were identified by NMR spectroscopy after partial resolution.

The [8 + 10] route was adapted for the preparation of hexaethynyl *carbo*-[6]cyclitol ether **34** from a C8 pentayne and a C10 heptaynedione.[37] The latter [8 + 10] ring formation step proceeded in 34% yield (**Scheme 1.14**).

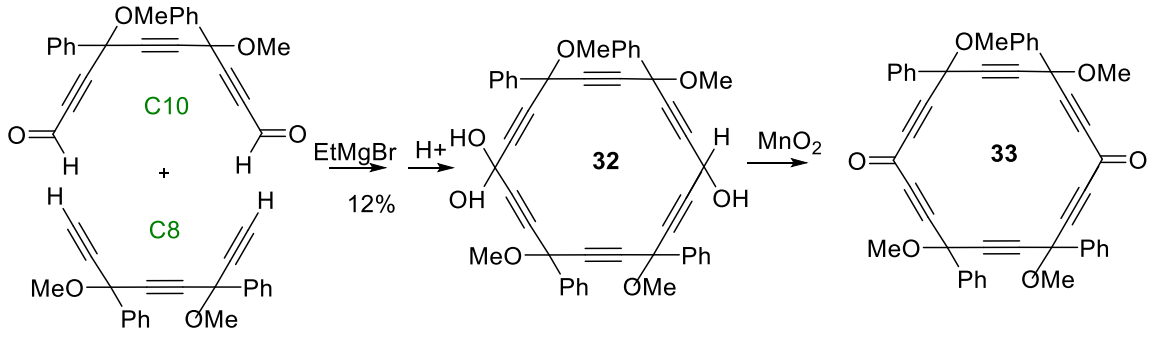

Scheme 1.13. [8 + 10] route for the preparation of a [6]pericyclynediol with two nonadjacent CH(OH) vertices and the corresponding pericyclynedione, as mixtures of steroisomers.[38]

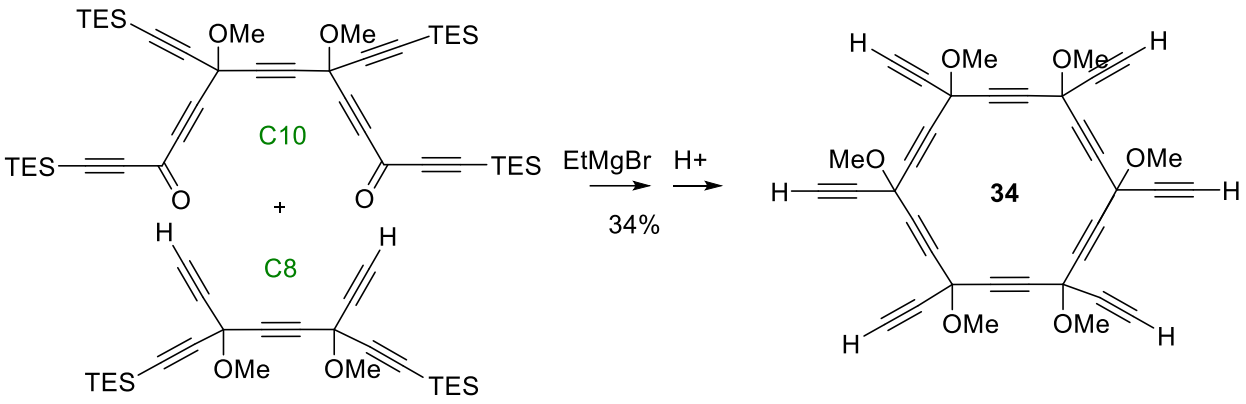

Scheme 1.14. Synthesis of hexaethynyl-*carbo*-[6]cyclitol hexamethyl ether **34**, as a mixture of steroisomers

A highly effective method has been developed for preparing functional [6]pericyclynes using substituted (9-oxo-nona-1,4,7-triyn-1-yl)lithium as a in situ formed reactant. This synthesis involves optimizing a process that forms a [9 + 9] ring structure (**Scheme 1.15**). The resulting [6]pericyclynes **35** are formed with a high yield up to 60%, as mixtures of diastereoisomers..

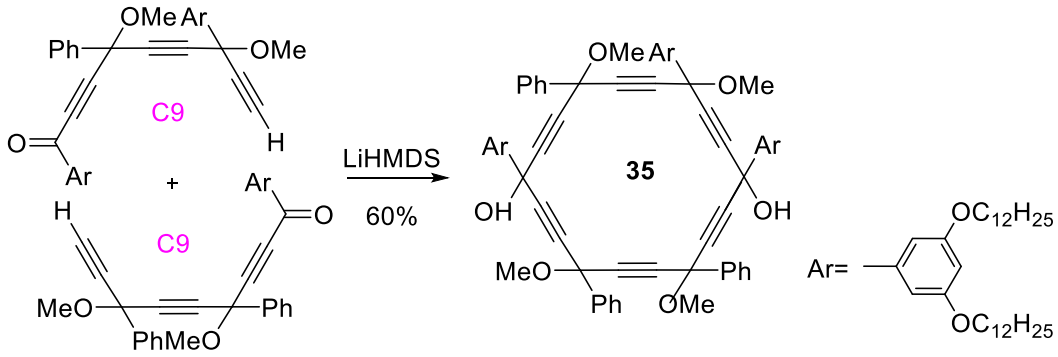

Scheme 1.15. Strategies proposed for the synthesis of substituted hexaoxy[6]pericyclyne precursors involve [9+9] approaches

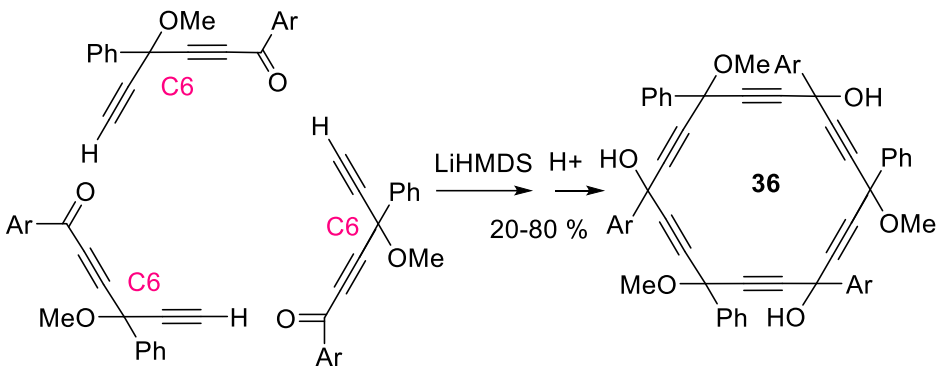

Scheme 1.16. Strategies envisioned for the synthesis of substituted hexaoxy[6]pericyclyne precursors through a [6+6+6] process.

Another trial has been developed for generating functional hexaoxy[6]pericyclynes using (6-hexa-2,5-diynal-1-yl)lithium as a starting point. This synthesis focuses on optimizing a process that yields from 20% to 80% with different subsituents though a [6+6+6] ring formation process (**Scheme 1.16**)[42]. Although the yield of the cyclization reaction fluctuated greatly, it brings the possibility of introducing more functional groups into hexaoxy[6]pericyclynes, and also opens up new perspectives for the development of alternative cyclization methods.

The synthetic methodologies involving the [9+9], [14+4], [6+6+6] and [8+10] cyclization strategies have shown promise and competitiveness compared to the [11 + 7] strategy previously developed by Kuwatani, Ueda *et al*[39,42]. While the [13 + 5], [16 + 2], and [17 + 1] strategies remain to be explored, the quite short synthesis of [6]pericyclynedione in just eight steps, along with its potential pivotal role, suggests that the [8 + 10] route is suitable for further scale-up studies. These studies are currently underway, indicating the ongoing progress and potential scalability of this synthetic route.[43] As a general trend, it may finally be concluded that the efficiencies of the ring formation schemes rank in the following order:

[11 + 7] < [6+6+6] < [8 + 10] < [14 + 4] < [9+9].

2.3.1.2. Pentaoxy[5]pericyclynes

The same process also enabled the synthesis of homologous pentaoxy[5]pericyclynes through [(15-k) + k] cyclization strategies from C_{15-k} diynes and C_k dicarbonyl compounds (k=1, 4, 10).[44]

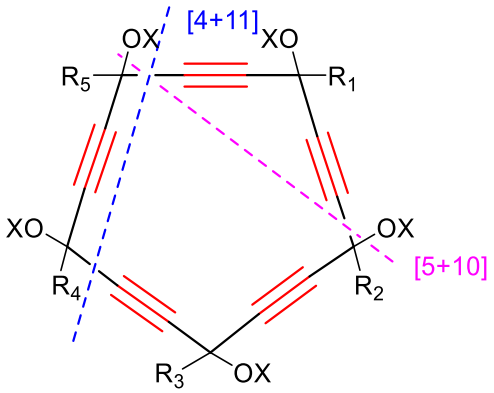

Figure 1. 7. Possible [k + (15 - k)] strategies for ring formation of [5]pericyclynes.

The formation of the C15 ring of *carbo*-[5]cyclitols resorted to two kinds of strategies: [11 + 4] , [5 + 10] (**Figure 1.7**).[41] The [11 + 4] route consisted in the reaction of dilithium salts of C11 tetraynes with two C4 synthons (**Scheme 1.23**).

Dibenzoylacetylene and the butyndial cobalt complex gave the [5]pericyclynediols **37a, 37b** and the [5]pericyclynediol complexes **38a, 38b** in 37-31% and 5-6% yield, respectively. Oxidative decomplexation of the latter afforded the free *carbo*-[5]cyclitol triethers **39a, 39b** as stable compounds. These compounds were obtained from statistical mixtures of the three diastereoisomers of the C11 tetraynes (as determined by HPLC analyses): all 10 diastereoisomers of the [5]pericyclynediols could therefore occur in the product mixture.

Symmetrization of **37a** was achieved by methylation of the remaining OH groups, which afforded all four possible diastereoisomers of **40a**. The reaction sequence was then repeated from a pure chiral diastereoisomer of the C11 tetrayne (i.e. the major (R*,R*) isomer, obtained by preparative HPLC): the three expected diastereoisomers of **40a** were formed in a statistical ratio, and two of them could be purified as crystalline solids by semipreparative HPLC (**Scheme 1.17**).

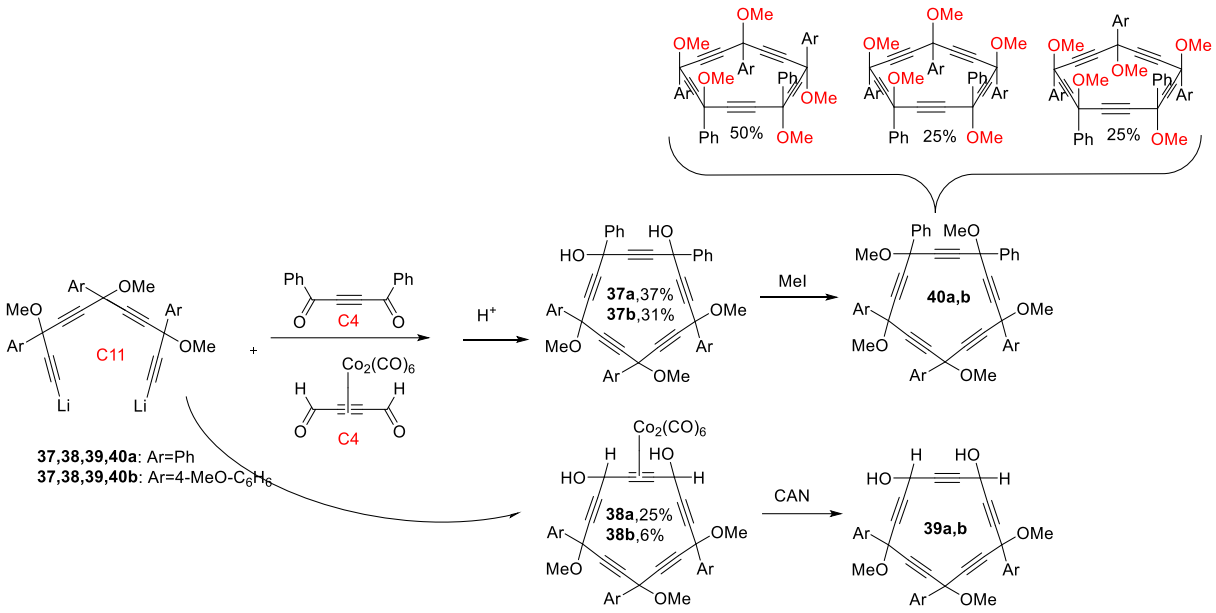

Scheme 1.17. Synthesis of pentaryl- and triaryl-*carbo*-[5]cyclitols ethers by a [11 + 4] route and statistical stereoisomeric ratio of the *carbo*-cyclitol pentamethyl ether **40a**.

The [5+10] route was first envisioned for preparing the regioisomer of [5]pericyclynediols **42a**, **42b** (**Scheme 1.18**) with nonadjacent CH(OH) vertices. It was finally tested from three C5 diynes and two C10 triyne dicarbaldehydes (**Scheme 1.18**): the *carbo*-[5]cyclitol products were obtained with a similar yield (15-19%) as mixtures of diastereoisomers (at most 10 for **42a, 42b** and 6 for **42c**). **42c** was regarded as a protected version of the corresponding [5]pericyclynone, itself a functional version of Scott's octamethyl[5]pericyclynone.[45] Nevertheless, treatment of **42c** with $SnCl_2$/HCl, followed by DCI/NH_3 MS analysis, allowed detection of a peak whose mass corresponds to the NH_3 adduct of a protonated cyclopentadienone **42d**: this can be considered as a sign of the existence of the ring *carbo*-mer of the *carbo*-aromatic cyclopentadienyl cation, which was predicted to indeed exist and be aromatic by DFT calculation.

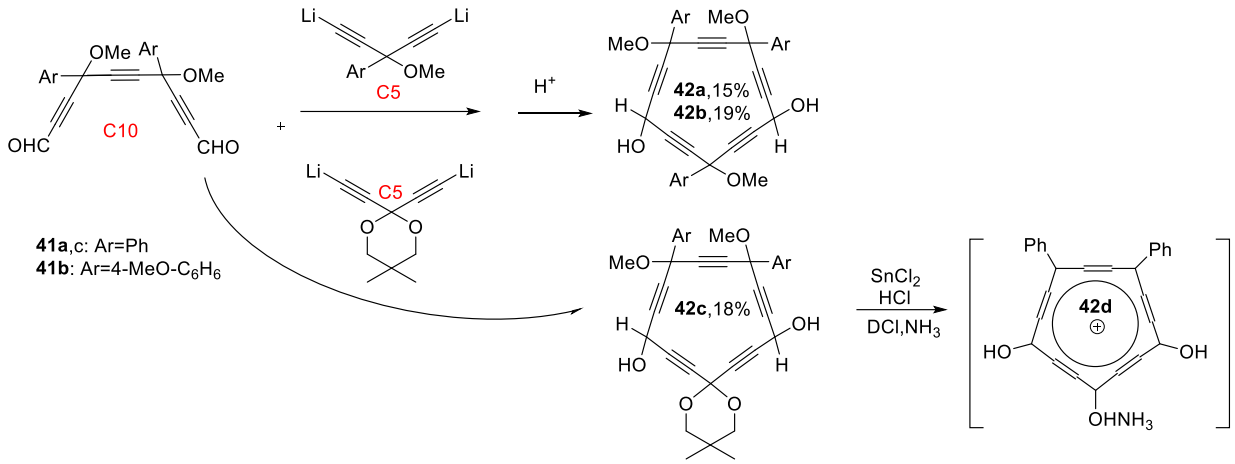

Scheme 1.18. [5 + 10] route to [5]pericyclynediols and a ketal-protected keto-*carbo*-[5]cyclitol ether with two nonadjacent CH(OH) vertices. After treatment of **42c** with $SnCl_2$ and HCl, a MS peak was assigned to an aromatic *carbo*-cyclopentadienyl adduct.

2.3.2. Synthesis of oxy[n]pericyclynes derivatives with one hetero atom in or on the ring.

Monophospha- and monosila[5]pericyclynes have been conceived as part of the functional series, as depicted in **Scheme 1.19**. A stereoisomeric mixture of a *carbo*-phospholane oxide **44a** was successfully obtained in high yield (86%) via a [14 + 1] ring formation route. However, a similar approach in the silicon series did not yield the desired outcome. Instead, analogous silolanes **44b** were synthesized using a [5 + 10] route, albeit with a lower yield of 20%. Notably, due to the presence of only four potentially stereogenic centers, chromatographic resolution allowed the isolation of two pure diastereoisomers. These compounds were considered as potential precursors of phosphole oxide and silole ring *carbo*-mers (**43ab**), the aromatic character of which was investigated at the theoretical level.[46,47]

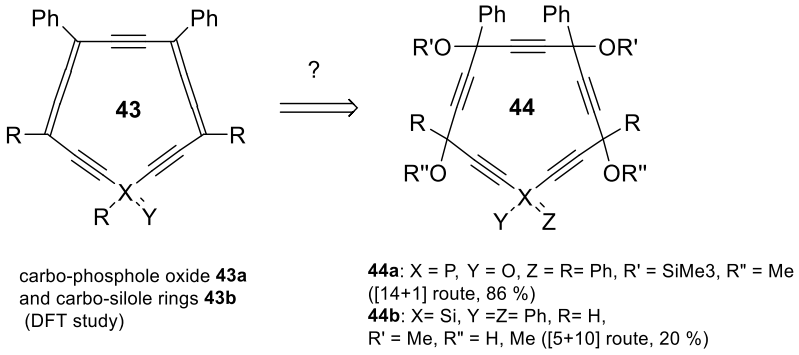

Scheme 1.19. *Carbo*-phospholane oxide **44a** and *carbo*-silolane **44b**, as possible precursors of phosphole oxide and silole ring *carbo*-mers **43b** and **43a**, respectively. The latter rings were predicted to be weakly aromatic by DFT calculations.[46–48]

Among all the work described before, the phospha[n]pericyclynes always appeared as derivatives having phosphorus atoms at every vertex until the synthesis of the first *carbo*-phospholane oxide was accomplished. The phospha[5]pericyclynic precursor **44a** was easily synthesized from the previously described pentadiyne (**section 2.3.1**) [11] by reacting the dimagnesium salt of pentayne **45** with one equivalent of dichlorophenylphosphine oxide, as outlined in **Scheme 1.20**. This two-step/one-pot [14+1] cyclization reaction proceeded with a high yield of 86%, which is notable for such a macrocyclization process conducted without a template. However, the formation of side-product **46** necessitated purification by silica gel chromatography. The presence of ethyl alkynylphosphinate **46** was likely due to contamination of the commercial ethylmagnesium bromide solution with ethoxymagnesium bromide. The resulting *carbo*-phospholane oxide **44a** was isolated as a mixture of 9 diastereoisomers, 5 of which being chiral. In ^{31}P NMR spectroscopy, the isomeric mixture exhibited a signal at -20 ppm, characteristic of the ≡C-P(O)(Ph)-C≡ environment.

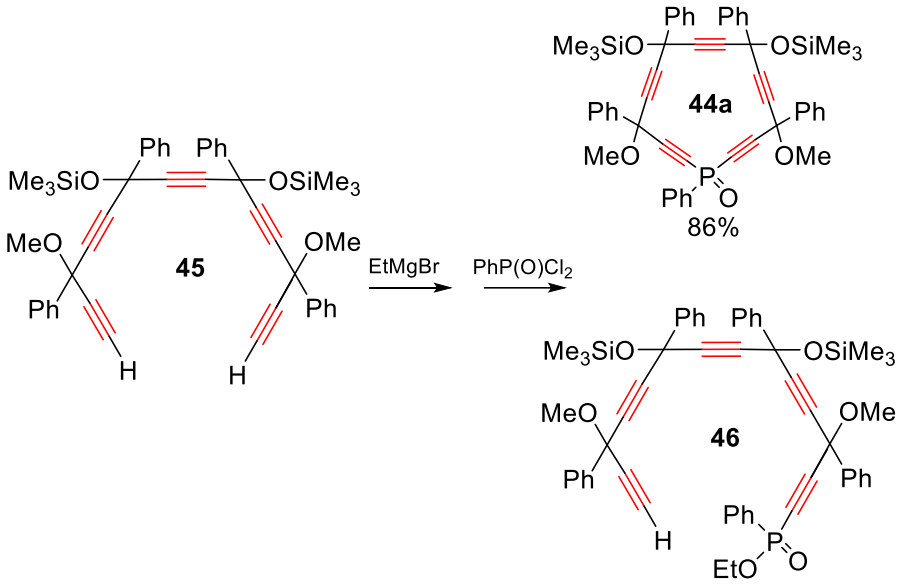

Scheme 1.20. Synthesis of the *carbo*-phospholane oxide **44a**.

While acetylenic macrocycles with phosphorus atom within the rings were widely investigated, much less attention has been paid to *carbo*-benzene derivatives featuring phosphorus atoms directly bonded to the C18 ring. Indeed, all the *carbo*-benzene derivatives described up to now have their a C18 ring bonded to H or C atoms only (aryl, alkyl, alkynyl

substituents) until first experimental examples of acetylenic macrocycles-exhibiting a direct bond with a heteroatom were synthesized in 2023, by Yao *et al.*[49,50].

The lithium salt of diphenylphosphine-borane was added to the [6]pericyclynedione **33** and gave the expected bis(phosphino-borane)-[6]pericyclyne **47** as a mixture of stereoisomers (14 in statistics) with a yield of 28%, which upon direct treatment with H_2O_2 gives the diphenyl phosphinoyl[6]pericyclynes 48 in 82% yield.

Addition to **33** of methyldiphenylphosphine oxide, upon deprotonation with *n*-BuLi, led to the bis(phosphinomethyl)-[6]pericyclynediol dioxide **49** in 70% yield (**Scheme 1.21**).

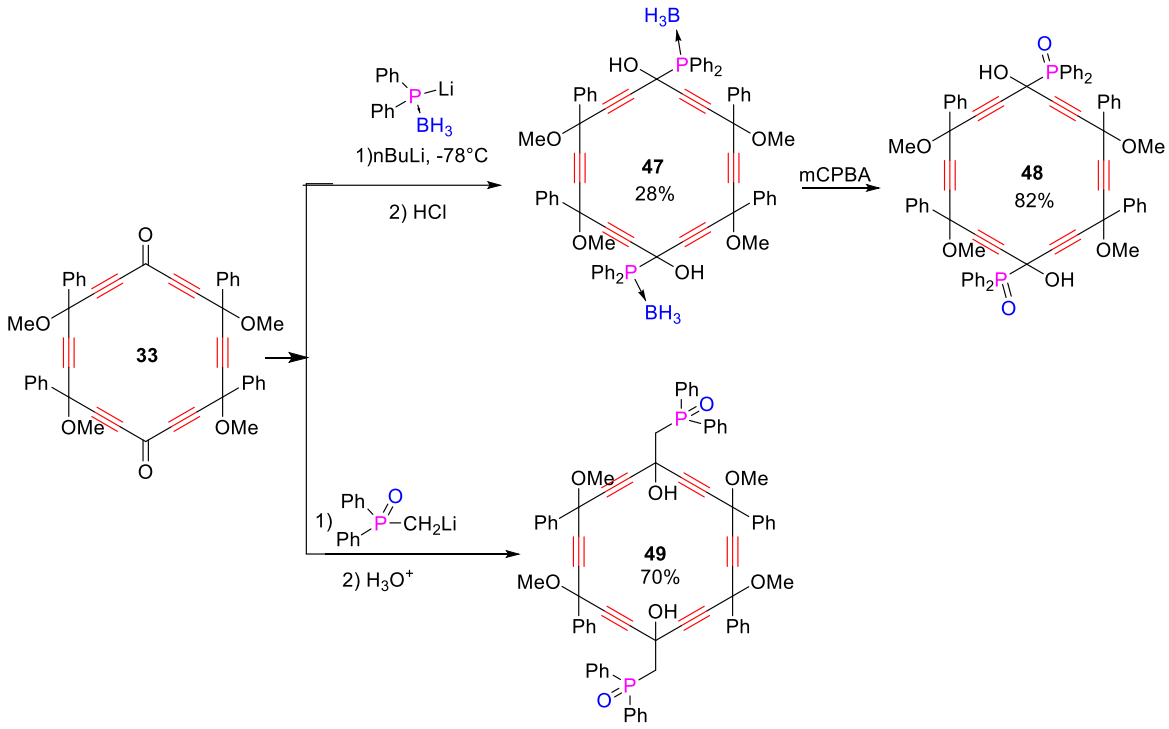

Scheme 1.21. Synthesis of acetylenic macrocycles having phosphorus atoms directly bonded to the C18 ring

2.3.3. Synthesis of expanded oxy[n]pericyclynes derivatives

Square and hexagonal expanded phospha[n]pericyclynes **51** and **52** were synthesized via oxidative Hay coupling of building block **50** (**Scheme 1.22**), which was derived from (i-Pr)$_2$NP(O)(C$\equiv$CH)$_2$ through oxidative coupling. Macrocycle **51** comprises several isomers, as indicated by the presence of four ^{31}P NMR resonances[57]. Conversely, the 30-membered ring structure **52** displays a distinct signal, likely due to the all-*cis* or all-*trans* isomer, along with a

broader signal representing other isomers. The elongated 'crystals' of **52** hint at the formation of nanotubes via one-dimensional stacking of the macrocycle in the solid phase[51].

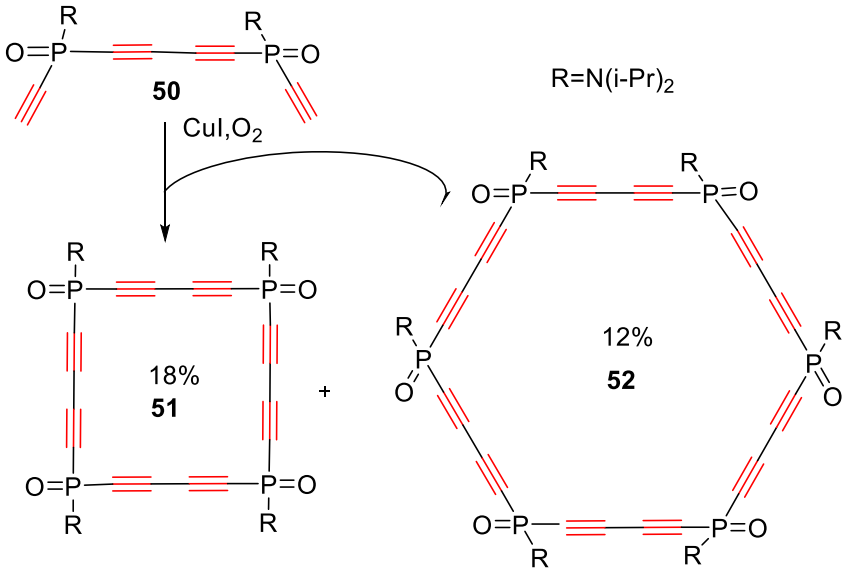

Scheme 1.22 Expanded phospha[n]pericyclynes oxides **51** (n = 4) and **52** (n = 6)

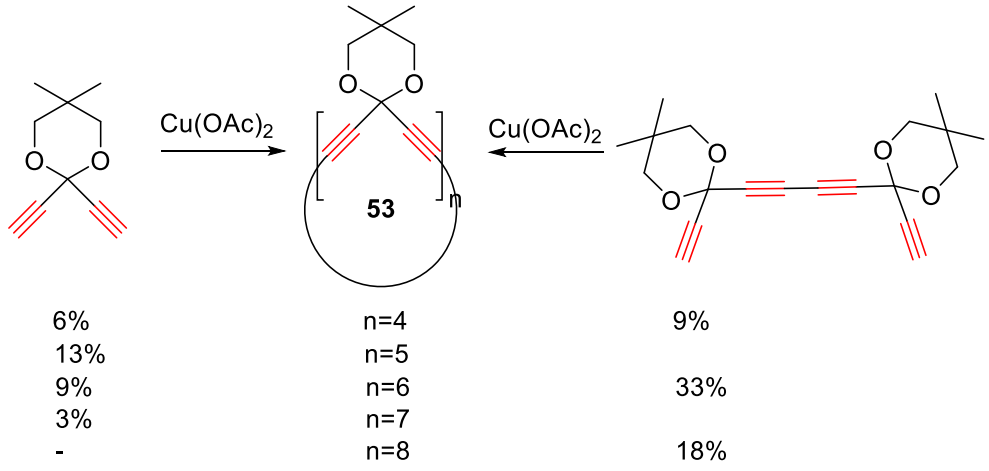

Scheme 1.23. Bunz's syntheses of ketal-protected versions of the challenging *carbo*$_2$-[n]oxocarbons **53**.

In 1996, Bunz *et al*. reported a significant synthesis milestone: the creation of nonstereogenic expanded dioxy[n]pericyclynes **53**, where n ranges from 4 to 8, each featuring a cyclic ketal function at every vertex (**Scheme 1.23**) [52]. The first method employed in this synthesis involved the oxidative coupling of n 1,4-diyne units. Notably, even-numbered representatives were obtained with higher yields when starting from 1,4,6,9-tetrayne units,

with a particularly high selectivity in the formation of the expanded dioxy[6]pericyclyne (33%). These molecules were strategically designed as protected versions of cyclic oligo-carbonylbutadiynylenes (referred to as "OCEs"), specifically aiming at the second *carbo*-mers of neutral oxocarbons.

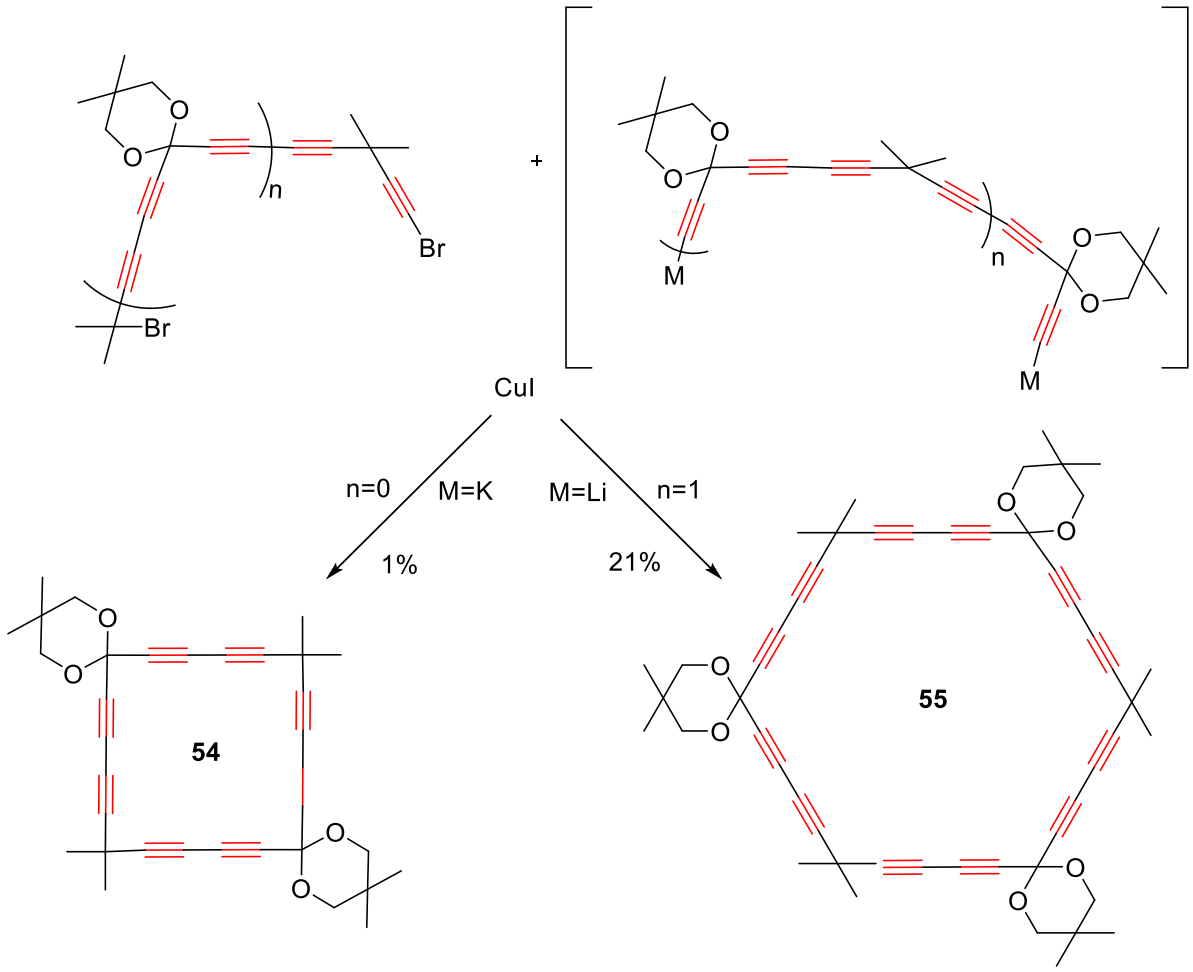

Scheme 1.24. Hirsch's synthesis of alternate functional expanded tri(dioxy)[n]pericyclynes.

In 2001, Hirsch *et al*. presented a noteworthy synthesis involving hybrid expanded pericyclynes characterized by alternating dimethylmethylene and dioxolane vertices.[53] Given that Glaser-type oxidative coupling wouldn't offer the desired selectivity, they turned to Cadiot-Chodkiewicz dehydrobromination between the 2-ethynyl-1,3-dioxolane termini of one reactant and the 2-bromoethynyl propane termini of the other (**Scheme 1.24**). Through the random coupling of single vertex units (where n=0), only a minute quantity of the four-membered ring **54** was obtained. However, by incrementally constructing two C15 units and

subsequently subjecting them to mutual cyclo-dehydrobromination, they successfully obtained the C30 six-membered ring **55** as a sensitive white crystalline solid.

In the pursuit of expanded cubanes, Diederich *et al*. later detailed the synthesis of per-alkynyl perhydroxylated expanded pericyclynes. The crucial ring formation step involved the oxidative coupling of a *meso*/*dl* mixture of an alkynyl-substituted bisterminal deca-1,4,6,9-tetrayne (**Scheme 1.25**)[54]. Remarkably, this reaction proceeded with exceptional selectivity, affording the tetraalkynyl expanded tetraoxy[4]pericyclyne **57** in a yield of 72%. The four stereoisomers resulting from this process could be separated, and one of them was further characterized via X-ray crystallography.

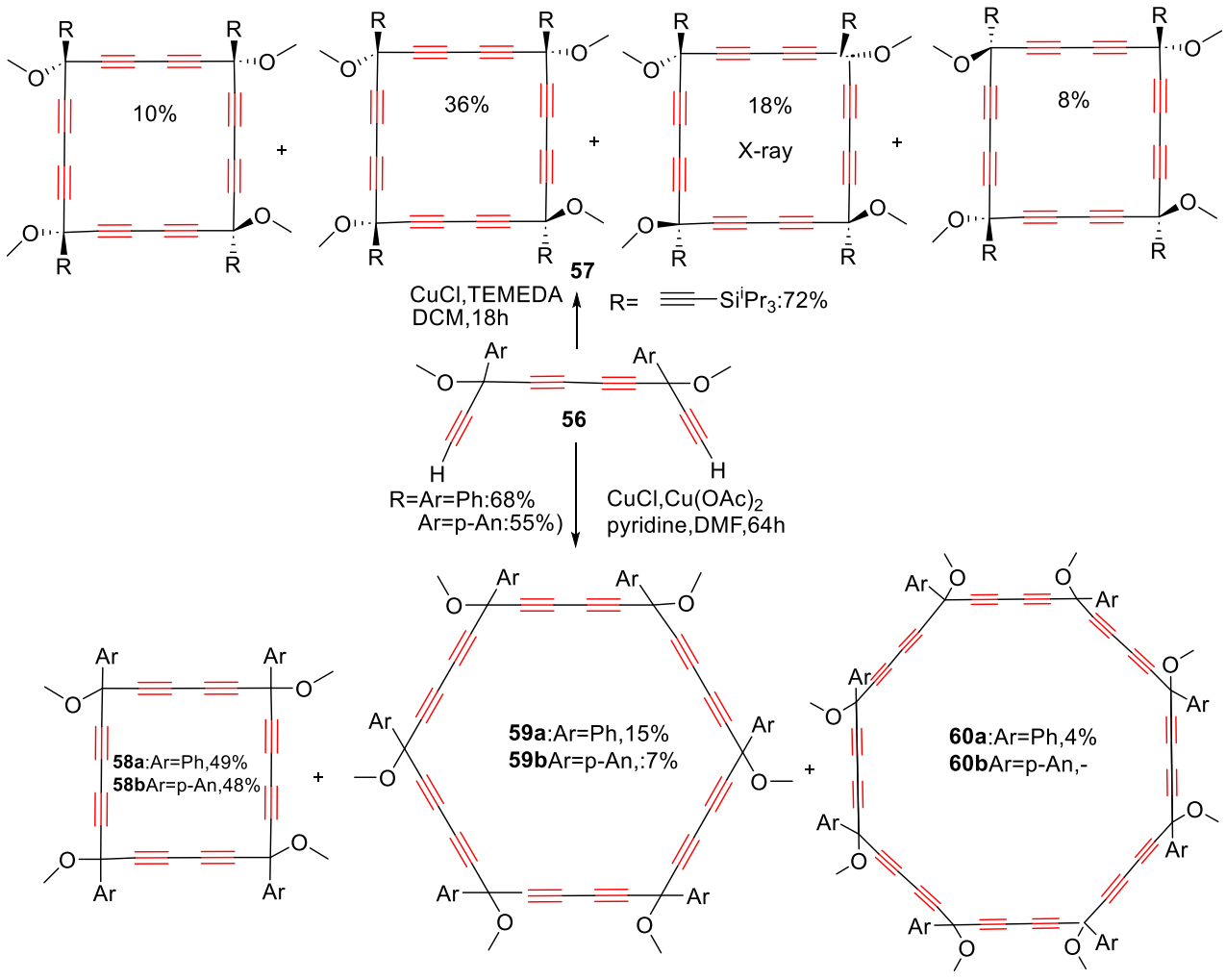

Scheme 1.25. Synthesis of expanded permethoxy[n]pericyclynes with alkynyl or aromatic substituents by oxidative coupling of bisterminal deca-1,4,6,9-tetrayne precursors[52,55].

On the path to hexaphenyl *carbo*$_2$-benzene, a similar oxidative coupling strategy was employed. Specifically, a *meso*/*dl* mixture of a phenyl-substituted bisterminal deca-1,4,6,9-tetrayne underwent oxidative coupling under slightly more concentrated conditions[49]. This process yielded the tetraphenyl expanded tetraoxy[4]pericyclyne **58** as the major product, with 49% yield. Additionally, the expanded hexaoxy[6]pericyclyne **59** was obtained as a trimeric product, albeit in lesser yield (15%), along with octaoxy[8]pericyclyne tetramer **60** (4%). It is worth noting that the reaction was also conducted using the analogous 4-anisyl substrate, as reported separately.

2.3.4. Poly macrocyclic oxy[n]pericyclynes derivatives

2.3.4.1. Synthesis of oxy[8]pericyclynediols - precursors of carbo-barrelene derivatives

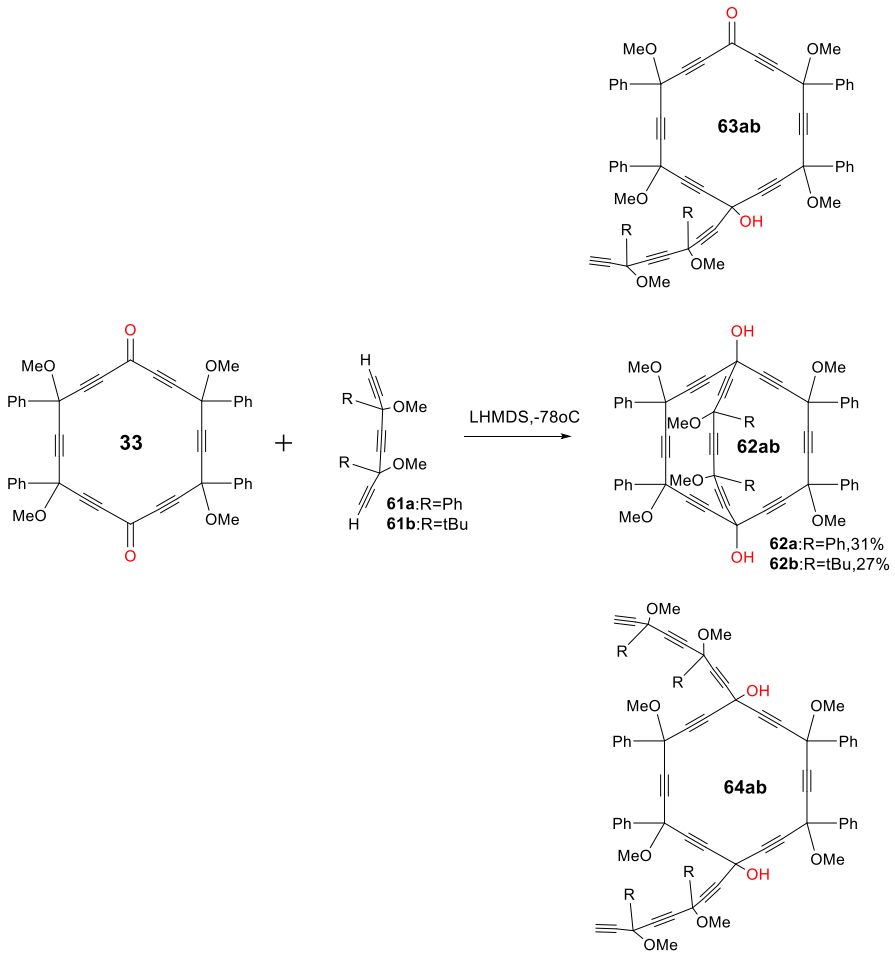

Schema 1.26. Synthesis of decaoxy-*carbo*-barellanes **62ab** by a [18 + 8] route from the [6]pericyclynedione [56,57].

Barrelene or bicyclo[2.2.2]octatriene, was first described by Zimmerman in 1960,[58] before the synthesis of its 3D version was envisaged in our group (**Scheme 1.26**). Deprotonation of diphenyltriyne led to the formation of bicyclic diol with a yield of 31% when using LiHMDS as base. Similarly, the preparation of **62** from di-tert-butyltriyne was performed with LiHMDS. However, in both cases, the reaction resulted in mixtures of stereoisomers, comprising 16 stereoisomers with 2 being achiral. This synthesis was accompanied by the formation of monocyclic [6]pericyclynediol side-products **63a,b** and **64a,b** resulting from the addition of one triyne on each carbonyl group of the [6]pericyclynedione

2.3.4.2. Synthesis of oxy[10]pericyclynediols – precursors of naphthalene

In 2016, a ring *carbo*-mer of decalin, precursor of the synthesis of a *carbo*-naphthalene, was synthesized using a [8+10] ring formation approach (**Scheme 1.27**).[59] The pentayne **66** was obtained using a procedure previously implemented (**section 2.3.1**). The diketone **65** was targeted from the triyne. An alternative method involved a Sonogashira-like coupling reaction with ArCOCl, providing access to the diketone **65** in one step with a 79% yield. In the presence of LiHMDS, the cycloaddition yielded the [6]pericyclynediol **67** in a 45% yield. After a methylation step, treatment of **68** with LiHMDS and the diketone **65** afforded the decaoxy *carbo*-decalin **70** in 23 % yield (theoretical mixture of 130 diastereoisomers).

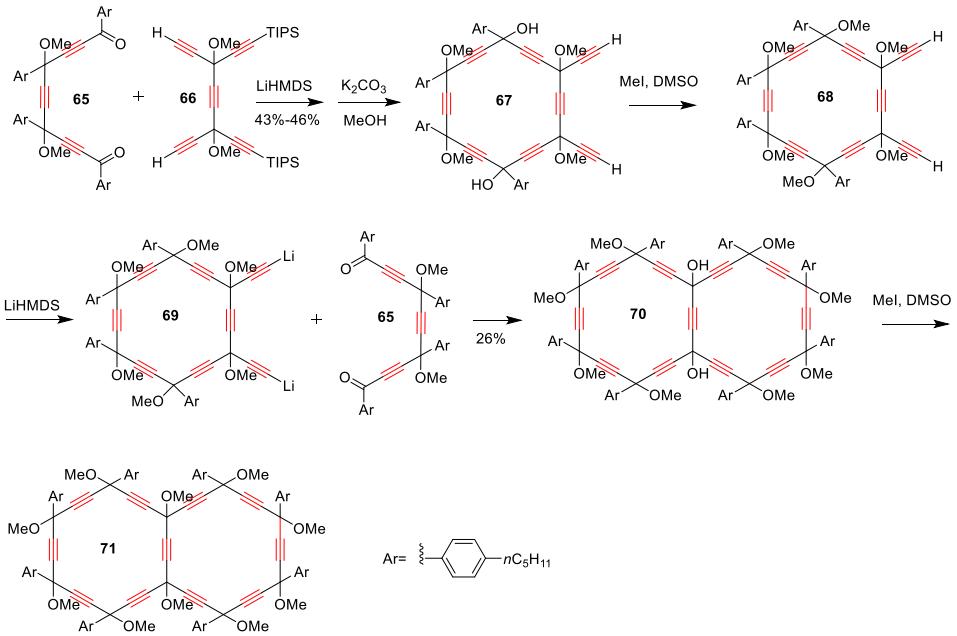

Scheme 1.27. Synthesis of a decaoxyperibicyclyne, ring *carbo*-mer of decalin [59].

2.3.4.3. Synthesis of poly-oxy[6]pericyclynes derivatives– precursors of carbo-biphenyl and carbo-terphenyl

Precursors of *carbo*-oligo(phenylene-ethynylene)s (*carbo*-OPEn, n = 1-2), namely poly-hexaoxy[6]pericyclynes which consist of C2-catenated C18 hexaoxy[6]pericyclynes, have been also synthesized [60]. After treating [6]pericyclynedione **33** by Grignard reagent, octyl-[6]pericyclynone **72a** and ethynyl[6]pericyclynol **72b** were synthesized using procedures previously implemented for the preparation of pericyclynedione (**Figure 8**). Then, n-octyllithium were applied to the sequential preparation of the [6]pericyclynediol **73a** and dimethyl diether **73b**, isolated in 42 % yield over three steps by the optimized route. Deprotonation of compound **73b** with LiHMDS in the presence of compound **72a** yielded crude bis-[6]pericyclynediol **74**, obtained as an intractable mixture of stereoisomers. The synthesis of *carbo*-terphenyls **76a-b** was approached using a similar strategy, initially focusing on the preparation of the respective tris-[6]pericyclynic precursors **75** and **73** (**Scheme 1.28**).

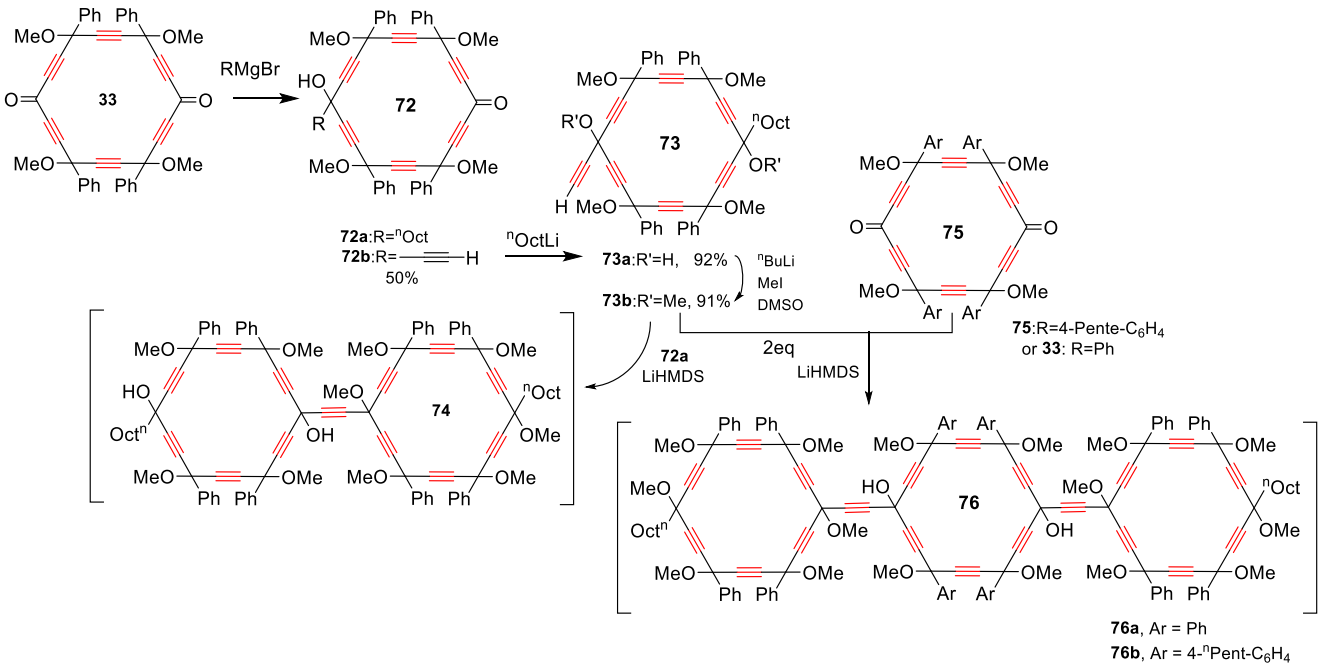

Scheme 1.28. Synthesis of pericyclynic precursors of *carbo*-biphenyl and *carbo*-terphenyl derivatives.

3. Reduction of n-oxy[n]pericyclyne derivatives

3.1. *Carbo*-benzene derivatives

Carbo-benzene derivatives constructure a captivating subset of organic compounds that have garnered significant interest within the realm of synthetic chemistry. These derivatives offer a vast array of molecular architectures with tailored properties and diverse applications. By introducing various substituents onto the *carbo*-benzene scaffold through intricate synthetic routes, researchers can fine-tune the physicochemical properties of *carbo*-benzene derivatives, influencing factors such as solubility, reactivity, and optical effects.

Ring *carbo*-benzenes with diverse substituents have been investigated. The initial representatives were synthesized in 15 steps by Ueda's research group in 1995[42]. Since then, more than 70 diversely substituted ring *carbo*-benzenes were synthesized[61–65]. All of them were synthesized from hexaoxy[6]pericyclyne precursors through a reductive elimination involving the elimination of groups such as hydroxyl or methoxy groups by reductive and acidic treatments. These compounds exhibited stability in both crystalline form and chloroform solution at room temperature. This stability was attributed to their aromatic nature, as evidenced by the presence of a diamagnetic ring current around the macrocycle in NMR spectral data. Additionally, the near D_{6h}-symmetry of the C18 ring further supported its aromatic character.

Several *carbo*-benzene derivatives have been prepared using a similar reductive aromatization method (as shown in **Scheme 1.29**). Hexaphenyl *carbo*-benzene **77** first described by Ueda and coworkers was later re-synthesized from the [6]periclynediol **31a** and [6]pericyclynetetraol **31b**, in 12% and 22% yield, respectively[42].

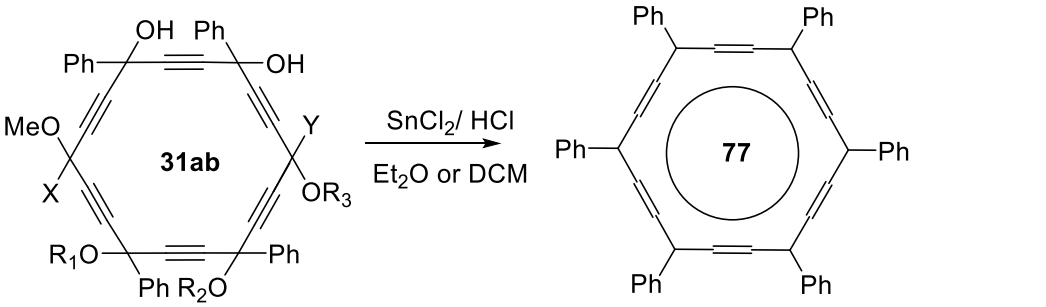

Scheme 1.29. The reductive aromatization of *carbo*-[6]cyclitol ethers into *carbo*-benzene derivatives

Aryl derivatives **79** were obtained through reductive aromatization of *carbo*[6]cyclitol ether precursors **78a-d**. Ueda, Kuwatani, *et al*[39,42]. successfully prepared hexasubstituted *carbo*-benzenes by treating crude triethers **78b-d** with $SnCl_2$ in etheral hydrochloric solution at 0℃ (**Scheme 1.30**). The hexaaryl derivatives **79b** and **79c** exhibited significantly better yields (59-67%) compared to the triaryl-trialkyl derivative **79d** (5%). Additionally, the same procedure yielded the trisubstituted (triaryl) *carbo*-benzene **79a** (29%) from **78a**, albeit at a much lower temperature (-50℃).

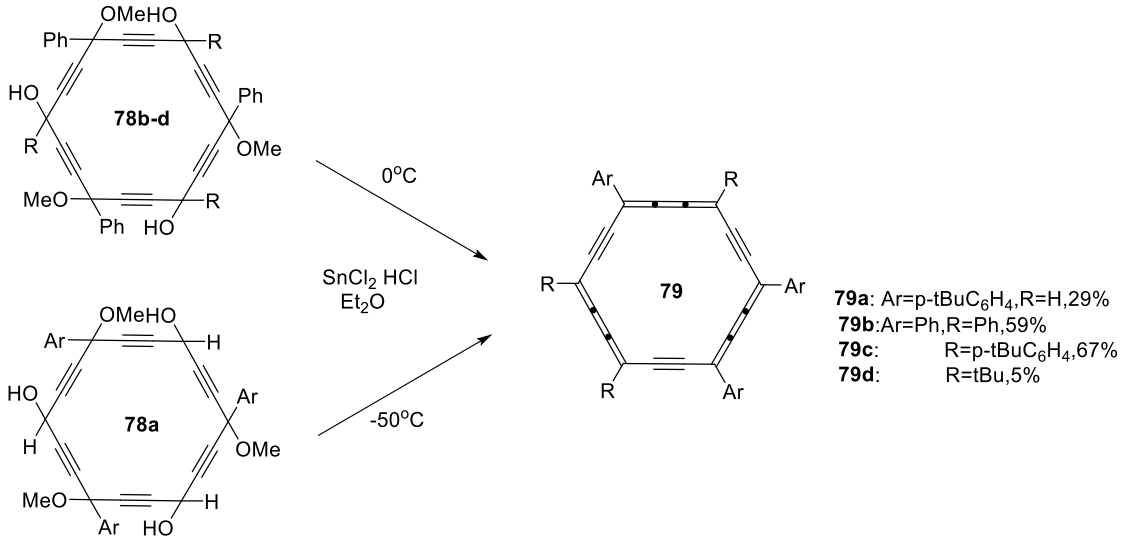

Scheme 1.30. Reductive aromatization of *carbo*-[6]cyclitol ethers

Among the *carbo*-benzene derivatives, most of them exhibit four phenyl substituents and two other substituents that can be either aryl, alkyl or alkynyl groups, in general at the 1,10-positions of the C_{18} macrocycle making the molecule centrosymmetric (ideally quadrupolar),

few examples of partially substituted *carbo*-benzenes (with 2 or 3 peripheral C-H bonds) were also described, such as the *ortho*-, *meta*- and *para*-di-unsubstituted derivatives, (**Figure 1.8**). [66,67]. In particular, the possibility of alkynyl substitution provides a firm basis for the possible functionalization of *carbo*-benzenes.

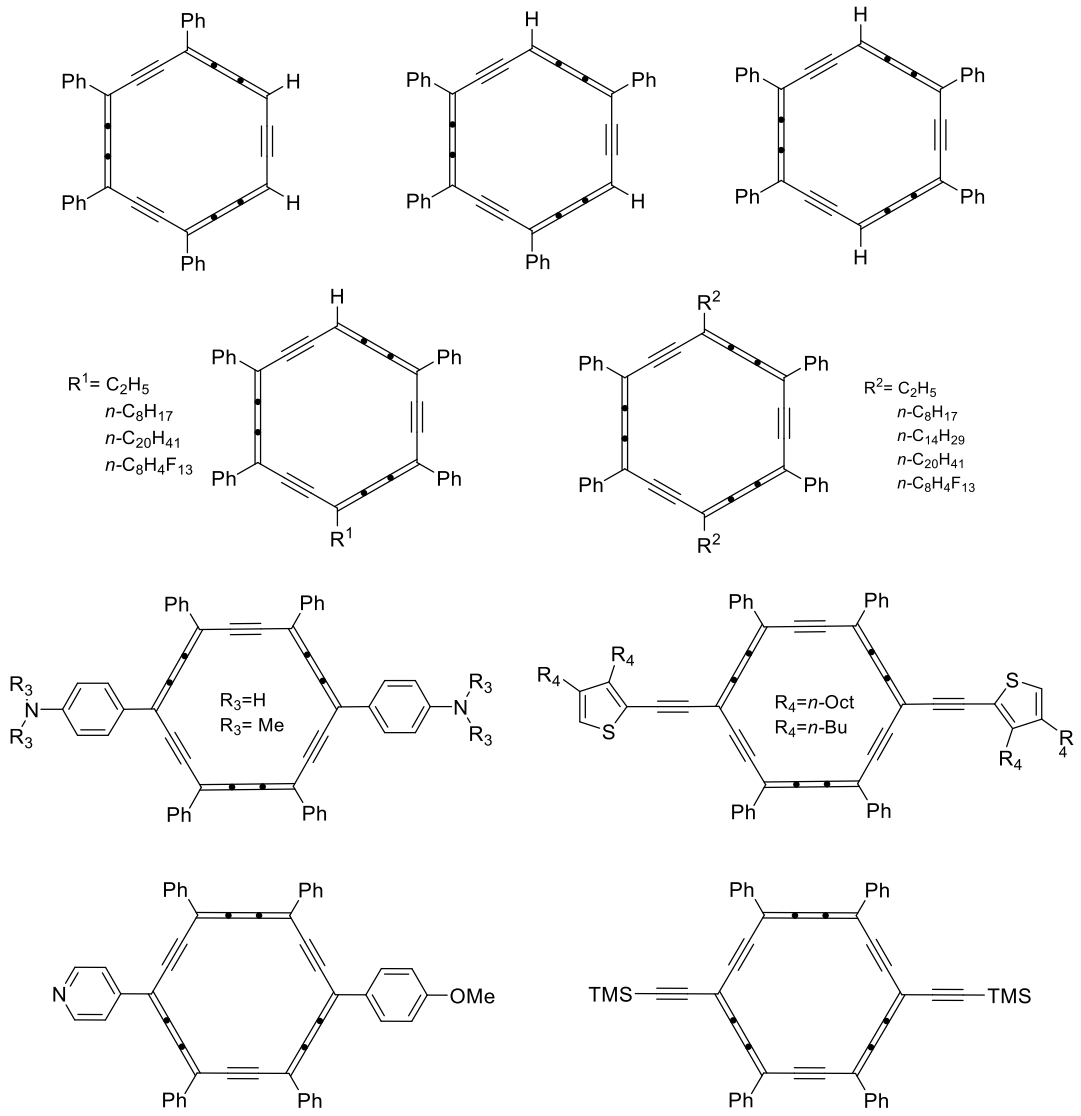

Figure 1.8. Examples of *para*-disubstituted tetraphenyl *carbo*-benzenes with various substituents at the *para* positions

In 2006, the synthesis of a hexa-alkynyl *carbo*-benzene was reported.[68] The reductive aromatization of hexaalkynyl hexaoxy[6]pericyclyne using $SnCl_2$/HCl necessitated the intermediate coordination of some triple bonds of the pericyclyne precursor with $Co_2(CO)_6$

units. This coordination facilitated the generation of stabilized cations, ultimately enabling the reduction process. Subsequently, the hexa-alkynyl *carbo*-benzene was obtained following the oxidative removal of the $Co_2(CO)_6$ moieties (**Scheme 1.31**). This *carbo*-benzene **80** represents a hexa-silylated protected version of the total *carbo*-mer of benzene. However, all attempts to deprotect the exocyclic triple bonds failed, preventing the isolation of the hexa-ethynyl target. This failure was likely due to its extremely low solubility due to a very high carbon content of the putative deprotected product $C_{30}H_6$ (C/H = 5).

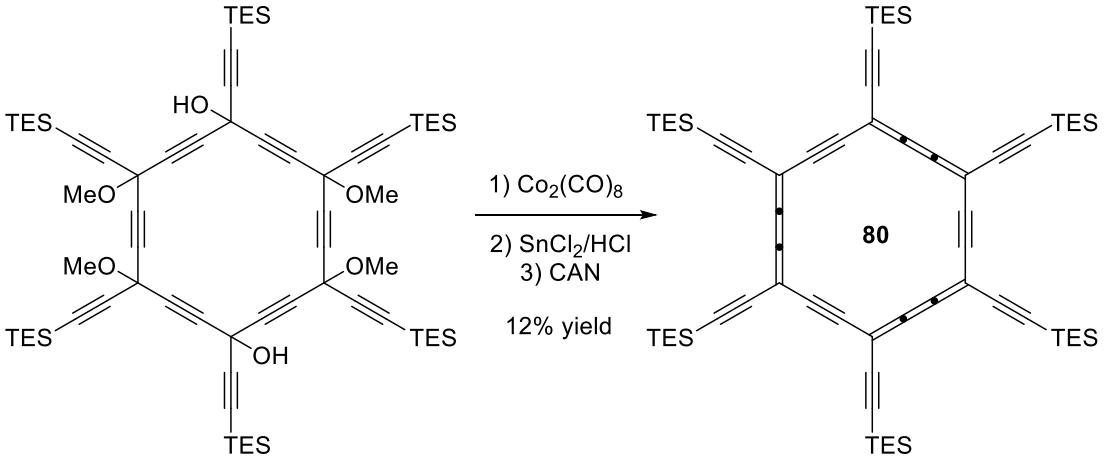

Scheme 1.31. Synthesis of a protected version of the total *carbo*-mer of benzene

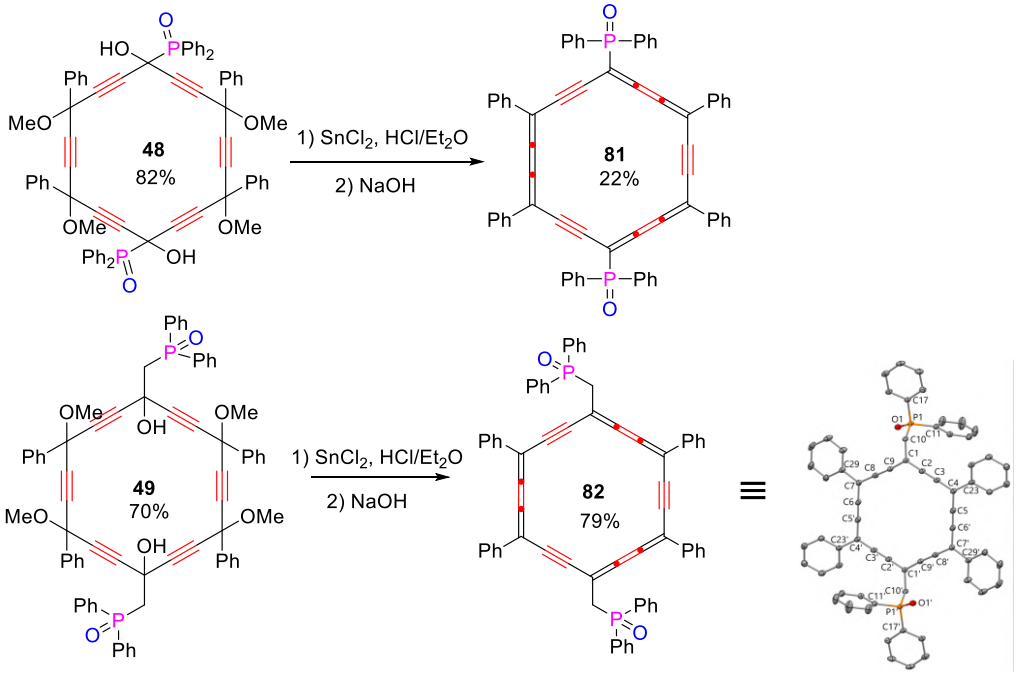

Scheme 1.32 Synthesis of *carbo*-benzene derivatives with *carbo*-benzene-heteroatom bond

The reduction of di(phosphinoyl)-[6]pericyclynediol **48** and di(phosphinoylmethyl)-[6]pericyclynediol **49** was also attempted using the classical procedure[50], and resulted in the formation of di(phosphinoyl)-*carbo*-benzene **81** with 22% yield and di(phosphinoylmethyl)-*carbo*-benzene **82** with a 79% yield respectively (**Scheme 1.32**). The di(phosphinoylmethyl)-*carbo*-benzene **82** was isolated as a poorly soluble bright purple solid, exhibiting solubility only in DCM or chloroform, producing red solutions. While the di(phosphinoyl)-*carbo*-benzene **81** was isolated as poorly soluble dark green solid (only slightly soluble in DCM, chloroform and THF, giving orange solutions).

3.2. Synthesis of *carbo*-barrelenes

Treating the octaoxy[6]peribicyclyne **62a** with $SnCl_2$/HCl in dichloromethane (DCM) at low temperature resulted in the formation of the first *carbo*-barrelene **83** as a brown solid with a yield of 28% (**Scheme 1.33**). As expected, the sp^3C-OH carbinol groups remained intact due to steric constraints preventing planarization of bridgehead carbon centers and facilitating the sequential formation of three Ph_2DAB edges. However, the moderate stability of **83** prompted an attempt at stabilization in the form of the diether. Ethers **84a** and **84b** were thus prepared by *o*-methylation of **62a** and **62b**, respectively. Treatment of **84a** and **84b** under the optimized reducing conditions with $SnCl_2$ and HCl**,** yielded *carbo*-barrelene **85a** and the partially reduced derivative **86b** of *carbo*-barrelene, isolated with approximately 30% and 17% yield, respectively[57].

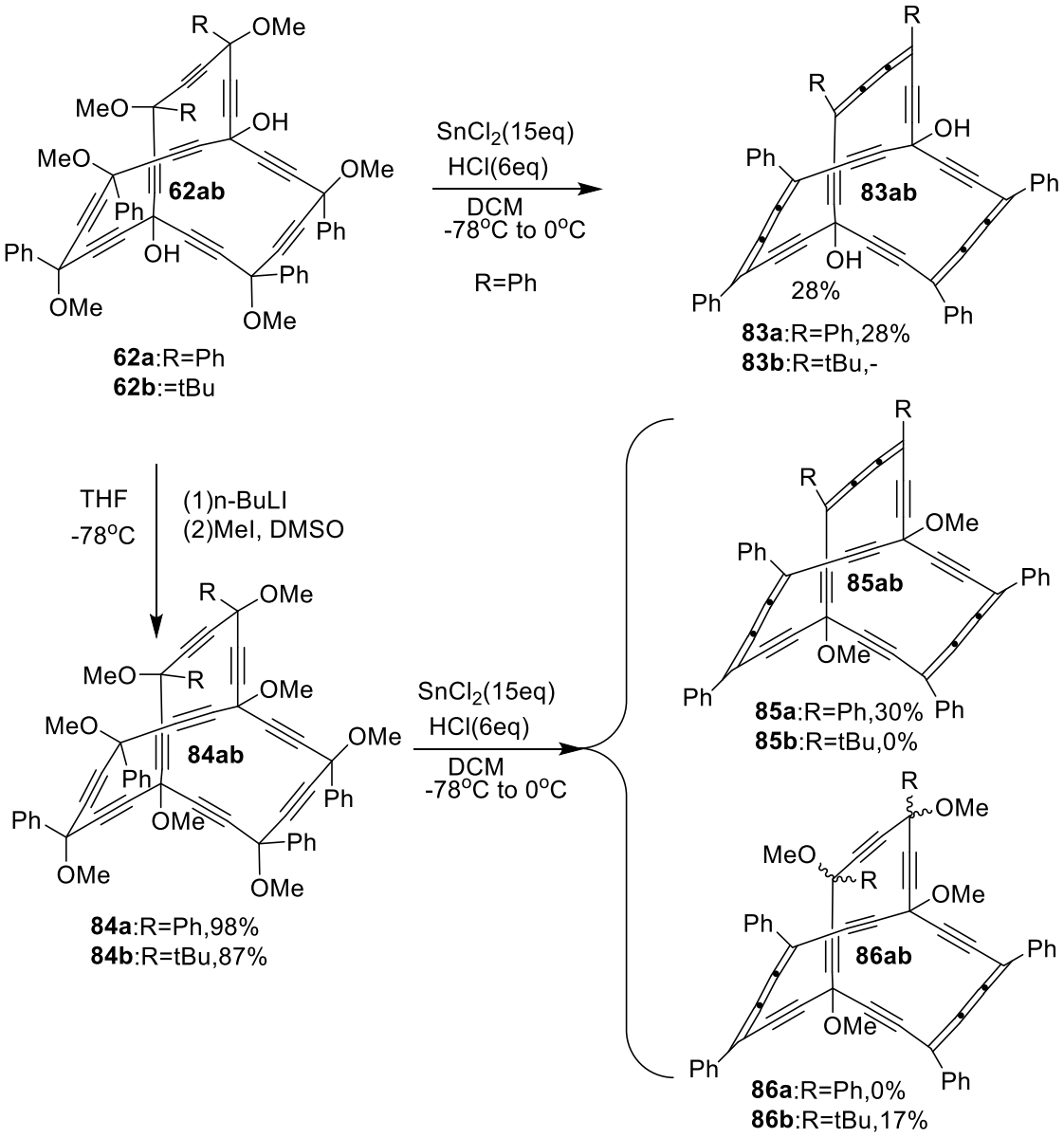

Scheme 1.33. Synthesis of the *carbo*-barrelenes **83** and **85**, and partially reduced derivative, functional *carbo*-dihydrobarrelene **86b** (**86a** was not isolated).

3.3. Synthesis of a *carbo*-naphthalene

The reductive aromatization with $SnCl_2$/HCl of **71** resulted in the formation of the *carbo*-naphthalene **87** (**Scheme 1.34**) which was isolated in a 7% yield as a poorly soluble blue solid. This solid demonstrated sufficient stability to be stored exposed to air and light at room temperature for several weeks and in solution for a few days[59]. The characteristics of the *carbo*-naphthalene

C32 molecule, including its availability, stability, structural features, and aromatic character, resemble those of the C10 naphthalene molecule. This similarity suggests the possibility of synthesizing larger *carbo*-benzenoid fragments. Despite the challenges posed by the long-initiated organic synthetic approach to infinite carbon allotropes, these findings also lend support to the existence of the α-graphyne allotrope[69,70].

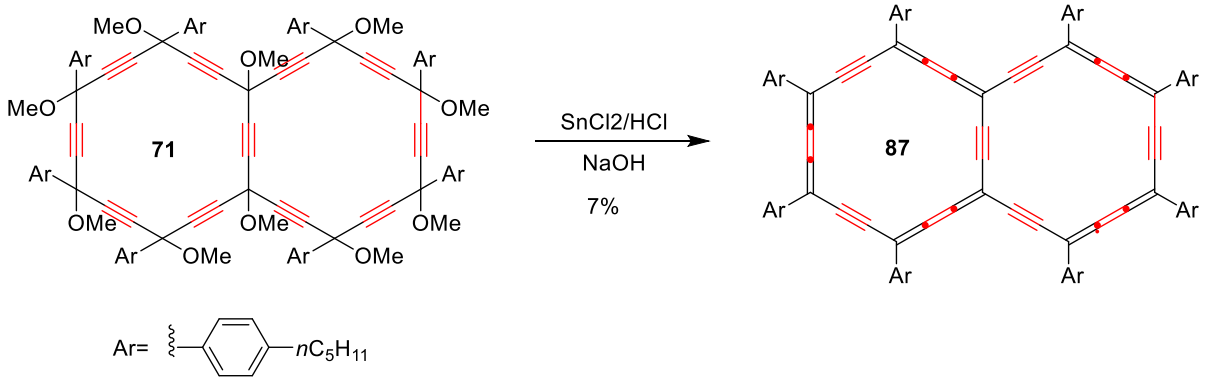

Scheme 1.34.Synthesis of a ring *carbo*-mer of naphthalene [59].

3.4. Synthesis of *carbo*-biphenyl and *carbo*-terphenyl derivatives

By treatment with $SnCl_2$/HCl, The bispericyclyne **74** afforded the *carbo*-biphenyl **88** with 18 % yield. The poorly soluble black solid **88** gave red-violet solutions in organic solvents. By the same method, **76a** and **76b** gave **89a** and **89b** with 20 % and 9 % yield over two steps, respectively. Just as **88**, the obtained black solids **89a-b** gave red solutions turning to red-violet upon increase of concentration in chlorinated solvents (e.g. chloroform). The poor solubility in other solvents (THF, toluene) makes the corresponding solutions remain red or light red, without indication of solvatochromism. As expected, however, **89b** was found to be more soluble than **89a** thanks to the presence of the pentylphenyl groups on the central *carbo*-benzene ring[60] (**Scheme 1.35**).

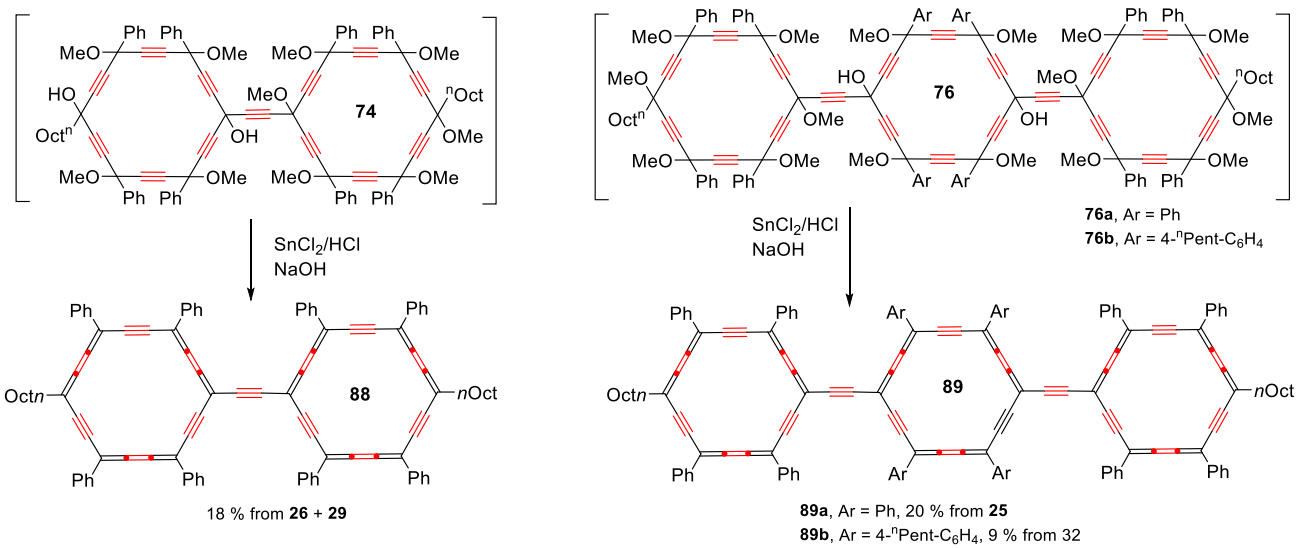

Scheme 1.35. Synthesis of *carbo*-mers of -biphenyl and terphenyl derivatives.

3.5. Synthesis of expanded *carbo*-benzene derivatives

Hexaphenyl-*carbo*$_2$-benzene **90** was targeted through the reductive aromatization of the expanded hexaoxy-[6]pericyclyne precursor **59a**.Treatment of **59a** with the $SnCl_2$/HCl system, which had been successfully used for preparing many ring *carbo*-mers of benzene derivatives, did not allow for the isolation and even detection of **90** under preparative conditions. To prevent solvent evaporation suspected to trigger decomposition, the aromatization was monitored in situ by ^{1}H NMR and UV – vis spectroscopy. Consequently, adding $SnCl_2$ into a solution of **59a** in a $CDCl_3$/DCl/D_2O mixture under quite diluted conditions resulted in a turquoise blue solution[71] (**Scheme 1.36**)

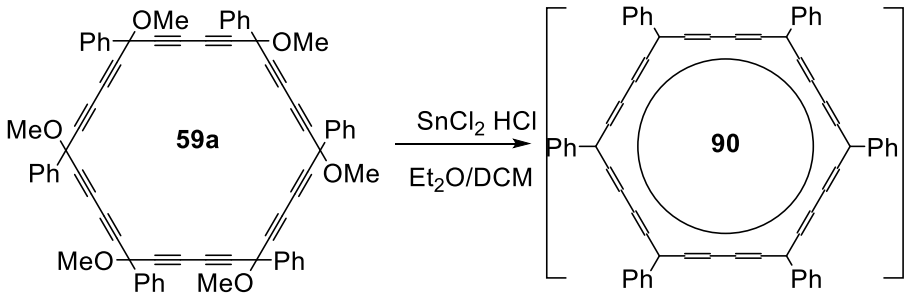

Scheme 1.36. Reductive aromatization of an expanded [6]pericyclyne to a *carbo*$_2$-benzene drrivatives

3.6. Synthesis of a *carbo*-phospholene

Via a reduction of the phospha-[5]pericyclyne **44a** with $SnCl_2$, the corresponding *carbo*-phospholene oxide **93** was obtained with an 11% yield. Although the ultimate *carbo*-phosphole oxide **91** couldn't be isolated, preliminary results on alternative strategies towards this 14 π-electron Hückel *carbo*-aromatic are reported.[41]

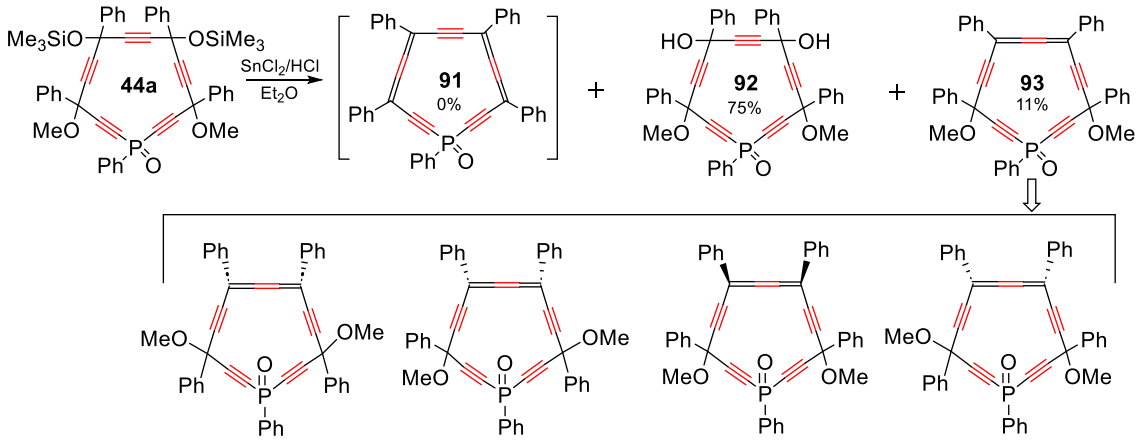

Scheme. 1.37. Reductive treatment of the *carbo*-phospholane oxide **93**

The procedure did not result in the formation of the *carbo*-phospholeoxide **91** but instead yielded the diol **92** as the main product, arising from the cleavage of the two silylether groups of **44a**. The appearance of a pink spot on silica gel TLC plates of the reaction mixture suggested the formation of another less polar side product, tentatively assigned to the targeted *carbo*-phosphole oxide **91**. However, the small amount formed prevented characterization of **91**. The reductive treatment of *carbo*-phospholane oxide **44a**, as illustrated in **Scheme 1.37**, also yielded *carbo*-phospholene oxide **93** in small quantity, but it could be isolated as a yellow solid and partly characterized. The ^{31}P and ^{1}H NMR spectra were fully consistent with the proposed structure. Regarding compound **44a**, the simplification into the spectra of **93** is indeed in accordance with the reduction of the number of isomers. The two remaining asymmetric carbon atoms of **93** thus generate four stereoisomers (two of them containing a pseudo-asymmetric P atom), which are found to be formed in statistically equal amounts. This mixture gives rise to two ^{31}P NMR signals (at –19.89 and –20.32 ppm) and four ^{1}H NMR signals for the non-equivalent methoxy groups of **93**.

4. The properties of *carbo*-benzenes

Numerous *para*-disubstituted ring *carbo*-benzenes, featuring various groups, have been extensively described and investigated for their distinctive properties. These properties include chromophore and dye characteristics, photosensitization capabilities, conductivity, charge transport (particularly for organic photovoltaics), nonlinear optical properties (specifically 2-Photon Absorption = 2PA), and more recently, supramolecular mesogenic properties, which are significant for liquid crystal design. In the following sections (2.1 to 2.4), the applications in which *carbo*-benzenes have been found to be involved will be addressed.

4.1. Electrical: single molecule conductance

Nitrogen-containing functional quadrupolar *carbo*-benzenes were synthesized in 2012 and 2013[72,73]. The aim was to investigate the formal "π-frustration" induced by two strongly π-donating substituents facing each other across the highly π-electron-rich *carbo*-benzene core. This π-frustration effect was examined in two series of *carbo*-benzene derivatives, where two nitrogen atoms are conjugated to the C18 macrocycle through either a p-phenylene linker or an indole ethenylene linker. Representatives containing p-phenylene linkers between the two N atoms and the C18 core were found to be stable, while those containing an ethenylene linker were poorly stable[74–77].

The dianilinyl-*carbo*-benzene, containing two NH_2 groups, exhibited a single molecule conductance (SMC) of 106 ns over 2 nm, recorded between gold electrodes by the STM break junction method. This value was 10 times higher than those measured for molecules with similar or shorter lengths between NH_2 anchoring groups, such as porphyrin or hexabenzocoronene counterparts. Moreover, it was about 40 times more conductive than a flexible linear *carbo*-n-butadiene reference. Additionally, the N-C_6H_4-$C_{18}Ph_4$-C_6H_4-N molecular junction was shown to exhibit field-effect transistor behavior under electrochemical gating conditions.

As a structurally related compound, the di(indol-3-yl)-*carbo*-benzene displayed significant UV-vis emission at 303 and 603 nm upon excitation at 242 and 503 nm, respectively. This unique fluorescent behavior was correlated with the particularly low molar extinction coefficient of the compound (**Figure.1.9**).

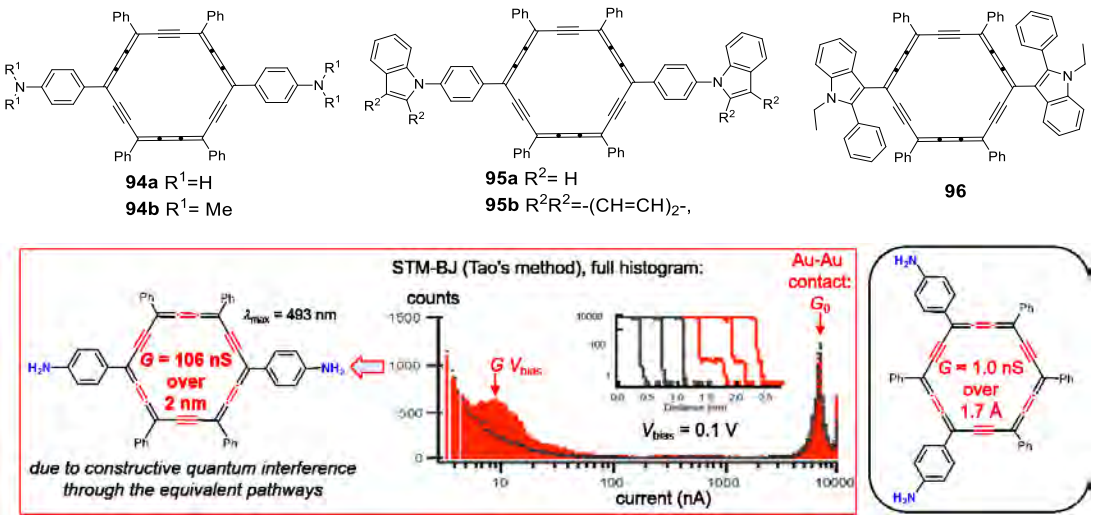

Figure.1.9. Structure and measurements of single molecule conductance (SMC) of *carbo*-benzene (bottom), structure of fluorescent and π-frustrated *carbo*-benzenes (top)

4.2. Two-photon absorption

Chromophores with two-photon absorption capabilities are substances that are able of absorbing two photons simultaneously. The absorbed photons create excited states that decay by emitting photons with double the energy of the absorbed photons. These compounds have attracted considerable attention over the past decades.

The synthesis of two quadrupolar fluorenyl-substituted tetraphenyl *carbo*-benzenes through the reductive aromatization of the [6]pericyclynediol precursor was reported [78]. To improve solubility, n-hexyl chains were introduced at the C-9 position of the selected 2-bromofluorene reactants. These chromophores, distinguished by the presence or absence of C2 expanders between the C18 core and the fluorenyl groups, broaden the range of quadrupolar *carbo*-benzenes for both linear and nonlinear optical properties in hydrocarbon-based and fluorophore-substituted series. The fluorophore-substituted *carbo*-benzenes exhibit low emission at around 650 nm (quantum yield undetermined) but show promise as candidates for two-photon absorption (2PA), with **97a** demonstrating twice the 2PA efficiency of **97b** **(Figure.1.10**), as assessed by the Z-scan technique. More recently, thienylethynyl-substituted *carbo*-benzenes **98b** were synthesized, with the 2PA cross-section of **98a** being five times higher than that of the corresponding parent benzenic model **99**, clearly demonstrating the impact of *carbo*-merization on optical properties.[79,80,62]

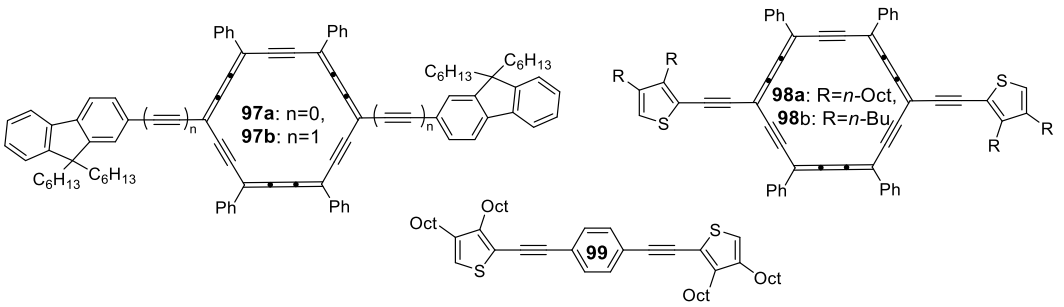

Figure.1.10. Structures of *carbo*-benzenes with 2PA properties

4.3. Mesogenic properties: liquid crystal (LC) properties

Since the initial report by S. Chandrasekhar *et al*. describing the mesomorphic properties of a hexa-substituted benzene derivative[81], a wide variety of rigid π-conjugated disc-shaped cores have been envisioned for the design of mesogenic molecules to be used in discotic liquid crystals. These cores feature two, three, four, five, six, or more dispersing groups, which confer self-assembly properties and govern the formation of mesophases. Typically, these groups are linear or branched alkyl chains. On the other hand, the most commonly used cores in discotic liquid crystals are macrocyclic or polycyclic in nature, such as porphyrins, phthalocyanines, triphenylenes, perylenes, and hexabenzocoronenes.

Given that the C_{18} core of a *carbo*-benzene bears a structural and chromophoric analogy to the $C_{16}N_2$ core of a porphyrin[82], *carbo*-benzenes have been envisioned as a new core for the design of discotic liquid crystals due to their hexagonal shape, aromatic character, and the possibility of anchoring dispersing groups at different positions of the macrocycle[83–85].

Recently, p-dialkyl-*carbo*-benzenes, or "lipidic *carbo*-benzenes" (p-$(C_nH_{2n+1})_2C_{18}Ph_4$) have been described[86], containing two alkyl chains of different lengths (n = 2, 8, 14, and 20), but none of them exhibited liquid crystal behavior. This suggests that the presence of only two alkyl chains is not sufficient to induce the formation of mesophases. Another important aspect to consider is the melting temperature of *carbo*-benzenes, which is above 200℃ in most derivatives. However, with the series of p-dialkyl-*carbo*-benzenes, it has been found that the

melting point decreases linearly with increasing the length of the alkyl chains, suggesting that an increase in the number of chains in *carbo*-benzenes could allow for achieving liquid crystal behavior.

p-Trialkoxyphenylethynyl-*carbo*-benzenes were synthesized and characterized, containing six alkyl chains of n-$C_{12}H_{25}$ and n-$C_{18}H_{37}$, respectively. The mesogenic behavior of the *carbo*-benzene having six alkyl chains of n-$C_{12}H_{25}$ was investigated and it was shown to exhibit a liquid crystal behavior in the range at 115 °C. Polarizing optical microscopy (POM), differential scanning calorimetry (DSC), and powder X-ray diffraction (PXRD) analyses revealed the formation of a rectangular columnar mesophase (**Figure 1.11**). The poor reversibility of the transition above 115℃ remains to be improved.[87]

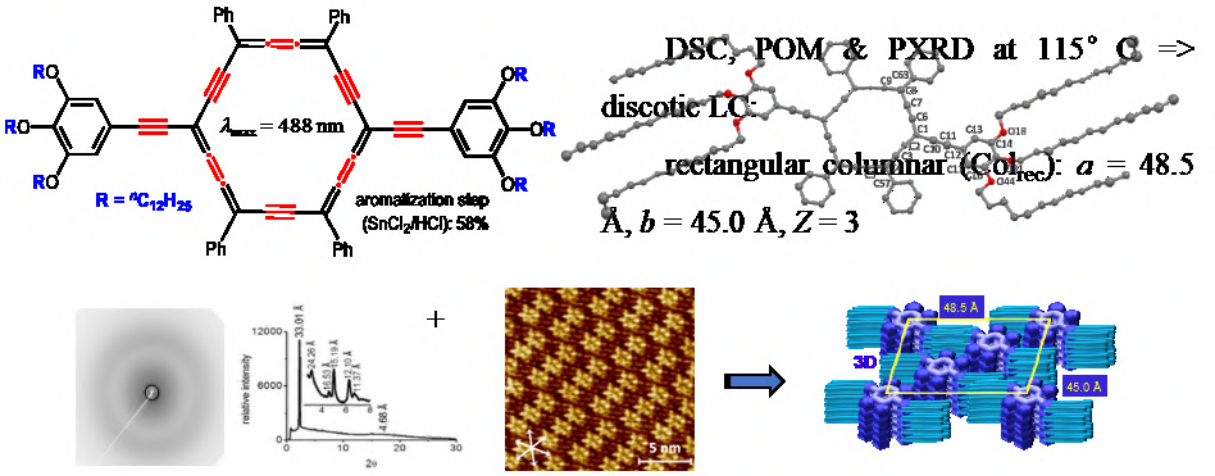

Figure 1.11. Molecular packing for a mesogenic *carbo*-benzene

4.4. Photosensitizers for hydrogen production

Among the processes for producing hydrogen, which represents one of the clean energy sources considered as an alternative to oil, photocatalysis is a heterogeneous catalysis process for producing hydrogen by the photo-reduction of water under solar irradiation. Photocatalysis differs from electrolysis, which is much more widely used, in that it requires no connection to the electrical grid, with solar energy being the only energy used to induce hydrogen production.

In this context, an efficient "triptych photocatalyst" was developed that combines a thin semiconductor film (TiO_2), a photosensitive macromolecule of *carbo*-benzene (Cbz) bearing two ethynylaniline substituents, and plasmonic noble metal nanoparticles (Ag). This tri-

component hybrid material, deposited on a glass plate contained in a device that can be filled with water, demonstrated its effectiveness in catalyzing hydrogen production under solar irradiation.

The structural characteristics of the (p-di(anilinylethynyl)-tetraphenyl-*carbo*-benzene) (quasi-D_6h persistent symmetry, residual flexibility), and its physicochemical properties motivated the use of this *carbo*-benzene as a redox-active photosensitizer. It indeed exhibits high molecular conductance and a high molar extinction coefficient (ε = 131,000 L mol-1 cm-1) at λ_{max} = 493 nm, which complements the plasmonic resonance frequency of silver nanoparticles. It is worth noting that the *carbo*-benzene selected as the photosensitizer in this work, like most other reported *carbo*-benzene molecules to date, is very weakly photoluminescent, so the possible contribution of its emission properties can be neglected in this study[72,73,88,89].

The TiO_2 / Ag / Cbz triptych photocatalyst was shown to be more effective than binary systems TiO_2 / Ag and TiO_2 / Cbz, highlighting the synergy among the three components of the nanocatalyst. The most efficient material, obtained after optimizing the quantities and assembly method of each component, achieved a hydrogen production rate of 0.18 $mmol.g^{-1}.h^{-1}$ under irradiation with a solar simulator, under pressure (2.2 bars) and temperature (ambient) conditions suitable for commercial applications (**Figure 1.12)**. This nanocatalyst also proved to be very stable and productive over time, for periods of up to 120 hours, unlike most systems described in the literature that deactivate after a few hours of use.

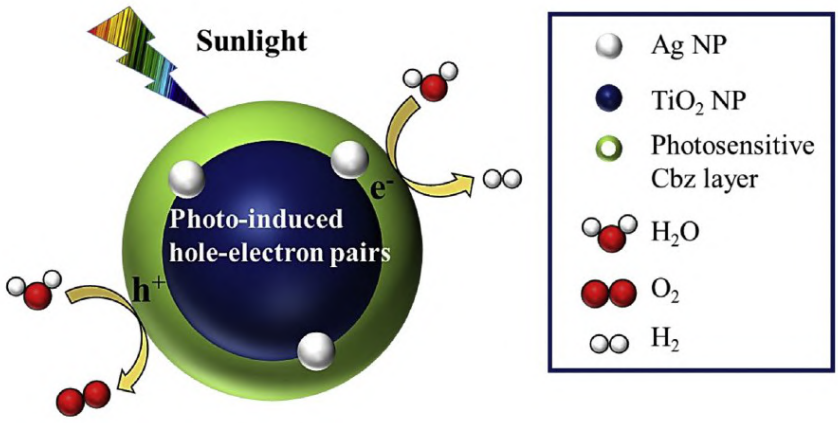

Figure1.12. Molecular packaging patterns for *carbo*-benzene photocatalysts of wata sphitting

5. Conclusion

Organophosphines and their corresponding complexes are intensively used in homogeneous catalysis [90, 91] because of the possibility of finely tuning their electronic and steric properties. Such catalysts frequently allow performance of some reactions in aqueous or biphasic media, provided that ionic or polar groups are attached to these phosphines.

By integrating phosphorus into *carbon*-mer chemistry, one can access a broader range of compounds with diverse properties and applications.[92–98] This interdisciplinary approach can lead to innovative solutions and open new avenues for exploration in synthetic chemistry and materials science.

Although phospha-[n]pericyclynes, having either a phosphorus atom at each vertex or only one phosphorus atom in the case of the *carbo*-phospholane derivative, were reported in the literature, the investigation of *carbo*-heterocycles containing two phosphorus atoms in their structure and butatriene edges has never been envisaged up to now. Their synthesis, characterization and properties are thus the aim of the following thesis work.

References

(1) *Carbon Rich Compounds II, Macrocyclic Oligoacetylenes and Other Linearly Conj ugated Systems*; A. de Meijer, Ed.; Springe; Vol. 201.

(2) Chauvin, R. “Carbomers”. I. A General Concept of Expanded Molecules. *Tetrahedr on Letters* **1995**, *36* (3), 397–400. https://doi.org/10.1016/0040-4039(94)02275-G.

(3) Cocq, K.; Lepetit, C.; Maraval, V.; Chauvin, R. “Carbo-Aromaticity” and Novel Car bo-Aromatic Compounds. *Chem. Soc. Rev.* **2015**, *44* (18), 6535–6559. https://doi.org/10.103 9/C5CS00244C.

(4) Zhu, C.; Saquet, A.; Maraval, V.; Bijani, C.; Cui, X.; Poater, A.; Chauvin, R. From S tilbenes to Carbo-Stilbenes: An Encouraging Prospect. *Chemistry – A European Journal* **202 4**, *30* (26), e202400451. https://doi.org/10.1002/chem.202400451.

(5) Chauvin, R. “Carbomers”. I. A General Concept of Expanded Molecules. *Tetrahedr on Letters* **1995**, *36* (3), 397–400. https://doi.org/10.1016/0040-4039(94)02275-G.

(6) Scott, L. T.; DeCicco, G. J.; Hyun, J. L.; Reinhardt, G. Decamethyl[5]Pericyclyne. A

Novel Homoconjugated Cyclic Polyacetylene. *J. Am. Chem. Soc.* **1983**, *105* (26), 7760–7761. https://doi.org/10.1021/ja00364a057.

(7) Scott, L. T.; DeCicco, G. J.; Hyun, J. L.; Reinhardt, G. Cyclynes. Part 4. Pericyclynes of the Order [5], [6], [7], and [8]. Simple Convergent Syntheses and Chemical Reactions of the First Homoconjugated Cyclic Polyacetylenes. *J. Am. Chem. Soc.* **1985**, *107* (23), 6546–6555. https://doi.org/10.1021/ja00309a021.

(8) Scherf, U. Oligo- and Polyarylenes, Oligo- and Polyarylenevinylenes. In *Carbon Rich Compounds II, Macrocyclic Oligoacetylenes and Other Linearly Conjugated Systems*; de Meijere, A., Ed.; Topics in Current Chemistry; Springer: Berlin, Heidelberg, 1999; pp 163–222. https://doi.org/10.1007/3-540-49451-0_5.

(9) Scott, L. T.; Cooney, M. J.; Johnels, D. Cyclynes. 7. Homoconjugated Cyclic Poly(Diacetylene)s. *J. Am. Chem. Soc.* **1990**, *112* (10), 4054–4055. https://doi.org/10.1021/ja00166a061.

(10) De Meijere, A.; Kozhushkov, S. I. Completely Spirocyclopropanated Macrocyclic Oligodiacetylenes and Their Permethylated Analogues: Preparation and Properties. *Chem. Eur. J.* **2002**, *8* (14), 3195. https://doi.org/10.1002/1521-3765(20020715)8:14<3195::AID-CHEM3195>3.0.CO;2-J.

(11) Williams, R. V. Homoaromaticity. *Chem. Rev.* **2001**, *101* (5), 1185–1204. https://doi.org/10.1021/cr9903149.

(12) de Meijere, A.; Kozhushkov, S.; Haumann, T.; Boese, R.; Puls, C.; Cooney, M. J.; Scott, L. T. Completely Spirocyclopropanated Macrocyclic Oligodiacetylenes: The Family of “Exploding” [n]Rotanes. *Chemistry – A European Journal* **1995**, *1* (2), 124–131. https://doi.org/10.1002/chem.19950010206.

(13) Scott, L. T.; Unno, M. Novel Heterocycles Comprised of Alternating Phosphorous Atoms and Alkyne Units. *J. Am. Chem. Soc.* **1990**, *112* (21), 7823–7825. https://doi.org/10.1021/ja00177a069.(14) Scott, L. T.; Cooney, M. J. Macrocyclic Homoconjugated Polyacetylenes. In *Modern Acetylene Chemistry*; John Wiley & Sons, Ltd, 1995; pp 321–351. https://doi.org/10.1002/9783527615278.ch09.

(15) Sakurai, H.; Eriyama, Y.; Hosomi, A.; Nakadaira, Y.; Kabuto, C. PREPARATION AND REACTIONS OF DODECAMETHYL-3,4,7,8,11,12-HEXASILACYCLODODECA-1,5,9-TRIYNE. *Chemistry Letters* **1984**, *13* (4), 595–598. https://doi.org/10.1246/cl.1984.59

5.

(16) Hengge, E.; Baumegger, A. Synthese Und Eigenschaften Einiger Ethinylsilane. *Jo urnal of Organometallic Chemistry* **1989**, *369* (3), C39–C42. https://doi.org/10.1016/0022-3 28X(89)85193-9.

(17) Gleiter, R.; Schaefer, W.; Sakurai, H. Evidence for a Strong .Sigma.,.Pi. Interaction in 3,4,7,8-Tetrasilacycloocta-1,5-Diyne and 3,4,7,8,11,12-Hexasilacyclododeca-1,5,9-Triyn e. *J. Am. Chem. Soc.* **1985**, *107* (11), 3046–3050. https://doi.org/10.1021/ja00297a009.

(18) Baumegger, A.; Hengge, E.; Gamper, S.; Hardtweck, E.; Janoschek, R. Molecular Properties of Some New Cyclic Ethynylsilanes. *Monatsh Chem* **1991**, *122* (8), 661–671. http s://doi.org/10.1007/BF00811465.

(19) Fluck, E.; Lange, K.; Heckmann, G. REAKTIONEN DES 1,1′,3,3′-TETRAKIS(DI METHYLAMINO)-1λ5,3Δ5-DIPHOSPHETS MIT ALKOHOLEN. ALK(PHEN)OXYCAR BODIPHOSPHORANE. *Phosphorus, Sulfur, and Silicon and the Related Elements* **1992**, *72* (1–4), 49–54. https://doi.org/10.1080/10426509208031538.

(20) Bortolin, R.; Parbhoo, B.; Brown, S. S. D. Pericyclynosilanes: Synthesis of a New Class of Cyclic Organosilicon Compounds. *J. Chem. Soc., Chem. Commun.* **1988**, No. 16, 10 79–1081. https://doi.org/10.1039/C39880001079.

(21) Unno, M.; Saito, T.; Matsumoto, H. Synthesis and Crystal Structures of Silapericyc lynes. *Bulletin of the Chemical Society of Japan* **2001**, *74* (12), 2407–2413. https://doi.org/1 0.1246/bcsj.74.2407.

(22) Bortolin, R.; Brown, S. S. D.; Parbhoo, B. Pericyclynosilanes: Single Xrystal x-Ra y Structure of Dodecamethyl(6)Pericyclynosilane, $(Me_2SiC{\equiv}C)_6$. *Inorganica Chimica Acta* **1989**, *158* (2), 137–139. https://doi.org/10.1016/S0020-1693(00)80826-9.

(23) Moonen, N. N. P.; Gist, R.; Boudon, C.; Gisselbrecht, J.-P.; Seiler, P.; Kawai, T.; K ishioka, A.; Gross, M.; Irie, M.; Diederich, F. Donor-Substituted Cyanoethynylethenes: Pow erful Chromophores for Opto-Electronic Applications. *Org. Biomol. Chem.* **2003**, *1* (12), 203 2–2034. https://doi.org/10.1039/B303879C.

(24) Michinobu, T.; May, J. C.; Lim, J. H.; Boudon, C.; Gisselbrecht, J.-P.; Seiler, P.; Gr oss, M.; Biaggio, I.; Diederich, F. A New Class of Organic Donor–Acceptor Molecules with Large Third-Order Optical Nonlinearities. *Chem. Commun.* **2005**, No. 6, 737–739. https://do i.org/10.1039/B417393G.

(25) Moonen, N. N. P.; Boudon, C.; Gisselbrecht, J.-P.; Seiler, P.; Gross, M.; Diederich, F. Cyanoethynylethenes: A Class of Powerful Electron Acceptors for Molecular Scaffolding. *Angewandte Chemie* **2002**, *114* (16), 3170–3173. https://doi.org/10.1002/1521-3757(20020816)114:16<3170::AID-ANGE3170>3.0.CO;2-N.

(26) Siemsen, P.; Livingston, R. C.; Diederich, F. Acetylenic Coupling: A Powerful Tool in Molecular Construction. *Angewandte Chemie International Edition* **2000**, *39* (15), 2632–2657. https://doi.org/10.1002/1521-3773(20000804)39:15<2632::AID-ANIE2632>3.0.CO;2-F.

(27) Diederich, F.; Gobbi, L. Cyclic and Linear Acetylenic Molecular Scaffolding. In *Carbon Rich Compounds II, Macrocyclic Oligoacetylenes and Other Linearly Conjugated Systems*; De Meijere, A., Ed.; De Meijere, A., Houk, K. N., Kessler, H., Lehn, J.-M., Ley, S. V., Schreiber, S. L., Thiem, J., Trost, B. M., Vögtle, F., Yamamoto, H., Series Eds.; Topics in Current Chemistry; Springer Berlin Heidelberg: Berlin, Heidelberg, 1999; Vol. 201, pp 43–79. https://doi.org/10.1007/3-540-49451-0_2.

(28) Dillon, K. B.; Mathey, F.; Nixon, J. F. *Phosphorus: The Carbon Copy: From Organophosphorus to Phospha-Organic Chemistry*; Wiley, 1998.

(29) Hissler, M.; Dyer, P. W.; Reau, R. The Rise of Organophosphorus Derivatives in π-Conjugated Materials Chemistry. In *New Aspects in Phosphorus Chemistry V*; Majoral, J.-P., Ed.; Topics in Current Chemistry; Springer: Berlin, Heidelberg, 2005; pp 127–163. https://doi.org/10.1007/b100984.

(30) Hissler, M.; Lescop, C.; Réau, R. Organophosphorus π-Conjugated Materials: The Rise of a New Field. *Journal of Organometallic Chemistry* **2005**, *690* (10), 2482–2487. https://doi.org/10.1016/j.jorganchem.2004.09.067.

(31) Hay, C.; Hissler, M.; Fischmeister, C.; Rault-Berthelot, J.; Toupet, L.; Nyulászi, L.; Réau, R. Phosphole-Containing π-Conjugated Systems: From Model Molecules to Polymer Films on Electrodes. *Chemistry – A European Journal* **2001**, *7* (19), 4222–4236. https://doi.org/10.1002/1521-3765(20011001)7:19<4222::AID-CHEM4222>3.0.CO;2-3.

(32) Kakiuchi, K.; Tsutsumi, T.; Suzuka, T.; Arai, Y.; Iseta, F. Jpn. Kokai Tokkyo Koho. JP 2006076959 A2 20060323.

(33) Werz, D. B.; Gleiter, R. [N]Chalcogena[N]Pericyclynes: DFT Studies on Binaric Carbon−Chalcogen Compounds. *Org. Lett.* **2004**, *6* (4), 589–592. https://doi.org/10.1021/ol03

6401b.

(34) Laporte, F.; Mercier, F.; Ricard, L.; Mathey, F. Tetraphosphorus Macrocycles from Phosphole Tetramers. *J. Am. Chem. Soc.* **1994**, *116* (8), 3306–3311. https://doi.org/10.1021/ja00087a017.

(35) Märkl, G.; Zollitsch, T.; Kreitmeier, P.; Prinzhorn, M.; Reithinger, S.; Eibler, E. Polyphospha[m]Cyclo[n]Carbons (M+n=15, 20, 25, 30, 40). *Chemistry – A European Journal* **2000**, *6* (20), 3806–3820. https://doi.org/10.1002/1521-3765(20001016)6:20<3806::AID-CHEM3806>3.0.CO;2-J.

(36) Scott, L. T.; DeCicco, G. J.; Hyun, J. L.; Reinhardt, G. Cyclynes. Part 4. Pericyclynes of the Order [5], [6], [7], and [8]. Simple Convergent Syntheses and Chemical Reactions of the First Homoconjugated Cyclic Polyacetylenes. *J. Am. Chem. Soc.* **1985**, *107* (23), 6546–6555. https://doi.org/10.1021/ja00309a021.

(37) Maraval, V.; Chauvin, R. From Macrocyclic Oligo-Acetylenes to Aromatic Ring Carbo-Mers. *Chem. Rev.* **2006**, *106* (12), 5317–5343. https://doi.org/10.1021/cr050964e.

(38) Saccavini, C.; Sui-Seng, C.; Maurette, L.; Lepetit, C.; Soula, S.; Zou, C.; Donnadieu, B.; Chauvin, R. Functional [6]Pericyclynes: Aromatization to Substituted Carbo-Benzenes. *Chem. – Eur. J.* **2007**, *13* (17), 4914–4931. https://doi.org/10.1002/chem.200601193.

(39) Suzuki, R.; Tsukuda, H.; Watanabe, N.; Kuwatani, Y.; Ueda, I. Synthesis, Structure and Properties of 3,9,15-Tri- and 3,6,9,12,15,18-Hexasubstituted Dodecadehydro[18]Annulenes ($C_{18}H_3R_3$ and $C_{18}R_6$) with D_6h-Symmetry. *Tetrahedron* **1998**, *54* (11), 2477–2496. https://doi.org/10.1016/S0040-4020(98)00011-8.

(40) Kuwatani, Y.; Watanabe, N.; Ueda, I. Synthesis of the First 3,6,9,15,18,18-Hexa-Substituted-1,2,4,5,7,8,10,11,13,14,16,17-Dodecadehydro [18] Annulenes with D6h-Symmetry. *Tetrahedron Lett.* **1995**, *36* (1), 119–122. https://doi.org/10.1016/0040-4039(94)02181-A.

(41) Maurette, L.; Saccavini, C.; Maraval, V.; Chauvin, R. First Insights into the Synthesis of Carbo-Phospholane and Carbo-Phospholene Oxides. *Fr. Ukr. J. Chem.* **2015**, *3* (2), 80–88. https://doi.org/10.17721/fujcV3I2P80-88.

(42) Kuwatani, Y.; Watanabe, N.; Ueda, I. Synthesis of the First 3,6,9,15,18,18-Hexa-Substituted-1,2,4,5,7,8,10,11,13,14,16,17-Dodecadehydro[18]Annulenes with D6h-Symmetry. *Tetrahedron Letters* **1995**, *36* (1), 119–122. https://doi.org/10.1016/0040-4039(94)02181-A.

(43) Saccavini, C.; Tedeschi, C.; Maurette, L.; Sui-Seng, C.; Zou, C.; Soleilhavoup, M.;

Vendier, L.; Chauvin, R. Functional [6]Pericyclynes: Synthesis through [14+4] and [8+10] Cyclization Strategies. *Chemistry - A European Journal* **2007**, *13*, 4895–4913. https://doi.org/10.1002/chem.200601191.

(44) Maurette, L.; Tedeschi, C.; Sermot, E.; Soleilhavoup, M.; Hussain, F.; Donnadieu, B.; Chauvin, R. Synthesis and Stereochemical Resolution of Functional [5] Pericyclynes. *Tetrahedron* **2004**, *60* (44), 10077–10098. https://doi.org/10.1016/j.tet.2004.07.052.

(45) de Meijere, A.; Kozhushkov, S. I. Macrocyclic Structurally Homoconjugated Oligoacetylenes: Acetylene- and Diacetylene-Expanded Cycloalkanes and Rotanes. In *Carbon Rich Compounds II, Macrocyclic Oligoacetylenes and Other Linearly Conjugated Systems*; de Meijere, A., Ed.; Topics in Current Chemistry; Springer: Berlin, Heidelberg, 1999; pp 1–42. https://doi.org/10.1007/3-540-49451-0_1.

(46) Maurette, L. Ph.D. Dissertation, Universite´ Paul Sabatier, Toulouse, 2001.

(47) Saccavini, C. Ph.D. Dissertation, Universite´ Paul Sabatier, Toulouse, 2004.

(48) Lepetit, C.; Peyrou, V.; Chauvin, R. Ring Carbo-Mers of "Aromatic" Heterocycles. *Phys Chem Chem Phys* **2004**, *6* (2), 303–309. https://doi.org/10.1039/B311790A.

(49) Z. Yao, V. Maraval, R. Chauvin. Unpublished Results.

(50) Yao, Z. Ph.D. Dissertation, Universite´ Paul Sabatier, Toulouse, 2023.

(51) van Assema, S. G. A.; de Jong, G. B.; Ehlers, A. W.; de Kanter, F. J. J.; Schakel, M.; Spek, A. L.; Lutz, M.; Lammertsma, K. Acetylene-Substituted Phosphane Oxides: Building Blocks for Macrocycles. *Eur. J. Org. Chem.* **2007**, *2007* (15), 2405–2412. https://doi.org/10.1002/ejoc.200600877.

(52) Brake, M.; Enkelmann, V.; Bunz, U. H. F. Synthesis and Characterization of Oxygen-Substituted Pericyclynes. *J. Org. Chem.* **1996**, *61* (4), 1190–1191. https://doi.org/10.1021/jo952087q.

(53) Leibrock, B.; Vostrowsky, O.; Hirsch, A. Synthesis of New Cyclic Homoconjugated Oligodiacetylenes. *European Journal of Organic Chemistry* **2001**, *2001* (23), 4401–4409. https://doi.org/10.1002/1099-0690(200112)2001:23<4401::AID-EJOC4401>3.0.CO;2-P.

(54) Manini, P.; Amrein, W.; Gramlich, V.; Diederich, F. Expanded Cubane: Synthesis of a Cage Compound with a C56 Core by Acetylenic Scaffolding and Gas-Phase Transformations into Fullerenes. *Angew. Chem. Int. Ed Engl.* **2002**, *41*, 4339–4343. https://doi.org/10.1002/1521-3773(20021115)41:22<4339::AID-ANIE4339>3.0.CO;2-8.

(55) Manini, P.; Amrein, W.; Gramlich, V.; Diederich, F. Cover Picture: Angew. Chem. In t. Ed. 22/2002. *Angew. Chem. Int. Ed.* **2002**, *41* (22), 4155–4155. https://doi.org/10.1002/152 1-3773(20021115)41:22<4155::AIDANIE4155>3.0. CO;2-3.

(56) Leroyer, L.; Zou, C.; Maraval, V.; Chauvin, R. Synthesis and Stereochemical Resolu tion of a [6]Pericyclynedione: Versatile Access to Pericyclynediol Precursors of *Carbo*-Benze nes. *Comptes Rendus Chim.* **2009**, *12* (3–4), 412–429. https://doi.org/10.1016/j.crci.2008.09.0 18.

(57) Zhu, C.; Poater, A.; Duhayon, C.; Kauffmann, B.; Saquet, A.; Rives, A.; Maraval, V.; Chauvin, R. *Carbo* -mer of Barrelene: A Rigid 3D-Carbon-Expanded Molecular Barrel. *Che m. – Eur. J.* **2021**, *27* (36), 9286–9291. https://doi.org/10.1002/chem.202100670.

(58) Zimmerman, H. E.; Paufler, R. M. BICYCLO[2,2,2]-2,5,7-OCTATRIENE (BARRE LENE), A UNIQUE CYCLIC SIX ELECTRON PI SYSTEM. *J. Am. Chem. Soc.* **1960**, *82* (6), 1514–1515. https://doi.org/10.1021/ja01491a071.

(59) Cocq, K.; Saffon-Merceron, N.; Coppel, Y.; Poidevin, C.; Maraval, V.; Chauvin, R. Carbo-Naphthalene: A Polycyclic Carbo-Benzenoid Fragment of α-Graphyne. *Angew. Chem. Int. Ed.* **2016**, *55* (48), 15133–15136. https://doi.org/10.1002/anie.201608300.

(60) Zhu, C.; Poater, A.; Duhayon, C.; Kauffmann, B.; Saquet, A.; Maraval, V.; Chauvin, R. Carbo-Biphenyls and Carbo-Terphenyls: Oligo(Phenylene Ethynylene) Ring Carbo-Mers. *Angew. Chem. Int. Ed.* **2018**, *57* (20), 5640–5644. https://doi.org/10.1002/anie.201713411.

(61) Barba-Barba, R. M.; Chammam, M.; Ramos-Ortiz, G.; Listunov, D.; Velusamy, J.; R odriguez, M.; Carriles, R.; Silva, C.; Duhayon, C.; Kauffmann, B.; Maraval, V.; Chauvin, R. Linear and Nonlinear Optical Properties of a Quadrupolar Carbo-Benzene and Its Benzenic P arent: The Carbo-Merization Effect. *Dyes Pigments* **2021**, *188*, 109133. https://doi.org/10.101 6/j.dyepig.2021.109133.

(62) Zhu, C.; Rives, A.; Duhayon, C.; Maraval, V.; Chauvin, R. Lipidic *Carbo* -Benzenes: Molecular Probes of Magnetic Anisotropy and Stacking Properties of α-Graphyne. *J. Org. C hem.* **2017**, *82* (2), 925–935. https://doi.org/10.1021/acs.joc.6b02397.

(63) Lepetit, C.; Peyrou, V.; Chauvin, R. Ring Carbo-Mers of "Aromatic" Heterocycles. *Phys. Chem. Chem. Phys.* **2004**, *6* (2), 303–309. https://doi.org/10.1039/B311790A.

(64) Cocq, K.; Barthes, C.; Rives, A.; Maraval, V.; Chauvin, R. Synthesis of Functional C arbo-Benzenes with Functional Properties: The C2 Tether Key. *Synlett* **2019**, *30* (01), 30–43. https://doi.org/10.1055/s-0037-1610269.

(65) Kuwatani, Y.; Watanabe, N.; Ueda, I. Synthesis of the First 3,6,9,15,18,18-Hexa-Sub stituted-1,2,4,5,7,8,10,11,13,14,16,17-Dodecadehydro[18]Annulenes with D6h-Symmetry. *Te trahedron Lett.* **1995**, *36* (1), 119–122. https://doi.org/10.1016/0040-4039(94)02181-A.

(66) Saccavini, C.; Sui-Seng, C.; Maurette, L.; Lepetit, C.; Soula, S.; Zou, C.; Donnadieu, B.; Chauvin, R. Functional [6]Pericyclynes: Aromatization to Substituted Carbo-Benzenes. *C hem. – Eur. J.* **2007**, *13* (17), 4914–4931. https://doi.org/10.1002/chem.200601193.

(67) Saccavini, C.; Tedeschi, C.; Maurette, L.; Sui-Seng, C.; Zou, C.; Soleilhavoup, M.; Vendier, L.; Chauvin, R. Functional [6]Pericyclynes: Synthesis through [14+4] and [8+10] C yclization Strategies. *Chem. – Eur. J.* **2007**, *13* (17), 4895–4913. https://doi.org/10.1002/chem. 200601191.

(68) Zou, C.; Duhayon, C.; Maraval, V.; Chauvin, R. Hexasilylated Total Carbomer of Be nzene. *Angew. Chem. Int. Ed.* **2007**, *46* (23), 4337–4341. https://doi.org/10.1002/anie.200605 262.

(69) Diederich, F.; Rubin, Y.; Diederich, F.; Rubin, Y. Strategien Zum Aufbau Molekulare r Und Polymerer Kohlenstoffallotrope. *Angew. Chem.* **1992**, *104* (9), 1123–1146. https://doi.o rg/10.1002/ange.19921040904.

(70) Diederich, F.; Rubin, Y. Synthetic Approaches toward Molecular and Polymeric Car bon Allotropes. *Angew. Chem. Int. Ed. Engl.* **1992**, *31* (9), 1101–1123. https://doi.org/10.1002 /anie.199211013.

(71) Zou, C.; Lepetit, C.; Coppel, Y.; Chauvin, R. Ring Carbo-Mers: From Questionable Homoaromaticity to Bench Aromaticity. *Pure Appl. Chem.* **2006**, *78* (4), 791–811. https://doi. org/10.1351/pac200678040791.

(72) Rives, A.; Baglai, I.; Malytskyi, V.; Maraval, V.; Saffon-Merceron, N.; Voitenko, Z.; Chauvin, R. Highly π Electron-Rich Macro-Aromatics: Bis(p-Aminophenyl)-Carbo-Benzene s and Their DBA Acyclic References. *Chem. Commun.* **2012**, *48* (70), 8763–8765. https://doi. org/10.1039/C2CC34176J.

(73) Baglai, I.; Maraval, V.; Bijani, C.; Saffon-Merceron, N.; Voitenko, Z.; Volovenko, Y. M.; Chauvin, R. Enhanced π-Frustration in Carbo-Benzenic Chromophores. *Chem. Commun.* **2013**, *49* (75), 8374–8376. https://doi.org/10.1039/C3CC43204A.

(74) Chen, F.; Li, X.; Hihath, J.; Huang, Z.; Tao, N. Effect of Anchoring Groups on Single-Molecule Conductance: Comparative Study of Thiol-, Amine-, and Carboxylic-Acid-Terminated Molecules. *J. Am. Chem. Soc.* **2006**, *128* (49), 15874–15881. https://doi.org/10.1021/ja065864k.

(75) Li, Z.; Borguet, E. Determining Charge Transport Pathways through Single Porphyrin Molecules Using Scanning Tunneling Microscopy Break Junctions. *J. Am. Chem. Soc.* **2012**, *134* (1), 63–66. https://doi.org/10.1021/ja208600v.

(76) Lu, Q.; Liu, K.; Zhang, H.; Du, Z.; Wang, X.; Wang, F. From Tunneling to Hopping: A Comprehensive Investigation of Charge Transport Mechanism in Molecular Junctions Based on Oligo(p-Phenylene Ethynylene)s. *ACS Nano* **2009**, *3* (12), 3861–3868. https://doi.org/10.1021/nn9012687.

(77) Xu, T.; Wu, Y.-K.; Luo, X.; Guo, L. J. Plasmonic Nanoresonators for High-Resolution Colour Filtering and Spectral Imaging. *Nat. Commun.* **2010**, *1* (1), 59. https://doi.org/10.1038/ncomms1058.

(78) Baglai, I.; de Anda-Villa, M.; Barba-Barba, R. M.; Poidevin, C.; Ramos-Ortíz, G.; Maraval, V.; Lepetit, C.; Saffon-Merceron, N.; Maldonado, J.-L.; Chauvin, R. Difluorenyl Carbo-Benzenes: Synthesis, Electronic Structure, and Two-Photon Absorption Properties of Hydrocarbon Quadrupolar Chromophores. *Chemistry* **2015**, *21* (40), 14186–14195. https://doi.org/10.1002/chem.201500482.

(79) M. Leckie, S.; J. Harkness, G.; L. Clarke, M. Catalytic Constructive Deoxygenation of Lignin-Derived Phenols: New C–C Bond Formation Processes from Imidazole-Sulfonates and Ether Cleavage Reactions. *Chem. Commun.* **2014**, *50* (78), 11511–11513. https://doi.org/10.1039/C4CC04939J.

(80) Wang, L.; Ren, X.; Yu, J.; Jiang, Y.; Cheng, J. Base-Promoted Formal Arylation of Benzo[d]Oxazoles with Acyl Chloride. *J. Org. Chem.* **2013**, *78* (23), 12076–12081. https://doi.org/10.1021/jo402106q.

(81) Chandrasekhar, S.; Sadashiva, B. K.; Suresh, K. A. Liquid Crystals of Disc-like Molecules. *Pramana* **1977**, *9* (5), 471–480. https://doi.org/10.1007/BF02846252.

(82) Poidevin, C.; Lepetit, C.; Ben Amor, N.; Chauvin, R. Truncated Transition Densities for Analysis of (Nonlinear) Optical Properties of Carbo-Chromophores. *J. Chem. Theory Co mput.* **2016**, *12* (8), 3727–3740. https://doi.org/10.1021/acs.jctc.6b00484.

(83) Roy, B.; De, N.; Majumdar, K. C. Advances in Metal-Free Heterocycle-Based Colu mnar Liquid Crystals. *Chem. – Eur. J.* **2012**, *18* (46), 14560–14588. https://doi.org/10.1002/c hem.201200483.

(84) Pisula, W.; Feng, X.; Müllen, K. Tuning the Columnar Organization of Discotic Po lycyclic Aromatic Hydrocarbons. *Adv. Mater.* **2010**, *22* (33), 3634–3649. https://doi.org/10.10 02/adma.201000585.

(85) Wöhrle, T.; Wurzbach, I.; Kirres, J.; Kostidou, A.; Kapernaum, N.; Litterscheidt, J.; Haenle, J. C.; Staffeld, P.; Baro, A.; Giesselmann, F.; Laschat, S. Discotic Liquid Crystals. *Ch em. Rev.* **2016**, *116* (3), 1139–1241. https://doi.org/10.1021/acs.chemrev.5b00190.

(86) Zhu, C.; Rives, A.; Duhayon, C.; Maraval, V.; Chauvin, R. Lipidic Carbo-Benzenes: Molecular Probes of Magnetic Anisotropy and Stacking Properties of α-Graphyne. *J. Org. C hem.* **2017**, *82* (2), 925–935. https://doi.org/10.1021/acs.joc.6b02397.

(87) Zhu, C.; Wang, T.-H.; Su, C.-J.; Lee, S.-L.; Rives, A.; Duhayon, C.; Kauffmann, B.; Maraval, V.; Chen, C.; Hsu, H.-F.; Chauvin, R. 3D and 2D Supramolecular Assemblies and T hermotropic Behaviour of a Carbo-Benzenic Mesogen. *Chem. Commun.* **2017**, *53* (43), 5902–5905. https://doi.org/10.1039/C7CC02430D.

(88) Baglai, I.; de Anda-Villa, M.; Barba-Barba, R. M.; Poidevin, C.; Ramos-Ortíz, G.; M araval, V.; Lepetit, C.; Saffon-Merceron, N.; Maldonado, J.-L.; Chauvin, R. Difluorenyl Carb o-Benzenes: Synthesis, Electronic Structure, and Two-Photon Absorption Properties of Hydro carbon Quadrupolar Chromophores. *Chem. – Eur. J.* **2015**, *21* (40), 14186–14195. https://doi. org/10.1002/chem.201500482.

(89) Zhu, C.; Poater, A.; Duhayon, C.; Kauffmann, B.; Saquet, A.; Maraval, V.; Chauvin, R. Carbo-Biphenyls and Carbo-Terphenyls: Oligo (Phenylene Ethynylene) Ring Carbo-Mers. *Angew. Chem. Int. Ed.* **2018**, *57* (20), 5640–5644. https://doi.org/10.1002/anie.201713411.

(90) Yao, Z.; Lin, X.; Chauvin, R.; Wang, L.; Gras, E.; Cui, X. Phosphine-Phosphonium Ylides as Ligands in Palladium-Catalysed C2-H Arylation of Benzoxazoles. *Chin. Chem. Let t.* **2020**, *31* (12), 3250–3254. https://doi.org/10.1016/j.cclet.2020.04.008.

(91) Zhu, C.; Gras, E.; Duhayon, C.; Lacassin, F.; Cui, X.; Chauvin, R. The Forgotten Nitroaromatic Phosphines as Weakly Donating P-ligands: An *N* -Aryl **-**benzimidazolyl Series in RhCl(CO) Complexes. *Chem. – Asian J.* **2017**, *12* (21), 2845–2856. https://doi.org/10.1002/asia.201701078.

(92) Hengefeld, A.; Kopf, J.; Nast, R. Kristall- und Molekülstruktur von Di-μ-iodo-tetrakis[tris(phenylethinyl)phosphin]dikupfer. *Chem. Ber.* **1977**, *110* (9), 3078–3083. https://doi.org/10.1002/cber.19771100913.

(93) Hengefeld, A.; Kopf, J.; Rehder, D. Pentacarbonyl[Tris(Phenylethynyl) Phosphine]Chromium(0), Cr(CO)5P(C.Tplbond.CPh)3: Spectral, Structural and MO Characteristics. *Organometallics* **1983**, *2* (1), 114–121. https://doi.org/10.1021/om00073a021.

(94) Hengefeld, A.; Nast, R. Komplexe Des Typs $Ni(CO)_4$-n(P(C≡CC_6H_5)$_m$(C_6H_5)$_{3-m}$)n (n = 2, 3, 4; m = 3, 2, 1). *J. Organomet. Chem.* **1983**, *252* (3), 375–379. https://doi.org/10.1016/S0022-328X(00)99838-3.

(95) Lang, H.; Leise, M.; Zsolnai, L. Bifunctional Neutral Phosphenium Ion Complexes: Synthesis of Phenylethynyl- and Styryl-Substituted (R)(R′)P=Mo- (H_5-C_5Me_5)$(CO)_2$ Compounds. Crystal Structure of [2,6-tBu_2-4-MeC_6H_2O)(PhC≡C)]P=Mo(H_5-C_5Me_5)$(CO)_2$. *J. Organomet. Chem.* **1990**, *389* (3), 325–332. https://doi.org/10.1016/0022-328X(90)85427-Z.

(96) Stulz, E.; Sanders, J. K. M.; Montalti, M.; Prodi, L.; Zaccheroni, N.; Fabrizi de Biani, F.; Grigiotti, E.; Zanello, P. Phosphine and Phosphonite Complexes of a Ru(II) Porphyrin. 2. Photophysical and Electrochemical Studies. *Inorg. Chem.* **2002**, *41* (20), 5269–5275. https://doi.org/10.1021/ic025728q.

(97) Hightower, S. E.; Corcoran, R. C.; Sullivan, B. P. Unusual, Bifurcated Photoreactivity of a Rhenium(I) Carbonyl Complex of Triethynylphosphine. *Inorg. Chem.* **2005**, *44* (26), 9601–9603. https://doi.org/10.1021/ic050901e.

(98) Mathur, P.; Rai, D. K.; Ji, R. S.; Pathak, B.; Boodida, S.; Mobin, S. M. Structural and Electrochemical Aspects of Tris(Ferrocenyl/Phenyl-Ethynyl)Phosphine Ligated Chalcogen Bridged Iron Carbonyl Clusters. *RSC Adv.* **2013**, *3* (48), 26025–26034. https://doi.org/10.1039/C3RA44788J.

Chapter 2. Synthesis of carbo-diphosphacyclohexane and carbo-diphosphinine derivatives

1. Introduction

It had been long suspected that heavier elements of group 15 could be engaged in multiple bonding, but no real demonstration of this became available until the preparation of 2,4,6-triphenylphosphinine in 1966 by Märkl[1], by a procedure involving the treatment of a pyrylium salt with tris(hydroxymethyl)phosphine. From then, a remarkable expansion of phosphorus heterocyclic chemistry has started. For the first time, the unsubstituted phosphinine (along with arsenine) was synthesized by Ashe[2] in 1976 by treating 1,1-dibutyl-1,4-dihydrostannabenzene with phosphorus tribromide (**Figure 2.1**).

Although nowadays phosphinines are well known, diphosphinines have been much less studied. The first case of diphosphinine was synthesized in 1976 by Kobayashi *et al.*, as the authors also reported the synthesis of a diphosphabarrelene[3]. In 1995, Biegger and coworkers synthezised the first case of 1,4-dihydro-dithiophosphinine, which could be desulfurized by action of tri-n-butylphosphine at high temperature[4].

Recently, a novel protocol of synthesis of the parent heterocycle via electrocyclization of *in situ*-generated phosphonium ylides followed by reduction of the resulting λ^5,σ^4-phosphinine has been published by A. Kostyuk *et al.*[5] While phosphinines have long been experimentally studied, in particular for the purpose of P-coordination chemistry, ring *carbo*-mers thereof have only been calculated[6].

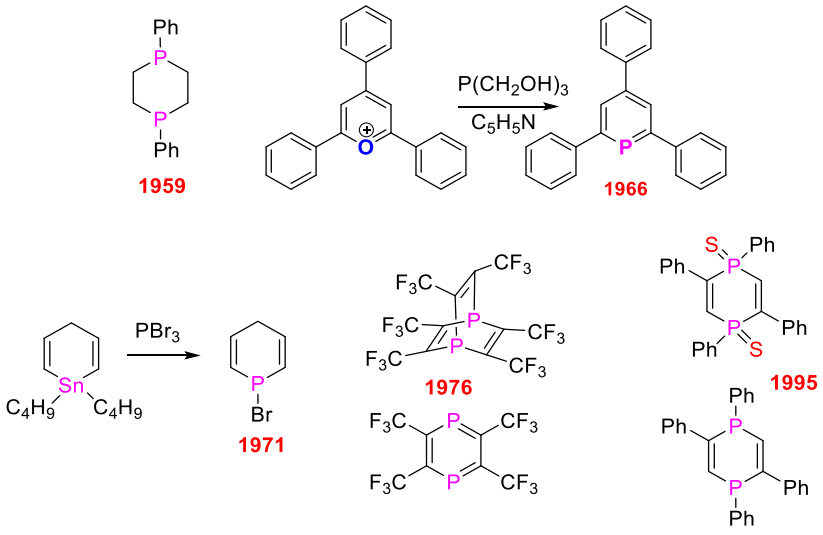

Figure 2.1. Early examples of phosphinine derivatives.

According to the Hückel rule, phosphinine, having 6 π-conjugated electrons in its ring, is an aromatic compound. Depending on the aromaticity index applied it can be shown that the aromaticity of the phosphinine is 80–97% of that of benzene.[7] In terms of reactivity, phosphinine differs significantly from both benzene and pyridine. By integrating phosphorus chemistry into *carbo*-mer chemistry (**Figure 2.2**), researchers can access a broad range of compounds with diverse properties and applications. Indeed, the introduction of phosphorus atoms in *carbo*-mer molecules opens prospects in areas such as catalysis and coordination chemistry, that have never been previously envisaged.

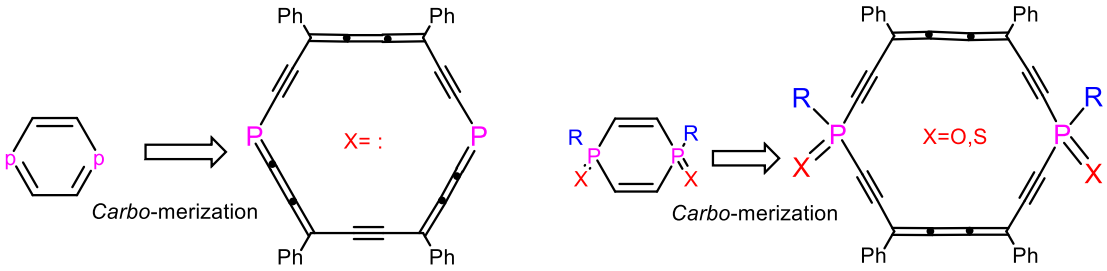

Figure 2.2. Ring *carbo*-merization of diphosphinine derivatives.

Therefore, the ring *carbo*-mers, i.e. C_2-expanded, of phosphinines (or phosphorines, or phosphabenzenes) were envisaged (**Figure 2.3**). Such "c*arbo*-phosphinines" are still unknown experimentally, [8] but a [8+1+8+1] route was envisaged as a reasonable synthetic strategy to access more symmetrical "*carbo*-1,4-diphosphinines". Their soft electrophilic character should allow evidence of original coordination chemistry (in particular regarding possible competition between P- and C_2- coordination), with related prospects for the catalytic properties of the complexes. In this context,[9–12] ruthenium complexes of *carbo*-diphosphinine derivatives were early envisaged as possible pre-catalysts, e.g. for transfer hydrogenation of acetophenones.

Owing to the paucity and poor stability of examples of λ^3, σ^2-phosphabutatrienes R – P=C=C=C(Ph)–R', first exemplified by Märkl *et al.* for R = 2,4,6-^{t}Bu$_3$C$_6$, R' = Ph [13], first reasonable derivatives of *carbo*-diphosphinines (where R and R' would be *a priori* reactive alkynyl groups) should contain λ^5,σ^4-P atoms, namely be 1*H*,10*H*-*carbo*-1,4-diphosphinines, or *carbo*-1,4-dihydro-1,4-diphosphinines.

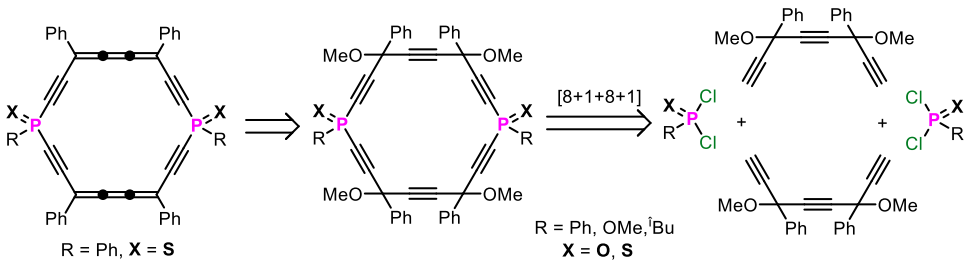

Figure 2.3. Proposed synthesis of ring *carbo*-mers of 1,4-dihydro-1,4-diphosphinine derivatives.

2. Results and discussion

The $C_{16}P_2$ macrocycle of ring *carbo*-mers of 1,4-diphosphinines or 1,4-dihydro-1,4-diphosphinines is targeted from two equivalents of C8 triyne dinucleophiles and two equivalents of P1 electrophiles.

2.1. Preparation of the triyne C_8 precursor of $C_{16}P_2$ macrocycles

From commercially available chemicals, the previously reported triyne **3** was obtained as a yellow solid by a 3-step sequence with an overall yield of 83%, the third step being a 3-step one-pot process [14,15](see **Scheme 2.1**).

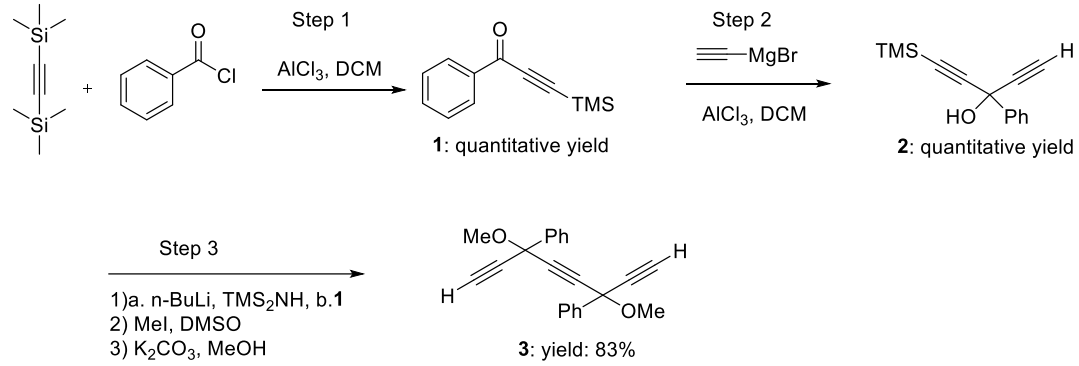

Scheme 2.1. Synthesis of the known triyne **3** in three steps.

2.2. Synthesis of diphospha-[6]pericyclyne derivatives

Given the interest of trivalent phosphorus atoms (λ^3-P) for coordination chemistry, the initial choice was to target diphosphane macrocycles despite their anticipated higher reactivity and sensitivity as compared to λ^5-P counterparts. Starting from **3**, many attempts have been made, and the first challenge came from the selection of the macrocyclization strategy. Firstly, a dicomponent [10+8] macrocyclization strategy, largely applied for the preparation of [6]pericyclyne derivatives,

was proposed to be used for the construction of the diphospha[6]pericyclynes (**Scheme 2.2**).

Initially, two equivalents of EtMgBr were used as base to doubly deprotonate the triyne **3** [16], followed by the slow addition of one equivalent of $PhPCl_2$ at low temperature. However, in these conditions, no trace of the diphosphine **3a** was observed in the ^{31}P NMR spectrum (expected at about 46 ppm). Instead, two broad signals in the range of -26 to -28 ppm were detected. n-Butyl lithium was then employed as an alternative base, resulting in the formation of a dark brown paste with extremely poor solubility: the ^{31}P and ^{1}H NMR spectra revealed complicated broad signals as well, suggesting the formation of polymers.

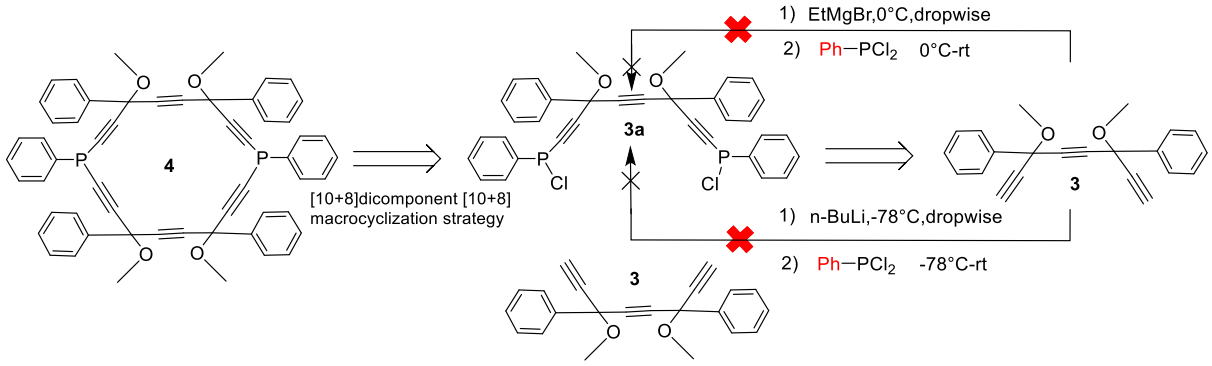

Scheme 2.2. Attempts at preparation of diphospha[6]pericyclynes by a dicomponent [10+8] macrocyclization strategy.

Drawing inspiration from a seminal report detailing the synthesis of parent dihydro-1,4-diphosphinines[17], a novel tetra-component [8+1+8+1] macrocyclization strategy was envisioned. Commencing with triyne **3**, two equivalents of lithium diisopropylamide (LDA) were employed as the deprotonating agent, followed by the addition of one equivalent of $PhPCl_2$ at low temperature and stirring overnight. In these conditions, a pioneering example of a macrocyclic acetylenic diphosphane, featuring phenyl substitution at the phosphorus atom, denoted as compound **4**, was obtained. The process is a tetracomponent [8+1+8+1] macrocyclization reaction, culminating in a promising yield of up to 40% (**Scheme 2.3**), after purification of the product by chromatography as a mixture of stereoisomers giving several signals in ^{31}P NMR and ^{1}H NMR as classically observed for hexaoxy-pericyclynes.

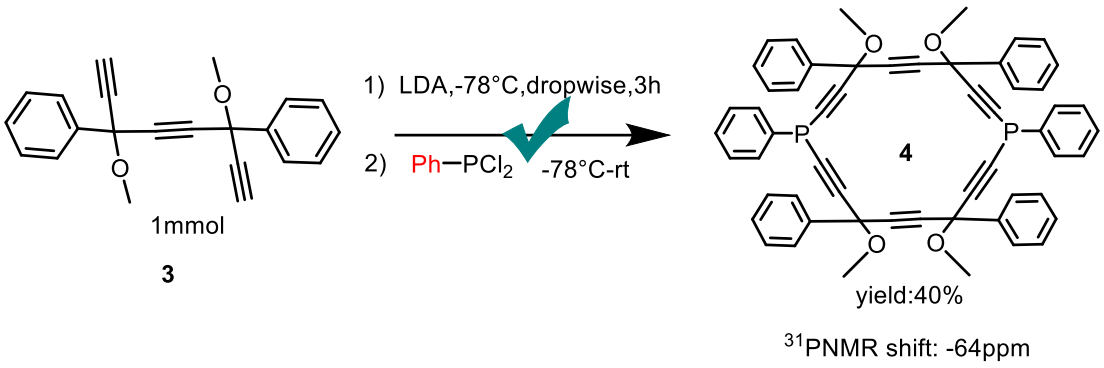

Scheme 2.3. Synthesis of the diphospha[6]pericyclyne **4** by a tetra-component [8+1+8+1] macrocyclization strategy.

With the final objective to prepare the fully aromatic *carbo*-diphosphinine, its precursor macrocyclic acetylenic diphosphane **5** having methoxy groups at the phosphorus atom was also targeted following the same [8+1+8+1] method. The hexaoxy-diphospha-[6]pericylyne **5** was thus obtained as a quasi-statistical mixture of stereoisomers (20 in theory, including 6 pairs of enantiomers, and 14 NMR-distinguishable diastereoisomers modulo their mirror image) but with a lower 5% yield, and fully characterized by ^{31}P NMR, ^{13}C NMR, ^{1}H NMR and HRMS. The much lower yield of **5** as compared to **4** may be attributed to the higher sensitivity toward hydrolysis of phosphinites as compared to phosphines (**Scheme 2.4**).

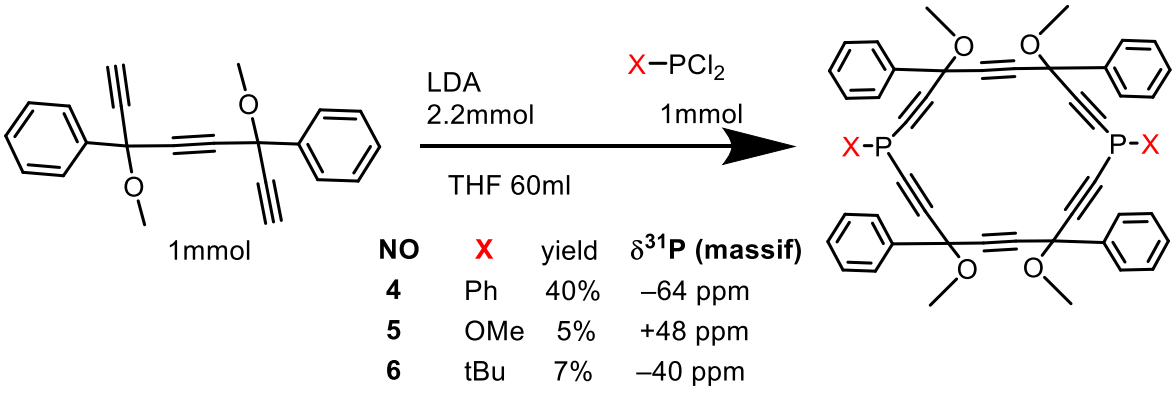

Scheme 2.4 Generalized access to diphospha-[6]pericyclyne derivatives.

During parallel investigations initiated from $tBuPCl_2$, three distinct products with different polarities were isolated by silica gel chromatography, all displaying nearly identical ^{1}H NMR chemical shifts, with two of them (**6** and **7**) even exhibiting similar ^{31}P NMR spectra (**Figure 2.4**). Subsequent analysis of high-resolution mass spectra revealed unexpected findings: alongside the originally targeted 18-membered ring compound **6**, side-products exhibiting a 27-membered ring,

designated as compounds **7** and **8**, were obtained, the second one resulting from the oxidation of the former. This unexpected outcome reveals a [8+1+8+1+8+1] cyclization process, highlighting the versatility of the reaction pathway (**Scheme 2.5**).

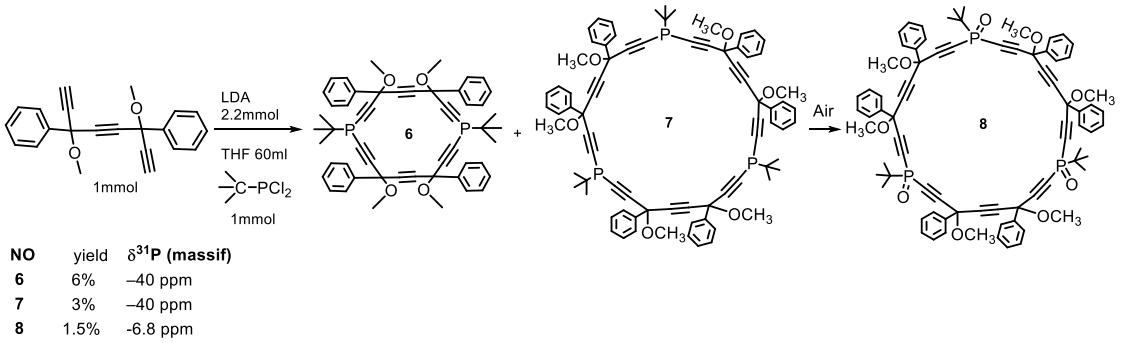

Scheme 2.5. Formation of triphospha-[9]pericyclyne derivatives as side-products of the synthesis of the diphospha[6]pericyclyne.

Comparison of the ^{31}P NMR spectra (**Figure 2.4a**) of diphospha-[6]pericyclyne **6** and triphospha-[9]pericyclyne **7** reveals notable differences. The 27-membered ring of **7** provides a higher number of stereoisomers but exhibits a smaller range of ^{31}P NNR chemical shifts， over 1.0 ppm for **7** *vs* 2.7 ppm for **6**. This difference can be explained by the increased flexibility in the larger-sized macrocycle, which makes less discernible the differences of ^{31}P environments between the different stereoisomers and thus decreases their influence on the chemical shifts. The same trend is observed in the ^{1}H NMR spectra (**Figure 2.4b**) as well, where the 27-membered ring of **7** exhibits a thinner range of signals.

Among the 14 theoretical diastereoisomers, 6 of them possess non-equivalent P atoms, thus making a total of 20 theoretically different ^{31}P chemical shifts: remarkably, one can count 19 resolved signals (top spectrum of **Figure 2.4.a**), one of them being quite broad around – 40.35 ppm, thus supporting the occurrence of all the stereoisomers.

Carbo-diphosphinine **5a** and *carbo*-dihydrodiphosphinine derivatives **4a** and **6a** (**Scheme 2.6**) were then targeted through reductive treatment with $SnCl_2$/HCl of the three putative precursors **5**, **4** and **6** featuring methoxy, phenyl, and tert-butyl groups respectively, as illustrated in **Scheme 2.6**. Despite extensive experiments involving varied reducing agents, acids, solvents and temperature conditions (**Table 2.1**), the desired reduced derivatives remained elusive. This failure can be

tentatively attributed to possible coordination interactions between the P(III) atoms within the macrocycle and the Sn(II) centers of the reducing agent $SnCl_2$. Such coordination phenomena are hypothesized to impede the desired chemical transformations, thereby explaining the unsuccessful outcome of the reaction.

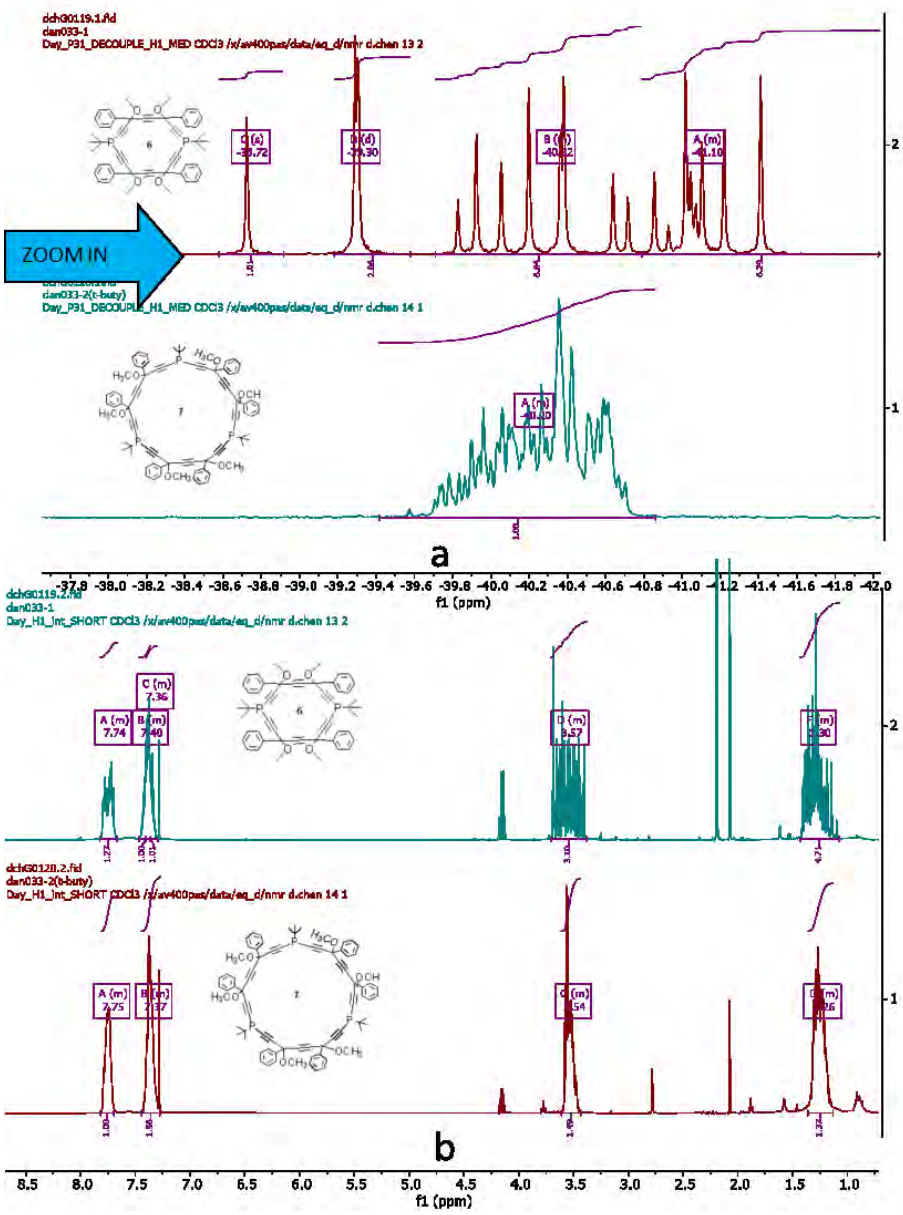

Figure 2.4 Comparison of the ^{31}P NMR spectra (a) and ^{1}H NMR spectra (b) of diphospha-[6]pericyclyne and triphospha-[9]pericyclyne derivatives

Table 2.1. Different conditions tested for the reductive elimination reaction of Scheme 2.6.

Condition / Trial	precursor	Solvent	Temperature	Acid	Time (h)
1	**4**	DCM	-78°C-rt	HCl	0.5
2	**4**	DCM	-78°C-rt	Acetic acid	0.5
3	**4**	DCM	0°C-30°C	None	2
4	**6**	DCM	-78°C-0°C	HCl	2
5	**5**	DCM	-78°C-rt	HCl	3
6	**5**	DCM	-78°C-rt	Acetic aid	3
7	**4**	DCM	0°C-30°C	None	5
8	**5**	DCM	-78°C-0°C	HCl	4
9	**4**	Et_2O	-78°C-rt	HCl	0.5
10	**4**	Et_2O	-78°C-rt	Acetic aid	0.5
11	**4**	Et_2O	0°C-30°C	None	2
12	**4**	Et_2O	-78°C-0°C	HCl	2
13	**4**	Et_2O	-78°C-rt	HCl	3
14	**4**	Et_2O	-78°C-rt	Acetic acid	3

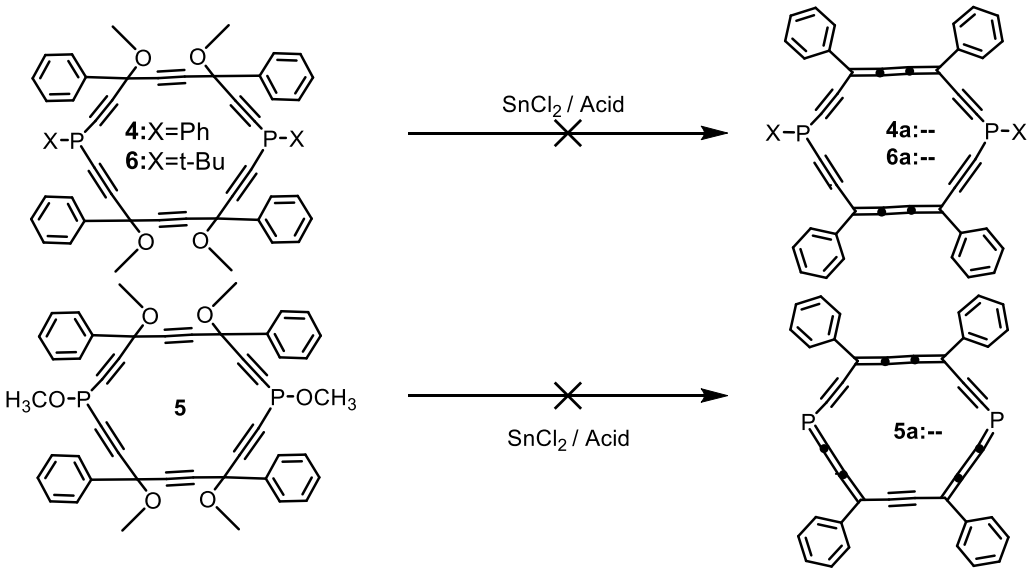

Scheme 2.6. Attempts at reduction of possible diphospha-[6]pericyclyne precursors of the corresponding *carbo*-dihydro-diphosphinine or *carbo*-diphosphinine derivatives.

2.3. Synthesis of the diphospha-[6]pericyclyne oxide and sulfide derivatives

To avoid the possible coordination of the Sn(II) center of the reducing agent by the λ^3,σ^3-P(III) atoms of **4**, **5** and **6** that could disrupt the reduction process, we explored λ^5,σ^4-P(IV) counterparts such as the corresponding phosphine oxides or phosphine sulfides. This strategic modification is expected not only to enhance the stability of the phosphorus-containing species but also to open alternative pathways to prepare the desired *carbo*-diphosphinines.

The target diphospha-[6]pericyclyne disulfide **9** and dioxide **10** can be accessed through two distinct routes. Firstly, the target could be obtained by sulfurization or oxidation of **4,** employing oxidative agents S_8 or H_2O_2, in 37% or quantitative yields, respectively. Alternatively, the same targets could be synthesized via the tetracomponent [8+1+8+1] macrocyclization strategy presented in Section 2.2 employing $S{=}PCl_2Ph$ or $O{=}PCl_2Ph$, affording **9** or **10** in 40% and 67% yield, respectively. These synthetic pathways offer versatile approaches to accessing the desired diphospha-[6]pericyclyne dioxide and disulfide compounds, each demonstrating their efficacy and potential for scalability in organic synthesis. In both cases, **9** and **10** were obtained as orange solid mixtures of stereoisomers, as can be seen in ^{31}P NMR (**Scheme 2.7** and **Figure 2.5**) by the presence of many signals between -9.97 ppm and -10.47 ppm for **9** and between -20.00 ppm and -20.73 ppm for **10** (14 diastereoisomers, 6 of them being chiral, and 6 of them containing non-equivalent P atoms, thus making a total of 20 theoretically different ^{31}P chemical shifts).

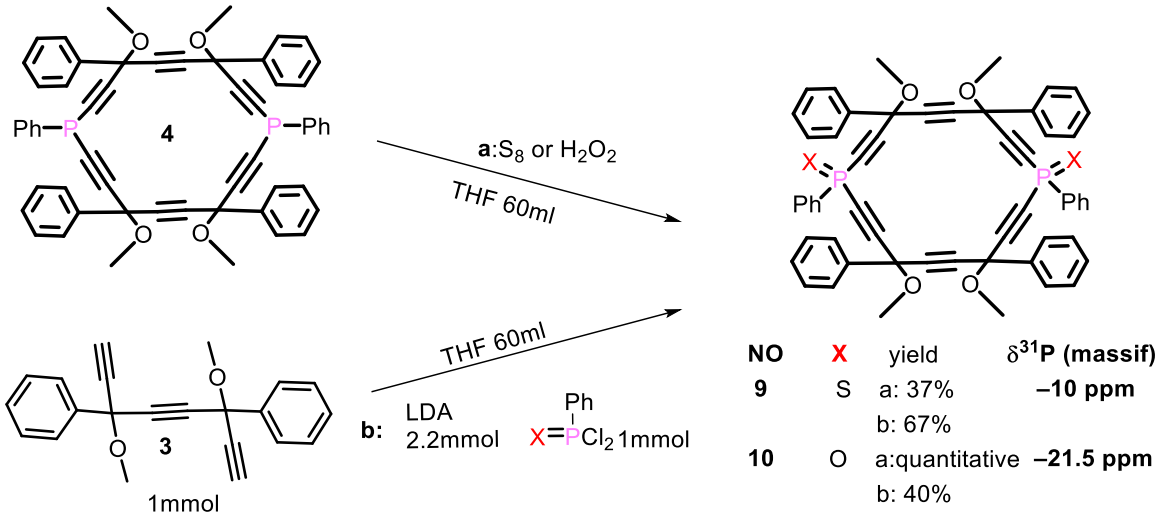

Scheme 2.7. Two routes to access diphospha-[6]pericyclyne dioxide and disulfide (see Scheme 2.5).

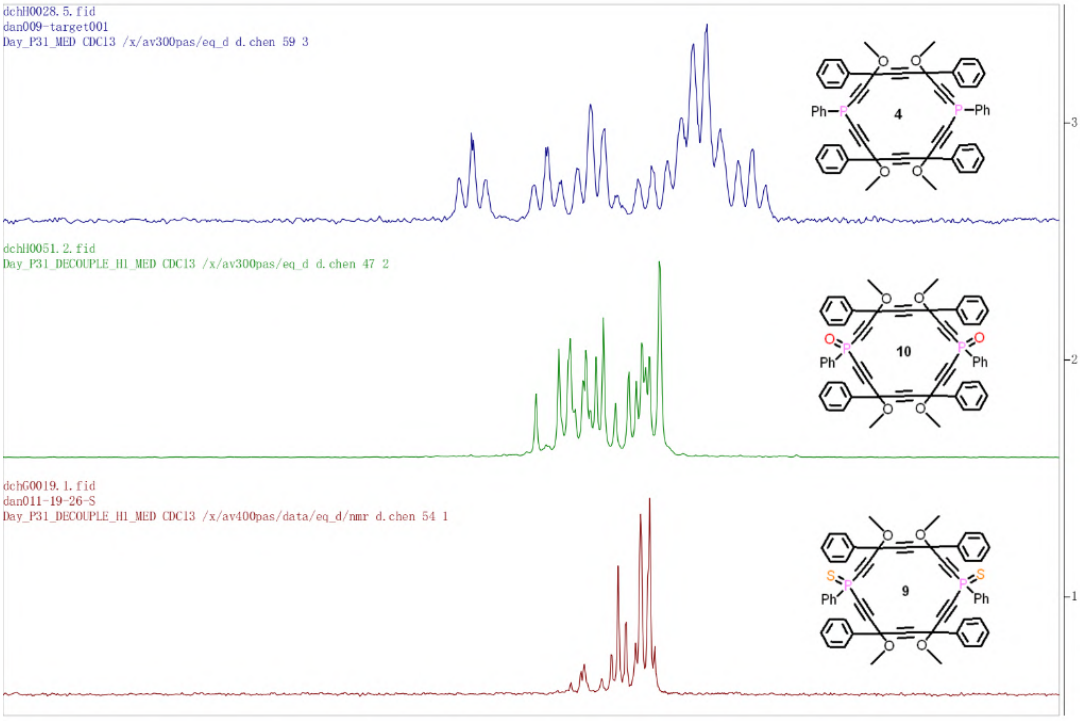

Figure 2.5. ^{31}P NMR spectra of diphospha-[6]pericyclyne dioxide and disulfide (compared with the corresponding diphosphine).

In **Figure 2.5**, we observe that the range of chemical shifts in the ^{31}P NMR spectrum of diphospha-[6]pericyclyne **4** is wider than that of the diphospha-[6]pericyclyne dioxide **10** and disulfide **9**, despite the identical size of the $C_{16}P_2$ macrocycle. The broadest range of ^{31}P NMR chemical shifts is observed for **4**, then for **10**, and finally for **9**. Therefore, the increase of the size of the substituent at the P atom (from an electron pair for **4**, to an oxygen atom for **9**, to a sulfur atom for **10**) induces a sharpening of the signal range in the ^{31}P NMR spectrum.

With the aim of preparing the fully aromatic *carbo*-diphosphinine dioxide **11a**, the possible precursor **11b** bearing a methoxy group at the two phosphorus atoms was targeted following the tetracomponent macrocyclization procedure. However, using LDA as base, starting from the triyne **3** and $O{=}PCl_2(OMe)$ did not allow formation of the target compound **11b**. Instead, the main product **11** and byproduct **12** were isolated with a yield of 17.3% and 10.8% respectively. Upon re-examining the starting methyl dichlorophosphonate reagent, it was evidenced that it was contaminated with dimethyl phosphorochloridate, $O{=}PCl(OMe)_2$. This impurity reacted with a

portion of the triyne **3** to form a singly substituted triyne **12**, while the remaining triyne **3** reacted with $O{=}PCl_2(OMe)$ to form the pentayne **11** (**Scheme 2.8**). However, no trace of the targeted macrocycle was observed, only a single end of the triyne precursor having reacted in each case.

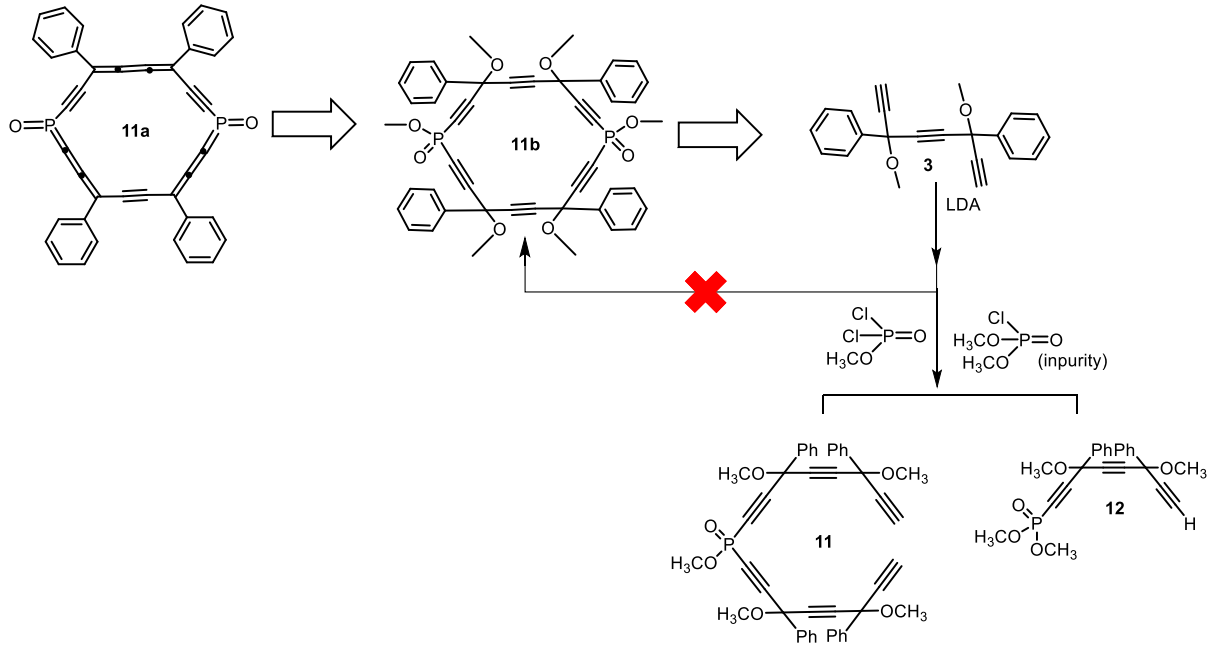

Scheme 2.8. Attempts at synthesis of aromatic *carbo*-diphosphinine dioxide.

2.4. Hexaphenyl-*carbo*-1,4-dithio-1,4-dihydro-1,4-diphosphinine and hexaphenyl-di(thiophosphinylethynyl)butatriene model thereof

2.4.1. *Synthesis of a carbo*-1,4-dithio-1,4-dihydro-1,4-diphosphinine and an acyclic model thereof

After subjecting **9** to $SnCl_2$/HCl in dichloromethane (DCM) at low temperatures, a treatment classically used for the synthesis of *carbo*-benzenes from hexaoxy[6]pericyclynes[18], hexaphenyl-*carbo*-1,4-dihydro-1,4-dithio-1,4-diphosphinine **13** was produced with 20 % yield as a bright orange solid (**Scheme 2.9**) and fully characterized by HRMS, NMR, IR and UV spectroscopy, electrochemistry, and X-ray crystallography.

Attempts at reducing the dioxybutyne edges of **10** were also made. After several trials, the diphosphine dioxide **14** could not be isolated. Only a broad massif in the aromatic region (6.8 - 8.0 ppm) and signals corresponding to remaining OCH_3 groups are observed in the ^1H NMR spectrum. It suggests the formation of polymers and the disappearance of the signals in ^{31}P NMR indicates a cleavage of the cyclic structure in the reaction conditions employed.

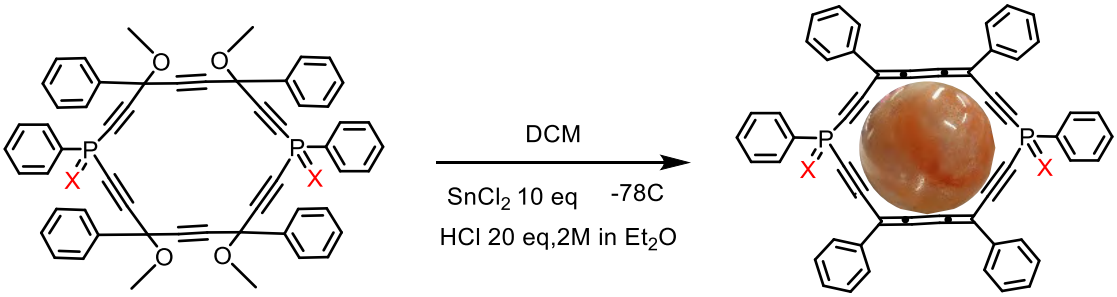

NO	X	δ^{31}P (massif)
9	S	–10 ppm
10	O	–21.5 ppm

NO	X	yield	δ^{31}P
13	S	20%	-9.08 ppm; -9.24 ppm
14	O	--	--

Scheme 2.9. Reductive acidic treatment of diphospha-[6]pericyclyne disulfide and dioxide with the view to forming the corresponding hexaphenyl-*carbo*-1,4-dihydro-1,4-phosphinine derivatives.

In order to analyze the properties of **13**, a half model thereof, i.e. hexaphenyl-di(thiophosphinylethynyl)butatriene **3b**, was synthesized within 3 steps from triyne **3** and $Ph_2P(S)Cl$, prepared from commercial Ph_2PCl in the presence of S_8 at 135℃ overnight. After treatment of **3** with LDA, an excess of $Ph_2P(S)Cl$ lead to the expected triyne **3a** in 59% yield. After subjecting **3a** to $SnCl_2$/HCl in DCM at low temperature, **3b** was produced with 23 % yield as a bright orange solid containing *E* and *Z* stereoisomers in a 2:1 ratio (**Scheme 2.10**), and was fully characterized by NMR, HRMS, UV, electrochemistry, single crystal X-ray diffraction.

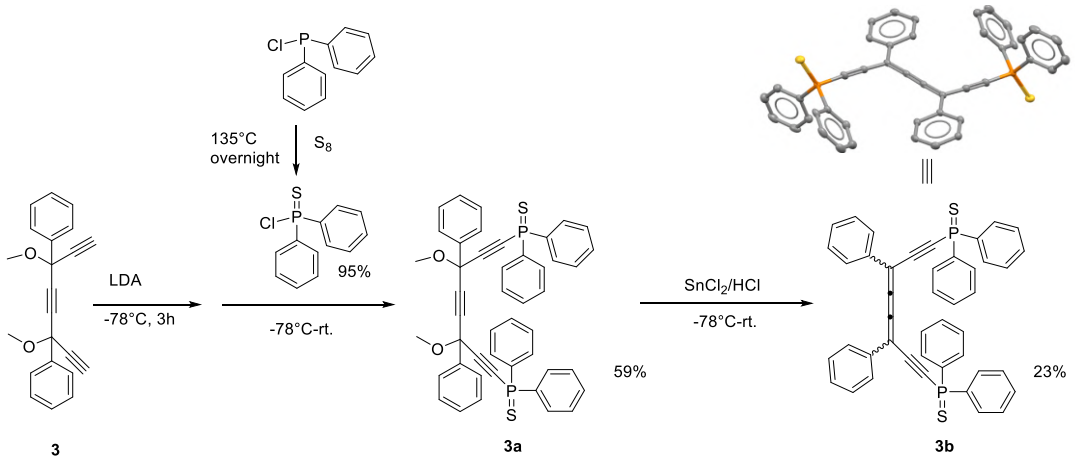

Scheme 2.10. Synthesis of hexaphenyl-di(thiophosphinylethynyl)butatriene **3b**, and X-ray crystal structure of *E*-isomer (CCDC number: 2352206)

2.4.2. Evolution of hexaphenyl-*carbo*-1,4-dithio-1,4-dihydro-1,4-phosphinine **13** in DCM without protection from light

An evolution of the title compound **13** can be observed when it is dissolved in DCM solution, under natural light at room temperature between several days and half a month. The color of the solution turned from bright orange for **13** to dark brown, while the solubility in either DCM or chloroform increased. Upon ^{31}P NMR monitoring, the spectrum progressively changed from a set of two singlets at -9.08 and -9.23 ppm for **13** to a unique singlet at 22 ppm (**Figure 2.6**), any other intermediate signal during the transformation. Regarding the ^{1}H NMR and ^{13}C NMR spectra, big differences can be observed between **13** and the final compound, including the appearance of new signals consistent with methylene groups, probably coming from a reaction with the solvent (this transformation occurring only in DCM), and the disappearance of the signals corresponding to C≡C units in the ^{13}C NMR spectrum. Many efforts were made to characterize the evolution compound, including ^{13}C and ^{1}H NMR spectra with or without ^{31}P-decoupling, ^{13}C and ^{31}P NMR spectra with or without ^{1}H-decoupling, as well as 2D NMR analysis (Cosy, HMBC, HSQC, HMQC (^{1}H-^{31}P)), and MS analysis. The exact structure of the evolution compound could not be elucidated until now, but efforts in this sense are still on the way.

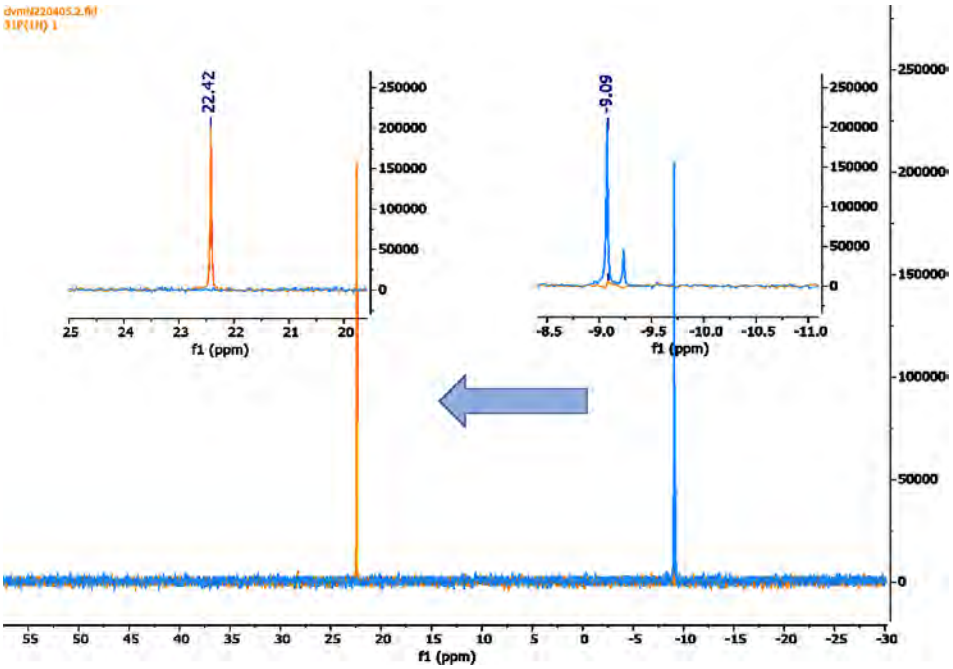

Figure 2.6. ^{31}P NMR spectra of **13** and its yet undetermined evolution product.

2.4.3. NMR characterization of **13** and **3b**

The hexaphenyl-*carbo*-1,4-dihydro-dithiodiphosphinine **13** is poorly soluble in most organic solvents, only allowing accurate characterization by ^{1}H and ^{31}P NMR spectroscopy in DCM solution. No consistent ^{13}C NMR spectrum could be recorded in solution, and **13** was thus characterized by solid state Magic Angle Spinning (MAS) NMR. The ^{1}H NMR spectrum in the 8.32–8.40 ppm and 8.26–8.30 ppm region, as well as the ^{31}P NMR spectrum giving a set of two singlets at -9.08 and -9.23 ppm indicate the presence of a mixture of *cis* and *trans* isomers, the *cis/trans* ratio being about 1:4.5 (**Figure 2.7a,b**).

The ^{31}P NMR spectrum of the model hexaphenyl-di(thiophosphinylethynyl)butatriene **3b** giving two singlets at 20.82 and 20.78 ppm indicates the presence of a mixture of *Z* and *E* isomers, the *Z/E* ratio being about 1:2 (**Figure 2.7 c,d**).

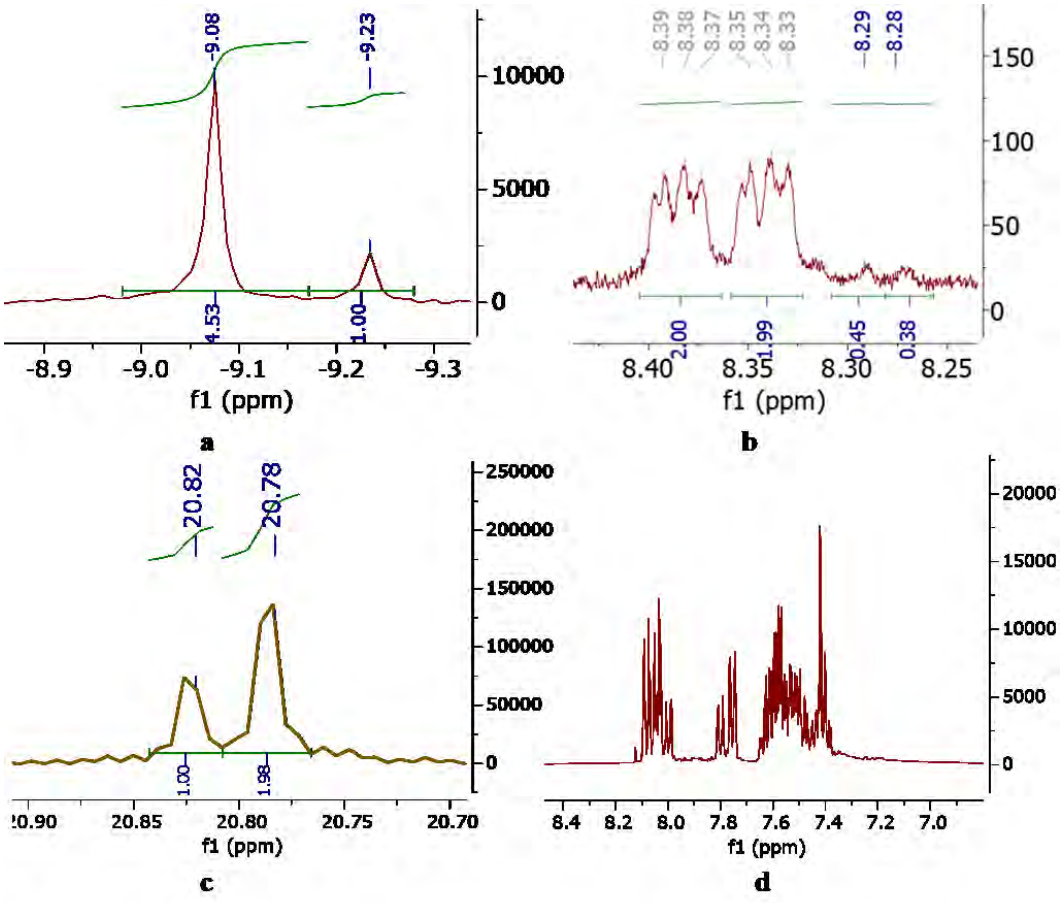

Figure 2.7. ^{31}P NMR spectrum (a) and 8.25-8.5 ppm region of the ^{1}H NMR spectrum (b) of **13** compared with ^{31}P NMR spectrum (c) and 7.3-8.2 ppm region of the ^{1}H NMR spectrum (d) of **3b**.

2.4.4. UV-VIS characterization of **13** and **3b**

The UV-vis absorption properties of **13** were investigated in DCM solution with a ε value of 28,800L· $mol^{-1}cm^{-1}$. Its absorption spectrum exhibits one main intense band at 438 nm with two shoulders at lower energies, making this band quite broad **(Figure 2.8)**. This spectral profile is comparable with that observed for the previously described *carbo*-dihydrobarrelene **15**,[19] having two dialkynylbutatriene motifs included in a C_{18} ring as in **13** (**Figure 2.8**). Though the two UV-vis spectra were not recorded in the same solvent, **13** being not soluble enough in $CHCl_3$ to allow using it, the 19 nm red shift of the maximum of absorption wavelength observed for **13** as compared to **15** can be explained by a more efficient π-delocalization through the P(S)Ph vertices in **13**. While the comparison was also done between **13** and the acylic butatriene model **3b**, the hexaphenyl-*carbo*-1,4-dihydro-dithio-1,4-diphosphinine **13**, which contains two butatriene motives, exhibits a blue shift of 35 nm in its UV-visible maximum absorption wavelength as compared to the monobutatriene model **3b,** for which the maximum absorption occurs at 473 nm, attributable to the main stereoisomer *E*-**3b** (~ 80 %), with a secondary broad band appearing as a pair of shoulders of the main band at 430-450 nm attributable to the minor stereoisomer *Z*-**3b** (~ 20 %). The blue shift to 430 ±10 nm is a priori consistent with a more efficient π-delocalization in the *cis*-configuration, enforced by the macrocycles of **13** and **15**, than in the *trans*-configuration of *E*-**3b**.

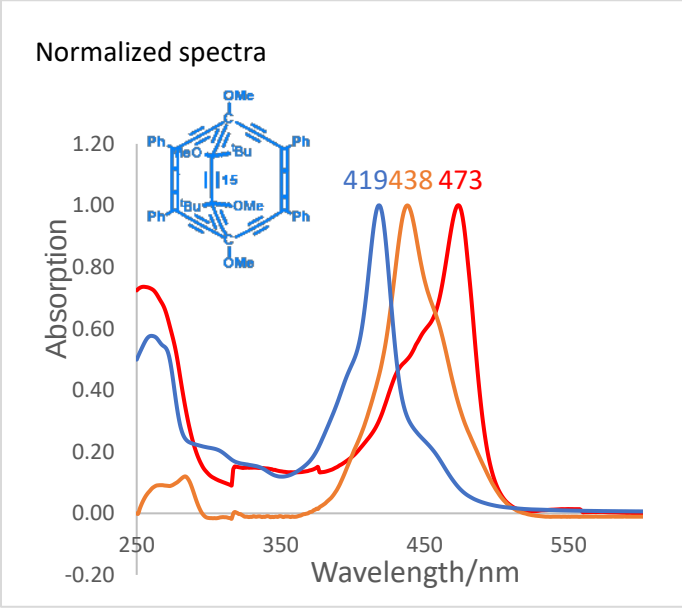

Figure 2.8. UV-vis absorption spectra of the hexaphenyl-*carbo*-1,4-dihydro-dithiodiphosphinine **13** and model **3b**, and partially reduced *carbo*-barrelene **15**.

2.4.5. Electrochemical behavior of **13** and **3b**

The electrochemical behavior of *carbo*-dihydro-1,4-dithiodiphosphinine **13** in DCM solutions was investigated using nBu$_4$NPF$_6$ as supporting electrolyte through cyclic and square-wave voltammetry with respect to a saturated calomel electrode (SCE) (**Figure 2.9**). As delineated in **Figure 2.10 ab**, cyclic voltammetry experiments show two reversible reductions at -0.57 and -0.70 V/SCE for **13** and one reversible reduction at -0.69 V/SCE for **3b**. Two other non-reversible reductions are also evidenced by square wave voltammetry at -1.15 and -1.42 V/SCE for **13** (**Figure 2.10 a**), and one at -1.006 V/SCE for **3b** (**Figure 2.10 b**). In contrast, the reduction potential of the model compound bis(3-methoxy-3,3-diphenylprop-1-yn-1-yl) (phenyl)phosphine, which contains a P(S)Ph motif, occurs at a very low potential of -2.17 V/SCE (**Figure 2.10 c**).

The two first reductions occur at quite high potentials as compared to the *carbo*-dihydro-barrelene **15** that displayed only two reductions at -1.11 and -1.28 V/SCE. The presence of two phosphorus atoms inside the macrocycle thus significantly affects the reduction behavior.

The compounds **13** and **3b**, both of which contain two P(S)Ph vertices, suggests that the reversible reductions at high potential of **13** and **3b** could correspond to a local reduction of butatriene motifs: only one is present in **3b** showing a single reversible reduction, while two are present in **13** showing two reversible reductions at close potentials.

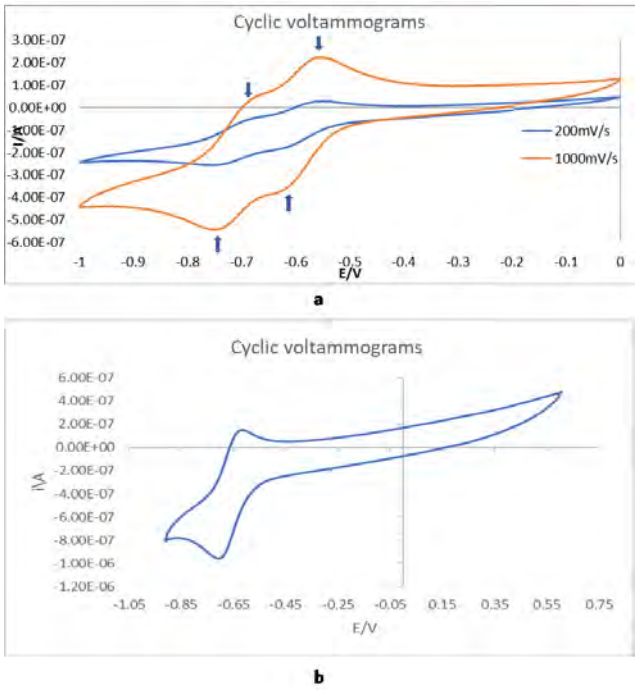

Figure 2.9. Cyclic voltammetry of the *carbo*-dihydro-dithiodiphosphinine **13** (a) and model **3b** (b),.

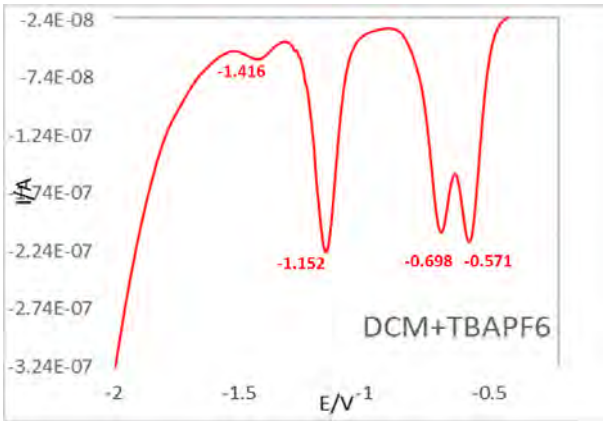

a

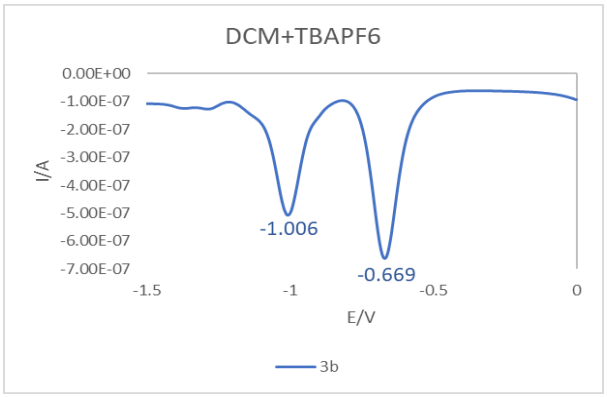

b

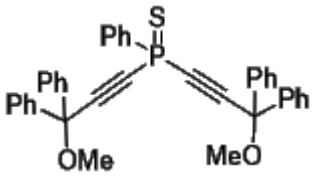

Model compound

Bis(3-methoxy-3,3-diphenylprop-1-yn-1-yl)(phenyl)phosphine

Reuction potential	**Position**	
01	-2.168	irreversible

c

Figure 2.10. Square wave voltammograms in reduction regime of the *carbo*-dihydro-dithiodiphosphinine **13** (a), half thereof **3b** (b) and comparision of its acyclic model **Bis(3-methoxy-3,3-diphenylprop-1-yn-1-yl)(phenyl)phosphine** (c).

While the first oxidation of both **13** (1.54 V/SCE) and **15** (1.58 V/SCE) occur at similar potentials, two oxidations are observed for **13**, the second one occurring at 1.72 V/SCE, none of them being reversible, as it is usually the case for *carbo*-mer molecules (**Figure 2.11 a**). By comparation with **3b** (1.509 V/SCE) (**Figure 2.11 b**), **13** is slightly less readily oxidized, possibly in line with its enhanced rigidity.

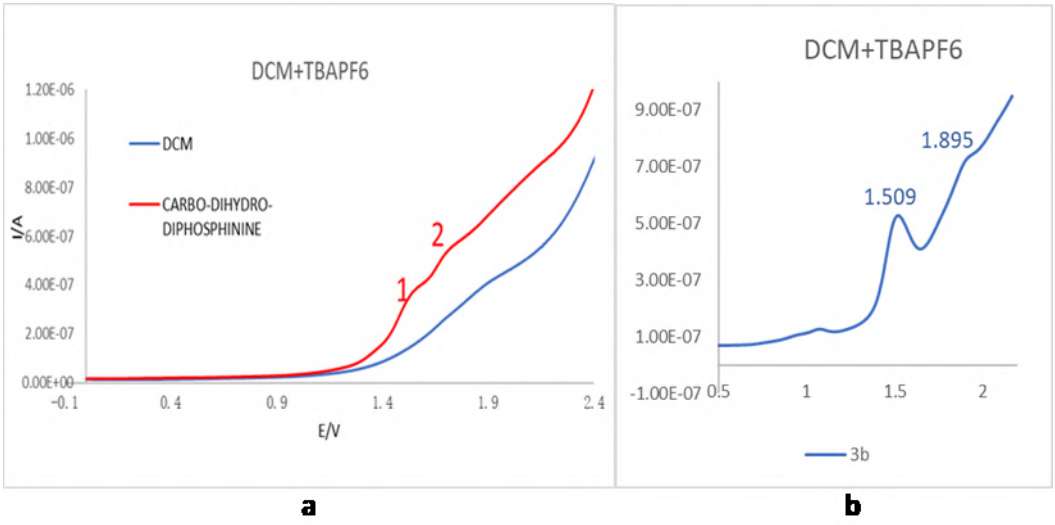

Figure 2.11. Square wave voltammetry in oxidation regime of the *carbo*-1,4-dihydro-1,4-dithiodiphosphinine 13 (a) and model molecule 3b (b).

2.4.6. X-ray diffraction of hexaphenyl-carbo-1,4-dihydro-1,4-dithiodiphosphinine

Single crystals of the *trans* isomer of the hexaphenyl-*carbo*-1,4-dihydro-dithiodiphosphinine **13** deposited from a DCM solution upon slow evaporation at room temperature and were analyzed by X-ray diffraction (**Figure 2.12**). In the crystal state, the macrocycle of **13** is almost planar, with a maximum deviation from the mean plane of 0.070 Å. The macrocycle does not exhibit a perfect hexagonal shape, and the distance between the opposite endpoints of the macrocycles are 8.03 Å and 8.44 Å for the C…C diagonals, 8.87 Å for the P…P diagonal. On the two butatriene edges, the Csp^2–Csp bond lengths are close to 1.35 Å, while the Csp–Csp bond lengths close to 1.25 Å. The Csp–Csp bonds of the phosphabutyne edges are significantly shorter, around 1.43 Å, while the P–Csp bonds are ca 1.76 Å long, the triplet bonds are ca 1.20 Å. All the angles at the Csp^2 vertices of the macrocycle are below 120°, those at the P atoms being the most closed at 103.15°. The angles between the C_{18} mean plane and the planes of the phenyl groups borne by C atoms are quite low, the maximum being 8.03°. The plane of the phenyl groups borne by the P atoms is almost perpendicular to the mean plane of the macrocycle, with an angle of 85.7°. In the crystal, the molecules are organized in two parallel interlocked columns slanted by 52.8° in which the mean planes of all the macrocycles are parallel.

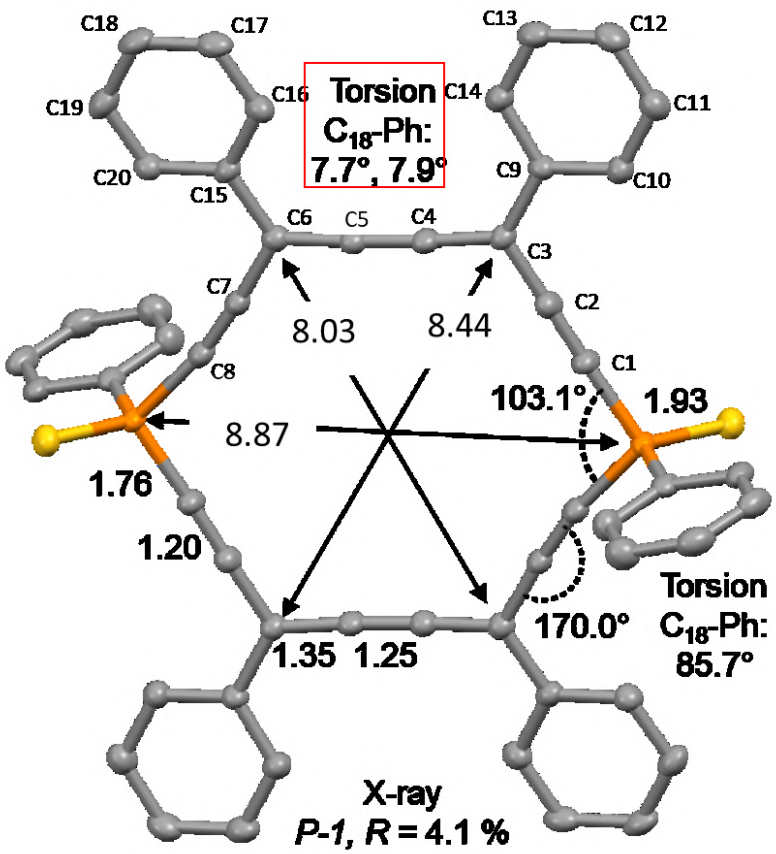

Figure 2.12. Molecular view of the X-ray crystal structure of the *trans* isomer of the *carbo*-dihydro-1,4-dithiodiphosphinine **13**.

2.4.7. Exploratory DFT calculations

2.4.7.1. Theoretical concern and context

Despite the prominent role of the phosphorus element in biochemistry at both the levels of structure (e.g. in nucleotides or phospholipids) and reactivity (e.g. in kinase-controlled phosphorylation events), by contrast to the wide occurrence of the pyridine ring, the phosphinine ring has not been found in Nature yet to the best of our knowledge. A natural explanation may reside in the fact that, contrary to most phosphines, phosphinines are quite reactive but not stabilized by P-oxidation due to their soft electrophilic character. Phosphinine P-oxides are indeed not known and perhaps not stable [20], while phosphinine P-sulfides are rare[21,22] and phosphinine P-selenides exemplified only once recently [23]just as phosphinine boranes[24] Even in lab, phosphinine

analogues of natural pyridine derivatives with possible biological properties (such as nicotine) have not attracted much attention.

A natural interest was however early focused on the analogy between pyridines and phosphinines by computational methods, regarding both their electronic structure and coordination chemistry [25–29].

In 2004 was reported a first theoretical comparison between phosphinine, pyridine and their respective ring *carbo*-mers using DFT-calculated structures and various indices to appraise basic electronic properties from the molecular orbitals and electron localization function (ELF), such as polarity (partition of ELF valence basins V(X) or V(X,Y) *vs* their population and size), polarizability (Pearson's hardness = HOMO-LUMO gap and relative localization), reactivity (HOMO/LUMO absolute energies and spatial localizations, bifurcation values of ELF localization domain) or aromaticity (ring planarity and bond length alternation, nucleus independent chemical shift at the ring center = NICS(0)) [30]. According to NICS(0) ratios, while phosphinine and pyridine are both *ca* 15 % less magnetically aromatic (NICS(0) = –17.5 ± 0.2 ppm) than benzene (NICS(0) =), their ring *carbo*-mers are just at most 5 % less magnetically aromatic (NICS(0) = –6.85 ± 0.05 ppm) than *carbo*-benzene (NICS(0) = -8.0 ppm). Nevertheless, *carbo*-phosphinine $PC_{17}H_5$ is as weakly nucleophilic as *carbo*-benzene $C_{18}H_6$ (V(P) and V(C,H) bifurcations at ELF = 0.67 ± 0.1) and much less than *carbo*-pyridine $NC_{17}H_5$ (V(N) bifurcation at ELF = 0.80).

To address the case of *carbo*-diphosphine and *carbo*-pyrazine counterparts, exploratory DFT calculations with the vacuum dielectric constant ($\varepsilon_r = 1$) were performed at the B3PW91/6-31G(d,p) level using the Firefly program v. 8.1.1[31,32] by Professor Remi CHAUVIN.

2.4.7.2. About model phosphinine, *carbo*-1,4-diphosphine, and their ring *carbo*-mers

To get preliminary insights into general trends of the structure of *carbo*-phosphinine $PC_{17}H_5$ *vs* the experimentally targeted *carbo*-1,4-diphosphinine $P_2C_{16}H_4$, static DFT calculations were carried out on both molecules and their respective parents, under C_{2v} or D_{2h} symmetry constraint. Selected results are listed in **Table 2.2**.

Table 2.2. Compared DFT-calculated nuclear and electronic structures of C_{2v}-symmetric phosphinine and *carbo*-phosphinine, and D_{2h}-symmetric 1,4-diphosphinine and *carbo*-1,4-diphosphinine. B3PW91/6-31G(d,p) level of calculation in the vacuum medium. Total energies are given without zero-point correction. Hardness: η = HOMO-LUMO gap.

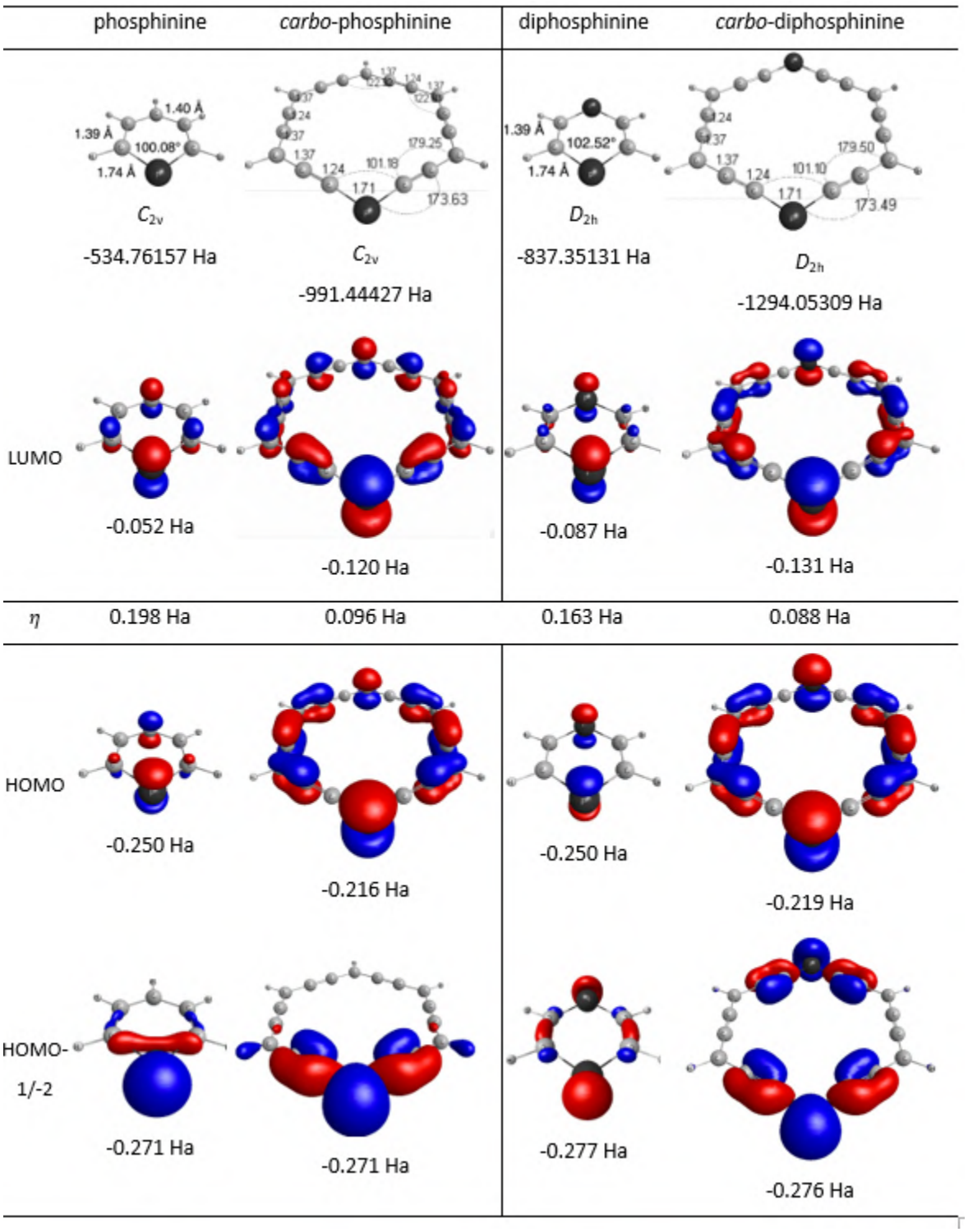

At first sight from **Table 2.2**, qualitative features of *carbo*-phosphinine are preserved in the experimentally targeted centrosymmetric *carbo*-diphosphinine counterpart.

In particular, while the HOMO and LUMO are concentrated on the P atoms in the parent phosphine (with a secondary component on the p-CH center) and diphosphinine, the HOMO and LUMO are spread out over the entire macrocycle in the corresponding ring *carbo*-mers.

In the four structures, the HOMO is π_z-oriented out-of-plane, as in benzene and *carbo*-benzene, while the in-plane P lone pairs occur in the HOMO-1 or HOMO-2. This is in contrast with the significantly harder pyridine and pyrazine (η = 0.229 Ha, 0.196 Ha), where the HOMO (–2.555 Ha, –2.252 Ha) is π_x-oriented in-plane and predicted to be less available for orbital overlap with sufficiently strong Lewis acids. The out-of-pane orientation of the HOMO is however restored in the *carbo*-mer series, i.e. in *carbo*-pyridine (η = 0.102 Ha) and *carbo*-pyrazine (η = 0.097 Ha) where the N lone pairs correspond to the HOMO-2 (-0.235 Ha) and HOMO-1 (-0.241 Ha) level, respectively, a situation similar to that of *carbo*-phosphinine and *carbo*-1,4-diphosphine.

The HOMO-LUMO gap is a primary quantitative descriptor of the electronic structure, which, at a strong approximation level, correlates with experimental observables such as the maximum absorption wavelength of electronic spectra. At the conceptual DFT level [33], the HOMO-LUMO gap is approximately proportional to molecular hardness η, defined as the second derivative of the total energy E vs the total number of electrons N at constant nuclear potential v, $\eta = c\,(\partial^2 E/\partial N^2)_v$ (c = 1/2, 1), which, for c = 1, is indeed approximated by the finite difference $\eta = \varepsilon_L - \varepsilon_H$, where ε_L and ε_H denote the LUMO ad HOMO energies, respectively, equivalent to the electron affinity and negative of the ionization potential of the Pearson's definition within the Koopmans' approximation.

From **Table 2.2**, it can been seen that *carbo*-diphosphinine (η = 0.088 a.u.) is ca 8 % softer than *carbo*-1,4-diphosphinine (η = 0.096 a.u.), and that the latter are twice softer than their parent diphosphinine (η = 0.163 a.u.) and phosphinine (η = 0.198 a.u.), respectively. This is consistent with expected effects: softness contamination by a second P atom, and increase of π-polarizability upon *carbo*-merization.

From a more conceptual standpoint, through their conclusive sentence "*hardness is a good indicator of the properties usually associated with aromatic character*", Paar *et al*. long proposed empirically that hardness can serve as a "quick" quantitative index of *energetic aromaticity*,[34] just as NICS serves as a "quick" quantitative index of *magnetic aromaticity* .

According the η index, the ring *carbo*-mers of phosphinine and 1,4-diphosphinine are thus twice less energetically aromatic than their respective parent, and *carbo*-1,4-diphosphinine is just

8% less energetically aromatic than *carbo*-phosphinine. Owing to the expected gain in synthesis efficiency for symmetric targets, *carbo*-1,4-diphosphinine targets could be regarded as reasonable objectives with the view to delineating experimental accessibility to the *carbo*-phosphinine family.

2.4.7.3. About hexaphenyl-*carbo*-1,4-dithio-1,4-dihydro-1,4-phosphinine **13**

The geometry of *trans*-**13** in the gas phase (ε_r = 1) has been optimized under C_i-symmetry constraint. In the calculated structure, the P_2C_{16} macrocycle is quasi-planar, with deviation from the mean plane in the range 0.006-0.070 Å (mean distance = 0.023 Å, standard deviation = (variance)$^{1/2}$ = 0.0224 Å), orthogonal to the P–Ph mean plane (dihedral angle = 89.98°), and slanted from the C–Ph means planes by 11.22-11.35°. Other geometrical data (bong lengths, bond angles) are depicted in **Figure 2.13**. As it can be seen by comparison to Figure the DFT-optimized structure of in the gas-phase reproduces quite satisfactorily the X-ray structure in the crystal state (**Figure 2.12**), a main difference being the irregularity of the hexagonal shape of the P_2C_{16} macrocycle. The P···P distance is however the greatest diagonal in both cases, just shrunken by 2 % in the gas phase (8.70 Å) with respect to the crystal phase (8.87 Å).

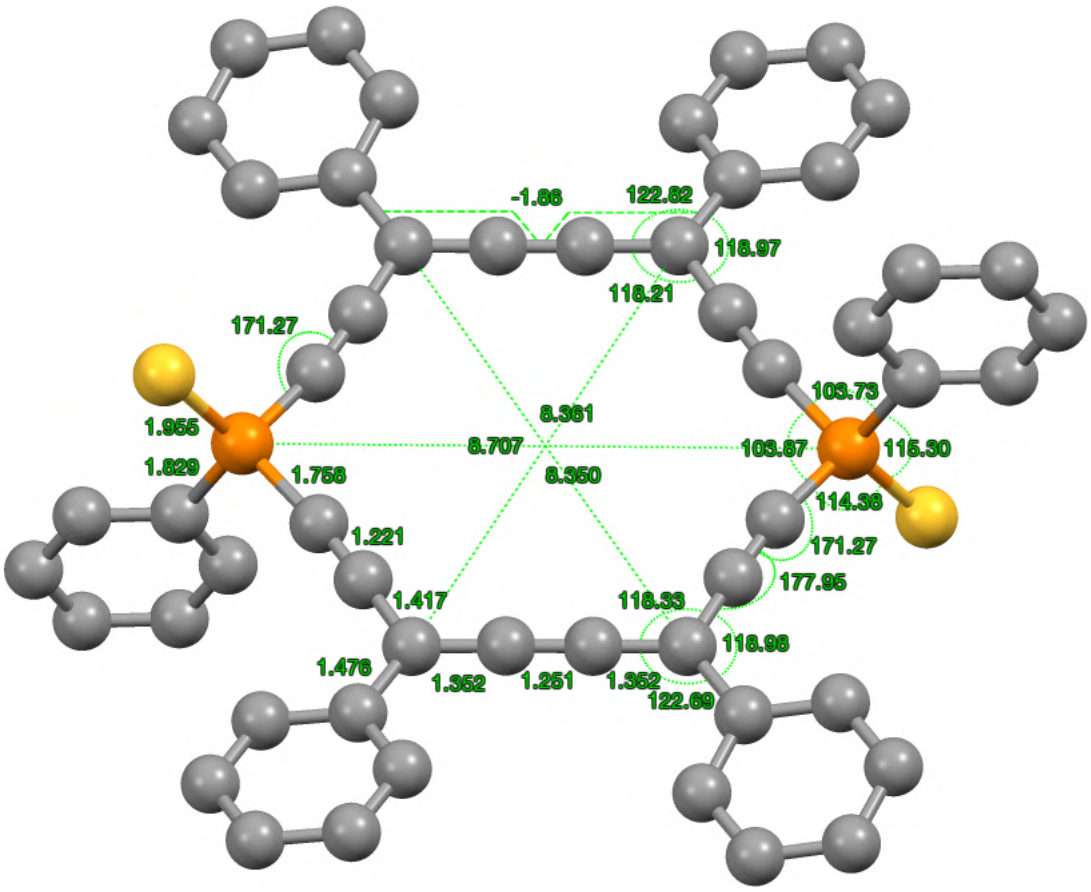

Figure 2.13. DFT-optimized structure of hexaphenyl-*carbo*-1,4-dihydro-1,4-dithiodiphosphinine *trans*-**13** in the gas phase (ε_r = 1) at the B3PW91/6-31G(d,p) calculation level, with final non-corrected energy components TOTAL = -3477.416524 a.u., NUCLEAR = 7134.122270 a.u., and ELECTRONIC = -10611.538793 a.u. Internuclear distances are given in Ångström, bond and dihedral angles in degrees. X-ray crystal structure in Figure 2.12.

The DFT frontier orbitals of *trans*-**13** are shown in **Figure 2.14**.

The four first frontier orbitals are located on the 16 C atoms of the P_2C_{16} macrocycle and are π_z-oriented out-of-plane, with a HOMO-LUMO gap of η = 0.85 a.u.

The occupied MOs featuring the P=S units are strongly localized and much deeper (HOMO-2/HOMO-5, in the range -0.233/-0.236 a.u.). The first in-plane π_{xy}-oriented MO, is the virtual LUMO+2/3 (-0.045 a.u.), involving the first contribution from the P OAs, also occurring in the degenerated LUMO+3/2 localized on the P–Ph units, and in the four next LUMO+n, n = 4-7.

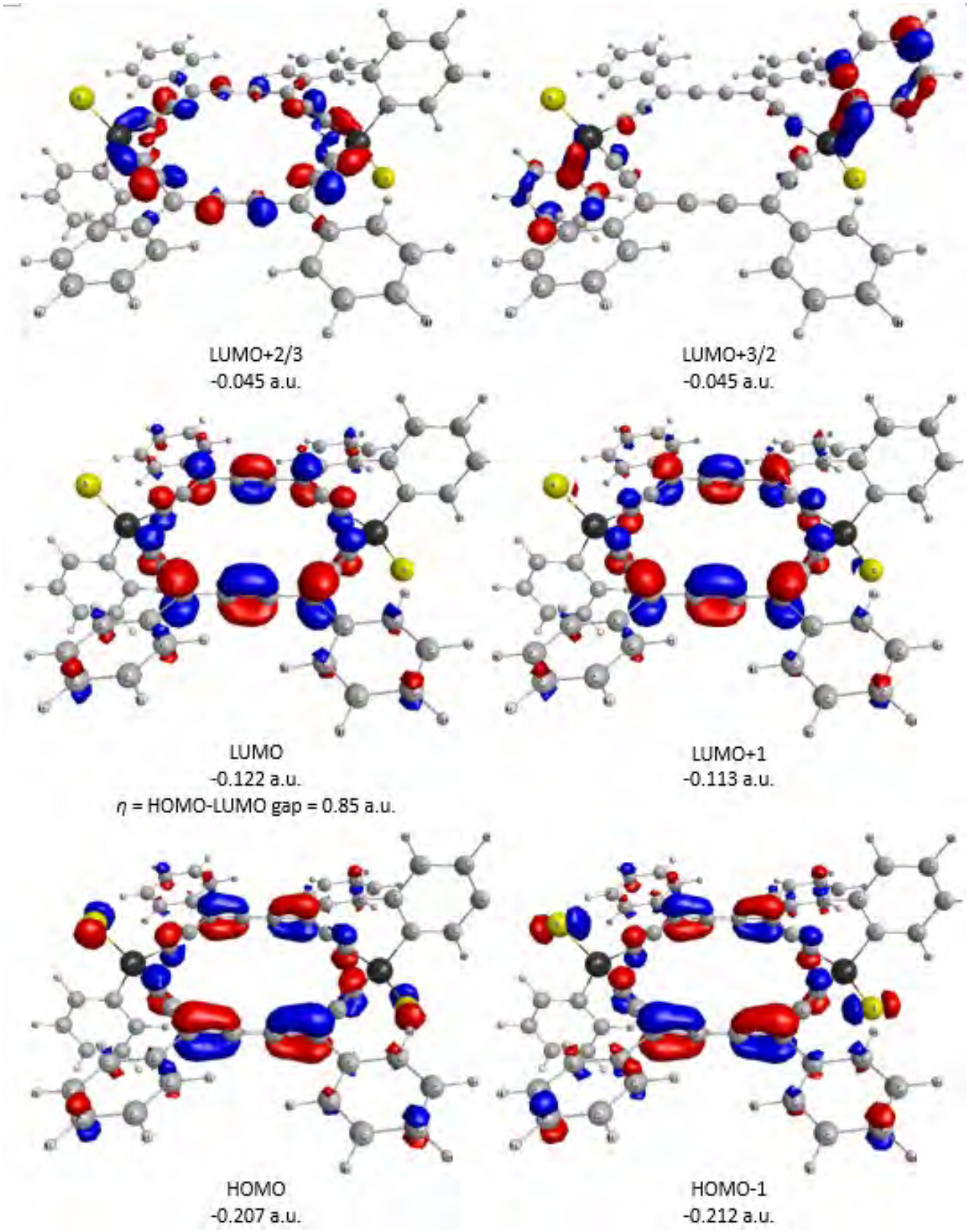
LUMO+2/3
-0.045 a.u.
LUMO+3/2
-0.045 a.u.
LUMO
-0.122 a.u.
η = HOMO-LUMO gap = 0.85 a.u.
LUMO+1
-0.113 a.u.
HOMO
-0.207 a.u.
HOMO-1
-0.212 a.u.

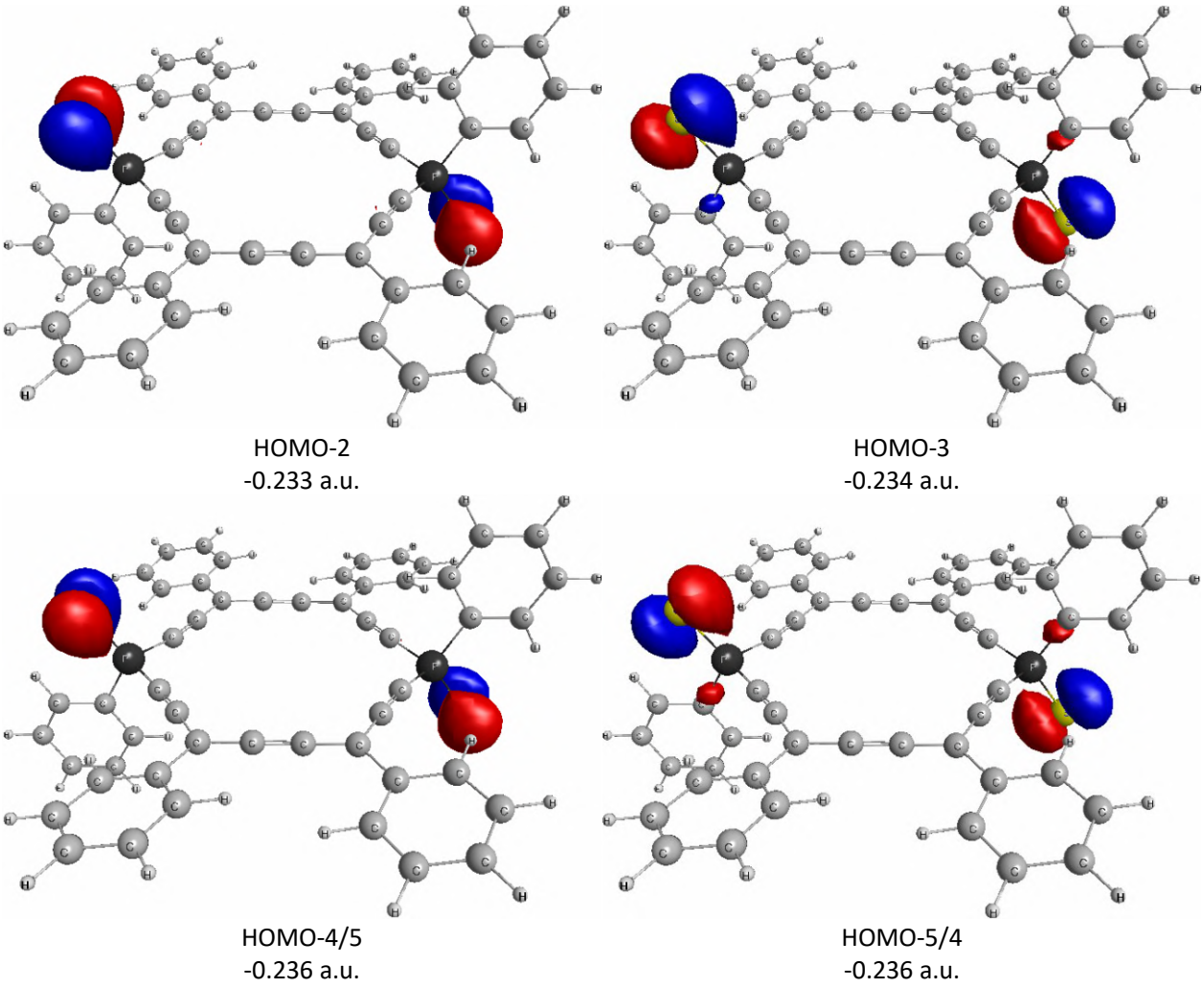

Figure 2.14. DFT frontier orbitals of hexaphenyl-*carbo*-1,4-dihydro-1,4-dithiodiphosphinine *trans*-**13** in the gas phase (ε_r = 1) at the B3PW91/6-31G(d,p) level of calculation, with final non-corrected energy components TOTAL = -3477.416524 a.u., NUCLEAR = 7134.122270 a.u., and ELECTRONIC = -10611.538793 a.u. (geometry in Figure 2.13).

From these data, one may anticipate that *trans*-**13** should not behave as an efficient S-nucleophile.

3. Conclusion

A first example of *carbo*-1,4-dihydro-1,4-dithio-1,4-diphosphinine and related macrocyclic *carbo*-diphosphacyclohexanes with different P-substituents and P-oxidation states were synthesized. Their preparation was achieved by a quite efficient and general method involving a

tetracomponent [8+1+8+1] macrocyclization process with up to 67 % yield. After a final reductive elimination step with $SnCl_2$/HCl, the hexaphenyl-*carbo*-1,4-dihydro-1,4-dithio-1,4-phosphinine was produced with 20 % yield and was fully characterized by NMR, HRMS, IR, UV, CV and SWvoltammetry, single crystal X-ray diffractometry.

4. Experimental Section

General remarks

THF and DCM were dried with a PureSolv-MD-5 Innovative Technology system for the purification of solvents. All other reagents were used as commercially available. In particular, commercial 2.5 M solutions of n-BuLi in hexane, 0.5 M solutions of HC_2MgBr (ethynylmagnesium bromide) in THF, 3.0 M solutions of EtMgBr in Et_2O, and 2.0 M solutions of hydrochloric acid in Et_2O were used. All reactions were carried out under nitrogen or argon using Schlenk tube and vacuum line techniques. Column chromatography was carried out with silica gel (60 P, 70–200 mm). Silica gel thin-layer chromatography plates (60F254; 0.25 mm) were developed by treatment with an ethanolic solution of phosphomolybdic acid (20%) or an aqueous potassium permanganate solution for fluorinated derivatives.

The following analytical instruments were used, ^1H and ^{13}C NMR: Avance 300, Avance 400, and Avance 400 HD spectrometers, 2D (^1H-^{13}C HSQC, ^1H-^{13}C HMBC): Avance 400 HD spectrometers; All the ^1H and ^{13}C signals were assigned according to chemical shifts, spin-spin coupling constants, splitting patterns, signal intensities, and 2D NMR experiments; All NMR spectra were recorded in $CDCl_3$ or CD_2Cl_2 solutions. NMR chemical shifts (δ) are given in ppm, with positive values to high frequency relative to the tetramethylsilane reference for ^1H and ^{13}C spectra, and ^{31}P spectra; coupling constants (J) are given in Hz. The symbols s, d, t, q and m refer to singlet, triplet, quadruplet and higher multiplet NMR signals, respectively, and can be associated for more complex coupling patterns. For compounds previously described in the literature, only ^1H NMR analysis was performed for purity control and the corresponding bibliographic references are given.

Mass spectra were recorded with a Quadrupolar Nermag R10–10H spectrometer.

UV spectra were recorded with a Perkin–Elmer UV/Vis Win-Lab Lambda 35 spectrometer with 1 cm quartz cell, UV-visible wave lengths λ are given in nm.

Voltammetric measurements were carried out with a potentiostat Autolab PGSTAT100 instrument controlled by GPES 4.09 software. Experiments were performed at room temperature in a homemade, air-tight, three-electrode cell connected to a vacuum/argon line. The reference electrode consisted of a saturated calomel electrode (SCE) separated from the solution by a bridge compartment. The counter electrode was a platinum wire of ca. 1 cm^2 apparent surface area. The working electrode was either a Pt microdisk (0.5 mm diameter) or a glassy carbon microdisk (1 mm diameter). The supporting electrolyte nBu$_4$NPF$_6$ (Fluka, 99% electrochemical grade) was used as received and simply degassed under argon. The DCM solvent was freshly distilled prior to use. Before each measurement, the solutions were degassed by bubbling Ar, and the working electrode was polished with a polishing machine (PresiP230). Typical instrumental parameters for recorded square-wave voltammograms were: SW frequency f = 20 Hz, SW amplitude Esw = 20 mV, and scan increment DE = 0.5 mV. All reported potentials are referenced to the formal potential of SCE.measured in the same electrolyte (ca. (0.45_0.02) V vs. SCE).

Experimental procedures and characterization

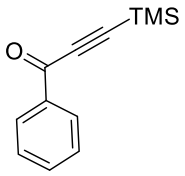

1-phenyl-1-trimethylsilyliprop-2-yn-1-one (1)

A solution of $AlCl_3$ (48 g, 160 mmol) in dry DCM (300 mL) was treated at 0°C with bis-trimethylsilylacetylene (60 g 352 mmol) then with benzoyl chloride (41 mL, 353 mmol) dropwise. The resulting mixture was stirred 15 min at 0°C and 18 h at room temperature (rt) before pooring the mixture into ice (400 g). After extractions with DCM, the combined organic layers were washed with brine, dried over $MgSO_4$ and concentrated under reduced pressure. Purification by distillation under reduced pressure afforded the expected compound as a paleyellow liquid (71 g, 351 mmol, quantitative yield).

^{1}H NMR (400 MHz, $CDCl_3$): δ 0.26 (8, 9H,), 7.38-7.44 (m, 2H) 7.50-7.54 (m, 1H), 8.06-8.10

(m, 2H).

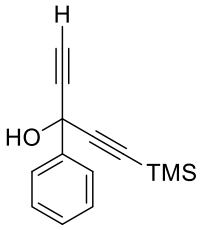

3-phenyl-1-(trimethylsilyl)penta-1,4- diyn-3-ol (2)

Pure **1** (6.036 g, 29.8 mmol) was treated neat at 0 °C with ethynylmagnesium bromide (0.5 M in Et_2O, 72 mL, 36 mmol). The resulting mixture was stirred at rt for 24 h. After treatment with a saturated aqueous solution of NH_4Cl and extractions with Et_2O, the combined organic layers were washed with brine, dried over $MgSO_4$, and concentrated under reduced pressure to afford the expected compound as a brown oil (6.85 g, 30.0 mmol, quantitative yield).

^1H NMR (400 MHz, $CDCl_3$): δ 0.21 (s, 9H), 2.74 (s, 1H,), 3.65 (s, 1H) 7.32-7.43 (m, 3H), 7.77-7.82 (m, 2H).

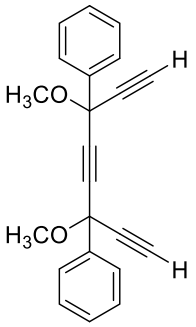

(3,6-dimethoxy-6-phenylocta-1.4.7-triyn-3-yl)benzene (3)

A solution of hexamethyldisilazane (14.0 mL, 67.1 mmol) in dry THF (100 mL) was treated at -78 °C with *n*-butyllithium (2.5 M in hexane, 26.0 mL, 65.0 mmol). The resulting mixture was stirred 30 min. at -78 °C, then a solution of **2** (6.59 g, 28.9 mmol) in dry THF (20 mL) was added at -78 °C. The resulting mixture was stirred at -78 °C, then pure **1** was added dropwise. The resulting mixture was allowed to warm up to rt over 18 h. After TLC control (disappearance of the diynol **2**: if not, let the reaction stirred at rt until complete consumption, and add more ketone **1** if necessary) methyl iodide (10.8 ml., 173.5 mmol) and dimethylsulfoxyde (4.50 mL, 63.4 mmol) were added at rt. The resulting mixture was stirred 18 h at rt before adding methanol (100 mL) and

K_2CO_3 (6.01g, 43.5 mmol) at rt. The resulting mixture was stirred 4 h at rt before addition of distilled water (50 mL) and filtration through a frit glass. Methanol was removed under reduced pressure, and after extractions with Et_2O, the combined organic layers were washed with brine, dried over anhydrous $MgSO_4$, and concentrated under reduced pressure Purification by silica gel chromatography (Pentane EtOAc: 95:5) afforded **3** as a yellow powder (7.52 g, 23.9 mmol, 83 %).
^{1}H NMR (300 MHz, $CDCl_3$) δ 7.87 – 7.73 (m, 4H), 7.45 – 7.34 (m, 6H), 3.58 (s, 6H), 2.81 (s, 2H).

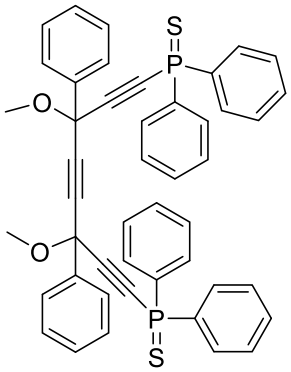

(3,6-dimethoxy-3,6-diphenylocta-1,4,7-triyne-1,8-diyl)bis(diphenylphosphine sulfide) (3a)

To a solution of **3** (682 mg, 2 mmol,) in 100 mL THF, under stirring at -78° C, was added dropwise LDA (1 M in THF; 4.2 mL, 4.2 mmol). After 3 h, $Ph_2P(S)Cl$ (1.4 mL, 6 mmol) was added, then the temperature was allowed to warm slowly up to rt overnight. After adding a saturated aqueous solution of NH_4Cl, after extractions with Et_2O, the combined organic layers were washed with brine, dried over anhydrous $MgSO_4$, and concentrated under reduced pressure and purification by a rapid chromatographic on silica gel with pentane and ethyl acetate 4:1, **3a** was isolated as a red-orange paste (0.872 g, 1.16 mmol, 58 %).

^{1}H NMR (300 MHz, $CDCl_3$) δ 7.98 – 7.88 (m, 8H), 7.79 – 7.74 (m, 4H), 7.52 – 7.37 (m, 18H), 3.59, 3.57 (2s, 6H).

^{31}P {^{1}H} NMR (121 MHz, $CDCl_3$) δ 20.37.

^{13}C NMR (75 MHz, $CDCl_3$) δ 138.2 (2d, J = 1.3 Hz), 133.1 (4d, J = 98.3 Hz), 132.2 (d, J = 3.2 Hz), 130.8 (d, J = 12.2 Hz), 129.6, 128.9, 128.8 (d, J = 13.8 Hz), 126.5, 102.4 (d, J = 20.6 Hz), 84.5 (2d, J = 9.1 Hz), 81.2 (d, J = 140.1 Hz), 72.4 (d, J = 2.9 Hz), 54.1.

HRMS (DCI-NH_3): *m/z* calculated for $C_{45}H_{36}OP_2S_2$ [M-OCH_3]: 715.1448, found 715.1443.

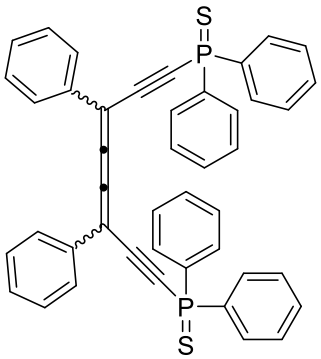

1,4-diphenyl-1,4-di(diphenyl-thiophosphinyl-ethynyl) butatriene (3b)

A solution of **3a** (0.134 mmol, 100 mg) in DCM (20 mL) was treated with anhydrous $SnCl_2$ (5 equiv, 120 mg, 0.67 mmol) and HCl (10 equiv, 0.6 mL, 2 mmol, 2 M in Et_2O) at -78 °C. The mixture was stirred at -78 °C for 30 min and then at rt for 3 h. After treatment with 1 M aqueous NaOH (10 equiv, 1.2 mL), and filtration through Celite®, the organic layer was separated, washed with brine (3x), dried over $MgSO_4$, and concentrated to dryness under reduced pressure. The residue was purified by chromatography on silica gel (Pentane/DCM:1/1) to give **3b** as a bright orange solid (21 mg, 0.03 mmol, 23 % yield).

^{1}H NMR (400 MHz, CD_2Cl_2) δ 8.09 – 7.99 (m, 7H), 7.81 – 7.74 (m, 4H), 7.63 – 7.38 (m, 19H).

^{31}P NMR (162 MHz, CD_2Cl_2) δ 20.82, 20.78.

^{13}C NMR (101 MHz, CD_2Cl_2) δ 150.5， 134.6 (d, *J* = 1.1 Hz), 133.5 (d, *J* = 98.6 Hz, *trans*), 133.3 (d, *J* = 98.6 Hz, *cis*),132.1 (d, *J* = 3.3 Hz, *trans*), 132.2 (d, *J* = 3.5 Hz, *cis*), 130.8 (d, *J* = 12.4 Hz, *trans*), 130.8 (d, *J* = 12.4 Hz, *cis*), 130.2 (*trans*), 130.1 (*cis*), 129.1 (*cis*), 129.0 (*trans*), 128.8 (d, *J* = 13.9 Hz), 127.6 (*cis*), 127.3 (*trans*), 104.9 (d, *J* = 7.2 Hz, *trans*), 104.9 (d, *J* = 7.2 Hz, *cis*), 101.7 (d, *J* = 23.3 Hz), 91.8 (d, *J* = 143.7 Hz, *trans*), 91.4 (d, *J* = 141.9 Hz, *cis*).

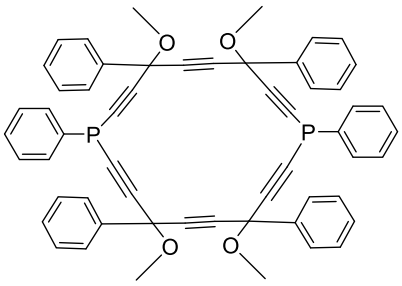

4,7,13,16-tetramethoxy-1,4,7,10,13,16-hexaphenyl-1,10-diphosphacyclooctadeca-

2,5,8,11,14,17-hexayne (4).

Pure**3** (943 mg, 3 mmol) in 200 mL THF, at -78° C, was added dropwise LDA (1 M, 6.5 mL, 6.5 mmol), under magnetic stirring. After 3 h, $PhPCl_2$ (0.42 mL, 3 mmol) was added, then the temperature was allowed to warm slowly up to room temperature overnight. After adding a saturated aqueous solution of NH_4Cl, after extractions with Et_2O, the combined organic layers were washed with brine, dried over anhydrous $MgSO_4$, evaporation of solvents and a rapid chromatographic purification on silica gel with pentane and diethyl acetate 15:1, **4** was isolated as a slightly yellow paste, (0.503 g, 0.59 mmol, 40 %). The product gives a brown spot in TLC after revealing with phosphomolybdic acid (pentane/ethyl acetate 5:1).

^{1}H NMR (400 MHz, $CDCl_3$) δ 7.92 – 7.63 (m, 12H), 7.53 – 7.24 (m, 18H), 3.75 – 3.37 (m, 12H).

^{31}P {^{1}H} NMR (121 MHz, $CDCl_3$) δ -63.3– -66.11 (m).

^{13}C NMR (75 MHz, $CDCl_3$) δ 139.4-139.1 (m), 132.8– 132.4 (m), 131.8 – 131.5 (one part of this dm is hidden) 130.2 – 129.9 (m), 129.2-128.4 (m), 126.6-126.5 (m), 103.8-103.0 (m), 84.7-84.2 (m), 82.0-81.5 (m), 72.5-72.4(m), 53.7 – 53.4 (m).

HRMS (MALDI-TOF/DCTB): *m/z* calculated for $C_{56}H_{43}O_4P_2$ $[M+H]^+$: 841.2558, found 840.2518.

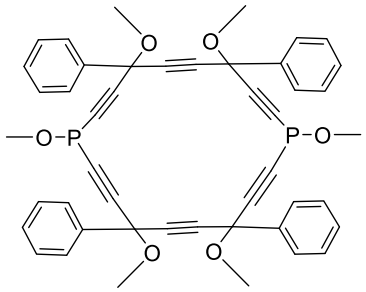

1,4,7,10,13,16-hexamethoxy-4,7,13,16-tetraphenyl-1,10-diphosphacyclooctadeca-2,5,8,11,14,17-hexayne (5).

To a solution of **3** (942 mg, 3 mmol) in 200 mL THF, was added dropwise at -78° C LDA (1 M, 6.5 mL, 6.5 mmol) under magnetic stirring. After 3 h, $P(OMe)Cl_2$ (0.304 mL, 3 mmol) was added, then the temperature was allowed to warm slowly up to room temperature overnight. After extractions with Et_2O, the combined organic layers were washed with brine, dried over anhydrous $MgSO_4$, evaporation of solvents and a rapid chromatographic purification on silica gel eluting with pentane/ethyl acetate 23:2, **4** was isolated as a pale yellow paste, (50 mg, 0.067 mmol, 5 %). The

product gives a brown spot on the TLC after revealing with phosphomolybdic acid (pentane/ethyl acetate 7:1).

^{1}H NMR (400 MHz, $CDCl_3$) δ 7.81 – 7.67 (m, 8H), 7.47 – 7.30 (m, 12H), 3.89 – 3.65(m, 6H), 3.63 – 3.39 (m, 12H).

^{31}P {^{1}H} NMR (162 MHz, $CDCl_3$) δ 49.1 – 47.4 (m).

^{13}C NMR (101 MHz, $CDCl_3$) δ 139.1-138.6 (m), 129.8-129.5 (m), 129.4-129.1 (m), 128.9-128.5 (m), 126.5-126.3 (m), 105.7-104.9 (m), 84.8-83.4 (m), 72.5-71.2 (m), 57.7-57.2 (m), 54.1-53.3 (m).

HRMS (MALDI-TOF/DCTB): *m/z*: calculated for $C_{46}H_{39}O_6P_2$ $[M+H]^+$: 749.2222, found 749.2193.

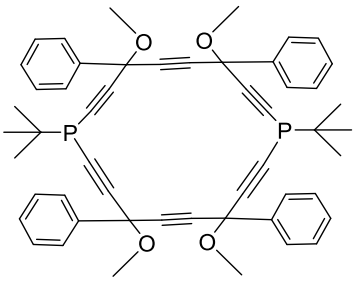

1,10-di-tert-butyl-4,7,13,16-tetramethoxy-4,7,13,16-tetraphenyl-1,10-diphosphacyclooctadeca-2,5,8,11,14,17-hexayne (6).

To a solution of **3** (942 mg, 3 mmol) in 200 mL THF, was added dropwise at -78° C, LDA (1 M, 6.5 mL, 6.5 mmol) under magnetic stirring. After 3 h, *t*-$BuPCl_2$ (1 M, 3.3 mL, 3.3 mmol) was added, then the temperature was allowed to warm slowly up to room temperature overnight. After treatment with a saturated aqueous solution of NH_4Cl, after extractions with Et_2O, the combined organic layers were washed with brine, dried over anhydrous $MgSO_4$, evaporation of solvents and a chromatographic purification on silica gel eluting with pentane/ethyl acetate 15:1, **6** was isolated as a slightly yellow paste (70 mg, 0.087 mmol, 6 %). The product **6** gives a brown spot on TLC after revealing with phosphomolybdic acid (pentane/ethyl acetate 9:1). R_f: 0.56.

^{1}H NMR (400 MHz, $CDCl_3$) δ 7.80 – 7.70 (m, 8H), 7.42 – 7.33 (m, 12H), 3.67 – 3.40 (m, 12H), 1.41 – 1.10 (m, 18H).

^{31}P {^{1}H} NMR (162 MHz, $CDCl_3$) δ -38.65-41.53 (m).

^{13}C NMR (101 MHz, $CDCl_3$) δ 139.7 – 139.2 (m), 129.1 – 128. 9 (m), 128.5 – 128.4 (m), 126.5 – 126.3 (m), 102.3 – 101.8 (m), 84.6-84.3 (m), 82.4-81.4 (m), 72.5-72.4 (m), 53.6 – 53.3 (m),

33.0-32.2 (m), 27.5 – 27.1 (m).

HRMS (MALDI-TOF/DCTB): *m/z*:: calculated for $C_{52}H_{51}O_4P_2$ $[M+H]^+$: 801.3163, found 801.3281.

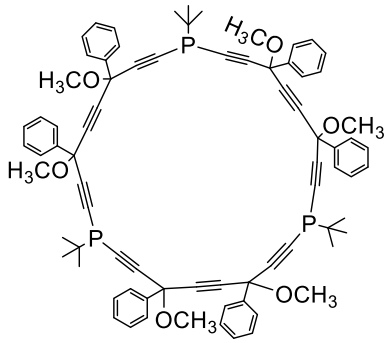

1,10,19-tri-tert-butyl-4,7,13,16,22,25-hexamethoxy-4,7,13,16,22,25-hexaphenyl-1,10,19-triphosphacycloheptacosa-2,5,8,11,14,17,20,23,26-nonayne(7)

The product **7** was isolated as side-product during the synthesis of **6**. It was isolated by silica gel chromatographic purification eluting with pentane/ethyl acetate 15:1, as a slightly yellow paste (30 mg, 0.025 mmol, 3 %). The product **7** gives a brown spot on TLC after revealing with phosphomolybdic acid (pentane/ethyl acetate 9:1). R_f: 0.18.

^{1}H NMR (400 MHz, $CDCl_3$) δ 7.79 – 7.72 (m, 12H), 7.41 – 7.32 (m, 18H), 3.58 – 3.47 (m, 18H), 1.32 – 1.17 (m, 27H).

^{31}P {^{1}H} NMR (162 MHz, $CDCl_3$) δ -39.64 – -40.76 (m).

^{13}C NMR (101 MHz, $CDCl_3$) δ 139.7 – 139.3 (m), 129.0 (m), 128.5 (m), 126.5 – 126.4 (m), 102.6 – 102.0 (m), 84.4 (m), 82.0– 81.3 (m), 72.4 (m), 53.5 (m), 32.7 (m), 27.4-27.2 (m).

HRMS (MALDI-TOF/DCTB): *m/z*: calculated for $C_{78}H_{76}O_6P_3$ $[M+H]^+$: 1201.4855, found 1201.4901

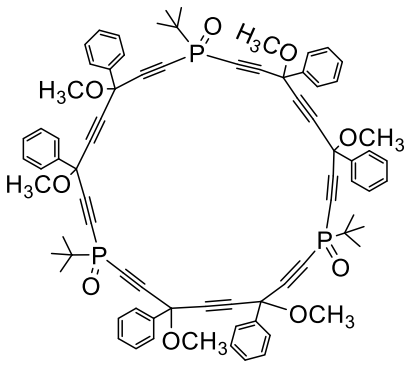

.

1,10,19-tri-tert-butyl-4,7,13,16,22,25-hexamethoxy-4,7,13,16,22,25-hexaphenyl-1,10,19-triphosphacycloheptacosa-2,5,8,11,14,17,20,23,26-nonayne 1,10,19-trioxide (8).

The product **8** was isolated as side-product during the synthesis of **6**. It was isolated by silica gel chromatography eluting with pentane/ethyl acetate 15:1, as a slightly yellow paste, (15 mg, 0.012 mmol, 1 %). The product **8** gives a brown spot on TLC after revealing with phosphomolybdic acid in TLC (pentane/ethyl acetate 9:1). R_f:0.09.

^{1}H NMR (400 MHz, $CDCl_3$) δ 7.76 – 7.64 (m, 12H), 7.45 – 7.36 (m, 18H), 3.71 – 3.38 (m, 18H), 1.40 – 1.08 (m, 27H).

^{31}P {^{1}H} NMR (162 MHz, $CDCl_3$) δ 6.76 – 6.19 (m).

HRMS (MALDI-TOF/DCTB):m/z calculated for $C_{78}H_{76}O_9P_3$[M+H]: 1249.4702, found 1249.4819.

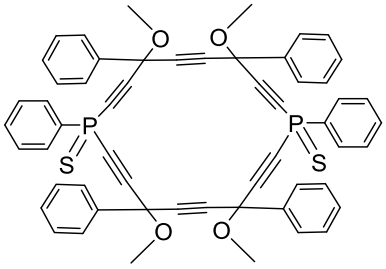

4,7,13,16-tetramethoxy-1,4,7,10,13,16-hexaphenyl-1,10-diphosphacyclooctadeca-2,5,8,11,14,17-hexayne 1,10-disulfide (9).

Method 1: To a solution of **4**（252 mg, 0.3 mmol）in the dry THF (10 mL), was added S_8（32 mg, 1 mmol) at room temperature. After stirring for 57 h, distilled water (50 mL) was added and the mixture was filtrated and concentrated under reduced pressure. The residue was purified by silica gel chromatography eluting with pentane/EtOAc 21:4, to give **9** as a slightly orange solid

(100 mg, 0.11 mmol, 37 %).

Method 2:

To a solution of triyne **3** (1.410 g, 4.5 mmol) in 400 mL of dry THF was added dropwise at -78 °C LDA (1 M, 9.8 mL, 9.8 mmol) under magnetic stirring. After 2.5 h, $PhSPCl_2$ (0.675 mL, 4.5 mmol) was added, then the mixture was slowly warmed to rt and stirring was maintained overnight. After treatment with a saturated aqueous NH_4Cl solution, the aqueous layer was extracted with ethyl acetate. The combined organic layers are dried over $MgSO_4$, filtrated and concentrated under reduced pressure. The residue was purified by silica gel chromatography eluting with pentane/EtOAc 21:4, to give **9** as a slightly orange solid (915 mg, 1.01 mmol, 67 %).

^{1}H NMR (400 MHz, $CDCl_3$) δ 8.22 – 7.85 (m, 4H), 7.77 – 7.54 (m, 12H), 7.49 – 7.28 (m, 14H), 3.75 – 3.28 (m, 12H).

$^{31}P\{^1H\}$ NMR (162 MHz, $CDCl_3$) δ -9.97 –-10.47 (m).

^{13}C NMR (101 MHz, $CDCl_3$) δ 138.8-137.1(m), 132.9(m), 130.5-130.3(m),129.8-129.6(m), 129.1-128.6 (m), 126.6-126.3(m), 100.8-100.3(m), 84.4-84.0 (m), 81.8-81.4(m), 80.1-79.7(m), 53.6-53.5(m), 54.3-54.2(m).

HRMS (DCl-CH_4) *m/z* calculated for $C_{56}H_{43}O_4S_2P_2$ $[M+H]^+$: 905.2078, found: 905.2121.

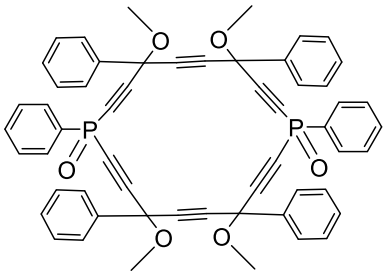

4,7,13,16-tetramethoxy-1,4,7,10,13,16-hexaphenyl-1,10-diphosphacyclooctadeca-2,5,8,11,14,17-hexayne 1,10-dioxide (10).

To a solution of **4** （84 mg 0.1 mmol in dry THF (10 mL), was added at 0° C H_2O_2（30%aq，0.25 mL), The stirring was maintained for 0.5 h at this temperature and then for 2 h at Rt before addition of distilled water (50 mL) and filtration through frit glass. The THF was removed under reduced pressure, and after extractions with Et_2O, the combined organic layers were washed with brine, dried over anhydrous $MgSO_4$ and concentrated under reduced pressure. Purification by silica gel chromatography (Pentane/ethyl acetate 4:1) afforded the expected compound as a pale yellow paste (87 mg, 0.1 mmol, quantitative yield).

^{1}H NMR (300 MHz, $CDCl_3$) δ 8.11 – 7.51 (m,16H), 7.49 – 7.26 (m, 14H), 3.75 – 3.29 (m,

12H).

^{31}P {^{1}H} NMR (121 MHz, $CDCl_3$) δ -20.00 – -20.74 (m).

^{13}C NMR (75 MHz, $CDCl_3$) δ 137.9 – 137.4 (m), 136.4 (dm, J= 97.5 Hz), 133.7 – 133.3 (m), 130.3 (dm, J = 12.9 Hz), 129.9-129.6 (m), 129.4-128.7 (m), 126.5 – 126.2 (m), 101.5-100.7 (m), 83.3 (dm, $J \approx$ 148.1 Hz), 79.9-79.3 (m), 72.2(m), 54.3 – 53.4 (m).

HRMS(MALDI-TOF/DCTB): m/z calculated for $C_{56}H_{43}O_6P_2[M+H]^+$: 873.2535, found 873.2568.

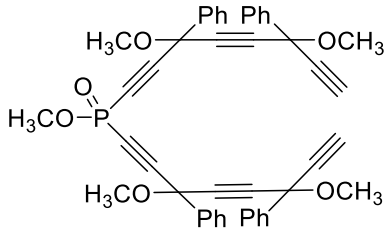

Methyl bis(3,6-dimethoxy-3,6-diphenylocta-1,4,7-triyn-1-yl) phosphinate (11)

To triyne **3** (3 mmol, 942 mg) in 200 mL of dry THF was added dropwise at -78 °C LDA (1 M, 6.2 mL, 6.2 mmol) under magnetic stirring. After 2.5 h, $OP(OMe)Cl_2$ (0.3 mL, 3 mmol) was added, then the mixture was slowly warmed to rt and stirring was maintained overnight. After treatment with a saturated aqueous NH_4Cl solution, the aqueous layer was extracted with ethyl acetate. The combined organic layers were dried over $MgSO_4$, filtrated and concentrated under reduced pressure. The residue was purified by silica gel chromatography eluting with pentane/EtOAc 4:1, R_f:0.4, to give **11** as a slightly yellow paste (180 mg,0.26 mmol, 17 %).

^{1}H NMR (400 MHz, $CDCl_3$) δ 7.87 – 7.58 (m, 8H), 7.39 (s, 12H), 3.88 – 3.74 (m, 3H), 3.56 (d, J = 11.4 Hz, 12H), 2.87 – 2.78 (m, 2H).

^{31}P NMR (162 MHz, $CDCl_3$) δ -19.86 (q, J = 13.8 Hz)MS: [M+H]: calculated for $C_{45}H_{38}O_6P$: 705.2, found 705.2.

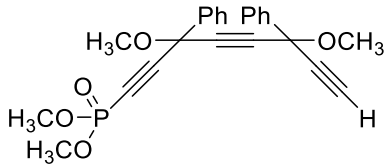

Dimethyl (3,6-dimethoxy-3,6-diphenylocta-1,4,7-triyn-1-yl)phosphonate (12)

The product **12** was isolated upon purification of the product **11**. The residue was purified by silica gel chromatography eluting with pentane/EtOAc 4:1 R_f: 0.2, to give **12** as a slightly yellow paste in (126.5 mg, 0.3 mmol, 11 %).

^{1}H NMR (400 MHz, $CDCl_3$) δ 7.79 – 7.72 (m, 4H), 7.46-7.37 (m, 6H), 3.81 (d, J = 12.2 Hz, 6H), 3.58 and 3.57 (2s, 6H), 2.84 (s, 1H).

^{31}P NMR (162 MHz, $CDCl_3$) δ -4.58 (hept, J = 12.4 Hz).

^{13}C NMR (101 MHz, $CDCl_3$) δ 139.3, 138.1, 129.5, 129.1, 128.7, 128.5, 126.4 (2s), 97.1 (d, J = 48.3 Hz), 86.3 (2s), 82.3 (2s), 80.3, 75.7, 74.9 (d, J = 291.8 Hz), 72.0 (d, J = 4.4 Hz), 71.7, 53.6 (d, J = 44.9 Hz), 53.6 (2s)

MS: [M+H]: calculated for $C_{24}H_{24}O_5P$: 423.1, found : 423.1.

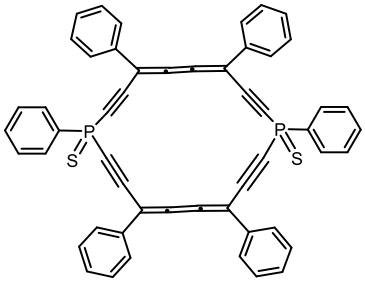

***Carbo*-1,4-dihydro-1,4-dithiodiphosphinine (13)**

A solution of **14** (50 mg, 0.055 mmol) in DCM (10 mL) was treated with anhydrous $SnCl_2$ (10 equiv, 104 mg, 0.55 mmol) and HCl (20 equiv, 2 M in Et_2O, 0.5 mL, 2 mmol) at -78 °C. The mixture was stirred at -78 °C for 0.5 h and then at room temperature for 3 h. After treatment with 1 M aqueous NaOH (20 equiv, 1 mL), and filtration through Celite®, the organic layer was separated, washed with brine (3x), dried over $MgSO_4$, and concentrated to dryness under reduced pressure. The residue was purified by chromatography on silica gel (Pentane/DCM:1/1) to give **12** as a bright orange solid (10 mg, 0.013 mmol, 21 % yield).

^{1}H NMR (400 MHz, CD_2Cl_2) δ 8.41 – 8.36 (m, 2H), 8.36 – 8.32 (m, 2H), 7.78 – 7.69 (m, 13H), 7.54 – 7.39 (m, 13H),

^{31}P {^{1}H} NMR (121 MHz, CD_2Cl_2) δ -9.08, -9.24.

^{13}C MAS NMR δ 147.3, 131.0, 126.3, 102.6, 99.0.

HRMS (MALDI-TOF DCTB + NaI matrix): m/z calculated for $C_{52}H_{30}NaP_2S_2$ [M+Na]: 803.1162, found: 803.1202.

References

(1) Märkl, G. 2,4,6-Triphenylphosphabenzene. *Angewandte Chemie International Editi on in English* **1966**, *5* (9), 846–847. https://doi.org/10.1002/anie.196608463.

(2) Ashe, A. J. I.; Gordon, M. D. Bismabenzene. Reaction of Group V Heteroaromatic Compounds with Hexafluorobutyne. *J. Am. Chem. Soc.* **1972**, *94* (21), 7596–7597. https://do i.org/10.1021/ja00776a063.

(3) Kobayashi, Y.; Kumadaki, I.; Ohsawa, A.; Hamana, H. 2,3,5,6-Tetrakis (Trifluorom ethyl)-1,4-Diphosphabenzene. *Tetrahedron Letters* **1976**, *17* (41), 3715–3716. https://doi.org /10.1016/S0040-4039(00)93089-2.

(4) Bieger, K.; Heckmann, G.; Fluck, E.; Weller, F.; Peters, K.; Peters, E.-M. 1,4-Dihyd ro-1λ5,4λ5-[1,4]Diphosphinine Und Ein 1,4-Dihydro-1λ3,4λ3-[1,4]Diphosphinin. *Zeitschrift für anorganische und allgemeine Chemie* **1995**, *621* (12), 1981–1988. https://doi.org/10.100 2/zaac.19956211202.

(5) Savateev, A.; Vlasenko, Y.; Shtil, N.; Kostyuk, A. Reduction of Λ5-Phosphinines. *E uropean Journal of Inorganic Chemistry* **2016**, *2016* (5), 628–632. https://doi.org/10.1002/ej ic.201500856.

(6) Lepetit, C.; Peyrou, V.; Chauvin, R. Ring Carbo-Mers of "Aromatic" Heterocycles. *Phys. Chem. Chem. Phys.* **2004**, *6* (2), 303–309. https://doi.org/10.1039/B311790A.

(7) Nyulászi, L. Aromaticity of Phosphorus Heterocycles. *Chem. Rev.* **2001**, *101* (5), 12 29–1246. https://doi.org/10.1021/cr990321x.

(8) J. Newland, R.; F. Wyatt, M.; L. Wingad, R.; M. Mansell, S. A Ruthenium(Ii) Bis(P hosphinophosphinine) Complex as a Precatalyst for Transfer-Hydrogenation and Hydrogen-Borrowing Reactions. *Dalton Transactions* **2017**, *46* (19), 6172–6176. https://doi.org/10.103 9/C7DT01022B.

(9) Märkl, G.; Dörges, C. 2,4,6-Triaryl-1,3,5λ3-Diazaphosphinines. *Angewandte Chemi e International Edition in English* **1991**, *30* (1), 106–107. https://doi.org/10.1002/anie.19910 1061.

(10) Clochard, M.; Grundy, J.; Donnadieu, B.; Mathey, F. A Straightforward Synthesis o f 3-Acylphospholes. *Org. Lett.* **2005**, *7* (20), 4511–4513. https://doi.org/10.1021/ol051816d.

(11) Müller, C.; Broeckx, L. E. E.; de Krom, I.; Weemers, J. J. M. Developments in the

Coordination Chemistry of Phosphinines. *European Journal of Inorganic Chemistry* **2013**, *2013* (2), 187–202. https://doi.org/10.1002/ejic.201200912.

(12) Tokarz, P.; Zagórski, P. M. Phosphinine – Synthesis of a Heavy Sibling of Pyridine (Microreview). *Chem Heterocycl Comp* **2017**, *53* (8), 858–860. https://doi.org/10.1007/s10593-017-2138-1.

(13) Märkl, G.; Sejpka, H.; Dietl, S.; Nuber, B.; Ziegler, M. L. 1-Phospha-1,2,3-Butatriene. *Angewandte Chemie* **1986**, *98* (11), 1020–1021. https://doi.org/10.1002/ange.19860981124.

(14) Maurette, L.; Tedeschi, C.; Sermot, E.; Soleilhavoup, M.; Hussain, F.; Donnadieu, B.; Chauvin, R. Synthesis and Stereochemical Resolution of Functional [5]Pericyclynes. *Tetrahedron* **2004**, *60* (44), 10077–10098. https://doi.org/10.1016/j.tet.2004.07.052.

(15) Leroyer, L.; Zou, C.; Maraval, V.; Chauvin, R. Synthesis and Stereochemical Resolution of a [6]Pericyclynedione: Versatile Access to Pericyclynediol Precursors of *Carbo*-Benzenes. *Comptes Rendus. Chimie* **2009**, *12* (3–4), 412–429. https://doi.org/10.1016/j.crci.2008.09.018.

(16) Hao, H.; Bagnol, T.; Pucheault, M.; Schafer, L. L. Using Catalysts To Make Catalysts: Titanium-Catalyzed Hydroamination To Access P,N-Ligands for Assembling Catalysts in One Pot. *Org. Lett.* **2021**, *23* (6), 1974–1979. https://doi.org/10.1021/acs.orglett.0c04212.

(17) Avarvari, N.; Fourmigué, M. 1,4-Dihydro-1,4-Diphosphinine Fused with Two Tetrathiafulvalenes. *Chem. Commun.* **2004**, No. 24, 2794–2795. https://doi.org/10.1039/B412193G.

(18) Leroyer, L.; Lepetit, C.; Rives, A.; Maraval, V.; Saffon-Merceron, N.; Kandaskalov, D.; Kieffer, D.; Chauvin, R. From Hexaoxy-[6]Pericyclynes to Carbo-Cyclohexadienes, Carbo-Benzenes, and Dihydro-Carbo-Benzenes: Synthesis, Structure, and Chromophoric and Redox Properties. *Chemistry* **2012**, *18* (11), 3226–3240. https://doi.org/10.1002/chem.201102993.

(19) Zhu, C.; Poater, A.; Duhayon, C.; Kauffmann, B.; Saquet, A.; Rives, A.; Maraval, V.; Chauvin, R. *Carbo* -mer of Barrelene: A Rigid 3D-Carbon-Expanded Molecular Barrel. *Chemistry A European J* **2021**, *27* (36), 9286–9291. https://doi.org/10.1002/chem.202100670.

(20) Dimroth, K.; Chatzidakis, A.; Schaffer, O. Photochemical Oxygenation of 2,4,6-Tri- *Tert* -butyl-λ^3 -phosphorin and 2,4,6-Tri- *Tert* -butyl-1,1-dimethoxy-λ^5 -phosphorin. *Ange*

w. Chem. Int. Ed. Engl. **1972**, *11* (6), 506–506. https://doi.org/10.1002/anie.197205061.

(21) Moores, A.; Cantat, T.; Ricard, L.; Mézailles, N.; Le Floch, P. Experimental and Th eoretical Study of Phosphinine Sulfides. *New J. Chem.* **2007**, *31* (8), 1493. https://doi.org/10. 1039/b702851b.

(22) Pfeifer, G.; Ribagnac, P.; Le Goff, X.; Wiecko, J.; Mézailles, N.; Müller, C. Reacti vity of Aromatic Phosphorus Heterocycles – Differences Between Nonfunctionalized and Py ridyl-Substituted 2,4,6-Triarylphosphinines. *Eur J Inorg Chem* **2015**, *2015* (2), 240–249. http s://doi.org/10.1002/ejic.201403048.

(23) Wossidlo, F.; Frost, D. S.; Lin, J.; Coles, N. T.; Klimov, K.; Weber, M.; Böttcher, T.; Müller, C. Making Aromatic Phosphorus Heterocycles More Basic and Nucleophilic: Synth esis, Characterization and Reactivity of the First Phosphinine Selenide. *Chemistry A Europe an J* **2021**, *27* (50), 12788–12795. https://doi.org/10.1002/chem.202102390.

(24) Lin, J.; Wossidlo., F.; Coles, N. T.; Weber, M.; Steinhauer, S.; Böttcher, T.; Müller, C. Borane Adducts of Aromatic Phosphorus Heterocycles: Synthesis, Crystallographic Chara cterization and Reactivity of a Phosphinine-$B(C_6F_5)_3$ Lewis Pair. *Chemistry – A European Jo urnal* **2022**, *28* (7), e202104135. https://doi.org/10.1002/chem.202104135.

(25) Priyakumar, U. D.; Dinadayalane, T. C.; Narahari Sastry, G. Structures, Energetics and Vibrational Spectra of the Valence Isomers of Phosphinine. An Ab Initio and DFT Study. *Chemical Physics Letters* **2001**, *336* (3–4), 343–348. https://doi.org/10.1016/S0009-2614(0 1)00148-8.

(26) Pfeifer, G.; Chahdoura, F.; Papke, M.; Weber, M.; Szűcs, R.; Geffroy, B.; Tondelie r, D.; Nyulászi, L.; Hissler, M.; Müller, C. Synthesis, Electronic Properties and OLED Devic es of Chromophores Based on λ^5 -Phosphinines. *Chemistry A European J* **2020**, *26* (46), 105 34–10543. https://doi.org/10.1002/chem.202000932.

(27) Zhang, J.; Hou, Y.; Liu, S.; Lin, J.; Li, Z. The Case of a M_2-P Aromatic Phosphinin e as a 4-Electron Donor Forming σ- and π-Three–Center-Two-Electron Bonds. *Dalton Trans.* **2024**, *53* (12), 5608–5615. https://doi.org/10.1039/D4DT00228H.

(28) Pham-Tran, N.-N.; Bouchoux, G.; Delaere, D.; Nguyen, M. T. Theoretical and Exp erimental Reevaluation of the Basicity of λ^3 -Phosphinine. *J. Phys. Chem. A* **2005**, *109* (12), 2957–2963. https://doi.org/10.1021/jp045339c.

(29) Coles, N. T.; Sofie Abels, A.; Leitl, J.; Wolf, R.; Grützmacher, H.; Müller, C. Phosp

hinine-Based Ligands: Recent Developments in Coordination Chemistry and Applications. *C oordination Chemistry Reviews* **2021**, *433*, 213729. https://doi.org/10.1016/j.ccr.2020.213729.

(30) Lepetit, C.; Peyrou, V.; Chauvin, R. Ring Carbo-Mers of "Aromatic" Heterocycles. *Phys. Chem. Chem. Phys.* **2004**, *6* (2), 303–309. https://doi.org/10.1039/B311790A.

(31) A. A. Granovsky. Firefly. http://classic.chem.msu.su:gran:firefly:index.html.

(32) Schmidt, M. W.; Baldridge, K. K.; Boatz, J. A.; Elbert, S. T.; Gordon, M. S.; Jensen, J. H.; Koseki, S.; Matsunaga, N.; Nguyen, K. A.; Su, S.; Windus, T. L.; Dupuis, M.; Montgomery Jr, J. A. General Atomic and Molecular Electronic Structure System. *Journal of Computational Chemistry* **1993**, *14* (11), 1347–1363. https://doi.org/10.1002/jcc.540141112.

(33) Geerlings, P.; De Proft, F.; Langenaeker, W. Conceptual Density Functional Theory. *Chem Rev* **2003**, *103* (5), 1793–1873. https://doi.org/10.1021/cr990029p.

(34) Zhou, Z.; Parr, R. G.; F. Garst, J. Absolute Hardness as a Measure of Aromaticity. *Tetrahedron Letters* **1988**, *29* (38), 4843–4846. https://doi.org/10.1016/S0040-4039(00)80623-1.

(35) Schleyer, P. V. R.; Maerker, C.; Dransfeld, A.; Jiao, H.; Van Eikema Hommes, N. J. R. Nucleus-Independent Chemical Shifts: A Simple and Efficient Aromaticity Probe. *J. Am. Chem. Soc.* **1996**, *118* (26), 6317–6318. https://doi.org/10.1021/ja960582d.

Chapter 3. Synthesis and properties of Carbo-diphosphabarrelene derivatives

1. Introduction

1.1. Barrelene

Barrelene is a fascinating bicyclic organic compound, characterized by its chemical formula C_8H_8 and systematic name bicyclo[2.2.2]octa-2,5,7-triene. It was first synthesized and described by H. E. Zimmerman in 1960[1] (**Figure 3.2**). The compound earned its name from its formal resemblance with a barrel, its three ethylene units attached to two methine groups featuring the staves of the barrel.

Essentially, barrelene can be considered as the formal Diels-Alder adduct of benzene and acetylene. Its unique molecular geometry attracted the attention of theoretical chemists worldwide. Similar to benzene, barrelene boasts a set of six cyclic, yet non-coplanar, but possibly overlapping p orbitals[2]. However, due to the inherent molecular arrangement, it is impossible to avoid a destabilizing overlap of opposite-sign lobes. This structural characteristic embodies Möbius aromaticity, here interrupted by bridgehead sp^3 vertices, adding another layer of intrigue to its chemical properties and behavior[3,4] (**Figure 3.1**).

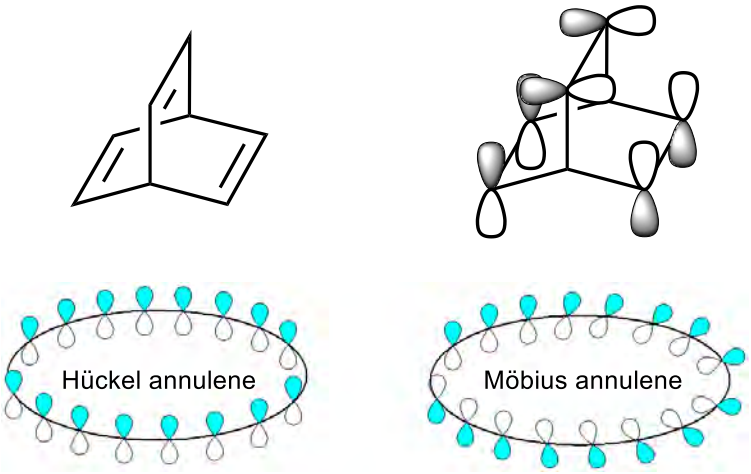

Figure 3.1. The barrel-shaped array of molecular orbitals and Möbius aromaticity.

1.2. Mono- and di-phospha-barrelene derivatives

The substitution of the bridgehead carbon atoms with a phosphorus atom in phospha-barrelene alters its electronic properties compared to barrelene. Specifically, the introduction of phosphorus

introduces a new element with different electronegativity, softness, and atomic size, which can affect the distribution of electron density within the molecule. Phosphorus typically has a lower electronegativity than carbon, leading to changes in the electron distribution and potentially altering the molecule's overall electronic structure, including changes in bond lengths, bond angles, and molecular orbitals. Additionally, the presence of phosphorus can introduce new electronic effects, such as lone pair interactions, that are absent in barrelene. Therefore, the electronic properties of phospha-barrelene can differ significantly from those of barrelene.

The first case of diphospha-barrenlene was reported in 1976 by Kobayashi *et al*.[5] (**Figure 3.2**). It is an intriguing molecule with unique structural and chemical properties, making it of interest in the field of organophosphorus chemistry and materials science.

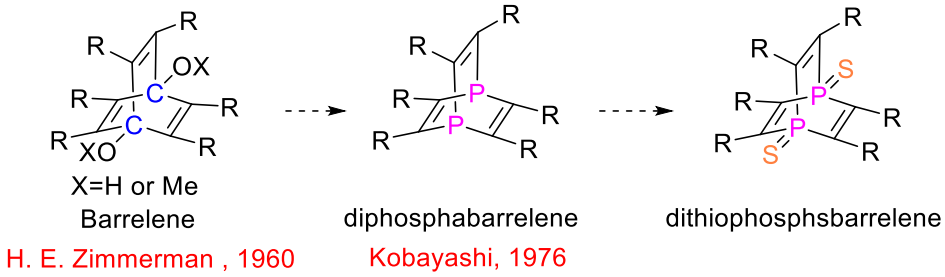

Figure 3.2. The development of (diphospha)barrelene derivatives.

1.3. *Carbo*-barrelene

In 2021, *carbo*-barrelene derivatives were synthesized in the group by Zhu *et al*.[6] and fully characterized using spectroscopic, electrochemical, and crystallographic methods (**Figure 3.3**). The emerging family of *carbo*-barrelenes suggests numerous potential applications, including their ability to encapsulate cations and exhibit high single molecule conductance (SMC) efficiency. Given that the *carbo*-benzene core has been shown to possess an unprecedented SMC value[7], and considering that SMC typically declines with the aromatic character, while it is expected to rise with the number of parallel conjugated pathways, the *carbo*-barrelene core featuring three parallel dialkynlbutatriene (DAB) conjugation paths could be an even more efficient single molecule conductor. This concept was explored computationally for parent barrelenes with bridgehead substituents Z = SH,[8] yet their experimental study remains elusive.

Lastly, the barrelene structure forms the foundational unit of the theoretical "hexagonite" 3D-

covalent carbon allotrope[9,10], diverging from diamond by containing sp^2-C atoms that enable a 3D honeycomb tessellation with intriguing features. Consequently, the *carbo*-meric version merits thorough investigation, akin to the exploration of "graphityne" for predicting unique electronic and mechanical attributes analogous to those of graphite[11].

Furthermore, beyond the thiolation of the sp^3 carbinol vertices[12–15], their replacement by P atoms holds promise for creating a P-gold junction, offering an alternative to classical S-gold junctions in SMC measurement via the STM-Break-Junction method (**Figure 3.4)** [16]. In the realm of coordination chemistry, these rigid bistrialkynylphosphines might also serve as bridging ligands in putative mixed-valence complexes.

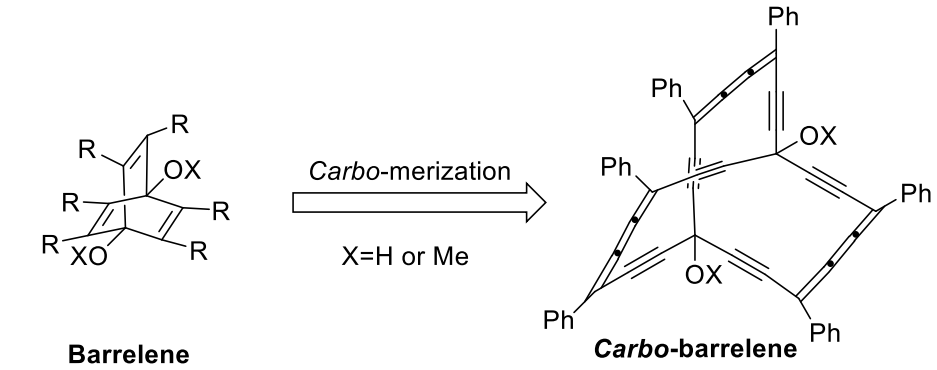

Figure 3.3. *Carbo*-merization of barrelene derivatives

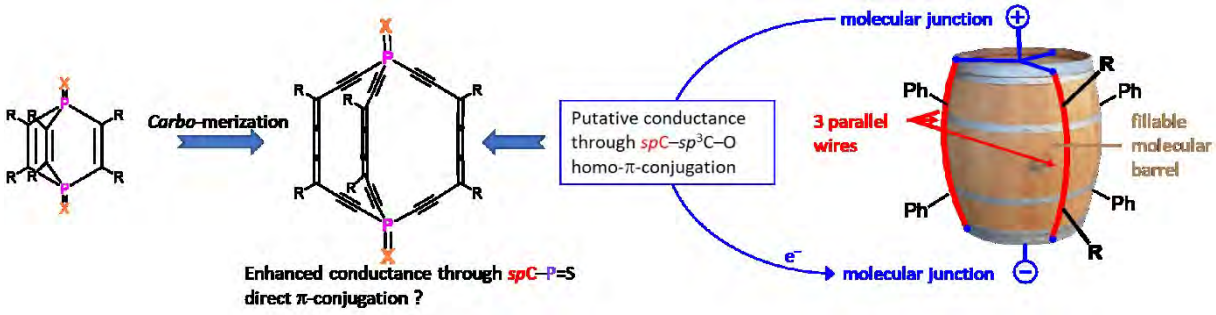

Figure 3.4. *Carbo*-merization of diphospha-barrelene derivatives

2. Results and discussion

2.1. Synthesis of a *carbo*-diphosphabarrelane dioxide

For stability reasons, *carbo*-diphosphabarrelane dioxide was first targeted following the strategy previously developed for the synthesis of diphospha-[6]pericyclyne dioxide (see Chapter 2) from [8+1+8+1] with $Cl_2P(O)Ph$ to [8+1+8+1+8] with $Cl_3P{=}O$ (**Scheme 3.1**). Starting from the same triyne **3** (which plays the role of the C_8 precursor), two equivalents of LDA and 2/3 equivalent of phosphorous oxychloride were added, and the reaction was monitored by ^{31}P NMR, revealing the appearance of a main signal at -55 ppm.

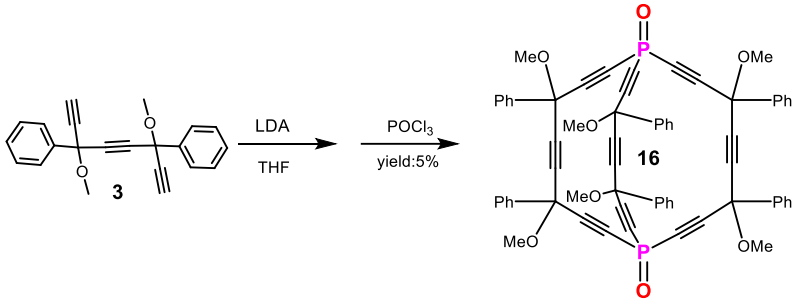

Scheme 3.1. Synthesis of *carbo*-diphospha barrelane dioxide by [8+1+8+1+8] from $Cl_3P{=}O$.

However, TLC analysis of the crude material revealed a significant dragging spot. Attempts to isolate *carbo*-diphosphabarrelane dioxide **1** through chromatography resulted in the degradation of the product on silica gel, each fraction displaying a spot with an R_f value of 0.8 (hexane/DCM: 2/1) on TLC plates (**Figure 3.5**). This observation suggests that the product **16** is highly sensitive to the weak acidity of silica gel. During silica gel column separation, partial decomposition may occur, leading to the continued generation of products with weak polarity, which are present in each fraction. Isolation of high purity products thus became exceedingly difficult due to the challenges posed by product decomposition during the separation process, further reducing the already modest reaction crude yields. We thus investigated different purification techniques to maximize product purity while minimizing decomposition. The use of neutral alumina helped to avoid the negative effects of acidity on the product, but the separation efficiency was still unsatisfactory. As a result, we tried preparative TLC plates to speed up the separation process, by neutralizing them with 5% triethylamine before loading the crude sample. Although the outcomes were not perfect and the method did not fully prevent decomposition, we were able to obtain a relatively pure *carbo*-diphospha barrelane dioxide **16** with a yield of 5%. This compound was characterized by NMR

and HRMS.

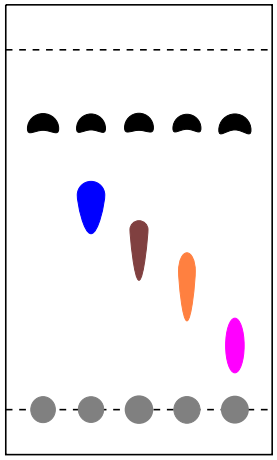

Figure 3.5. TLC plates of column chromatography fractions obtained upon purification of *carbo*-diphosphabarrelene dioxide **16(**pink spot**)**, each fraction showing a spot at R_f = 0.8.

2.2. Attempt at synthesis of *carbo*-dithiophosphabarrelane

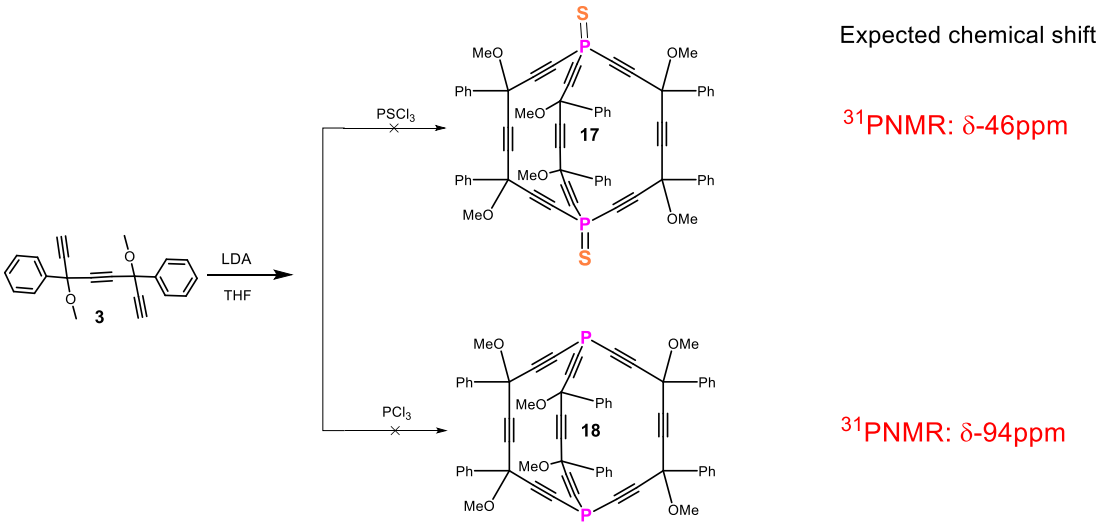

Scheme 3.2. Failed attempts at synthesis of *carbo*-diphosphabarrelane **18** and *carbo*-dithiodiphospha barrelane **17** following the strategy of Scheme 3.1.

After obtaining the *carbo*-diphospha-barrelane dioxide product **16**, the established [8+1+8+1+8] synthesis method was tested from $Cl_3P{=}S$ to prepare the *carbo*-

dithiodiphosphabarrelane **17**. However, ^{31}P NMR spectra of the crude reaction mixtures did not fit our expectations to get signals around -46 ppm that should correspond to the *carbo*-dithiodiphosphabarrelane **17**, but gave signals around 31.7 ppm instead. The preparation of *carbo*-diphospha-barrelane **18** was also attempted from PCl_3 in the same conditions, but only polymers were obtained.

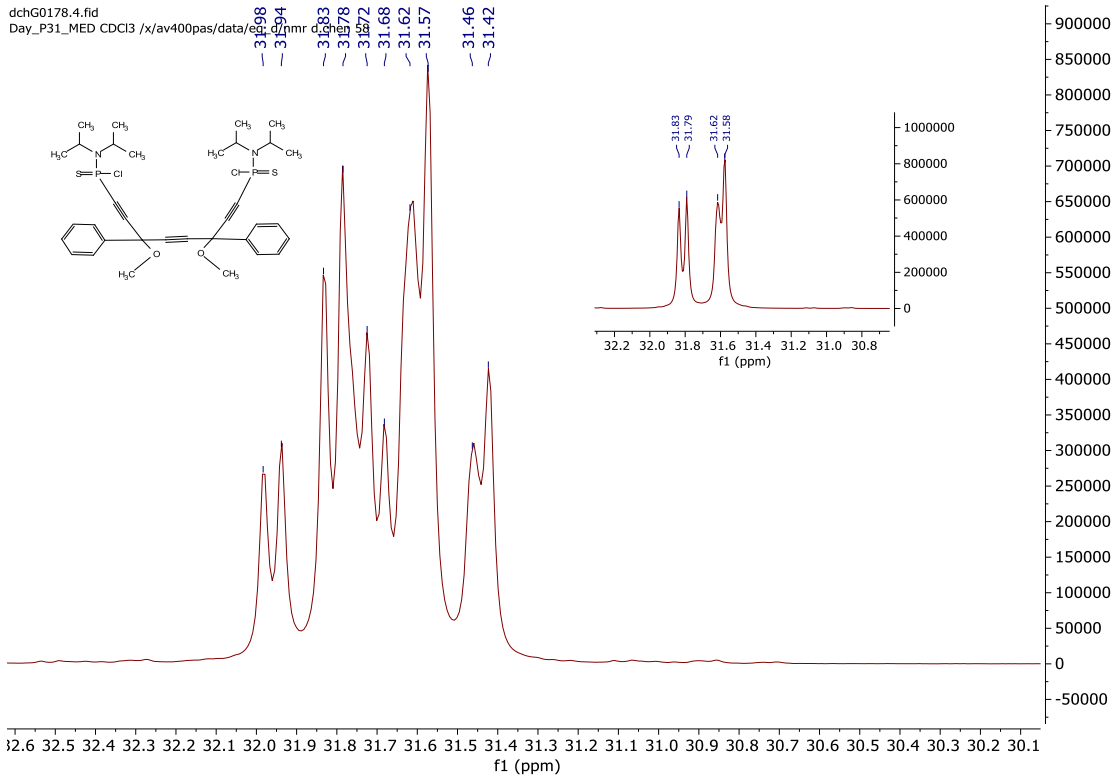

Figure 3.6. ^{31}P NMR spectrum of by-product **19**, coupled (main picture) and decoupled (in upper right) from ^{1}H.

After purification, the unexpected product obtained from the triyne **3**, LDA and $P(S)Cl_3$ instead of **17** (**Scheme 3.2**) could be determined to possess the structure **19** (**Scheme 3.3**), thanks to a full characterization by NMR and mass analyses. The ^{31}P NMR spectra, coupled and decoupled from ^{1}H, indicated the presence of ^{1}H nuclei coupled with ^{31}P nuclei at short distance (**Figure 3.6**). Additionally, signals corresponding to isopropyl groups were observed on the ^{1}H NMR spectrum. The N, N-diisopropylamino group, which originates from the LDA reagent used to deprotonate the triyne 3, was thus speculated to be part of the structure. The structure of **19** was finally confirmed

through MS and elemental analysis.

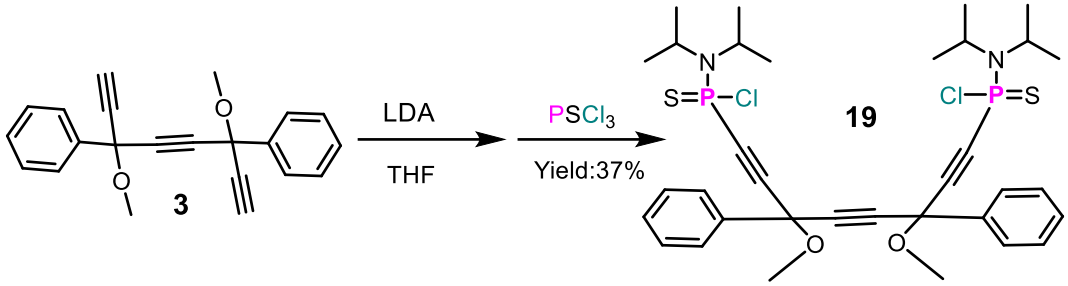

Scheme 3.3. Synthesis of the by-product **19** unexpectedly obtained, instead of **17** (Scheme 2.2), as a mixture of steerosiomers (7 diasteoroisomers in theory, 2 of them achiral).

To confirm the hypothesis, we prepared the model terminal alkyne **21** in two steps with an overall yield of 88% in order to study its reactivity in the reaction conditions previously applied to the triyne **3**. The model product **21** was thus treated with one equivalent of LDA and 1/3 equivalent of $P(S)Cl_3$, and observed to give the product **22**, analogue of **19** (**Scheme 3.4**). The model reaction thus showed that one of the chlorides of $P(S)Cl_3$ was substituted by the model alkyne, and one was unexpectedly substituted by the diisopropylamino group of LDA.

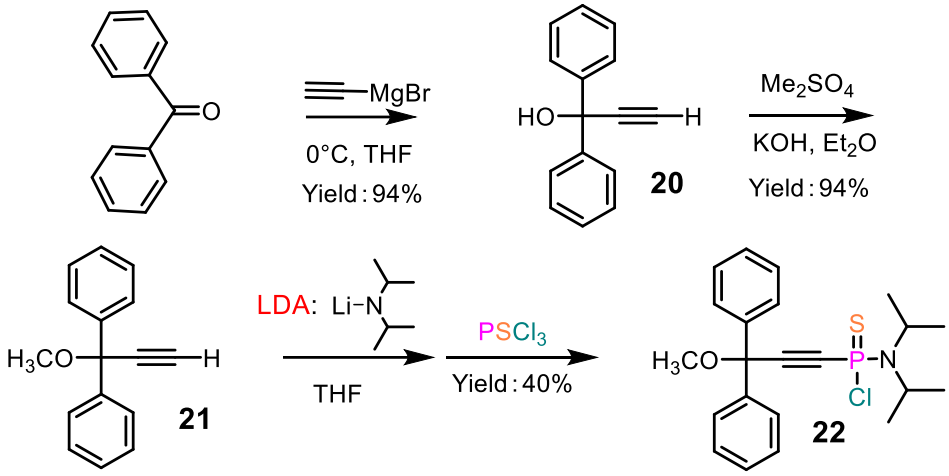

Scheme 3.4. Synthesis of the model alkyne **21** and control experiment with LDA.

2.3. Alternative access to *carbo*-dithiodiphosphabarrelanes

The use of LDA to deprotonate the triyne and react with $(S)PCl_3$ was found to be inefficient

for the preparation of the *carbo*-dithiodiphospha-barrelane, as demonstrated experimentally in the previous section. Therefore, it became necessary to search for a more suitable base for the deprotonation of the triyne **3** that is compatible with a selective reaction with (S)PCl_3. Trials were conducted on triyne **3** using classical deprotonation reagents, including, beyond LDA, LiHMDS, and n-butyl-lithium. For comparison, **Figure 3.7** shows a zoomed region of the obtained ^{31}P NMR spectra around the chemical shift of -46 ppm. Both reactions with LiHMDS and n-butyllithium as base produced signals around -46 ppm, among which a broad signal presumably corresponding to trialkynyl-substituted phosphorus sulfide polymeric compounds. In the case of LiHMDS, however, a set of sharp signals is observed at slightly higher field (around -47 ppm), as expected for the stereoisomers of the *carbo*-dithiodiphospha-barrelane **17**. In contrast, the reaction with LDA produces no signals in this area, as previously mentioned. Notably, all three bases lead to a more or less intense secondary signal at + 41.9 ppm.

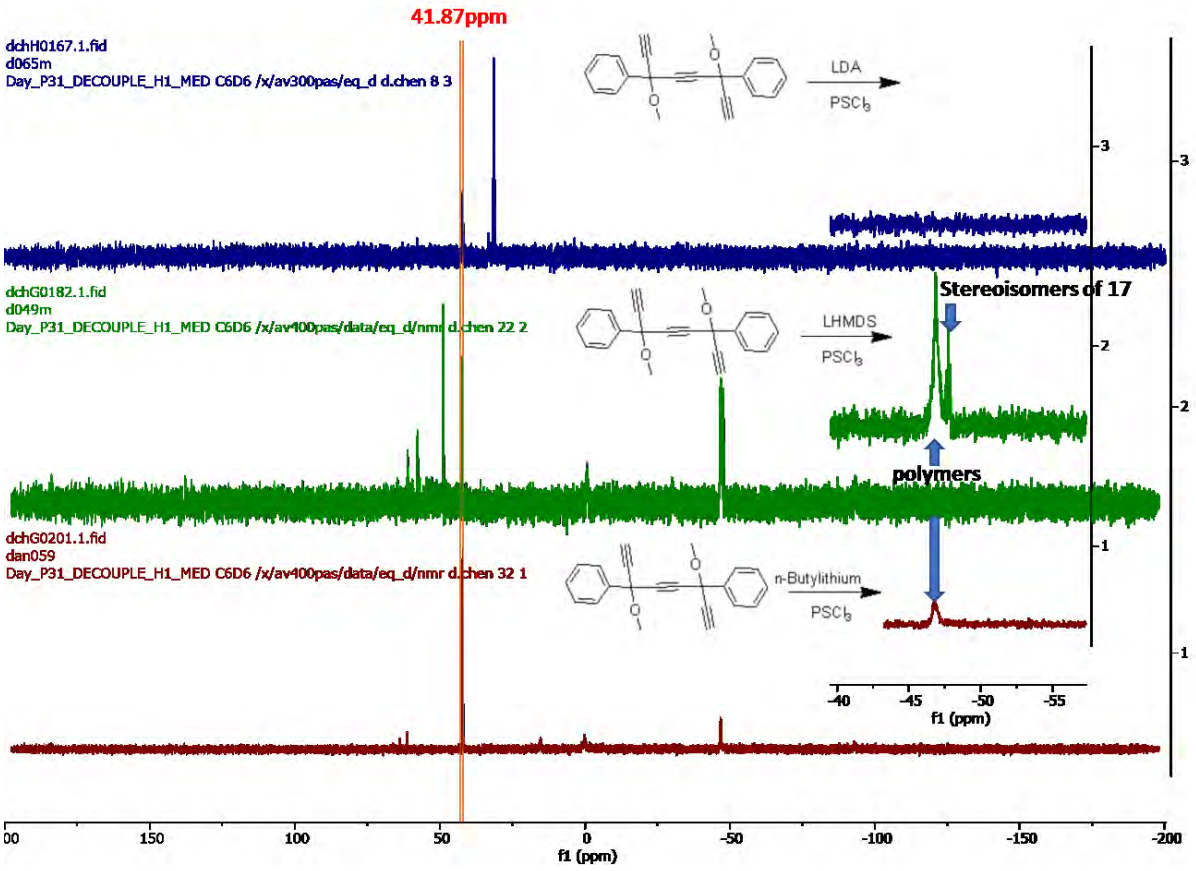

Figure 3.7. Comparison of the ^{31}P NMR spectra obtained by reaction of the triyne **3** with (S)PCl_3 using different bases.

After comparing different deprotonation reagents on the reaction outcome, LiHMDS was assessed to be the optimal choice for constructing *carbo*-dithiodiphospha-barrelanes.

The reaction was also tested on the model compound **21** to allow interpretation of the results. Three products were obtained upon reaction of **21**[17] with 1.1 equivalent LiHMDS and 0.33 equivalent of (S)PCl_3: the expected thiophosphine **23**, the phosphine **24**, and the phosphine oxide **2**, which were each separated and characterized, as shown in **Scheme 3.5**.

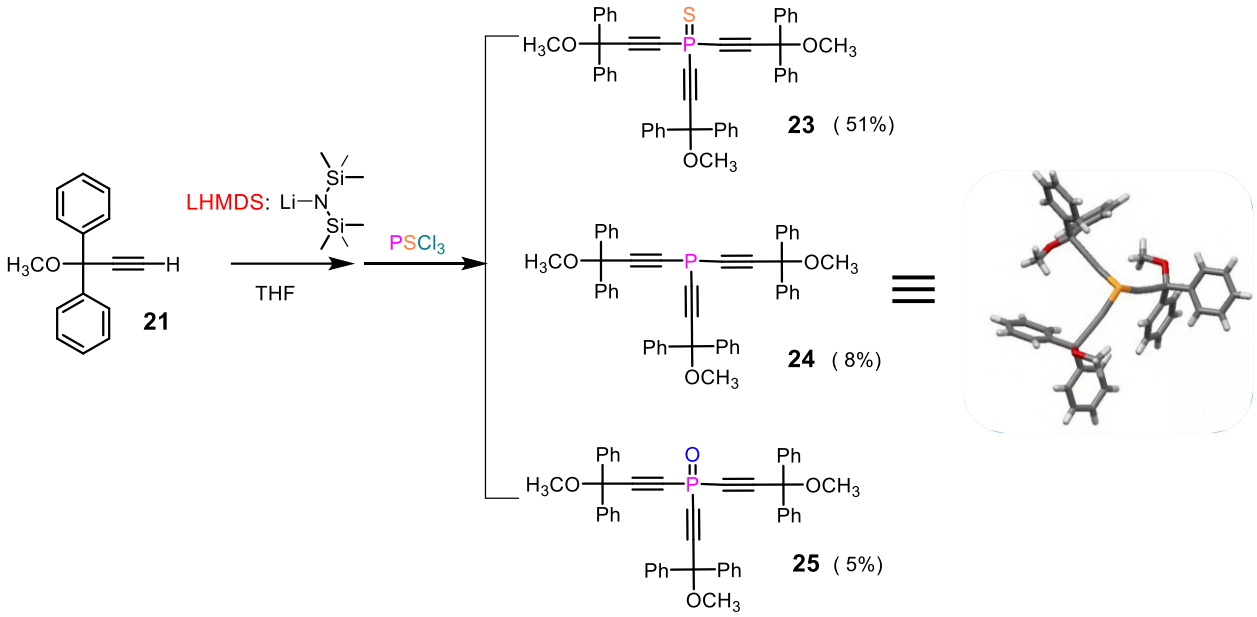

Scheme 3.5. Reaction of the model terminal alkyne **21** with P(S)Cl_3 in the presence of LiHMDS.

During the reaction, partial desulfurization of the product **23** thus occurred, giving the phosphine **24**, which was in turn partially oxidized into **25** (**Figure 3.8**). The structure of **24** was confirmed by X-ray diffraction analysis of single crystals deposited from a pentane solution. The purity of the starting material P(S)Cl_3 was checked by ^{31}P NMR analysis to rule out that the obtained side-products were not due to any impurities coming from the reagent. The reaction was also conducted using PCl_3 under identical conditions, but it did not result in the formation of **24** (**Scheme 3.6**). Based on these observations and the crude ratio **23**/**24**/**25** ≈ 80/10/10 suggested by ^{31}P NMR (**Figure 3.8**), it is reasonable to assume that approximately 20% of the thiophosphine **23** underwent desulfurization in the reaction conditions, and that some of the formed reduced product was subsequently oxidized by oxygen in the air during the work-up. However, further investigations deserve to be undertaken to better understand this process.

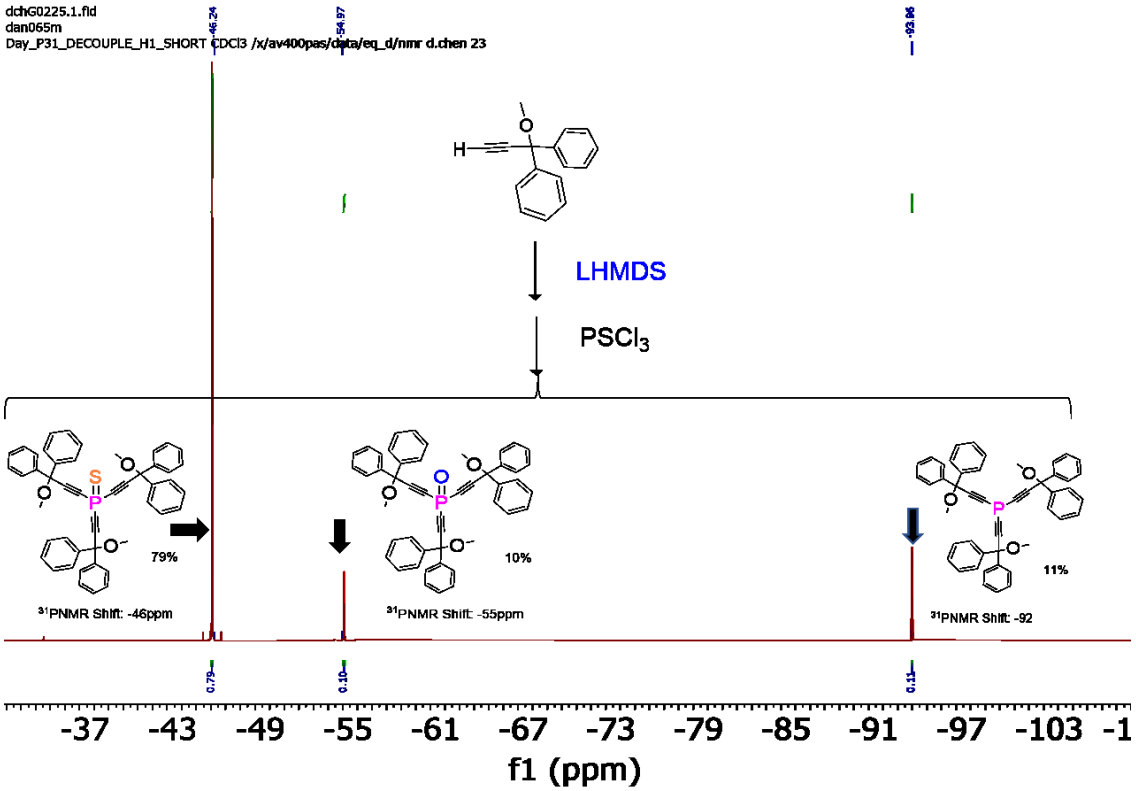

Figure 3.8. ^{31}P NMR spectrum of the crude material after reaction of the model alkyne with $P(S)Cl_3$ using LiHMDS (Scheme 3.5).

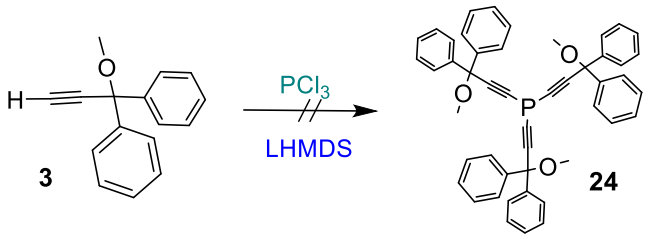

Scheme 3.6. Attempt at synthesis of the functional trialkynylphosphine **24** from PCl_3

As shown above LiHMDS is definitely the most promising base for preparing *carbo*-dithiodiphospha-barrelane **17** though the same [8+1+8+1+8] strategy previously used for the synthesis of the *carbo*-diphospha-barrelane dioxide with LDA (section 2.1). The use of two equivalents of LiHMDS as base and 2/3 equivalent of $Cl_3P{=}S$ thus lead to the *carbo*-dithiodiphospha-barrelane **17** with a yield of 5% after purification by flash chromatography. The product was obtained as a mixture of stereoisomers, as shown in **Figure 3.9**, giving multiple signals between -45.62 ppm and -47.39 ppm in the ^{31}P NMR spectrum.

In theory, there are 14 stereoisomers, 2 of which are achiral with equivalent P atoms, the remaining 12 stereoisomers consisting of 6 pairs of enantiomers, 2 of them being C_2-symmetric with equivalent P atoms, the 4 last ones with unequivalent P atoms. The total number of possible distinct ^{31}P resonance is therefore 2 + 2 + 4 x 2 = 12, with possible pairs of doublets between nonequivalent ^{31}P nuclei albeit quite unlikely due to expected very small $^{9}J_{PP}$ values.

As previously shown with the model alkyne **21**, partial desulfurization was observed in this reaction, the reduced diphosphine **18** accounting for approximately 17% of the crude product, with ^{31}P NMR chemical shifts around -94 ppm, 11 signals were observed in the ^{31}P nmr spectrum. After work-up, the phosphine **18** was partially oxidized into **16**, giving signals around -55 ppm in the ^{31}P NMR spectrum. Due to the far distance between two phosphorus, the mono-desulfurated sideproduct is difficult to identify in NMR specta, along with its oxidation state.

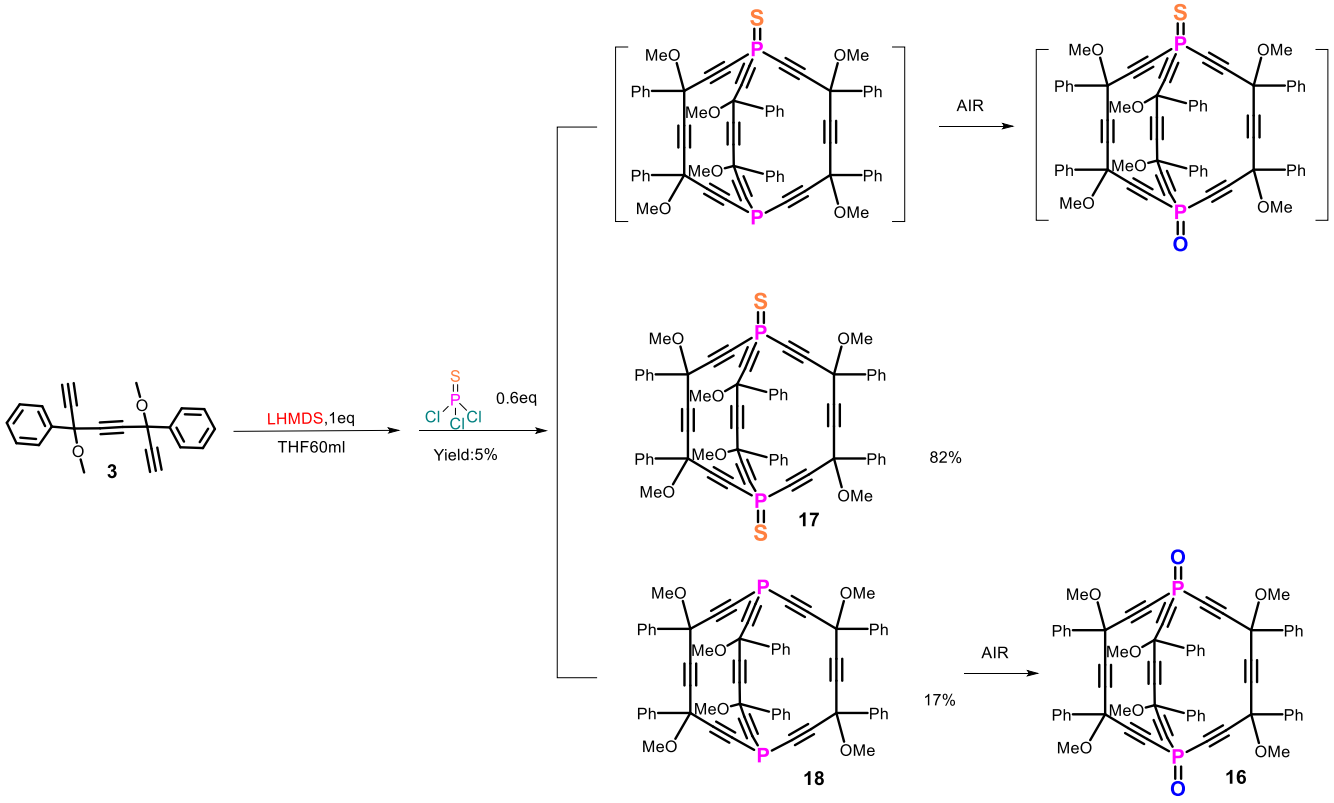

Scheme 3.7. Synthesis of *carbo*-dithiodiphospha barrelane **17**,and *carbo*-diphospha barrelane **18** and *carbo*-diphospha-barrelane dioxide **16**

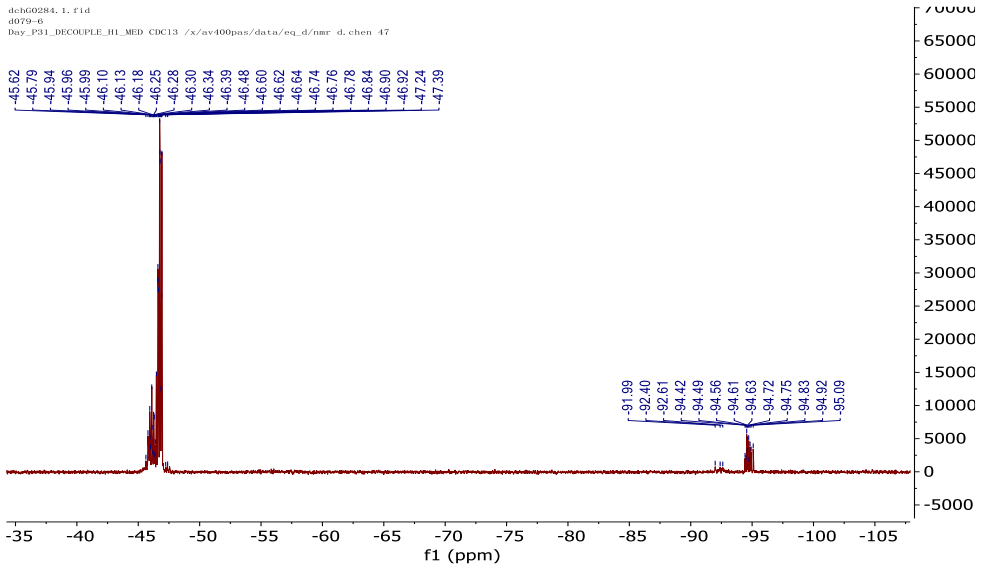

Figure 3.9. ^{31}P NMR spectrum of the crude mixture obtained by reaction of the triyne **3** and $P(S)Cl_3$ with LiHMDS (Scheme 3.7).

2.4. Synthesis and partial characterization of a *carbo*-dithiodiphospha-barrelene

2.4.1. Synthesis of a *carbo*-dithiodiphospha-barrelene

After subjecting **17** to $SnCl_2$/HCl in DCM at low temperature under the conditions classically used for the synthesis of *carbo*-benzenes from hexaoxy[6]pericyclynic precursors[18], the hexaphenyl-*carbo*-dithiodiphospha-barrelene **26** was produced and isolated with 20 % yield as a colored dark orange solid (**Scheme 3.8**) which could be partially characterized by NMR and UV-vis spectroscopy.

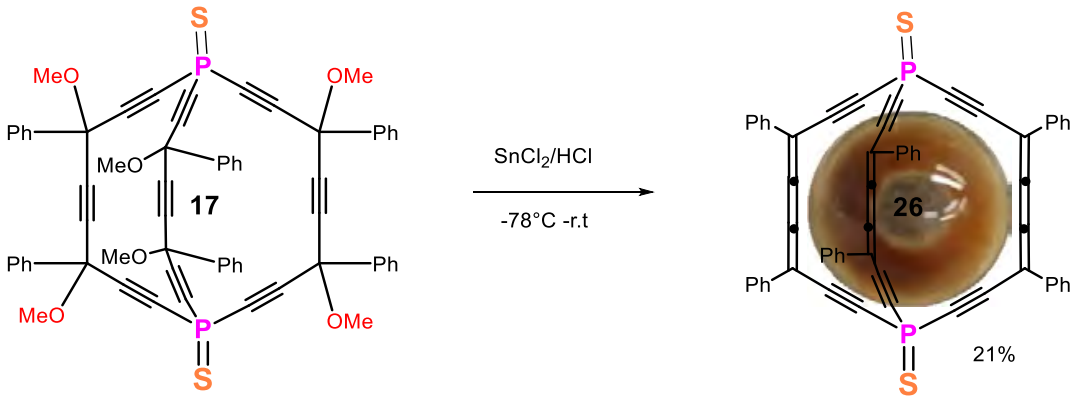

Scheme 3.8. Reduction of the *carbo*-dithiodiphospha barrelane **17** to the hexaphenyl-*carbo*-

dithiodiphospha-barrelene **26**.

2.4.2. NMR characterization

The hexaphenyl-*carbo*-dithiodiphospha-barrelene **26** is poorly soluble in most organic solvents, only allowing accurate characterization by ^{1}H and ^{31}P NMR spectroscopy in CD_2Cl_2 as solvent.

The reductive-elimination reaction from **17** to **26** induces the simplification of the ^{31}P NMR spectrum, because of the elimination of the stereogenic centers originally giving rise to mutliple signals around -46/47 ppm, resulting in a single signal at -44.6 ppm. Indeed, the formation of the butatriene motifs, induces a low field shifting of the ^{31}P NMR signal, in this case of 1.4 ppm only because the formed butatrienes are quite far (through bonds) from the P atoms, which are thus moderately affected by the transformation (see **Figure 3.10**).

The ^{1}H NMR spectrum shows clear signals in the 7.46–7.56 ppm and 7.79–7.83 ppm regions, corresponding to the aromatic protons of **26**. This is in contrast with the broad signals of **17**, which are due to the presence of stereoisomers. Additionally, the resonances around 3.5 ppm, which correspond to the OCH_3 groups, disappeared after the reductive elimination (**Figure 3.11**).

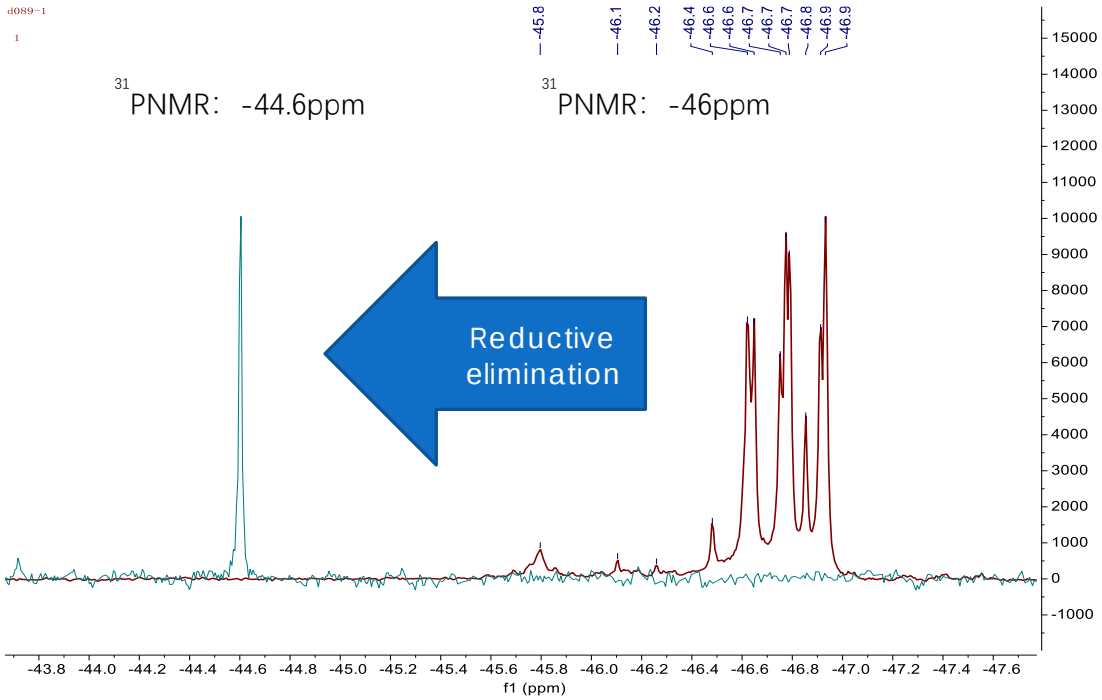

Figure 3.10. ^{31}P NMR spectrum of the hexaphenyl *carbo*-dithiodiphospha-barrelene **26** (with green line)

vs that of the stereoisomeric mixture of hexaphenyl *carbo*-dithiodiphospha-barrelane **17** (with red line).

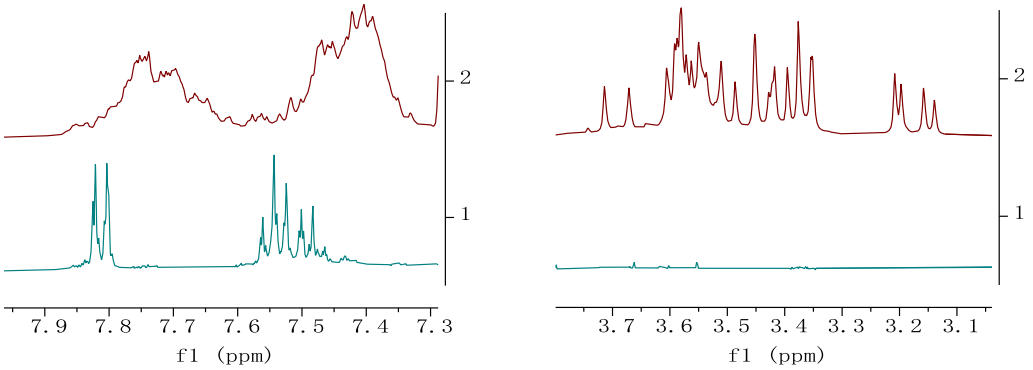

Figure 3.11. ^{1}H NMR spectrum of hexaphenyl-*carbo*- dithiodiphospha-barrelene **26** (with green line) *vs* that of the stereoisomeric mixture of hexaphenyl *carbo*-dithiodiphospha-barrelane **17** (with red line).

2.4.3. UV-visible spectroscopy

The UV-vis absorption properties of **26** were investigated in DCM solution. Its absorption spectrum exhibits one main intense absorption band at 418 nm with two shoulders at lower energies, making this band quite broad (**Figure 3.12**). This spectral profile is comparable with that observed for the previously described 1,4-diphenyl-1,4-di(diphenylthiophosphinylethynyl) butatriene **3b** and *carbo*-1,4-dithio-1,4-dihydro-1,4-diphosphinine **13** (see Chapter 2), having one and two DAB motifs, respectively, two or one less than in **26**. By comparison to **13**, the 19 nm blue shift of the maximum absorption wavelength of **26** can be explained by the presence of one more DAB motif in **26**. This is in line with an observations of Zhu *et al.* in 2021[6] regarding the UV-visible maximum absorption wavelengths of *carbo*-barrelene derivatives **27** and **15**: (**Figure 3.12 a**) the *carbo*-barrelene **27**, which contains three butatriene edges, exhibits a blue shift of 17 nm of its UV-visible maximum absorption wavelength as compared to the partially reduced derivative **15**.

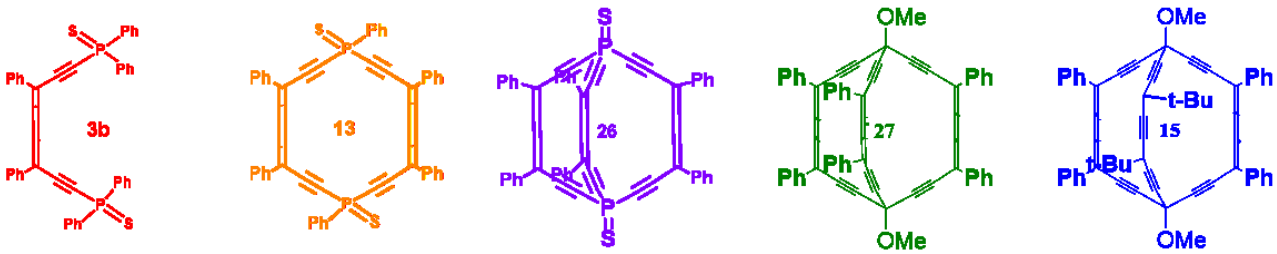

a

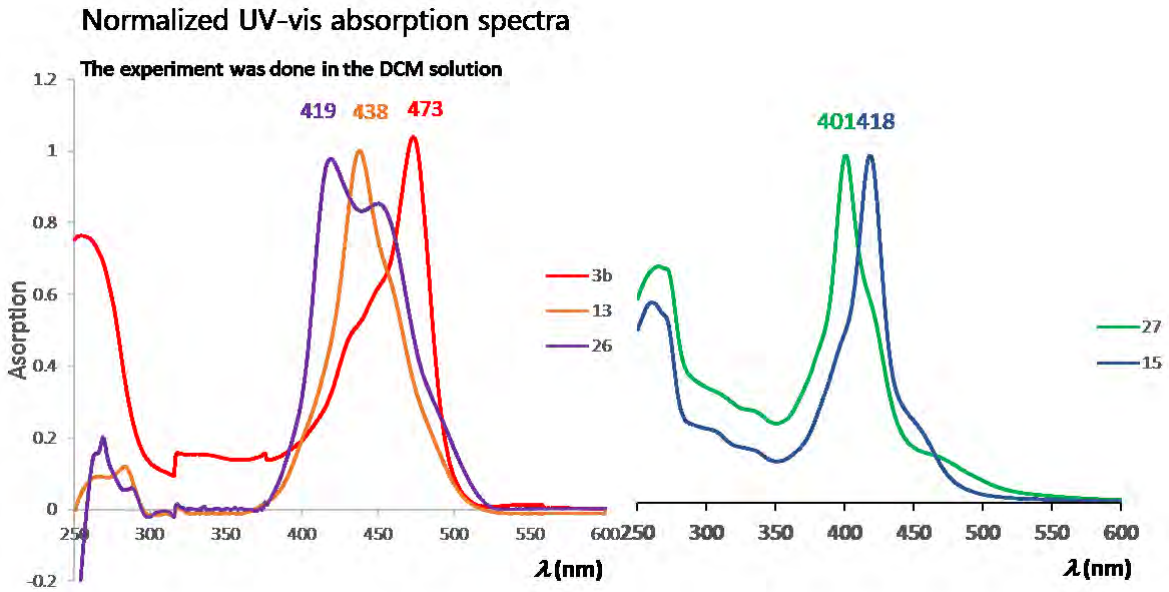

b

Figure 3.12. Normalized UV-vis absorption spectra of the hexaphenyl-*carbo*-dithiodiphosphabarrelene **26**, hexaphenyl-*carbo*-1,4-dihydro-dithiophosphinine **13** and **3b,** compared with UV-vis absorption spectra of **27** and **15**(**b**) and their structure (**a**).

2.4.4. Theoretical calculation

In the absence of X-ray crystal structure of hexaphenyl-*carbo*-dithiodiphosphabarrelene **26,** DFT calculations were performed at the B3PW91/6-31G(d,p) level with the vacuum dielectric constant ($\varepsilon_r = 1$) under D_3 symmetry constraint, using the Firefly program v. 8.1.1[19,20] by Professor Remi CHAUVIN.

Selected structural data of D_3-symmetric **26** as compared to those of C_2-symmetric hexaphenyl-dihydroxy-*carbo*-barrelene **15** [6] are shown in **Figure 3.13**.

The transannular P···P distance of 7.457 Å in **17** is 7% greater that sp^3C-sp^3C distance in **15** (6.983 Å). The three P_2DAB blades (P_2C_8) of **26** are quasi-planar, with deviation from their mean plane in the range 0.004-0.022 Å (mean distance = 0.021 Å, standard deviation = (variance)$^{1/2}$ = 0.017 Å), slightly more distorted than the C_2DAB blades of **15** in the range 0.001-0.017 Å (mean distance = 0.010 Å, standard deviation = (variance)$^{1/2}$ = 0.0064 Å). The C–Ph means planes are almost coplanar with the P_2DAB blades of **26**, just slanted by 1.53°, significantly less than the angle of 10.06° between the C–Ph mean planes and C_2DAB blades of **15**.

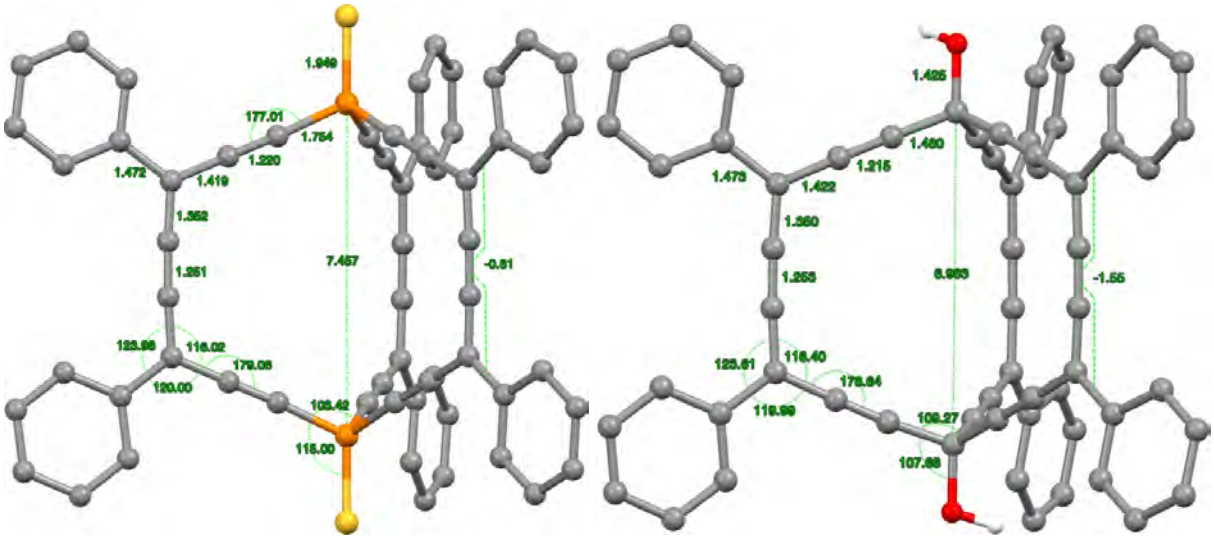

Figure 3.13. DFT-optimized structures of hexaphenyl-*carbo*-dithiodiphosphabarrelene **26** under D_3-symmetry constraint (*left*) and hexaphenyl-dihydroxy-*carbo*-barrelene **15** under C_2-symmetry constraint (*right*), in the gas phase (ε_r = 1) at the B3PW91/6-31G(d,p) calculation level. Final non-corrected energy components for **26**: TOTAL = -3781.942829 a.u., NUCLEAR = 8541.896763 a.u., ELECTRONIC = -12323.839593 a.u. Final non-corrected energy components for **15**: TOTAL = -2530.745403 a.u., NUCLEAR = 7574.216290a.u., ELECTRONIC = -10104.961693 a.u. Internuclear distances are given in Ångström, bond and dihedral angles in degrees.

The frontier orbitals of **26** (**Table 3.1**) from HOMO-2 to LUMO+1 are localized on the carbon core, with the HOMO (-0.206 a.u.) and LUMO (-0.127 a.u.) giving the quite low hardness η = 0.79 a.u., slightly lower than that of **15** (η = 0.191 - (-0.107) = 0.84 a.u.), as expected from the softness of the P atoms in **26**. Noteworthy is the depth the orbitals localized on the P=S vertices at -0.237 a.u for HOMO-3/HOMO-4, and -0.238 a.u. for HOMO-5/HOMO-6.

Table 3.1. DFT frontier orbitals of the putative hexaphenyl-*carbo*-dithio-diphosphabarrelene **26** in the gas phase (ε_r = 1) at the B3PW91/6-31G(d,p) level of calculation under D_3 symmetry constraint. Final non-corrected energy components for **26**: TOTAL = -3781.942829 a.u., NUCLEAR = 8541.896763 a.u., ELECTRONIC = -12323.839593 a.u.

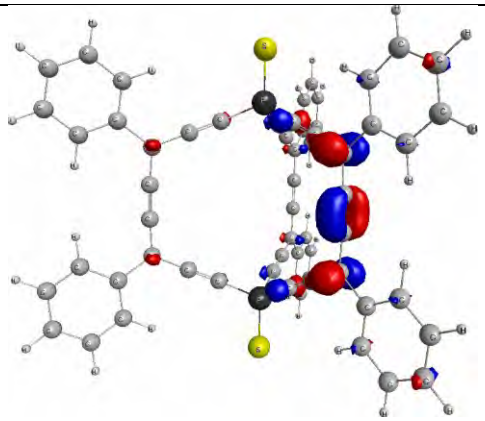

LUMO
-0.127 a.u. (*E* symmetry)
η = HOMO-LUMO gap = 0.790 a.u.

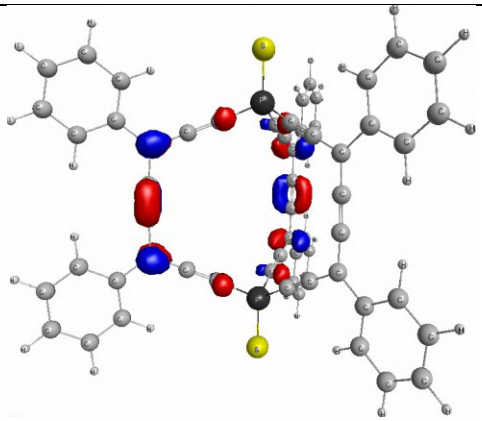

LUMO(+1)
-0.127 a.u. (*E* symmetry)

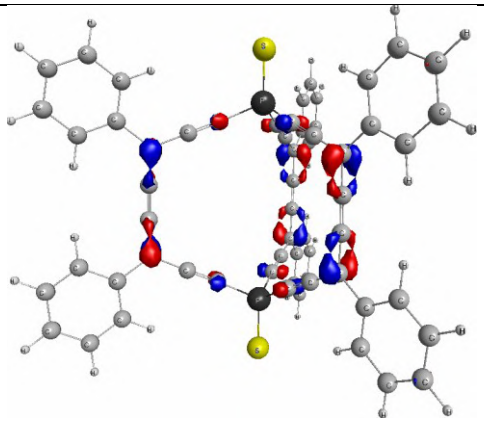

HOMO
-0.206 a.u. (A_1 symmetry)

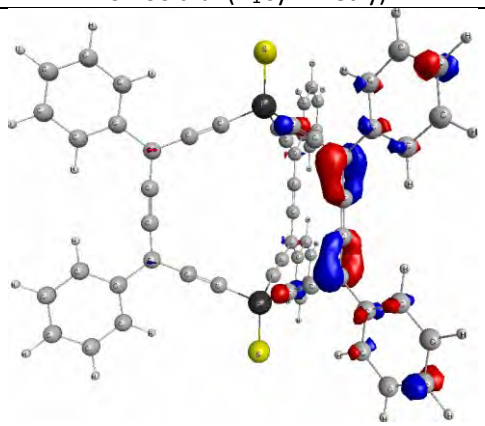

HOMO-1/2
-0.218 a.u. (*E* symmetry)

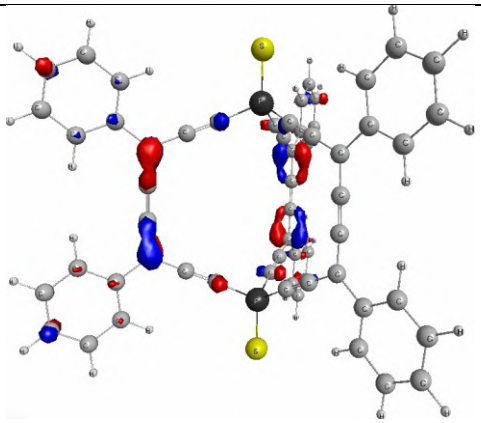

HOMO-2/1
-0.218 a.u. (*E* symmetry)

Table 3.1(continued）

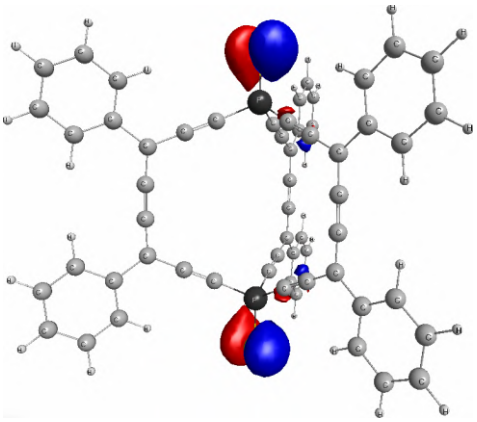 HOMO-3/4 -0.237 a.u. (*E* symmetry)	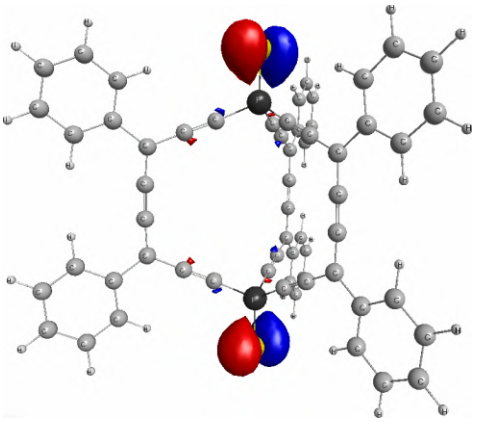 HOMO-4/3 -0.237 a.u. (*E* symmetry)
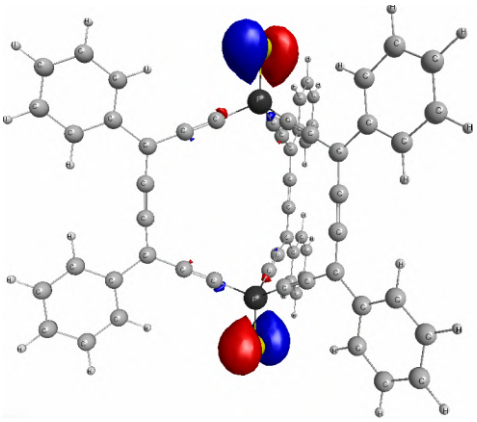 HOMO-5/6 -0.238 a.u. (*E* symmetry)	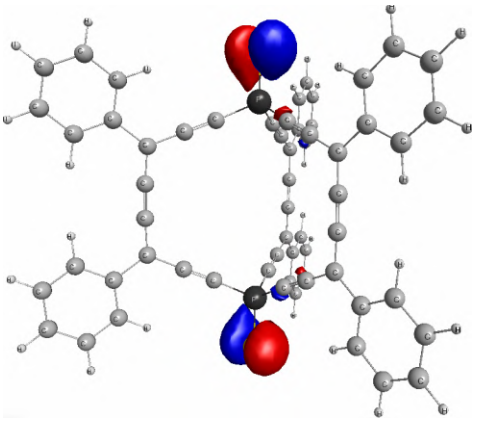 HOMO-6/5 -0.238 a.u. (*E* symmetry)

As a prospect, the reduced diphosphine hexaphenyl-*carbo*-diphosphabarrelene was also calculated (**Figure 3.14**). The frontiers orbitals are listed in **Table 3.2**.

The transannular P···P distance of 7.476 Å is 0.02 Å greater than that of the disulfide counterpart **26** (7.457 Å). The three P_2DAB blades (P_2C_8) are also quasi-planar, with deviation from their mean plane in the range 0.003-0.022 Å (mean distance = 0.012 Å, standard deviation = (variance)$^{1/2}$ = 0.0082 Å). The C–Ph means planes are almost coplanar with the P_2DAB blades with exactly the same inclination angle (1.53°) as in the disulfide counterpart **26**.

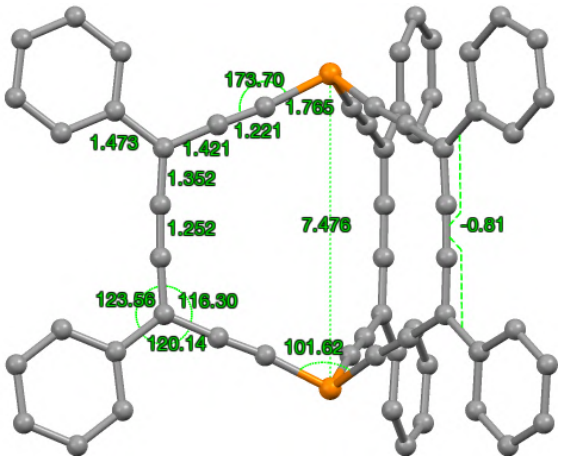

Figure 3.14. DFT-optimized structures of the putative hexaphenyl-*carbo*-diphosphabarrelene in the gas phase (ε_r = 1) at the B3PW91/6-31G(d,p) level of calculation under D_3 symmetry constraint. Final non-corrected energy components: TOTAL = -2985.630529 a.u., NUCLEAR = 7446.6943091 a.u., ELECTRONIC = -10432.3248378 a.u. Internuclear distances are given in Ångström, bond and dihedral angles in degrees.

The frontier orbitals of hexaphenyl-*carbo*-diphosphabarrelene from HOMO-2 to LUMO+1 are localized on the carbon core, with a HOMO-LUMO gap η = 0.80 a.u. (**Table 3.2**), a situation very similar to the one occurring in the disulfide counterpart **26** (**Table 3.1**). The P lone pair orbitals are also as deep as in **26**, starting from the non-degenerated HOMO-3 (-0.233 Å) and HOMO-4 (-0.237 a.u.), raising questions about the P/C chemoselectivity of the coordination to soft Lewis acids. The issue is addressed experimentally in Chapter 4.

Table 3.2. DFT frontier orbitals of the putative hexaphenyl-*carbo*-diphosphabarrelene in the gas phase (ε_r = 1) at the B3PW91/6-31G(d,p) level of calculation under D_3 symmetry constraint. Final non-corrected energy components: TOTAL = -2985.630529 a.u., NUCLEAR = 7446.6943091 a.u., ELECTRONIC = -10432.3248378 au.

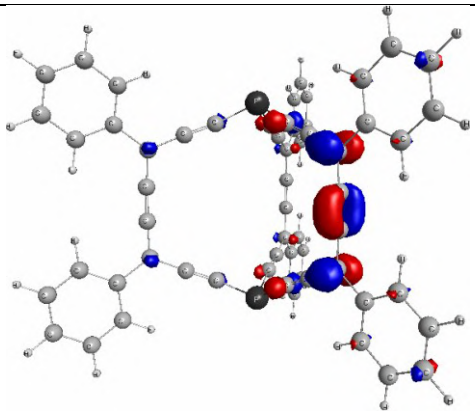	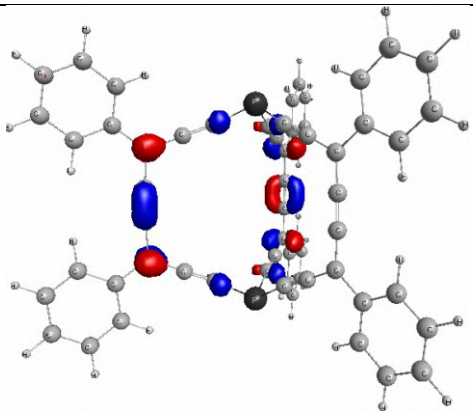
LUMO -0.115 a.u. (*E* symmetry) η = HOMO-LUMO gap = 0.800 a.u.	LUMO(+1) -0.115 a.u. (*E* symmetry)

Table 3.2(continued).

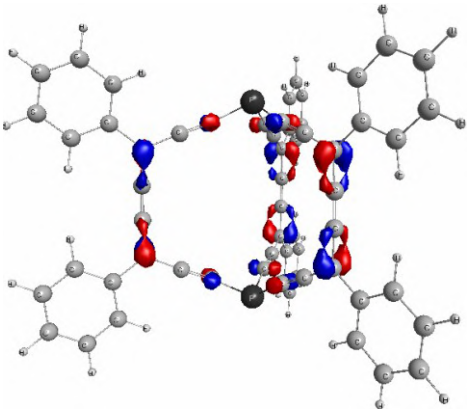

HOMO
-0.195 a.u. (A_1 symmetry)

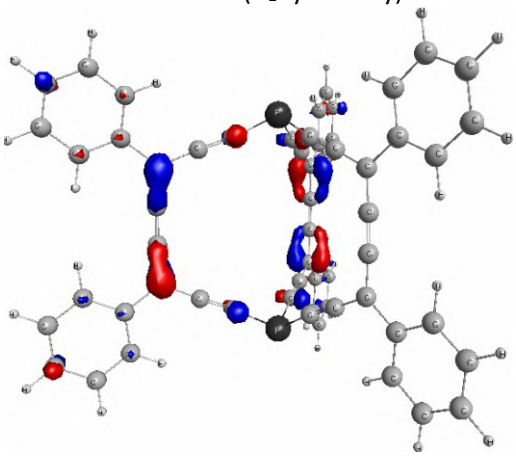

HOMO-1
-0.208 a.u. (*E* symmetry)

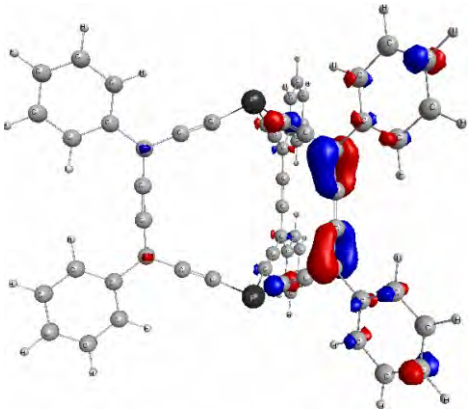

HOMO-2
-0.208 a.u. (*E* symmetry)

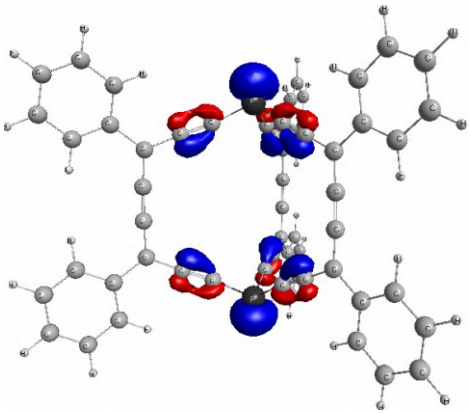

HOMO-3
-0.233 a.u. (A_1 symmetry)

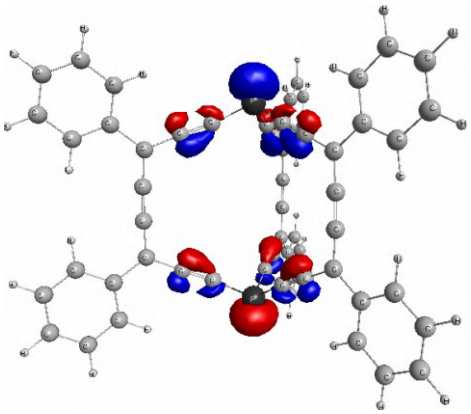

HOMO-4
-0.237 a.u. (A_2 symmetry)

3. Conclusion

A first hexaphenyl-*carbo*-dithiodiphosphabarrelene **26** and related *carbo*-diphospha-barrelane derivatives **16**, **17**, **18** have been synthesized. Their preparation was achieved by a general method involving a penta-component [8+1+8+1+8] macrocyclization process with *ca* 5 % yield. Hexaphenyl-*carbo*-dithiodiphospha-barrelene **26** was obtained after $SnCl_2$/HCl-mediated reductive elimination from the hexamethoxy-hexaphenyl-*carbo*-dithiodiphosphabarrelane **17** with 20 % yield as a colored dark orange solid, and was partially characterized by NMR and UV-vis spectroscopy.

The family of *carbo*-diphospha-barrelenes has several potential applications by comparison to the all-carbon *carbo*-barrelenes, including cage behavior towards cations and enhanced single molecule conductance (SMC).

By reduction of **26**, the corresponding *carbo*-diphosphabarrelene could henceforth be envisaged as an intriguing bis-macrocyclic diphosphine for putative original uses in coordination chemistry and catalysis.

4. Experimental section

General remarks

General: THF and DCM were dried with a PureSolv-MD-5 Innovative Technology system for the purification of solvents. All other reagents were used as commercially available. In particular, commercial 2.5M solutions of n-BuLi in hexane, 0.5M solutions of ethynylmagnesium bromide in THF, 3.0 M solutions of ethylmagnesium bromide in Et_2O, and 2.0 M solutions of hydrochloric acid in Et_2O were used. All reactions were carried out under nitrogen or Argon using schlenk and vacuum line techniques. Column chromatography was carried out with silica gel (60 P, 70–200 mm). Silica gel thin-layer chromatography plates (60F254; 0.25 mm) were developed by treatment with an ethanolic solution of phosphomolybdic acid (20%) or an aqueous potassium permanganate solution for fluorinated derivatives.

Bruker Avance 300, or Avance 400 spectrometers were used; all NMR spectra were recorded in $CDCl_3$ or CD_2Cl_2 solutions. NMR chemical shifts (d) are given in ppm, with positive values to

high frequency relative to the tetramethylsilane reference for ^{1}H and ^{13}C spectra, and ^{31}P spectra; coupling constants (J) are given in Hz. For compounds previously described in the literature, only 'H NMR was performed to purity control and the corresponding bibliographic references are given.

Mass spectra were recorded with a Quadrupolar Nermag R10–10H spectrometer.

UV spectra were recorded with a Perkin–Elmer UV/Vis Win-Lab Lambda 35 spectrometer with 1 cm quartz cell, UV-Visible wave length is in nm;

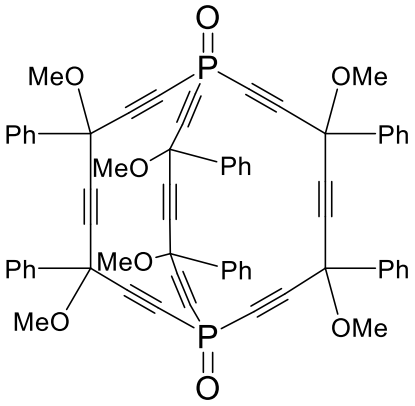

4,7,13,16,21,24-hexamethoxy-4,7,13,16,21,24-hexaphenyl-1,10-diphosphabicyclo[8.8.8] hexacosa-2,5,8,11,14,17,19,22,25-nonayne1,10-dioxide (16).

To a solution of triyne **3** (3 mmol, 942 mg) in 200 mL THF at -78°C, LDA (6.5 mmol, 6.5 mL) was added dropwise under magnetic stirring. After a period of 3 h, $POCl_3$ (2 mmol, 0.187 mL) was added, then the temperature was allowed to warm slowly up to room temperature overnight. After adding distilled water, the THF was partially evaporated and the mixture wasextracted with Et_2O. The combined organic extracts were washed by brine, dried with $MgSO_4$ and concentrated under reduced pressure. A preparative TLC purification was done with hexane/Ethyl acetate 2:1 as eluent, R_f = 0.4, to give **1** as a slightly yellow paste with 8% yield (82.5 mg, 0.08mmol).

^{1}H NMR (400 MHz, $CDCl_3$) δ 7.86 – 7.57 (m, 12H), 7.47 – 7.30 (m, 18H), 3.74 – 3.31 (m, 18H).

^{31}P NMR (121 MHz, $CDCl_3$) δ -55.74 – -56.11 (m).

HRMS (DCI-CH_4): *m/z*: calculated for $[M+H]^+$ $C_{66}H_{49}O_8P_2$:1031.2903, found 1031.2938.

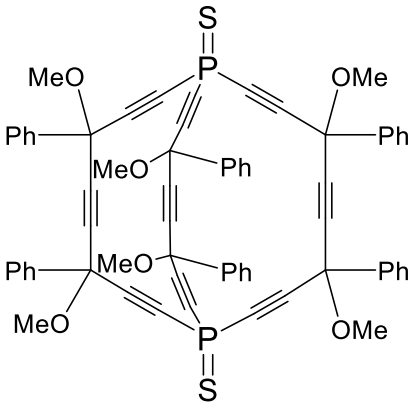

4,7,13,16,21,24-hexamethoxy-4,7,13,16,21,24-hexaphenyl-1,10-diphosphabicyclo[8.8.8] hexacosa-2,5,8,11,14,17,19,22,25-nonayne 1,10-disulfide(17)

To a solution of HMDS (6.5 mmol, 1.3 mL) in 200 mL THF, at -78° C, was added dropwise *n*-butyl lithium (2.5 M, 6.5 mmol, 2.6 mL) under magnetic stirring. After 1 h, the triyne **3** (3 mmol, 942 mg) was added under argon. After 3 h, $PSCl_3$ (0.2 mL, 2 mmol) was added, then the temperature was allowed to warm slowly up to room temperature overnight. After addition of water, the THF was partially evaporated and the mixture was extracted with ethyl acetate. The combined organic extracts were washed by brine, and dried with $MgSO_4$. A preparative TLC purification was done with hexane/ethyl acetate 4:1 as elution mixture, allowing the isolation of **2** (R_f = 0.31) as a slightly yellow paste with 5 % yield (53 mg, 0.05mmol).

^{1}H NMR (400 MHz, $CDCl_3$) δ 7.84 – 7.58 (m, 12H), 7.54 – 7.32 (m, 18H), 3.82 – 3.05 (m, 18H).

^{31}P NMR (162 MHz, $CDCl_3$) δ -46.57 – -46.99 (m).

^{13}C NMR (101 MHz, $CDCl_3$) δ 137.47 – 136.79 (m), 129.99 – 129.42 (m), 129.39 – 128.31 (m), 126.91 – 125.95 (m), 99.85 – 98.19 (m), 84.36 – 83.48 (m), 80.61-78.52 (dm, J = 198.2 Hz), 72.70-71.86 (dm, J = 12.2 Hz), 54.04 – 53.44 (m).

HRMS (DCI/CH_4): m/z calculated for $[M+NH_4]^+$ $C_{66}H_{52}NO_6P_2S_2$: 1080.2711, found 1080.2723.

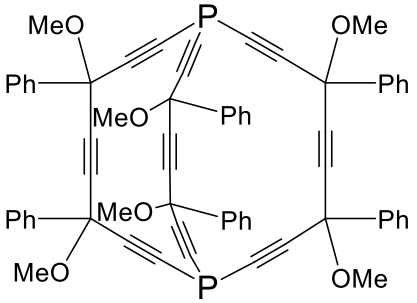

4,7,13,16,21,24-hexamethoxy-4,7,13,16,21,24-hexaphenyl-1,10-diphosphabicyclo[8.8.8] hexacosa-2,5,8,11,14,17,19,22,25-nonayne(18)

18 was obtained as a sideproduct during the synthesis of **17**, isolated by a preparative TLC purification with hexane/ethyl acetate 4:1 as elution mixture (R_f = 0.42) as slightly yellow paste with 1% yield (10 mg, 0.01 mmol).

^{1}H NMR (300 MHz, $CDCl_3$) δ ^{1}H NMR (400 MHz, $CDCl_3$) δ 7.84 – 7.52 (m, 12H), 7.48 – 7.28 (m, 18H), 3.47 (d, *J* = 1664.9 Hz, 18H).

^{31}P NMR (162 MHz, $CDCl_3$) δ -94.31 – -95.26 (m).

HRMS (DCI/CH_4): *m/z* calculated for $C_{66}H_{49}O_6P_2$ $[M+H]^+$: 999.3004, found: 999.2325.

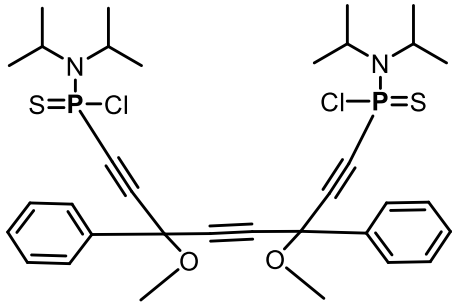

N,N'-(3,6-dimethoxy-3,6-diphenylocta-1,4,7-triyne-1,8-diyl)bis(N,N-diethylphosphona midothioic chloride) (19).

To a solution of the triyne **3** (3 mmol, 942 mg) in 200 mL THF, at -78° C, was added dropwise LDA (6.5 mmol, 6.5 mL) under magnetic stirring. After 3 h, $PSCl_3$ (0.2 mL, 2 mmol) was added, then the temperature was allowed to warm slowly up to room temperature overnight before adding a saturated aqueous NH_4Cl solution and extracted with ethyl acetate (2×50 mL). evaporation of solvents and a rapid chromatographic purification on silica gel eluting with pentane/ethyl acetate 98:2 gave **4** as a yellow paste with 17% yield (350 mg, 0.49 mmol). R_f = 0.5 (pentane/ethyl acetate 95:5).

^{1}H NMR (400 MHz, $CDCl_3$) δ 7.82 – 7.75 (m, 4H), 7.45 – 7.41 (m, 6H), 4.00 (hept, *J* = 7.0 Hz, 4H), 3.63 (m, 6H), 1.43 (dd, *J* = 7.0, 3.0 Hz, 12H), 1.38 (d, *J* = 7.0 Hz, 12H).

^{31}P NMR (162 MHz, $CDCl_3$) δ 31.81 (d, *J* = 7.0 Hz), 31.60 (d, *J* = 6.6 Hz).

^{13}C NMR (75 MHz, $CDCl_3$) δ 129.72 – 128.40 (m), 126.60 – 126.43 (m),96.47(d, *J* = 40.7 Hz), 96.05(d, *J* = 40.7 Hz), 86.41 – 86.14 (m), 84.84, 83.56 (d, *J* = 202.6 Hz), 83.34 (dm, *J* = 205.03 Hz), 72.14 (d, *J* = 3.0 Hz),71.69, 54.07, 53.97 (d, *J* = 1.7 Hz), 53.43, 31.88 (d, *J* = 11.4 Hz), 22.44

(d, J = 3.3 Hz),21.68 (d, J = 4.2 Hz).

MS (MALDI-TOF DCTB/NaI): *m/z* $[M+Na]^+$ found: 731.3.

Elemental analysis: C: 63%, H: 6.4%, N: 3.3%.

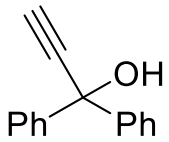

1,1-diphenylprop-2-yn-1-ol (20)

Neat benzophenone (3 g, 16 mmol) was treated at 0 °C with ethynylmagnesium bromide (0.5 M in THF, 66 mL, 32 mmol, 2 equiv) under argon. The mixture was stirred overnight at room temperature. After the completion of the reaction (determined by TLC), the reaction mixture was quenched by addition of an aqueous saturated solution of NH_4Cl (35 mL) and extracted with ethyl acetate (2×50 mL). The combined organic layers were washed with brine, dried over $MgSO_4$, and concentrated under reduced pressure. Purification by silica gel chromatography afforded the expected compound **20** with 94% yield (3.12 g, mm 15mmol).

^{1}H NMR (400 MHz, $CDCl_3$) δ 7.64 (m, J = 8.0, 3.0, 1.4 Hz, 4H), 7.42 - 7.34 (m, 4H), 7.33 - 7.29 (m, 2H), 2.91 (s, 1H), 2.91 (s, 1H).

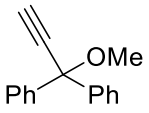

1-methoxyprop-2-yne-1,1-diyl) dibenzene (21)

KOH (33 mmol, 1.8 g) was added in one portion to a solution of **20** (9.6 mmol, 2g) in anhydrous diethyl ether. To this suspension dimethyl sulfate (14 mmol, 1.36 mL) was added slowly with stirring at 0 °C. After the completion of the reaction determined by TLC (1-2 days), water was added to the reaction mixture and organic phase was separated, washed with water and brine and dried over $MgSO_4$ Purification by silica gel chromatography afforded the expected compound **21** with 94% yield (2 g, mm 9mmol).

^{1}H NMR (300 MHz, $CDCl_3$) δ 7.63 - 7.52 (m, 4H), 7.41 - 7.22 (m, 6H,), 3.38 (s, 3H,), 2.92 (s, 1H,).

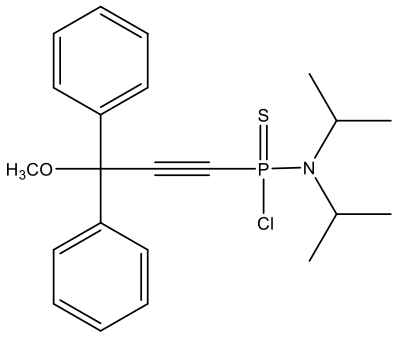

N, N-diethyl-P-(3-methoxy-3,3-diphenylprop-1-yn-1-yl)phosphonamidothioic chloride (22)

To a solution of the alkyne **21** (1.34 g, 6mmol) in 50 mL THF at -78° C, was added dropwise LDA (6.5 mmol, 6.5 mL) under magnetic stirring. After 3 h, $PSCl_3$ (0.2 mL, 2 mmol) was added, then the temperature was allowed to warm slowly up to room temperature overnight. After adding a saturated aqueous NH_4Cl solution, and partial evaporation of the THF, extractions with diethyl ether were performed. The combined organic extracts were washed by brine, dried over $MgSO_4$ and evaporated under reduced pressure. The residue was purified on preparative TLC eluting with pentane/ethyl acetate 98:2, to afford **22** as a yellow paste with 40% yield (1.01 g, 2.4 mmol). R_f = 0.2 (pentane/ethyl acetate 98:2).

^{1}H NMR (300 MHz, $CDCl_3$) δ 7.52 (ddd, J = 8.1, 2.1, 1.2 Hz, 4H), 7.39 – 7.27 (m, 6H), 3.99 (ddq, J = 23.8, 13.7, 6.9 Hz, 2H), 3.41 (s, 3H), 1.37 (dd, J = 25.1, 6.9 Hz, 12H).

^{31}P NMR (121 MHz, $CDCl_3$) δ 32.53.

^{13}C NMR (75 MHz, $CDCl_3$) δ 141.48 – 141.41 (m), 128.43, 128.34 – 128.15 (m), 126.78 – 126.61 (m), 100.51 (d, J = 38.7 Hz), 86.27 (d, J = 233.2 Hz), 81.09 (d, J = 3.6 Hz), 53.25, 49.79 (d, J = 4.7 Hz), 29.87 – 29.53 (m), 29.51 – 29.24 (m), 22.45 (d, J = 4.2 Hz), 21.58 (d, J = 4.3 Hz).

HRMS (DCl-CH_4): *m/z* calculated for $[M+H]^+$: $C_{22}H_{28}ClNOPS$: 420.1318, found: 420.1316.

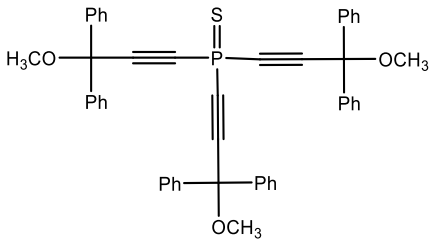

tris(3-methoxy-3,3-diphenylprop-1-yn-1-yl)phosphine sulfide (23)

To a solution of HMDS (0.68 mL, 1.62 mmol) in 50 mL THF, at -78° C, was added dropwise *n*-butyllitium (2.5 M, 1.3 mL, 1.62 mmol) under magnetic stirring. After 1 h, **22** (670 mg, 3 mmol) was added under argon. After 3 h, $PSCl_3$ (0.1 mL, 1 mmol) was added, then the temperature was allowed to warm slowly up to room temperature overnight. After adding a saturated aqueous NH_4Cl solution and partial evaporation of the THF, the mixture was extracted with diethyl ether. The combines organic extracts were washed with brine, dried over $MgSO_4$ and concentrated under reduced pressure. The residue was purified by preparative TLC eluting with pentane/ethyl acetate 96:4. The product eluting at $R_f = 0.48$ was recovered as a slightly yellow solid with 51% yield (371 mg, 0.51 mmol).

^{1}H NMR (400 MHz, $CDCl_3$) δ 7.53 – 7.49 (m, 12H), 7.33 – 7.28 (m, 18H), 3.35 (s, 9H).
^{31}P NMR (162 MHz, $CDCl_3$) δ -45.98.
^{13}C NMR (75 MHz, $CDCl_3$) δ 141.18 (d, J = 1.3 Hz), 128.49, 128.30, 126.63, 103.35 (d, J = 35.6 Hz), 83.93 (d, J = 199.0 Hz), 81.26 (d, J = 3.4 Hz), 53.17.
HRMS (DCl-CH_4): *m/z* calculated for $[M+C_2H_5]^+$ $C_{50}H_{44}O_3PS$: 755.2749, found: 755.2773.

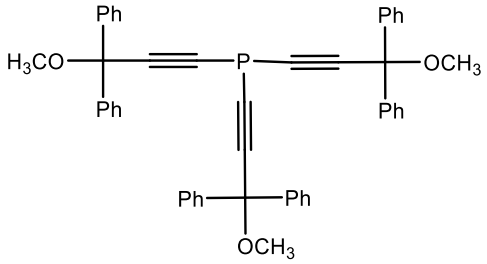

Tris(3-methoxy-3,3-diphenylprop-1-yn-1-yl) phosphane (24)

24 was obtained as a sideproduct during the synthesis of **23**, isolated by a preparative TLC eluting with Pentane/ethyl acetate 96:4. The product **24** eluting at $R_f = 0.65$ was recovered as a slightly yellow solid with 8% yield (55 mg, 0.08 mmol).
^{1}H NMR (400 MHz, $CDCl_3$) δ 7.57 – 7.53 (m, 12H), 7.30 – 7.27 (m, 18H), 3.36 (s, 9H).
^{31}P NMR (162 MHz, $CDCl_3$) δ -93.88.
^{13}C NMR (75 MHz, $CDCl_3$) δ 142.30 (d, J = 1.1 Hz), 128.27, 127.87, 126.65, 105.50 (t, J = 7.0 Hz), 81.44(d, J = 1.5 Hz), 78.66 (d, J = 220.2 Hz), 52.79.

HRMS (DCl-CH_4): *m/z* calculated for $[M]^+$ $C_{48}H_{39}O_3P$: 694.2637, found: 694.2671.

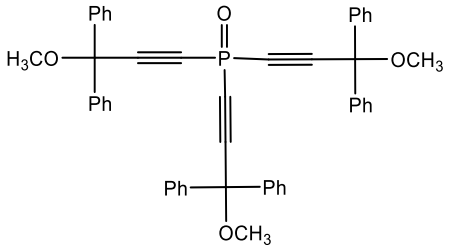

Tris(3-methoxy-3,3-diphenylprop-1-yn-1-yl)phosphine oxide (25)

25 was obtained as a sideproduct during the synthesis of **23**, isolated by a preparative TLC eluting with Pentane/ethyl acetate 96:4. The product **24** eluting at R_f = 0.4 was recovered as a slightly yellow solid with 5% yield (35 mg, 0.05 mmol).

^{1}H NMR (400 MHz, $CDCl_3$) δ 7.49 – 7.45 (m, 12H), 7.33 – 7.25 (m, 18H), 3.31 (s, 9H).

^{31}P NMR (162 MHz, $CDCl_3$) δ -55.06.

^{13}C NMR (75 MHz, $CDCl_3$) δ 140.94 (d, J = 1.35 Hz), δ 128.47, 128.34, 126.60, 103.55 (d, J = 42.5 Hz), 83.44(d, J = 233.0 Hz), 77.20(d, J = 3.5 Hz), 53.12.

HRMS(MALDI-TOF DCTB/NaI): *m/z* calculated for $[M+H]^+$ $C_{48}H_{40}O_4P$: 711.2664, found: 711.2646.

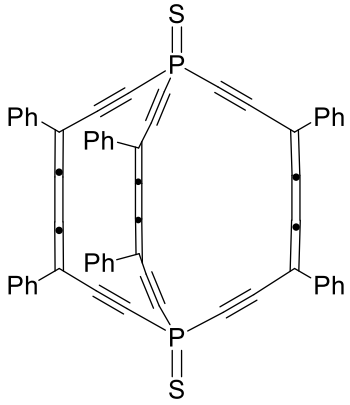

.

(5Z,14Z,22Z)-4,7,13,16,21,24-hexaphenyl-1,10-diphosphabicyclo[8.8.8]hexacosa-4,5,6, 13,14,15,21,22,23-nonaen-2,8,11,17,19,25-hexayne 1,10-disulfide (26)

A solution of **10**（20 mg, 0.024 mmol in DCM (10 mL) was treated with anhydrous $SnCl_2$（60 mg, 1 mmol, 10 equiv) and HCl（2 M in Et_2O, 0.3 mL, 0.6 mmol, 20 equiv) at-78 °C. The mixture was stirred at-78℃ for 30 min and then the temperature was increased slowly in the cooling bath for 4.5 h before adding of 1 M aqueous NaOH (1 mL, 20 equiv). After filtration through Celite®, the organic layer was separated, washed with brine (3x), dried over $MgSO_4$, and concentrated to dryness under reduced pressure. The residue was purified by chromatography on silica gel (Pentane/DCM 1:1) to give the **26** as a strongly colored a bright orange solid with 20 % yield (4 mg, 0.0045mmol).

^{1}H NMR (400 MHz, CD_2Cl_2) δ 7.88 – 7.74 (m, 12H), 7.57 – 7.46 (m, 18H).

^{31}P NMR (162 MHz, CD_2Cl_2) δ -44.61.

References

(1) Zimmerman, H. E.; Paufler, R. M. BICYCLO[2,2,2]-2,5,7-OCTATRIENE (BARRE LENE), A UNIQUE CYCLIC SIX ELECTRON PI SYSTEM. *J. Am. Chem. Soc.* **1960**, *82* (6), 1514–1515. https://doi.org/10.1021/ja01491a071.

(2) Day, A. R.; Edinger, J. M. Protonation and Methylation of Dianions Derived from 1, 4-Bisbiphenylenebutatriene-and 1,4-Bisbiphenylene-1,3-Butadiene. *J. Org. Chem.* **1971**, *36* (1), 240–242. https://doi.org/10.1021/jo00800a064.

(3) Zimmerman, H. E.; Grunewald, G. L.; Paufler, R. M.; Sherwin, M. A. Synthesis and Physical Properties of Barrelene, a Unique Moebius-like Molecule. *J. Am. Chem. Soc.* **1969**, *91* (9), 2330–2338. https://doi.org/10.1021/ja01037a024.

(4) Hine, J.; Brown, J. A.; Zalkow, L. H.; Gardner, W. E.; Hine, M. The Synthesis of Bi cyclo [2,2,2]-2,5-Octadiene [1,2]. *J. Am. Chem. Soc.* **1955**, *77* (3), 594–598. https://doi.org/10.1 021/ja01608a022.

(5) Kobayashi, Y.; Kumadaki, I.; Ohsawa, A.; Hamana, H. 2,3,5,6-Tetrakis (Trifluorom ethyl)-1,4-Diphosphabenzene. *Tetrahedron Letters* **1976**, *17* (41), 3715–3716. https://doi.org /10.1016/S0040-4039(00)93089-2.

(6) Zhu, C.; Poater, A.; Duhayon, C.; Kauffmann, B.; Saquet, A.; Rives, A.; Maraval, V.; Chauvin, R. *Carbo* -mer of Barrelene: A Rigid 3D-Carbon-Expanded Molecular Barrel. *Che*

mistry A European J **2021**, *27* (36), 9286–9291. https://doi.org/10.1002/chem.202100670.

(7) Li, Z.; Smeu, M.; Rives, A.; Maraval, V.; Chauvin, R.; Ratner, M. A.; Borguet, E. To wards Graphyne Molecular Electronics. *Nat Commun* **2015**, *6* (1), 6321. https://doi.org/10.1 038/ncomms7321.

(8) Garcia-Lekue, A.; Wang, L.-W. Elastic Quantum Transport Calculations for Molecu lar Nanodevices Using Plane Waves. *Phys. Rev. B* **2006**, *74* (24), 245404. https://doi.org/10.1 103/PhysRevB.74.245404.

(9) Bucknum, M. J.; Castro, E. A. The Carbon Allotrope Hexagonite and Its Potential S ynthesis from Cold Compression of Carbon Nanotubes. *J. Chem. Theory Comput.* **2006**, *2* (3), 775–781. https://doi.org/10.1021/ct060003n.

(10) Karfunkel, H. R.; Dressler, T. New Hypothetical Carbon Allotropes of Remarkable Stability Estimated by MNDO Solid-State SCF Computations. *J. Am. Chem. Soc.* **1992**, *114* (7), 2285–2288. https://doi.org/10.1021/ja00033a001.

(11) Ducéré, J.-M.; Lepetit, C.; Chauvin, R. Carbo-Graphite: Structural, Mechanical, an d Electronic Properties. *J. Phys. Chem. C* **2013**, *117* (42), 21671–21681. https://doi.org/10.1 021/jp4067795.

(12) Baglai, I.; de Anda-Villa, M.; Barba-Barba, R. M.; Poidevin, C.; Ramos-Ortíz, G.; Maraval, V.; Lepetit, C.; Saffon-Merceron, N.; Maldonado, J.-L.; Chauvin, R. Difluorenyl C arbo-Benzenes: Synthesis, Electronic Structure, and Two-Photon Absorption Properties of H ydrocarbon Quadrupolar Chromophores. *Chemistry – A European Journal* **2015**, *21* (40), 14 186–14195. https://doi.org/10.1002/chem.201500482.

(13) Leroyer, L.; Lepetit, C.; Rives, A.; Maraval, V.; Saffon-Merceron, N.; Kandaskalov, D.; Kieffer, D.; Chauvin, R. From Hexaoxy-[6]Pericyclynes to Carbo-Cyclohexadienes, Car bo-Benzenes, and Dihydro-Carbo-Benzenes: Synthesis, Structure, and Chromophoric and R edox Properties. *Chemistry – A European Journal* **2012**, *18* (11), 3226–3240. https://doi.org/ 10.1002/chem.201102993.

(14) Vallejos, M. M.; Pellegrinet, S. C. Theoretical Study of the BF3-Promoted Rearran gement of Oxiranyl N-Methyliminodiacetic Acid Boronates. *J. Org. Chem.* **2017**, *82* (11), 59 17–5925. https://doi.org/10.1021/acs.joc.7b01096.

(15) Zhu, C.; Wang, T.-H.; Su, C.-J.; Lee, S.-L.; Rives, A.; Duhayon, C.; Kauffmann, B.; Maraval, V.; Chen, C.; Hsu, H.-F.; Chauvin, R. 3D and 2D Supramolecular Assemblies and

Thermotropic Behaviour of a Carbo-Benzenic Mesogen. *Chem. Commun.* **2017**, *53* (43), 5902–5905. https://doi.org/10.1039/C7CC02430D.

(16) Xu, B.; Tao, N. J. Measurement of Single-Molecule Resistance by Repeated Formation of Molecular Junctions. *Science* **2003**, *301* (5637), 1221–1223. https://doi.org/10.1126/science.1087481.

(17) Gawel, P.; Dengiz, C.; Finke, A. D.; Trapp, N.; Boudon, C.; Gisselbrecht, J.-P.; Diederich, F. Synthesis of Cyano-Substituted Diaryltetracenes from Tetraaryl[3]Cumulenes. *Angewandte Chemie International Edition* **2014**, *53* (17), 4341–4345. https://doi.org/10.1002/anie.201402299.

(18) Leroyer, L.; Lepetit, C.; Rives, A.; Maraval, V.; Saffon-Merceron, N.; Kandaskalov, D.; Kieffer, D.; Chauvin, R. From Hexaoxy-[6]Pericyclynes to Carbo-Cyclohexadienes, Carbo-Benzenes, and Dihydro-Carbo-Benzenes: Synthesis, Structure, and Chromophoric and Redox Properties. *Chemistry* **2012**, *18* (11), 3226–3240. https://doi.org/10.1002/chem.201102993.

(19) A. A. Granovsky. Firefly. http://classic.chem.msu.su:gran:firefly:index.html.

(20) Schmidt, M. W.; Baldridge, K. K.; Boatz, J. A.; Elbert, S. T.; Gordon, M. S.; Jensen, J. H.; Koseki, S.; Matsunaga, N.; Nguyen, K. A.; Su, S.; Windus, T. L.; Dupuis, M.; Montgomery Jr, J. A. General Atomic and Molecular Electronic Structure System. *Journal of Computational Chemistry* **1993**, *14* (11), 1347–1363. https://doi.org/10.1002/jcc.540141112.

(21) Rives, A.; Baglai, I.; Malytskyi, V.; Maraval, V.; Saffon-Merceron, N.; Voitenko, Z.; Chauvin, R. Highly π Electron-Rich Macro-Aromatics: Bis(p-Aminophenyl)-Carbo-Benzenes and Their DBA Acyclic References. *Chem. Commun.* **2012**, *48* (70), 8763–8765. https://doi.org/10.1039/C2CC34176J.

(22) Baglai, I.; Maraval, V.; Bijani, C.; Saffon-Merceron, N.; Voitenko, Z.; Volovenko, Y. M.; Chauvin, R. Enhanced π-Frustration in Carbo-Benzenic Chromophores. *Chem. Commun.* **2013**, *49* (75), 8374–8376. https://doi.org/10.1039/C3CC43204A.

Chapter 4. Reactivity and coordination chemistry of ring carbo-mers of P-heterocyles and acyclic model thereof

1. Introduction

Research conducted over the past decades on 1,4-diphosphinine and diphosphacyclohexane derivatives has revealed unexpected features of these unique phosphorus-containing heterocycles in coordination chemistry. For instance, the saturated analog **28** of 1,4-diphosphinine, namely 1,4-diphosphacyclohexane, first described in 1959[1], was later reported to behave as a versatile κ^2 bidentate ligand, bridging in dinuclear complexes **28-M₂**, chelating in complexes **28-M**, or doubly bridging in dimeric complexes **28₂-M₂**.[2,3] (**Figure 4.1**). Such diphosphines could also be used to prepare coordination polymers.

Only a few reports have been published on the coordination chemistry of diphosphabarrelene derivatives **29**, despite their key rigidity offering a strong potential to form polymeric materials where organic substrates and metal moieties are arranged alternately. In 1993, a complex **29-M₂** was first reported to be produced from **29** and $W(CO)_5(THF)$ at room temperature in 72 % yield [4]. The same year, Lang *et al*. reported a monometallic chromium(0) complexs **30-M** of 1-phenyl-4-benzyl-1,4-dihydro-1,4-diphosphinine **30** [5], but no dimetallic complex **30-M₂** was described.

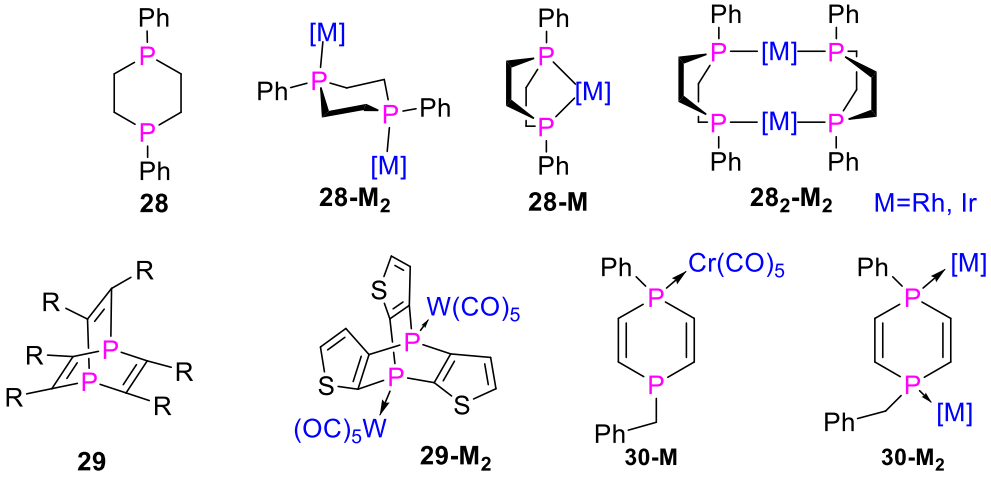

Figure 4.1. Examples of known metal complexes prepared from 1,4-diphosphacyclohexane, diphosphabarrelene, and 1,4-dihydro-1,4-diphosphinine derivatives[2,3,4,6,7].

The use of phosphabarrelenes as ligands in catalytic reactions has previously been reported by the group of Mezailles and Le Floch [6,7]. Developing their work on Pd-catalysed Suzuki coupling reactions, Mezailles, Le Floch *et al*. investigated the reduction of a Pd(II) complex precursor to

give the highly active Pd(0) species [8]: from their previous work, indeed, both the Pd(II) **31-M** and Pd(0) **31$_2$-M** complexes (**Figure 4.2**) showed similar catalytic reactivity. In order to understand the catalytic process in more details, a stepwise reduction of the Pd(II) complex **31-M** was conducted (**Scheme 4.1**).

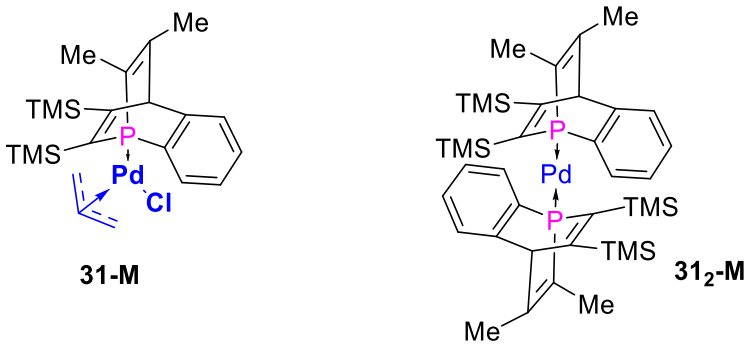

Figure 4.2. Phosphabarrelene complexes used in Suzuki coupling reactions (see ref. 8).

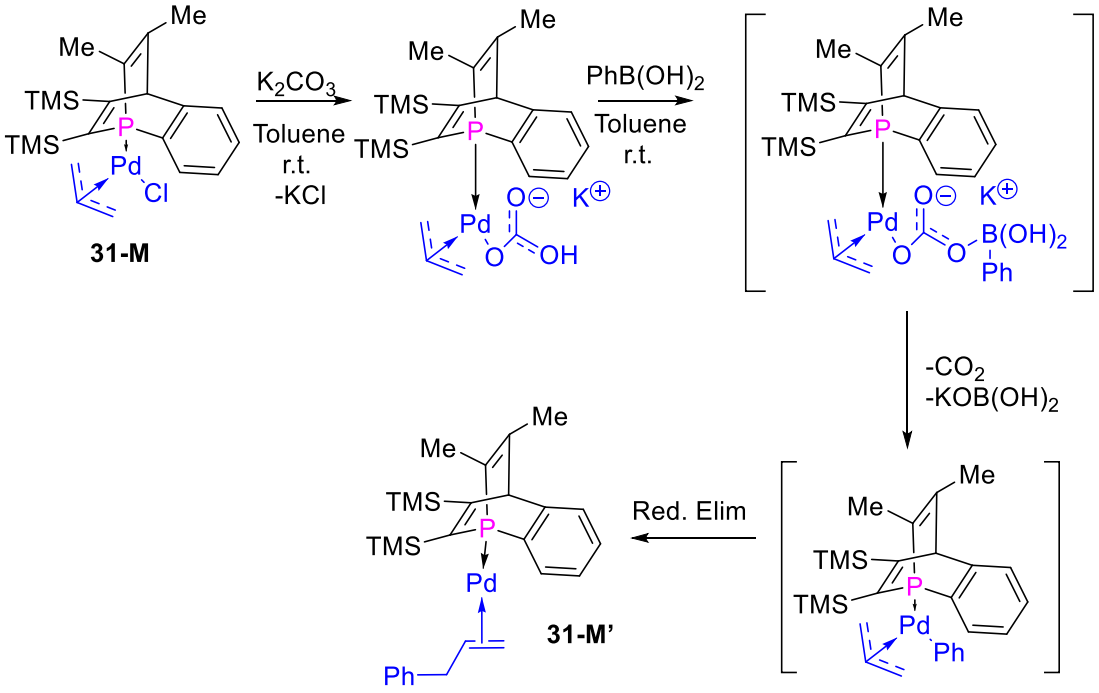

Scheme 4.1. Stepwise reduction of **31-M** to **31-M'** according to ref. 8

In 2019, researchers investigated the cycloisomerisation of N-benzoyl propargylamine **32** using gold complexes and a selection of phosphabarrelenes as ligands (**Scheme 4.2**).[9] They

observed a high selectivity (> 98%) in 5-methylidene-2-phenyl-4*H*-1,3-oxazole **33** over 5-methyl-2-phenyl-1,3-oxazole **34**, using [(**L**)AuCl]-complexes of strongly donating and bulky ligands **L** = **35-38** (**Scheme 4.2**), in combination with $AgSbF_6$ as a chloride abstracting reagent. In the absence of $AgSbF_6$, the ligands **35** and **37** showed no reactivity, while **38** gave much lower selectivity than **36**. As previously stated, a switch in selectivity to form **34** was achievable without $AgSbF_6$, albeit with low conversion. The addition of $AgSbF_6$ resulted in a change in selectivity back to **33** (4:1, **33:34**), again with low conversion. This emphasizes a significant role that the ligands' steric properties play in this process.

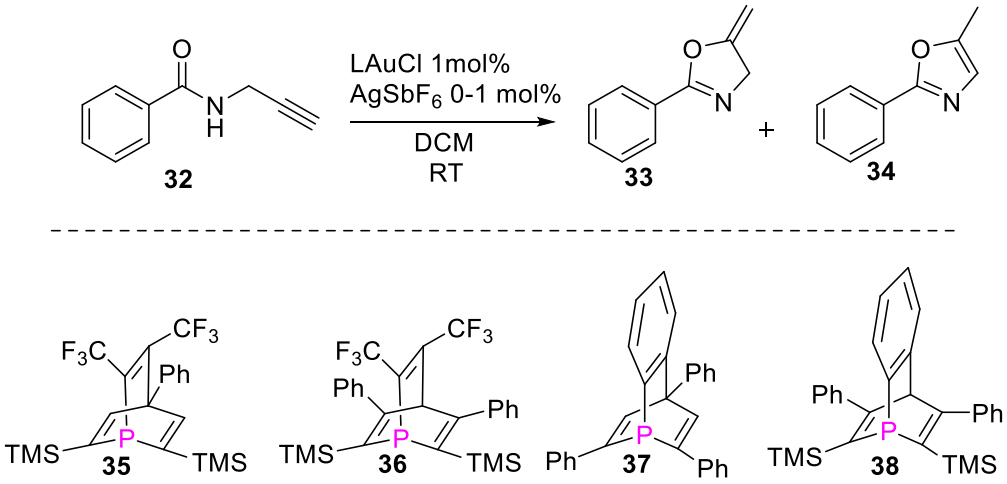

Scheme 4.2. Au(I)-catalyzed cycloisomerisation reaction (top) and ligands **L** investigated in the study (bottom).

While phosphabarrelene and diphosphacyclohexane derivatives[2,3,4,6,7] were thus investigated for their coordination and catalytic properties, the corresponding ring *carbo*-mers[10] deserve consideration regarding the competing coordination of the P(III) atoms and triple bonds towards metals (**Figure 4.3**). This is envisaged hereafter, first on model di- and tri-alkynyl-monophosphine.

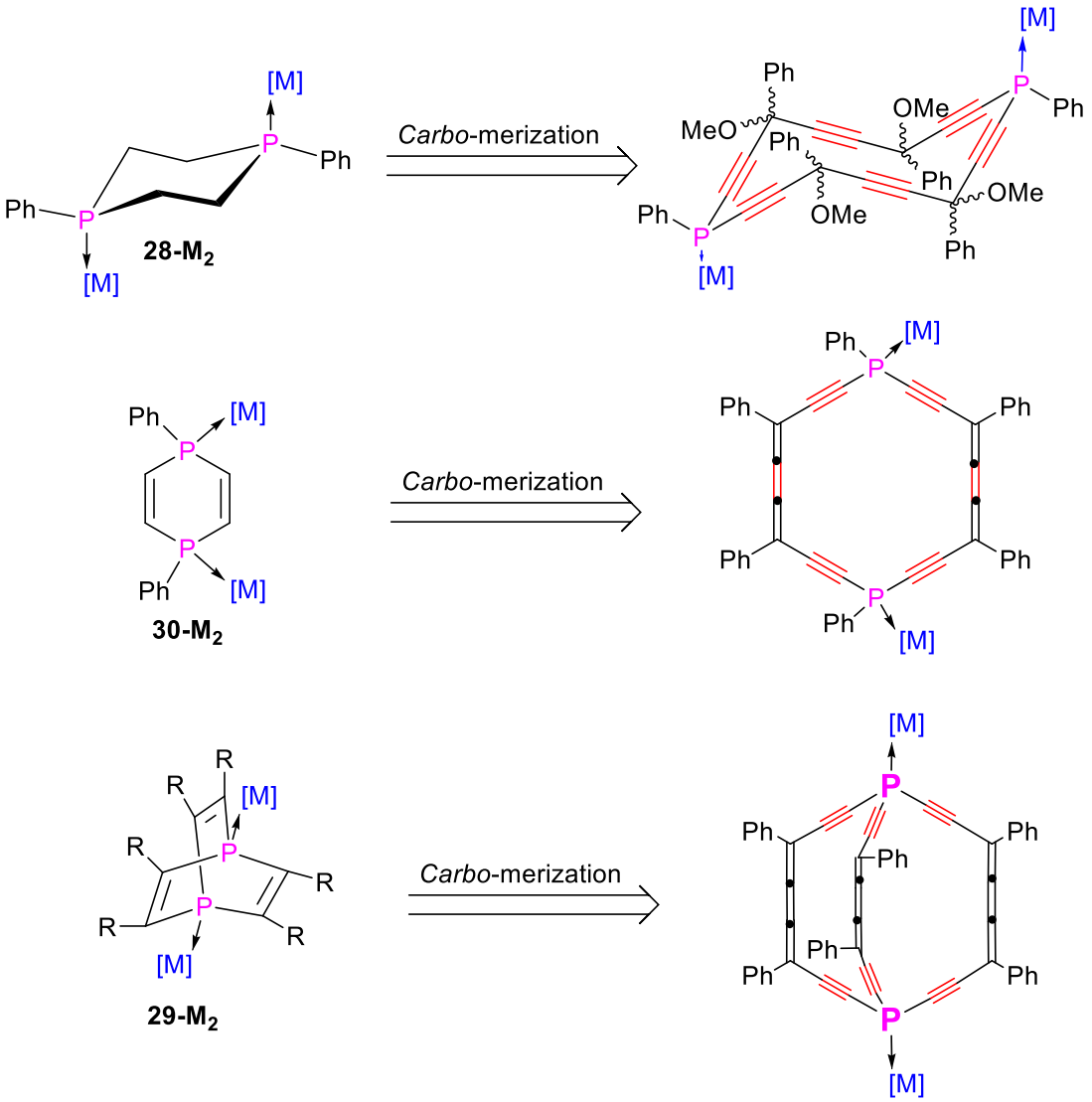

Figure 4. 3. Ring *carbo*-merization of diphosphacyclohexane, dihydrodiphosphinine and diphosphabarrelene derivatives[2,3,4].

2. Reduction of dialkynylthiophosphines to corresponding phosphines

One of the classical protection method of phosphine P(III) centers consists in their oxidation into the corresponding P=O or P=S derivatives, followed by their ultimate reduction back to P(III) centers suitable for selective coordination to transition metals.[11,12,13] Following incidental observations (Chapters 2), the possibility to desulfurize the *carbo*-1,4-diphenyl-1,4-dihydro-1,4-dithio-1,4-diphosphinine **13** in a preparative way was studied with the view to preparing P-coordination complexes.

Phosphine sulfides can actually be reduced by various organic and inorganic reagents. Sodium[14], copper[15], or iron[16] were initially used to produce corresponding phosphines. However, these metals could only be used to reduce highly resistant phosphine sulfides due to the extreme reaction conditions required, such as very high temperatures and long reaction times. Reductions utilizing strongly nucleophilic P(III) reagents, such as tri-*n*-butyl-phosphine[17], tris(2-cyanoethyl)phosphine[18], or hexamethyl-phosphorous triamide (HMPT, $P(NMe_2)_3$), also require high-temperatures .

The available amounts of **13** being limited, the reactions were first tested from the model dialkynyl(phenyl)thiophosphine **39**, which could be prepared in one step with 86 % yield by addition of 2 equivalents of the lithium reagent of the previously described propargylic ether **21**[19–21] to $P(S)PhCl_2$ using LiHMDS as base (**Scheme 4.3**). The structure of **39** was confirmed by X-ray diffraction analysis of light yellow single crystals that deposited from an EtOAc/pentane mixture (**Scheme 4.3**).

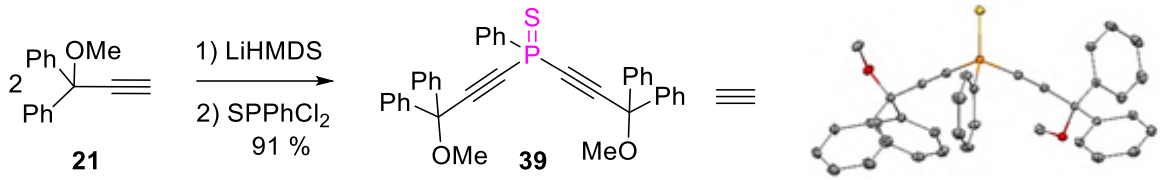

Scheme 4. 3. Synthesis of the model dialkynyl(phenyl)thiophosphine **39** and its X-ray crystal structure (CCDC deposition number 2342365).

Various procedures were attempted to reduce the model dialkynylthiophosphine **39** to the corresponding phosphine 40 (**Scheme 4.4**).

A two-step process was fist attempted, involving initial methylation of the sulfur atom with MeOTf,[22] followed by treatment with $P(NMe_2)_3$[23,24]. ^{31}P NMR monitoring of the reaction suggested that the S-methylated product was indeed formed, according a new up-field signal at -22.31 ppm (top **Figure 4.3**). After full conversion of **39** to the putative (methylsulfinyl)phosphonium triflate, desulfurization was attempted using $P(NMe_2)_3$[24] or $NaSCH_3$[25]. However, both reagents caused the disappearance of all ^{31}P NMR signals, indicating the likely decomposition of the product.

Desulfurization of **39** was also attempted using $LiAlH_4$,[26] but it resulted in the disappearance of the signal of **39** accompanied by a fast appearance of three main downfield signals far from the – 64 ppm region expected for the desulfurized product **40** (middle **Figure 4.3**).

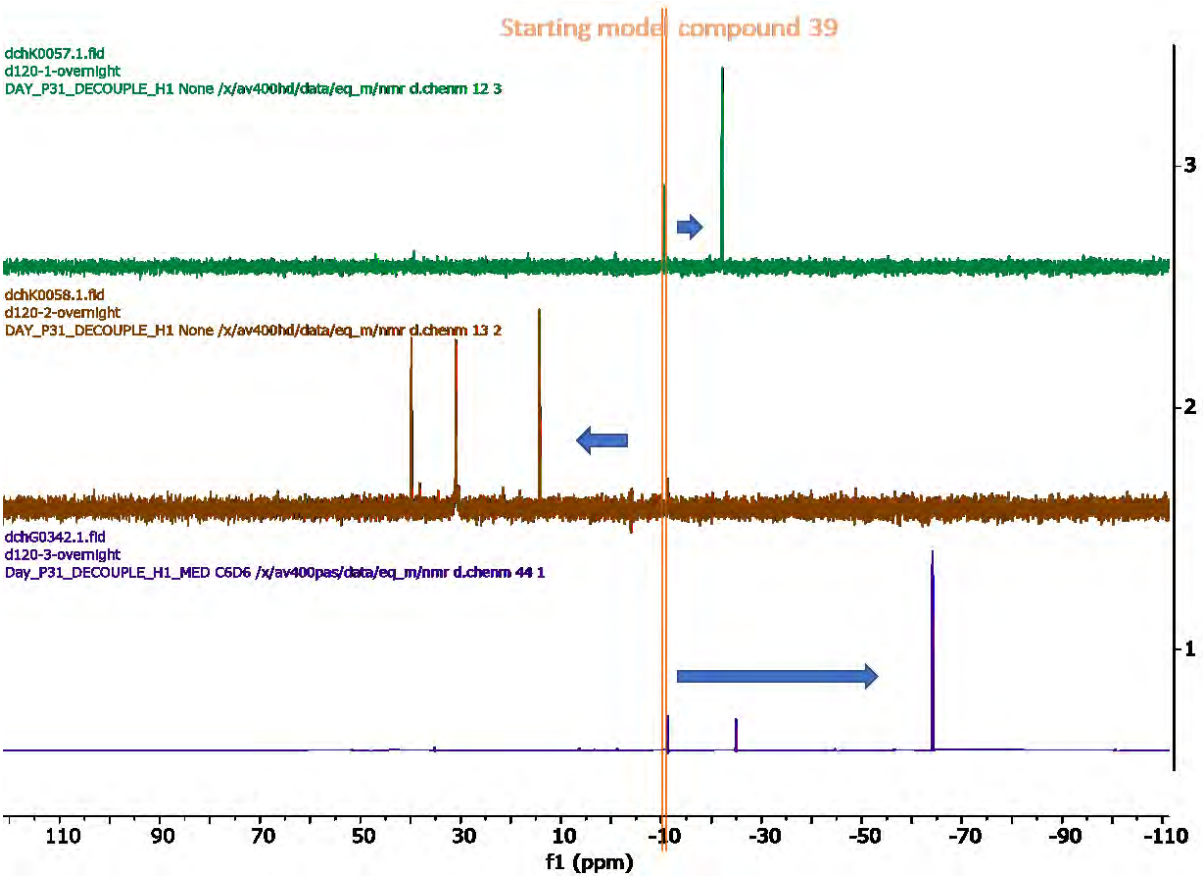

Figure 4.3. ^{31}P NMR monitoring of attempted reduction of the model dialkynylthiophosphine **39** to the corresponding phosphine **40**: *top*: with MeOTf/HMPT, *middle*: with $LiAlH_4$, *bottom*: with $(Me_3Si)_3SiH$.

Finally, the radical-based reduction with $(Me_3Si)_3SiH$ in the presence of AIBN as radical initiator at 70° C [27] appeared to be efficient. The ^{31}P NMR monitoring indeed shows the progressive decrease of the signal of **39** at -10.8 ppm and the appearance of a main signal at ca -64 ppm as expected for the desulfurization product **40**, along with small by-product signals near -25 ppm, (bottom **Figure 4.3**).

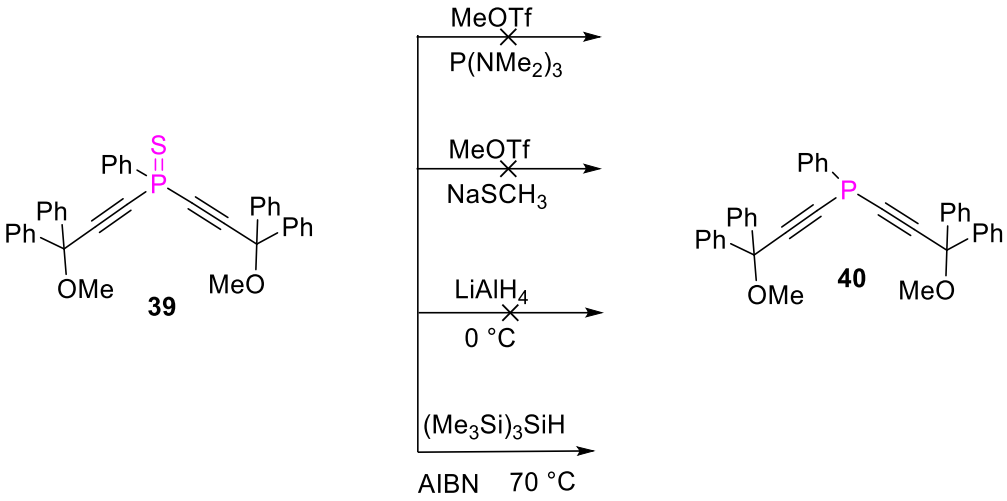

Scheme 4.4. Different methods attempted for the desulfurization of the model dialkynylthiophosphine **39.**[22,24,28,29,27,26]

Though quite air-sensitive, the phosphine **40** could be isolated as a yellow liquid with a 75% yield after purification on preparative TLC eluting with pentane/EtOAc 98/2.

In the presence of air, the corresponding phosphine oxide **41** was readily formed and isolated quantitatively as a white paste. (**Scheme 4.5**).

Both products were fully characterized, including by X-ray diffraction analysis for **41**.

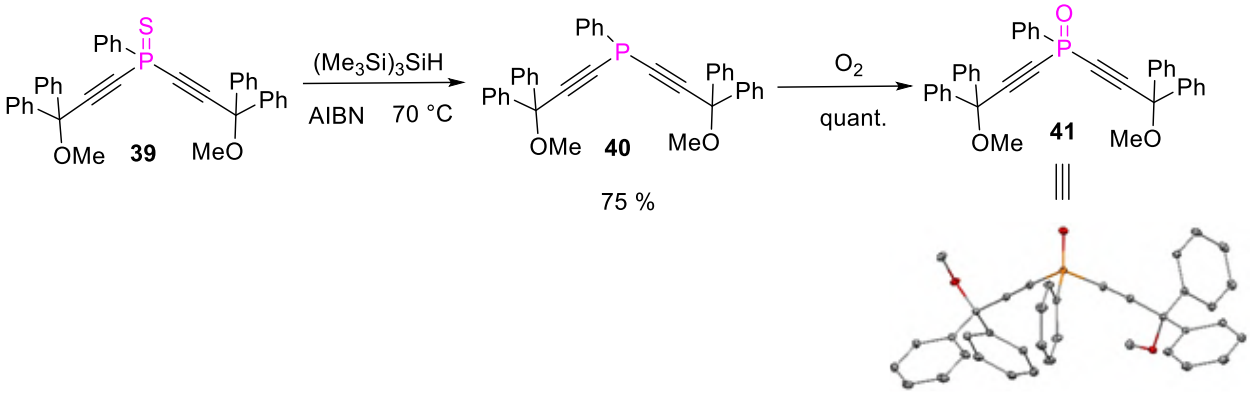

Scheme 4.5. Reduction of the model dialkynylthiophosphine **39** to the corresponding phosphine **40**, and X-ray crystal structure of its oxide **41** (CCDC deposition number 2342364).

The same methodology was therefore attempted for the desulfurization of the *carbo*-dithiodiphosphacyclohexane **17** using two equivalents of $(Me_3Si)_3SiH$ and 5% AIBN. The reaction took 50 hours to reach 100% conversion, which is significantly longer than the 3 hours required

for the desulfurization of the model compound **39**. In the presence of the oxygen of air, the formed *carbo*-diphosphacyclohexane **18** was partially or completely oxidized to the monoxide **16** and dioxide **42** (**Scheme 4.6**). The ^{31}P NMR spectrum gives two massives, with the shift around -23 ppm which are corresponding to the phosphine oxide group and around -64 ppm which are corresponding to the phosphine group respectively, The MS result also validated the formation of **42**.

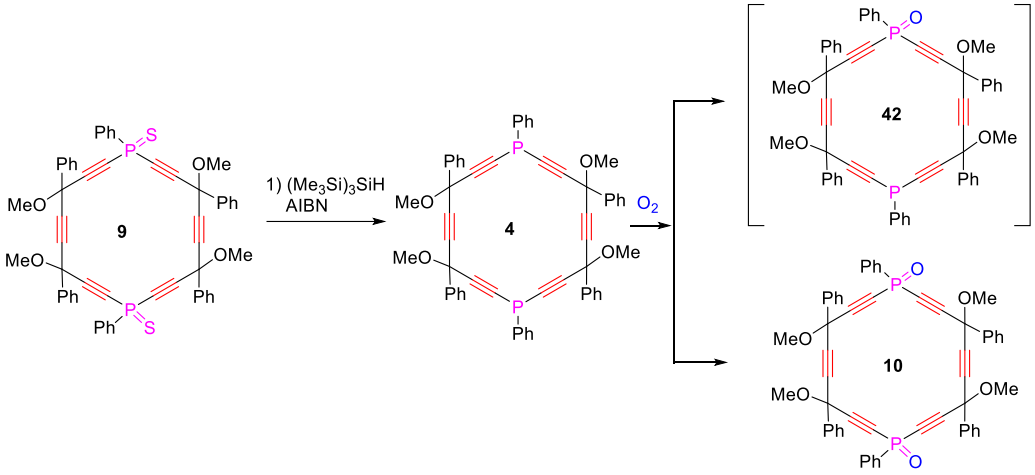

Scheme 4.6. Redox reactivity of the *carbo*-dithiodiphosphacyclohexane **9**.

3. Explorations in coordination chemistry

Preliminary studies of the coordination chemistry of the model dialkynylphosphine **40** were also performed, with the synthesis of the ruthenium complex **43** and rhodium complex **44**. Their preparation was achieved through a two-step one-pot process from the thiophosphine **39**, without isolation of the phosphine intermediate **40** to prevent the formation of the phosphine oxide **41** as a side-product (**Scheme 4.7**).

The ruthenium complex **43** was isolated as a red-orange solid with 71 % yield, while the rhodium complex **44** was obtained in mixture with impurities showing a very similar solubility, thus preventing their separation.

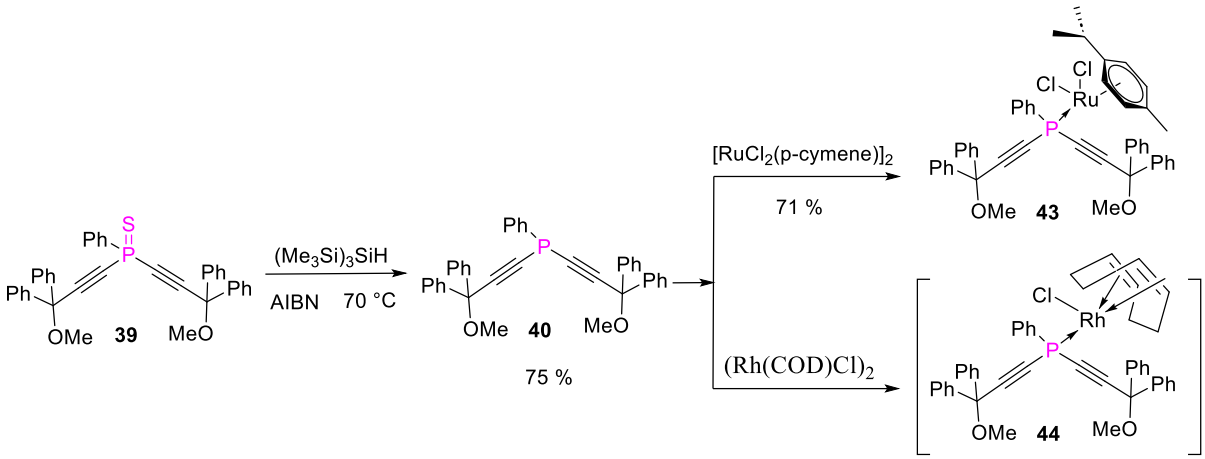

(a)

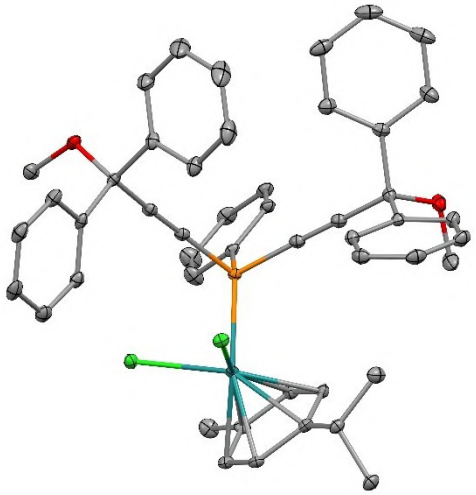

(b)

Scheme 4.7. Synthesis of the ruthenium complex **43** and rhodium complex **44** (a), and X-ray structure of the ruthenium complex **43** (CCDC number:2331290) (b).

The ^{31}P NMR spectrum of the Ru(II) complex **43** and Rh(I) complex **44** shows signals at very close chemical shifts, the Ru(II) complex exhibiting a singlet at -18.83 ppm, while the Rh(I) complex displays a doublet at -18.49 ppm with a ^{103}Rh-^{31}P coupling constant J_{RhP} = 163.9 Hz (**Figure 4.4**). In both spectra, a signal was detected at -21 ppm, corresponding to the phosphine oxide **41**, which could be removed then by washing with diethyl ether.

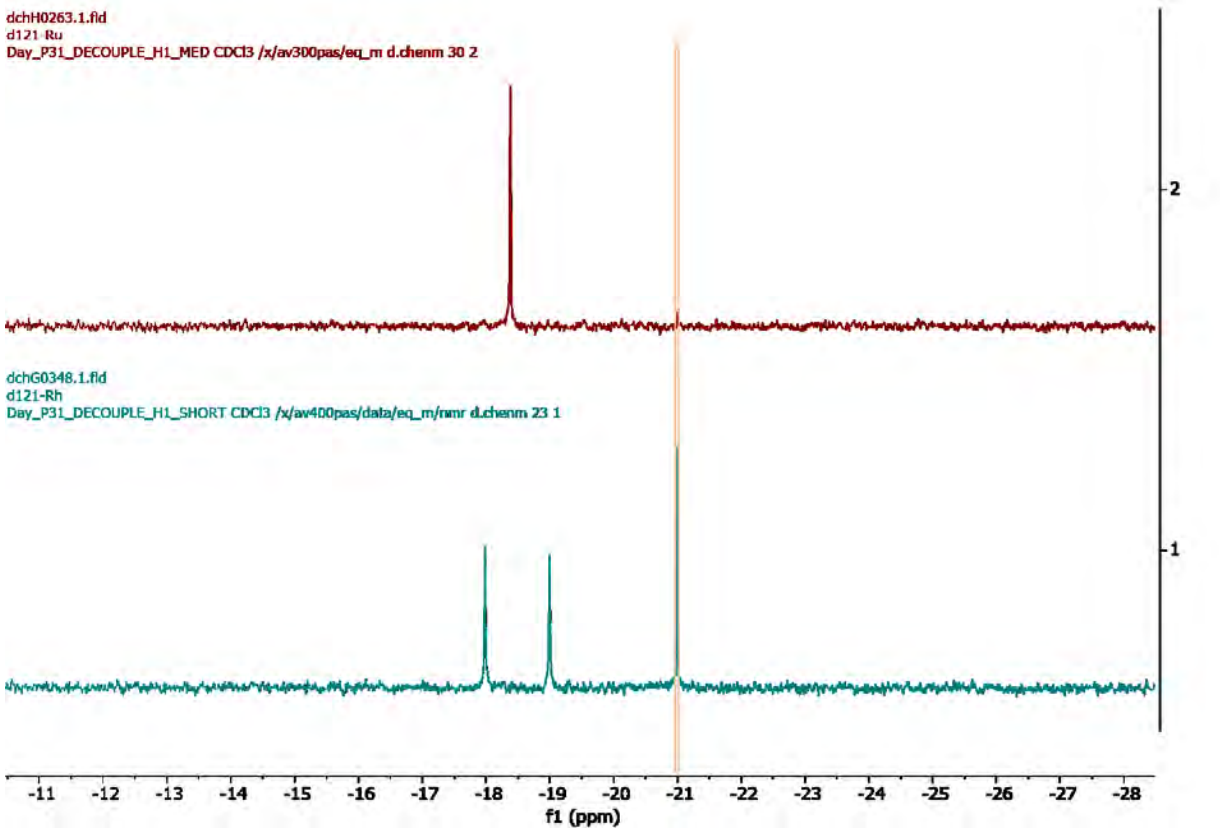

Figure 4.4. ^{31}P NMR monitoring of the preparation of the ruthenium complex **43**, and rhodium complex **44**.

The same two-step methodology was thus attempted first on the *carbo*-dihydro-dithiodiphosphinine **13** to prepare the corresponding diruthenium complex **45**. However, treatment of **13** with $(Me_3Si)_3SiH$ and AIBN was found to induce the decomposition of the macrocycle, probably because of the diradical character of the butatriene units (which are not present in the model phosphine **40**),[30] making them sensitive to radical reaction conditions.

The synthesis of a diruthenium complex **46** was thus attempted from the stereoisomeric mixture of *carbo*-dithiodiphosphacyclohexane **9** (**Scheme 4.8**). By successive treatments with 2 equivalents of $(Me_3Si)_3SiH$ and 1 equivalent $[RuCl_2(p\text{-cymene})]_2$, the Ru(II) complex **46** was obtained as a mixture of stereoisomers as main product, along with the mono-oxidized by-product **47** whose formation was confirmed by NMR and HRMS.

Attempts at reduction of **46** to **45** using various acidic and reductive reagents failed only inducing degradation of the product as indicated by the disappearance of all sharp ^{31}P NMR signals in trials #1 and trial# 2 (**Table 4.1**). In the absence of Brønsted acid (trial # **3**), no reaction was

observed, while the use of the reductive reagents P_2I_4 instead of $SnCl_2$ (trial # 4) also provoked decomposition of **13**.

Table 4.1. Different conditions tested for the reductive elimination reaction.

Condition / Trial	Precursor	Solvent	Reducing reagents	Brønsted acid
1	**13**	DCM	$SnCl_2$	HCl
2	**13**	DCM	$SnCl_2$	Acetic acid
3	**13**	DCM	$SnCl_2$	None
4	**13**	DCM	P_2I_4	None

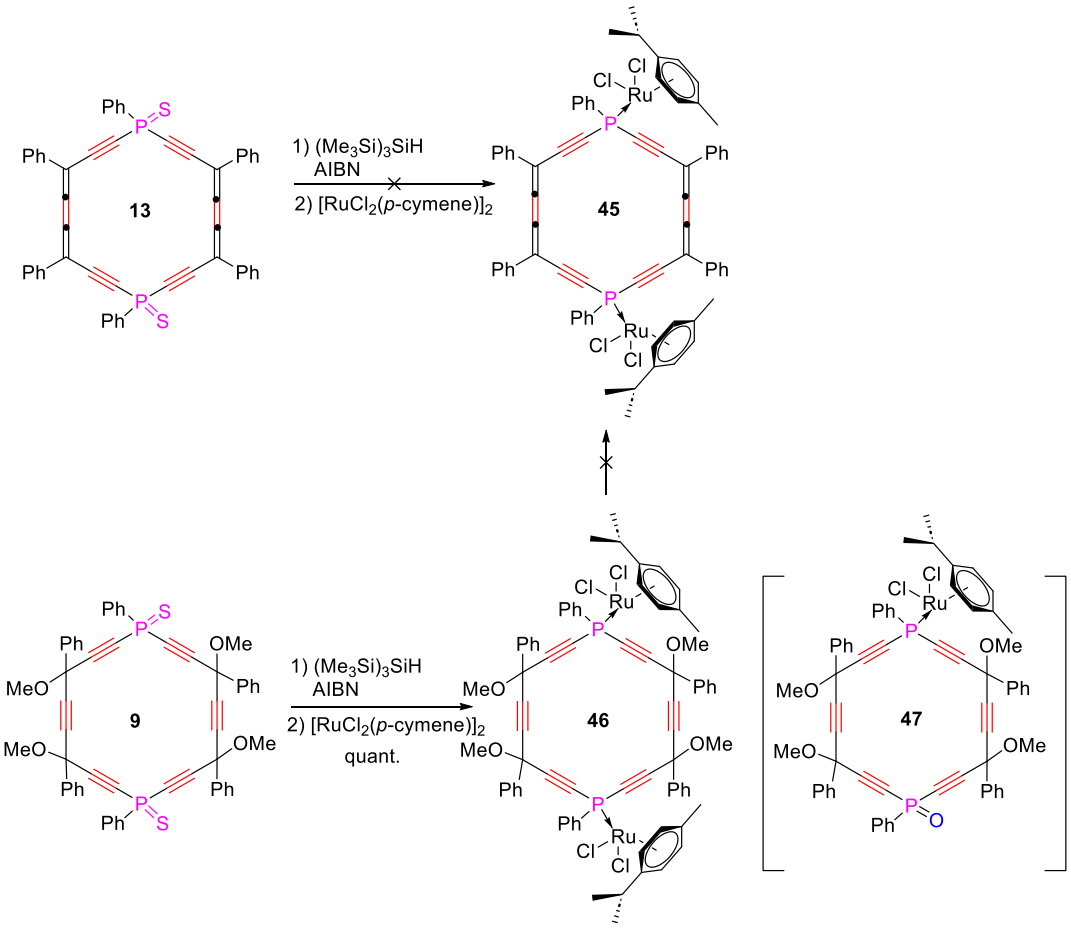

Scheme 4.8. Synthesis of a stereoisomeric mixture of the diruthenium complex **46** and attempts at reduction to the hexaphenyl-*carbo*-1,4-diphenyl-1,4-dihydro-1,4-diphosphine complex **45**.

4. Perspectives of alkynylphosphine complexes in catalysis

Complexes of alkynylphosphines were reported as active and selective catalysts for hydroboration of a wide range of alkenes[31]. From a more basic standpoint, coordination chemistry of alkynylphosphines is an area of significant interest:[32–70] while phosphines are typical η^1-P-ligands of transition metals, alkynes also bind to such metals in a η^2-π fashion.

Rhodium phosphine complexes are highly efficient catalysts for hydroboration of alkenes using catecholborane ("HBcat"), and in 2006, C. M. Vogels *et al*. reported acetylacetonate rhodium complexes of monodentate alkynylphosphines and examined their ability to catalyze the hydroboration of vinylarenes (**Figure 4. 5**).

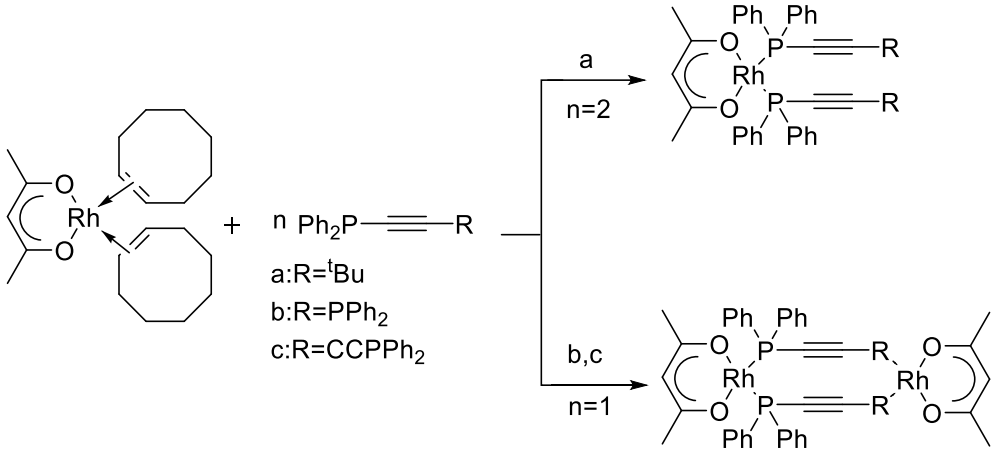

Figure 4. 5. Acetylacetonate rhodium complexes of monodentate alkynylphosphine ligands.

The chemistry of Ru(II) complexes of highly unsaturated ligands, and in particular alkynyl-phosphines, has not been studied in a systematic manner. In 2000, Ru(II) with allyl phosphine ligands were reported by Nelson *et al.*[71 72], who showed that some of them exhibit unusual reactivity. A noteworthy aspect of this kind of complexes is the possibility of simultaneous coordination of both the phosphine and alkene or alkyne moieties to the ruthenium center. Such ligands PPh_2–C⁝C–R associated to metal centers have revealed remarkable catalytic activity for P−C bond cleavages, insertion, or C-C coupling reactions. In particular, P-cooordination of such Ph_2P–Cα⁝Cβ−R ligands typically induces polarization of the alkyne moiety. As a result, the Cα center becomes partially negatively charged, making the triple bond prone to undergo heteropolar addition of simple

molecules such as water, ethanol, XH, $HPPh_2$, or non-tertiary amines.[54]

The ring *carbo*-mer of diphosphacyclohexane **4** and diphosphabarrelane **18** are respectively a bis(dialkynylphosphine) and a bis(trialkynylphosphine) exhibiting similar features that could be both compatible with P-coordination to transition metals. However, they possess large molecular sizes, more or less flexible spatial configurations, and are π-electron rich molecules (**Figure 4.6**). These unique features for potential diphosphine ligands open prospects in catalysis, e.g. for hydrogen transfer, C–C bond formation or hydroboration reactions, while remaining aware of the competitivity of the constitutive unsaturations of the ligands.

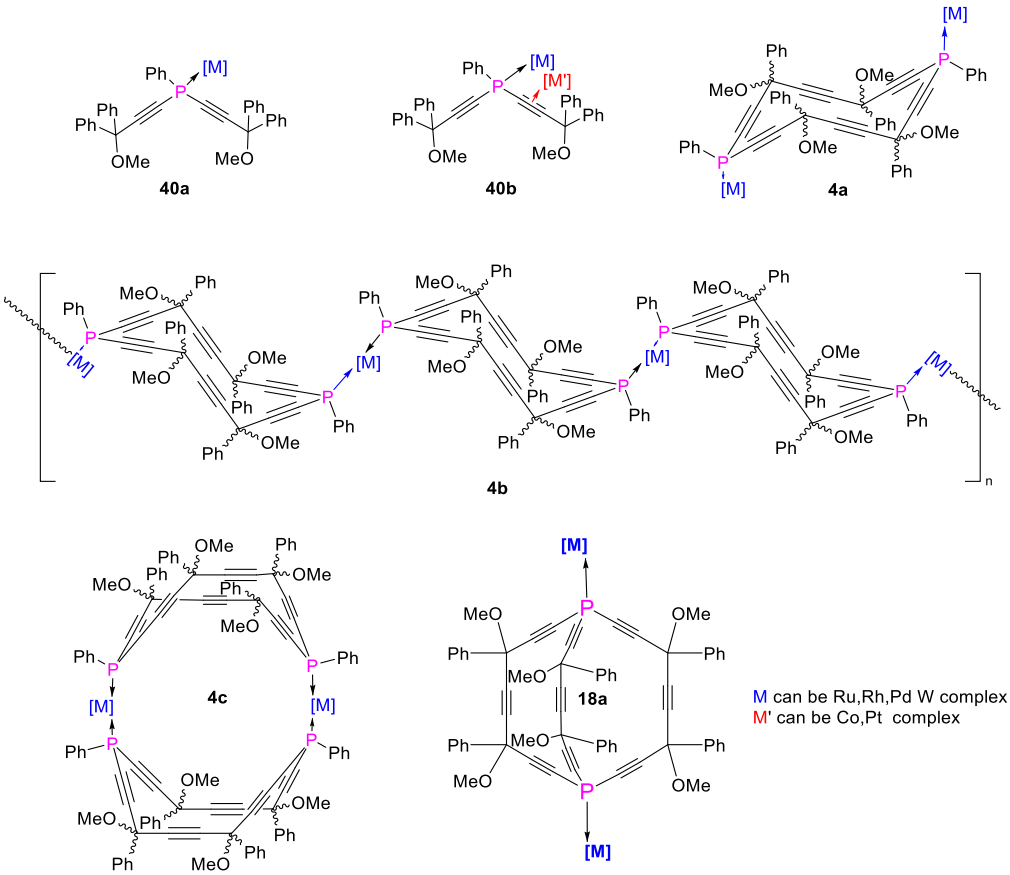

Figure 4.6. Possible coordination complexes of *carbo*-diphosphacyclohexane and *carbo*-diphosphabarrelane derivatives for use in catalysis.

5. Conclusion

The model functional dialkynylphenylphosphine bis(3-methoxy-3,3-diphenylprop-1-yn-1-yl)(phenyl)phosphine **40** and its oxidized analogue **41** were obtained by an efficient radical desulfurization process, which happen to be remarkably compatible with the carbon-carbon triple bonds of the starting phosphine sulfide **39**. The coordination of **40** in a Ru(II) complex **43** open prospects for a related κ^2 P,P-coordination of the *carbo*-diphosphacyclohexane **4** and c*arbo*-diphosphabarrelane **18**. The new products were characterized by NMR, HRMS and X-ray diffraction analysis for **39**, **41** and **43**.

With the same method through a two-step-one-pot process, the diruthenium complex **46** was thus prepared from the hexaphenyl-tetramethoxy-*carbo*-1,4-diphosphacyclohexane **4** as a stereoisomeric mixture. Unlike its parent diphosphacyclohexane, **46** is the first example of coordination complex of a phosphorus-containing ring *carbo*-mer, and its catalytic properties would deserve to be investigated in the future. *Carbo*-diphosphacyclohexane derivatives could also be used as building blocks of axial coordination polymers such as **4b**, or simpler dimeric complexes like **4c** (**Figure 4.6**).

6. Experimental section

THF, diethyl ether (Et_2O), pentane and dichloromethane (DCM) were dried with a PureSolv-MD-5 Innovative Technology system for the purification of solvents. All other reagents were used as commercially available. In particular, commercial solutions of *n*-BuLi were 2.5 M in hexane, solutions of EtMgBr were 3 M in THF, solutions of HCl were 2 M in diethyl ether, solutions of LDA were 1 M in THF, $SnCl_2$ was anhydrous. Silica gel (60 P, 70-200 μm) was used for column chromatography. Silica gel thin layer chromatography plates (60F254, 0.25 mm) were revealed under UV-light and/or by treatment with an ethanolic solution of phosphomolybdic acid (20%). The following analytical instruments were used, ^{1}H and ^{13}C NMR: Avance 300, Avance 400, and Avance 400 HD spectrometers, 2D (^{1}H-^{13}C HSQC, ^{1}H-^{13}C HMBC): Avance 400 HD spectrometers; UV-Visible: Perkin-Elmer UV-Vis Win-Lab Lambda 35 with 1 cm quartz cell; IR: Perkin-Elmer Spectrum 100 FT-IR spectrometer. Dual Syringe Infusion Pump was used for cyclization. All the ^{1}H and ^{13}C signals were assigned according to chemical shifts, spin-spin coupling constants, splitting patterns, signal intensities, and 2D NMR experiments; NMR chemical shifts are given in

ppm with positive values to high frequency relative to the tetramethylsilane reference. Coupling constants J are in Hertz. UV-Visible extinction molar coefficient ε is in $L{\cdot}mol^{-1}{\cdot}cm^{-1}$ and wavelengths λ in nm.

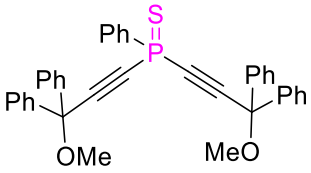

Bis(3-methoxy-3,3-diphenylprop-1-yn-1-yl)(phenyl)phosphine sulfide (39)

To HMDS (22 mmol, 4.4 mL) in 50 mL dry THF at -78 °C, was added *n*-butyllithium (2.5 M, 22 mmol, 8.8 mL) dropwise under magnetic stirring. After one hour, **21** (20 mmol, 4.44 g) was added under argon. After 3 h, $PhSPCl_2$ (1.5 mL, 10 mmol) was added, then the temperature was allowed to warm slowly up to room temperature for 2.5 h. The reaction was treated by addition of distilled water (100 mL), and extracted with Et_2O (30 mL x 3). The combined organic extracts were washed with brine (30 mL x 2), dried over $MgSO_4$ and evaporated under reduced pressure. The residue was purified by column chromatography on silica gel (Pentane: EtOAc 96/4) to give **39** as a yellow solid with 91 % yield (9.12 mmol, 5.312 g).

Melting Point: 126° C

^{1}H NMR (300 MHz, $CDCl_3$) δ 8.15 – 8.03 (m, 2H), 7.60 – 7.50 (m, 11H), 7.38 – 7.24 (m, 14H), 3.35 (s, 6H).

^{31}P NMR (121 MHz, $CDCl_3$) δ -10.49.

^{13}C NMR (75 MHz, $CDCl_3$) δ 141.4 (d, J =3.0Hz), 132.6 (d, J =2.2 Hz), 130.5 (d, J =10.5 Hz), 128.9 (d, J =11.2 Hz), 128.4, 128.3, 128.2, 126.6 (d, J =1.0 Hz), 104.5 (d, J =21.0 Hz), 83.3 (d, J= 125.2 Hz), 81.3, 53.1.

HRMS (DCI/CH_4): *m/z* calculated for $C_{38}H_{32}O_2SP$ $[M+H]^+$: 583.1861, found: 583.1862.

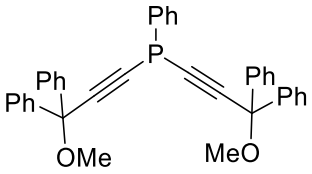

Bis(3-methoxy-3,3-diphenylprop-1-yn-1-yl)(phenyl)phosphine (40)

To a solution of **39** (0.2 mmol, 116.5 mg) in dry THF (100 mL) was added AIBN (3 %, 5 mg) under magnetic stirring. Then, tris(trimethylsilyl)silane (0.22 mmol, 62 µL) was injected dropwise,

and the reaction mixture was heated at 70 °C for 3 h. The reaction was monitored by ^{31}P NMR. After full consumption of **39**, the reaction mixture was concentrated under reduced pressure and purified by preparative TLC eluting with Pentane:EtOAc 96/4, R_f = 0.8 to give **40** as light yellow liquid with 75 % yield with 75 % yield (82.4 mg, 0.149 mmol).

^{1}H NMR (400 MHz, $CDCl_3$) δ 7.79 (3, 2H), 7.56 – 7.54 (m, 8H), 7.43 – 7.40 (m, 3H), 7.32 – 6.25 (m, 12H), 3.37 (s, 6H).

^{31}P NMR (162 MHz, $CDCl_3$) δ -63.96.

^{13}C NMR (101 MHz, $CDCl_3$) δ 142.7, 132.3 (d, J = 22.2 Hz), 129.7, 128.8 (d, J =8.1 Hz), 128.4, 128.2, 127.8, 126.7 (d, J =1.0 Hz), 105.9 (d, J =3.0 Hz), 84.0 (d, J = 9.1 Hz), 81.5, 52.75.

HRMS (DCI/CH_4): *m/z* calculated for $C_{38}H_{32}O_2P$ $[M+H]^+$: 551.2140, found: 551.2141.

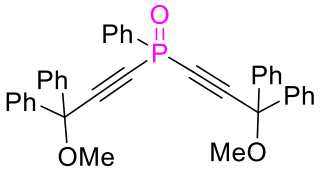

Bis(3-methoxy-3,3-diphenylprop-1-yn-1-yl)(phenyl)phosphine oxide (41)

To a solution of **39**(0.2 mmol, 116.5 mg) in dry THF (100 mL) was added AIBN (3 %, 5 mg) under magnetic stirring. Then tris(trimethylsilyl)silane (0.22 mmol, 62 µL) was injected dropwise, and the mixture was heated at 70 °C for 3 h under argon before opening to air. The oxidation was monitored by ^{31}P NMR. After full conversion, the mixture was concentrated under reduced pressure and purified by preparative TLC eluting with Pentane: EtOAc 96/4, R_f = 0, to give **41** as a white solid with in quantitative yield (112 mg, 0.198 mmol).

^{1}H NMR (300 MHz, $CDCl_3$) δ 7.97 – 7.88 (m, 2H), 7.62 – 7.59 (m, 1H), 7.54 – 7.46 (m, 10H), 7.33 – 7.28 (m, 12H), 3.33 (s, 6H).

^{31}P NMR (162 MHz, $CDCl_3$) δ -20.99.

^{13}C NMR (101 MHz, $CDCl_3$) δ 141.2 (d, J =4.0 Hz), 133.0 (d, J = 3.0 Hz), 130.3 (d, J =13.1 Hz), 129.9 (d, J = 15.2 Hz), 128.4, 128.3, 128.6 (d, J =2.0 Hz), 104.4 (d, J = 32.0 Hz), 84.0 (d, J =195.0 Hz), 81.3, 53.1.

HRMS (DCI/CH_4): *m/z* calculated for $C_{38}H_{32}O_3P$ $[M+H]^+$: 567.2089, found: 567.2095.

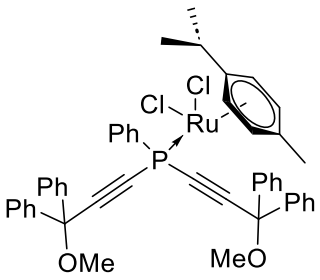

Bis(3-methoxy-3,3-diphenylprop-1-yn-1-yl) (phenyl)phosphine dichloro(*p*-cymene) ruthenium (43)

To a solution of **39** (0.2 mmol, 116.5 mg) in dry THF (100 mL) was added with AIBN (3 %, 5 mg) under magnetic stirring. Then tris(trimethylsilyl)silane (0.22 mmol, 62 μL) was injected dropwise, and the reaction mixture was heated at 70 °C for 3 h. The reaction was monitored by ^{31}P NMR. After full consumption of **39**, of solution of [Ru(*p*-cymene)Cl_2]$_2$ (0.1 mmol, 61.2 mg) in dry DCM was added at room temperature. After 30min, the reaction mixture was concentrated under reduced pressure. The residue was purified by washings with Et_2O: pentane (3:1) mixtures to give **43** as an orange to brown solid with 71% (124.6mg,0.145mmol).

Melting Point: 156℃.

^1H NMR (400 MHz, $CDCl_3$) δ 8.02 – 7.96 (m, 2H), 7.62 – 7.59 (m, 7H), 7.48 – 7.42 (m, 3H), 7.31 (m, 13H), 5.21 – 5.14 (m, 4H), 3.38 (s, 6H), 2.64 (p, J =7.0, 1H), 1.84 (s, 3H), 1.01 (d, J= 7.0, 6H).

^{31}P NMR (162 MHz, $CDCl_3$) δ -18.29.

^{13}C NMR (75 MHz, $CDCl_3$) δ 142.1 (d, J =3.3 Hz), 131.3 (d, J =11.1 Hz), 131.0 (d, J =2.9 Hz), 130.7 (d, J= 65.1 Hz), 128.5, 128.4, 128.0, 126.9, 109.2, 107.2 (d, J= 11.2 Hz), 98.1, 89.5 (d, J =5.0 Hz), 86.8 (d, J =5.0 Hz), 81.3 (d, J= 101.7 Hz), 81.5 (d, J =1.5 Hz), 53.2, 30.3, 21.9, 17.6.

HRMS (DCI/CH_4): *m/z* calculated for formula $C_{39}H_{34}Cl_2O_2PRu$ $[M+NH_4]^+$: 874.1917 (100%), found: 874.1929.

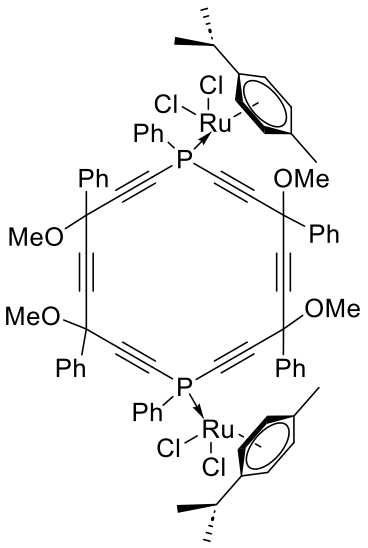

4,7,13,16-Tetramethoxy-1,4,7,10,13,16-hexaphenyl-1,10-diphospha-cyclooctadeca-2,5,8,11,14,17-hexayne bis-dichloro(*p*-cymene) ruthenium (46)

To a solution of **9** (0.05 mmol, 45 mg) in dry THF (10 mL) was added with AIBN (5 %, 3 mg) under magnetic stirring. Then tris(trimethylsilyl)silane (0.11 mmol, 31 μL) was injected dropwise, and the reaction mixture was heated at 70 °C for 51 h. The reaction was monitored by ^{31}P NMR. After full consumption of **9**, the solution of [Ru(*p*-cymene)Cl_2]$_2$ (0.1 mmol, 61.2 mg) in dry DCM was added at room temperature. After 30min, the reaction mixture was concentrated under reduced pressure. The residue was purified by washings with Toluene to give **46** as a red solid with in quantitative yield (72 mg and 0.048 mmol).

^{1}H NMR (400 MHz, $CDCl_3$) δ 7.92-7.66 (m, 12H), 7.52 –7.16 (m, 18H), 5.55 – 5.10 (m, 8H), 3.73 – 3.32 (m, 12H), 2.80 – 2.62 (m, 2H), 2.14 – 1.82 (m, 6H), 1.28 – 0.85 (m, 12H).

^{31}P NMR (162 MHz, $CDCl_3$) δ -17.61- -25.98.

^{13}C NMR (101 MHz, $CDCl_3$) δ 138.6-137.9 (m), 132.6-131.0 (m), 129.6-128.5 (m), 128.4 - 128.0 (m), 127.0-126.5 (m), 125.3 (s), 110.4-109.7 (m), 103.7-102.6 (m), 98.0-96.7 (m), 90.7-89.1 (m), 87.7-86.6 (m), 84.7-84.0 (m), 72.5-72.2 (m), 54.5-53.5 (m), 31.9-29.7 (m), 25.0- 21.5 (m), 18.0-17.7 (m).

HRMS (DCI/CH_4): *m/z* calculated for formula $C_{76}H_{70}Cl_4O_4P_2Ru_2NH_4[M+NH_4]^+$:1472.1943 (100%), found: 1472.1931.

References

(1) Hinton, R. C.; Mann, F. G. 569. Triethylenediphosphine (1 : 4-Diphosphabicyclo[2 : 2 : 2]-Octane). *J. Chem. Soc.* **1959**, 2835–2843. https://doi.org/10.1039/JR9590002835.

(2) De Felice, V.; Fraldi, N.; Roviello, G.; Ruffo, F.; Tuzi, A. Coordination Modes of 1,2,3,4-Tetrahydro-1,4-Diphenyl-1,4-Benzodiphosphinine (*Bedip*) to Pt and Pd Metal Ions: Synthesis and Structural Characterization of Mono- and Bi-Nuclear Complexes. *Journal of Organometallic Chemistry* **2007**, *692* (23), 5211–5220. https://doi.org/10.1016/j.jorganchem.2007.08.003.

(3) Sussman, J. E.; Morey, T. S.; Miller, S. M.; Helm, M. L. Group 9 Half-Sandwich Complexes Containing the Unique *P*,*P*′-Diphenyl-1,4-Diphospha-Cyclohexane Ligand: Synthesis, X-Ray Structure Analyses and Spectroscopic Studies. *Journal of Organometallic Chemistry* **2009**, *694* (21), 3506–3510. https://doi.org/10.1016/j.jorganchem.2009.06.023.

(4) Ishii, A.; Yoshioka, R.; Nakayama, J.; Hoshino, M. 4,8-Diphosphathiophenetriptycenes. *Tetrahedron Letters* **1993**, *34* (51), 8259–8262. https://doi.org/10.1016/S0040-4039(00)61405-3.

(5) Lang, H.; Lay, U.; Imhof, W. Additionsreaktionen von $(CO)_5CrEPhH_2$(E = P As) an di(ethinyl)-phosphane und stannane; stufenweise darstellung von komplex-gebundenen 1,4-dihetero-cyclohexa-2,5-dienen *Journal of Organometallic Chemistry* **1993**, *444* (1), 53–59. https://doi.org/10.1016/0022-328X(93)83054-Y.

(6) Deberitz, J.; Nöth, H. 2,4,6-Triphenylphosphorin-Metall(0)-Carbonyle Des Chroms, Molybdäns Und Wolframs. *Journal of Organometallic Chemistry* **1973**, *49* (2), 453–468. https://doi.org/10.1016/S0022-328X(00)84236-9.

(7) Rigo, M.; Sklorz, J. a. W.; Hatje, N.; Noack, F.; Weber, M.; Wiecko, J.; Müller, C. 2,4,6-Triphenylphosphinine and 2,4,6-Triphenylposphabarrelene Revisited: Synthesis, Reactivity and Coordination Chemistry. *Dalton Trans.* **2016**, *45* (5), 2218–2226. https://doi.org/10.1039/C5DT03609G.

(8) Ortiz, D.; Blug, M.; Le Goff, X.-F.; Le Floch, P.; Mézailles, N.; Maître, P. Mechanistic Investigation of the Generation of a Palladium(0) Catalyst from a Palladium(II) Allyl Complex: A Combined Experimental and DFT Study. *Organometallics* **2012**, *31* (17), 5975–5978. https://doi.org/10.1021/om300375b.

(9) Rigo, M.; Habraken, E. R. M.; Bhattacharyya, K.; Weber, M.; Ehlers, A. W.; Mézailles, N.; Slootweg, J. C.; Müller, C. Phosphinine-Based Ligands in Gold-Catalyzed Reactions. *Chemistry*

– *A European Journal* **2019**, *25* (37), 8769–8779. https://doi.org/10.1002/chem.201900938.

(10) Chauvin, R. "Carbomers". I. A General Concept of Expanded Molecules. *Tetrahedron Le tters* **1995**, *36* (3), 397–400. https://doi.org/10.1016/0040-4039(94)02275-G.

(11) Quin, L. D. *A Guide to Organophosphorus Chemistry*; John Wiley & Sons, 2000.

(12) Zon, G.; DeBruin, K. E.; Naumann, K.; Mislow, K. Stereospecific Desulfurization of Ac yclic Phosphine Sulfides with Hexachlorodisilane and the Alkaline Hydrolysis of Monoalkoxy- an d Monoalkylthiophosphonium Salts. *J. Am. Chem. Soc.* **1969**, *91* (25), 7023–7027. https://doi.org/ 10.1021/ja01053a022.

(13) Naumann, K.; Zon, G.; Mislow, K. Use of Hexachlorodisilane as a Reducing Agent. Ster eospecific Deoxygenation of Acyclic Phosphine Oxides. *J. Am. Chem. Soc.* **1969**, *91* (25), 7012–7 023. https://doi.org/10.1021/ja01053a021.

(14) King, R. B.; Cloyd, J. C. Jr.; Reimann, R. H. Poly(Tertiary Phosphines and Arsines). XII I. Neopentyl Poly(Tertiary Phosphines). *J. Org. Chem.* **1976**, *41* (6), 972–977. https://doi.org/10.1 021/jo00868a016.

(15) Niebergall, H.; Langenfeld, B. Synthese von Tetraorgano-Diphosphinen, Diorgano-Phos phinen Und Tetraorgano-Diphosphindisulfiden. *Chemische Berichte* **1962**, *95* (1), 64–76. https://d oi.org/10.1002/cber.19620950114.

(16) SCHMUTZLER, R.; STELZER, O.; WEFERLING, N. A New Method for the Formation of P-P Bonds-Synthesis of Cyclic Diphosphine Monosulfides. *ChemInform* **1988**, *19* (24), 134. ht tps://doi.org/10.1002/chin.198824275.

(17) Niemi, T.-A.; Coe, P. L.; Till, S. J. The Synthesis of Stable 1,3,4-Triphenylphospholes. *J. Chem. Soc., Perkin Trans.* **2000**, 10, 1519–1528. https://doi.org/10.1039/B000692K.

(18) Kanemura, S.; Kondoh, A.; Yorimitsu, H.; Oshima, K. Carbocupration of 1-Alkynylphos phines Followed by Trapping with Electrophiles. *Org. Lett.* **2007**, *9* (10), 2031–2033. https://doi.o rg/10.1021/ol0706657.

(19) Gawel, P.; Dengiz, C.; Finke, A. D.; Trapp, N.; Boudon, C.; Gisselbrecht, J.-P.; Diederic h, F. Synthesis of Cyano-Substituted Diaryltetracenes from Tetraaryl[3]Cumulenes. *Angewandte Chemie International Edition* **2014**, *53* (17), 4341–4345. https://doi.org/10.1002/anie.201402299.

(20) Ried, W.; Neidhardt, R. Über Ringschlußreaktionen Im Anschluß an Die Allenumlagerun g von 1-Methoxy-1.1.5.5-Tetraaryl-Pentin-(2)-Onen-(4) Mit Anorganischen Säurehalogeniden. *Ch emische Berichte* **1970**, *103* (7), 2208–2224. https://doi.org/10.1002/cber.19701030725.

(21) Ried, W.; Schlegelmilch, W.; Piesch, S. Äthinierungsreaktionen, XX. Über Alkindiole U nd Kumulene. *Chemische Berichte* **1963**, *96* (5), 1221–1228. https://doi.org/10.1002/cber.196309 60508.

(22) Omelańczuk, J. A New Synthesis of Unsymmetrically Substituted Halophosphines. *Hete roatom Chemistry* **1992**, *3* (4), 403–405. https://doi.org/10.1002/hc.520030414.

(23) Neumann, P.; Dib, H.; Sournia-Saquet, A.; Grell, T.; Handke, M.; Caminade, A.-M.; Hey -Hawkins, E. Ruthenium Complexes with Dendritic Ferrocenyl Phosphanes: Synthesis, Character ization, and Application in the Catalytic Redox Isomerization of Allylic Alcohols. *Chemistry – A European Journal* **2015**, *21* (17), 6590–6604. https://doi.org/10.1002/chem.201406489.

(24) Mikolajczyk, M.; Graczyk, P. P. Synthesis and Conformational Behavior of 2-Phosphoni o- and 2-Phosphinyl-1,3-Dithianes. Operation of the Generalized Anomeric Effect in the S-C-P+ System. *J. Org. Chem.* **1995**, *60* (16), 5190–5208. https://doi.org/10.1021/jo00121a043.

(25) Omelanczuk, J.; Mikolajczyk, M. Optically Active Trivalent Phosphorus Compounds. 2. Reactivity of Alkylthio- and Alkylselenophosphonium Salts. The First Stereospecific Synthesis of a Chiral Phosphinite. *J. Am. Chem. Soc.* **1979**, *101* (24), 7292–7295. https://doi.org/10.1021/ja00 518a026.

(26) Griffiths, D. V.; Groombridge, H. J.; Mahoney, P. M.; Swetnam, S. P.; Walton, G.; York, D. C. Nucleophilic Addition to Dimethylvinylphosphine Sulfide as a Convenient Route to Polyde ntate Ligands Containing the 2-Dimethylphosphinoethyl Unit. *Tetrahedron* **2005**, *61* (19), 4595–4 600. https://doi.org/10.1016/j.tet.2005.03.012.

(27) Romeo, R.; Wozniak, L. A.; Chatgilialoglu, C. Radical-Based Reduction of Phosphine S ulfides and Phosphine Selenides by $(Me_3Si)_3SiH$. *Tetrahedron Letters* **2000**, *41* (50), 9899–9902. https://doi.org/10.1016/S0040-4039(00)01759-7.

(28) Demchuk, O. M.; Świerczyńska, W.; Dziuba, K.; Frynas, S.; Flis, A.; Pietrusiewicz, K. M. Raney-Ni Reduction of Phosphine Sulfides. *Phosphorus, Sulfur, and Silicon and the Related E lements* **2017**, *192* (1), 64–68. https://doi.org/10.1080/10426507.2016.1225052.

(29) Arisawa, M.; Tazawa, T.; Ichinose, W.; Kobayashi, H.; Yamaguchi, M. Rhodium-Catalyz ed Synthesis of Dialkyl(Heteroaryl)Phosphine Sulfides by Phosphinylation of Heteroaryl Sulfides. *Adv Synth Catal* **2018**, *360* (18), 3488–3491. https://doi.org/10.1002/adsc.201800630.

(30) Auffrant, A.; Jaun, B.; Jarowski, P. D.; Houk, K. N.; Diederich, F. Peralkynylated Buta-1, 2,3-Trienes: Exceptionally Low Rotational Barriers of Cumulenic C=C Bonds in the Range of Th

ose of Peptide C-N Bonds. *Chemistry – A European Journal* **2004**, *10* (12), 2906–2911. https://doi.org/10.1002/chem.200400218.

(31) Vogels, C. M.; Decken, A.; Westcott, S. A. Rhodium(I) Acetylacetonato Complexes Containing Phosphinoalkynes as Catalysts for the Hydroboration of Vinylarenes. *Can. J. Chem.* **2006**, *84* (2), 146–153. https://doi.org/10.1139/v05-242.

(32) Carty, A. J.; Ng, T. W. A Monosubstituted Derivative of Dicobalt Octacarbonyl Containing Bridging Carbonyl Groups: $[Co_2(CO)_7]_2Ph_2PCCPPh_2$. *J. Chem. Soc. D* **1970**, No. 3, 149–150. https://doi.org/10.1039/C29700000149.

(33) Carty, A. J.; Efraty, A. A New Class of Palladium and Platinum Complexes: Diphosphine Bridged $M_2X_4L_2$ Species. (L=Bis Diphenylphosphinoacetylene). *Inorganic and Nuclear Chemistry Letters* **1968**, *4* (7), 427–431. https://doi.org/10.1016/0020-1650(68)80052-2.

(34) Rodewald, D.; Schulzke, C.; Rehder, D. Alkyne-Niobium(I) Complexes with Functionalized Alkynes: Synthesis, Structure and Reactivity. *Journal of Organometallic Chemistry* **1995**, *498* (1), 29–35. https://doi.org/10.1016/0022-328X(95)05493-9.

(35) Carty, A. J.; Efraty, A. Binuclear Copper(I) Complexes with Bridging Bis(Diphenylphosphino)Acetylene Groups. *Can. J. Chem.* **1968**, *46* (9), 1598–1599. https://doi.org/10.1139/v68-267.

(36) Dillinger, K.; Oberhauser, W.; Bachmann, C.; Brüggeller, P. Binuclear Platinum(II) Complexes of 1,1,4,7,10,10-Hexaphenyl-1,4,7,10-Tetraphosphadecane (P_4) Containing Various Bridging Ligands as Spacers between the P4 Coordination Units. *Inorganica Chimica Acta* **1994**, *223* (1), 13–20. https://doi.org/10.1016/0020-1693(94)03979-8.

(37) Hong, F.-E.; Chang, Y.-C.; Chang, R.-E.; Chen, S.-C.; Ko, B.-T. Bis(Diphenylphosphino) Acetylene as Bifunctional Ligand in Dicobalt Carbonyl Complexes. *Organometallics* **2002**, *21* (5), 961–967. https://doi.org/10.1021/om0106783.

(38) Holm, R. H.; Eaton, G. R. Bridged binuclear bis(dithiolene) complexes of iron and cobalt. *Inorg. Chem.* **1971**, 10(4), 805–811. https://doi.org/10.1021/ic50098a028.

(39) Adams, C. J.; Bruce, M. I.; Skelton, B. W.; White, A. H. Cluster Chemistry: LXXXVII. Some Homo- and Hetero-Nuclear Complexes Derived from $C_2(PPh_2)_2$: Crystal Structures of $Re_3(\mu\text{-}H)_3(\mu\text{-}Dppa)(CO)_{10}$ {dppa = $C_2(PPh_2)_2$}, $Re_3(\mu\text{-}H)_3(CO)_{11}\{PPh_2[\mu\text{-}C_2Ru_2(\mu\text{-}PPh_2)(CO)_6]\}$ and $Os_3Ru_2(M_5\text{-}C_2PPh_2)(\mu\text{-}PPh_2)(CO)_{13}$. *Journal of Organometallic Chemistry* **1993**, *447* (1), 91–101. https://doi.org/10.1016/0022-328X(93)80277-I.

(40) King, R. B.; Houk, L. W.; Kapoor, R. N. Complexes of Trivalent Phosphorus Derivatives. X. Reactions of Ditertiary Phosphines with Alkyl Derivatives of Cyclopentadienylmolybdenum Tricarbonyl. *Inorg. Chem.* **1969**, *8* (8), 1792–1794. https://doi.org/10.1021/ic50078a053.

(41) Carty, A. J.; Efraty, A. Coordination Complexes of Acetylene Diphosphines. I. Diphosphine-Bridged Binuclear Copper(I) and Gold(I) Complexes of Bis(Diphenylphosphino)Acetylene. *Inorg. Chem.* **1969**, *8* (3), 543–550. https://doi.org/10.1021/ic50073a026.

(42) Carty, A. J.; Efraty, A. Coordination Complexes of Acetylene Diphosphines. II. Diphosphine Bridged Palladium(II) and Platinum(II) Derivatives. *Can. J. Chem.* **1969**, *47* (14), 2573–2578. https://doi.org/10.1139/v69-425.

(43) Coordination complexes of acetylene diphosphines. Part III. Silver(I) and mercury(II) complexes. *Can. J. Chem.* **1969**, 47 (18), 3361-3366. https://cdnsciencepub.com/doi/abs/10.1139/v69-557.

(44) Carty, A. J.; Efraty, A.; Ng, T. W.; Birchall, T. Coordination Complexes of Acetylenic Phosphines and Diphosphines. IV. Characterization and Moessbauer Spectra of Derivatives of Cyclopentadienyliron Dicarbonyl Dimer and Cyclopentadienyliron Dicarbonyl Halides. *Inorg. Chem.* **1970**, *9* (5), 1263–1268. https://doi.org/10.1021/ic50087a051..

(45) Semmelmann, M.; Fenske, D.; Corrigan, J. F. Copper-Chalcogenide Clusters Stabilised with Linear Bidentate Phosphine Ligands. *Journal of the Chemical Society, Dalton Transactions* **1998**, 15, 2541–2546. https://doi.org/10.1039/A802007H.

(46) Cifeuntes, M. P.; Humphrey, M. G.; Willis, A. C. High Nuclearity Ruthenium Carbonyl Cluster Chemistry IV1. Reactivity of $[Ru_{10}(\mu\text{-}H)(M_6\text{-}C)(CO)_{24}]$-towards Trimethylphosphite or Bis(Diphenylphosphino)Acetylene; X-Ray Crystal Structure of $[PPh_4][Ru_{10}(\mu\text{-}H)(M_6\text{-}C)22\{P(OMe)_3\}_2]$. *Journal of Organometallic Chemistry* **1996**, *513* (1), 85–95. https://doi.org/10.1016/0022-328X(95)05896-W.

(47) Hogarth, G.; Norman, T. Linking Metal Centres with 1,4-Bis(Diphenylphosphino)-2,5-Difluorobenzene (Dpfb): Syntheses and Molecular Structures of $[\{Mo(CO)_4(\mu\text{-}Dpfb)\}_2]$ and $[\{Mo(CO)_4\}_2(\mu\text{-}Dpfb)(\mu\text{-}Dppa)]$(Dppa = $Ph_2PCCPPh_2$). *J. Chem. Soc., Dalton Trans.* **1996**, No. 6, 1077–1085. https://doi.org/10.1039/DT9960001077.

(48) Elschenbroich, C.; Sebbach, J.; Metz, B.; Heikenfeld, G. Metal-π-Complexes of Benzene Derivatives. Part 39. Di (1, 4-Bis (Diphenylphosphano) H_6-Benzene) Chromium: A Building Block for Polynuclear Bimetal Complexes? *ChemInform* **1992**, *23* (24), 236-236.

(49) Wong, Y. S.; Jacobson, S.; Chieh, P. C.; Carty, A. J. Mixed Thiocyanate Complexes of Pl atinum(II). Crystal Structure of Cis-Thiocyanatoisothiocyanatobis(3,3-Dimethylbutynldiphenylp hosphine)Platinum(II). *Inorg. Chem*. **1974**, 13 (2), 284–290. https://doi.org/10.1021/ic50132a007.

(50) Lee, J.; Humphrey, M. G.; Hockless, D. C. R.; Skelton, B. W.; White, A. H. Mixed-metal cluster chemistry. Site-selective reactions of tungsten-iridium cluster CpWIr3(CO)11 with PPh3 a nd bidentate phosphines: x-ray crystal structures of $CpWIr_3$(.mu.-dppe)(.mu.-$CO)_3(CO)_6$, $CpWIr_3$ (.mu.-dppm)(.mu.-$CO)_3(CO)_6$, and $CpWIr_3$(.mu.-dppa)(.mu.-$CO)_3(CO)_6$. *Organometallics* **1993**, *1 2* (9), 3468–3473. https://doi.org/10.1021/om00033a017.

(51) Draper, S. M.; Housecroft, C. E.; Humphrey, J. S.; Rheingold, A. L. Mono- and Di-Dent ate Tertiary Phosphine and Monodentate Tertiary Phosphite Derivatives of $[Ru_4H(CO)_{12}BH_2]$. *J. C hem. Soc., Dalton Trans.* **1995**, No. 23, 3789–3799. https://doi.org/10.1039/DT9950003789.

(52) Nelson, J. H.; Jonassen, H. B. Monoolefin and Acetylene Complexes of Nickel, Palladiu m and Platinum. *Coordination Chemistry Reviews* **1971**, *6* (1), 27–63. https://doi.org/10.1016/S00 10-8545(00)80033-8.

(53) Jia, G.; Puddephatt, R. J.; Scott, J. D.; Vittal, J. J. Organometallic Polymers with Gold(I) Centers Bridged by Diphosphines and Diacetylides. *Organometallics* **1993**, *12* (9), 3565–3574. h ttps://doi.org/10.1021/om00033a032.

(54) Berenguer, J. R.; Bernechea, M.; Forniés, J.; García, A.; Lalinde, E. (P-Cymene)Rutheni um(II)(Diphenylphosphino)Alkyne Complexes: Preparation of (μ-Cl)(μ-PPh_2C∶CR)-Bridged Ru/ Pt Heterobimetallic Complexes. *Organometallics* **2004**, *23* (18), 4288–4300. https://doi.org/10.10 21/om049676j.

(55) Hong, F.-E.; Ho, Y.-J.; Chang, Y.-C.; Lai, Y.-C. Palladium Catalyzed Suzuki Coupling R eactions Using Cobalt-Containing Bulky Phosphine Ligands. *Tetrahedron* **2004**, *60* (11), 2639–26 45. https://doi.org/10.1016/j.tet.2004.01.071.

(56) Xu, D.; Murfee, H. J.; van der Veer, W. E.; Hong, B. Photoluminescent Macrocyclic Pd(I I) and Pt(II) Dimeric Complexes with Ph_2P–C□C–PPh_2 Spacer. *Journal of Organometallic Chem istry* **2000**, *596* (1), 53–63. https://doi.org/10.1016/S0022-328X(99)00538-0.

(57) Brandys, M.-C.; Puddephatt, R. J. Polymeric Complexes of Silver(I) with Diphosphine L igands: Self-Assembly of a Puckered Sheet Network Structure. *J. Am. Chem. Soc.* **2002**, *124* (15), 3946–3950. https://doi.org/10.1021/ja0113293.

(58) Galsworthy, J. R.; Housecroft, C. E.; Rheingold, A. L. Reactions of [RhRu3H(H5-C_5Me

$_5$) (CO)$_9$ BH$_2$] with Didentate Phosphines and the Synthesis and Crystal Structure of [RhRu$_3$H$_2$(H$_5$-C$_5$Me$_5$) (CO)$_8$(μ-Dppf-P,P′)AuB][Dppf = 1,1′-Bis(Diphenylphosphino)Ferrocene]. *J. Chem. Soc., Dalton Trans.* **1996**, No. 14, 2917–2922. https://doi.org/10.1039/DT9960002917.

(59) Carty, A. J.; Efraty, A.; Ng, T. W. Some New Diphosphine-Bridged Nickel Carbonyl and Cyclopentadienyl Compounds. *Can. J. Chem.* **1969**, *47* (8), 1429–1431. https://doi.org/10.1139/v69-233.

(60) Carty, A. J.; Ng, T. W.; Carter, W.; Palenik, G. J.; Birchall, T. Structural Characterisation of an Acetylenic Diphosphine Derivative of π-Cyclopentadienyliron Dicarbonyl Dimer: An Unusual Mössbauer Effect. *J. Chem. Soc. D* **1969**, No. 19, 1101–1102. https://doi.org/10.1039/C2969000 1101.

(61) Carty, A. J.; MacLaughlin, S. A.; Wagner, J. V.; Taylor, N. J. *Structural versatility of Ru4 butterflies. The molecular structures of Ru$_4$(CO)$_{13}$(.mu.-PPh$_2$)(.mu.-.eta.2-C.tplbond.C-t-Bu) and Ru$_4$(CO)$_8$(.mu.-PPh$_2$)$_2$(.mu.-.eta.2-C.tplbond.C-t-Bu)(.mu.3-.eta.2-C.tplbond.C-t-Bu)(Ph$_2$PC.tplbond.C-t-Bu).1/2C$_6$H$_{14}$: clusters with almost planar metal frameworks*. *Organometallics* **1982**, 1 (7), 1013–1015.https://doi.org/10.1021/om00067a024.

(62) Chen, J.-L.; Zhang, L.-Y.; Chen, Z.-N.; Gao, L.-B.; Abe, M.; Sasaki, Y. Syntheses, Structures, and Redox Properties of Dimeric Triruthenium Clusters Bridged by Bis(Diphenylphosphino) Acetylene and -Ethylene. *Inorg. Chem.* **2004**, *43* (4), 1481–1490. https://doi.org/10.1021/ic0344968.

(63) Louattani, E.; Suades, J.; Urtiaga, K.; Arriortua, M. I.; Solans, X. Synthesis of a Zwitteronic P-Coordinated Complex with Bis (Diphenylphosphino)Acetylene. *Organometallics* **1996**, *15* (1), 468–471. https://doi.org/10.1021/om950507w.

(64) Clark, H. C.; Ferguson, G.; Kapoor, P. N.; Parvez, M. *Synthesis of heterobimetallic bis(diphenylphosphino)acetylene-bridged palladium-platinum complexes. Crystal and molecular structure of [PdPtCl$_4$(Ph$_2$PC.tplbond.CPPh$_2$)$_2$].2CHCl$_3$*. *Inorg. Chem.* **1985**, *24* (23), 3924–3928. https://doi.org/10.1021/ic00217a046.

(65) Jones, D. F.; Dixneuf, P. H.; Southern, T. G.; Le Marouille, J. Y.; Grandjean, D.; Guenot, P. Synthesis of Novel Halo-Bridged Trinuclear Ruthenium-Iron Derivatives. X-Ray Structure of FeRu$_2$(Mu.-Cl)$_2$(CO)$_8$(Ph$_2$PC.Tplbond.C-Tert-Bu)$_2$. *Inorg. Chem.* **1981**, *20* (10), 3247–3252. https://doi.org/10.1021/ic50224a022.

(66) Wright, M. E.; Lawson, L.; Baker, R. T.; Roe, D. C. Synthesis of the New Metalloligand

s [η 6-(PPh2)xC6H6−x]Cr(CO)2(L) [*x* = 1,2; L = CO and PR3] and Some Rhodium(I) Complexes. *Polyhedron* **1992**, *11* (3), 323–329. https://doi.org/10.1016/S0277-5387(00)83176-9.

(67) Li, L.; Reginato, N.; Urschey, M.; Stradiotto, M.; Liarakos, J. D. The Synthesis and Structural Characterization of Linear and Macrocyclic Bis(Dinitrosyliron) Complexes Supported by Bis(Phosphine) Bridging Ligands. *Can. J. Chem.* **2003**, *81* (6), 468–475. https://doi.org/10.1139/v03-040.

(68) Amoroso, A. J.; Johnson, B. F. G.; Lewis, J.; Massey, A. D.; Raithby, P. R.; Wong, W. T. The Use of Bis(Diphenylphosphinoacetylene) and Its Digold Derivative as Linking Groups in Osmium Cluster Chemistry. Crystal Structures of [{Os3(CO)11}2(Dppa)], [Os3,(CO)10(Dppa)]2 and [Os4H(CO)12Au(Dppa)]2 (Dppa = Ph2PC≡CPPh2). *Journal of Organometallic Chemistry* **1992**, *440* (1), 219–231. https://doi.org/10.1016/0022-328X(92)83498-7.

(69) Wallbank, A. I.; Corrigan, J. F. Triply Bridged Dicopper-Bis (Trimethylsilylchalcogenolates): Synthesis and Characterization of the Series of Helical Complexes [(Me3SiE-Cu)2(μ-Ph2PCCPPh2-κ2P)3] (E = S, Se, Te). *CJC Western University Virtual Compilation* **2014**, *1* (2), 1592–1599. https://doi.org/10.1139/v02-032@cjc0102.

(70) Jones, D. F.; Dixneuf, P. H.; Southern, T. G.; Marouille, J. Y. L.; Grandjean, D.; Guenot, P. *Synthesis of novel halo-bridged trinuclear ruthenium-iron derivatives. X-ray structure of FeRu2(.mu.-Cl)2(CO)8(Ph2PC.tplbond.C-tert-Bu)2*. *Inorg. Chem.* **1981**, *20* (10), 3247–3252. https://doi.org/10.1021/ic50224a022.

(71) Redwine, Kent D.; Hansen, Heather D.; Bowley, Sarah; Isbell, Jamie; Sanchez, Michael; Vodak, David; Nelson, John H. Synthesis and Characterization of [(η 6-Arene) Ru(R3P) Cl2] Complexes. *Synthesis and Reactivity in Inorganic and Metal-Organic Chemistry*; **2000**; 30, 379–407.

(72) Ghebreyessus, K. Y.; Nelson, J. H. Base-Promoted Hydroalkylation Reactions of 1,3,5-Me 3 C 6 H 3, *p* -MeC 6 H 4 CHMe 2, C 6 Me 6, *p* -MeC 6 H 4 Me, and MeC 6 H 5 Ligands Coordinated to Ruthenium (II). *Organometallics* **2000**, *19* (17), 3387–3392. https://doi.org/10.1021/om000375t.

General Conclusion

General Conclusion

In the four chapter of the thesis, ring *carbo*-mers of diphosphaheterocycles, *carbo*-diphosphinines, *carbo*-diphosphacyclohexanes and *carbo*-diphosphabarrelene, were considered, and a preliminary study of their possible use as ligands towards metal centers was envisaged (**Scheme 1**).

Carbo-diphosphaheterocycles were unknown experimentally before this work, though they could be attractive for their diverse possible properties and applications. Indeed, P atoms inside *carbo*-meric macrocycles open new prospects in coordination chemistry, the P and C atoms sharing complementary functional and constitutional roles.

The first chapter provides an overview of the definition and synthetic approaches for '*carbo*-mers'. Additionally, it includes an update on pericyclyne derivatives, including hydrocarbon and hetero-pericyclynes, as well as their construction by general and accelerated synthesis methods. The synthesis of *carbo*-benzenes with various substituents is then described, followed by a comprehensive study of their properties and applications.

The personal work is presented in the following three chapters, with an experimental part attached at the end of each chapter.

In the second chapter, the synthesis of a first example of *carbo*-1,4-dihydro-dithiodiphosphinine and related macrocyclic *carbo*-diphosphacyclohexane derivatives with different substituents and oxidation states is described. Their preparation was achieved by a quite efficient and general method involving a tetracomponent [8+1+8+1] macrocyclization process with up to 67 % yield. After a final reductive elimination step with $SnCl_2$/HCl, the hexaphenyl-*carbo*-1,4-dihydro-1,4-dithio-1,4-diphosphinine target was produced with 20 % yield and was fully characterized by NMR, IR and UV spectroscopy, HRMS, electrochemistry and single crystal X-ray diffractometry.

The third chapter reports on the synthesis of hexaphenyl-*carbo*-dithiodiphospha-barrelene and related *carbo*-dithiodiphosphabarrelane derivatives. The preparation of the latter was achieved by a pentacomponent [8+1+8+1+8] process with low yields. After a final reductive elimination step with $SnCl_2$/HCl, the hexaphenyl-*carbo*-1,4-dihydro-dithiodiphosphabarrelene was produced with

20 % yield as a colored dark orange solid, and was partially characterized by NMR and UV-vis spectroscopy.

In the fourth chapter, the reactivity and coordination chemistry of *carbo*-diphosphaheterocycles described in the previous chapters are studied. After preliminary investigations on model dialkynylphosphine ligands, a first example of coordination complex of a phosphorus-containing *carbo*-mer, the *carbo*-diphosphacyclohexane di-ruthenium complex was prepared through a two-step one-pot process and fully characterized as a quasi-statistical mixture of diastereoisomers.

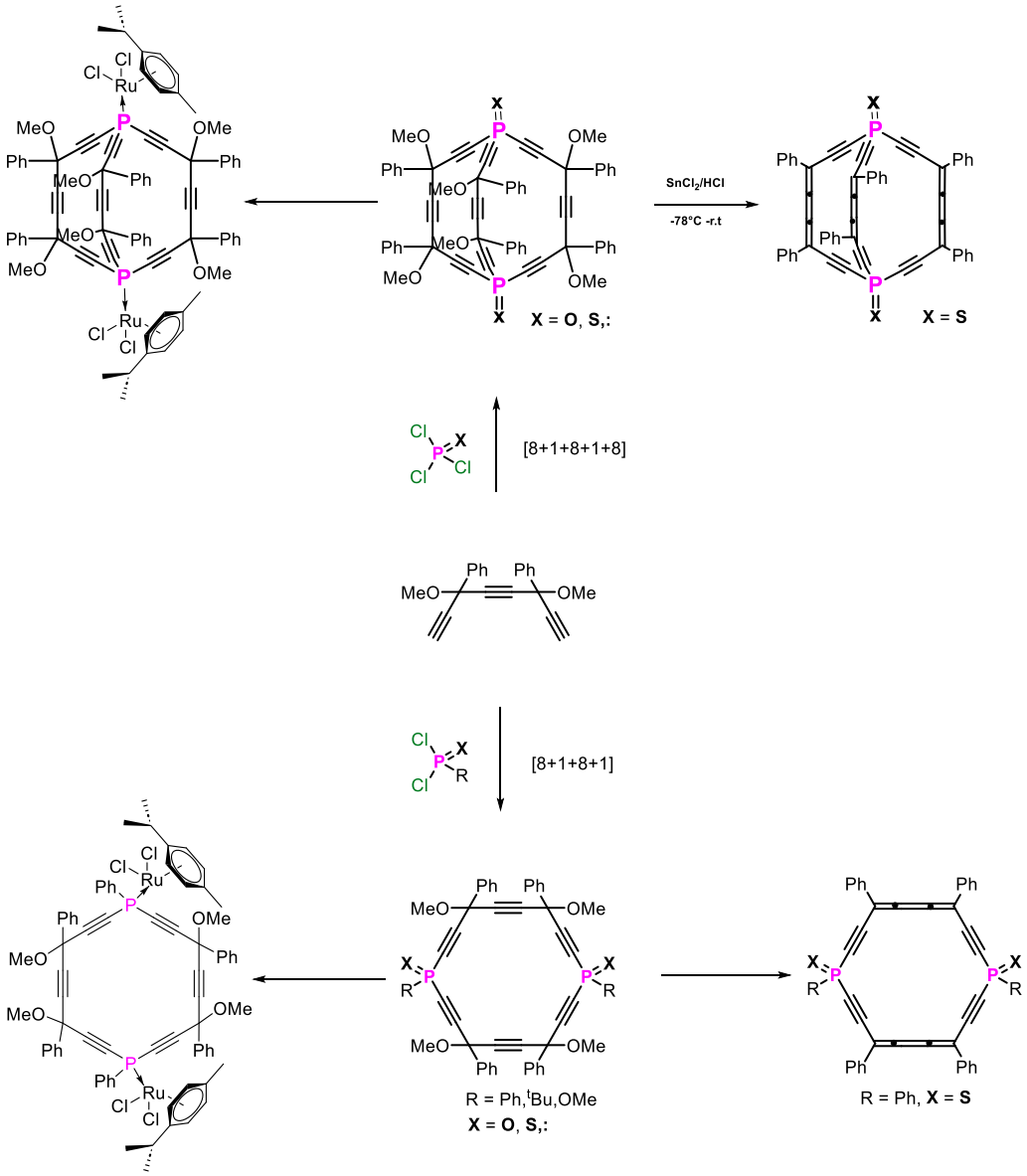

Scheme 1. Main results of the thesis.

While *carbo*-benzene derivatives have been extensively studied in the past few decades, *carbo*-mers of heterocycles received very little experimental attention before this work. The provided examples of *carbo*-dihydro-dithiodiphosphine and *carbo*-diphosphabarrelenes also provide a revival of the long-envisioned chemistry of *carbo*-heterocycles, which started with *carbo*-phosphole derivative targets.

As basically intended by the *carbo*-merization definition, ring *carbo*-mers of diphosphacyclohexane and diphosphabarrelane derivatives exhibit similar basic structural features as their parent diphosphacyclohexane and diphosphabarrelane derivatives, but offer larger molecular sizes and carbon and π electron-richness, thus in distinct spatial configurations.

Beyond coordination chemistry with transition metals for the design of a new type of coordination polymer materials, *carbo*-P-heterocycle complexes might also be envisaged for catalytic transformation of unsaturated substrates (alkenes, alkynes, ketones or aldehydes), but one must keep aware of the competition with the Csp-Csp and Csp-Csp^2 unsaturations of the ligands themselves.This research could thus result in the design of versatile and novel catalysts, making it a valuable long-term investment.

The family of *carbo*-diphosphabarrelenes provides specific prospects of potential applications, including cage behavior towards cations (such as NH_4^+) and enhanced single molecule conductance or conductivity (SMC). Indeed, the *carbo*-benzene core was reported to have an unprecedented SMC value. Since SMC is known to increase with a lesser aromatic character of the π-conjugation pathway, with a greater number of parallel π-conjugated pathways (e.g. from 2 to 3), and with the electronic communication at STM tips, the *carbo*-diphosphabarrelene core could be anticipated to act as a quite efficient single molecule conductor.

Résumé en Français

Résumé en Français

1.Introduction

L'unité acétylène, historiquement utilisée comme une entité utilitaire en chimie organique de synthèse, a subi un changement de paradigme au cours des dernières décennies. L'augmentation rapide du nombre d'outils s'accompagne d'un nombre croissant de publications concernant l'élaboration de réseaux impressionnants - cycliques, bidimensionnels et même tridimensionnels – composés d'unités acétyléniques et diacétyléniques reliées par des connecteurs aliphatiques, aromatiques ou organométalliques. [1] Elle a transcendé son rôle conventionnel et s'est élevée au rang de motif structurel distinctif dans le domaine de la physico-chimie organique. Cette transformation a notamment fait de la chimie acétylénique un champ d'investigation scientifique à part entière.

Le terme "*carbo*-mère" fait référence à un concept chimique dans lequel une unité C_2 (un fragment de deux atomes de carbone) est insérée dans chaque liaison covalente (ou dans une partie sélectionnée de celles-ci) d'une structure de Lewis représentative d'une molécule mère[2]. Le processus de *carbo*-mérisation induit l'augmentation de la teneur en carbone par rapport à la molécule parente et conduit à des molécules plus grandes, présentant potentiellement des propriétés différentes. Les caractéristiques fondamentales de la molécule mère, cruciales pour le contrôle de ses propriétés physiques, sont a priori préservées dans son *carbo*-mère. Il s'agit notamment de la connectivité, de la forme, de la symétrie, de la résonance π et des configurations des éléments de chiralité.

Les organophosphines et leurs complexes de métaux de transition sont intensivement utilisés en catalyse homogène [3 4]en raison de la possibilité d'ajuster finement leurs propriétés électroniques et stériques. Ces catalyseurs permettent souvent de réaliser des réactions en milieu aqueux ou biphasique, à condition que des groupes ioniques ou polaires soient attachés à ces phosphines.

On soupçonnait depuis longtemps que les éléments du groupe 15 tels que le phosphore pouvaient être engagés dans des liaisons multiples, mais aucune démonstration réelle n'en avait été

faite jusqu'à la préparation de la 2,4,6-triphénylphosphinine en 1966 [5], par une procédure impliquant le traitement du sel de pyrylium avec de la tris(hydroxyméthyl)phosphine. Depuis lors, la chimie des hétérocycles phosphorés a connu une expansion remarquable. Pour la première fois, la phosphinine non substituée (de même que l'arsenine) a été synthétisée par Ashe[6] en 1971 en traitant le 1,1-dibutyl-1,4-dihydrostannabenzène avec du tribromure de phosphore.

En intégrant le phosphore dans la chimie des *carbo*-mères (**Figure 1**), les chercheurs peuvent accéder à une plus large gamme de composés aux propriétés et applications diverses.[7–13]Cette approche pourrait conduire à des solutions innovantes et à de nouvelles voies d'exploration en chimie de synthèse et en science des matériaux.

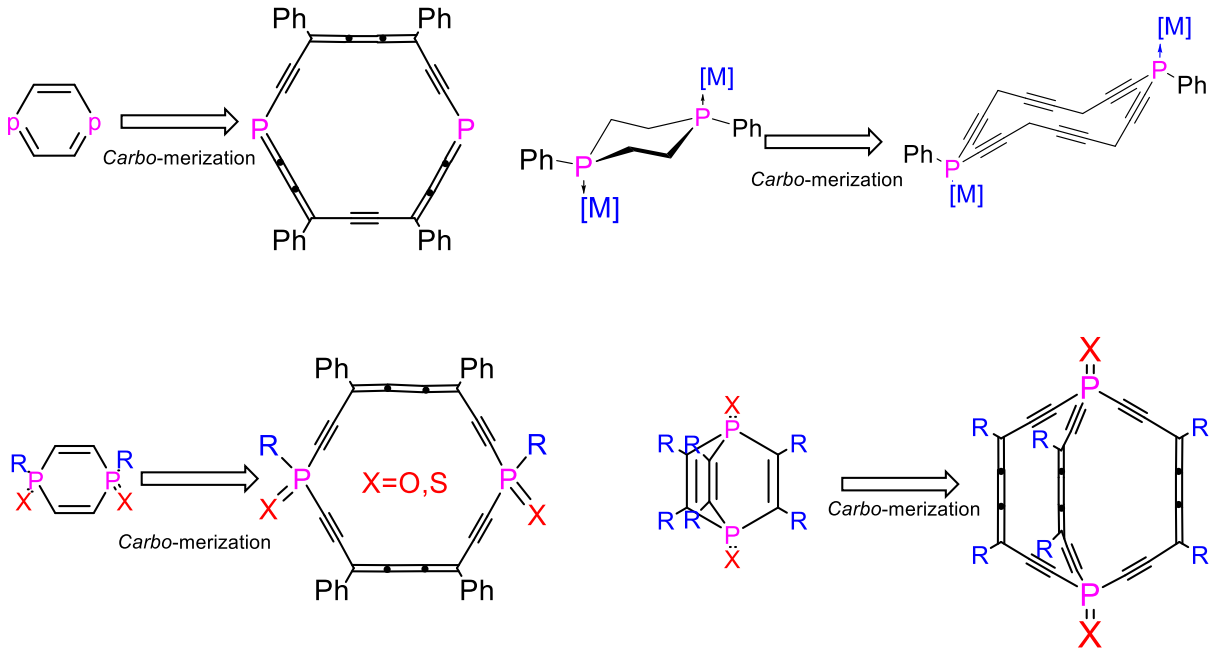

Figure 1 *Carbo*-mérisation de cycle de dérivés de la diphosphinine

Bien que des phospha-[n]péricyclynes, ayant soit un atome de phosphore à chaque sommet de la molécule, soit un seul atome de phosphore dans le cas du dérivé *carbo*-phospholane, aient été rapportés dans la littérature, l'étude de *carbo*-hétérocycles et de *carbo*-hétérobarrelènes contenant deux atomes de phosphore dans leur structure n'a jamais été envisagée jusqu'à présent. Leur synthèse, leur caractérisation et leurs propriétés sont donc les objectifs de cette thèse **(Figure 1**).

2. Synthèse de dérivés du carbo-diphosphacyclohexane et de la carbo-diphosphinine

Après la première synthèse d'une phosphinine par Märkl [5], une expansion remarquable de la chimie des hétérocycles phosphorés a commencé. Alors que les phosphinines sont bien connues et ont été largement étudiées, en particulier en ce qui concerne leur chimie de coordination[14] , les 1,4-diphosphinines ont été moins considérées. Elles ont été illustrées pour la première fois par Kobayashi en 1976, qui a également décrit le premier diphospha-barrelène. [15] Les 1,4-dihydro-diphosphinines non aromatiques ont été signalées pour la première fois en 1975, [16] et leurs analogues dithio ont été décrits pour la première fois en 1992 (**Figure 2**). [17] L'analogue saturé des 1,4-diphosphinines, à savoir le diphosphacyclohexane, a été signalé pour la première fois en 1959. [18] La version expansée de ces molécules, dans laquelle une unité C2 est insérée dans chaque liaison covalente de la structure de Lewis de ces hétérocycles insaturés, conduisant ainsi aux *carbo*-mères cycliques correspondants,[2] n'a jamais été envisagée. En effet, alors que les *carbo*-mères de dérivés du benzène ont été largement étudiés au cours des dernières décennies, [19–21] les *carbo*-mères d'hétérocycles n'ont été que très peu considérés au niveau expérimental.

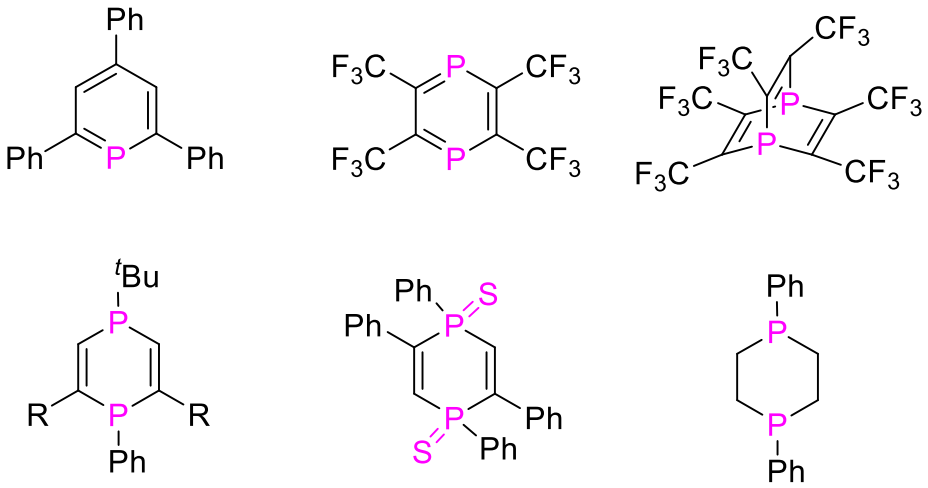

Figure 2. Exemples de phosphinines, diphosphinines et diphosphacyclohexanes connus.

Compte tenu de l'efficacité de la synthèse des *carbo*-benzènes centrosymétriques, les *carbo*-mères cycliques centrosymétriques des 1,4-diphosphinines sont apparus comme des cibles expérimentales "raisonnables", attrayantes en raison de leur intérêt potentiel notamment en tant que ligands P-P pontants.

S'inspirant d'un rapport fondateur détaillant la synthèse des dihydro-1,4-diphosphinines parentes[22], une réaction de macro-cyclisation à quatre composants [8+1+8+1] sans précédent a été envisagée entre deux équivalents du triyne connu, [23,24] intermédiaire classique utilisé pour la synthèse des *carbo*-benzènes, [25] et deux équivalents de $RP(X)Cl_2$ (**schéma 1**). Plusieurs bases ont été testées pour réaliser la double déprotonation du triyne et sa réaction avec $RP(X)Cl_2$, parmi lesquelles EtMgBr et *n*-Buli sont apparues inefficaces. Finalement, l'utilisation de LDA ou de LiHMDS a permis la formation du macrocycle attendu avec différents substituants et degrés d'oxydation du phosphore qui ont tous été isolés sous forme de mélanges de diastéréoisomères avec des rendements allant jusqu'à 67 % (avec $PhP(S)Cl_2$, en utilisant LDA comme base) après purification par chromatographie sur gel de silice.

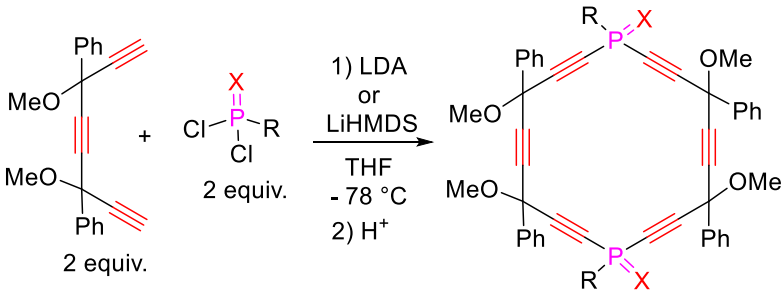

	X	R	Rendement	$\delta^{31}P$ (massif)
a		Ph	40%	–64 ppm
b		OMe	5%	+48 ppm
c		tBu	7%	–40 ppm
d	S	Ph	67%	–10 ppm
e	O	Ph	40%	–21.5 ppm

Schéma 1. Synthèse des macrocycles derivés de diphosphacyclohexanes.

En soumettant **d** à un traitement réducteur et acide avec un mélange $SnCl_2$/HCl dans du dichlorométhane à basse température, l'hexaphényl-*carbo*-1,4-dihydro-dithiodiphosphinine, premier exemple de dérivé de la *carbo*-diphosphinine, a été isolé avec un rendement de 20 % sous la forme d'un solide orange vif. La réduction de **d** à **f** induit une simplification des spectres RMN en raison de la diminution du nombre de stéréoisomères (seulement deux pour **f**). En RMN ^{31}P, deux singlets à -9 ppm correspondant aux deux diastéréoisomères sont observés, leur rapport étant d'environ 1:4,5. La solubilité limitée de **f** dans les solvants organiques courants n'a pas permis d'enregistrer un spectre RMN ^{13}C lisible en solution et il a donc été enregistré par RMN à rotation d'angle magique (RMN MAS).

Des monocristaux de l'isomère *trans* de **f** se sont formés à partir d'une solution de DCM par évaporation lente à température ambiante et ont été analysés par diffraction des rayons X (**schéma**

2). À l'état cristallin, le macrocycle de **f** est presque plan, avec une déviation maximale du plan moyen de 0,070 Å. Le macrocycle ne présente pas une forme hexagonale parfaite, les angles aux atomes P étant les plus fermés à 103,15°.

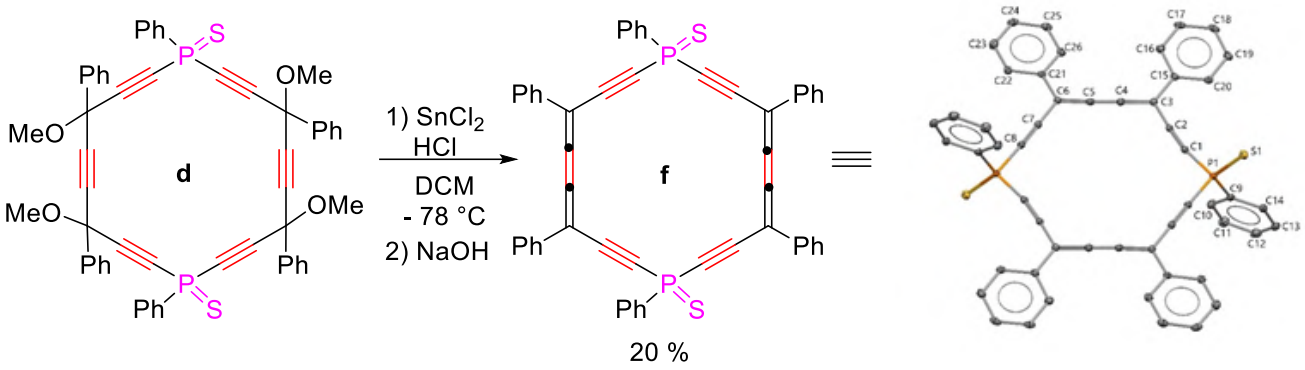

Schéma 2. Synthèse de la *carbo*-dihydro-1,4-dithiodiphosphinine et vue moléculaire de la structure cristalline aux rayons X de l'isomère *trans* de la *carbo*-dihydro-1,4-dithiodiphosphinine **f** (numéro de dépôt CCDC 2331290).

Les propriétés d'absorption UV-vis de **f** ont été étudiées en solution dans le DCM. Son spectre d'absorption présente une bande d'absorption principale intense à 438 nm avec deux épaulements à des énergies plus basses, ce qui rend cette bande assez large (**Figure 3**). Ce profil spectral est comparable à celui observé pour le *carbo*-dihydrobarrelène, [26] précédemment décrit, ayant deux motifs dialkynylbutatriènes inclus dans un macrocycle en C_{18} comme dans **f**. Bien que les deux spectres UV-vis n'aient pas été enregistrés dans le même solvant, **f** n'étant pas suffisamment soluble dans $CHCl_3$ pour permettre son utilisation, le décalage de 20 nm vers le rouge de la longueur d'onde d'absorption maximale observé pour **f** par rapport au *carbo*-dihydrobarrelène peut s'expliquer par un système π-conjugué légèrement plus étendu à travers les deux liaisons P=S dans **f**.

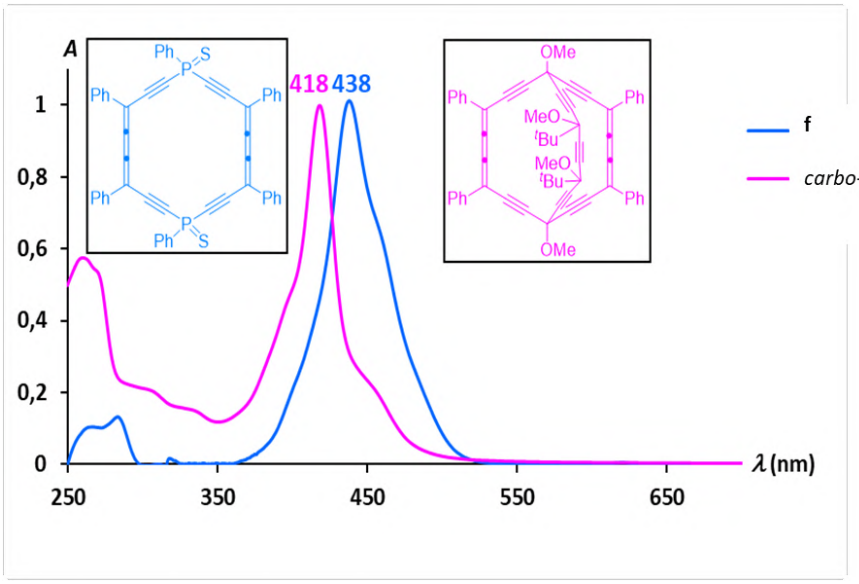

Figure 3. Spectres d'absorption normalisés de la *carbo*-dihydro-1,4-dithiodiphosphinine **f** (en solution dans DCM) et du *carbo*-dihydrobarrelène (en solution dans $CHCl_3$).

Le comportement redox de la *carbo*-dihydro-1,4-dithiodiphosphinine **f** a également été étudié par voltampérométrie à vague carrée et cyclique dans une solution de chloroforme en utilisant le nBu_4NPF_6 comme électrolyte support. Quatre réductions sont observées pour **f**, à -0,57, -0,70, -1,15 et -1,42 V/SCE, les deux premières étant réversibles et se produisant à des potentiels assez élevés par rapport au *carbo*-dihydrobarrelène qui ne présente que deux réductions à -1,11 et -1,28 V/SCE. La présence des deux atomes de phosphore à l'intérieur du macrocycle affecte donc de manière significative son comportement de réduction, tandis que la première oxydation de **f** (1,54 V/SCE) et du *carbo*-dihydrobarrelène (1,58 V/SCE) se produisent à des potentiels comparables. Deux oxydations sont observées pour **f**, la seconde se produisant à 1,72 V/SCE, aucune d'entre elles n'étant réversible, comme c'est généralement le cas pour les *carbo*-mères.

3 Synthèse et propriétés des dérivés du carbo-diphosphabarrelène

Le barrelène est un composé organique bicyclique fascinant, caractérisé par sa formule chimique C_8H_8 et son nom systématique bicyclo[2.2.2]octa-2,5,7-triène. Il a été synthétisé et décrit pour la première fois par H. E. Zimmerman en 1960[27]. Ce composé doit son nom à sa ressemblance

frappante avec un tonneau, ses trois unités éthylène attachées à deux groupes méthine représentant les douelles du tonneau.

La substitution d'un atome de carbone par un atome de phosphore dans le phospha-barrelène modifie ses propriétés électroniques par rapport au barrelène. Plus précisément, l'introduction du phosphore introduit un nouvel élément dont l'électronégativité et la taille atomique sont différentes, ce qui peut affecter la distribution de la densité électronique au sein de la molécule. Le phosphore a une électronégativité inférieure à celle du carbone, ce qui entraîne des changements dans la distribution des électrons et peut modifier la structure électronique globale de la molécule, ainsi que les longueurs de liaison, les angles de liaison et les orbitales moléculaires. En outre, la présence de phosphore peut introduire de nouveaux effets électroniques, liés à la présence de paires libres d'électrons, qui sont absentes dans le barrelène.

Le premier exemple de diphospha-barrelène a été synthétisé en 1976 par Kobayashi et ses collègues[15]. Il s'agit d'une molécule intrigante aux propriétés structurelles et chimiques uniques, qui présente un intérêt dans le domaine de la chimie des organophosphorés et de la science des matériaux.

En 2021, Zhu *et al.* [26] ont réussi à synthétiser des dérivés de *carbo*-barrelènes et les ont entièrement caractérisé. La famille émergente des *carbo*-barrelènes offre de nombreuses possibilités d'applications potentielles, notamment à travers leur capacité à encapsuler des cations et à présenter une efficacité élevée en matière de conductance de molécule unique (SMC). Au-delà de la thiolation des sommets carbinol sp^3 [25,28–30], leur substitution par des atomes de P est prometteuse pour la création d'une jonction P-or, offrant une alternative aux jonctions S-or classiques dans la mesure de la SMC par la méthode de rupture de jonction STM (STM-Break-Junction)[31]. (**Figure 4**) Dans le domaine de la chimie de coordination, ces bis-trialkynylphosphines rigides pourraient également servir de ligands dans des complexes à valence mixte.

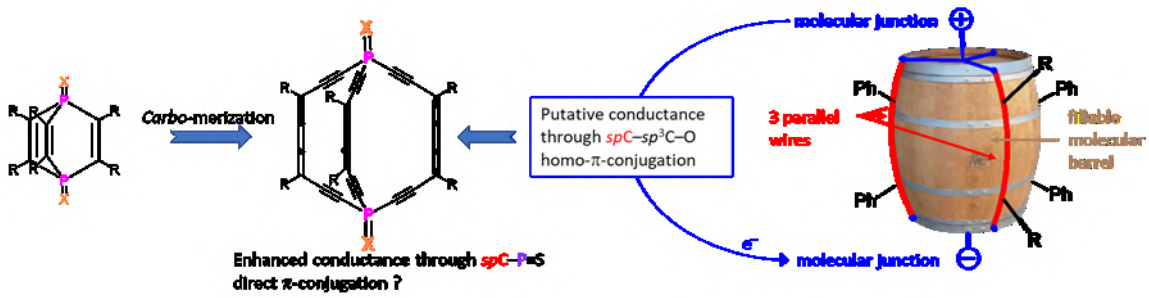

Figure 4. *Carbo-mérisation de dérivés de diphospha-barrelane et de diphospha-barrelène*

Pour des raisons de stabilité, le dioxyde de *carbo*-diphospha-barrelane a d'abord été ciblé en utilisant le LDA comme base, en suivant la stratégie développée précédemment pour la synthèse du *carbo*-diphosphacyclohexane (voir section 2). Dans ce cas, une mcrocyclisation [8+1+8+1+8] est utilisée (**schéma 3**). A partir du triyne précédemment utilisé (qui joue le rôle de précurseur en C_8), deux équivalents de LDA et 2/3 équivalents d'oxychlorure de phosphore sont ajoutés, et la réaction est suivie par RMN P^{31}, révélant l'apparition d'un signal principal à -55 ppm qui correspond au dioxyde de *carbo*-diphospha-barrelane **g**. Après une purification par chromatographie flash, le dioxyde de *carbo*-diphospha-barrelane **g** a été obtenu avec un rendement de 5 %. Ce composé a été caractérisé par RMN et HRMS.

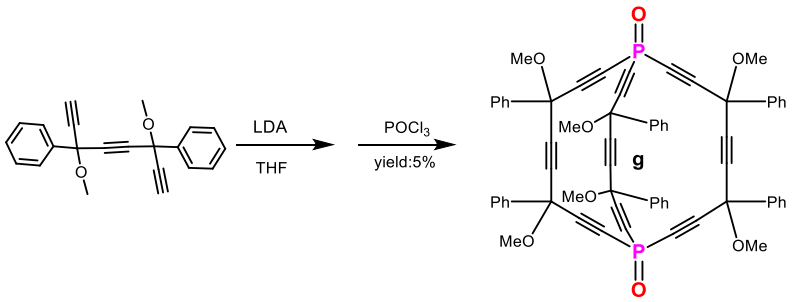

Schéma 3. Synthèse du dioxyde de *carbo*-diphospha-barrelane par réaction [8+1+8+1+8] entre le triyne et $Cl_3P{=}O$

Cependant, lorsque la réaction est réalisée avec $PSCl_3$ dans l'objectif de préparer l'analogue soufré *carbo*-dithiodiphospha-barrelane, seul le sous-produit **h** est obtenu. Dans ce cas, le groupe N, N-diisopropylamino, qui provient du réactif LDA utilisé pour déprotoner le triyne, a substitué

un atome de chlore du $SPCl_3$, conduisant au sous-produit **h** (**Schéma 4**), dont la structure a finalement été confirmée par MS et analyse élémentaire.

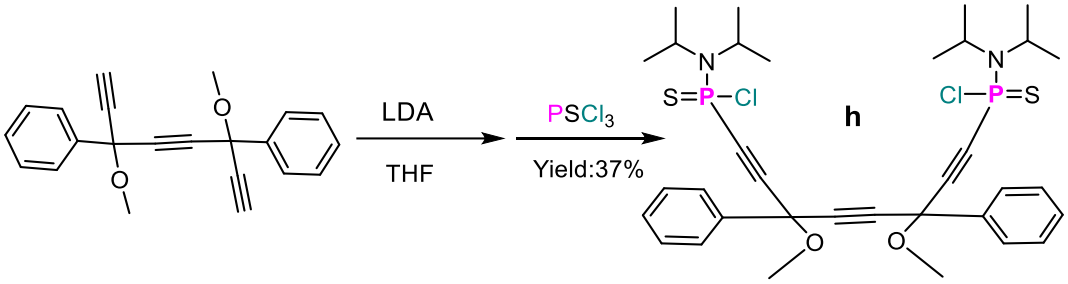

Schéma 4. Synthèse du sous-produit **h**

La réaction a également été testée sur le composé modèle **i**[32] afin de permettre une interprétation plus simple des résultats et de comparer les effets des différents réactifs utilisés pour la déprotonation de l'alcyne. Trois produits ont été obtenus à partir du composé modèle **i**, après réaction avec 1,1 équivalent de LiHMDS et 0,33 équivalent de (S)PCl_3 : la thiophosphine **j** attendue, le phosphane **k** et l'oxyde de phosphine **l** qui ont été séparés et caractérisés (**schéma 5)**.

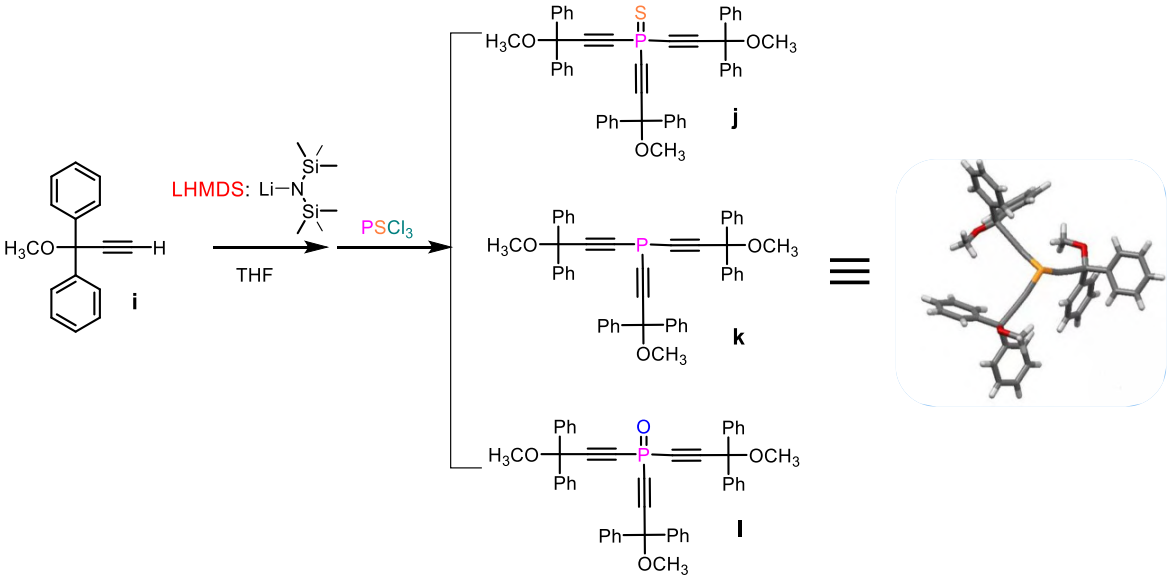

Schéma 5. Réaction de la molécule modèle avec $SPCl_3$ en présence de LiHMDS.

Après avoir testé différents réactifs de déprotonation sur un composé modèle, il a été déterminé que le LiHMDS est la base la plus prometteuse pour préparer le *carbo*-dithiodiphospha-

barrelane. En utilisant la stratégie [8+1+8+1+8] précédemment utilisée pour la synthèse du dioxyde de *carbo*-diphospha-barrelane avec deux équivalents de LiHMDS comme base et 2/3 équivalents de $Cl_3P{=}S$, le *carbo*-dithiodiphospha-barrelane **m** a été obtenu avec un rendement de 5% après purification par chromatographie flash. Le produit a été isolé sous la forme d'un mélange de stéréoisomères (16 stéréoisomères, dont 2 sont achiraux), donnant des signaux multiples entre -45,62 ppm et -47,39 ppm en RMN ^{31}P.

Une désulfuration partielle a été observée lors de cette réaction, comme cela a été observé précédemment avec le composé modèle, le produit réduit **n** représentant environ 17% du produit total. Le déplacement chimique en RMN ^{31}P du produit désulfuré est de -94 ppm. Lors du traitement de la réaction, le produit réduit **n** a été partiellement oxydé en **g**, donnant des signaux autour de -55 ppm dans le spectre RMN ^{31}P (**schéma 6**).

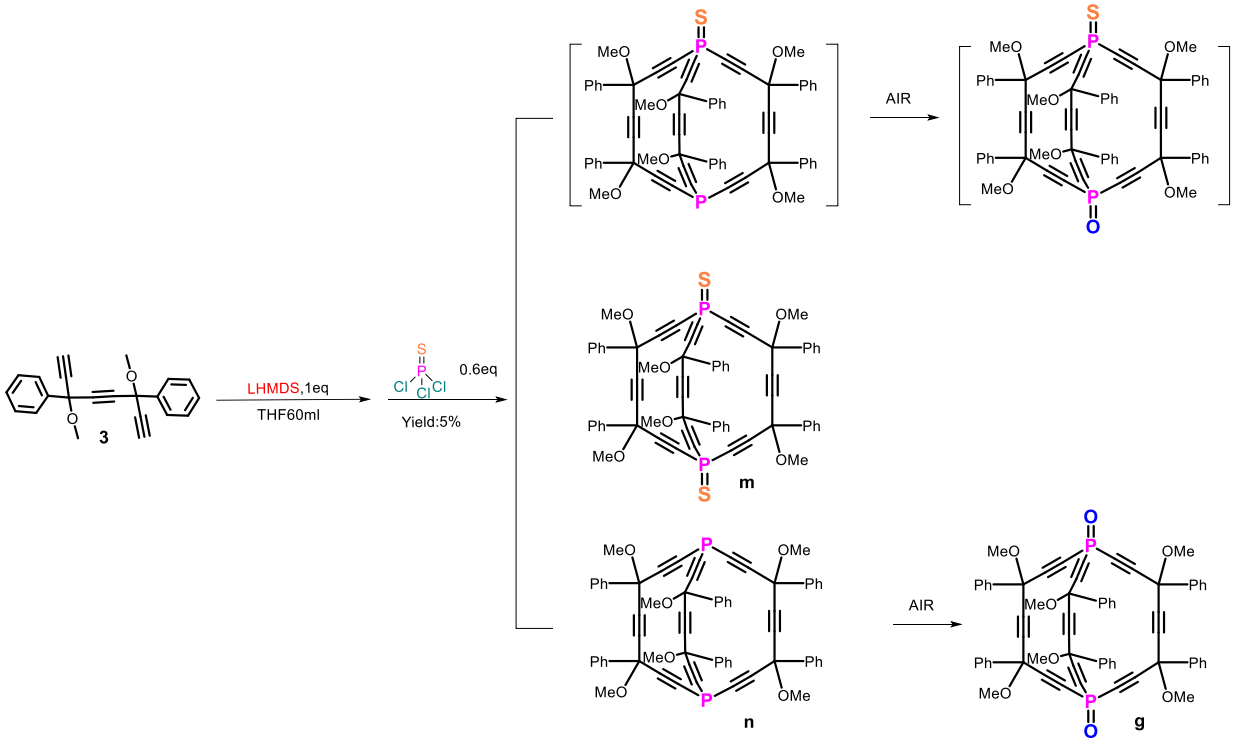

Schéma 6. Synthèse du *carbo*-dithiodiphospha-barrelane **m**, du *carbo*-diphospha-barrelane **n** et du dioxyde de *carbo*-diphospha-barrelane **g**

Après avoir soumis **m** à un traitement par $SnCl_2$/HCl dans du dichlorométhane (DCM) à basse température dans les conditions classiquement utilisées pour la synthèse de *carbo*-benzènes à partir

de précurseurs hexaoxy[6]péricyclyniques[33], l'hexaphényl-*carbo*-dithiodiphospha-barrelène **o** a été formé et isolé avec un rendement de 20 % sous la forme d'un solide orange foncé coloré (**schéma 7**) qui a pu être partiellement caractérisé par RMN et spectroscopie UV-vis.

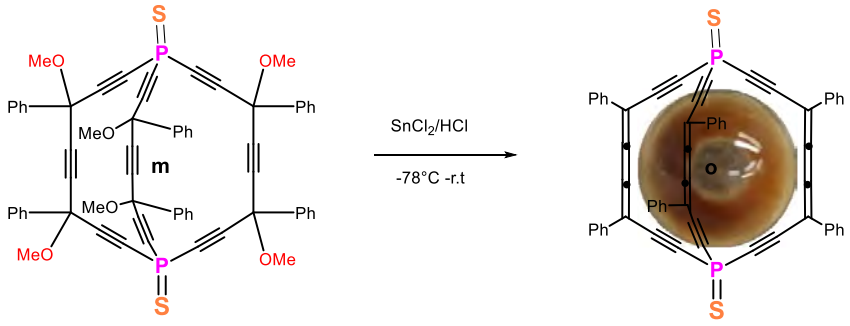

Schéma 7. Réduction du *carbo*-dithiodiphospha-barrelane **m** en hexaphényl-*carbo*-dithiodiphospha-barrelene **o**

L'hexaphényl-*carbo*-dithiodiphospha-barrelene **o** est peu soluble dans la plupart des solvants organiques, ce qui a permis sa caractérisation partielle en solution par spectroscopie RMN ^{1}H et ^{31}P.

La réaction d'élimination réductrice de **m** en **o** a induit la simplification du spectre RMN ^{31}P, en raison de l'élimination des stéréoisomères, conduisant à un signal unique avec un déplacement chimique de -44,6 ppm.

Le spectre RMN ^{1}H montre des signaux bien définis dans les régions 7,46-7,56 ppm et 7,79-7,83 ppm, correspondant aux protons aromatiques de **o**. Ceci contraste avec les signaux larges de **m**, qui sont dus à la présence de nombreux stéréoisomères. En outre, les pics autour de 3,5 ppm, qui correspondent aux groupes méthoxy de **m**, ont disparu après l'élimination réductrice.

Les propriétés d'absorption UV-vis de **o** ont été étudiées en solution dans le DCM. Son spectre d'absorption présente une bande d'absorption principale intense à 418 nm avec deux épaulements à des énergies plus basses, ce qui rend cette bande assez large. Ce profil spectral est comparable à celui observé pour la *carbo*-dihydrodithiodiphosphinine décrite précédemment (voir section 2), qui comportait deux motifs dialkynylbutatriènes inclus dans un macrocycle en C_{18}, c'est-à-dire un de moins que dans **o**. Le décalage de 20 nm vers le bleu de la longueur d'onde d'absorption maximale observé pour **o** par rapport à **f** est conforme aux observations de Zhu *et al*. en 2021[26] concernant les longueurs d'onde d'absorption UV-visible maximales des dérivés du *carbo*-barrelène et du

carbo-dihydrobarrelène. En effet, le *carbo*-barrelène, qui contient trois motifs butatriènes, présente un décalage vers le bleu de 17 nm de sa longueur d'onde d'absorption maximale UV-visible par rapport au dérivé partiellement réduit qu'est le *carbo*-dihydrobarrelène.

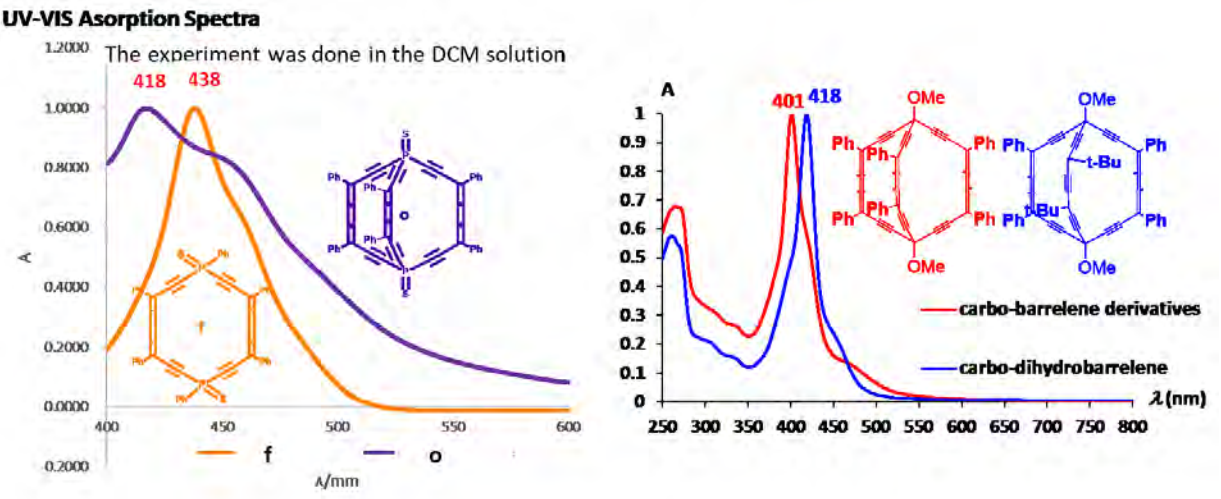

Figure 5. Spectres d'absorption UV-vis de l'hexaphényl-*carbo*-dithiodiphospha-barrelène **o** et de l'hexaphényl-*carbo*-1,4-dihydro-dithiodiphosphinine **f**, comparés aux spectres d'absorption UV-vis du *carbo*-barrelène et du *carbo*-dihydrobarrelène.

4. *Réactivité et chimie de coordination des dérivés macrocycliques diphosphorés et de leurs molécules modèles*

La réactivité de la *carbo*-1,4-dihydrodithidiphosphinine **f** a également été étudiée, et en particulier la possibilité de la réduire (ou désulfurer) en vue d'obtenir la diphosphine correspondante et de l'utiliser pour préparer des complexes de coordination. Les quantités disponibles de **f** étant limitées, les réactions ont d'abord été testées sur le composé modèle **p**, qui a été préparé en une étape par addition de deux équivalents du lithium de l'éther propargylique **i**[32,34,35]précédemment décrit sur $SPPhCl_2$ (**schéma 7**). La structure du composé modèle **p** a été confirmée par RMN, SM et analyse par diffraction des rayons X de monocristaux qui se sont déposés à partir d'une solution de **p** dans un mélange d'acétate d'éthyle et de pentane (**Figure 6**). La réaction a été effectuée en utilisant le LiHMDS comme base pour générer le lithien et le composé modèle **p** a été isolé avec un rendement de 86 %. Ensuite, diverses procédures ont été testées pour réduire cette thiophosphine en phosphine correspondante, parmi lesquelles la réduction

radicalaire mettant en jeu l'utilisation de $(Me_3Si)_3SiH$ en présence d'AIBN comme initiateur de radicaux s'est avérée la plus efficace.[36] Dans ces conditions, la phosphine ciblée **q** a été isolée avec un rendement de 75 %, et l'oxyde de phosphine correspondant **r** a été obtenu quantitativement par simple oxydation de **q** en présence d'air. Les deux produits ont été entièrement caractérisés, notamment par une analyse de diffraction des rayons X pour **r** (**figure 6**). Des études préliminaires de la chimie de coordination de **q** ont également été réalisées, avec la synthèse du complexe de Ruthénium **s**. Sa préparation a été réalisée par un processus en deux étapes à partir de la thiophosphine **p**, sans isolation de l'intermédiaire phosphine **q** pour éviter son oxydation partielle en oxyde de phosphine **r**. Le complexe de ruthénium ainsi obtenu a été isolé sous la forme d'un solide rouge-orange avec un rendement de 71 %.

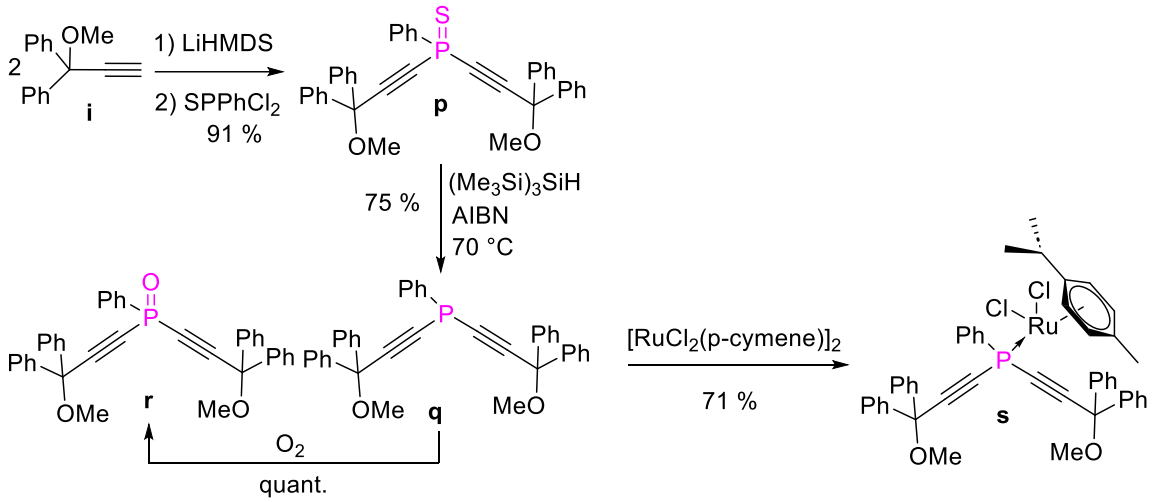

Schéma 7. Synthèse du composé modèle **p** et sa réactivité.

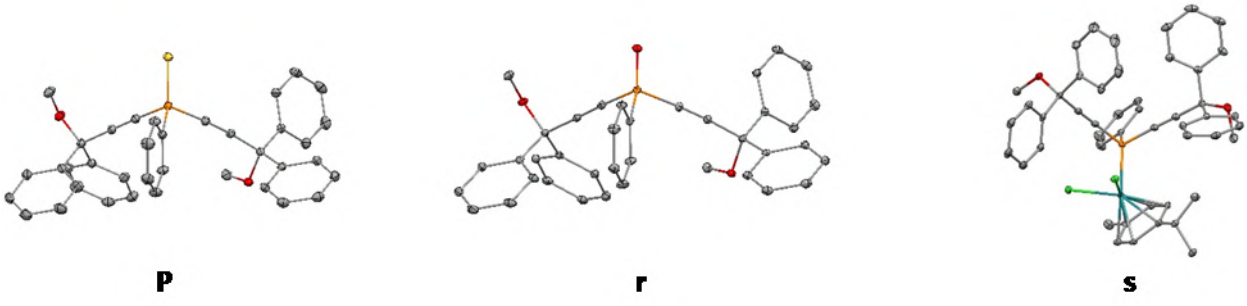

Figure 6. Vue moléculaire de la structure cristalline aux rayons X de **p** (en haut, numéro de dépôt CCDC 2342365), **r** (au milieu, numéro de dépôt CCDC 2342364) et **s** (en 2347595).

La même méthodologie a donc été appliquée dans un premier temps à la *carbo*-dihydro-dithiodiphosphinine **f** pour préparer le di-complexe de ruthénium correspondant **t**. Cependant, le traitement de **f** avec $(Me_3Si)_3SiH$ et AIBN induit la décomposition du macrocycle, probablement en raison du caractère diradical des unités butatriènes[37], les rendant sensibles aux conditions réactionnelles radicalaires. La synthèse du dicomplexe de ruthénium **u** a donc été testée à partir du macrocycle **d** (**schéma 8**).

Le dicomplexe de ruthénium **u** a été obtenu sous la forme d'un mélange de stéréoisomères, avec un rendement quantitatif. Les tentatives de réduction de **u** en **t** à l'aide de divers réactifs acides et réducteurs ont échoué, probablement en raison de la sensibilité des complexes dans de telles conditions.

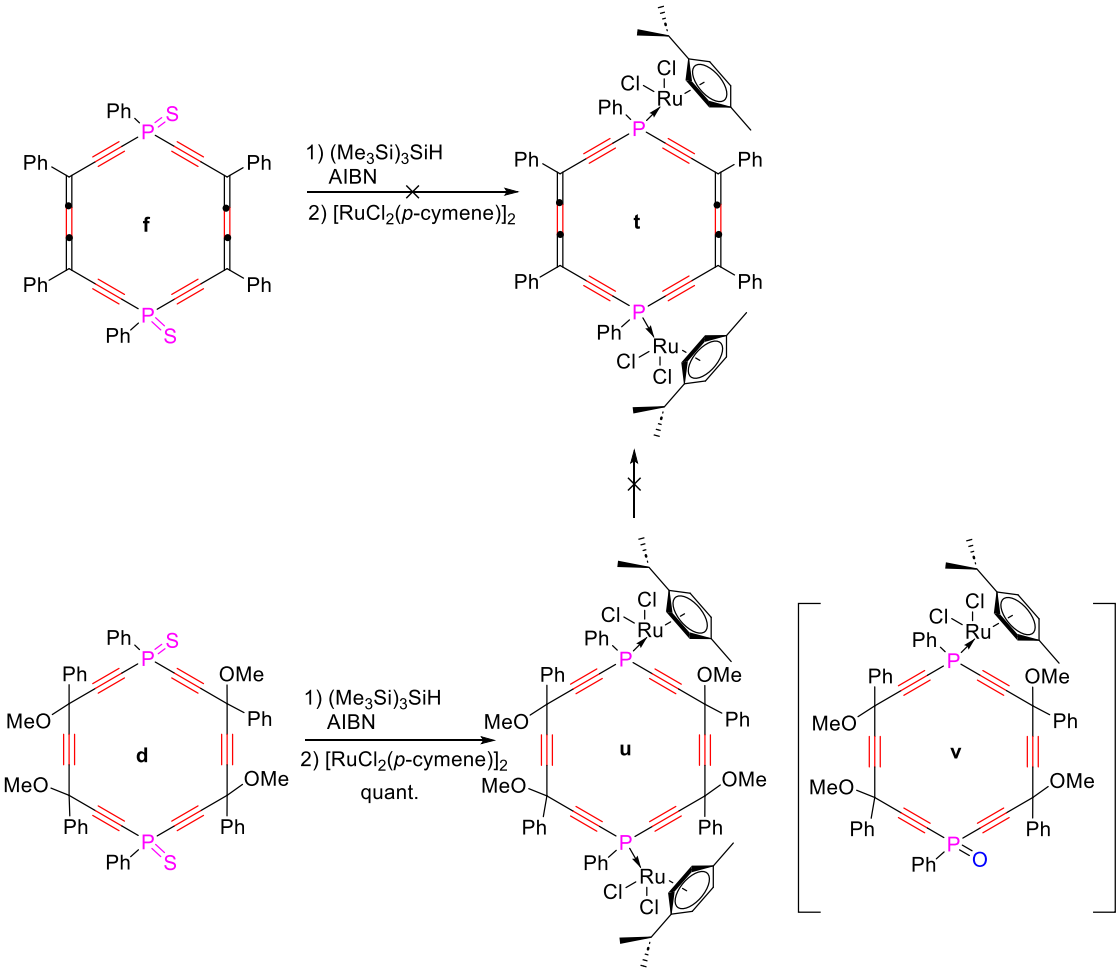

Schéma 8. Synthèse du dicomplexe de ruthénium **u** et tentatives de synthèse de **t**.

5. *Conclusion et perspectives*

Les *carbo*-mères de dérivés benzéniques ont été largement étudiés au cours des dernières décennies, tandis que les *carbo*-mères d'hétérocycles ont reçu peu d'attention expérimentale. La première synthèse de *carbo*-dihydro-dithiodiphosphine et de *carbo*-diphospha-barrelènes présentés dans ce manuscrit offre une nouvelle opportunité d'étudier les propriétés des *carbo*-hétérocycles- . L'impact de l'insertion de phosphore dans la structure des *carbo*-mères et ses effets sur le comportement redox, l'absorption UV-Vis et les caractéristiques des molécules à l'état solide obtenues par diffraction des rayons X représentent des informations d'intérêt sur cette nouvelle famille de molécules.

Les ligands phosphine macrocycliques insaturés, *carbo*-mères du diphosphacyclohexane et du diphosphabarrelane, présentent des propriétés de base similaires à celles du diphosphacyclohexane et du diphosphabarrelane parents, mais présentent des tailles moléculaires plus importantes, des propriétés de transfert d'électrons uniques et des configurations spatiales distinctes. La littérature concernant la synthèse de complexes de coordination avec des ligands de de type diphosphacyclohexane et diphosphabarrelane et leur utilisation en catalyse sont discutées. La synthèse de leurs analogues expansés, tels que ceux décrits dans ce manuscrit, ouvre la perspective d'utiliser ces *carbo*-phosphahétérocycles comme catalyseurs dans l'hydrogénation d'alcènes ou d'alcynes, les réactions de transfert et les réactions de formation de liaisons carbone-carbone, ainsi que dans l'hydroboration (**Figure 7**). Les résultats du travail présenté dans ce mémoire pourraient donc conduire à la conception et la synthèse de nouveaux catalyseurs plus polyvalents, ce qui en fait un investissement précieux à long terme.

La famille des *carbo*-diphospha-barrelènes est intéressante à plusieurs égards : elle pourrait d'une part être étudiée pour son comportement de cage vis-à-vis de cations et d'autre part pour ses propriétés de transport de charge, et en particulier elle pourrait présenter une conductance de molécule unique (SMC) élevée. En effet, macrocycle des *carbo*-benzènes a été rapporté comme ayant une valeur de SMC sans précédent. La SMC diminuant avec le caractère aromatique et augmentant avec le nombre de ces chemins conjugués parallèles, on peut s'attendre à ce que le

carbo-barrelène, avec trois unités dialcynylbutatriènes parallèles possède une conductance moléculaire encore plus élevée que les *carbo*-benzènes.

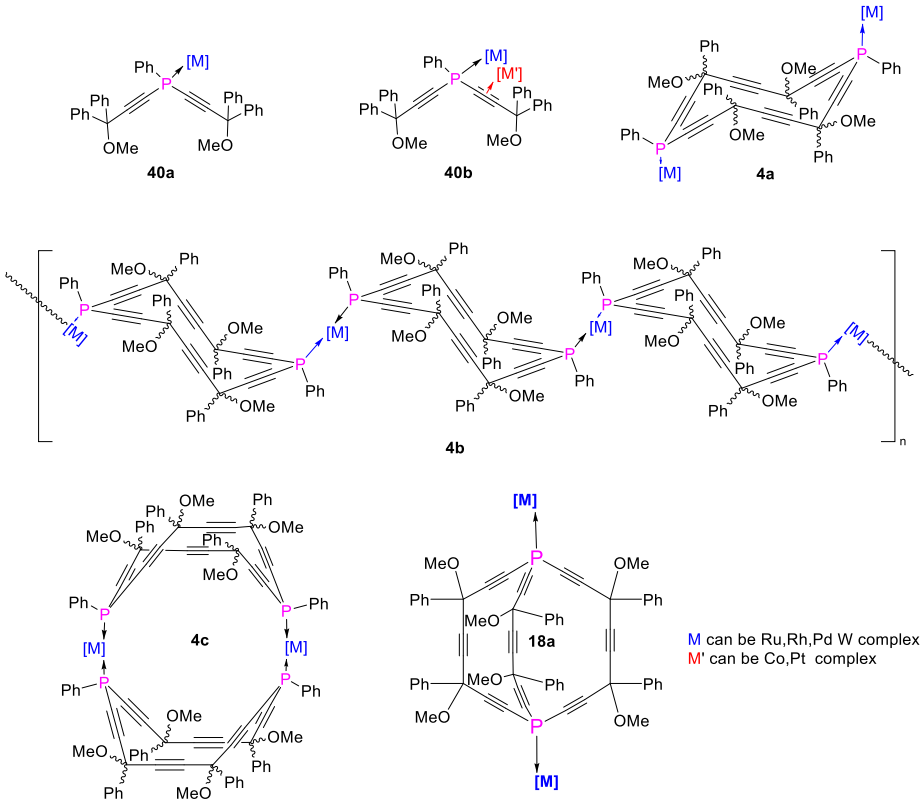

Figure 7. Complexes de métaux de transition pouvant être envisagés à partir de la molécule modèle et des *carbo*-diphosphacyclohexanes et *carbo*-diphosphabarrelènes en vue de les utiliser en catalyse.

References

(1) *Carbon Rich Compounds II, Macrocyclic Oligoacetylenes and Other Linearly Conjugated S ystems*; A. de Meijer, Ed.; Springe; Vol. 201.

(2) Chauvin, R. “Carbomers”. I. A General Concept of Expanded Molecules. *Tetrahedron Lett.* **1 995**, *36* (3), 397–400. https://doi.org/10.1016/0040-4039(94)02275-G.

(3) Yao, Z.; Lin, X.; Chauvin, R.; Wang, L.; Gras, E.; Cui, X. Phosphine-Phosphonium Ylides as Ligands in Palladium-Catalysed C2-H Arylation of Benzoxazoles. *Chin. Chem. Lett.* **2020**, *31* (12), 3250–3254. https://doi.org/10.1016/j.cclet.2020.04.008.

(4) Zhu, C.; Gras, E.; Duhayon, C.; Lacassin, F.; Cui, X.; Chauvin, R. The Forgotten Nitroaroma tic Phosphines as Weakly Donating P-ligands: An *N* -Aryl -benzimidazolyl Series in RhCl(C O) Complexes. *Chem. – Asian J.* **2017**, *12* (21), 2845–2856. https://doi.org/10.1002/asia.201 701078.

(5) Märkl, G. 2,4,6-Triphenylphosphabenzene. *Angewandte Chemie International Edition in En glish* **1966**, *5* (9), 846–847. https://doi.org/10.1002/anie.196608463.

(6) Ashe, A. J. I.; Gordon, M. D. Bismabenzene. Reaction of Group V Heteroaromatic Compou nds with Hexafluorobutyne. *J. Am. Chem. Soc.* **1972**, *94* (21), 7596–7597. https://doi.org/10. 1021/ja00776a063.

(7) Hengefeld, A.; Kopf, J.; Nast, R. Kristall- und Molekülstruktur von Di-μ-iodo-tetrakis[tris(p henylethinyl)phosphin]dikupfer. *Chemische Berichte* **1977**, *110* (9), 3078–3083. https://doi.o rg/10.1002/cber.19771100913.

(8) Hengefeld, A.; Kopf, J.; Rehder, D. Pentacarbonyl[Tris(Phenylethynyl)Phosphine]Chromium (0), Cr(CO)5P(C.Tplbond.CPh)3: Spectral, Structural and MO Characteristics. *Organometal lics* **1983**, *2* (1), 114–121. https://doi.org/10.1021/om00073a021.

(9) Hengefeld, A.; Nast, R. Komplexe Des Typs $Ni(CO)_4$-n($P(C{\equiv}CC6H5)m(C_6H_5)_{3-m})_n$ (*n* = 2, 3, 4; *m* = 3, 2, 1). *J. Organomet. Chem.* **1983**, *252* (3), 375–379. https://doi.org/10.1016/S00 22-328X(00)99838-3.

(10) Lang, H.; Leise, M.; Zsolnai, L. Bifunctional Neutral Phosphenium Ion Complexes: Synthes is of Phenylethynyl- and Styryl-Substituted (R)(R′)P=Mo- $(H_5\text{-}C_5Me_5)(CO)_2$ Compounds. C rystal Structure of $[2,6\text{-}tBu_2\text{-}4\text{-}MeC_6H_2O)(PhC{\equiv}C)]P{=}Mo(H_5\text{-}C_5Me_5)(CO)_2$. *J. Organomet. Chem.* **1990**, *389* (3), 325–332. https://doi.org/10.1016/0022-328X(90)85427-Z.

(11) Stulz, E.; Sanders, J. K. M.; Montalti, M.; Prodi, L.; Zaccheroni, N.; Fabrizi de Biani, F.; Gri giotti, E.; Zanello, P. Phosphine and Phosphonite Complexes of a Ru(II) Porphyrin. 2. Photo physical and Electrochemical Studies. *Inorg. Chem.* **2002**, *41* (20), 5269–5275. https://doi.or g/10.1021/ic025728q.

(12) Hightower, S. E.; Corcoran, R. C.; Sullivan, B. P. Unusual, Bifurcated Photoreactivity of a R henium(I) Carbonyl Complex of Triethynylphosphine. *Inorg. Chem.* **2005**, *44* (26), 9601–96 03. https://doi.org/10.1021/ic050901e.

(13) Mathur, P.; Rai, D. K.; Ji, R. S.; Pathak, B.; Boodida, S.; Mobin, S. M. Structural and Electro chemical Aspects of Tris(Ferrocenyl/Phenyl-Ethynyl)Phosphine Ligated Chalcogen Bridged Iron Carbonyl Clusters. *RSC Adv.* **2013**, *3* (48), 26025–26034. https://doi.org/10.1039/C3RA 44788J.

(14) Coles, N. T.; Sofie Abels, A.; Leitl, J.; Wolf, R.; Grützmacher, H.; Müller, C. Phosphinine-B ased Ligands: Recent Developments in Coordination Chemistry and Applications. *Coord. Ch em. Rev.* **2021**, *433*, 213729. https://doi.org/10.1016/j.ccr.2020.213729.

(15) Kobayashi, Y.; Kumadaki, I.; Ohsawa, A.; Hamana, H. 2,3,5,6-Tetrakis (Trifluoromethyl)-1, 4-Diphosphabenzene. *Tetrahedron Lett.* **1976**, *17* (41), 3715–3716. https://doi.org/10.1016/S 0040-4039(00)93089-2.

(16) Märkl, G.; Matthes, D.; Donaubauer, A.; Baier, H. 1.4 -Diphospha-, 1-Phospha-4-Arsa-Dihy drobenzole. *Tetrahedron Lett.* **1975**, *16* (36), 3171–3174. https://doi.org/10.1016/S0040-403 9(00)91487-4.

(17) Fluck, E.; Lange, K.; Heckmann, G. REAKTIONEN DES 1,1′,3,3′-TETRAKIS(DIMETHY LAMINO)-1λ5,3Δ5-DIPHOSPHETS MIT ALKOHOLEN. ALK(PHEN)OXYCARBODIPH OSPHORANE. *Phosphorus Sulfur Silicon Relat. Elem.* **1992**, *72* (1–4), 49–54. https://doi.or g/10.1080/10426509208031538.

(18) Hinton, R. C.; Mann, F. G. 569. Triethylenediphosphine (1 : 4-Diphosphabicyclo[2 : 2 : 2]-O ctane). *J. Chem. Soc. Resumed* **1959**, No. 0, 2835–2843. https://doi.org/10.1039/JR95900028 35.

(19) Cocq, K.; Lepetit, C.; Maraval, V.; Chauvin, R. "Carbo-Aromaticity" and Novel Carbo-Aro matic Compounds. *Chem. Soc. Rev.* **2015**, *44* (18), 6535–6559. https://doi.org/10.1039/C5CS 00244C.

(20) Cocq, K.; Barthes, C.; Rives, A.; Maraval, V.; Chauvin, R. Synthesis of Functional Carbo-Be nzenes with Functional Properties: The C2 Tether Key. *Synlett* **2019**, *30* (01), 30–43. https:// doi.org/10.1055/s-0037-1610269.

(21) Bucknum, M. J.; Castro, E. A. The Carbon Allotrope Hexagonite and Its Potential Synthesis from Cold Compression of Carbon Nanotubes. *J. Chem. Theory Comput.* **2006**, *2* (3), 775–7 81. https://doi.org/10.1021/ct060003n.

(22) Avarvari, N.; Fourmigué, M. 1,4-Dihydro-1,4-Diphosphinine Fused with Two Tetrathiafulva lenes. *Chem. Commun.* **2004**, No. 24, 2794–2795. https://doi.org/10.1039/B412193G.

(23) Maurette, L.; Tedeschi, C.; Sermot, E.; Soleilhavoup, M.; Hussain, F.; Donnadieu, B.; Chauvin, R. Synthesis and Stereochemical Resolution of Functional [5]Pericyclynes. *Tetrahedron* **2004**, *60* (44), 10077–10098. https://doi.org/10.1016/j.tet.2004.07.052.

(24) Leroyer, L.; Zou, C.; Maraval, V.; Chauvin, R. Synthesis and Stereochemical Resolution of a [6]Pericyclynedione: Versatile Access to Pericyclynediol Precursors of *Carbo*-Benzenes. *Comptes Rendus Chim.* **2009**, *12* (3–4), 412–429. https://doi.org/10.1016/j.crci.2008.09.018.

(25) Leroyer, L.; Lepetit, C.; Rives, A.; Maraval, V.; Saffon-Merceron, N.; Kandaskalov, D.; Kieffer, D.; Chauvin, R. From Hexaoxy-[6]Pericyclynes to Carbo-Cyclohexadienes, Carbo-Benzenes, and Dihydro-Carbo-Benzenes: Synthesis, Structure, and Chromophoric and Redox Properties. *Chem. – Eur. J.* **2012**, *18* (11), 3226–3240. https://doi.org/10.1002/chem.201102993.

(26) Zhu, C.; Poater, A.; Duhayon, C.; Kauffmann, B.; Saquet, A.; Rives, A.; Maraval, V.; Chauvin, R. *Carbo* -mer of Barrelene: A Rigid 3D-Carbon-Expanded Molecular Barrel. *Chem. – Eur. J.* **2021**, *27* (36), 9286–9291. https://doi.org/10.1002/chem.202100670.

(27) Zimmerman, H. E.; Paufler, R. M. BICYCLO[2,2,2]-2,5,7-OCTATRIENE (BARRELENE), A UNIQUE CYCLIC SIX ELECTRON PI SYSTEM. *J. Am. Chem. Soc.* **1960**, *82* (6), 1514–1515. https://doi.org/10.1021/ja01491a071.

(28) Baglai, I.; de Anda-Villa, M.; Barba-Barba, R. M.; Poidevin, C.; Ramos-Ortíz, G.; Maraval, V.; Lepetit, C.; Saffon-Merceron, N.; Maldonado, J.-L.; Chauvin, R. Difluorenyl Carbo-Benzenes: Synthesis, Electronic Structure, and Two-Photon Absorption Properties of Hydrocarbon Quadrupolar Chromophores. *Chem. – Eur. J.* **2015**, *21* (40), 14186–14195. https://doi.org/10.1002/chem.201500482.

(29) Vallejos, M. M.; Pellegrinet, S. C. Theoretical Study of the BF3-Promoted Rearrangement of Oxiranyl N-Methyliminodiacetic Acid Boronates. *J. Org. Chem.* **2017**, *82* (11), 5917–5925. https://doi.org/10.1021/acs.joc.7b01096.

(30) Zhu, C.; Wang, T.-H.; Su, C.-J.; Lee, S.-L.; Rives, A.; Duhayon, C.; Kauffmann, B.; Maraval, V.; Chen, C.; Hsu, H.-F.; Chauvin, R. 3D and 2D Supramolecular Assemblies and Thermotropic Behaviour of a Carbo-Benzenic Mesogen. *Chem. Commun.* **2017**, *53* (43), 5902–5905. https://doi.org/10.1039/C7CC02430D.

(31) Xu, B.; Tao, N. J. Measurement of Single-Molecule Resistance by Repeated Formation of Molecular Junctions. *Science* **2003**, *301* (5637), 1221–1223. https://doi.org/10.1126/science.1087481.

(32) Gawel, P.; Dengiz, C.; Finke, A. D.; Trapp, N.; Boudon, C.; Gisselbrecht, J.-P.; Diederich, F. Synthesis of Cyano-Substituted Diaryltetracenes from Tetraaryl[3]Cumulenes. *Angew. Chem. Int. Ed.* **2014**, *53* (17), 4341–4345. https://doi.org/10.1002/anie.201402299.

(33) Leroyer, L.; Lepetit, C.; Rives, A.; Maraval, V.; Saffon-Merceron, N.; Kandaskalov, D.; Kief fer, D.; Chauvin, R. From Hexaoxy-[6]Pericyclynes to Carbo-Cyclohexadienes, Carbo-Benz enes, and Dihydro-Carbo-Benzenes: Synthesis, Structure, and Chromophoric and Redox Pro perties. *Chem. Weinh. Bergstr. Ger.* **2012**, *18* (11), 3226–3240. https://doi.org/10.1002/chem. 201102993.

(34) Ried, W.; Schlegelmilch, W.; Piesch, S. Äthinierungsreaktionen, XX. Über Alkindiole Und K umulene. *Chem. Ber.* **1963**, *96* (5), 1221–1228. https://doi.org/10.1002/cber.19630960508.

(35) Ried, W.; Neidhardt, R. Über Ringschlußreaktionen Im Anschluß an Die Allenumlagerung v on 1-Methoxy-1.1.5.5-Tetraaryl-Pentin-(2)-Onen-(4) Mit Anorganischen Säurehalogeniden. *Chem. Ber.* **1970**, *103* (7), 2208–2224. https://doi.org/10.1002/cber.19701030725.

(36) Romeo, R.; Wozniak, L. A.; Chatgilialoglu, C. Radical-Based Reduction of Phosphine Sulfid es and Phosphine Selenides by (Me3Si)3SiH. *Tetrahedron Lett.* **2000**, *41* (50), 9899–9902. h ttps://doi.org/10.1016/S0040-4039(00)01759-7.

(37) Auffrant, A.; Jaun, B.; Jarowski, P. D.; Houk, K. N.; Diederich, F. Peralkynylated Buta-1,2,3 -Trienes: Exceptionally Low Rotational Barriers of Cumulenic C≡C Bonds in the Range of Those of Peptide C≡N Bonds. *Chem. – Eur. J.* **2004**, *10* (12), 2906–2911. https://doi.org/10. 1002/chem.200400218.

Annexes

Crystallographic Data and Structural Refinement Parameters for Compounds

	20240226-Dan soufre	20240304-Dan oxygène	20240402-Dan Ru	DanAvril2022-Brice	20240429-Dan
Chemical formula	$C_{38}H_{31}O_2PS$	$C_{38}H_{31}O_3P$	$C_{48.50}H_{46}Cl_3O_2PRu$	$C_{52}H_{30}P_2S_2$	$C_{44}H_{30}P_2S_2$
M ($g.mol^{-1}$)	582.70	566.64	899.30	780.89	684.80
Crystal system	Monoclinic	Monoclinic	Triclinic	Triclinic	Monoclinic
Space group	P $2_1/c$	P $2_1/c$	P -1	P -1	P $2_1/c$
a (Å)	9.9630(1)	9.8457(1)	13.1192(1)	8.3477(6)	8.3168(1)
b (Å)	28.8565(2)	28.5483(3)	16.7850(1)	11.1327(7)	12.4724(1)
c (Å)	11.7084(1)	11.6095(2)	19.3142(1)	11.2423(8)	16.7109(1)
α (°)	90	90	90.655(1)	97.136(5)	90
β (°)	113.679(1)	112.998(2)	90.347(1)	94.354(5)	92.310(1)
γ (°)	90	90	92.415(1)	104.652(6)	90
V ($Å^3$)	3082.74(5)	3003.81(8)	4248.95(5)	996.68(12)	1732.02(3)
Z	4	4	4	1	2
d_{calcd}	1.255	1.253	1.406	1.301	1.313
μ (mm^{-1})	1.673	1.096	5.375	2.247	2.503
Refl. measured	10605	27672	148264	9992	28504
Refl. unique	5973	5900	18179	4012	3735
R_{int}	0.101	0.037	0.049	0.037	0.031
Refl. with $I > 2\sigma(I)$	5819	5338	16201	3053	3284
Nb. parameters	379	379	1111	253	217
R with $I > 2\sigma(I)$	0.0349	0.0366	0.0298	0.0410	0.0325
Rw with $I > 2\sigma(I)$	0.0942	0.0963	0.0792	0.1000	0.0829
Residual electron density ($ē.Å^{-3}$)	0.32/-0.37	0.32/-0.46	0.86/-0.83	0.40/-0.67	0.55/-0.37
CCDC number	2342365	2342364	2347595	2331290	2352206

Crystal Data 3b

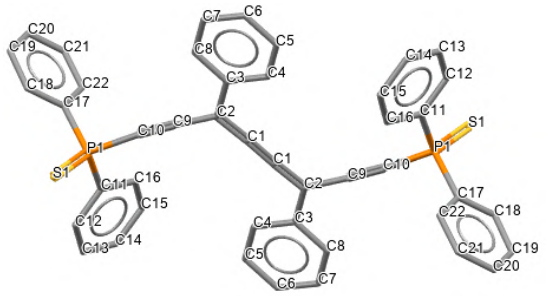

a = 8.31680(10) Å α = 90°

b = 12.47240(10) Å β = 92.3100(10)°

c = 16.71090(10) Å γ = 90°

Volume	1732.02(3) Å³	Crystal Class	monoclinic
Space group	P 1 2_1/c 1	Z =	2
Formula	C_{44} H_{30} P_2 S_2	M_r	684.80
Cell determined from	20077 reflections	Cell θ range =	4 - 79°
Temperature	100K		
Shape	block		
Colour	orange	Size	0.05 × 0.06 × 0.17 mm
D_x	1.31	F000	712.000
μ	2.503 mm^{-1}		
Absorption correction	multi-scan		
T_{min}	0.64	T_{max}	0.88

Data Collection

Diffractometer	multi-scan
Scan type	ϕ and ω scans
Reflections measured	28504
Independent reflections	3735
Rint	0.0306
$θ_{max}$	79.9687
h =	-10 → 9
k =	-15 → 15
l =	-21 → 21

Refinement

$Δρ_{min}$ =	-0.37 e $Å^{-3}$
$Δρ_{max}$ =	0.55 e $Å^{-3}$
Reflections used	3410
Cutoff: I >	-3.00σ(I)
Parameters refined	217
S =	0.99

R-factor	0.033
weighted R-factor	0.083
Δ/σ_{max}	0.0009
Refinement on	F^2
w =	$1/[\sigma^2(F_{obs}^2) + (0.038 \times P)^2 + 1.560 \times P + 0.000 + 0.000 \times \sin\theta]$, $P = 0.333 \times \max(F_{obs}^2,0) + 0.667 \times F_{calc}^2$

Parameters

Label	*x*	*y*	*z*	$U_{iso/equiv}$	Occupancy
C1	0.54870(18)	0.52589(13)	0.52171(9)	0.0206	1.0000
C2	0.64929(18)	0.58144(12)	0.57155(9)	0.0197	1.0000
C3	0.81381(18)	0.61298(12)	0.55110(9)	0.0190	1.0000
C4	0.86433(19)	0.60222(12)	0.47238(9)	0.0210	1.0000
C5	1.0176(2)	0.63149(12)	0.45341(9)	0.0232	1.0000
C6	1.12541(19)	0.67186(13)	0.51259(10)	0.0243	1.0000
C7	1.07688(19)	0.68233(12)	0.59124(9)	0.0218	1.0000
C8	0.92147(19)	0.65375(13)	0.61004(9)	0.0214	1.0000
C9	0.58874(17)	0.60961(12)	0.64756(9)	0.0207	1.0000
C10	0.53136(18)	0.63197(13)	0.71063(9)	0.0212	1.0000
C11	0.25068(17)	0.58191(13)	0.78791(9)	0.0197	1.0000
C12	0.10876(18)	0.62165(14)	0.81864(9)	0.0239	1.0000
C13	0.02795(19)	0.55950(16)	0.81573(10)	0.0306	1.0000
C14	-0.0255(2)	0.45717(16)	0.78335(10)	0.0328	1.0000
C15	0.1154(2)	0.41727(15)	0.75241(10)	0.0318	1.0000
C16	0.25292(19)	0.47992(14)	0.75370(9)	0.0247	1.0000
C17	0.55679(17)	0.60214(12)	0.87757(9)	0.0188	1.0000
C18	0.6311(2)	0.66711(14)	0.93553(10)	0.0271	1.0000
C19	0.7335(2)	0.62048(16)	0.99449(10)	0.0347	1.0000
C20	0.7563(2)	0.51193(17)	0.99632(10)	0.0340	1.0000
C21	0.6798(2)	0.44694(15)	0.93967(11)	0.0306	1.0000
C22	0.58061(19)	0.49116(13)	0.88009(10)	0.0243	1.0000
P1	0.43174(4)	0.66230(3)	0.79841(2)	0.0170	1.0000
S1	0.39275(5)	0.81487(3)	0.81386(2)	0.0262	1.0000
H41	0.79076(19)	0.57417(12)	0.43159(9)	0.0251	1.0000
H51	1.0505(2)	0.62365(12)	0.40170(9)	0.0275	1.0000
H61	1.22958(19)	0.69072(13)	0.50043(10)	0.0283	1.0000
H71	1.14584(19)	0.70742(12)	0.63038(9)	0.0266	1.0000
H81	0.88632(19)	0.66107(13)	0.66309(9)	0.0263	1.0000

H121	0.10855(18)	0.68983(14)	0.84007(9)	0.0277	1.0000
H131	0.12172(19)	0.58686(16)	0.83552(10)	0.0364	1.0000
H141	-0.1184(2)	0.41481(16)	0.78311(10)	0.0403	1.0000
H151	0.1195(2)	0.34949(15)	0.73062(10)	0.0371	1.0000
H161	0.34554(19)	0.45345(14)	0.73208(9)	0.0293	1.0000
H181	0.6135(2)	0.74195(14)	0.93356(10)	0.0328	1.0000
H191	0.7836(2)	0.66491(16)	1.03339(10)	0.0437	1.0000
H201	0.8237(2)	0.48238(17)	1.03655(10)	0.0417	1.0000
H211	0.6941(2)	0.37348(15)	0.94092(11)	0.0379	1.0000
H221	0.53237(19)	0.44524(13)	0.84142(10)	0.0287	1.0000

Thermal Parameters

Label	U_{11}	U_{22}	U_{33}	U_{23}	U_{13}	U_{12}
C1	0.0199(7)	0.0241(8)	0.0183(7)	0.0032(6)	0.0051(5)	-0.0007(6)
C2	0.0204(7)	0.0216(7)	0.0171(7)	0.0024(6)	0.0025(5)	-0.0015(6)
C3	0.0192(7)	0.0201(7)	0.0180(7)	0.0011(5)	0.0024(5)	-0.0011(6)
C4	0.0241(7)	0.0215(7)	0.0174(7)	-0.0007(6)	0.0015(6)	-0.0009(6)
C5	0.0298(8)	0.0203(7)	0.0202(7)	0.0006(6)	0.0110(6)	0.0007(6)
C6	0.0197(7)	0.0239(8)	0.0298(8)	0.0018(6)	0.0060(6)	-0.0029(6)
C7	0.0219(7)	0.0228(8)	0.0206(7)	-0.0009(6)	-0.0011(6)	-0.0036(6)
C8	0.0233(8)	0.0249(8)	0.0163(7)	-0.0001(6)	0.0022(6)	-0.0020(6)
C9	0.0170(7)	0.0236(8)	0.0216(8)	0.0019(6)	0.0005(6)	-0.0035(6)
C10	0.0165(7)	0.0275(8)	0.0197(7)	0.0021(6)	0.0030(6)	-0.0022(6)
C11	0.0158(7)	0.0282(8)	0.0151(7)	0.0041(6)	-0.0000(5)	-0.0016(6)
C12	0.0202(7)	0.0354(9)	0.0163(7)	0.0050(6)	0.0018(6)	0.0046(6)
C13	0.0161(7)	0.0549(11)	0.0208(8)	0.0089(7)	0.0015(6)	0.0027(7)
C14	0.0202(8)	0.0515(11)	0.0263(8)	0.0096(8)	-0.0034(6)	-0.0136(8)
C15	0.0357(9)	0.0343(9)	0.0253(8)	0.0014(7)	-0.0011(7)	-0.0114(8)
C16	0.0205(7)	0.0316(9)	0.0220(7)	-0.0004(6)	0.0012(6)	-0.0011(6)
C17	0.0131(6)	0.0250(8)	0.0185(7)	0.0036(6)	0.0028(5)	-0.0003(6)
C18	0.0279(8)	0.0279(8)	0.0253(8)	0.0019(7)	-0.0024(6)	-0.0049(7)
C19	0.0367(10)	0.0428(11)	0.0239(8)	0.0016(7)	-0.0080(7)	-0.0115(8)
C20	0.0245(8)	0.0522(12)	0.0251(8)	0.0163(8)	-0.0027(7)	0.0003(8)
C21	0.0253(8)	0.0297(9)	0.0375(9)	0.0134(7)	0.0096(7)	0.0079(7)
C22	0.0206(7)	0.0267(8)	0.0257(8)	0.0004(6)	0.0029(6)	0.0011(6)
P1	0.01429(18)	0.0203(2)	0.01658(18)	0.00167(13)	0.00262(13)	0.00049(13)
S1	0.0265(2)	0.02017(19)	0.0321(2)	0.00223(15)	0.00482(16)	0.00302(15)

Distances

C1	C1 2_666	1.246(3)Å		C1	C2	1.348(2)Å
C2	C3	1.477(2)Å		C2	C9	1.429(2)Å
C3	C4	1.403(2)Å		C3	C8	1.400(2)Å
C4	C5	1.375(2)Å		C4	H41	0.963Å
C5	C6	1.401(2)Å		C5	H51	0.922Å
C6	C7	1.396(2)Å		C6	H61	0.928Å
C7	C8	1.389(2)Å		C7	H71	0.908Å
C8	H81	0.949Å		C9	C10	1.207(2)Å
C10	P1	1.7547(15)Å		C11	C12	1.397(2)Å
C11	C16	1.395(2)Å		C11	P1	1.8118(15)Å
C12	C13	1.375(2)Å		C12	H121	0.923Å
C13	C14	1.387(3)Å		C13	H131	0.925Å
C14	C15	1.392(3)Å		C14	H141	0.936Å
C15	C16	1.385(2)Å		C15	H151	0.922Å
C16	H161	0.925Å		C17	C18	1.389(2)Å
C17	C22	1.399(2)Å		C17	P1	1.8121(15)Å
C18	C19	1.402(2)Å		C18	H181	0.945Å
C19	C20	1.367(3)Å		C19	H191	0.939Å
C20	C21	1.382(3)Å		C20	H201	0.934Å
C21	C22	1.382(2)Å		C21	H211	0.924Å
C22	H221	0.941Å		P1	S1	1.9493(5)Å

Angles

C1 2_666	C1	C2	177.3(2)°		C1	C2	C3	123.47(13)°
C1	C2	C9	116.32(13)°		C3	C2	C9	120.21(13)°
C2	C3	C4	120.44(13)°		C2	C3	C8	120.41(13)°
C4	C3	C8	119.15(14)°		C3	C4	C5	120.40(14)°
C3	C4	H41	119.494°		C5	C4	H41	120.106°
C4	C5	C6	120.36(14)°		C4	C5	H51	120.063°
C6	C5	H51	119.574°		C5	C6	C7	119.78(14)°
C5	C6	H61	120.857°		C7	C6	H61	119.351°
C6	C7	C8	119.73(14)°		C6	C7	H71	120.806°
C8	C7	H71	119.467°		C3	C8	C7	120.58(14)°
C3	C8	H81	118.674°		C7	C8	H81	120.747°
C2	C9	C10	177.28(15)°		C9	C10	P1	175.11(14)°
C12	C11	C16	119.98(14)°		C12	C11	P1	118.64(12)°
C16	C11	P1	121.30(12)°		C11	C12	C13	119.77(16)°

C11	C12	H121	118.981°		C13	C12	H121	121.244°
C12	C13	C14	120.49(16)°		C12	C13	H131	119.173°
C14	C13	H131	120.333°		C13	C14	C15	119.99(16)°
C13	C14	H141	119.753°		C15	C14	H141	120.250°
C14	C15	C16	119.98(17)°		C14	C15	H151	121.343°
C16	C15	H151	118.678°		C11	C16	C15	119.76(15)°
C11	C16	H161	120.706°		C15	C16	H161	119.533°
C18	C17	C22	119.87(14)°		C18	C17	P1	119.59(12)°
C22	C17	P1	120.54(12)°		C17	C18	C19	119.25(16)°
C17	C18	H181	119.201°		C19	C18	H181	121.531°
C18	C19	C20	120.41(16)°		C18	C19	H191	118.812°
C20	C19	H191	120.752°		C19	C20	C21	120.37(16)°
C19	C20	H201	119.068°		C21	C20	H201	120.558°
C20	C21	C22	120.31(17)°		C20	C21	H211	120.696°
C22	C21	H211	118.999°		C17	C22	C21	119.75(16)°
C17	C22	H221	121.713°		C21	C22	H221	118.520°
C10	P1	C11	102.62(7)°		C10	P1	C17	104.16(7)°
C11	P1	C17	106.97(7)°		C10	P1	S1	114.07(6)°
C11	P1	S1	114.27(5)°		C17	P1	S1	113.65(5)°

Crystal Data 13

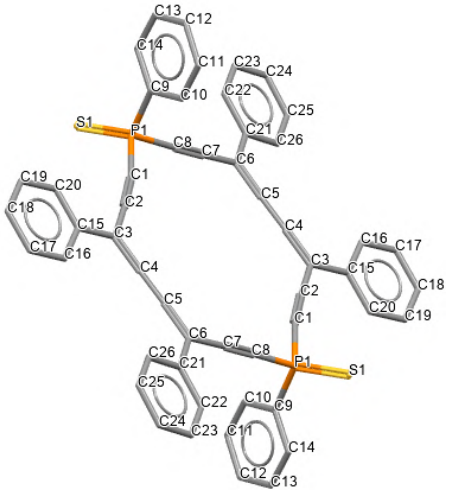

a = 8.3477(6) Å α = 97.136(5)°

b = 11.1327(7) Å β = 94.354(5)°

c = 11.2423(8) Å γ = 104.652(6)°

Volume	996.68(12) Å³	Crystal Class	triclinic
Space group	P -1	Z =	1
Formula	C_{52} H_{30} P_2 S_2	M_r	780.89
Cell determined from	3627 reflections	Cell θ range =	4 - 77°
Temperature	100K		
Shape	block		
Colour	colorless	Size	0.00 × 0.02 × 0.02 mm
D_x	1.30	F000	404.000
μ	2.247 mm^{-1}		
Absorption correction	multi-scan		
T_{min}	0.87	T_{max}	0.99

Data Collection

Diffractometer	multi-scan
Scan type	ϕ and ω scans
Reflections measured	9992
Independent reflections	4012
Rint	0.0374
θ_{max}	76.9907
h =	-9 → 10
k =	-13 → 13
l =	-14 → 13

Refinement

$\Delta\rho_{min}$ = -0.67 e $Å^{-3}$

$\Delta\rho_{max}$ =	0.40 e Å^{-3}
Reflections used	3812
Cutoff: I >	-3.00σ(I)
Parameters refined	253
S =	0.98
R-factor	0.054
weighted R-factor	0.112
Δ/σ_{max}	0.0004
Refinement on	F^2
w =	$1/[\sigma^2(F_{obs}^2) + (0.014 \times P)^2 + 2.155 \times P + 0.000 + 0.000 \times \sin\theta]$, $P = 0.333 \times \max(F_{obs}^2,0) + 0.667 \times F_{calc}^2$

Parameters

Label	*x*	*y*	*z*	$U_{iso/equiv}$	Occupancy
C1	0.3253(3)	0.1871(2)	0.7077(2)	0.0213	1.0000
C2	0.2932(3)	0.2630(2)	0.6490(2)	0.0197	1.0000
C3	0.2663(3)	0.3597(2)	0.5838(2)	0.0199	1.0000
C4	0.1498(3)	0.3295(2)	0.4871(2)	0.0210	1.0000
C5	0.0471(3)	0.3032(2)	0.3953(2)	0.0213	1.0000
C6	-0.0613(3)	0.2807(2)	0.2942(2)	0.0194	1.0000
C7	-0.1662(3)	0.1556(2)	0.2595(2)	0.0223	1.0000
C8	-0.2570(3)	0.0513(2)	0.2325(2)	0.0209	1.0000
C9	0.5904(3)	0.0862(2)	0.7666(2)	0.0229	1.0000
C10	0.6158(3)	0.0778(3)	0.6448(3)	0.0276	1.0000
C11	0.7633(4)	0.0614(3)	0.6082(3)	0.0322	1.0000
C12	0.8878(4)	0.0519(3)	0.6933(3)	0.0334	1.0000
C13	0.8655(3)	0.0620(2)	0.8148(3)	0.0298	1.0000
C14	0.7168(3)	0.0799(2)	0.8525(3)	0.0250	1.0000
C15	0.3726(3)	0.4887(2)	0.6236(2)	0.0200	1.0000
C16	0.3418(3)	0.5891(2)	0.5713(2)	0.0246	1.0000
C17	0.4415(4)	0.7098(2)	0.6085(3)	0.0271	1.0000
C18	0.5722(4)	0.7328(2)	0.7000(3)	0.0288	1.0000
C19	0.6032(3)	0.6333(2)	0.7530(3)	0.0275	1.0000
C20	0.5047(3)	0.5127(2)	0.7151(2)	0.0233	1.0000
C21	-0.0780(3)	0.3807(2)	0.2232(2)	0.0199	1.0000
C22	-0.2091(3)	0.3599(2)	0.1321(2)	0.0232	1.0000
C23	-0.2294(4)	0.4567(3)	0.0706(3)	0.0287	1.0000
C24	-0.1190(4)	0.5755(3)	0.0995(3)	0.0290	1.0000
C25	0.0142(4)	0.5956(2)	0.1881(3)	0.0281	1.0000

C26	0.0353(3)	0.5001(2)	0.2490(2)	0.0243	1.0000
P1	0.39182(8)	0.09963(6)	0.81140(6)	0.0195	1.0000
S1	0.38958(9)	0.16826(6)	0.97774(6)	0.0273	1.0000
H101	0.5306(3)	0.0836(3)	0.5886(3)	0.0331	1.0000
H111	0.7803(4)	0.0550(3)	0.5270(3)	0.0393	1.0000
H121	0.9871(4)	0.0392(3)	0.6680(3)	0.0422	1.0000
H131	0.9503(3)	0.0572(2)	0.8718(3)	0.0382	1.0000
H141	0.7040(3)	0.0884(2)	0.9354(3)	0.0307	1.0000
H161	0.2540(3)	0.5762(2)	0.5104(2)	0.0300	1.0000
H171	0.4176(4)	0.7752(2)	0.5719(3)	0.0335	1.0000
H181	0.6378(4)	0.8139(2)	0.7241(3)	0.0352	1.0000
H191	0.6907(3)	0.6483(2)	0.8144(3)	0.0346	1.0000
H201	0.5272(3)	0.4471(2)	0.7514(2)	0.0286	1.0000
H221	-0.2840(3)	0.2811(2)	0.1142(2)	0.0283	1.0000
H231	-0.3167(4)	0.4408(3)	0.0106(3)	0.0364	1.0000
H241	-0.1345(4)	0.6418(3)	0.0595(3)	0.0352	1.0000
H251	0.0911(4)	0.6738(2)	0.2063(3)	0.0364	1.0000
H261	0.1268(3)	0.5149(2)	0.3090(2)	0.0296	1.0000

Thermal Parameters

Label	U_{11}	U_{22}	U_{33}	U_{23}	U_{13}	U_{12}
C1	0.0199(12)	0.0150(12)	0.0265(13)	0.0014(10)	-0.0018(10)	0.0021(9)
C2	0.0179(12)	0.0149(11)	0.0243(13)	0.0011(10)	-0.0016(10)	0.0026(9)
C3	0.0192(13)	0.0170(12)	0.0242(13)	0.0031(10)	0.0020(10)	0.0061(10)
C4	0.0212(13)	0.0161(12)	0.0266(14)	0.0052(10)	0.0011(10)	0.0060(10)
C5	0.0223(13)	0.0133(11)	0.0282(14)	0.0054(10)	0.0004(10)	0.0041(10)
C6	0.0174(12)	0.0155(12)	0.0252(13)	0.0023(10)	-0.0001(10)	0.0050(9)
C7	0.0204(13)	0.0207(13)	0.0266(13)	0.0076(10)	-0.0018(10)	0.0063(10)
C8	0.0198(13)	0.0155(12)	0.0273(13)	0.0052(10)	-0.0020(10)	0.0046(10)
C9	0.0234(13)	0.0118(11)	0.0325(14)	0.0064(10)	-0.0034(11)	0.0034(10)
C10	0.0227(14)	0.0298(14)	0.0314(15)	0.0065(11)	-0.0025(11)	0.0097(11)
C11	0.0302(15)	0.0318(15)	0.0368(16)	0.0089(13)	0.0056(12)	0.0101(12)
C12	0.0232(14)	0.0235(14)	0.054(2)	0.0099(13)	0.0053(13)	0.0051(11)
C13	0.0205(14)	0.0200(13)	0.0481(18)	0.0086(12)	-0.0060(12)	0.0053(10)
C14	0.0227(13)	0.0153(12)	0.0338(15)	0.0067(10)	-0.0063(11)	0.0003(10)
C15	0.0198(12)	0.0155(12)	0.0227(13)	0.0006(9)	0.0018(10)	0.0026(9)
C16	0.0303(15)	0.0212(13)	0.0234(13)	0.0054(10)	0.0021(11)	0.0083(11)

C17	0.0342(15)	0.0163(12)	0.0334(15)	0.0061(11)	0.0109(12)	0.0081(11)
C18	0.0300(15)	0.0152(12)	0.0367(16)	-0.0014(11)	0.0074(12)	-0.0008(11)
C19	0.0222(14)	0.0230(14)	0.0328(15)	-0.0027(11)	0.0000(11)	0.0020(11)
C20	0.0259(14)	0.0186(12)	0.0263(14)	0.0047(10)	0.0011(11)	0.0073(10)
C21	0.0221(13)	0.0147(11)	0.0231(13)	0.004(1)	0.0011(10)	0.0053(10)
C22	0.0230(13)	0.0198(12)	0.0252(13)	0.0035(10)	-0.0018(10)	0.0039(10)
C23	0.0276(15)	0.0307(15)	0.0292(15)	0.0090(12)	0.0001(11)	0.0090(12)
C24	0.0366(16)	0.0225(14)	0.0330(15)	0.0108(11)	0.0061(12)	0.0132(12)
C25	0.0331(15)	0.0170(13)	0.0333(15)	0.0050(11)	0.0057(12)	0.0038(11)
C26	0.0237(13)	0.0197(13)	0.0271(14)	0.0041(10)	-0.0010(11)	0.0023(10)
P1	0.0199(3)	0.0139(3)	0.0230(3)	0.0034(2)	-0.0037(2)	0.0032(2)
S1	0.0316(4)	0.0241(3)	0.0241(3)	0.0009(3)	-0.0026(3)	0.0066(3)

Distances

C1	C2	1.204(4)Å		C1	P1	1.752(3)Å
C2	C3	1.428(3)Å		C3	C4	1.350(4)Å
C3	C15	1.479(3)Å		C4	C5	1.244(4)Å
C5	C6	1.354(4)Å		C6	C7	1.433(3)Å
C6	C21	1.476(3)Å		C7	C8	1.203(4)Å
C8	P1 2_556	1.757(2)Å		C9	C10	1.396(4)Å
C9	C14	1.397(4)Å		C9	P1	1.805(3)Å
C10	C11	1.375(4)Å		C10	H101	0.936Å
C11	C12	1.391(4)Å		C11	H111	0.931Å
C12	C13	1.387(5)Å		C12	H121	0.934Å
C13	C14	1.394(4)Å		C13	H131	0.934Å
C14	H141	0.942Å		C15	C16	1.395(4)Å
C15	C20	1.399(4)Å		C16	C17	1.383(4)Å
C16	H161	0.934Å		C17	C18	1.392(4)Å
C17	H171	0.935Å		C18	C19	1.391(4)Å
C18	H181	0.925Å		C19	C20	1.381(4)Å
C19	H191	0.933Å		C20	H201	0.930Å
C21	C22	1.394(4)Å		C21	C26	1.404(3)Å
C22	C23	1.388(4)Å		C22	H221	0.928Å
C23	C24	1.391(4)Å		C23	H231	0.920Å
C24	C25	1.389(4)Å		C24	H241	0.941Å
C25	C26	1.374(4)Å		C25	H251	0.930Å
C26	H261	0.947Å		P1	S1	1.9336(10)Å

Angles

C2	C1	P1	169.9(2)°		C1	C2	C3	175.7(3)°
C2	C3	C4	119.2(2)°		C2	C3	C15	117.9(2)°
C4	C3	C15	122.9(2)°		C3	C4	C5	177.6(3)°
C4	C5	C6	177.0(3)°		C5	C6	C7	117.6(2)°
C5	C6	C21	122.2(2)°		C7	C6	C21	120.1(2)°
C6	C7	C8	178.3(3)°		C7	C8	P1 2_556	178.1(2)°
C10	C9	C14	119.8(3)°		C10	C9	P1	119.8(2)°
C14	C9	P1	120.4(2)°		C9	C10	C11	120.6(3)°
C9	C10	H101	118.766°		C11	C10	H101	120.587°
C10	C11	C12	119.6(3)°		C10	C11	H111	120.896°
C12	C11	H111	119.452°		C11	C12	C13	120.4(3)°
C11	C12	H121	119.422°		C13	C12	H121	120.157°
C12	C13	C14	120.1(3)°		C12	C13	H131	120.118°
C14	C13	H131	119.734°		C9	C14	C13	119.3(3)°
C9	C14	H141	121.236°		C13	C14	H141	119.428°
C3	C15	C16	120.5(2)°		C3	C15	C20	120.7(2)°
C16	C15	C20	118.8(2)°		C15	C16	C17	120.5(3)°
C15	C16	H161	120.771°		C17	C16	H161	118.730°
C16	C17	C18	120.3(3)°		C16	C17	H171	118.532°
C18	C17	H171	121.136°		C17	C18	C19	119.5(2)°
C17	C18	H181	119.478°		C19	C18	H181	121.007°
C18	C19	C20	120.2(3)°		C18	C19	H191	119.776°
C20	C19	H191	120.064°		C15	C20	C19	120.7(2)°
C15	C20	H201	120.178°		C19	C20	H201	119.086°
C6	C21	C22	120.8(2)°		C6	C21	C26	120.4(2)°
C22	C21	C26	118.8(2)°		C21	C22	C23	120.4(2)°
C21	C22	H221	119.202°		C23	C22	H221	120.392°
C22	C23	C24	120.2(3)°		C22	C23	H231	118.938°
C24	C23	H231	120.854°		C23	C24	C25	119.5(2)°
C23	C24	H241	120.273°		C25	C24	H241	120.244°
C24	C25	C26	120.6(3)°		C24	C25	H251	120.333°
C26	C25	H251	119.102°		C21	C26	C25	120.5(2)°
C21	C26	H261	119.684°		C25	C26	H261	119.770°
C1	P1	C8 2_556	103.11(12)°		C1	P1	C9	103.59(12)°
C8 2_556	P1	C9	104.59(12)°		C1	P1	S1	113.51(9)°
C8 2_556	P1	S1	113.97(10)°		C9	P1	S1	116.59(9)°

Crystal Data 24

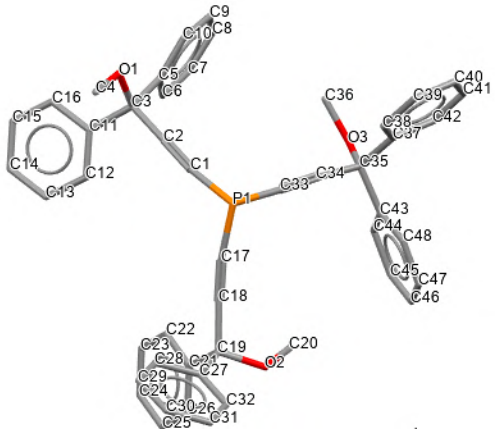

a = 13.9425(3) Å α = 90°

b = 17.2855(3) Å β = 110.712(2)°

c = 16.7324(2) Å γ = 90°

Volume	3771.94(12) Å³	Crystal Class	monoclinic
Space group	P 1 2_1 1	Z =	4
Formula	C_{48} H_{39} O_3 P_1	M_r	694.81
Cell determined from	33795 reflections	Cell θ range =	3 - 78°
Temperature	100K		
Shape	planar		
Colour	colorless	Size	0.02 × 0.07 × 0.20 mm
D_x	1.22	F000	1464.000
μ	0.968 mm^{-1}		
Absorption correction	multi-scan		
T_{min}	0.93	T_{max}	0.98

Data Collection

Diffractometer	multi-scan
Scan type	ϕ and ω scans
Reflections measured	111897
Independent reflections	16196
Rint	0.1095
$θ_{max}$	80.7077
h =	-17 → 17
k =	-22 → 22

l =	-13 → 20

Refinement

$\Delta\rho_{min}$ =	-0.52 e Å^{-3}
$\Delta\rho_{max}$ =	0.79 e Å^{-3}
Reflections used	15328
Cutoff: I >	-3.00σ(I)
Parameters refined	938
S =	0.97
R-factor	0.087
weighted R-factor	0.224
Δ/σ_{max}	0.0012
Flack parameter	0.448(8) Parsons, Flack & Wagner (2013)
Refinement on	F^2
w =	$1/[\sigma^2(F_{obs}^2) + (0.156 \times P)^2 + 4.580 \times P + 0.000 + 0.000 \times \sin\theta]$, $P = 0.333 \times \max(F_{obs}^2,0) + 0.667 \times F_{calc}^2$

Parameters

Label	*x*	*y*	*z*	$U_{iso/equiv}$	Occupancy
P1	0.02143(8)	0.72585(7)	0.04091(5)	0.0228	1.0000
P2	1.02588(8)	0.72968(7)	0.46229(5)	0.0224	1.0000
C1	-0.0871(3)	0.7406(2)	-0.1346(2)	0.0262	1.0000
C2	-0.1680(3)	0.7504(2)	-0.1895(2)	0.0247	1.0000
C3	-0.2673(3)	0.7655(2)	-0.2598(2)	0.0246	1.0000
C4	-0.3332(4)	0.6404(3)	-0.2423(3)	0.0339	1.0000
C5	-0.2939(3)	0.8509(3)	-0.2551(2)	0.0274	1.0000
C6	-0.2563(4)	0.9069(3)	-0.2958(3)	0.0366	1.0000
C7	-0.2771(4)	0.9840(3)	-0.2902(4)	0.0425	1.0000
C8	-0.3321(5)	1.0081(3)	-0.2415(3)	0.0450	1.0000
C9	-0.3696(5)	0.9516(3)	-0.1991(3)	0.0474	1.0000
C10	-0.3520(5)	0.8740(3)	-0.2059(3)	0.0410	1.0000
C11	-0.2601(4)	0.7442(2)	-0.3468(2)	0.0253	1.0000
C12	-0.1686(3)	0.7277(3)	-0.3575(2)	0.0290	1.0000
C13	-0.1674(4)	0.7086(3)	-0.4384(3)	0.0343	1.0000
C14	-0.2574(4)	0.7074(3)	-0.5076(3)	0.0360	1.0000
C15	-0.3497(4)	0.7237(3)	-0.4977(2)	0.0326	1.0000
C16	-0.3521(4)	0.7415(3)	-0.4172(3)	0.0292	1.0000
C17	0.1236(3)	0.7170(3)	-0.0800(2)	0.0262	1.0000

C18	0.2031(4)	0.7066(2)	-0.0911(2)	0.0287	1.0000
C19	0.3044(4)	0.6930(2)	-0.0990(2)	0.0256	1.0000
C20	0.3669(4)	0.8163(3)	-0.0319(3)	0.0364	1.0000
C21	0.3068(4)	0.7175(3)	-0.1866(2)	0.0285	1.0000
C22	0.2219(4)	0.7496(3)	-0.2501(3)	0.0331	1.0000
C23	0.2282(4)	0.7726(3)	-0.3273(2)	0.0325	1.0000
C24	0.3200(4)	0.7656(3)	-0.3417(3)	0.0352	1.0000
C25	0.4046(4)	0.7338(3)	-0.2784(3)	0.0308	1.0000
C26	0.3978(3)	0.7108(3)	-0.2012(2)	0.0292	1.0000
C27	0.3299(4)	0.6069(3)	-0.0829(2)	0.0275	1.0000
C28	0.2636(4)	0.5526(3)	-0.1362(4)	0.0416	1.0000
C29	0.2816(5)	0.4744(3)	-0.1204(5)	0.0548	1.0000
C30	0.3662(6)	0.4504(3)	-0.0519(4)	0.0554	1.0000
C31	0.4335(5)	0.5039(3)	0.0007(4)	0.0459	1.0000
C32	0.4144(4)	0.5815(3)	-0.0149(3)	0.0360	1.0000
C33	0.0412(3)	0.8213(3)	-0.0019(2)	0.0287	1.0000
C34	0.0520(3)	0.8841(2)	0.0327(2)	0.0243	1.0000
C35	0.0719(3)	0.9612(2)	0.0748(2)	0.0258	1.0000
C36	-0.0938(4)	1.0078(3)	-0.0148(3)	0.0364	1.0000
C37	0.0458(3)	0.9621(2)	0.1561(2)	0.0252	1.0000
C38	0.0120(4)	0.8981(3)	0.1878(3)	0.0294	1.0000
C39	-0.0137(4)	0.9030(3)	0.2606(3)	0.0322	1.0000
C40	-0.0082(4)	0.9733(3)	0.3018(3)	0.0359	1.0000
C41	0.0253(4)	1.0387(3)	0.2697(3)	0.0314	1.0000
C42	0.0522(4)	1.0335(2)	0.1979(2)	0.0290	1.0000
C43	0.1858(4)	0.9775(2)	0.0921(2)	0.0271	1.0000
C44	0.2158(4)	1.0236(3)	0.0366(2)	0.0343	1.0000
C45	0.3196(4)	1.0333(3)	0.0508(3)	0.0411	1.0000
C46	0.3933(4)	0.9960(3)	0.1169(3)	0.0387	1.0000
C47	0.3634(4)	0.9508(3)	0.1724(3)	0.0371	1.0000
C48	0.2612(4)	0.9411(3)	0.1592(3)	0.0305	1.0000
C51	0.9194(3)	0.7162(3)	0.3661(2)	0.0246	1.0000
C52	0.8391(3)	0.7053(2)	0.3098(2)	0.0244	1.0000
C53	0.7358(3)	0.6951(3)	0.2430(2)	0.0248	1.0000
C54	0.6815(4)	0.8200(3)	0.2764(3)	0.0368	1.0000
C55	0.7048(4)	0.6094(3)	0.2415(2)	0.0262	1.0000

C56	0.6409(4)	0.5853(3)	0.2833(3)	0.0367	1.0000
C57	0.6169(5)	0.5067(4)	0.2838(3)	0.0467	1.0000
C58	0.6563(5)	0.4531(3)	0.2422(4)	0.0508	1.0000
C59	0.7207(4)	0.4778(3)	0.2007(3)	0.0396	1.0000
C60	0.7454(4)	0.5559(3)	0.2002(3)	0.0312	1.0000
C61	0.7364(3)	0.7189(3)	0.1554(2)	0.0240	1.0000
C62	0.6417(3)	0.7258(3)	0.0887(2)	0.0282	1.0000
C63	0.6386(4)	0.7420(3)	0.0067(3)	0.0338	1.0000
C64	0.7282(5)	0.7505(3)	-0.0099(3)	0.0421	1.0000
C65	0.8207(5)	0.7456(4)	0.0554(3)	0.0498	1.0000
C66	0.8254(4)	0.7306(4)	0.1387(3)	0.0397	1.0000
C67	1.1300(3)	0.7469(2)	0.4268(2)	0.0234	1.0000
C68	1.2092(3)	0.7586(2)	0.4174(2)	0.0247	1.0000
C69	1.3093(3)	0.7744(3)	0.4078(2)	0.0239	1.0000
C70	1.3746(4)	0.6477(3)	0.4595(3)	0.0322	1.0000
C71	1.3057(3)	0.7564(2)	0.3173(2)	0.0243	1.0000
C72	1.2190(3)	0.7279(3)	0.2542(2)	0.0277	1.0000
C73	1.2213(4)	0.7095(3)	0.1738(3)	0.0354	1.0000
C74	1.3109(4)	0.7178(3)	0.1567(2)	0.0355	1.0000
C75	1.3982(4)	0.7457(3)	0.2191(3)	0.0347	1.0000
C76	1.3965(4)	0.7659(3)	0.2993(3)	0.0276	1.0000
C77	1.3362(3)	0.8595(3)	0.4319(2)	0.0251	1.0000
C78	1.2664(4)	0.9171(3)	0.3883(3)	0.0328	1.0000
C79	1.2881(4)	0.9941(3)	0.4091(3)	0.0352	1.0000
C80	1.3796(4)	1.0147(3)	0.4728(3)	0.0403	1.0000
C81	1.4492(4)	0.9590(3)	0.5156(3)	0.0399	1.0000
C82	1.4269(4)	0.8801(3)	0.4953(3)	0.0366	1.0000
C83	1.0000(3)	0.8254(3)	0.4848(2)	0.0258	1.0000
C84	0.9813(3)	0.8877(2)	0.5100(2)	0.0228	1.0000
C85	0.9559(3)	0.9646(2)	0.5357(2)	0.0241	1.0000
C86	1.1230(4)	1.0127(3)	0.5536(3)	0.0330	1.0000
C87	0.9732(3)	0.9671(2)	0.6321(2)	0.0245	1.0000
C88	0.9590(3)	1.0376(3)	0.6672(3)	0.0284	1.0000
C89	0.9753(4)	1.0426(3)	0.7531(3)	0.0313	1.0000
C90	1.0068(4)	0.9794(3)	0.8066(3)	0.0360	1.0000
C91	1.0204(4)	0.9089(3)	0.7723(3)	0.0313	1.0000

C92	1.0056(3)	0.9027(3)	0.6858(3)	0.0286	1.0000
C93	0.8436(3)	0.9798(2)	0.4828(2)	0.0269	1.0000
C94	0.7674(4)	0.9310(3)	0.4906(3)	0.0316	1.0000
C95	0.6654(4)	0.9430(3)	0.4428(3)	0.0402	1.0000
C96	0.6367(4)	1.0027(3)	0.3822(3)	0.0431	1.0000
C97	0.7122(4)	1.0503(3)	0.3745(3)	0.0440	1.0000
C98	0.8141(4)	1.0399(3)	0.4236(3)	0.0340	1.0000
O1	-0.3469(2)	0.72232(19)	0.24577(17)	0.0269	1.0000
O2	0.3804(2)	0.73419(19)	0.03157(17)	0.0296	1.0000
O3	0.0137(3)	1.01860(18)	0.01501(17)	0.0312	1.0000
O51	0.6627(2)	0.73793(19)	0.26665(18)	0.0285	1.0000
O52	1.3881(2)	0.72941(19)	0.46845(16)	0.0257	1.0000
O53	1.0149(2)	1.02242(18)	0.51442(17)	0.0287	1.0000
H41	-0.3897(4)	0.6170(3)	-0.2290(3)	0.0602	1.0000
H42	-0.3346(4)	0.6220(3)	-0.2986(3)	0.0601	1.0000
H43	-0.2690(4)	0.6263(3)	-0.1966(3)	0.0601	1.0000
H61	-0.2181(4)	0.8904(3)	-0.3319(3)	0.0512	1.0000
H71	-0.2506(4)	1.0215(3)	-0.3199(4)	0.0623	1.0000
H81	-0.3479(5)	1.0597(3)	-0.2380(3)	0.0626	1.0000
H91	-0.4047(5)	0.9710(3)	-0.1609(3)	0.0742	1.0000
H101	-0.3767(5)	0.8365(3)	-0.1760(3)	0.0588	1.0000
H121	-0.1074(3)	0.7299(3)	-0.3095(2)	0.0392	1.0000
H131	-0.1042(4)	0.6994(3)	-0.4457(3)	0.0471	1.0000
H141	-0.2560(4)	0.6991(3)	-0.5637(3)	0.0490	1.0000
H151	-0.4106(4)	0.7248(3)	-0.5457(2)	0.0399	1.0000
H161	-0.4151(4)	0.7483(3)	-0.4087(3)	0.0399	1.0000
H201	0.4189(4)	0.8391(3)	0.0170(3)	0.0692	1.0000
H202	0.3715(4)	0.8382(3)	-0.0855(3)	0.0691	1.0000
H203	0.2989(4)	0.8293(3)	-0.0303(3)	0.0691	1.0000
H221	0.1595(4)	0.7515(3)	-0.2381(3)	0.0440	1.0000
H231	0.1681(4)	0.7872(3)	-0.3718(2)	0.0425	1.0000
H241	0.3231(4)	0.7779(3)	-0.3958(3)	0.0440	1.0000
H251	0.4661(4)	0.7273(3)	-0.2890(3)	0.0432	1.0000
H261	0.4556(3)	0.6959(3)	-0.1573(2)	0.0407	1.0000
H281	0.2076(4)	0.5689(3)	-0.1861(4)	0.0584	1.0000
H291	0.2319(5)	0.4380(3)	-0.1556(5)	0.0795	1.0000

H301	0.3798(6)	0.3968(3)	-0.0428(4)	0.0764	1.0000
H311	0.4921(5)	0.4862(3)	0.0492(4)	0.0637	1.0000
H321	0.4597(4)	0.6183(3)	0.0233(3)	0.0497	1.0000
H361	-0.1286(4)	1.0489(3)	-0.0538(3)	0.0583	1.0000
H362	-0.1193(4)	1.0075(3)	0.0334(3)	0.0577	1.0000
H363	-0.1139(4)	0.9604(3)	-0.0469(3)	0.0586	1.0000
H381	0.0041(4)	0.8507(3)	0.1578(3)	0.0395	1.0000
H391	-0.0326(4)	0.8593(3)	0.2837(3)	0.0418	1.0000
H401	-0.0228(4)	0.9776(3)	0.3546(3)	0.0530	1.0000
H411	0.0297(4)	1.0846(3)	0.2980(3)	0.0446	1.0000
H421	0.0720(4)	1.0767(2)	0.1754(2)	0.0427	1.0000
H441	0.1661(4)	1.0457(3)	-0.0117(2)	0.0486	1.0000
H451	0.3400(4)	1.0621(3)	0.0115(3)	0.0542	1.0000
H461	0.4630(4)	1.0021(3)	0.1240(3)	0.0563	1.0000
H471	0.4148(4)	0.9285(3)	0.2209(3)	0.0492	1.0000
H481	0.2409(4)	0.9104(3)	0.1987(3)	0.0415	1.0000
H541	0.6285(4)	0.8446(3)	0.2924(3)	0.0681	1.0000
H542	0.7483(4)	0.8306(3)	0.3200(3)	0.0682	1.0000
H543	0.6807(4)	0.8414(3)	0.2206(3)	0.0679	1.0000
H561	0.6165(4)	0.6214(3)	0.3154(3)	0.0526	1.0000
H571	0.5742(5)	0.4891(4)	0.3157(3)	0.0639	1.0000
H581	0.6388(5)	0.4007(3)	0.2429(4)	0.0657	1.0000
H591	0.7474(4)	0.4418(3)	0.1709(3)	0.0566	1.0000
H601	0.7885(4)	0.5705(3)	0.1700(3)	0.0472	1.0000
H621	0.5807(3)	0.7209(3)	0.1011(2)	0.0381	1.0000
H631	0.5740(4)	0.7445(3)	-0.0378(3)	0.0433	1.0000
H641	0.7244(5)	0.7605(3)	-0.0671(3)	0.0589	1.0000
H651	0.8823(5)	0.7499(4)	0.0432(3)	0.0632	1.0000
H661	0.8883(4)	0.7290(4)	0.1843(3)	0.0491	1.0000
H701	1.4248(4)	0.6221(3)	0.5087(3)	0.0554	1.0000
H702	1.3821(4)	0.6310(3)	0.4060(3)	0.0549	1.0000
H703	1.3051(4)	0.6342(3)	0.4582(3)	0.0551	1.0000
H721	1.1579(3)	0.7220(3)	0.2665(2)	0.0399	1.0000
H731	1.1606(4)	0.6970(3)	0.1289(3)	0.0502	1.0000
H741	1.3120(4)	0.7089(3)	0.1003(2)	0.0520	1.0000
H751	1.4594(4)	0.7481(3)	0.2075(3)	0.0461	1.0000

H761	1.4559(4)	0.7812(3)	0.3427(3)	0.0374	1.0000
H781	1.2039(4)	0.9027(3)	0.3431(3)	0.0435	1.0000
H791	1.2419(4)	1.0335(3)	0.3795(3)	0.0535	1.0000
H801	1.3941(4)	1.0665(3)	0.4866(3)	0.0565	1.0000
H811	1.5141(4)	0.9744(3)	0.5597(3)	0.0593	1.0000
H821	1.4745(4)	0.8413(3)	0.5262(3)	0.0547	1.0000
H861	1.1575(4)	1.0558(3)	0.5387(3)	0.0535	1.0000
H862	1.1433(4)	1.0095(3)	0.6157(3)	0.0530	1.0000
H863	1.1452(4)	0.9670(3)	0.5315(3)	0.0535	1.0000
H881	0.9423(3)	1.0800(3)	0.6324(3)	0.0373	1.0000
H891	0.9638(4)	1.0883(3)	0.7759(3)	0.0407	1.0000
H901	1.0184(4)	0.9839(3)	0.8684(3)	0.0488	1.0000
H911	1.0387(4)	0.8659(3)	0.8078(3)	0.0367	1.0000
H921	1.0159(3)	0.8563(3)	0.6621(3)	0.0377	1.0000
H941	0.7875(4)	0.8901(3)	0.5305(3)	0.0435	1.0000
H951	0.6129(4)	0.9118(3)	0.4533(3)	0.0566	1.0000
H961	0.5660(4)	1.0107(3)	0.3466(3)	0.0581	1.0000
H971	0.6933(4)	1.0885(3)	0.3332(3)	0.0654	1.0000
H981	0.8657(4)	1.0720(3)	0.4150(3)	0.0486	1.0000

Thermal Parameters

Label	U_{11}	U_{22}	U_{33}	U_{23}	U_{13}	U_{12}
P1	0.0338(5)	0.0257(5)	0.0084(4)	0.0000(4)	0.0066(3)	0.0015(4)
P2	0.0311(5)	0.0262(5)	0.0110(4)	-0.0003(4)	0.0088(3)	0.0004(4)
C1	0.039(2)	0.024(2)	0.0161(18)	-0.0017(14)	0.0097(16)	0.0035(17)
C2	0.036(2)	0.026(2)	0.0120(17)	0.0011(14)	0.0082(16)	0.0011(17)
C3	0.033(2)	0.026(2)	0.0155(18)	0.0022(15)	0.0104(16)	0.0038(17)
C4	0.047(3)	0.029(2)	0.028(2)	0.0109(18)	0.0159(19)	0.004(2)
C5	0.037(2)	0.025(2)	0.0152(17)	-0.0006(15)	0.0028(16)	0.0051(18)
C6	0.037(3)	0.034(3)	0.044(3)	0.000(2)	0.021(2)	0.003(2)
C7	0.039(3)	0.030(3)	0.056(3)	0.004(2)	0.013(2)	-0.004(2)
C8	0.055(3)	0.029(3)	0.039(3)	-0.012(2)	0.003(2)	0.008(2)
C9	0.077(4)	0.046(3)	0.021(2)	0.001(2)	0.020(2)	0.026(3)
C10	0.069(3)	0.040(3)	0.022(2)	0.0059(19)	0.026(2)	0.012(2)
C11	0.041(2)	0.024(2)	0.0124(16)	0.0041(14)	0.0112(16)	-0.0013(17)
C12	0.037(2)	0.036(2)	0.0162(17)	0.0028(18)	0.0121(15)	-0.001(2)
C13	0.048(3)	0.044(3)	0.0174(19)	-0.0006(17)	0.0189(18)	-0.004(2)

C14	0.062(3)	0.034(3)	0.0152(18)	-0.0012(16)	0.0183(19)	-0.005(2)
C15	0.048(3)	0.034(2)	0.0114(16)	0.0036(17)	0.0049(16)	-0.005(2)
C16	0.034(2)	0.033(2)	0.0192(19)	0.0043(16)	0.0071(16)	0.0008(18)
C17	0.037(2)	0.028(2)	0.0126(15)	-0.0020(15)	0.0081(15)	0.0044(18)
C18	0.047(3)	0.027(2)	0.0125(16)	0.0002(14)	0.0107(16)	0.0032(18)
C19	0.039(2)	0.025(2)	0.0117(17)	-0.0007(14)	0.0086(16)	0.0036(17)
C20	0.059(3)	0.026(2)	0.021(2)	-0.0050(17)	0.0104(19)	0.000(2)
C21	0.043(2)	0.031(2)	0.0131(17)	-0.0016(16)	0.0118(15)	-0.0006(19)
C22	0.042(3)	0.046(3)	0.0146(18)	-0.0040(17)	0.0138(17)	0.002(2)
C23	0.045(3)	0.042(3)	0.0088(17)	-0.0021(16)	0.0079(16)	0.002(2)
C24	0.047(3)	0.044(3)	0.0157(18)	-0.0065(17)	0.0125(18)	-0.004(2)
C25	0.037(2)	0.038(3)	0.0208(18)	-0.0059(17)	0.0141(16)	-0.0047(19)
C26	0.033(2)	0.036(2)	0.0155(17)	-0.0020(16)	0.0055(15)	0.0002(18)
C27	0.040(2)	0.029(2)	0.0176(18)	-0.0009(15)	0.0162(17)	0.0022(18)
C28	0.044(3)	0.031(2)	0.052(3)	-0.010(2)	0.020(2)	-0.002(2)
C29	0.053(3)	0.037(3)	0.086(5)	-0.018(3)	0.038(3)	-0.012(3)
C30	0.081(5)	0.032(3)	0.078(4)	0.009(3)	0.058(4)	0.011(3)
C31	0.074(4)	0.035(3)	0.043(3)	0.017(2)	0.039(3)	0.018(3)
C32	0.057(3)	0.036(3)	0.0178(19)	0.0072(17)	0.017(2)	0.011(2)
C33	0.039(2)	0.036(2)	0.0137(16)	0.0024(16)	0.0122(16)	0.0047(18)
C34	0.042(2)	0.0225(19)	0.0121(16)	-0.0060(14)	0.0145(15)	-0.0018(16)
C35	0.046(2)	0.0204(18)	0.0120(16)	-0.0003(14)	0.0116(15)	0.0010(17)
C36	0.045(3)	0.042(3)	0.024(2)	0.0061(18)	0.0142(18)	0.009(2)
C37	0.036(2)	0.028(2)	0.0112(16)	-0.0008(14)	0.0085(15)	0.0006(17)
C38	0.049(3)	0.026(2)	0.0167(17)	0.0033(15)	0.0156(17)	-0.0002(18)
C39	0.049(3)	0.036(2)	0.0162(18)	0.0092(17)	0.0174(18)	0.000(2)
C40	0.050(3)	0.042(3)	0.0174(19)	0.0012(18)	0.0147(18)	0.004(2)
C41	0.053(3)	0.028(2)	0.0158(18)	-0.0038(16)	0.0154(18)	0.0038(19)
C42	0.048(3)	0.022(2)	0.0175(18)	-0.0009(15)	0.0129(17)	0.0005(18)
C43	0.044(2)	0.028(2)	0.0137(16)	-0.0052(14)	0.0151(16)	-0.0016(17)
C44	0.058(3)	0.038(2)	0.0093(17)	0.0011(16)	0.0154(17)	-0.010(2)
C45	0.067(3)	0.046(3)	0.019(2)	-0.0061(19)	0.026(2)	-0.016(3)
C46	0.049(3)	0.042(3)	0.034(2)	-0.011(2)	0.027(2)	-0.009(2)
C47	0.048(3)	0.033(2)	0.032(2)	0.0031(18)	0.015(2)	0.004(2)
C48	0.043(2)	0.028(2)	0.0223(19)	0.0019(16)	0.0142(17)	0.0007(18)
C51	0.036(2)	0.029(2)	0.0122(16)	-0.0025(15)	0.0129(15)	-0.0011(18)

C52	0.034(2)	0.028(2)	0.0152(17)	-0.0016(14)	0.0140(16)	-0.0013(17)
C53	0.036(2)	0.029(2)	0.0120(17)	-0.0040(15)	0.0127(16)	0.0002(17)
C54	0.056(3)	0.032(2)	0.022(2)	-0.0094(18)	0.012(2)	0.006(2)
C55	0.038(2)	0.031(2)	0.0088(16)	0.0004(15)	0.0076(15)	-0.0024(18)
C56	0.055(3)	0.045(3)	0.0154(19)	0.0034(17)	0.0189(19)	-0.007(2)
C57	0.056(3)	0.053(3)	0.029(2)	0.008(2)	0.013(2)	-0.019(3)
C58	0.055(3)	0.033(3)	0.051(3)	0.006(2)	0.002(3)	-0.010(2)
C59	0.044(3)	0.033(3)	0.032(2)	-0.0060(19)	0.000(2)	-0.004(2)
C60	0.043(3)	0.029(2)	0.023(2)	-0.0053(16)	0.0120(18)	-0.0033(19)
C61	0.037(2)	0.0251(19)	0.0105(16)	-0.0032(15)	0.0096(14)	0.0003(18)
C62	0.041(2)	0.033(2)	0.0118(16)	-0.0058(16)	0.0104(15)	-0.0014(19)
C63	0.053(3)	0.033(2)	0.0119(17)	-0.0003(15)	0.0070(17)	0.005(2)
C64	0.066(3)	0.049(3)	0.017(2)	0.0044(18)	0.020(2)	-0.005(3)
C65	0.055(3)	0.077(4)	0.027(2)	0.004(2)	0.026(2)	-0.013(3)
C66	0.036(2)	0.065(4)	0.0171(19)	0.001(2)	0.0090(16)	-0.007(3)
C67	0.034(2)	0.027(2)	0.0107(15)	-0.0019(13)	0.0092(14)	0.0008(16)
C68	0.035(2)	0.025(2)	0.0131(16)	-0.0046(14)	0.0070(15)	-0.0018(16)
C69	0.030(2)	0.032(2)	0.0114(17)	0.0021(15)	0.0086(15)	0.0029(17)
C70	0.047(3)	0.030(2)	0.0219(19)	0.0064(17)	0.0148(18)	0.0053(19)
C71	0.029(2)	0.0259(19)	0.0167(18)	0.0044(15)	0.0060(15)	0.0029(16)
C72	0.035(2)	0.033(2)	0.0144(16)	-0.0008(16)	0.0082(15)	0.0003(19)
C73	0.051(3)	0.034(3)	0.0169(18)	0.0027(17)	0.0064(18)	0.005(2)
C74	0.066(3)	0.031(2)	0.0116(17)	0.0059(16)	0.0170(18)	0.011(2)
C75	0.045(3)	0.044(3)	0.022(2)	0.0116(18)	0.0208(18)	0.010(2)
C76	0.034(2)	0.035(2)	0.0147(18)	0.0029(15)	0.0089(16)	0.0027(17)
C77	0.039(2)	0.030(2)	0.0104(16)	-0.0019(15)	0.0133(15)	0.0023(17)
C78	0.043(3)	0.034(2)	0.0199(19)	0.0047(17)	0.0087(17)	-0.0001(19)
C79	0.042(3)	0.030(2)	0.037(2)	0.0089(19)	0.018(2)	0.0035(19)
C80	0.045(3)	0.031(2)	0.049(3)	-0.008(2)	0.022(2)	-0.003(2)
C81	0.039(3)	0.037(3)	0.042(3)	-0.015(2)	0.012(2)	-0.007(2)
C82	0.037(2)	0.038(3)	0.032(2)	-0.0085(19)	0.0083(19)	0.003(2)
C83	0.032(2)	0.036(2)	0.0093(15)	0.0007(15)	0.0073(14)	-0.0003(17)
C84	0.037(2)	0.027(2)	0.0056(14)	-0.0046(13)	0.0091(13)	-0.0000(16)
C85	0.038(2)	0.0217(19)	0.0149(17)	0.0001(14)	0.0125(15)	0.0010(16)
C86	0.043(2)	0.037(2)	0.0228(19)	-0.0046(17)	0.0162(18)	-0.0104(19)
C87	0.035(2)	0.0260(19)	0.0167(18)	-0.0030(15)	0.0141(15)	0.0017(16)

C88	0.041(2)	0.026(2)	0.0213(19)	-0.0058(15)	0.0145(17)	-0.0047(17)
C89	0.049(3)	0.035(2)	0.0183(19)	-0.0036(17)	0.0219(18)	-0.004(2)
C90	0.048(3)	0.049(3)	0.0164(19)	-0.0065(18)	0.0182(18)	-0.008(2)
C91	0.046(3)	0.040(2)	0.0120(18)	0.0066(16)	0.0155(17)	-0.002(2)
C92	0.044(2)	0.029(2)	0.0167(18)	0.0021(15)	0.0155(17)	0.0013(18)
C93	0.044(2)	0.028(2)	0.0102(16)	-0.0032(14)	0.0110(15)	0.0041(17)
C94	0.041(2)	0.038(2)	0.0156(18)	-0.0007(16)	0.0101(16)	-0.0021(19)
C95	0.038(3)	0.052(3)	0.032(2)	-0.016(2)	0.014(2)	0.001(2)
C96	0.045(3)	0.044(3)	0.032(2)	-0.014(2)	0.002(2)	0.008(2)
C97	0.060(3)	0.041(3)	0.021(2)	0.0010(19)	0.003(2)	0.015(2)
C98	0.054(3)	0.029(2)	0.0179(18)	0.0014(16)	0.0115(18)	0.003(2)
O1	0.0364(15)	0.0297(15)	0.0170(12)	0.0020(12)	0.0125(11)	0.0003(14)
O2	0.0414(17)	0.0269(16)	0.0168(13)	-0.0003(12)	0.0058(11)	0.0015(14)
O3	0.0504(19)	0.0280(15)	0.0153(13)	0.0038(11)	0.0116(12)	0.0046(13)
O51	0.0352(16)	0.0337(18)	0.0192(13)	-0.0058(11)	0.0127(11)	0.0025(13)
O52	0.0373(15)	0.0280(15)	0.0115(11)	0.0048(11)	0.0084(10)	0.0030(13)
O53	0.0473(18)	0.0264(15)	0.0164(13)	0.0005(10)	0.0163(12)	-0.0043(13)

Distances

P1	C1	1.770(4)Å		P1	C17	1.771(4)Å
P1	C33	1.760(5)Å		P2	C51	1.778(4)Å
P2	C67	1.778(4)Å		P2	C83	1.762(5)Å
C1	C2	1.188(6)Å		C2	C3	1.489(6)Å
C3	C5	1.532(6)Å		C3	C11	1.538(5)Å
C3	O1	1.424(5)Å		C4	O1	1.427(6)Å
C4	H41	0.979Å		C4	H42	0.988Å
C4	H43	0.981Å		C5	C6	1.389(7)Å
C5	C10	1.402(6)Å		C6	C7	1.373(7)Å
C6	H61	0.979Å		C7	C8	1.367(8)Å
C7	H71	0.966Å		C8	C9	1.413(9)Å
C8	H81	0.925Å		C9	C10	1.374(8)Å
C9	H91	0.990Å		C10	H101	0.956Å
C11	C12	1.379(6)Å		C11	C16	1.402(6)Å
C12	C13	1.399(5)Å		C12	H121	0.943Å
C13	C14	1.375(7)Å		C13	H131	0.945Å
C14	C15	1.384(7)Å		C14	H141	0.956Å
C15	C16	1.394(6)Å		C15	H151	0.941Å

C16	H161	0.945Å		C17	C18	1.202(6)Å
C18	C19	1.482(6)Å		C19	C21	1.538(5)Å
C19	C27	1.532(6)Å		C19	O2	1.434(5)Å
C20	O2	1.431(5)Å		C20	H201	0.965Å
C20	H202	0.996Å		C20	H203	0.984Å
C21	C22	1.397(6)Å		C21	C26	1.380(6)Å
C22	C23	1.383(6)Å		C22	H221	0.959Å
C23	C24	1.390(7)Å		C23	H231	0.938Å
C24	C25	1.390(7)Å		C24	H241	0.946Å
C25	C26	1.387(6)Å		C25	H251	0.942Å
C26	H261	0.915Å		C27	C28	1.395(7)Å
C27	C32	1.388(6)Å		C28	C29	1.384(8)Å
C28	H281	0.961Å		C29	C30	1.387(10)Å
C29	H291	0.966Å		C30	C31	1.388(10)Å
C30	H301	0.947Å		C31	C32	1.374(7)Å
C31	H311	0.975Å		C32	H321	0.963Å
C33	C34	1.214(6)Å		C34	C35	1.488(5)Å
C35	C37	1.527(5)Å		C35	C43	1.536(6)Å
C35	O3	1.438(5)Å		C36	O3	1.415(6)Å
C36	H361	0.971Å		C36	H362	0.989Å
C36	H363	0.966Å		C37	C38	1.380(6)Å
C37	C42	1.407(6)Å		C38	C39	1.389(5)Å
C38	H381	0.946Å		C39	C40	1.384(7)Å
C39	H391	0.928Å		C40	C41	1.400(7)Å
C40	H401	0.978Å		C41	C42	1.383(5)Å
C41	H411	0.914Å		C42	H421	0.921Å
C43	C44	1.395(6)Å		C43	C48	1.387(6)Å
C44	C45	1.392(7)Å		C44	H441	0.940Å
C45	C46	1.375(8)Å		C45	H451	0.945Å
C46	C47	1.387(7)Å		C46	H461	0.941Å
C47	C48	1.372(7)Å		C47	H471	0.954Å
C48	H481	0.966Å		C51	C52	1.196(6)Å
C52	C53	1.488(6)Å		C53	C55	1.541(6)Å
C53	C61	1.525(5)Å		C53	O51	1.424(5)Å
C54	O51	1.440(6)Å		C54	H541	0.969Å
C54	H542	0.976Å		C54	H543	1.001Å

C55	C56	1.378(6)Å		C55	C60	1.389(6)Å
C56	C57	1.399(8)Å		C56	H561	0.961Å
C57	C58	1.385(9)Å		C57	H571	0.978Å
C58	C59	1.382(9)Å		C58	H581	0.940Å
C59	C60	1.394(7)Å		C59	H591	0.952Å
C60	H601	0.945Å		C61	C62	1.399(6)Å
C61	C66	1.380(6)Å		C62	C63	1.386(6)Å
C62	H621	0.949Å		C63	C64	1.378(8)Å
C63	H631	0.946Å		C64	C65	1.367(8)Å
C64	H641	0.957Å		C65	C66	1.396(6)Å
C65	H651	0.953Å		C66	H661	0.938Å
C67	C68	1.186(6)Å		C68	C69	1.485(6)Å
C69	C71	1.530(5)Å		C69	C77	1.536(6)Å
C69	O52	1.433(5)Å		C70	O52	1.426(6)Å
C70	H701	0.978Å		C70	H702	0.981Å
C70	H703	0.989Å		C71	C72	1.384(6)Å
C71	C76	1.411(6)Å		C72	C73	1.392(6)Å
C72	H721	0.950Å		C73	C74	1.385(7)Å
C73	H731	0.937Å		C74	C75	1.381(7)Å
C74	H741	0.962Å		C75	C76	1.395(6)Å
C75	H751	0.940Å		C76	H761	0.926Å
C77	C78	1.404(6)Å		C77	C82	1.379(6)Å
C78	C79	1.381(7)Å		C78	H781	0.963Å
C79	C80	1.389(7)Å		C79	H791	0.948Å
C80	C81	1.375(8)Å		C80	H801	0.929Å
C81	C82	1.414(7)Å		C81	H811	0.980Å
C82	H821	0.956Å		C83	C84	1.217(6)Å
C84	C85	1.480(5)Å		C85	C87	1.544(5)Å
C85	C93	1.525(6)Å		C85	O53	1.418(5)Å
C86	O53	1.424(6)Å		C86	H861	0.965Å
C86	H862	0.977Å		C86	H863	0.969Å
C87	C88	1.396(6)Å		C87	C92	1.403(6)Å
C88	C89	1.377(5)Å		C88	H881	0.914Å
C89	C90	1.382(7)Å		C89	H891	0.915Å
C90	C91	1.388(7)Å		C90	H901	0.992Å
C91	C92	1.391(5)Å		C91	H911	0.928Å

C92	H921	0.928Å		C93	C94	1.399(6)Å
C93	C98	1.392(6)Å		C94	C95	1.379(7)Å
C94	H941	0.944Å		C95	C96	1.402(8)Å
C95	H951	0.973Å		C96	C97	1.377(8)Å
C96	H961	0.965Å		C97	C98	1.380(7)Å
C97	H971	0.924Å		C98	H981	0.959Å

Angles

C1	P1	C17	103.47(19)°		C1	P1	C33	99.5(2)°
C17	P1	C33	100.2(2)°		C51	P2	C67	103.77(18)°
C51	P2	C83	98.5(2)°		C67	P2	C83	99.63(19)°
P1	C1	C2	170.3(4)°		C1	C2	C3	177.6(4)°
C2	C3	C5	107.6(3)°		C2	C3	C11	110.6(3)°
C5	C3	C11	112.2(3)°		C2	C3	O1	109.8(3)°
C5	C3	O1	106.2(3)°		C11	C3	O1	110.3(3)°
O1	C4	H41	108.285°		O1	C4	H42	108.910°
H41	C4	H42	109.674°		O1	C4	H43	110.569°
H41	C4	H43	107.788°		H42	C4	H43	111.553°
C3	C5	C6	120.4(4)°		C3	C5	C10	120.4(4)°
C6	C5	C10	119.1(4)°		C5	C6	C7	121.2(5)°
C5	C6	H61	118.713°		C7	C6	H61	119.958°
C6	C7	C8	120.8(5)°		C6	C7	H71	119.319°
C8	C7	H71	119.837°		C7	C8	C9	118.3(5)°
C7	C8	H81	121.902°		C9	C8	H81	119.693°
C8	C9	C10	121.6(5)°		C8	C9	H91	116.468°
C10	C9	H91	121.796°		C5	C10	C9	119.0(5)°
C5	C10	H101	120.248°		C9	C10	H101	120.755°
C3	C11	C12	123.1(4)°		C3	C11	C16	117.1(4)°
C12	C11	C16	119.8(4)°		C11	C12	C13	120.2(4)°
C11	C12	H121	118.734°		C13	C12	H121	121.066°
C12	C13	C14	119.9(4)°		C12	C13	H131	119.700°
C14	C13	H131	120.292°		C13	C14	C15	120.4(4)°
C13	C14	H141	120.004°		C15	C14	H141	119.397°
C14	C15	C16	120.2(4)°		C14	C15	H151	119.882°
C16	C15	H151	119.889°		C11	C16	C15	119.4(4)°
C11	C16	H161	119.545°		C15	C16	H161	120.885°
P1	C17	C18	167.7(4)°		C17	C18	C19	176.4(4)°

C18	C19	C21	112.6(4)°		C18	C19	C27	108.0(4)°
C21	C19	C27	110.7(3)°		C18	C19	O2	108.2(3)°
C21	C19	O2	110.7(4)°		C27	C19	O2	106.5(3)°
O2	C20	H201	110.121°		O2	C20	H202	109.314°
H201	C20	H202	109.791°		O2	C20	H203	110.699°
H201	C20	H203	109.021°		H202	C20	H203	107.860°
C19	C21	C22	122.5(4)°		C19	C21	C26	118.5(4)°
C22	C21	C26	119.0(4)°		C21	C22	C23	120.5(4)°
C21	C22	H221	116.189°		C23	C22	H221	123.174°
C22	C23	C24	120.3(4)°		C22	C23	H231	119.007°
C24	C23	H231	120.337°		C23	C24	C25	119.2(4)°
C23	C24	H241	120.235°		C25	C24	H241	120.301°
C24	C25	C26	120.3(4)°		C24	C25	H251	119.189°
C26	C25	H251	120.515°		C21	C26	C25	120.7(4)°
C21	C26	H261	119.081°		C25	C26	H261	119.848°
C19	C27	C28	118.7(4)°		C19	C27	C32	121.9(4)°
C28	C27	C32	119.4(5)°		C27	C28	C29	120.0(5)°
C27	C28	H281	120.610°		C29	C28	H281	119.241°
C28	C29	C30	119.6(6)°		C28	C29	H291	118.490°
C30	C29	H291	121.741°		C29	C30	C31	120.7(5)°
C29	C30	H301	119.279°		C31	C30	H301	119.935°
C30	C31	C32	119.2(6)°		C30	C31	H311	119.779°
C32	C31	H311	120.949°		C27	C32	C31	121.0(5)°
C27	C32	H321	120.214°		C31	C32	H321	118.766°
P1	C33	C34	172.5(3)°		C33	C34	C35	176.3(4)°
C34	C35	C37	111.5(3)°		C34	C35	C43	105.1(3)°
C37	C35	C43	112.7(3)°		C34	C35	O3	108.9(3)°
C37	C35	O3	111.1(3)°		C43	C35	O3	107.2(3)°
O3	C36	H361	110.825°		O3	C36	H362	110.803°
H361	C36	H362	108.218°		O3	C36	H363	111.769°
H361	C36	H363	105.560°		H362	C36	H363	109.479°
C35	C37	C38	123.8(4)°		C35	C37	C42	117.2(4)°
C38	C37	C42	118.8(3)°		C37	C38	C39	121.1(4)°
C37	C38	H381	118.764°		C39	C38	H381	120.052°
C38	C39	C40	120.3(4)°		C38	C39	H391	121.002°
C40	C39	H391	118.695°		C39	C40	C41	119.1(4)°

C39	C40	H401	121.570°		C41	C40	H401	119.253°
C40	C41	C42	120.7(4)°		C40	C41	H411	118.247°
C42	C41	H411	121.076°		C37	C42	C41	120.0(4)°
C37	C42	H421	118.895°		C41	C42	H421	121.067°
C35	C43	C44	120.7(4)°		C35	C43	C48	120.4(4)°
C44	C43	C48	118.6(4)°		C43	C44	C45	119.5(4)°
C43	C44	H441	120.183°		C45	C44	H441	120.223°
C44	C45	C46	121.2(4)°		C44	C45	H451	119.623°
C46	C45	H451	118.930°		C45	C46	C47	119.1(5)°
C45	C46	H461	119.599°		C47	C46	H461	121.303°
C46	C47	C48	120.1(5)°		C46	C47	H471	118.981°
C48	C47	H471	120.841°		C43	C48	C47	121.4(4)°
C43	C48	H481	118.763°		C47	C48	H481	119.739°
P2	C51	C52	169.5(3)°		C51	C52	C53	176.1(4)°
C52	C53	C55	108.4(4)°		C52	C53	C61	111.0(3)°
C55	C53	C61	109.9(3)°		C52	C53	O51	109.1(3)°
C55	C53	O51	106.2(3)°		C61	C53	O51	112.0(4)°
O51	C54	H541	109.771°		O51	C54	H542	110.889°
H541	C54	H542	109.286°		O51	C54	H543	108.467°
H541	C54	H543	109.685°		H542	C54	H543	108.721°
C53	C55	C56	120.7(4)°		C53	C55	C60	119.1(4)°
C56	C55	C60	120.1(4)°		C55	C56	C57	119.7(5)°
C55	C56	H561	120.487°		C57	C56	H561	119.652°
C56	C57	C58	120.6(5)°		C56	C57	H571	119.937°
C58	C57	H571	119.444°		C57	C58	C59	119.3(5)°
C57	C58	H581	119.150°		C59	C58	H581	121.593°
C58	C59	C60	120.6(5)°		C58	C59	H591	120.207°
C60	C59	H591	119.184°		C55	C60	C59	119.8(5)°
C55	C60	H601	122.409°		C59	C60	H601	117.811°
C53	C61	C62	117.7(4)°		C53	C61	C66	123.0(4)°
C62	C61	C66	119.2(4)°		C61	C62	C63	119.8(4)°
C61	C62	H621	118.963°		C63	C62	H621	121.220°
C62	C63	C64	120.5(4)°		C62	C63	H631	118.379°
C64	C63	H631	121.069°		C63	C64	C65	119.9(4)°
C63	C64	H641	119.179°		C65	C64	H641	120.881°
C64	C65	C66	120.4(5)°		C64	C65	H651	119.426°

C66	C65	H651	120.063°		C61	C66	C65	120.1(4)°
C61	C66	H661	118.683°		C65	C66	H661	121.210°
P2	C67	C68	168.8(4)°		C67	C68	C69	178.5(4)°
C68	C69	C71	111.5(3)°		C68	C69	C77	107.4(3)°
C71	C69	C77	112.0(3)°		C68	C69	O52	109.8(3)°
C71	C69	O52	109.8(3)°		C77	C69	O52	106.2(3)°
O52	C70	H701	109.393°		O52	C70	H702	109.529°
H701	C70	H702	111.046°		O52	C70	H703	109.196°
H701	C70	H703	108.438°		H702	C70	H703	109.208°
C69	C71	C72	122.8(4)°		C69	C71	C76	118.0(4)°
C72	C71	C76	119.1(4)°		C71	C72	C73	120.4(4)°
C71	C72	H721	118.699°		C73	C72	H721	120.866°
C72	C73	C74	120.4(4)°		C72	C73	H731	120.400°
C74	C73	H731	118.807°		C73	C74	C75	119.9(4)°
C73	C74	H741	121.053°		C75	C74	H741	118.769°
C74	C75	C76	120.3(4)°		C74	C75	H751	118.701°
C76	C75	H751	120.937°		C71	C76	C75	119.9(4)°
C71	C76	H761	119.213°		C75	C76	H761	120.647°
C69	C77	C78	118.9(4)°		C69	C77	C82	121.4(4)°
C78	C77	C82	119.7(4)°		C77	C78	C79	120.2(4)°
C77	C78	H781	119.546°		C79	C78	H781	120.277°
C78	C79	C80	120.1(5)°		C78	C79	H791	120.813°
C80	C79	H791	119.081°		C79	C80	C81	120.4(5)°
C79	C80	H801	119.925°		C81	C80	H801	119.629°
C80	C81	C82	119.8(5)°		C80	C81	H811	119.693°
C82	C81	H811	120.547°		C77	C82	C81	119.9(5)°
C77	C82	H821	120.428°		C81	C82	H821	119.705°
P2	C83	C84	171.6(3)°		C83	C84	C85	176.9(4)°
C84	C85	C87	111.3(3)°		C84	C85	C93	106.7(3)°
C87	C85	C93	110.6(3)°		C84	C85	O53	109.9(3)°
C87	C85	O53	110.7(3)°		C93	C85	O53	107.5(3)°
O53	C86	H861	109.466°		O53	C86	H862	110.981°
H861	C86	H862	109.576°		O53	C86	H863	110.425°
H861	C86	H863	105.973°		H862	C86	H863	110.291°
C85	C87	C88	118.0(4)°		C85	C87	C92	122.9(3)°
C88	C87	C92	119.0(3)°		C87	C88	C89	119.9(4)°

C87	C88	H881	118.340°		C89	C88	H881	121.656°
C88	C89	C90	121.5(4)°		C88	C89	H891	120.052°
C90	C89	H891	118.382°		C89	C90	C91	119.0(4)°
C89	C90	H901	120.639°		C91	C90	H901	120.318°
C90	C91	C92	120.4(4)°		C90	C91	H911	118.934°
C92	C91	H911	120.681°		C87	C92	C91	120.1(4)°
C87	C92	H921	118.385°		C91	C92	H921	121.516°
C85	C93	C94	120.0(4)°		C85	C93	C98	121.7(4)°
C94	C93	C98	118.3(4)°		C93	C94	C95	121.1(4)°
C93	C94	H941	118.171°		C95	C94	H941	120.675°
C94	C95	C96	120.1(5)°		C94	C95	H951	119.933°
C96	C95	H951	119.885°		C95	C96	C97	118.4(5)°
C95	C96	H961	121.366°		C97	C96	H961	120.200°
C96	C97	C98	121.7(5)°		C96	C97	H971	118.175°
C98	C97	H971	120.012°		C93	C98	C97	120.3(5)°
C93	C98	H981	119.381°		C97	C98	H981	120.257°
C3	O1	C4	115.2(3)°		C19	O2	C20	115.5(3)°
C35	O3	C36	114.9(3)°		C53	O51	C54	115.1(3)°
C69	O52	C70	115.1(3)°		C85	O53	C86	114.5(3)°

Crystal Data 39

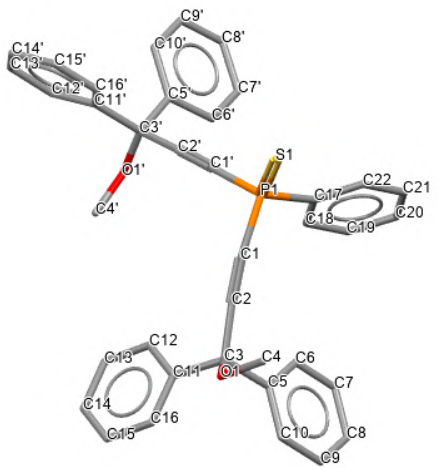

a = 9.96300(10) Å α = 90°

b = 28.8565(2) Å β = 113.6790(10)°

c = 11.70840(10) Å γ = 90°

Volume	3082.74(5) Å³	Crystal Class	monoclinic
Space group	P 1 2_1/c 1	Z =	4
Formula	C_{38} H_{31} O_2 P_1 S_1	M_r	582.70
Cell determined from	30299 reflections	Cell θ range =	3 - 75°
Temperature	180K		
Shape	block		
Colour	colorless	Size	0.05 × 0.09 × 0.22 mm
D_x	1.26	F000	1224.000
μ	1.673 mm^{-1}		
Absorption correction	multi-scan		
T_{min}	0.65	T_{max}	0.92

Data Collection

Diffractometer	multi-scan
Scan type	ϕ and ω scans
Reflections measured	10605
Independent reflections	5973
Rint	0.1012
θ_{max}	75.7918
h =	-12 → 11
k =	-35 → 26
l =	0 → 14

Refinement

$\Delta\rho_{min}$ = -0.37 e $Å^{-3}$

$\Delta\rho_{max}$ =	0.32 e Å^{-3}
Reflections used	5819
Cutoff: I >	-3.00σ(I)
Parameters refined	379
S =	0.98
R-factor	0.038
weighted R-factor	0.098
Δ/σ_{max}	0.0010
Refinement on	F^2
w =	$1/[\sigma^2(F_{obs}^2) + (0.057 \times P)^2 + 1.203 \times P + 0.000 + 0.000 \times \sin\theta]$, $P = 0.333 \times \max(F_{obs}^2,0) + 0.667 \times F_{calc}^2$

Parameters

Label	*x*	*y*	*z*	$U_{iso/equiv}$	Occupancy
C1	0.26760(15)	0.40257(5)	0.44130(13)	0.0312	1.0000
P1	0.22228(4)	.361560(12)	0.53060(3)	0.0272	1.0000
S1	0.06444(4)	.379729(13)	0.57740(4)	0.0361	1.0000
O1	0.23242(12)	0.49771(4)	0.25292(11)	0.0420	1.0000
C2	0.29207(15)	0.42746(5)	0.37032(13)	0.0318	1.0000
C3	0.31672(16)	0.45618(5)	0.27553(14)	0.0334	1.0000
C4	0.07954(19)	0.49097(7)	0.2196(2)	0.0532	1.0000
C5	0.27795(16)	0.42744(6)	0.15538(14)	0.0367	1.0000
C6	0.2856(2)	0.37955(6)	0.15773(16)	0.0449	1.0000
C7	0.2545(2)	0.35415(8)	0.04904(18)	0.0575	1.0000
C8	0.2162(2)	0.37648(9)	0.06291(18)	0.0598	1.0000
C9	0.2098(2)	0.42372(9)	0.06632(16)	0.0617	1.0000
C10	0.24013(19)	0.44989(7)	0.04162(16)	0.0503	1.0000
C11	0.47660(16)	0.47213(5)	0.32196(14)	0.0329	1.0000
C12	0.58851(18)	0.44810(6)	0.41345(16)	0.0408	1.0000
C13	0.73320(19)	0.46201(6)	0.44876(17)	0.0476	1.0000
C14	0.76652(19)	0.49973(6)	0.39321(17)	0.0463	1.0000
C15	0.6551(2)	0.52405(6)	0.30350(17)	0.0471	1.0000
C16	0.51052(19)	0.51049(6)	0.26705(16)	0.0433	1.0000
C17	0.18990(15)	0.30984(5)	0.43640(13)	0.0306	1.0000
C18	0.29910(17)	0.29329(6)	0.40126(16)	0.0408	1.0000
C19	0.2701(2)	0.25617(6)	0.32061(19)	0.0515	1.0000
C20	0.1337(2)	0.23539(6)	0.27521(18)	0.0529	1.0000
C21	0.0264(2)	0.25102(7)	0.31257(18)	0.0521	1.0000
C22	0.05384(17)	0.28840(6)	0.39290(16)	0.0407	1.0000

C1’	0.39202(16)	0.35183(5)	0.65490(13)	0.0327	1.0000
O1’	0.76138(11)	0.33779(3)	0.77084(9)	0.0328	1.0000
C2’	0.50990(15)	0.34315(5)	0.73528(13)	0.0306	1.0000
C3’	0.65837(14)	0.33006(5)	0.82701(12)	0.0283	1.0000
C4’	0.77628(19)	0.38518(6)	0.74138(17)	0.0431	1.0000
C5’	0.65988(14)	0.27729(5)	0.84422(13)	0.0292	1.0000
C6’	0.61667(17)	0.24956(5)	0.73772(14)	0.0366	1.0000
C7’	0.62141(19)	0.20188(6)	0.74728(17)	0.0440	1.0000
C8’	0.66792(19)	0.18090(6)	0.86323(17)	0.0447	1.0000
C9’	0.70844(19)	0.20792(6)	0.96871(16)	0.0429	1.0000
C10’	0.70420(17)	0.25599(5)	0.95989(14)	0.0354	1.0000
C11’	0.70219(15)	0.35734(5)	0.94834(13)	0.0300	1.0000
C12’	0.84832(17)	0.35589(6)	1.03340(15)	0.0399	1.0000
C13’	0.8915(2)	0.37923(7)	1.14575(16)	0.0496	1.0000
C14’	0.7913(2)	0.40470(7)	1.17394(17)	0.0532	1.0000
C15’	0.6475(2)	0.40668(6)	1.08973(17)	0.0488	1.0000
C16’	0.60259(17)	0.38316(5)	0.97699(15)	0.0371	1.0000
H41	0.03361(19)	0.52060(7)	0.2021(2)	0.0792	1.0000
H42	0.06722(19)	0.47677(7)	0.2912(2)	0.0796	1.0000
H43	0.03549(19)	0.47116(7)	0.1441(2)	0.0800	1.0000
H61	0.3132(2)	0.36502(6)	0.23644(16)	0.0546	1.0000
H71	0.2567(2)	0.32104(8)	0.05155(18)	0.0736	1.0000
H81	0.1934(2)	0.35931(9)	0.13975(18)	0.0727	1.0000
H91	0.1870(2)	0.43822(9)	0.14185(16)	0.0745	1.0000
H101	0.23825(19)	0.48342(7)	0.03864(16)	0.0627	1.0000
H121	0.56922(18)	0.42160(6)	0.45679(16)	0.0489	1.0000
H131	0.80770(19)	0.44604(6)	0.51394(17)	0.0587	1.0000
H141	0.86781(19)	0.50819(6)	0.41585(17)	0.0543	1.0000
H151	0.6774(2)	0.55091(6)	0.26469(17)	0.0562	1.0000
H161	0.43268(19)	0.52754(6)	0.20229(16)	0.0525	1.0000
H181	0.39538(17)	0.30782(6)	0.43385(16)	0.0500	1.0000
H191	0.3411(2)	0.24421(6)	0.29489(19)	0.0612	1.0000
H201	0.1124(2)	0.20962(6)	0.21729(18)	0.0637	1.0000
H211	-0.0687(2)	0.23658(7)	0.28358(18)	0.0633	1.0000
H221	0.01999(17)	0.29971(6)	0.41645(16)	0.0492	1.0000
H541	0.84312(19)	0.38513(6)	0.70421(17)	0.0649	1.0000

H542	0.81592(19)	0.40299(6)	0.81680(17)	0.0645	1.0000
H543	0.68380(19)	0.39798(6)	0.68486(17)	0.0665	1.0000
H561	0.58666(17)	0.26440(5)	0.65739(14)	0.0462	1.0000
H571	0.58893(19)	0.18401(6)	0.67207(17)	0.0531	1.0000
H581	0.67291(19)	0.14756(6)	0.86784(17)	0.0556	1.0000
H591	0.74049(19)	0.19404(6)	1.04917(16)	0.0537	1.0000
H601	0.73449(17)	0.27533(5)	1.03357(14)	0.0427	1.0000
H621	0.92139(17)	0.33842(6)	1.01374(15)	0.0491	1.0000
H631	0.9917(2)	0.37654(7)	1.20339(16)	0.0588	1.0000
H641	0.8167(2)	0.42035(7)	1.25041(17)	0.0656	1.0000
H651	0.5783(2)	0.42413(6)	1.10785(17)	0.0587	1.0000
H661	0.50104(17)	0.38371(5)	0.92019(15)	0.0460	1.0000

Thermal Parameters

Label	U_{11}	U_{22}	U_{33}	U_{23}	U_{13}	U_{12}
C1	0.0286(7)	0.0336(8)	0.0310(7)	0.0001(6)	0.0116(6)	0.0001(6)
P1	0.02330(17)	0.0306(2)	0.02715(18)	0.00278(13)	0.00951(14)	0.00080(13)
S1	0.03142(19)	0.0405(2)	0.0412(2)	0.00044(15)	0.01971(16)	0.00280(14)
O1	0.0365(6)	0.0361(6)	0.0562(7)	0.0114(5)	0.0216(5)	0.0081(4)
C2	0.0308(7)	0.0319(7)	0.0320(7)	-0.0003(6)	0.0121(6)	-0.0002(6)
C3	0.0331(7)	0.0334(8)	0.0357(7)	0.0077(6)	0.0158(6)	0.0048(6)
C4	0.0358(9)	0.0523(11)	0.0732(12)	0.0130(9)	0.0237(8)	0.0113(8)
C5	0.0270(7)	0.0515(9)	0.0316(7)	0.0045(6)	0.0118(6)	0.0026(6)
C6	0.0482(9)	0.0498(10)	0.0376(8)	-0.0028(7)	0.0181(7)	-0.0023(7)
C7	0.0570(11)	0.0663(13)	0.0512(11)	-0.0179(9)	0.0238(9)	-0.0048(9)
C8	0.0424(10)	0.0926(17)	0.0406(10)	-0.0137(10)	0.0128(8)	0.0073(10)
C9	0.0435(10)	0.1113(19)	0.0292(8)	0.0128(10)	0.0134(7)	0.0206(11)
C10	0.0442(9)	0.0684(12)	0.0386(9)	0.0138(8)	0.0169(7)	0.0134(8)
C11	0.0349(7)	0.0312(7)	0.0356(7)	0.0004(6)	0.0174(6)	0.0015(6)
C12	0.0369(8)	0.0376(8)	0.0468(9)	0.0058(7)	0.0156(7)	0.0035(6)
C13	0.0354(8)	0.0477(10)	0.0550(10)	0.0001(8)	0.0131(7)	0.0041(7)
C14	0.0368(8)	0.0481(10)	0.0576(10)	-0.0127(8)	0.0228(8)	-0.0065(7)
C15	0.0486(10)	0.0429(9)	0.0580(10)	-0.0004(8)	0.0299(8)	-0.0081(7)
C16	0.0427(9)	0.0418(9)	0.0471(9)	0.0086(7)	0.0197(7)	0.0008(7)
C17	0.0282(7)	0.0322(7)	0.0311(7)	0.0020(6)	0.0115(5)	0.0012(5)
C18	0.0326(8)	0.0409(9)	0.0519(9)	-0.0038(7)	0.0201(7)	0.0005(6)
C19	0.0526(10)	0.0454(10)	0.0652(11)	-0.0096(8)	0.0329(9)	0.0047(8)

C20	0.0625(12)	0.0424(10)	0.0551(10)	-0.0145(8)	0.0250(9)	-0.0053(8)
C21	0.0444(9)	0.0503(10)	0.0598(11)	-0.0162(8)	0.0191(8)	-0.0143(8)
C22	0.0306(7)	0.0457(9)	0.0476(9)	-0.0068(7)	0.0175(7)	-0.0060(6)
C1’	0.0301(7)	0.0344(8)	0.0326(7)	0.0016(6)	0.0114(6)	-0.0001(6)
O1’	0.0327(5)	0.0337(5)	0.0373(5)	0.0019(4)	0.0197(4)	-0.0002(4)
C2’	0.0296(7)	0.0310(7)	0.0309(7)	-0.0001(5)	0.0118(6)	-0.0006(6)
C3’	0.0244(6)	0.0329(7)	0.0279(6)	0.0012(5)	0.0109(5)	0.0010(5)
C4’	0.0451(9)	0.0398(9)	0.0505(9)	0.0067(7)	0.0255(8)	-0.0037(7)
C5’	0.0240(6)	0.0323(7)	0.0334(7)	0.0004(6)	0.0136(5)	0.0007(5)
C6’	0.0389(8)	0.0367(8)	0.0349(8)	-0.0028(6)	0.0156(6)	-0.0011(6)
C7’	0.0484(9)	0.0366(9)	0.0500(9)	-0.0092(7)	0.0230(8)	-0.0047(7)
C8’	0.0478(9)	0.0301(8)	0.0639(11)	0.0024(7)	0.0305(8)	-0.0003(7)
C9’	0.0454(9)	0.0404(9)	0.0474(9)	0.0116(7)	0.0233(7)	0.0046(7)
C10’	0.0364(8)	0.0371(8)	0.0344(7)	0.0023(6)	0.0158(6)	0.0023(6)
C11’	0.0303(7)	0.0294(7)	0.0300(7)	-0.0002(5)	0.0119(6)	-0.0014(5)
C12’	0.0325(8)	0.0450(9)	0.0374(8)	-0.0047(7)	0.0090(6)	-0.0017(7)
C13’	0.0446(9)	0.0565(11)	0.0381(9)	-0.0073(8)	0.0066(7)	-0.0143(8)
C14’	0.0693(12)	0.0524(11)	0.0409(9)	-0.0176(8)	0.0254(9)	-0.0192(9)
C15’	0.0617(11)	0.0440(10)	0.0520(10)	-0.0109(8)	0.0347(9)	-0.0022(8)
C16’	0.0372(8)	0.0372(8)	0.0400(8)	-0.0010(6)	0.0186(7)	0.0018(6)

Distances

C1	P1	1.7541(15)Å		C1	C2	1.195(2)Å
P1	S1	1.9340(5)Å		P1	C17	1.8061(15)Å
P1	C1’	1.7550(15)Å		O1	C3	1.4258(18)Å
O1	C4	1.426(2)Å		C2	C3	1.482(2)Å
C3	C5	1.543(2)Å		C3	C11	1.533(2)Å
C4	H41	0.953Å		C4	H42	0.984Å
C4	H43	0.995Å		C5	C6	1.384(2)Å
C5	C10	1.390(2)Å		C6	C7	1.391(2)Å
C6	H61	0.947Å		C7	C8	1.370(3)Å
C7	H71	0.956Å		C8	C9	1.365(3)Å
C8	H81	0.971Å		C9	C10	1.397(3)Å
C9	H91	0.921Å		C10	H101	0.968Å
C11	C12	1.383(2)Å		C11	C16	1.388(2)Å
C12	C13	1.390(2)Å		C12	H121	0.979Å
C13	C14	1.375(3)Å		C13	H131	0.944Å

C14	C15	1.375(3)Å		C14	H141	0.966Å
C15	C16	1.385(2)Å		C15	H151	0.968Å
C16	H161	0.973Å		C17	C18	1.393(2)Å
C17	C22	1.388(2)Å		C18	C19	1.380(2)Å
C18	H181	0.973Å		C19	C20	1.382(3)Å
C19	H191	0.939Å		C20	C21	1.383(3)Å
C20	H201	0.971Å		C21	C22	1.384(2)Å
C21	H211	0.964Å		C22	H221	0.942Å
C1’	C2’	1.200(2)Å		O1’	C3’	1.4415(16)Å
O1’	C4’	1.4326(18)Å		C2’	C3’	1.4859(19)Å
C3’	C5’	1.535(2)Å		C3’	C11’	1.5264(19)Å
C4’	H541	0.930Å		C4’	H542	0.959Å
C4’	H543	0.966Å		C5’	C6’	1.396(2)Å
C5’	C10’	1.388(2)Å		C6’	C7’	1.380(2)Å
C6’	H561	0.965Å		C7’	C8’	1.385(2)Å
C7’	H571	0.958Å		C8’	C9’	1.377(2)Å
C8’	H581	0.964Å		C9’	C10’	1.390(2)Å
C9’	H591	0.953Å		C10’	H601	0.968Å
C11’	C12’	1.396(2)Å		C11’	C16’	1.386(2)Å
C12’	C13’	1.384(2)Å		C12’	H621	0.986Å
C13’	C14’	1.382(3)Å		C13’	H631	0.958Å
C14’	C15’	1.376(3)Å		C14’	H641	0.942Å
C15’	C16’	1.389(2)Å		C15’	H651	0.944Å
C16’	H661	0.962Å				

Angles

P1	C1	C2	173.25(13)°	C1	P1	S1	114.79(5)°
C1	P1	C17	102.66(7)°	S1	P1	C17	115.52(5)°
C1	P1	C1’	102.08(7)°	S1	P1	C1’	115.52(5)°
C17	P1	C1’	104.51(7)°	C3	O1	C4	114.90(12)°
C1	C2	C3	176.18(15)°	O1	C3	C2	110.28(12)°
O1	C3	C5	111.69(12)°	C2	C3	C5	109.03(12)°
O1	C3	C11	105.32(12)°	C2	C3	C11	111.30(12)°
C5	C3	C11	109.19(12)°	O1	C4	H41	107.723°
O1	C4	H42	107.983°	H41	C4	H42	110.112°
O1	C4	H43	111.294°	H41	C4	H43	108.789°
H42	C4	H43	110.888°	C3	C5	C6	121.82(14)°

C3	C5	C10	119.69(15)°		C6	C5	C10	118.43(16)°
C5	C6	C7	121.17(17)°		C5	C6	H61	116.978°
C7	C6	H61	121.852°		C6	C7	C8	120.1(2)°
C6	C7	H71	120.287°		C8	C7	H71	119.589°
C7	C8	C9	119.31(18)°		C7	C8	H81	121.201°
C9	C8	H81	119.486°		C8	C9	C10	121.54(18)°
C8	C9	H91	118.198°		C10	C9	H91	120.248°
C5	C10	C9	119.45(19)°		C5	C10	H101	119.617°
C9	C10	H101	120.905°		C3	C11	C12	121.61(13)°
C3	C11	C16	119.12(13)°		C12	C11	C16	119.21(15)°
C11	C12	C13	120.20(15)°		C11	C12	H121	121.897°
C13	C12	H121	117.888°		C12	C13	C14	120.43(16)°
C12	C13	H131	118.984°		C14	C13	H131	120.526°
C13	C14	C15	119.40(16)°		C13	C14	H141	119.608°
C15	C14	H141	120.960°		C14	C15	C16	120.79(16)°
C14	C15	H151	119.984°		C16	C15	H151	119.226°
C11	C16	C15	119.96(16)°		C11	C16	H161	119.878°
C15	C16	H161	120.161°		P1	C17	C18	119.64(11)°
P1	C17	C22	120.08(11)°		C18	C17	C22	120.16(14)°
C17	C18	C19	119.64(15)°		C17	C18	H181	120.014°
C19	C18	H181	120.348°		C18	C19	C20	120.24(16)°
C18	C19	H191	121.810°		C20	C19	H191	117.949°
C19	C20	C21	120.16(16)°		C19	C20	H201	120.388°
C21	C20	H201	119.452°		C20	C21	C22	120.15(16)°
C20	C21	H211	121.541°		C22	C21	H211	118.305°
C17	C22	C21	119.61(15)°		C17	C22	H221	120.065°
C21	C22	H221	120.310°		P1	C1’	C2’	175.88(14)°
C3’	O1’	C4’	114.78(11)°		C1’	C2’	C3’	175.22(15)°
O1’	C3’	C2’	108.38(11)°		O1’	C3’	C5’	104.00(11)°
C2’	C3’	C5’	107.54(11)°		O1’	C3’	C11’	110.79(11)°
C2’	C3’	C11’	111.79(11)°		C5’	C3’	C11’	113.91(11)°
O1’	C4’	H541	105.911°		O1’	C4’	H542	109.509°
H541	C4’	H542	108.910°		O1’	C4’	H543	111.542°
H541	C4’	H543	110.186°		H542	C4’	H543	110.646°
C3’	C5’	C6’	117.90(13)°		C3’	C5’	C10’	123.34(13)°
C6’	C5’	C10’	118.74(14)°		C5’	C6’	C7’	120.72(15)°

C5’	C6’	H561	118.670°		C7’	C6’	H561	120.575°
C6’	C7’	C8’	120.17(16)°		C6’	C7’	H571	118.331°
C8’	C7’	H571	121.472°		C7’	C8’	C9’	119.57(15)°
C7’	C8’	H581	118.733°		C9’	C8’	H581	121.680°
C8’	C9’	C10’	120.61(15)°		C8’	C9’	H591	120.642°
C10’	C9’	H591	118.744°		C5’	C10’	C9’	120.16(15)°
C5’	C10’	H601	118.515°		C9’	C10’	H601	121.298°
C3’	C11’	C12’	118.37(13)°		C3’	C11’	C16’	122.52(13)°
C12’	C11’	C16’	119.11(14)°		C11’	C12’	C13’	120.05(16)°
C11’	C12’	H621	120.335°		C13’	C12’	H621	119.614°
C12’	C13’	C14’	120.47(17)°		C12’	C13’	H631	117.951°
C14’	C13’	H631	121.563°		C13’	C14’	C15’	119.67(16)°
C13’	C14’	H641	122.516°		C15’	C14’	H641	117.791°
C14’	C15’	C16’	120.41(16)°		C14’	C15’	H651	120.336°
C16’	C15’	H651	119.250°		C11’	C16’	C15’	120.27(15)°
C11’	C16’	H661	119.882°		C15’	C16’	H661	119.792°

Crystal Data 41

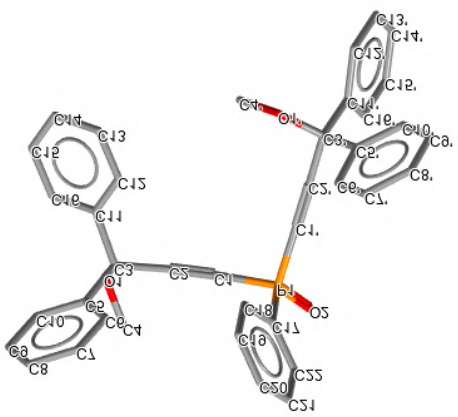

a = 9.84570(10) Å α = 90°
b = 28.5483(3) Å β = 112.998(2)°
c = 11.6095(2) Å γ = 90°

Volume	3003.81(8) Å³	Crystal Class	monoclinic
Space group	P 1 2_1/c 1	Z =	4
Formula	C_{38} H_{31} O_3 P_1	M_r	566.64
Cell determined from	18399 reflections	Cell θ range =	3 - 76°
Temperature	100K		
Shape	block		
Colour	colorless	Size	0.09 × 0.18 × 0.25 mm
D_x	1.25	F000	1192.000
μ	1.096 mm^{-1}		
Absorption correction	multi-scan		
T_{min}	0.48	T_{max}	0.91

Data Collection

Diffractometer	multi-scan
Scan type	ϕ and ω scans
Reflections measured	27672
Independent reflections	5900
Rint	0.0374
$θ_{max}$	76.0323
h =	-12 → 11
k =	-35 → 28
l =	-14 → 13

Refinement

$Δρ_{min}$ =	-0.46 e $Å^{-3}$
$Δρ_{max}$ =	0.32 e $Å^{-3}$

Reflections used	5756
Cutoff: I >	-3.00σ(I)
Parameters refined	379
S =	0.93
R-factor	0.039
weighted R-factor	0.096
Δ/σ_{max}	0.0007
Refinement on	F^2
w =	$1/[\sigma^2(F_{obs}^2) + (0.050 \times P)^2 + 2.095 \times P + 0.000 + 0.000 \times \sin\theta]$, $P = 0.333 \times \max(F_{obs}^2,0) + 0.667 \times F_{calc}^2$

Parameters

Label	*x*	*y*	*z*	$U_{iso/equiv}$	Occupancy
C1	0.27764(15)	0.40064(5)	0.43603(13)	0.0211	1.0000
P1	0.23617(4)	.357500(11)	0.52536(3)	0.0184	1.0000
O2	0.11599(11)	0.36920(3)	0.56630(9)	0.0245	1.0000
O1	0.24781(11)	0.50128(3)	0.26719(10)	0.0245	1.0000
C2	0.30574(14)	0.42713(5)	0.36828(12)	0.0200	1.0000
C3	0.33219(15)	0.45944(5)	0.27954(13)	0.0206	1.0000
C4	0.09312(16)	0.49396(5)	0.23048(16)	0.0296	1.0000
C5	0.29220(14)	0.43508(5)	0.15207(13)	0.0227	1.0000
C6	0.29012(16)	0.38664(5)	0.14008(14)	0.0274	1.0000
C7	0.25699(18)	0.36617(6)	0.02333(16)	0.0359	1.0000
C8	0.22661(17)	0.39408(7)	0.08148(15)	0.0392	1.0000
C9	0.23077(18)	0.44231(7)	0.06928(15)	0.0382	1.0000
C10	0.26258(17)	0.46294(6)	0.04600(14)	0.0311	1.0000
C11	0.49361(15)	0.47523(5)	0.32824(13)	0.0207	1.0000
C12	0.60644(16)	0.44730(5)	0.40766(13)	0.0241	1.0000
C13	0.75325(16)	0.46100(5)	0.44393(14)	0.0284	1.0000
C14	0.78699(16)	0.50298(5)	0.40129(14)	0.0274	1.0000
C15	0.67407(16)	0.53132(5)	0.32317(14)	0.0261	1.0000
C16	0.52793(16)	0.51760(5)	0.28636(14)	0.0250	1.0000
C17	0.20665(15)	0.30603(5)	0.42970(12)	0.0202	1.0000
C18	0.31453(16)	0.29034(5)	0.38852(15)	0.0292	1.0000
C19	0.28594(18)	0.25238(6)	0.30901(16)	0.0338	1.0000
C20	0.15084(18)	0.22962(5)	0.27006(15)	0.0302	1.0000
C21	0.04480(17)	0.24484(6)	0.31221(15)	0.0317	1.0000
C22	0.07197(16)	0.28314(5)	0.39187(14)	0.0260	1.0000
C1’	0.40901(15)	0.34922(5)	0.64814(13)	0.0228	1.0000

O1’	0.78295(10)	0.33707(3)	0.76644(9)	0.0210	1.0000
C2’	0.52831(15)	0.34172(5)	0.72909(13)	0.0209	1.0000
C3’	0.67730(14)	0.32930(5)	0.82235(12)	0.0188	1.0000
C4’	0.79706(17)	0.38484(5)	0.73484(15)	0.0277	1.0000
C5’	0.68017(14)	0.27601(5)	0.84120(13)	0.0195	1.0000
C6’	0.63671(16)	0.24781(5)	0.73461(14)	0.0238	1.0000
C7’	0.64321(17)	0.19946(5)	0.74469(15)	0.0290	1.0000
C8’	0.69265(17)	0.17865(5)	0.86203(15)	0.0296	1.0000
C9’	0.73347(17)	0.20616(5)	0.96831(14)	0.0280	1.0000
C10’	0.72715(16)	0.25497(5)	0.95810(13)	0.0233	1.0000
C11’	0.71734(15)	0.35766(4)	0.94266(13)	0.0195	1.0000
C12’	0.86368(16)	0.35708(5)	1.02919(14)	0.0250	1.0000
C13’	0.90390(17)	0.38209(6)	1.13970(14)	0.0303	1.0000
C14’	0.79970(18)	0.40825(5)	1.16493(14)	0.0313	1.0000
C15’	0.65516(18)	0.40943(5)	1.07926(15)	0.0287	1.0000
C16’	0.61376(16)	0.38403(5)	0.96825(13)	0.0231	1.0000
H41	0.04951(16)	0.52546(5)	0.21982(16)	0.0449	1.0000
H42	0.07388(16)	0.47607(5)	0.29560(16)	0.0447	1.0000
H43	0.05143(16)	0.47645(5)	0.15000(16)	0.0446	1.0000
H61	0.31221(16)	0.36692(5)	0.21417(14)	0.0331	1.0000
H71	0.25732(18)	0.33241(6)	0.01652(16)	0.0424	1.0000
H81	0.20372(17)	0.37986(7)	0.16102(15)	0.0465	1.0000
H91	0.21200(18)	0.46147(7)	0.14196(15)	0.0452	1.0000
H101	0.26414(17)	0.49688(6)	0.05335(14)	0.0378	1.0000
H121	0.58338(16)	0.41787(5)	0.43753(13)	0.0289	1.0000
H131	0.83248(16)	0.44086(5)	0.49944(14)	0.0337	1.0000
H141	0.88945(16)	0.51312(5)	0.42670(14)	0.0323	1.0000
H151	0.69625(16)	0.56186(5)	0.29511(14)	0.0317	1.0000
H161	0.44987(16)	0.53817(5)	0.23107(14)	0.0299	1.0000
H181	0.40956(16)	0.30661(5)	0.41726(15)	0.0356	1.0000
H191	0.36011(18)	0.24138(6)	0.27917(16)	0.0415	1.0000
H201	0.12950(18)	0.20229(5)	0.21277(15)	0.0359	1.0000
H211	0.04860(17)	0.22828(6)	0.28539(15)	0.0376	1.0000
H221	0.00191(16)	0.29459(5)	0.42076(14)	0.0326	1.0000
H541	0.86922(17)	0.38564(5)	0.69553(15)	0.0411	1.0000
H542	0.83077(17)	0.40474(5)	0.81215(15)	0.0403	1.0000

H543	0.70225(17)	0.39754(5)	0.67550(15)	0.0400	1.0000
H561	0.60104(16)	0.26300(5)	0.65252(14)	0.0287	1.0000
H571	0.61225(17)	0.18047(5)	0.66843(15)	0.0346	1.0000
H581	0.69836(17)	0.14500(5)	0.86962(15)	0.0351	1.0000
H591	0.76779(17)	0.19164(5)	1.05154(14)	0.0341	1.0000
H601	0.75621(16)	0.27432(5)	1.03437(13)	0.0279	1.0000
H621	0.93654(16)	0.33806(5)	1.01081(14)	0.0294	1.0000
H631	1.00567(17)	0.38091(6)	1.20072(14)	0.0372	1.0000
H641	0.82748(18)	0.42550(5)	1.24320(14)	0.0376	1.0000
H651	0.58128(18)	0.42790(5)	1.09438(15)	0.0351	1.0000
H661	0.51330(16)	0.38549(5)	0.90831(13)	0.0278	1.0000

Thermal Parameters

Label	U_{11}	U_{22}	U_{33}	U_{23}	U_{13}	U_{12}
C1	0.0192(6)	0.0203(6)	0.0228(6)	-0.0019(5)	0.0072(5)	-0.0005(5)
P1	0.01644(17)	0.01866(17)	0.01983(17)	0.00127(12)	0.00670(13)	0.00107(12)
O2	0.0235(5)	0.0259(5)	0.0273(5)	-0.0013(4)	0.0135(4)	-0.0019(4)
O1	0.0214(5)	0.0180(5)	0.0364(6)	0.0036(4)	0.0137(4)	0.0030(4)
C2	0.0196(6)	0.0182(6)	0.0217(6)	-0.0022(5)	0.0075(5)	0.0001(5)
C3	0.0228(7)	0.0174(6)	0.0232(7)	0.0026(5)	0.0107(5)	0.0025(5)
C4	0.0222(7)	0.0253(7)	0.0429(9)	0.0037(6)	0.0144(6)	0.0036(6)
C5	0.0170(6)	0.0289(7)	0.0227(7)	-0.0006(6)	0.0083(5)	0.0003(5)
C6	0.0261(7)	0.0307(8)	0.0270(7)	-0.0040(6)	0.0122(6)	-0.0042(6)
C7	0.0299(8)	0.0426(9)	0.0384(9)	-0.0157(7)	0.0168(7)	-0.0076(7)
C8	0.0223(7)	0.0700(12)	0.0252(8)	-0.0127(8)	0.0092(6)	-0.0016(7)
C9	0.0271(8)	0.0637(12)	0.0244(8)	0.0065(7)	0.0105(6)	0.0123(8)
C10	0.0276(8)	0.0390(9)	0.0283(8)	0.0070(6)	0.0125(6)	0.0081(6)
C11	0.0224(7)	0.0191(6)	0.0229(7)	-0.0018(5)	0.0112(5)	0.0004(5)
C12	0.0258(7)	0.0230(7)	0.0243(7)	0.0006(5)	0.0107(6)	0.0010(5)
C13	0.0243(7)	0.0324(8)	0.0277(7)	-0.0007(6)	0.0092(6)	0.0016(6)
C14	0.0240(7)	0.0328(8)	0.0283(7)	-0.0075(6)	0.0131(6)	-0.0053(6)
C15	0.0308(8)	0.0226(7)	0.0310(7)	-0.0036(6)	0.0186(6)	-0.0037(6)
C16	0.0274(7)	0.0218(7)	0.0291(7)	0.0022(6)	0.0146(6)	0.0013(6)
C17	0.0186(6)	0.0200(6)	0.0210(6)	0.0018(5)	0.0067(5)	-0.0005(5)
C18	0.0209(7)	0.0282(7)	0.0408(8)	-0.0048(6)	0.0146(6)	-0.0017(6)
C19	0.0304(8)	0.0306(8)	0.0469(9)	-0.0071(7)	0.0223(7)	0.0013(6)
C20	0.0344(8)	0.0239(7)	0.0329(8)	-0.0055(6)	0.0138(7)	-0.0020(6)

C21	0.0264(7)	0.0309(8)	0.0387(9)	-0.0081(7)	0.0136(7)	-0.0102(6)
C22	0.0204(7)	0.0289(7)	0.0307(7)	-0.0042(6)	0.0120(6)	-0.0041(6)
C1’	0.0237(7)	0.0201(6)	0.0242(7)	0.0018(5)	0.0089(6)	-0.0016(5)
O1’	0.0237(5)	0.0178(5)	0.0254(5)	0.0010(4)	0.0138(4)	-0.0009(4)
C2’	0.0227(7)	0.0173(6)	0.0226(7)	-0.0005(5)	0.0089(6)	-0.0011(5)
C3’	0.0168(6)	0.0188(6)	0.0216(6)	0.0006(5)	0.0083(5)	-0.0001(5)
C4’	0.0333(8)	0.0201(7)	0.0333(8)	0.0033(6)	0.0168(6)	-0.0040(6)
C5’	0.0169(6)	0.0189(6)	0.0245(7)	-0.0005(5)	0.0101(5)	-0.0002(5)
C6’	0.0257(7)	0.0216(7)	0.0260(7)	-0.0020(5)	0.0121(6)	-0.0017(5)
C7’	0.0327(8)	0.0225(7)	0.0361(8)	-0.0065(6)	0.0180(7)	-0.0041(6)
C8’	0.0352(8)	0.0172(7)	0.0450(9)	0.0028(6)	0.0251(7)	0.0002(6)
C9’	0.0327(8)	0.0241(7)	0.0328(8)	0.0074(6)	0.0189(6)	0.0031(6)
C10’	0.0250(7)	0.0232(7)	0.0242(7)	0.0012(5)	0.0122(6)	0.0006(5)
C11’	0.0206(6)	0.0166(6)	0.0217(6)	0.0001(5)	0.0088(5)	-0.0017(5)
C12’	0.0221(7)	0.0260(7)	0.0264(7)	-0.0026(6)	0.0088(6)	-0.0011(5)
C13’	0.0279(8)	0.0341(8)	0.0262(7)	-0.0056(6)	0.0076(6)	-0.0099(6)
C14’	0.0413(9)	0.0286(8)	0.0285(8)	-0.0098(6)	0.0183(7)	-0.0129(7)
C15’	0.0368(8)	0.0224(7)	0.0349(8)	-0.0037(6)	0.0225(7)	-0.0018(6)
C16’	0.0239(7)	0.0207(6)	0.0264(7)	0.0016(5)	0.0118(6)	0.0013(5)

Distances

C1	P1	1.7578(14)Å		C1	C2	1.199(2)Å
P1	O2	1.4755(10)Å		P1	C17	1.7958(14)Å
P1	C1’	1.7573(14)Å		O1	C3	1.4298(16)Å
O1	C4	1.4274(17)Å		C2	C3	1.4796(18)Å
C3	C5	1.5406(19)Å		C3	C11	1.5319(19)Å
C4	H41	0.983Å		C4	H42	0.990Å
C4	H43	0.996Å		C5	C6	1.389(2)Å
C5	C10	1.398(2)Å		C6	C7	1.393(2)Å
C6	H61	0.979Å		C7	C8	1.386(3)Å
C7	H71	0.967Å		C8	C9	1.383(3)Å
C8	H81	0.952Å		C9	C10	1.382(2)Å
C9	H91	0.961Å		C10	H101	0.972Å
C11	C12	1.3856(19)Å		C11	C16	1.3935(19)Å
C12	C13	1.394(2)Å		C12	H121	0.969Å
C13	C14	1.386(2)Å		C13	H131	0.981Å
C14	C15	1.387(2)Å		C14	H141	0.978Å

C15	C16	1.388(2)Å		C15	H151	0.985Å
C16	H161	0.981Å		C17	C18	1.398(2)Å
C17	C22	1.3867(19)Å		C18	C19	1.379(2)Å
C18	H181	0.979Å		C19	C20	1.388(2)Å
C19	H191	0.974Å		C20	C21	1.385(2)Å
C20	H201	0.993Å		C21	C22	1.389(2)Å
C21	H211	0.971Å		C22	H221	0.969Å
C1’	C2’	1.203(2)Å		O1’	C3’	1.4423(15)Å
O1’	C4’	1.4330(16)Å		C2’	C3’	1.4862(18)Å
C3’	C5’	1.5358(18)Å		C3’	C11’	1.5270(18)Å
C4’	H541	0.983Å		C4’	H542	1.003Å
C4’	H543	0.987Å		C5’	C6’	1.3959(19)Å
C5’	C10’	1.3877(19)Å		C6’	C7’	1.385(2)Å
C6’	H561	0.979Å		C7’	C8’	1.388(2)Å
C7’	H571	0.980Å		C8’	C9’	1.383(2)Å
C8’	H581	0.964Å		C9’	C10’	1.398(2)Å
C9’	H591	0.982Å		C10’	H601	0.986Å
C11’	C12’	1.3980(19)Å		C11’	C16’	1.3897(19)Å
C12’	C13’	1.384(2)Å		C12’	H621	0.987Å
C13’	C14’	1.390(2)Å		C13’	H631	0.976Å
C14’	C15’	1.382(2)Å		C14’	H641	0.974Å
C15’	C16’	1.394(2)Å		C15’	H651	0.968Å
C16’	H661	0.963Å				

Angles

P1	C1	C2	174.51(12)°		C1	P1	O2	115.58(6)°
C1	P1	C17	103.14(6)°		O2	P1	C17	115.35(6)°
C1	P1	C1’	101.44(6)°		O2	P1	C1’	114.42(6)°
C17	P1	C1’	105.25(6)°		C3	O1	C4	114.71(10)°
C1	C2	C3	176.88(14)°		O1	C3	C2	109.70(11)°
O1	C3	C5	111.12(11)°		C2	C3	C5	109.81(11)°
O1	C3	C11	105.64(10)°		C2	C3	C11	111.46(11)°
C5	C3	C11	109.04(11)°		O1	C4	H41	105.444°
O1	C4	H42	110.345°		H41	C4	H42	111.308°
O1	C4	H43	110.742°		H41	C4	H43	109.962°
H42	C4	H43	109.014°		C3	C5	C6	122.26(13)°
C3	C5	C10	118.45(13)°		C6	C5	C10	119.24(14)°

C5	C6	C7	120.26(15)°		C5	C6	H61	119.666°
C7	C6	H61	120.077°		C6	C7	C8	120.09(16)°
C6	C7	H71	119.388°		C8	C7	H71	120.511°
C7	C8	C9	119.66(15)°		C7	C8	H81	119.657°
C9	C8	H81	120.677°		C8	C9	C10	120.66(16)°
C8	C9	H91	119.266°		C10	C9	H91	120.073°
C5	C10	C9	120.08(16)°		C5	C10	H101	119.946°
C9	C10	H101	119.970°		C3	C11	C12	121.51(12)°
C3	C11	C16	118.99(12)°		C12	C11	C16	119.41(13)°
C11	C12	C13	120.43(13)°		C11	C12	H121	119.868°
C13	C12	H121	119.695°		C12	C13	C14	119.98(14)°
C12	C13	H131	119.904°		C14	C13	H131	120.119°
C13	C14	C15	119.67(14)°		C13	C14	H141	120.744°
C15	C14	H141	119.574°		C14	C15	C16	120.42(13)°
C14	C15	H151	120.518°		C16	C15	H151	119.031°
C11	C16	C15	120.07(13)°		C11	C16	H161	120.882°
C15	C16	H161	119.048°		P1	C17	C18	120.84(11)°
P1	C17	C22	119.02(11)°		C18	C17	C22	120.07(13)°
C17	C18	C19	119.80(14)°		C17	C18	H181	118.958°
C19	C18	H181	121.244°		C18	C19	C20	120.32(14)°
C18	C19	H191	120.388°		C20	C19	H191	119.287°
C19	C20	C21	119.79(14)°		C19	C20	H201	120.746°
C21	C20	H201	119.460°		C20	C21	C22	120.45(14)°
C20	C21	H211	118.969°		C22	C21	H211	120.585°
C17	C22	C21	119.56(13)°		C17	C22	H221	119.058°
C21	C22	H221	121.375°		P1	C1’	C2’	176.84(13)°
C3’	O1’	C4’	114.88(10)°		C1’	C2’	C3’	175.20(14)°
O1’	C3’	C2’	108.40(10)°		O1’	C3’	C5’	103.90(10)°
C2’	C3’	C5’	107.35(10)°		O1’	C3’	C11’	110.87(10)°
C2’	C3’	C11’	111.62(11)°		C5’	C3’	C11’	114.28(11)°
O1’	C4’	H541	107.507°		O1’	C4’	H542	109.952°
H541	C4’	H542	110.843°		O1’	C4’	H543	111.609°
H541	C4’	H543	108.981°		H542	C4’	H543	107.964°
C3’	C5’	C6’	117.56(12)°		C3’	C5’	C10’	123.27(12)°
C6’	C5’	C10’	119.15(13)°		C5’	C6’	C7’	120.79(14)°
C5’	C6’	H561	118.475°		C7’	C6’	H561	120.735°

C6’	C7’	C8’	119.76(14)°		C6’	C7’	H571	119.171°
C8’	C7’	H571	121.065°		C7’	C8’	C9’	120.03(13)°
C7’	C8’	H581	120.101°		C9’	C8’	H581	119.866°
C8’	C9’	C10’	120.17(14)°		C8’	C9’	H591	120.403°
C10’	C9’	H591	119.421°		C5’	C10’	C9’	120.07(13)°
C5’	C10’	H601	120.307°		C9’	C10’	H601	119.618°
C3’	C11’	C12’	118.44(12)°		C3’	C11’	C16’	122.27(12)°
C12’	C11’	C16’	119.29(13)°		C11’	C12’	C13’	120.08(14)°
C11’	C12’	H621	118.892°		C13’	C12’	H621	121.011°
C12’	C13’	C14’	120.35(14)°		C12’	C13’	H631	119.730°
C14’	C13’	H631	119.917°		C13’	C14’	C15’	119.93(14)°
C13’	C14’	H641	120.463°		C15’	C14’	H641	119.604°
C14’	C15’	C16’	119.98(14)°		C14’	C15’	H651	121.202°
C16’	C15’	H651	118.814°		C11’	C16’	C15’	120.37(13)°
C11’	C16’	H661	120.109°		C15’	C16’	H661	119.506°

Crystal Data 43

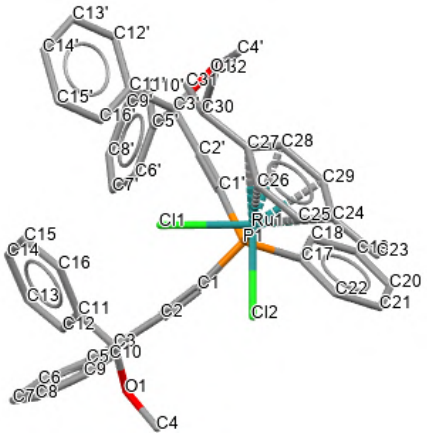

a = 13.11920(10) Å α = 90.6550(10)°

b = 16.78500(10) Å β = 90.3470(10)°

c = 19.31420(10) Å γ = 92.41°

Volume	4248.95(5) Å³	Crystal Class	triclinic
Space group	P -1	Z =	4
Formula	$C_{48.50}$ H_{46} Cl_3 O_2 P Ru	M_r	899.30
Cell determined from	102200 reflections	Cell θ range =	3 - 80°
Temperature	100K		
Shape	plate		
Colour	dark red	Size	0.03 × 0.16 × 0.22 mm
D_x	1.41	F000	1852.000
μ	5.375 mm^{-1}		
Absorption correction	multi-scan		
T_{min}	0.50	T_{max}	0.85

Data Collection

Diffractometer	multi-scan
Scan type	ϕ and ω scans
Reflections measured	148264
Independent reflections	18179
Rint	0.0489
$θ_{max}$	82.2684
h =	-16 → 16
k =	-16 → 21
l =	-24 → 24

Refinement

$Δρ_{min}$ =	-0.83 e $Å^{-3}$
$Δρ_{max}$ =	0.86 e $Å^{-3}$

Reflections used	16914
Cutoff: I >	-3.00σ(I)
Parameters refined	1111
S =	0.99
R-factor	0.031
weighted R-factor	0.080
Δ/σ_{max}	0.0029
Refinement on	F^2
w =	$1/[\sigma^2(F_{obs}^2) + (0.045 \times P)^2 + 5.350 \times P + 0.000 + 0.000 \times \sin\theta]$, $P = 0.333 \times \max(F_{obs}^2,0) + 0.667 \times F_{calc}^2$

Parameters

Label	*x*	*y*	*z*	$U_{iso/equiv}$	Occupancy
C1’	0.69039(16)	0.19968(12)	0.95662(10)	0.0194	1.0000
C2’	0.77429(16)	0.18898(12)	0.93481(10)	0.0193	1.0000
C3’	0.87723(15)	0.17550(13)	0.90723(10)	0.0194	1.0000
C4’	0.95161(19)	0.21412(17)	1.01717(12)	0.0342	1.0000
C5’	0.87284(16)	0.10319(12)	0.85767(11)	0.0210	1.0000
C6’	0.78721(18)	0.08489(14)	0.81735(12)	0.0269	1.0000
C7’	0.7874(2)	0.02246(16)	0.76939(13)	0.0365	1.0000
C8’	0.8727(2)	0.02253(15)	0.76181(13)	0.0392	1.0000
C9’	0.9581(2)	0.00454(15)	0.80200(14)	0.0401	1.0000
C10’	0.9593(2)	0.05839(15)	0.84959(13)	0.0316	1.0000
C11’	0.91811(15)	0.24818(12)	0.86695(10)	0.0190	1.0000
C12’	1.02322(16)	0.26229(14)	0.86175(12)	0.0246	1.0000
C13’	1.06207(18)	0.32470(14)	0.82224(13)	0.0292	1.0000
C14’	0.99726(18)	0.37364(13)	0.78743(12)	0.0287	1.0000
C15’	0.89245(18)	0.35963(13)	0.79209(12)	0.0272	1.0000
C16’	0.85295(16)	0.29726(13)	0.83170(11)	0.0218	1.0000
Ru1	.560027(10)	.350638(8)	.029241(7)	0.0138	1.0000
Ru2	.062385(11)	.154562(8)	.527569(7)	0.0163	1.0000
P1	0.56717(4)	0.22297(3)	0.98409(2)	0.0145	1.0000
P2	0.0793(3)	0.2807(4)	0.4872(3)	0.0140	0.5000
P3	0.0521(3)	0.2846(4)	0.4850(3)	0.0146	0.5000
C1	0.49867(15)	0.20577(11)	0.90612(10)	0.0174	1.0000
C2	0.46048(15)	0.20199(11)	0.84964(10)	0.0181	1.0000
C3	0.42163(15)	0.19938(12)	0.77766(10)	0.0185	1.0000
C4	0.25212(16)	0.15040(13)	0.80623(13)	0.0269	1.0000
C5	0.38008(15)	0.27977(12)	0.75579(11)	0.0194	1.0000

C6	0.35749(17)	0.28907(14)	0.68590(12)	0.0263	1.0000
C7	0.31266(19)	0.35747(15)	0.66285(13)	0.0325	1.0000
C8	0.29135(18)	0.41763(14)	0.70977(13)	0.0313	1.0000
C9	0.31676(17)	0.40978(13)	0.77895(13)	0.0277	1.0000
C10	0.36102(16)	0.34086(13)	0.80242(11)	0.0219	1.0000
C11	0.50974(16)	0.17780(14)	0.73030(11)	0.0226	1.0000
C12	0.50513(19)	0.10881(17)	0.68981(13)	0.0342	1.0000
C13	0.5841(2)	0.0934(2)	0.64428(15)	0.0504	1.0000
C14	0.6678(2)	0.1464(2)	0.63966(15)	0.0529	1.0000
C15	0.67304(19)	0.2143(2)	0.68119(14)	0.0430	1.0000
C16	0.59482(17)	0.23025(15)	0.72676(12)	0.0296	1.0000
C17	0.52995(15)	0.14001(11)	1.03969(10)	0.0175	1.0000
C18	0.58620(16)	0.07153(12)	1.04257(11)	0.0207	1.0000
C19	0.55686(17)	0.01044(13)	1.08715(12)	0.0252	1.0000
C20	0.47114(19)	0.01633(13)	1.12736(12)	0.0290	1.0000
C21	0.4140(2)	0.08347(15)	1.12340(15)	0.0376	1.0000
C22	0.44384(18)	0.14601(14)	1.08010(13)	0.0303	1.0000
C23	0.45151(18)	0.32236(14)	1.18606(12)	0.0296	1.0000
C24	0.53470(16)	0.35884(13)	1.14246(10)	0.0204	1.0000
C25	0.52525(16)	0.43642(12)	1.11388(10)	0.0193	1.0000
C26	0.60174(15)	0.47184(12)	1.07303(10)	0.0183	1.0000
C27	0.69339(15)	0.43070(12)	1.05844(10)	0.0182	1.0000
C28	0.70471(15)	0.35512(12)	1.08734(10)	0.0188	1.0000
C29	0.62521(16)	0.31898(12)	1.12814(10)	0.0205	1.0000
C30	0.77393(15)	0.47147(12)	1.01371(11)	0.0207	1.0000
C31	0.85070(17)	0.41431(14)	0.98507(13)	0.0289	1.0000
C32	0.82808(17)	0.53891(13)	1.05584(12)	0.0253	1.0000
C134	0.0030(2)	0.29457(13)	0.40623(11)	0.0299	1.0000
C135	-0.0372(2)	0.29567(13)	0.35066(12)	0.0299	1.0000
C136	-0.0837(2)	0.29576(13)	0.28073(11)	0.0290	1.0000
C137	-0.2410(3)	0.34923(19)	0.31886(19)	0.0620	1.0000
C138	0.13839(18)	0.21558(13)	0.26263(11)	0.0249	1.0000
C139	-0.1497(2)	0.15294(14)	0.30844(12)	0.0361	1.0000
C140	-0.2037(2)	0.08315(15)	0.28811(14)	0.0400	1.0000
C141	-0.2481(2)	0.07612(14)	0.22310(13)	0.0341	1.0000
C142	-0.2354(2)	0.13824(16)	0.17704(13)	0.0355	1.0000

C143	0.18024(19)	0.20688(15)	0.19656(12)	0.0313	1.0000
C144	0.0011(2)	0.31316(14)	0.22816(11)	0.0300	1.0000
C145	-0.0025(2)	0.37690(17)	0.18335(13)	0.0406	1.0000
C146	0.0730(3)	0.3874(2)	0.13355(14)	0.0498	1.0000
C147	0.1508(2)	0.3354(2)	0.12793(14)	0.0509	1.0000
C148	0.1551(2)	0.27231(19)	0.17336(15)	0.0464	1.0000
C149	0.0809(2)	0.26109(16)	0.22353(13)	0.0365	1.0000
C67	-0.0050(3)	0.3603(2)	0.5409(2)	0.0139	0.5000
C68	-0.1111(4)	0.3615(3)	0.5456(3)	0.0279	0.5000
C69	-0.1551(4)	0.4194(3)	0.5856(3)	0.0365	0.5000
C70	-0.0931(5)	0.4764(3)	0.6211(3)	0.0336	0.5000
C71	0.0129(5)	0.4766(3)	0.6154(3)	0.0293	0.5000
C72	0.0563(3)	0.4170(2)	0.5765(2)	0.0212	0.5000
C73	0.0370(4)	0.3631(3)	0.5401(2)	0.0182	0.5000
C74	-0.0604(4)	0.3556(3)	0.5693(2)	0.0222	0.5000
C75	-0.0962(4)	0.4180(3)	0.6103(2)	0.0284	0.5000
C76	-0.0336(5)	0.4849(3)	0.6221(2)	0.0244	0.5000
C77	0.0634(4)	0.4927(3)	0.5921(2)	0.0263	0.5000
C78	0.0977(3)	0.4317(2)	0.5514(2)	0.0214	0.5000
C79	0.2033(6)	0.3110(5)	0.4638(5)	0.0183	0.5000
C80	0.2886(4)	0.3263(3)	0.4419(2)	0.0214	0.5000
C81	0.3895(3)	0.3434(3)	0.4100(2)	0.0225	0.5000
C82	0.1740(7)	0.3292(5)	0.4697(5)	0.0194	0.5000
C83	0.2579(4)	0.3574(3)	0.4592(2)	0.0181	0.5000
C84	0.3585(3)	0.3996(2)	0.4449(2)	0.0191	0.5000
C85	0.3108(4)	0.5201(3)	0.5041(3)	0.0309	0.5000
C86	0.4787(6)	0.3154(5)	0.5159(4)	0.0294	0.5000
C87	0.3548(4)	0.4407(3)	0.3748(3)	0.0184	0.5000
C88	0.2753(5)	0.4262(4)	0.3271(3)	0.0203	0.5000
C89	0.2840(2)	0.46751(15)	0.26289(12)	0.0339	1.0000
C90	0.3565(2)	0.52773(16)	0.25612(15)	0.0392	1.0000
C91	0.4340(2)	0.53755(16)	0.30415(18)	0.0450	1.0000
C92	0.4395(2)	0.48795(18)	0.35988(14)	0.0394	1.0000
C93	0.3779(4)	0.4131(3)	0.3590(3)	0.0204	0.5000
C94	0.3022(5)	0.4075(4)	0.3098(3)	0.0257	0.5000
C95	0.4262(5)	0.2700(3)	0.3706(3)	0.0218	0.5000

C96	0.3571(3)	0.2139(3)	0.3404(2)	0.0247	0.5000
C97	0.3931(4)	0.1495(3)	0.3031(2)	0.0288	0.5000
C98	0.4944(4)	0.1390(3)	0.2961(2)	0.0316	0.5000
C99	0.5644(4)	0.1952(3)	0.3252(3)	0.0344	0.5000
C100	0.5293(4)	0.2608(3)	0.3618(3)	0.0293	0.5000
C101	0.4440(5)	0.3406(4)	0.4480(4)	0.0214	0.5000
C102	0.4604(5)	0.2902(4)	0.3924(4)	0.0359	0.5000
C103	0.5385(5)	0.2367(4)	0.3934(4)	0.0461	0.5000
C104	0.6017(4)	0.2346(4)	0.4522(4)	0.0492	0.5000
C105	0.5858(5)	0.2830(4)	0.5072(4)	0.0545	0.5000
C106	0.5072(7)	0.3374(6)	0.5057(5)	0.0408	0.5000
C107	0.04231(17)	0.18198(13)	0.68329(11)	0.0248	1.0000
C108	0.04050(16)	0.14855(13)	0.64096(10)	0.0195	1.0000
C109	0.03223(16)	0.06928(12)	0.61320(10)	0.0191	1.0000
C110	0.10755(16)	0.03804(12)	0.57128(11)	0.0213	1.0000
C111	0.19739(16)	0.08506(14)	0.55449(12)	0.0273	1.0000
C112	0.20857(16)	0.16324(14)	0.58295(13)	0.0286	1.0000
C113	0.13059(16)	0.19466(13)	0.62497(11)	0.0225	1.0000
C133	1.1465(2)	0.06323(19)	1.02007(17)	0.0494	1.0000
O1	0.34393(11)	0.13721(9)	0.76906(8)	0.0218	1.0000
O1’	0.94476(11)	0.15620(9)	0.96249(8)	0.0246	1.0000
O3	0.3793(2)	0.45688(18)	0.49938(15)	0.0239	0.5000
O4	0.4622(4)	0.3697(3)	0.4617(2)	0.0234	0.5000
O5	0.15362(16)	0.35907(10)	0.27580(9)	0.0393	1.0000
Cl1	0.59012(3)	0.38588(3)	0.91059(2)	0.0182	1.0000
Cl2	0.38009(3)	0.33366(3)	1.00476(2)	0.0198	1.0000
Cl3	1.20739(5)	0.15745(4)	1.00462(4)	0.0423	1.0000
Cl4	1.16563(5)	0.00398(4)	0.95128(5)	0.0500	1.0000
Cl5	0.08807(5)	0.11781(3)	0.40835(3)	0.0299	1.0000
Cl6	0.11834(4)	0.15760(3)	0.50567(2)	0.0224	1.0000
C118	0.2732(3)	0.0567(4)	0.4991(3)	0.0213	0.5000
C114	0.2800(3)	0.0421(4)	0.5166(3)	0.0213	0.5000
C116	0.3264(4)	-0.0260(3)	0.5564(3)	0.0243	0.5000
C119	0.3374(4)	-0.0025(3)	0.5384(3)	0.0243	0.5000
C117	0.3393(4)	0.1196(3)	0.4630(3)	0.0374	0.5000
C115	0.3620(4)	0.1032(3)	0.4921(3)	0.0374	0.5000

H541	0.99749(19)	0.19424(17)	1.05173(12)	0.0522	1.0000
H543	0.97766(19)	0.26595(17)	1.00094(12)	0.0523	1.0000
H542	0.88500(19)	0.21923(17)	1.03815(12)	0.0516	1.0000
H561	0.72872(18)	0.11485(14)	0.82381(12)	0.0333	1.0000
H571	0.7296(2)	0.01075(16)	0.74234(13)	0.0436	1.0000
H581	0.8723(2)	0.06488(15)	0.73038(13)	0.0461	1.0000
H591	1.0154(2)	0.03625(15)	0.79727(14)	0.0478	1.0000
H601	1.0182(2)	0.07101(15)	0.87631(13)	0.0390	1.0000
H621	1.06726(16)	0.22852(14)	0.88678(12)	0.0300	1.0000
H631	1.13358(18)	0.33443(14)	0.81764(13)	0.0355	1.0000
H641	1.02381(18)	0.41589(13)	0.75978(12)	0.0342	1.0000
H651	0.84701(18)	0.39268(13)	0.76819(12)	0.0339	1.0000
H661	0.78132(16)	0.28756(13)	0.83607(11)	0.0269	1.0000
H41	0.20779(16)	0.10357(13)	0.80044(13)	0.0412	1.0000
H43	0.26709(16)	0.15941(13)	0.85446(13)	0.0410	1.0000
H42	0.21888(16)	0.19618(13)	0.78783(13)	0.0407	1.0000
H61	0.37378(17)	0.24839(14)	0.65390(12)	0.0322	1.0000
H71	0.29666(19)	0.36295(15)	0.61524(13)	0.0382	1.0000
H81	0.26022(18)	0.46404(14)	0.69523(13)	0.0375	1.0000
H91	0.30441(17)	0.45158(13)	0.81034(13)	0.0333	1.0000
H101	0.37728(16)	0.33568(13)	0.84971(11)	0.0262	1.0000
H121	0.44713(19)	0.07249(17)	0.69213(13)	0.0413	1.0000
H131	0.5804(2)	0.0466(2)	0.61610(15)	0.0593	1.0000
H141	0.7197(2)	0.1362(2)	0.60871(15)	0.0624	1.0000
H151	0.72943(19)	0.2504(2)	0.67842(14)	0.0524	1.0000
H161	0.59689(17)	0.27723(15)	0.75522(12)	0.0360	1.0000
H181	0.64339(16)	0.06651(12)	1.01367(11)	0.0255	1.0000
H191	0.59590(17)	0.03608(13)	1.09040(12)	0.0304	1.0000
H201	0.45191(19)	0.02524(13)	1.15701(12)	0.0345	1.0000
H211	0.3544(2)	0.08643(15)	1.14909(15)	0.0448	1.0000
H221	0.40610(18)	0.19230(14)	1.07805(13)	0.0366	1.0000
H231	0.45215(18)	0.34834(14)	1.23116(12)	0.0441	1.0000
H233	0.46267(18)	0.26745(14)	1.19225(12)	0.0431	1.0000
H232	0.38609(18)	0.32955(14)	1.16393(12)	0.0438	1.0000
H251	0.46004(16)	0.46262(12)	1.11963(10)	0.0229	1.0000
H261	0.58944(15)	0.52305(12)	1.05170(10)	0.0228	1.0000

H281	0.76297(15)	0.32328(12)	1.07253(10)	0.0234	1.0000
H291	0.63170(16)	0.26463(12)	1.14405(10)	0.0234	1.0000
H301	0.73836(15)	0.49536(12)	0.97471(11)	0.0244	1.0000
H312	0.89386(17)	0.44131(14)	0.95167(13)	0.0440	1.0000
H311	0.89283(17)	0.39522(14)	1.02238(13)	0.0436	1.0000
H313	0.81550(17)	0.37027(14)	0.96271(13)	0.0434	1.0000
H322	0.87925(17)	0.56578(13)	1.02791(12)	0.0389	1.0000
H323	0.85997(17)	0.51703(13)	1.09669(12)	0.0392	1.0000
H321	0.77970(17)	0.57795(13)	1.07191(12)	0.0388	1.0000
H1371	-0.2831(3)	0.39400(19)	0.31113(19)	0.0916	1.0000
H1373	-0.2184(3)	0.34913(19)	0.36627(19)	0.0917	1.0000
H1372	-0.2768(3)	0.30018(19)	0.30669(19)	0.0923	1.0000
H1391	-0.1224(2)	0.15703(14)	0.35223(12)	0.0426	1.0000
H1401	-0.2111(2)	0.04026(15)	0.31914(14)	0.0484	1.0000
H1411	-0.2867(2)	0.02947(14)	0.21041(13)	0.0412	1.0000
H1421	-0.2633(2)	0.13367(16)	0.13239(13)	0.0419	1.0000
H1431	0.16986(19)	0.24840(15)	0.16472(12)	0.0370	1.0000
H1451	-0.0549(2)	0.41378(17)	0.18813(13)	0.0505	1.0000
H1461	0.0714(3)	0.4310(2)	0.10402(14)	0.0597	1.0000
H1471	0.1996(2)	0.3427(2)	0.09408(14)	0.0605	1.0000
H1481	0.2079(2)	0.23604(19)	0.16970(15)	0.0566	1.0000
H1491	0.0831(2)	0.21693(16)	0.25468(13)	0.0442	1.0000
H681	-0.1517(4)	0.3238(3)	0.5208(3)	0.0340	0.5000
H691	-0.2260(4)	0.4203(3)	0.5898(3)	0.0443	0.5000
H701	-0.1225(5)	0.5157(3)	0.6484(3)	0.0410	0.5000
H711	0.0534(5)	0.5155(3)	0.6382(3)	0.0362	0.5000
H721	0.1262(3)	0.4146(2)	0.5738(2)	0.0267	0.5000
H741	-0.1009(4)	0.3095(3)	0.5618(2)	0.0275	0.5000
H751	-0.1603(4)	0.4135(3)	0.6297(2)	0.0349	0.5000
H761	-0.0564(5)	0.5260(3)	0.6501(2)	0.0300	0.5000
H771	0.1043(4)	0.5388(3)	0.5998(2)	0.0321	0.5000
H781	0.1614(3)	0.4359(2)	0.5311(2)	0.0259	0.5000
H853	0.3289(4)	0.5492(3)	0.5442(3)	0.0447	0.5000
H852	0.3165(4)	0.5534(3)	0.4655(3)	0.0448	0.5000
H851	0.2429(4)	0.4997(3)	0.5085(3)	0.0451	0.5000
H861	0.5202(6)	0.3401(5)	0.5524(4)	0.0437	0.5000

H862	0.4140(6)	0.2971(5)	0.5345(4)	0.0430	0.5000
H863	0.5132(6)	0.2701(5)	0.4979(4)	0.0433	0.5000
H903	0.3547(2)	0.56622(16)	0.21979(15)	0.0580	1.0000
H911	0.4835(2)	0.57820(16)	0.29912(18)	0.0528	1.0000
H961	0.2876(3)	0.2194(3)	0.3451(2)	0.0301	0.5000
H971	0.3459(4)	0.1132(3)	0.2830(2)	0.0352	0.5000
H981	0.5167(4)	0.0948(3)	0.2724(2)	0.0381	0.5000
H991	0.6340(4)	0.1881(3)	0.3208(3)	0.0413	0.5000
H1001	0.5755(4)	0.2985(3)	0.3811(3)	0.0353	0.5000
H1021	0.4185(5)	0.2920(4)	0.3538(4)	0.0417	0.5000
H1031	0.5492(5)	0.2034(4)	0.3560(4)	0.0543	0.5000
H1041	0.6542(4)	0.1996(4)	0.4540(4)	0.0592	0.5000
H1051	0.6274(5)	0.2795(4)	0.5459(4)	0.0631	0.5000
H1061	0.4965(7)	0.3717(6)	0.5438(5)	0.0512	0.5000
H1071	0.03459(17)	0.16554(13)	0.73031(11)	0.0385	1.0000
H1072	0.03894(17)	0.23901(13)	0.68201(11)	0.0381	1.0000
H1073	0.10740(17)	0.16216(13)	0.66576(11)	0.0383	1.0000
H1091	0.03196(16)	0.03871(12)	0.61929(10)	0.0236	1.0000
H1101	0.09630(16)	0.01402(12)	0.54836(11)	0.0257	1.0000
H1121	0.26483(16)	0.19920(14)	0.56751(13)	0.0352	1.0000
H1131	0.13614(16)	0.25081(13)	0.64160(11)	0.0270	1.0000
H1332	1.1763(2)	0.04298(19)	1.06406(17)	0.0597	1.0000
H1331	1.0720(2)	0.07036(19)	1.02530(17)	0.0596	1.0000
H921	0.4827(2)	0.50147(18)	0.39824(14)	0.0474	0.5000
H922	0.4998(2)	0.48606(18)	0.38720(14)	0.0474	0.5000
H891	0.2233(2)	0.46643(15)	0.23581(12)	0.0403	0.5000
H892	0.2401(2)	0.45287(15)	0.22517(12)	0.0403	0.5000
H881	0.2182(5)	0.3917(4)	0.3372(3)	0.0251	0.5000
H941	0.2589(5)	0.3607(4)	0.3086(3)	0.0280	0.5000
H1181	0.2352(3)	0.0280(4)	0.4642(3)	0.0238	0.5000
H1141	0.2489(3)	0.0190(4)	0.4762(3)	0.0238	0.5000
H1171	0.2973(4)	0.1548(3)	0.4387(3)	0.0431	0.5000
H1172	0.3779(4)	0.1487(3)	0.4973(3)	0.0431	0.5000
H1173	0.3843(4)	0.0954(3)	0.4315(3)	0.0431	0.5000
H1151	0.3309(4)	0.1447(3)	0.4677(3)	0.0431	0.5000
H1152	0.3989(4)	0.1250(3)	0.5308(3)	0.0431	0.5000

H1153	0.4073(4)	0.0769(3)	0.4621(3)	0.0431	0.5000
H1161	0.3775(4)	-0.0493(3)	0.5291(3)	0.0274	0.5000
H1162	0.3557(4)	-0.0061(3)	0.5986(3)	0.0274	0.5000
H1163	0.2741(4)	-0.0651(3)	0.5661(3)	0.0274	0.5000
H1191	0.2933(4)	-0.0416(3)	0.5591(3)	0.0274	0.5000
H1192	0.3760(4)	0.0255(3)	0.5734(3)	0.0274	0.5000
H1193	0.3823(4)	-0.0278(3)	0.5075(3)	0.0274	0.5000

Thermal Parameters

Label	U_{11}	U_{22}	U_{33}	U_{23}	U_{13}	U_{12}
C1’	0.0232(10)	0.0163(9)	0.0189(9)	0.0013(7)	0.0008(8)	0.0002(8)
C2’	0.0229(10)	0.0163(9)	0.0189(9)	0.0025(7)	0.0015(8)	-0.0001(8)
C3’	0.0174(9)	0.0229(10)	0.0182(9)	0.0011(8)	0.0004(7)	0.0036(8)
C4’	0.0324(12)	0.0492(15)	0.0216(11)	-0.0066(10)	-0.0058(9)	0.0111(11)
C5’	0.0267(10)	0.0162(10)	0.0203(10)	0.0027(8)	0.0051(8)	0.0007(8)
C6’	0.0277(11)	0.0246(11)	0.0280(11)	-0.0005(9)	0.0057(9)	-0.0046(9)
C7’	0.0456(14)	0.0324(13)	0.0298(12)	-0.0054(10)	0.0074(11)	-0.0173(11)
C8’	0.0655(18)	0.0223(12)	0.0290(12)	-0.0056(10)	0.0181(12)	-0.0067(12)
C9’	0.0581(17)	0.0265(13)	0.0370(14)	0.0005(11)	0.0177(12)	0.0142(12)
C10’	0.0358(13)	0.0307(12)	0.0293(12)	-0.0005(10)	0.0053(10)	0.0116(10)
C11’	0.0201(9)	0.0190(10)	0.0177(9)	-0.0036(8)	0.0012(7)	-0.0010(8)
C12’	0.0195(10)	0.0268(11)	0.0272(11)	-0.0025(9)	-0.0021(8)	-0.0015(8)
C13’	0.0253(11)	0.0273(12)	0.0339(12)	-0.0049(9)	0.0026(9)	-0.0090(9)
C14’	0.0359(12)	0.0196(11)	0.0299(12)	-0.0006(9)	0.0049(9)	-0.0078(9)
C15’	0.0343(12)	0.0211(11)	0.0265(11)	0.0013(9)	0.0006(9)	0.0032(9)
C16’	0.0211(10)	0.0219(10)	0.0223(10)	-0.0006(8)	0.0007(8)	0.0005(8)
Ru1	0.01583(7)	0.01049(7)	0.01513(8)	0.00244(5)	0.00141(5)	0.00097(5)
Ru2	0.02153(8)	0.01092(7)	0.01569(8)	0.00247(5)	0.00545(6)	0.00755(5)
P1	0.0163(2)	0.0114(2)	0.0156(2)	0.00204(17)	0.00088(17)	0.00064(17)
P2	0.0182(17)	0.0115(8)	0.0118(7)	-0.0001(5)	-0.0002(13)	-0.0059(13)
P3	0.0163(16)	0.0118(8)	0.0151(8)	0.0010(5)	-0.0008(13)	-0.0057(13)
C1	0.0209(9)	0.0122(9)	0.0192(10)	0.0024(7)	0.0016(7)	-0.0010(7)
C2	0.0207(9)	0.0116(9)	0.0220(10)	0.0025(7)	0.0032(8)	-0.0010(7)
C3	0.0189(9)	0.0164(9)	0.0197(10)	0.0005(7)	-0.0010(7)	-0.0053(7)
C4	0.0221(10)	0.0208(11)	0.0373(12)	0.0004(9)	0.0058(9)	-0.0052(8)
C5	0.0165(9)	0.0186(10)	0.0226(10)	0.0042(8)	-0.0026(7)	-0.0070(7)
C6	0.0280(11)	0.0261(11)	0.0242(11)	0.0032(9)	-0.0077(9)	-0.0071(9)

C7	0.0353(12)	0.0294(12)	0.0321(12)	0.0097(10)	-0.0158(10)	-0.0075(10)
C8	0.0296(12)	0.0192(11)	0.0444(14)	0.0112(10)	-0.0141(10)	-0.0079(9)
C9	0.0274(11)	0.0183(10)	0.0369(12)	0.0021(9)	-0.0054(9)	-0.0046(8)
C10	0.0209(10)	0.0200(10)	0.0245(10)	0.0038(8)	-0.0027(8)	-0.0044(8)
C11	0.0202(10)	0.0306(11)	0.0170(9)	0.0029(8)	-0.0020(8)	-0.0002(8)
C12	0.0277(12)	0.0456(15)	0.0288(12)	-0.0125(11)	0.0010(9)	-0.0019(10)
C13	0.0371(15)	0.076(2)	0.0373(15)	-0.0272(15)	0.0039(12)	0.0037(14)
C14	0.0307(14)	0.097(3)	0.0308(14)	-0.0116(15)	0.0110(11)	0.0026(15)
C15	0.0240(12)	0.0665(19)	0.0381(14)	0.0054(13)	0.0052(10)	-0.0055(12)
C16	0.0230(11)	0.0369(13)	0.0286(12)	0.0031(10)	0.0000(9)	-0.0039(9)
C17	0.0211(9)	0.0139(9)	0.0170(9)	0.0022(7)	-0.0031(7)	-0.0035(7)
C18	0.0242(10)	0.0143(9)	0.0233(10)	0.0006(8)	-0.0045(8)	-0.0016(8)
C19	0.0303(11)	0.0148(10)	0.0303(11)	0.0040(8)	-0.0098(9)	-0.0024(8)
C20	0.0375(12)	0.0198(11)	0.0291(11)	0.0102(9)	-0.0025(9)	-0.0088(9)
C21	0.0375(13)	0.0298(13)	0.0459(15)	0.0140(11)	0.0167(11)	-0.0007(10)
C22	0.0304(12)	0.0193(11)	0.0416(13)	0.0115(10)	0.0118(10)	0.0028(9)
C23	0.0327(12)	0.0290(12)	0.0273(11)	0.0091(9)	0.0104(9)	0.0007(9)
C24	0.0244(10)	0.0217(10)	0.0152(9)	-0.0004(8)	0.0055(8)	0.0011(8)
C25	0.0244(10)	0.0166(9)	0.0166(9)	-0.0017(7)	-0.0003(8)	-0.0004(8)
C26	0.0233(10)	0.0133(9)	0.0180(9)	-0.0023(7)	0.0000(8)	-0.0023(7)
C27	0.0202(9)	0.0170(9)	0.0170(9)	-0.0013(7)	-0.0022(7)	-0.0033(7)
C28	0.0165(9)	0.0210(10)	0.0188(9)	0.0000(8)	-0.0046(7)	-0.0001(7)
C29	0.0261(10)	0.0196(10)	0.0159(9)	0.0027(8)	-0.0014(8)	0.0010(8)
C30	0.0207(9)	0.0191(10)	0.0219(10)	0.0009(8)	0.0005(8)	-0.0039(8)
C31	0.0271(11)	0.0256(11)	0.0335(12)	-0.0032(9)	0.0100(9)	-0.0046(9)
C32	0.0238(10)	0.0229(11)	0.0286(11)	-0.0003(9)	-0.0007(8)	-0.0067(8)
C134	0.0568(15)	0.0146(10)	0.0174(11)	-0.0010(8)	0.0073(10)	-0.0098(10)
C135	0.0564(15)	0.0125(10)	0.0203(11)	-0.0005(8)	0.0060(10)	-0.0062(10)
C136	0.0506(14)	0.0161(10)	0.0206(10)	0.0011(8)	0.0028(10)	0.0038(10)
C137	0.090(3)	0.0335(16)	0.065(2)	0.0074(14)	0.0358(19)	0.0266(17)
C138	0.0363(12)	0.0172(10)	0.0216(10)	-0.0003(8)	0.0004(9)	0.0050(9)
C139	0.0655(17)	0.0216(11)	0.0206(11)	0.0014(9)	-0.0095(11)	-0.0042(11)
C140	0.0674(18)	0.0179(11)	0.0341(13)	0.0020(10)	-0.0115(12)	-0.0020(11)
C141	0.0422(14)	0.0211(11)	0.0391(14)	-0.0081(10)	-0.0139(11)	0.0063(10)
C142	0.0407(14)	0.0344(13)	0.0317(12)	-0.0020(10)	-0.0163(11)	0.0082(11)
C143	0.0381(13)	0.0294(12)	0.0269(12)	0.0050(9)	-0.0084(10)	0.0063(10)

C144	0.0483(14)	0.0240(11)	0.0167(10)	-0.0015(8)	-0.0004(9)	-0.0090(10)
C145	0.0584(17)	0.0350(14)	0.0275(12)	0.0092(11)	-0.0028(12)	-0.0087(12)
C146	0.065(2)	0.0566(19)	0.0261(13)	0.0142(12)	-0.0031(13)	-0.0225(16)
C147	0.0500(17)	0.073(2)	0.0262(13)	-0.0058(13)	0.0045(12)	-0.0311(16)
C148	0.0423(15)	0.0525(18)	0.0428(16)	-0.0111(13)	0.0060(12)	-0.0127(13)
C149	0.0465(15)	0.0306(13)	0.0315(13)	-0.0034(10)	0.0003(11)	-0.0065(11)
C67	0.0189(10)	0.0081(5)	0.0146(6)	-0.0009(5)	0.0049(6)	-0.0022(7)
C68	0.0329(10)	0.0221(5)	0.0286(6)	-0.0007(5)	0.0050(6)	-0.0017(7)
C69	0.0415(10)	0.0307(5)	0.0372(6)	-0.0006(5)	0.0051(6)	-0.0013(7)
C70	0.0386(10)	0.0278(5)	0.0343(6)	-0.0007(5)	0.0050(6)	-0.0014(7)
C71	0.0343(10)	0.0235(5)	0.0300(6)	-0.0007(5)	0.0050(6)	-0.0016(7)
C72	0.0262(10)	0.0154(5)	0.0219(6)	-0.0008(5)	0.0050(6)	-0.0019(7)
C73	0.0231(10)	0.0123(5)	0.0189(6)	-0.0008(5)	0.0049(6)	-0.0021(7)
C74	0.0271(10)	0.0163(5)	0.0229(6)	-0.0008(5)	0.0050(6)	-0.0019(7)
C75	0.0333(10)	0.0225(5)	0.0291(6)	-0.0007(5)	0.0050(6)	-0.0016(7)
C76	0.0293(10)	0.0185(5)	0.0251(6)	-0.0008(5)	0.0050(6)	-0.0018(7)
C77	0.0312(10)	0.0205(5)	0.0270(6)	-0.0007(5)	0.0050(6)	-0.0017(7)
C78	0.0264(10)	0.0156(5)	0.0221(6)	-0.0008(5)	0.0050(6)	-0.0019(7)
C79	0.027(4)	0.008(4)	0.019(3)	0.000(2)	0.003(3)	-0.007(3)
C80	0.028(3)	0.019(2)	0.017(2)	0.0011(18)	0.0035(19)	-0.008(2)
C81	0.022(2)	0.020(2)	0.024(2)	-0.0036(17)	0.002(2)	-0.0113(17)
C82	0.029(4)	0.012(4)	0.017(3)	-0.000(2)	0.003(3)	0.002(2)
C83	0.025(2)	0.016(2)	0.014(2)	-0.0010(17)	0.0019(17)	0.001(2)
C84	0.024(2)	0.0171(19)	0.0157(18)	0.0006(15)	0.0007(15)	-0.0055(16)
C85	0.035(2)	0.024(2)	0.032(2)	-0.0074(19)	0.012(2)	-0.0084(19)
C86	0.036(4)	0.030(4)	0.021(3)	0.005(3)	-0.004(3)	-0.009(3)
C87	0.025(3)	0.013(3)	0.018(3)	0.0021(19)	0.0073(19)	-0.002(2)
C88	0.022(3)	0.018(3)	0.021(3)	-0.001(2)	0.006(2)	-0.000(2)
C89	0.0532(15)	0.0270(12)	0.0219(11)	-0.0002(9)	-0.0057(10)	0.0052(11)
C90	0.0414(14)	0.0345(14)	0.0434(15)	0.0224(12)	0.0205(12)	0.0117(11)
C91	0.0284(13)	0.0289(13)	0.078(2)	0.0231(14)	0.0112(13)	-0.0053(10)
C92	0.0289(12)	0.0488(16)	0.0391(14)	0.0061(12)	0.0042(10)	-0.0174(11)
C93	0.024(3)	0.018(3)	0.019(3)	-0.001(2)	0.0068(19)	-0.004(2)
C94	0.027(3)	0.021(3)	0.029(4)	-0.001(2)	0.002(2)	-0.004(2)
C95	0.028(3)	0.016(3)	0.021(3)	0.003(2)	0.007(2)	-0.002(2)
C96	0.029(2)	0.020(2)	0.025(2)	0.0011(17)	0.0040(17)	-0.0072(17)

C97	0.042(3)	0.019(2)	0.025(2)	-0.0040(17)	0.0005(19)	-0.0099(19)
C98	0.042(3)	0.026(2)	0.027(2)	-0.0051(18)	0.002(2)	0.008(2)
C99	0.028(2)	0.033(3)	0.042(3)	-0.001(2)	0.002(2)	0.003(2)
C100	0.026(3)	0.024(3)	0.038(3)	-0.007(2)	-0.002(2)	-0.006(2)
C101	0.019(3)	0.019(3)	0.025(4)	0.009(3)	0.001(3)	-0.009(2)
C102	0.036(4)	0.031(4)	0.041(4)	0.014(3)	0.011(3)	0.005(3)
C103	0.041(3)	0.029(3)	0.069(5)	0.015(3)	0.025(3)	0.008(3)
C104	0.023(2)	0.039(3)	0.087(5)	0.028(3)	0.009(3)	0.005(2)
C105	0.041(3)	0.052(4)	0.071(4)	0.022(3)	-0.019(3)	0.002(3)
C106	0.035(4)	0.041(5)	0.046(4)	0.014(3)	-0.005(4)	-0.001(3)
C107	0.0302(11)	0.0232(11)	0.0211(10)	-0.0004(8)	0.0064(8)	-0.0005(9)
C108	0.0223(10)	0.0222(10)	0.0140(9)	-0.0002(8)	0.0029(7)	-0.0012(8)
C109	0.0240(10)	0.0174(10)	0.0156(9)	0.0037(7)	-0.0003(7)	-0.0038(8)
C110	0.0246(10)	0.0151(9)	0.0242(10)	-0.0008(8)	-0.0036(8)	0.0008(8)
C111	0.0194(10)	0.0282(12)	0.0338(12)	-0.0111(9)	0.0008(9)	-0.0007(9)
C112	0.0154(9)	0.0303(12)	0.0389(13)	-0.0130(10)	-0.0001(9)	-0.0093(8)
C113	0.0239(10)	0.0204(10)	0.0226(10)	-0.0058(8)	-0.0038(8)	-0.0064(8)
C133	0.0448(16)	0.0462(17)	0.0577(19)	0.0201(14)	0.0108(14)	0.0018(13)
O1	0.0195(7)	0.0175(7)	0.0278(8)	-0.0021(6)	0.0006(6)	-0.0057(6)
O1’	0.0238(7)	0.0311(8)	0.0193(7)	0.0023(6)	-0.0023(6)	0.0078(6)
O3	0.0269(15)	0.0228(15)	0.0210(14)	-0.0027(12)	-0.0059(12)	-0.0090(12)
O4	0.027(2)	0.022(3)	0.020(2)	-0.0023(18)	-0.0029(15)	-0.0131(18)
O5	0.0660(13)	0.0179(8)	0.0349(9)	0.0049(7)	0.0096(9)	0.0109(8)
Cl1	0.0233(2)	0.0152(2)	0.0160(2)	0.00366(16)	0.00134(16)	0.00256(17)
Cl2	0.0168(2)	0.0173(2)	0.0252(2)	0.00316(17)	0.00066(17)	0.00075(16)
Cl3	0.0356(3)	0.0451(4)	0.0461(4)	0.0070(3)	0.0033(3)	0.0001(3)
Cl4	0.0380(3)	0.0347(3)	0.0783(5)	0.0130(3)	-0.0026(3)	0.0106(3)
Cl5	0.0534(3)	0.0162(2)	0.0192(2)	0.00512(18)	0.0125(2)	-0.0088(2)
Cl6	0.0263(2)	0.0183(2)	0.0221(2)	0.00241(18)	0.00255(18)	0.00180(18)
C118	0.0183(8)	0.0229(16)	0.0229(18)	-0.0000(12)	0.0047(9)	0.0005(8)
C114	0.0183(8)	0.0229(16)	0.0229(18)	-0.0000(12)	0.0047(9)	0.0005(8)
C116	0.0212(8)	0.0258(16)	0.0258(18)	0.0000(12)	0.0047(9)	0.0006(8)
C119	0.0212(8)	0.0258(16)	0.0258(18)	0.0000(12)	0.0047(9)	0.0006(8)
C117	0.0343(8)	0.0389(16)	0.0389(18)	0.0002(12)	0.0048(9)	0.0012(8)
C115	0.0343(8)	0.0389(16)	0.0389(18)	0.0002(12)	0.0048(9)	0.0012(8)

Distances

C1’	C2’	1.201(3)Å		C1’	P1	1.763(2)Å
C2’	C3’	1.480(3)Å		C3’	C5’	1.536(3)Å
C3’	C11’	1.534(3)Å		C3’	O1’	1.432(2)Å
C4’	O1’	1.427(3)Å		C4’	H541	0.968Å
C4’	H543	0.977Å		C4’	H542	0.972Å
C5’	C6’	1.385(3)Å		C5’	C10’	1.395(3)Å
C6’	C7’	1.391(3)Å		C6’	H561	0.943Å
C7’	C8’	1.384(4)Å		C7’	H571	0.931Å
C8’	C9’	1.380(4)Å		C8’	H581	0.929Å
C9’	C10’	1.392(4)Å		C9’	H591	0.943Å
C10’	H601	0.943Å		C11’	C12’	1.394(3)Å
C11’	C16’	1.392(3)Å		C12’	C13’	1.385(3)Å
C12’	H621	0.959Å		C13’	C14’	1.383(3)Å
C13’	H631	0.950Å		C14’	C15’	1.389(3)Å
C14’	H641	0.948Å		C15’	C16’	1.388(3)Å
C15’	H651	0.952Å		C16’	H661	0.951Å
Ru1	P1	2.3101(5)Å		Ru1	C24	2.218(2)Å
Ru1	C25	2.228(2)Å		Ru1	C26	2.2393(19)Å
Ru1	C27	2.2266(19)Å		Ru1	C28	2.1973(19)Å
Ru1	C29	2.169(2)Å		Ru1	Cl1	2.4041(4)Å
Ru1	Cl2	2.4092(5)Å		Ru2	P2	2.267(6)Å
Ru2	P3	2.351(6)Å		Ru2	C108	2.2135(19)Å
Ru2	C109	2.2261(19)Å		Ru2	C110	2.240(2)Å
Ru2	C111	2.224(2)Å		Ru2	C112	2.189(2)Å
Ru2	C113	2.166(2)Å		Ru2	Cl5	2.4065(5)Å
Ru2	Cl6	2.4087(5)Å		P1	C1	1.764(2)Å
P1	C17	1.820(2)Å		P2	P3	0.367(5)Å
P2	C134	1.874(5)Å		P2	C67	2.046(7)Å
P2	C73	1.818(7)Å		P2	C79	1.747(10)Å
P2	C82	1.499(11)Å		P3	C134	1.661(6)Å
P3	C67	1.844(7)Å		P3	C73	1.704(7)Å
P3	C79	2.057(9)Å		P3	C82	1.764(11)Å
C1	C2	1.197(3)Å		C2	C3	1.477(3)Å
C3	C5	1.539(3)Å		C3	C11	1.531(3)Å
C3	O1	1.435(2)Å		C4	O1	1.430(3)Å
C4	H41	0.963Å		C4	H43	0.960Å

C4	H42	0.969Å		C5	C6	1.392(3)Å
C5	C10	1.389(3)Å		C6	C7	1.388(3)Å
C6	H61	0.948Å		C7	C8	1.388(4)Å
C7	H71	0.948Å		C8	C9	1.384(3)Å
C8	H81	0.940Å		C9	C10	1.395(3)Å
C9	H91	0.942Å		C10	H101	0.943Å
C11	C12	1.389(3)Å		C11	C16	1.395(3)Å
C12	C13	1.394(4)Å		C12	H121	0.956Å
C13	C14	1.387(5)Å		C13	H131	0.950Å
C14	C15	1.384(5)Å		C14	H141	0.929Å
C15	C16	1.389(3)Å		C15	H151	0.938Å
C16	H161	0.955Å		C17	C18	1.393(3)Å
C17	C22	1.383(3)Å		C18	C19	1.390(3)Å
C18	H181	0.944Å		C19	C20	1.377(3)Å
C19	H191	0.954Å		C20	C21	1.382(4)Å
C20	H201	0.935Å		C21	C22	1.394(3)Å
C21	H211	0.932Å		C22	H221	0.940Å
C23	C24	1.497(3)Å		C23	H231	0.969Å
C23	H233	0.948Å		C23	H232	0.969Å
C24	C25	1.430(3)Å		C24	C29	1.415(3)Å
C25	C26	1.397(3)Å		C25	H251	0.985Å
C26	C27	1.439(3)Å		C26	H261	0.976Å
C27	C28	1.405(3)Å		C27	C30	1.515(3)Å
C28	C29	1.430(3)Å		C28	H281	0.993Å
C29	H291	0.973Å		C30	C31	1.522(3)Å
C30	C32	1.534(3)Å		C30	H301	0.982Å
C31	H312	0.965Å		C31	H311	0.971Å
C31	H313	0.953Å		C32	H322	0.964Å
C32	H323	0.974Å		C32	H321	0.981Å
C134	C135	1.193(3)Å		C135	C136	1.479(3)Å
C136	C138	1.534(3)Å		C136	C144	1.532(3)Å
C136	O5	1.437(3)Å		C137	O5	1.425(4)Å
C137	H1371	0.963Å		C137	H1373	0.961Å
C137	H1372	0.956Å		C138	C139	1.386(3)Å
C138	C143	1.390(3)Å		C139	C140	1.394(4)Å
C139	H1391	0.917Å		C140	C141	1.383(4)Å

C140	H1401	0.944Å		C141	C142	1.384(4)Å
C141	H1411	0.944Å		C142	C143	1.382(4)Å
C142	H1421	0.936Å		C143	H1431	0.941Å
C144	C145	1.386(3)Å		C144	C149	1.395(4)Å
C145	C146	1.392(4)Å		C145	H1451	0.948Å
C146	C147	1.374(5)Å		C146	H1461	0.934Å
C147	C148	1.386(5)Å		C147	H1471	0.923Å
C148	C149	1.387(4)Å		C148	H1481	0.944Å
C149	H1491	0.961Å		C67	C68	1.396(7)Å
C67	C72	1.393(6)Å		C67	C73	0.551(5)Å
C67	C74	0.915(6)Å		C68	C69	1.382(7)Å
C68	C74	0.815(6)Å		C68	C75	1.565(7)Å
C68	H681	0.936Å		C68	H741	0.944Å
C69	C70	1.399(8)Å		C69	C74	1.703(7)Å
C69	C75	0.907(7)Å		C69	H691	0.935Å
C69	H751	0.860Å		C70	C71	1.395(7)Å
C70	C75	0.999(7)Å		C70	C76	0.788(6)Å
C70	H701	0.937Å		C70	H761	1.092Å
C71	C72	1.389(7)Å		C71	C75	1.704(7)Å
C71	C76	0.644(5)Å		C71	C77	0.841(6)Å
C71	H711	0.929Å		C72	C73	1.157(6)Å
C72	C77	1.301(6)Å		C72	C78	0.765(5)Å
C72	H721	0.921Å		C73	C74	1.401(6)Å
C73	C78	1.387(6)Å		C74	C75	1.404(6)Å
C74	H741	0.929Å		C75	C76	1.380(7)Å
C75	H751	0.922Å		C76	C77	1.403(7)Å
C76	H711	1.267Å		C76	H761	0.932Å
C77	C78	1.376(6)Å		C77	H711	0.977Å
C77	H771	0.933Å		C78	H721	0.648Å
C78	H781	0.925Å		C79	C80	1.218(11)Å
C79	C82	0.513(7)Å		C79	C83	1.041(9)Å
C80	C81	1.481(6)Å		C80	C82	1.603(9)Å
C80	C83	0.749(5)Å		C80	C84	1.503(6)Å
C81	C84	1.237(6)Å		C81	C93	1.550(7)Å
C81	C95	1.538(7)Å		C81	C101	1.024(8)Å
C81	C102	1.358(8)Å		C81	O4	1.429(5)Å

C82	C83	1.199(11)Å		C83	C84	1.500(6)Å
C84	C87	1.528(6)Å		C84	C93	1.697(6)Å
C84	C101	1.528(8)Å		C84	O3	1.435(5)Å
C84	O4	1.504(6)Å		C85	O3	1.422(6)Å
C85	H853	0.936Å		C85	H852	0.939Å
C85	H851	0.945Å		C86	C101	1.459(10)Å
C86	C105	1.537(11)Å		C86	C106	0.553(7)Å
C86	O4	1.418(9)Å		C86	H861	0.966Å
C86	H862	0.963Å		C86	H863	0.964Å
C86	H1061	1.097Å		C87	C88	1.399(8)Å
C87	C92	1.372(6)Å		C87	C93	0.640(5)Å
C87	C94	1.518(9)Å		C88	C89	1.430(7)Å
C88	C93	1.502(8)Å		C88	C94	0.585(5)Å
C88	H881	0.950Å		C88	H941	1.162Å
C89	C90	1.366(4)Å		C89	C94	1.389(7)Å
C89	H891	0.950Å		C89	H892	0.950Å
C90	C91	1.376(4)Å		C90	H903	0.960Å
C91	C92	1.372(4)Å		C91	H911	0.928Å
C92	C93	1.465(6)Å		C92	H921	0.950Å
C92	H922	0.950Å		C93	C94	1.370(9)Å
C94	H881	1.245Å		C94	H941	0.950Å
C95	C96	1.398(7)Å		C95	C100	1.378(8)Å
C95	C102	0.691(7)Å		C95	C103	1.656(9)Å
C95	H1021	0.508Å		C96	C97	1.393(6)Å
C96	H961	0.926Å		C97	C98	1.356(7)Å
C97	H971	0.930Å		C98	C99	1.398(7)Å
C98	H981	0.926Å		C99	C100	1.398(7)Å
C99	C103	1.530(9)Å		C99	H991	0.931Å
C99	H1031	0.644Å		C100	C102	1.203(8)Å
C100	C103	0.748(7)Å		C100	H1001	0.930Å
C100	H1031	1.015Å		C101	C102	1.382(10)Å
C101	C106	1.388(12)Å		C101	O4	0.594(5)Å
C102	C103	1.391(9)Å		C102	H1021	0.926Å
C103	C104	1.404(11)Å		C103	H1001	1.154Å
C103	H1031	0.923Å		C104	C105	1.353(10)Å
C104	H1041	0.924Å		C105	C106	1.405(12)Å

C105	H863	0.982Å		C105	H1051	0.927Å
C106	O4	1.182(10)Å		C106	H861	0.918Å
C106	H863	1.144Å		C106	H1061	0.943Å
C107	C108	1.488(3)Å		C107	H1071	0.958Å
C107	H1072	0.957Å		C107	H1073	0.962Å
C108	C109	1.429(3)Å		C108	C113	1.423(3)Å
C109	C110	1.397(3)Å		C109	H1091	0.976Å
C110	C111	1.431(3)Å		C110	H1101	0.980Å
C111	C112	1.418(3)Å		C111	C118	1.550(6)Å
C111	C114	1.514(6)Å		C112	C113	1.424(3)Å
C112	H1121	0.984Å		C113	H1131	0.992Å
C133	Cl3	1.771(3)Å		C133	Cl4	1.759(4)Å
C133	H1332	1.002Å		C133	H1331	0.995Å
C118	C114	0.431(7)Å		C118	C119	1.534(5)Å
C118	C117	1.516(6)Å		C118	C115	1.382(8)Å
C118	H1181	0.950Å		C118	H1141	0.820Å
C114	C116	1.530(5)Å		C114	C119	1.164(8)Å
C114	C115	1.535(6)Å		C114	H1181	1.184Å
C114	H1141	0.950Å		C116	C119	0.545(5)Å
C116	H1161	0.950Å		C116	H1162	0.950Å
C116	H1163	0.950Å		C116	H1191	0.500Å
C116	H1192	1.105Å		C116	H1193	1.201Å
C119	H1161	0.979Å		C119	H1162	1.190Å
C119	H1191	0.950Å		C119	H1192	0.950Å
C119	H1193	0.950Å		C117	C115	0.698(6)Å
C117	H1171	0.950Å		C117	H1172	0.950Å
C117	H1173	0.950Å		C117	H1151	0.449Å
C117	H1153	1.168Å		C115	H1172	0.790Å
C115	H1173	1.215Å		C115	H1151	0.950Å
C115	H1152	0.950Å		C115	H1153	0.950Å
H861	H1061	0.648Å		H921	H922	0.408Å
H891	H892	0.382Å		H1181	H1141	0.333Å
H1171	H1151	0.736Å		H1172	H1151	0.838Å
H1172	H1152	0.815Å		H1173	H1153	0.741Å
H1161	H1193	0.557Å		H1162	H1192	0.766Å
H1163	H1191	0.480Å				

Angles

C2’	C1’	P1	174.95(19)°		C1’	C2’	C3’	179.4(2)°
C2’	C3’	C5’	109.88(17)°		C2’	C3’	C11’	110.96(16)°
C5’	C3’	C11’	108.08(16)°		C2’	C3’	O1’	109.95(16)°
C5’	C3’	O1’	106.32(16)°		C11’	C3’	O1’	111.52(17)°
O1’	C4’	H541	107.002°		O1’	C4’	H543	111.859°
H541	C4’	H543	109.740°		O1’	C4’	H542	109.716°
H541	C4’	H542	108.316°		H543	C4’	H542	110.098°
C3’	C5’	C6’	121.26(19)°		C3’	C5’	C10’	119.3(2)°
C6’	C5’	C10’	119.3(2)°		C5’	C6’	C7’	120.3(2)°
C5’	C6’	H561	118.660°		C7’	C6’	H561	121.019°
C6’	C7’	C8’	120.5(3)°		C6’	C7’	H571	119.720°
C8’	C7’	H571	119.818°		C7’	C8’	C9’	119.4(2)°
C7’	C8’	H581	120.412°		C9’	C8’	H581	120.200°
C8’	C9’	C10’	120.7(2)°		C8’	C9’	H591	118.852°
C10’	C9’	H591	120.470°		C5’	C10’	C9’	119.9(2)°
C5’	C10’	H601	119.813°		C9’	C10’	H601	120.306°
C3’	C11’	C12’	119.14(18)°		C3’	C11’	C16’	121.52(18)°
C12’	C11’	C16’	119.2(2)°		C11’	C12’	C13’	120.2(2)°
C11’	C12’	H621	118.391°		C13’	C12’	H621	121.373°
C12’	C13’	C14’	120.5(2)°		C12’	C13’	H631	121.066°
C14’	C13’	H631	118.389°		C13’	C14’	C15’	119.5(2)°
C13’	C14’	H641	120.586°		C15’	C14’	H641	119.877°
C14’	C15’	C16’	120.3(2)°		C14’	C15’	H651	120.366°
C16’	C15’	H651	119.373°		C11’	C16’	C15’	120.3(2)°
C11’	C16’	H661	118.549°		C15’	C16’	H661	121.191°
P1	Ru1	C24	115.58(6)°		P1	Ru1	C25	152.12(5)°
C24	Ru1	C25	37.53(7)°		P1	Ru1	C26	163.54(5)°
C24	Ru1	C26	67.31(7)°		C25	Ru1	C26	36.46(7)°
P1	Ru1	C27	125.94(5)°		C24	Ru1	C27	80.81(8)°
C25	Ru1	C27	67.13(7)°		C26	Ru1	C27	37.60(7)°
P1	Ru1	C28	98.53(6)°		C24	Ru1	C28	68.36(8)°
C25	Ru1	C28	79.08(8)°		C26	Ru1	C28	66.83(7)°
C27	Ru1	C28	37.03(7)°		P1	Ru1	C29	93.69(6)°
C24	Ru1	C29	37.61(8)°		C25	Ru1	C29	67.10(7)°
C26	Ru1	C29	79.43(8)°		C27	Ru1	C29	68.11(8)°
P1	Ru1	Cl1	82.199(16)°		C24	Ru1	Cl1	162.21(6)°

C25	Ru1	Cl1	124.98(5)°		C26	Ru1	Cl1	95.47(5)°
C27	Ru1	Cl1	88.05(5)°		P1	Ru1	Cl2	84.192(17)°
C24	Ru1	Cl2	92.59(6)°		C25	Ru1	Cl2	89.29(5)°
C26	Ru1	Cl2	112.16(5)°		C27	Ru1	Cl2	149.10(5)°
C28	Ru1	C29	38.23(8)°		C28	Ru1	Cl1	110.01(5)°
C29	Ru1	Cl1	147.27(6)°		C28	Ru1	Cl2	160.09(6)°
C29	Ru1	Cl2	122.14(6)°		Cl1	Ru1	Cl2	89.893(16)°
P2	Ru2	P3	8.88(15)°		P2	Ru2	C108	113.68(16)°
P3	Ru2	C108	112.76(16)°		P2	Ru2	C109	151.04(15)°
P3	Ru2	C109	148.46(15)°		C108	Ru2	C109	37.54(7)°
P2	Ru2	C110	158.91(10)°		P3	Ru2	C110	167.72(10)°
C108	Ru2	C110	67.49(8)°		C109	Ru2	C110	36.44(8)°
P2	Ru2	C111	121.65(10)°		P3	Ru2	C111	130.53(10)°
C108	Ru2	C111	81.25(8)°		C109	Ru2	C111	67.04(8)°
C110	Ru2	C111	37.40(8)°		P2	Ru2	C112	93.34(12)°
P3	Ru2	C112	101.32(12)°		C108	Ru2	C112	68.69(8)°
C109	Ru2	C112	79.14(9)°		C110	Ru2	C112	66.98(8)°
P2	Ru2	C113	89.61(15)°		P3	Ru2	C113	93.51(15)°
C108	Ru2	C113	37.89(8)°		C109	Ru2	C113	67.15(8)°
C110	Ru2	C113	79.51(8)°		P2	Ru2	Cl5	83.76(15)°
P3	Ru2	Cl5	84.73(15)°		C108	Ru2	Cl5	162.48(6)°
C109	Ru2	Cl5	125.14(5)°		C110	Ru2	Cl5	95.68(6)°
P2	Ru2	Cl6	88.71(8)°		P3	Ru2	Cl6	79.87(9)°
C108	Ru2	Cl6	92.48(5)°		C109	Ru2	Cl6	89.59(5)°
C110	Ru2	Cl6	112.38(6)°		C111	Ru2	C112	37.49(8)°
C111	Ru2	C113	68.45(8)°		C112	Ru2	C113	38.18(8)°
C111	Ru2	Cl5	88.09(6)°		C112	Ru2	Cl5	110.25(6)°
C113	Ru2	Cl5	147.41(6)°		C111	Ru2	Cl6	149.04(6)°
C112	Ru2	Cl6	160.22(6)°		C113	Ru2	Cl6	122.28(6)°
Cl5	Ru2	Cl6	89.53(2)°		C1’	P1	Ru1	113.01(7)°
C1’	P1	C1	99.86(9)°		Ru1	P1	C1	115.03(7)°
C1’	P1	C17	103.40(9)°		Ru1	P1	C17	117.97(7)°
C1	P1	C17	105.43(9)°		Ru2	P2	P3	98.7(19)°
Ru2	P2	C134	112.3(3)°		P3	P2	C134	49.8(18)°
Ru2	P2	C67	113.4(3)°		P3	P2	C67	52.1(17)°
C134	P2	C67	91.8(2)°		Ru2	P2	C73	119.5(3)°

P3	P2	C73	66.3(18)°		C134	P2	C73	100.7(3)°
C67	P2	C73	14.93(16)°		Ru2	P2	C79	114.8(3)°
P3	P2	C79	145(2)°		C134	P2	C79	103.7(4)°
C67	P2	C79	117.8(4)°		C73	P2	C79	103.7(4)°
Ru2	P2	C82	129.6(3)°		P3	P2	C82	131(2)°
C134	P2	C82	99.8(5)°		C67	P2	C82	102.9(4)°
C73	P2	C82	89.5(4)°		C79	P2	C82	15.9(3)°
Ru2	P3	P2	72.4(19)°		Ru2	P3	C134	117.4(3)°
P2	P3	C134	120.4(20)°		Ru2	P3	C67	118.1(3)°
P2	P3	C67	118.8(19)°		C134	P3	C67	106.9(3)°
Ru2	P3	C73	120.6(3)°		P2	P3	C73	102.4(19)°
C134	P3	C73	115.4(3)°		C67	P3	C73	17.28(17)°
Ru2	P3	C79	100.5(3)°		P2	P3	C79	29.5(18)°
C134	P3	C79	99.4(4)°		C67	P3	C79	112.8(4)°
C73	P3	C79	96.0(4)°		Ru2	P3	C82	111.8(3)°
P2	P3	C82	39.5(18)°		C134	P3	C82	98.3(4)°
C67	P3	C82	101.4(4)°		C73	P3	C82	85.1(4)°
C79	P3	C82	12.7(3)°		P1	C1	C2	171.28(18)°
C1	C2	C3	175.3(2)°		C2	C3	C5	111.93(17)°
C2	C3	C11	107.85(16)°		C5	C3	C11	109.70(16)°
C2	C3	O1	110.60(16)°		C5	C3	O1	109.96(16)°
C11	C3	O1	106.64(16)°		O1	C4	H41	107.775°
O1	C4	H43	110.194°		H41	C4	H43	109.934°
O1	C4	H42	110.138°		H41	C4	H42	109.399°
H43	C4	H42	109.380°		C3	C5	C6	117.19(19)°
C3	C5	C10	123.22(18)°		C6	C5	C10	119.5(2)°
C5	C6	C7	120.7(2)°		C5	C6	H61	119.305°
C7	C6	H61	120.033°		C6	C7	C8	119.7(2)°
C6	C7	H71	120.069°		C8	C7	H71	120.229°
C7	C8	C9	119.8(2)°		C7	C8	H81	120.920°
C9	C8	H81	119.259°		C8	C9	C10	120.6(2)°
C8	C9	H91	119.547°		C10	C9	H91	119.816°
C5	C10	C9	119.6(2)°		C5	C10	H101	120.299°
C9	C10	H101	120.117°		C3	C11	C12	121.5(2)°
C3	C11	C16	118.6(2)°		C12	C11	C16	119.9(2)°
C11	C12	C13	119.9(2)°		C11	C12	H121	120.291°

C13	C12	H121	119.795°		C12	C13	C14	120.2(3)°
C12	C13	H131	119.831°		C14	C13	H131	119.936°
C13	C14	C15	119.7(2)°		C13	C14	H141	119.823°
C15	C14	H141	120.518°		C14	C15	C16	120.6(3)°
C14	C15	H151	120.136°		C16	C15	H151	119.230°
C11	C16	C15	119.7(2)°		C11	C16	H161	118.720°
C15	C16	H161	121.579°		P1	C17	C18	121.63(16)°
P1	C17	C22	118.61(15)°		C18	C17	C22	119.76(19)°
C17	C18	C19	119.8(2)°		C17	C18	H181	119.785°
C19	C18	H181	120.357°		C18	C19	C20	120.4(2)°
C18	C19	H191	120.490°		C20	C19	H191	119.083°
C19	C20	C21	119.8(2)°		C19	C20	H201	119.715°
C21	C20	H201	120.534°		C20	C21	C22	120.5(2)°
C20	C21	H211	119.738°		C22	C21	H211	119.795°
C17	C22	C21	119.7(2)°		C17	C22	H221	119.544°
C21	C22	H221	120.729°		C24	C23	H231	109.529°
C24	C23	H233	109.619°		H231	C23	H233	108.468°
C24	C23	H232	109.467°		H231	C23	H232	108.979°
H233	C23	H232	110.755°		Ru1	C24	C23	130.31(16)°
Ru1	C24	C25	71.64(11)°		C23	C24	C25	120.60(19)°
Ru1	C24	C29	69.33(11)°		C23	C24	C29	122.01(19)°
C25	C24	C29	117.39(18)°		Ru1	C25	C24	70.84(11)°
Ru1	C25	C26	72.21(11)°		C24	C25	C26	121.76(19)°
Ru1	C25	H251	125.185°		C24	C25	H251	118.184°
C26	C25	H251	119.773°		Ru1	C26	C25	71.33(11)°
Ru1	C26	C27	70.72(11)°		C25	C26	C27	120.49(18)°
Ru1	C26	H261	126.785°		C25	C26	H261	118.646°
C27	C26	H261	120.692°		Ru1	C27	C26	71.68(11)°
Ru1	C27	C28	70.35(11)°		C26	C27	C28	118.41(18)°
Ru1	C27	C30	130.39(14)°		C26	C27	C30	118.52(18)°
C28	C27	C30	123.05(18)°		Ru1	C28	C27	72.62(11)°
Ru1	C28	C29	69.81(11)°		C27	C28	C29	120.54(18)°
Ru1	C28	H281	121.361°		C27	C28	H281	118.853°
C29	C28	H281	119.780°		Ru1	C29	C24	73.06(12)°
Ru1	C29	C28	71.96(11)°		C24	C29	C28	121.37(19)°
Ru1	C29	H291	124.611°		C24	C29	H291	119.231°

C28	C29	H291	119.296°		C27	C30	C31	113.06(17)°
C27	C30	C32	108.96(17)°		C31	C30	C32	110.73(18)°
C27	C30	H301	107.201°		C31	C30	H301	108.595°
C32	C30	H301	108.125°		C30	C31	H312	109.803°
C30	C31	H311	109.976°		H312	C31	H311	109.090°
C30	C31	H313	109.643°		H312	C31	H313	108.699°
H311	C31	H313	109.608°		C30	C32	H322	109.951°
C30	C32	H323	109.656°		H322	C32	H323	109.678°
C30	C32	H321	111.287°		H322	C32	H321	108.842°
H323	C32	H321	107.379°		P2	C134	P3	9.7(3)°
P2	C134	C135	170.9(3)°		P3	C134	C135	174.3(3)°
C134	C135	C136	177.9(3)°		C135	C136	C138	111.89(18)°
C135	C136	C144	108.3(2)°		C138	C136	C144	109.40(18)°
C135	C136	O5	109.98(19)°		C138	C136	O5	110.1(2)°
C144	C136	O5	107.01(18)°		O5	C137	H1371	107.419°
O5	C137	H1373	108.352°		H1371	C137	H1373	109.920°
O5	C137	H1372	108.979°		H1371	C137	H1372	110.957°
H1373	C137	H1372	111.101°		C136	C138	C139	123.9(2)°
C136	C138	C143	117.2(2)°		C139	C138	C143	118.9(2)°
C138	C139	C140	119.8(2)°		C138	C139	H1391	120.614°
C140	C139	H1391	119.545°		C139	C140	C141	120.8(2)°
C139	C140	H1401	120.004°		C141	C140	H1401	119.181°
C140	C141	C142	119.3(2)°		C140	C141	H1411	120.245°
C142	C141	H1411	120.476°		C141	C142	C143	120.0(2)°
C141	C142	H1421	120.223°		C143	C142	H1421	119.749°
C138	C143	C142	121.1(2)°		C138	C143	H1431	118.973°
C142	C143	H1431	119.950°		C136	C144	C145	121.6(2)°
C136	C144	C149	118.7(2)°		C145	C144	C149	119.7(2)°
C144	C145	C146	119.5(3)°		C144	C145	H1451	119.533°
C146	C145	H1451	120.971°		C145	C146	C147	121.1(3)°
C145	C146	H1461	119.473°		C147	C146	H1461	119.418°
C146	C147	C148	119.5(3)°		C146	C147	H1471	119.988°
C148	C147	H1471	120.555°		C147	C148	C149	120.3(3)°
C147	C148	H1481	120.133°		C149	C148	H1481	119.567°
C144	C149	C148	120.0(3)°		C144	C149	H1491	119.493°
C148	C149	H1491	120.504°		P2	C67	P3	9.0(2)°

P2	C67	C68	127.7(3)°		P3	C67	C68	119.1(3)°
P2	C67	C72	112.1(3)°		P3	C67	C72	120.7(4)°
C68	C67	C72	120.2(4)°		P2	C67	C73	58.3(7)°
P3	C67	C73	66.8(7)°		C68	C67	C73	173.8(9)°
C72	C67	C73	53.9(7)°		P2	C67	C74	134.2(5)°
P3	C67	C74	129.5(5)°		C68	C67	C74	33.8(4)°
C72	C67	C74	101.6(5)°		C73	C67	C74	144.6(10)°
C67	C68	C69	119.7(5)°		C67	C68	C74	38.7(4)°
C69	C68	C74	98.3(6)°		C67	C68	C75	88.1(4)°
C69	C68	C75	35.1(3)°		C74	C68	C75	63.4(5)°
C67	C68	H681	119.594°		C69	C68	H681	120.652°
C74	C68	H681	129.866°		C75	C68	H681	149.080°
C67	C68	H741	80.307°		C69	C68	H741	122.760°
C74	C68	H741	63.273°		C75	C68	H741	105.768°
H681	C68	H741	69.123°		C68	C69	C70	119.8(5)°
C68	C69	C74	28.3(3)°		C70	C69	C74	95.6(4)°
C68	C69	C75	83.5(5)°		C70	C69	C75	45.4(4)°
C74	C69	C75	55.4(4)°		C68	C69	H691	120.492°
C70	C69	H691	119.704°		C74	C69	H691	141.230°
C75	C69	H691	143.361°		C68	C69	H751	120.036°
C70	C69	H751	69.225°		C74	C69	H751	99.461°
C75	C69	H751	62.870°		H691	C69	H751	80.663°
C69	C70	C71	120.8(5)°		C69	C70	C75	40.3(4)°
C71	C70	C75	89.2(5)°		C69	C70	C76	132.5(7)°
C71	C70	C76	11.8(5)°		C75	C70	C76	100.4(7)°
C69	C70	H701	120.177°		C71	C70	H701	118.999°
C75	C70	H701	143.160°		C76	C70	H701	107.283°
C69	C70	H761	170.477°		C71	C70	H761	68.450°
C75	C70	H761	147.791°		C76	C70	H761	56.723°
H701	C70	H761	50.560°		C70	C71	C72	118.9(5)°
C70	C71	C75	35.9(3)°		C72	C71	C75	85.4(4)°
C70	C71	C76	14.5(6)°		C72	C71	C76	133.3(8)°
C75	C71	C76	49.8(6)°		C70	C71	C77	145.0(7)°
C72	C71	C77	66.2(5)°		C75	C71	C77	142.3(6)°
C76	C71	C77	141.4(10)°		C70	C71	H711	120.226°
C72	C71	H711	120.900°		C75	C71	H711	150.301°

C76	C71	H711	105.841°		C77	C71	H711	66.848°
C67	C72	C71	120.5(4)°		C67	C72	C73	22.6(2)°
C71	C72	C73	143.1(5)°		C67	C72	C77	142.0(4)°
C71	C72	C77	36.2(3)°		C73	C72	C77	153.9(5)°
C67	C72	C78	107.0(6)°		C71	C72	C78	114.8(6)°
C73	C72	C78	89.9(5)°		C77	C72	C78	78.8(5)°
C67	C72	H721	119.213°		C71	C72	H721	120.249°
C73	C72	H721	96.634°		C77	C72	H721	91.484°
C78	C72	H721	43.947°		P2	C73	P3	11.4(2)°
P2	C73	C67	106.8(8)°		P3	C73	C67	95.9(8)°
P2	C73	C72	149.5(4)°		P3	C73	C72	160.6(5)°
C67	C73	C72	103.5(8)°		P2	C73	C74	117.7(4)°
P3	C73	C74	108.6(4)°		C67	C73	C74	22.2(6)°
C72	C73	C74	89.8(4)°		P2	C73	C78	121.9(4)°
P3	C73	C78	130.5(4)°		C67	C73	C78	127.2(8)°
C72	C73	C78	33.5(3)°		C74	C73	C78	120.4(4)°
C67	C74	C68	107.5(7)°		C67	C74	C69	130.8(5)°
C68	C74	C69	53.4(5)°		C67	C74	C73	13.2(4)°
C68	C74	C73	120.4(6)°		C69	C74	C73	134.8(4)°
C67	C74	C75	124.3(5)°		C68	C74	C75	85.4(5)°
C69	C74	C75	32.1(3)°		C73	C74	C75	119.6(4)°
C67	C74	H741	114.182°		C68	C74	H741	65.159°
C69	C74	H741	98.187°		C73	C74	H741	120.273°
C75	C74	H741	120.168°		C68	C75	C69	61.3(5)°
C68	C75	C70	138.5(5)°		C69	C75	C70	94.3(6)°
C68	C75	C71	117.8(4)°		C69	C75	C71	134.7(6)°
C70	C75	C71	54.9(4)°		C68	C75	C74	31.3(2)°
C69	C75	C74	92.4(5)°		C70	C75	C74	147.2(6)°
C71	C75	C74	99.1(4)°		C68	C75	C76	131.9(4)°
C69	C75	C76	122.4(6)°		C70	C75	C76	34.2(4)°
C71	C75	C76	20.9(2)°		C74	C75	C76	119.0(5)°
C68	C75	H751	100.784°		C69	C75	H751	56.107°
C70	C75	H751	89.832°		C71	C75	H751	140.104°
C74	C75	H751	120.153°		C76	C75	H751	120.789°
C70	C76	C71	153.7(10)°		C70	C76	C75	45.4(5)°
C71	C76	C75	109.2(8)°		C70	C76	C77	153.9(7)°

C71	C76	C77	22.0(6)°		C75	C76	C77	121.2(4)°
C70	C76	H711	161.095°		C71	C76	H711	44.863°
C75	C76	H711	149.419°		C77	C76	H711	42.574°
C70	C76	H761	78.324°		C71	C76	H761	127.737°
C75	C76	H761	119.442°		C77	C76	H761	119.334°
H711	C76	H761	82.897°		C71	C77	C72	77.5(5)°
C71	C77	C76	16.7(4)°		C72	C77	C76	88.6(4)°
C71	C77	C78	110.4(6)°		C72	C77	C78	33.1(2)°
C76	C77	C78	119.5(4)°		C71	C77	H711	60.897°
C72	C77	H711	125.208°		C76	C77	H711	61.254°
C78	C77	H711	149.030°		C71	C77	H771	127.161°
C72	C77	H771	148.892°		C76	C77	H771	120.216°
C78	C77	H771	120.292°		H711	C77	H771	67.914°
C72	C78	C73	56.6(5)°		C72	C78	C77	68.1(5)°
C73	C78	C77	120.2(4)°		C72	C78	H721	80.954°
C73	C78	H721	92.959°		C77	C78	H721	99.449°
C72	C78	H781	157.931°		C73	C78	H781	119.192°
C77	C78	H781	120.568°		H721	C78	H781	77.608°
P2	C79	P3	5.9(3)°		P2	C79	C80	173.1(7)°
P3	C79	C80	171.1(7)°		P2	C79	C82	53.4(19)°
P3	C79	C82	49.0(19)°		C80	C79	C82	131(2)°
P2	C79	C83	148.0(7)°		P3	C79	C83	144.0(7)°
C80	C79	C83	37.7(4)°		C82	C79	C83	95(2)°
C79	C80	C81	175.7(6)°		C79	C80	C82	13.9(6)°
C81	C80	C82	166.0(5)°		C79	C80	C83	58.2(6)°
C81	C80	C83	123.7(7)°		C82	C80	C83	45.2(6)°
C79	C80	C84	133.4(6)°		C81	C80	C84	49.0(3)°
C82	C80	C84	120.5(5)°		C83	C80	C84	75.4(6)°
C80	C81	C84	66.4(4)°		C80	C81	C93	107.6(4)°
C84	C81	C93	74.0(4)°		C80	C81	C95	111.1(4)°
C84	C81	C95	176.3(5)°		C93	C81	C95	109.5(4)°
C80	C81	C101	108.0(5)°		C84	C81	C101	84.5(5)°
C93	C81	C101	125.8(5)°		C95	C81	C101	93.9(6)°
C80	C81	C102	127.5(5)°		C84	C81	C102	152.9(6)°
C93	C81	C102	115.4(4)°		C95	C81	C102	26.7(3)°
C101	C81	C102	69.3(6)°		C80	C81	O4	110.3(4)°

C84	C81	O4	68.2(4)°		C93	C81	O4	107.3(4)°
C95	C81	O4	110.9(4)°		C101	C81	O4	20.7(4)°
C102	C81	O4	84.6(5)°		P2	C82	P3	9.0(3)°
P2	C82	C79	111(2)°		P3	C82	C79	118(2)°
P2	C82	C80	145.3(6)°		P3	C82	C80	152.0(6)°
C79	C82	C80	34.9(18)°		P2	C82	C83	169.4(7)°
P3	C82	C83	178.1(7)°		C79	C82	C83	59.8(19)°
C80	C82	C83	26.3(3)°		C79	C83	C80	84.1(7)°
C79	C83	C82	25.2(4)°		C80	C83	C82	108.5(8)°
C79	C83	C84	159.6(7)°		C80	C83	C84	75.7(6)°
C82	C83	C84	174.9(6)°		C80	C84	C81	64.6(4)°
C80	C84	C83	28.9(2)°		C81	C84	C83	93.2(4)°
C80	C84	C87	108.5(4)°		C81	C84	C87	83.3(4)°
C83	C84	C87	110.0(4)°		C80	C84	C93	99.6(3)°
C81	C84	C93	61.5(3)°		C83	C84	C93	112.2(3)°
C87	C84	C93	22.09(19)°		C80	C84	C101	84.8(4)°
C81	C84	C101	41.8(4)°		C83	C84	C101	109.9(4)°
C87	C84	C101	111.6(4)°		C93	C84	C101	91.0(4)°
C80	C84	O3	131.2(4)°		C81	C84	O3	147.3(4)°
C83	C84	O3	108.3(3)°		C87	C84	O3	110.6(4)°
C93	C84	O3	126.7(3)°		C80	C84	O4	105.2(4)°
C81	C84	O4	62.0(3)°		C83	C84	O4	126.2(4)°
C87	C84	O4	112.8(4)°		C93	C84	O4	97.0(3)°
C101	C84	O3	106.3(4)°		C101	C84	O4	22.6(2)°
O3	C84	O4	85.4(3)°		O3	C85	H853	106.501°
O3	C85	H852	111.028°		H853	C85	H852	109.618°
O3	C85	H851	110.634°		H853	C85	H851	108.773°
H852	C85	H851	110.193°		C101	C86	C105	107.6(6)°
C101	C86	C106	71.6(17)°		C105	C86	C106	66.0(17)°
C101	C86	O4	23.8(2)°		C105	C86	O4	108.1(6)°
C106	C86	O4	54.1(15)°		C101	C86	H861	134.659°
C105	C86	H861	74.086°		C106	C86	H861	68.218°
O4	C86	H861	111.169°		C101	C86	H862	98.821°
C105	C86	H862	137.367°		C106	C86	H862	156.281°
O4	C86	H862	109.406°		H861	C86	H862	109.550°
C101	C86	H863	94.117°		C105	C86	H863	38.255°

C106	C86	H863	93.918°		O4	C86	H863	109.422°
H861	C86	H863	108.602°		C101	C86	H1061	103.920°
C105	C86	H1061	101.156°		C106	C86	H1061	59.351°
O4	C86	H1061	80.625°		H861	C86	H1061	35.941°
H862	C86	H863	108.648°		H862	C86	H1061	104.186°
H863	C86	H1061	139.368°		C84	C87	C88	122.7(5)°
C84	C87	C92	114.7(4)°		C88	C87	C92	122.4(5)°
C84	C87	C93	93.9(8)°		C88	C87	C93	86.4(9)°
C92	C87	C93	85.3(8)°		C84	C87	C94	126.0(4)°
C88	C87	C94	22.7(2)°		C92	C87	C94	112.0(4)°
C93	C87	C94	64.5(8)°		C87	C88	C89	116.2(5)°
C87	C88	C93	25.1(2)°		C89	C88	C93	111.9(5)°
C87	C88	C94	90.1(12)°		C89	C88	C94	74.1(11)°
C93	C88	C94	65.7(11)°		C87	C88	H881	121.772°
C89	C88	H881	122.031°		C93	C88	H881	120.684°
C94	C88	H881	106.005°		C87	C88	H941	117.680°
C89	C88	H941	102.018°		C93	C88	H941	96.530°
C94	C88	H941	54.455°		H881	C88	H941	51.569°
C88	C89	C90	119.5(3)°		C88	C89	C94	23.9(2)°
C90	C89	C94	118.2(4)°		C88	C89	H891	114.646°
C90	C89	H891	120.821°		C94	C89	H891	121.020°
C88	C89	H892	120.194°		C90	C89	H892	120.332°
C94	C89	H892	115.774°		H891	C89	H892	23.222°
C89	C90	C91	120.3(2)°		C89	C90	H903	122.787°
C91	C90	H903	116.864°		C90	C91	C92	120.9(2)°
C90	C91	H911	120.026°		C92	C91	H911	119.087°
C87	C92	C91	117.7(3)°		C87	C92	C93	25.8(2)°
C91	C92	C93	118.7(3)°		C87	C92	H921	115.314°
C91	C92	H921	120.878°		C93	C92	H921	120.403°
C87	C92	H922	120.917°		C91	C92	H922	121.403°
C93	C92	H922	113.620°		H921	C92	H922	24.814°
C81	C93	C84	44.5(3)°		C81	C93	C87	107.9(8)°
C84	C93	C87	64.0(7)°		C81	C93	C88	119.3(4)°
C84	C93	C88	106.8(4)°		C87	C93	C88	68.4(8)°
C81	C93	C92	125.4(4)°		C84	C93	C92	100.9(4)°
C87	C93	C92	68.9(7)°		C88	C93	C92	109.8(5)°

C81	C93	C94	119.1(5)°		C84	C93	C94	124.2(5)°
C87	C93	C94	90.6(9)°		C88	C93	C94	22.9(2)°
C92	C93	C94	115.4(5)°		C87	C94	C88	67.2(11)°
C87	C94	C89	111.4(5)°		C88	C94	C89	82.0(12)°
C87	C94	C93	24.9(2)°		C88	C94	C93	91.4(12)°
C89	C94	C93	123.4(5)°		C87	C94	H881	96.177°
C88	C94	H881	47.167°		C89	C94	H881	105.245°
C93	C94	H881	110.392°		C87	C94	H941	124.038°
C88	C94	H941	95.495°		C89	C94	H941	118.441°
C93	C94	H941	118.097°		H881	C94	H941	48.347°
C81	C95	C96	121.4(5)°		C81	C95	C100	119.6(5)°
C96	C95	C100	119.0(5)°		C81	C95	C102	62.0(8)°
C96	C95	C102	164.6(10)°		C100	C95	C102	60.8(9)°
C81	C95	C103	117.0(5)°		C96	C95	C103	116.1(5)°
C100	C95	C103	26.6(3)°		C102	C95	C103	55.8(9)°
C81	C95	H1021	69.591°		C96	C95	H1021	94.986°
C100	C95	H1021	103.022°		C102	C95	H1021	100.015°
C103	C95	H1021	128.603°		C95	C96	C97	119.9(5)°
C95	C96	H961	120.326°		C97	C96	H961	119.797°
C96	C97	C98	121.3(4)°		C96	C97	H971	118.517°
C98	C97	H971	120.179°		C97	C98	C99	119.4(4)°
C97	C98	H981	119.931°		C99	C98	H981	120.636°
C98	C99	C100	119.8(5)°		C98	C99	C103	119.3(5)°
C100	C99	C103	29.2(3)°		C98	C99	H991	119.822°
C100	C99	H991	120.341°		C103	C99	H991	112.148°
C98	C99	H1031	107.729°		C100	C99	H1031	41.947°
C103	C99	H1031	15.082°		H991	C99	H1031	115.383°
C95	C100	C99	120.5(5)°		C95	C100	C102	30.1(4)°
C99	C100	C102	147.8(6)°		C95	C100	C103	97.9(8)°
C99	C100	C103	85.2(8)°		C102	C100	C103	87.7(8)°
C95	C100	H1001	119.269°		C99	C100	H1001	120.177°
C102	C100	H1001	90.525°		C103	C100	H1001	86.152°
C95	C100	H1031	114.289°		C99	C100	H1031	25.096°
C102	C100	H1031	131.827°		C103	C100	H1031	60.928°
H1001	C100	H1031	119.884°		C81	C101	C84	53.7(4)°
C81	C101	C86	151.9(7)°		C84	C101	C86	118.1(6)°

C81	C101	C102	66.8(6)°		C84	C101	C102	120.1(6)°
C86	C101	C102	117.3(6)°		C81	C101	C106	172.3(8)°
C84	C101	C106	120.9(7)°		C86	C101	C106	22.2(3)°
C102	C101	C106	118.9(7)°		C81	C101	O4	121.9(12)°
C84	C101	O4	76.4(10)°		C86	C101	O4	74.2(10)°
C102	C101	O4	140.3(11)°		C106	C101	O4	57.6(10)°
C81	C102	C95	91.3(10)°		C81	C102	C100	159.7(7)°
C95	C102	C100	89.2(10)°		C81	C102	C101	43.9(4)°
C95	C102	C101	130.5(11)°		C100	C102	C101	140.3(7)°
C81	C102	C103	164.6(8)°		C95	C102	C103	99.9(11)°
C100	C102	C103	32.5(4)°		C101	C102	C103	121.4(7)°
C81	C102	H1021	75.638°		C95	C102	H1021	32.708°
C100	C102	H1021	94.370°		C101	C102	H1021	119.348°
C103	C102	H1021	119.281°		C95	C103	C99	98.3(6)°
C95	C103	C100	55.5(7)°		C99	C103	C100	65.6(8)°
C95	C103	C102	24.3(3)°		C99	C103	C102	117.6(7)°
C100	C103	C102	59.8(7)°		C95	C103	C104	139.1(6)°
C99	C103	C104	122.5(5)°		C100	C103	C104	141.7(10)°
C102	C103	C104	118.8(7)°		C95	C103	H1001	89.152°
C99	C103	H1001	97.414°		C100	C103	H1001	53.516°
C102	C103	H1001	73.085°		C104	C103	H1001	88.467°
C95	C103	H1031	99.150°		C99	C103	H1031	10.460°
C100	C103	H1031	73.954°		C102	C103	H1031	120.912°
C104	C103	H1031	120.318°		H1001	C103	H1031	107.821°
C103	C104	C105	120.4(5)°		C103	C104	H1041	120.373°
C105	C104	H1041	119.206°		C86	C105	C104	117.8(6)°
C86	C105	C106	21.1(3)°		C104	C105	C106	120.5(7)°
C86	C105	H863	37.448°		C104	C105	H863	84.536°
C106	C105	H863	53.796°		C86	C105	H1051	118.862°
C104	C105	H1051	118.784°		C106	C105	H1051	120.692°
H863	C105	H1051	133.915°		C86	C106	C101	86.1(17)°
C86	C106	C105	93.0(19)°		C101	C106	C105	120.0(9)°
C86	C106	O4	103.6(19)°		C101	C106	O4	25.1(3)°
C105	C106	O4	135.2(10)°		C86	C106	H861	77.754°
C101	C106	H861	153.224°		C105	C106	H861	82.497°
O4	C106	H861	141.328°		C86	C106	H863	57.232°

C101	C106	H863	90.465°		C105	C106	H863	43.831°
O4	C106	H863	115.038°		H861	C106	H863	98.375°
C86	C106	H1061	90.344°		C101	C106	H1061	119.386°
C105	C106	H1061	120.637°		O4	C106	H1061	100.856°
H861	C106	H1061	40.738°		H863	C106	H1061	135.447°
C108	C107	H1071	109.026°		C108	C107	H1072	110.653°
H1071	C107	H1072	108.831°		C108	C107	H1073	109.450°
H1071	C107	H1073	109.229°		H1072	C107	H1073	109.628°
Ru2	C108	C107	128.50(15)°		Ru2	C108	C109	71.71(11)°
C107	C108	C109	121.55(19)°		Ru2	C108	C113	69.25(11)°
C107	C108	C113	121.55(19)°		C109	C108	C113	116.88(18)°
Ru2	C109	C108	70.75(11)°		Ru2	C109	C110	72.33(12)°
C108	C109	C110	122.25(19)°		Ru2	C109	H1091	124.265°
C108	C109	H1091	118.137°		C110	C109	H1091	119.177°
Ru2	C110	C109	71.23(11)°		Ru2	C110	C111	70.68(12)°
C109	C110	C111	120.66(19)°		Ru2	C110	H1101	124.970°
C109	C110	H1101	120.505°		C111	C110	H1101	118.443°
Ru2	C111	C110	71.92(12)°		Ru2	C111	C112	69.93(13)°
C110	C111	C112	118.11(19)°		Ru2	C111	C118	122.3(2)°
C110	C111	C118	121.3(3)°		C112	C111	C118	120.1(3)°
Ru2	C111	C114	137.6(2)°		C110	C111	C114	116.2(3)°
C112	C111	C114	125.0(3)°		C118	C111	C114	16.1(3)°
Ru2	C112	C111	72.58(13)°		Ru2	C112	C113	70.04(12)°
C111	C112	C113	120.6(2)°		Ru2	C112	H1121	121.437°
C111	C112	H1121	119.665°		C113	C112	H1121	118.963°
Ru2	C113	C108	72.86(11)°		Ru2	C113	C112	71.78(12)°
C108	C113	C112	121.46(19)°		Ru2	C113	H1131	125.277°
C108	C113	H1131	118.123°		C112	C113	H1131	120.319°
Cl3	C133	Cl4	111.44(16)°		Cl3	C133	H1332	106.820°
Cl4	C133	H1332	110.510°		Cl3	C133	H1331	108.676°
Cl4	C133	H1331	108.901°		H1332	C133	H1331	110.475°
C3	O1	C4	114.36(16)°		C3’	O1’	C4’	114.36(16)°
C84	O3	C85	115.8(3)°		C81	O4	C84	49.8(3)°
C81	O4	C86	115.7(5)°		C84	O4	C86	122.6(5)°
C81	O4	C101	37.5(9)°		C84	O4	C101	81.0(10)°
C86	O4	C101	82.0(10)°		C81	O4	C106	134.1(6)°

C84	O4	C106	141.6(6)°		C86	O4	C106	22.3(4)°
C101	O4	C106	97.2(11)°		C136	O5	C137	114.08(19)°
C111	C118	C114	77.1(14)°		C111	C118	C119	103.4(3)°
C114	C118	C119	26.6(12)°		C111	C118	C117	117.9(4)°
C114	C118	C117	130.0(10)°		C119	C118	C117	111.86(10)°
C111	C118	C115	116.0(5)°		C114	C118	C115	102.7(10)°
C119	C118	C115	87.0(3)°		C117	C118	C115	27.4(2)°
C111	C118	H1181	108.036°		C114	C118	H1181	112.405°
C119	C118	H1181	108.124°		C117	C118	H1181	107.225°
C115	C118	H1181	128.378°		C111	C118	H1141	111.576°
C114	C118	H1141	93.564°		C119	C118	H1141	88.298°
C117	C118	H1141	118.741°		C115	C118	H1141	131.935°
H1181	C118	H1141	19.989°		C111	C114	C118	86.7(14)°
C111	C114	C116	115.2(4)°		C118	C114	C116	157.5(17)°
C111	C114	C119	128.8(6)°		C118	C114	C119	143.8(16)°
C116	C114	C119	17.4(3)°		C111	C114	C115	109.4(4)°
C118	C114	C115	61.4(10)°		C116	C114	C115	111.84(10)°
C119	C114	C115	95.3(3)°		C111	C114	H1181	98.422°
C118	C114	H1181	47.900°		C116	C114	H1181	119.488°
C119	C114	H1181	120.643°		C115	C114	H1181	100.850°
C111	C114	H1141	106.488°		C118	C114	H1141	59.479°
C116	C114	H1141	106.696°		C119	C114	H1141	108.232°
C115	C114	H1141	106.675°		H1181	C114	H1141	12.829°
C114	C116	C119	39.8(9)°		C114	C116	H1161	109.630°
C119	C116	H1161	76.536°		C114	C116	H1162	109.859°
C119	C116	H1162	102.035°		H1161	C116	H1162	109.476°
C114	C116	H1163	108.910°		C119	C116	H1163	142.938°
H1161	C116	H1163	109.476°		H1162	C116	H1163	109.476°
C114	C116	H1191	94.923°		C119	C116	H1191	130.637°
H1161	C116	H1191	117.364°		H1162	C116	H1191	114.514°
H1163	C116	H1191	14.075°		C114	C116	H1192	78.478°
C119	C116	H1192	59.262°		H1161	C116	H1192	94.379°
H1162	C116	H1192	42.938°		H1163	C116	H1192	149.860°
C114	C116	H1193	83.124°		C119	C116	H1193	50.288°
H1161	C116	H1193	26.932°		H1162	C116	H1193	116.269°
H1163	C116	H1193	124.906°		H1191	C116	H1192	147.731°

H1191	C116	H1193	126.492°		H1192	C116	H1193	84.466°
C118	C119	C114	9.6(4)°		C118	C119	C116	131.0(11)°
C114	C119	C116	122.8(12)°		C118	C119	H1161	139.470°
C114	C119	H1161	146.711°		C116	C119	H1161	70.694°
C118	C119	H1162	129.709°		C114	C119	H1162	121.796°
C116	C119	H1162	51.355°		H1161	C119	H1162	90.819°
C118	C119	H1191	109.173°		C114	C119	H1191	102.112°
C116	C119	H1191	23.564°		H1161	C119	H1191	81.629°
H1162	C119	H1191	70.078°		C118	C119	H1192	109.028°
C114	C119	H1192	106.495°		C116	C119	H1192	91.204°
H1161	C119	H1192	103.148°		H1162	C119	H1192	40.011°
C118	C119	H1193	110.196°		C114	C119	H1193	119.346°
C116	C119	H1193	103.532°		H1161	C119	H1193	33.525°
H1162	C119	H1193	117.282°		H1191	C119	H1192	109.476°
H1191	C119	H1193	109.475°		H1192	C119	H1193	109.476°
C118	C117	C115	65.6(7)°		C118	C117	H1171	109.690°
C115	C117	H1171	156.030°		C118	C117	H1172	108.129°
C115	C117	H1172	54.707°		H1171	C117	H1172	109.476°
C118	C117	H1173	110.571°		C115	C117	H1173	93.696°
H1171	C117	H1173	109.476°		H1172	C117	H1173	109.475°
C118	C117	H1151	114.036°		C115	C117	H1151	109.914°
H1171	C117	H1151	48.786°		H1172	C117	H1151	61.937°
H1173	C117	H1151	134.944°		C118	C117	H1153	90.475°
C115	C117	H1153	54.432°		H1171	C117	H1153	148.552°
H1172	C117	H1153	85.380°		H1173	C117	H1153	39.283°
H1151	C117	H1153	143.392°		C118	C115	C114	15.9(3)°
C118	C115	C117	87.0(7)°		C114	C115	C117	102.9(8)°
C118	C115	H1172	135.727°		C114	C115	H1172	139.333°
C117	C115	H1172	79.106°		C118	C115	H1173	104.257°
C114	C115	H1173	113.768°		C117	C115	H1173	51.306°
H1172	C115	H1173	99.238°		C118	C115	H1151	95.272°
C114	C115	H1151	109.905°		C117	C115	H1151	26.385°
H1172	C115	H1151	56.721°		H1173	C115	H1151	73.096°
C118	C115	H1152	122.397°		C114	C115	H1152	109.804°
C117	C115	H1152	133.919°		H1172	C115	H1152	54.917°
H1173	C115	H1152	132.185°		C118	C115	H1153	109.532°

C114	C115	H1153	108.687°		C117	C115	H1153	88.859°
H1172	C115	H1153	111.967°		H1173	C115	H1153	37.572°
H1151	C115	H1152	109.476°		H1151	C115	H1153	109.476°
H1152	C115	H1153	109.476°		C71	H711	C76	29.296°
C71	H711	C77	52.255°		C76	H711	C77	76.173°
C72	H721	C78	55.099°		C68	H741	C74	51.568°
C69	H751	C75	61.023°		C70	H761	C76	44.953°
C86	H861	C106	34.028°		C86	H861	H1061	83.047°
C106	H861	H1061	71.719°		C86	H863	C105	104.297°
C86	H863	C106	28.850°		C105	H863	C106	82.374°
C100	H1001	C103	40.332°		C95	H1021	C102	47.277°
C99	H1031	C100	112.957°		C99	H1031	C103	154.459°
C100	H1031	C103	45.117°		C86	H1061	C106	30.304°
C86	H1061	H861	61.013°		C106	H1061	H861	67.543°
C92	H921	H922	77.592°		C92	H922	H921	77.594°
C89	H891	H892	78.387°		C89	H892	H891	78.391°
C88	H881	C94	26.829°		C88	H941	C94	30.050°
C118	H1181	C114	19.695°		C118	H1181	H1141	57.373°
C114	H1181	H1141	39.332°		C118	H1141	C114	26.957°
C118	H1141	H1181	102.637°		C114	H1141	H1181	127.839°
C117	H1171	H1151	27.310°		C117	H1172	C115	46.187°
C117	H1172	H1151	28.207°		C115	H1172	H1151	71.332°
C117	H1172	H1152	118.715°		C115	H1172	H1152	72.601°
H1151	H1172	H1152	139.611°		C117	H1173	C115	34.998°
C117	H1173	H1153	86.425°		C115	H1173	H1153	51.445°
C117	H1151	C115	43.701°		C117	H1151	H1171	103.903°
C115	H1151	H1171	145.829°		C117	H1151	H1172	89.856°
C115	H1151	H1172	51.948°		H1171	H1151	H1172	160.288°
C115	H1152	H1172	52.482°		C117	H1153	C115	36.709°
C117	H1153	H1173	54.293°		C115	H1153	H1173	90.983°
C116	H1161	C119	32.770°		C116	H1161	H1193	102.489°
C119	H1161	H1193	70.387°		C116	H1162	C119	26.611°
C116	H1162	H1192	79.389°		C119	H1162	H1192	52.895°
C116	H1163	H1191	14.681°		C116	H1191	C119	25.799°
C116	H1191	H1163	151.245°		C119	H1191	H1163	167.943°
C116	H1192	C119	29.535°		C116	H1192	H1162	57.673°

C119	H1192	H1162	87.093°		C116	H1193	C119	26.180°
C116	H1193	H1161	50.579°		C119	H1193	H1161	76.088°

Electrochemistry Data of **3b**

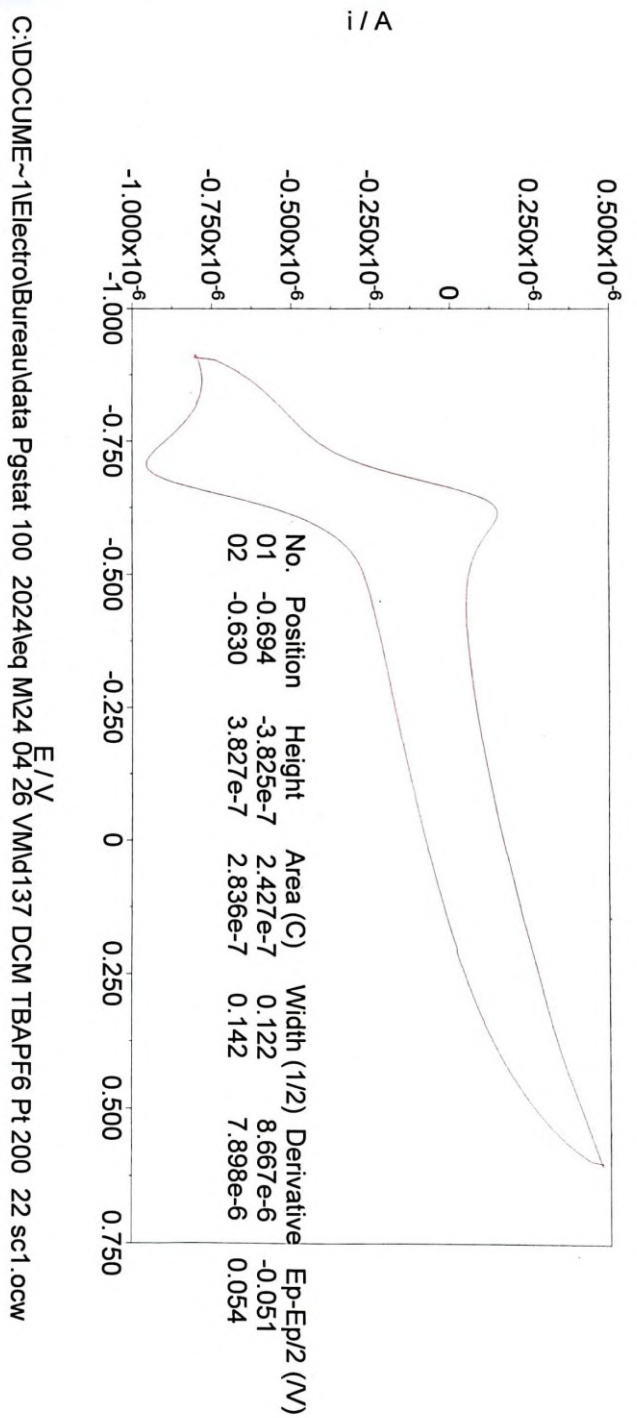

Overlay legends:
blanc dcm tbapf6 pt sqw 20 20 5 ox1 (Line-blue)
d137 dcm tbapf6 pt sqw 20 20 5 ox2 (Line-green)

DCM + TBAPF6

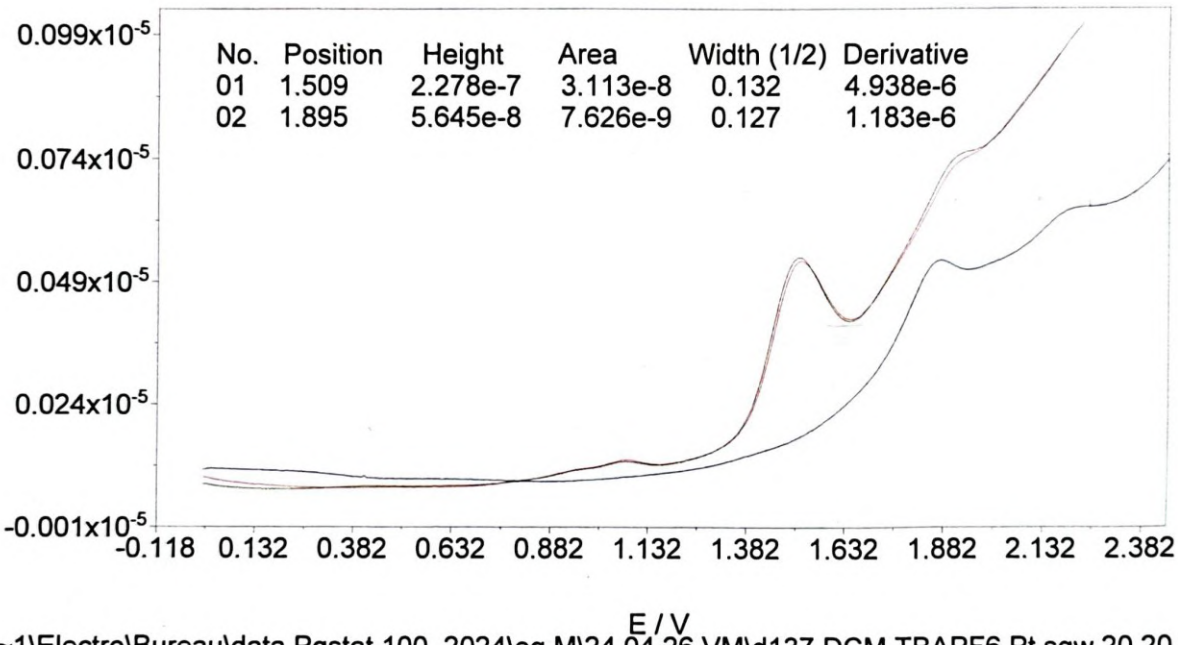

C:\DOCUME~1\Electro\Bureau\data Pgstat 100 2024\eq M\24 04 26 VM\d137 DCM TBAPF6 Pt sqw 20 20 5 ox1.oew

Overlay legends:
blanc dcm tbapf6 pt sqw 20 20 5 red1 (Line-blue)

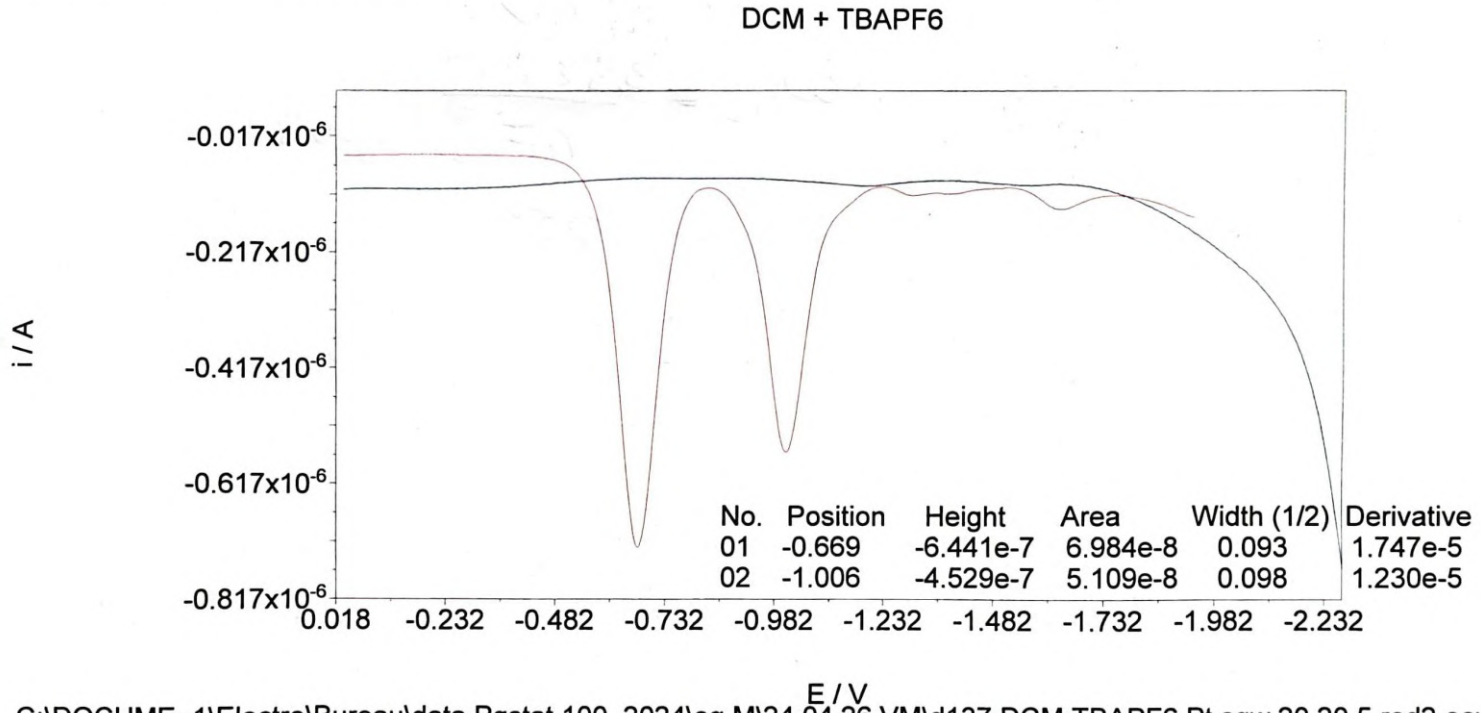

C:\DOCUME~1\Electro\Bureau\data Pgstat 100 2024\eq M\24 04 26 VM\d137 DCM TBAPF6 Pt sqw 20 20 5 red2.oew

Overlay legends:
d134 dcm tbapf6 pt 200 01 sc1 (Line-blue)
d134 dcm tbapf6 pt 200 03 sc1 red (Line-green)

No.	Position	Height	Area (C)	Width (1/2)	Derivative	Ep-Ep/2 (/V)
01	-1.568	-1.496e-7	1.359e-7	0.200	3.850e-6	-0.082
02	-1.680	-5.754e-8	3.018e-8	0.107	1.757e-6	-0.063

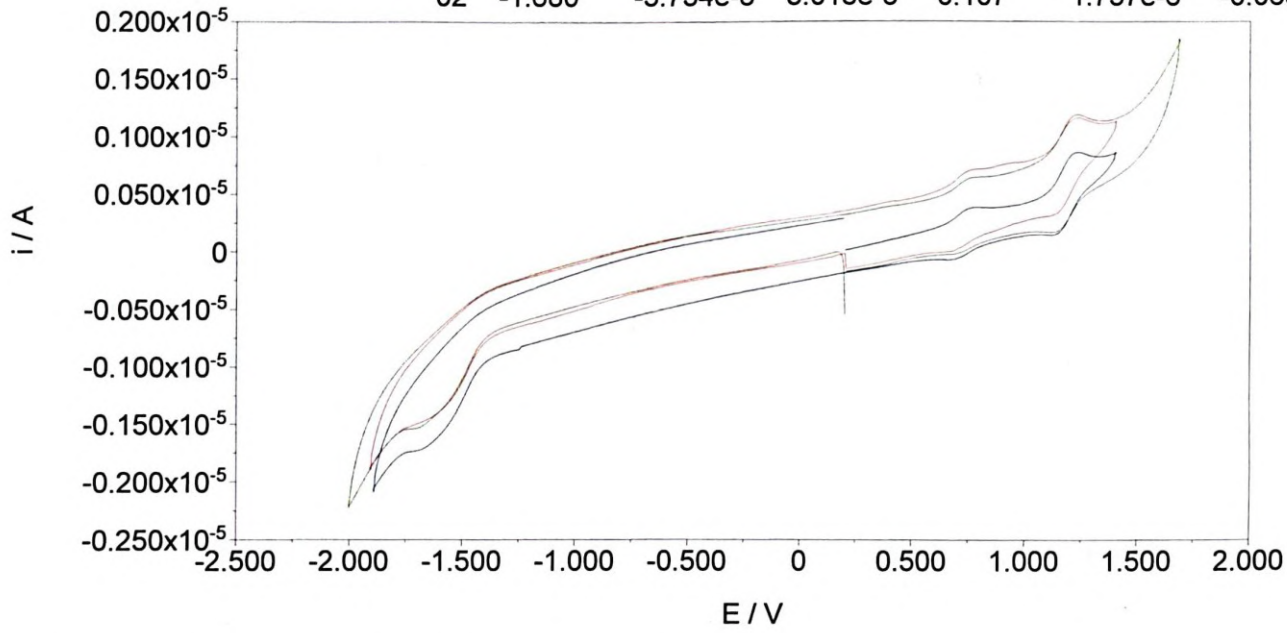

C:\DOCUME~1\Electro\Bureau\data Pgstat 100 2024\eq M\24 04 19 VM\d134 DCM TBAPF6 Pt 200 04 sc1 red.ocw

Electrochemistry Data of **13**

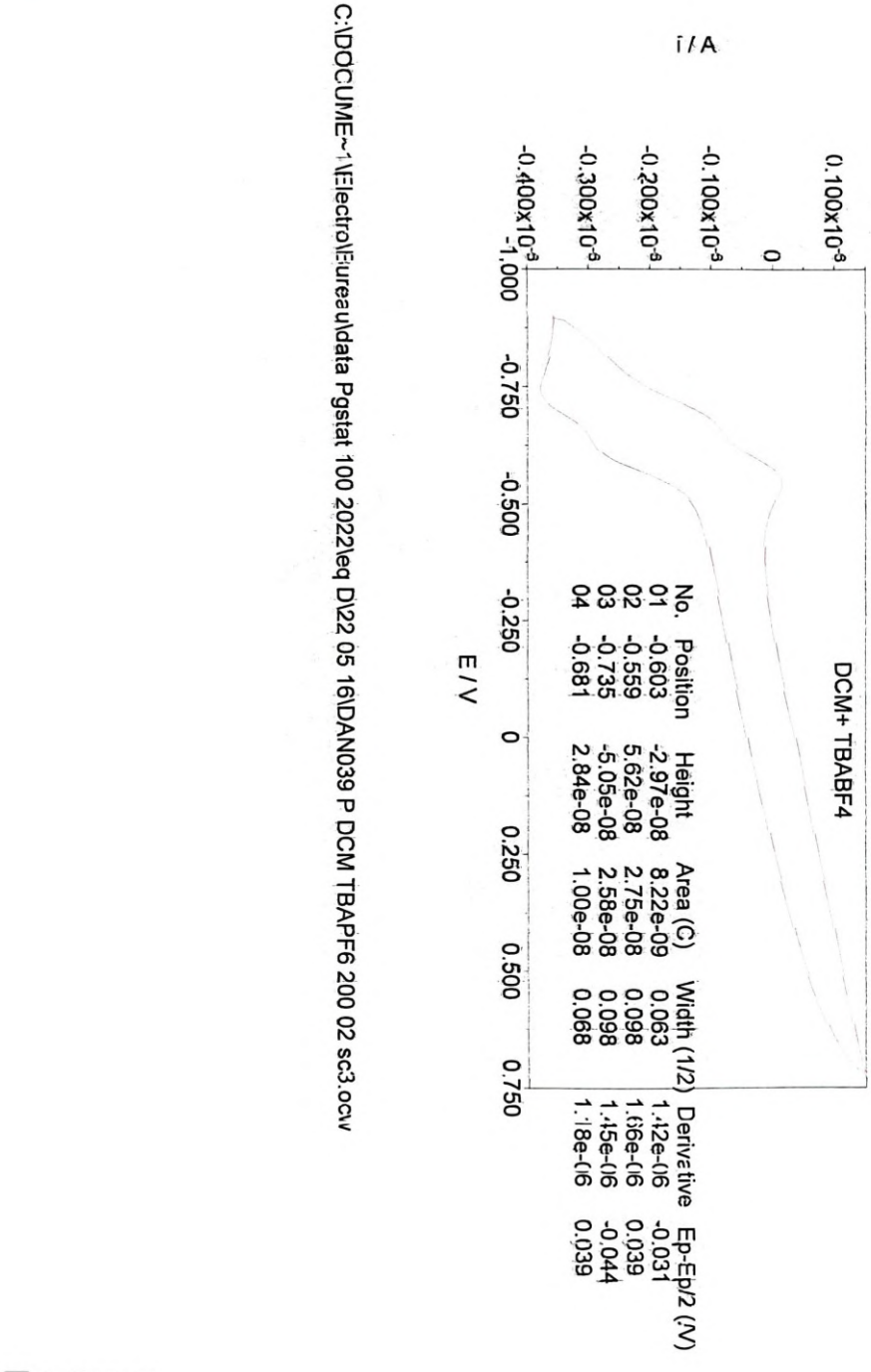

Overlay legends:
blanc dcm tbapf6 sqw 20 20 5 ox1 (Line-blue)
dan039 p dcm tbapf6 sqw 20 20 5 ox1 (Line-green)

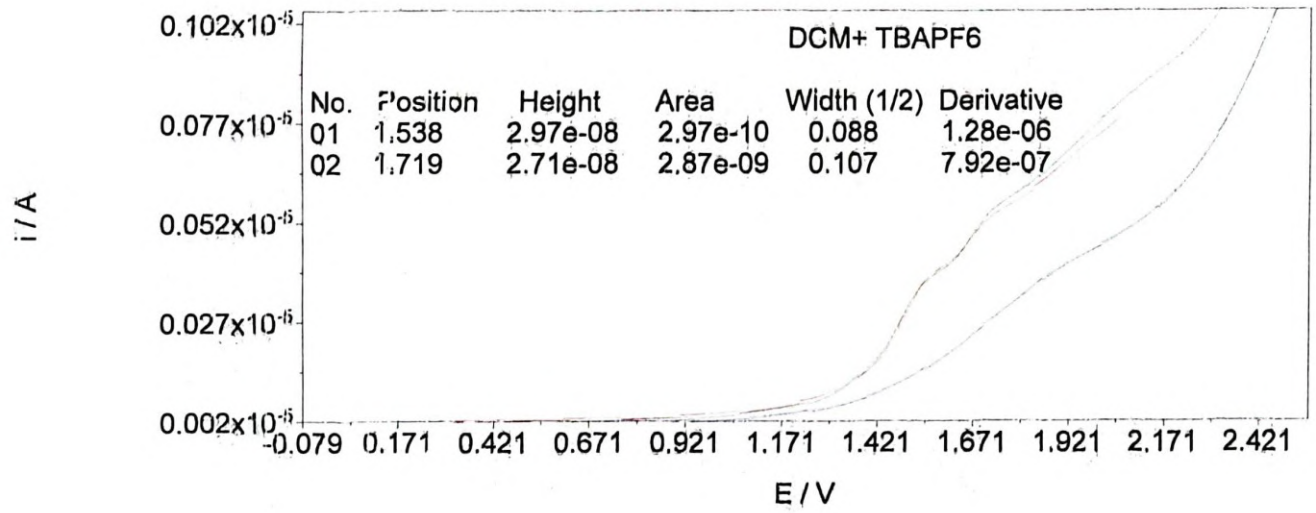

C:\DOCUME~1\Electro\Bureau\data Pgstat 100 2022\eq D\22 05 16\DAN039 P DCM TBAPF6 sqw 20 20 5 ox2.oew

No.	Position	Height	Area	Width (1/2	Derivative
01	-0.571	-1.03e-07	7.26e-09	0.068	4.13e-06
02	-0.698	-8.50e-08	5.80e-09	0.068	3.47e-06
03	-1.152	-1.86e-07	2.04e-08	0.098	5.11e-06
04	-1.416	-1.13e-08	1.12e-09	0.093	3.29e-07

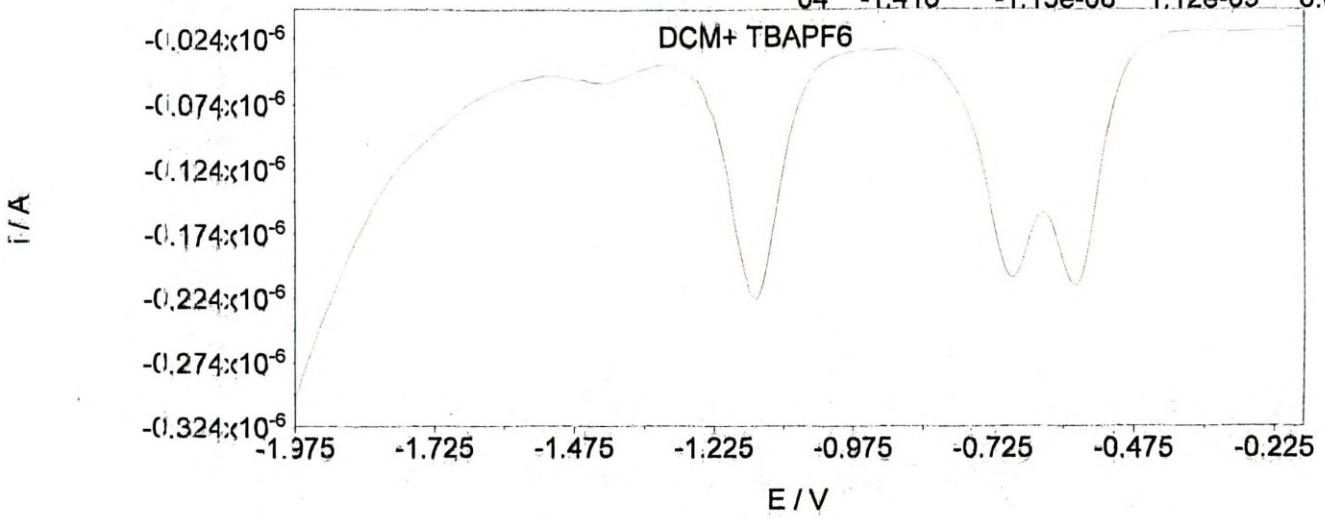

C:\DOCUME~1\Electro\Eureau\data Pgstat 100 2022\eq D\22 05 16\DAN039 P DCM TBAPF6 sqw 20 20 5 re11.oew

No.	Position	Height	Area (C)	Width (1/2)	Derivative	Ep-Ep/2 (/V)
01	1.538	2.382e-7	1.497e-7	0.132	5.694e-6	0.058

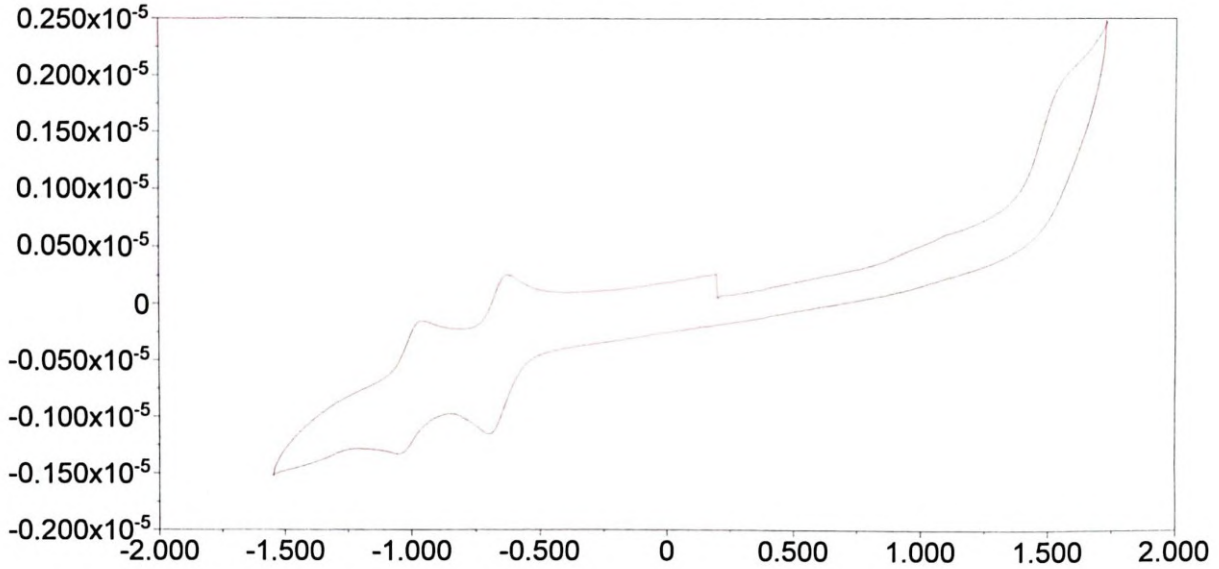

C:\DOCUME~1\Electro\Bureau\data Pgstat 100 2024\eq M\24 04 26 VM\d137 DCM TBAPF6 Pt 200 20 sc1.ocw

Electrochemistry Data of 39

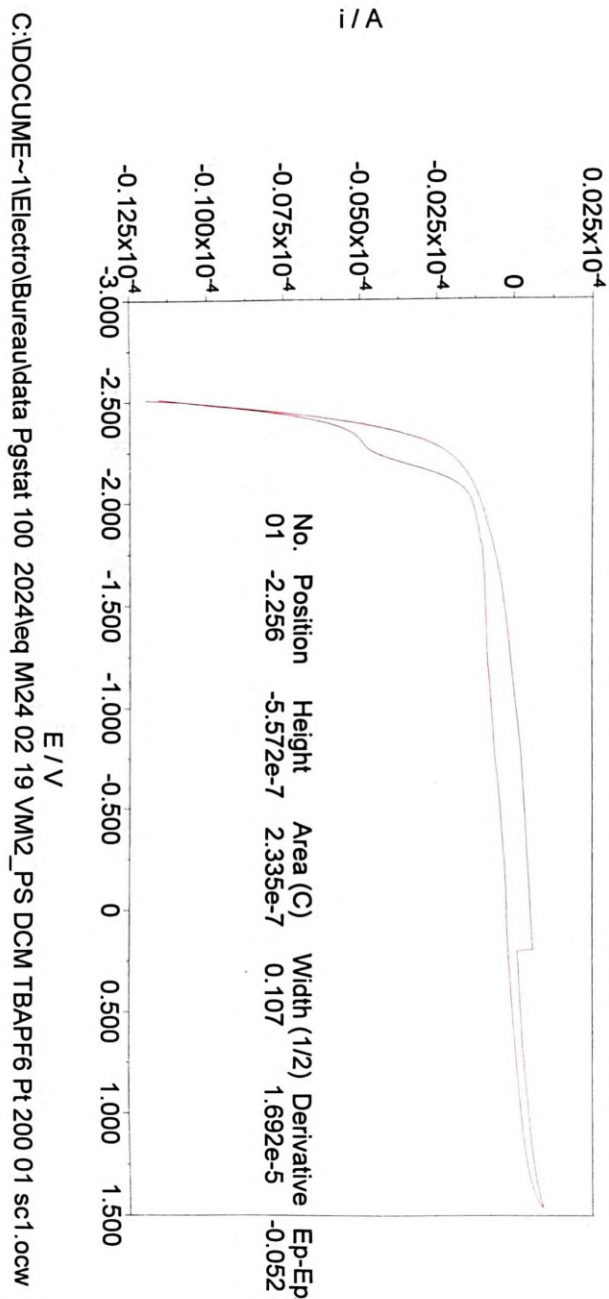

Overlay legends:
blanc dcm tbapf6 pt sqw 20 20 5 ox2 (Line-blue)
ps dcm tbapf6 pt sqw 20 20 5 ox1 (Line-green)

DCM + TBAPF6

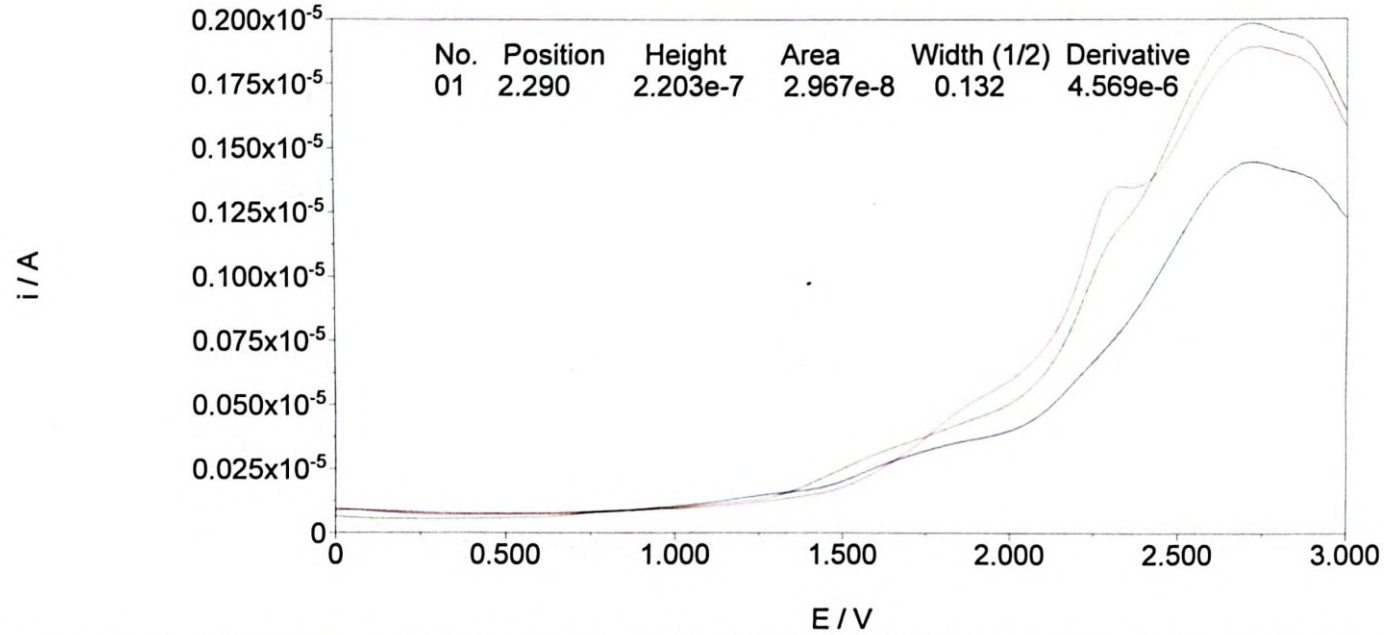

C:\DOCUME~1\Electro\Bureau\data Pgstat 100 2024\eq M\24 02 19 VM\PS DCM TBAPF6 Pt sqw 20 20 5 ox2.oew

Overlay legends:
blanc dcm tbapf6 pt sqw 20 20 5 red1 (Line-blue)
ps dcm tbapf6 pt sqw 20 20 5 red1 (Line-green)

DCM + TBAPF6

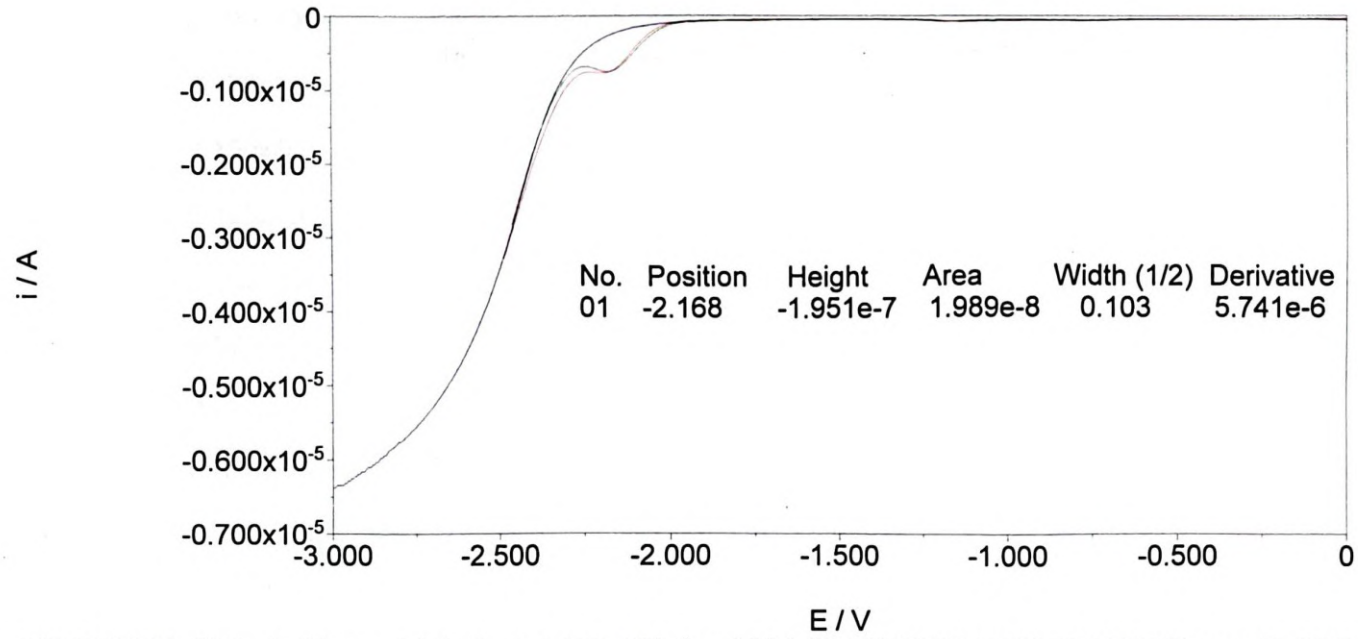

C:\DOCUME~1\Electro\Bureau\data Pgstat 100 2024\eq M\24 02 19 VM\PS DCM TBAPF6 Pt sqw 20 20 5 red2.oew

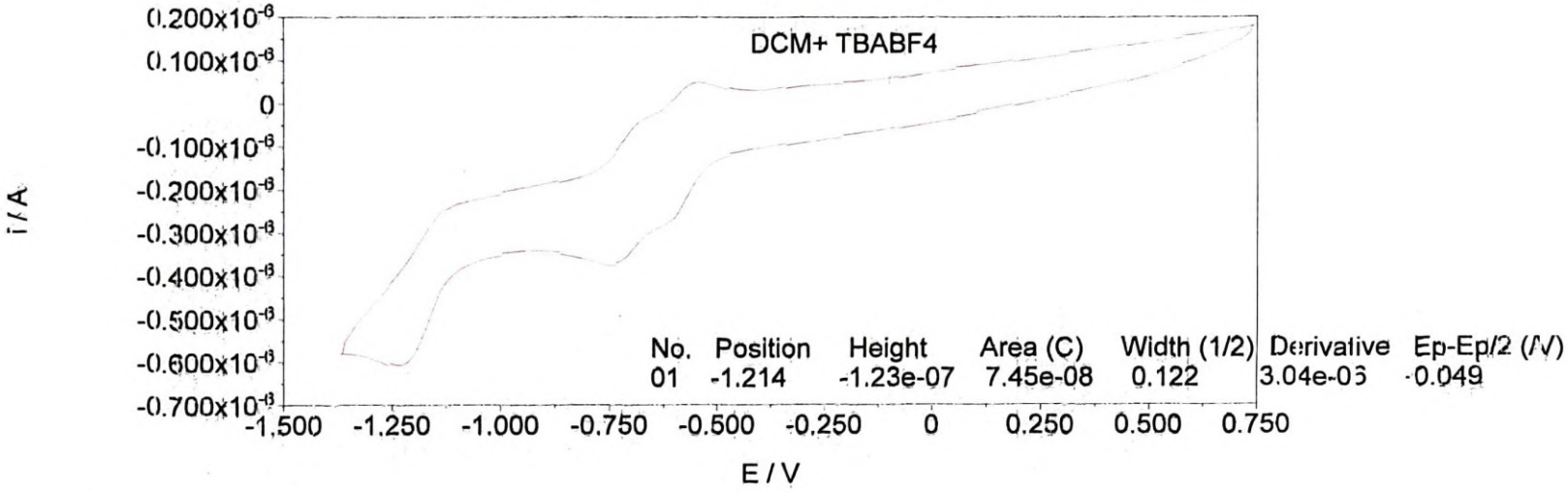

C:\DOCUME~1\Electro\Bureau\data Pgstat 100 2022\eq D\22 05 16\DAN039 P DCM TBAPF6 200 02 sc4.ocw

Electrochemistry Data of **43**

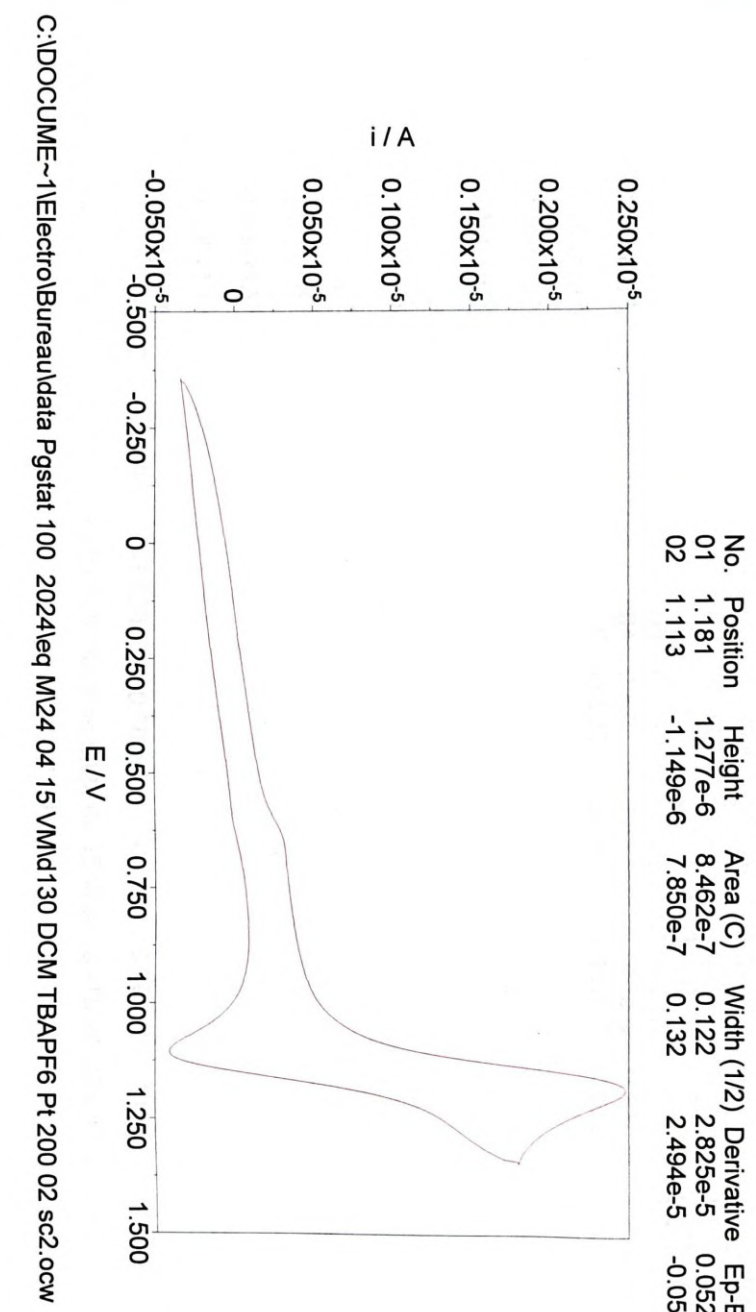

Overlay legends:
d130 dcm tbapf6 pt sqw 20 20 5 ox2 (Line-blue)

DCM + TBAPF6

No.	Position	Height	Area	Width (1/2)	Derivative
01	0.376	8.193e-7	8.191e-8	0.093	2.349e-5

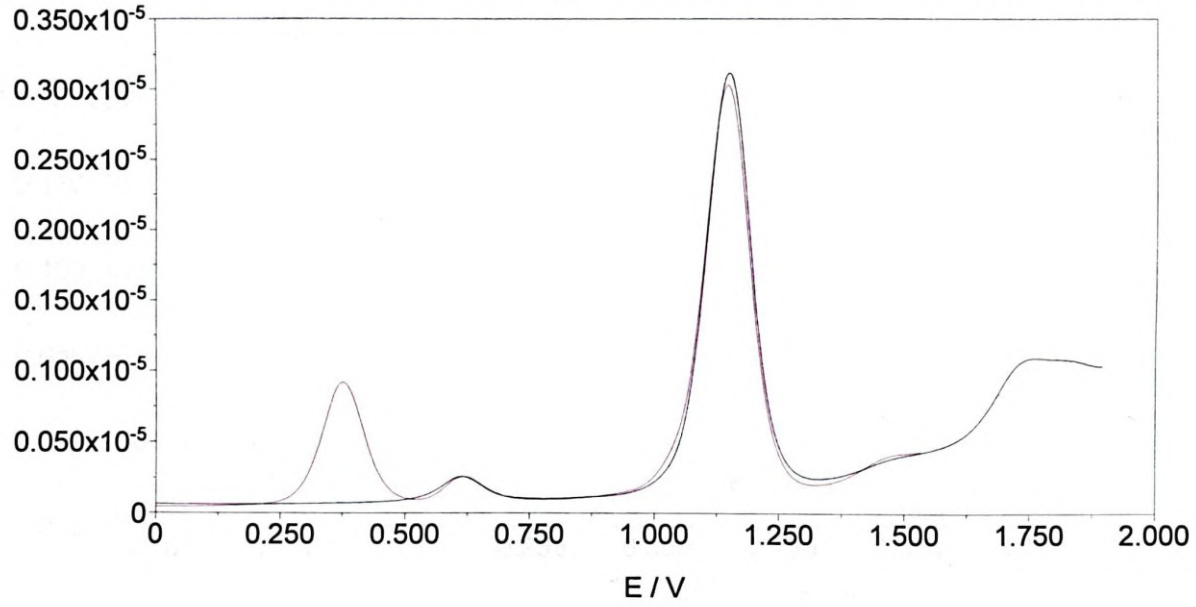

Overlay legends:
blanc dcm tbapf6 pt sqw 20 20 5 red1 (Line-blue)
d130 dcm tbapf6 pt sqw 20 20 5 red1 (Line-green)

DCM + TBAPF6

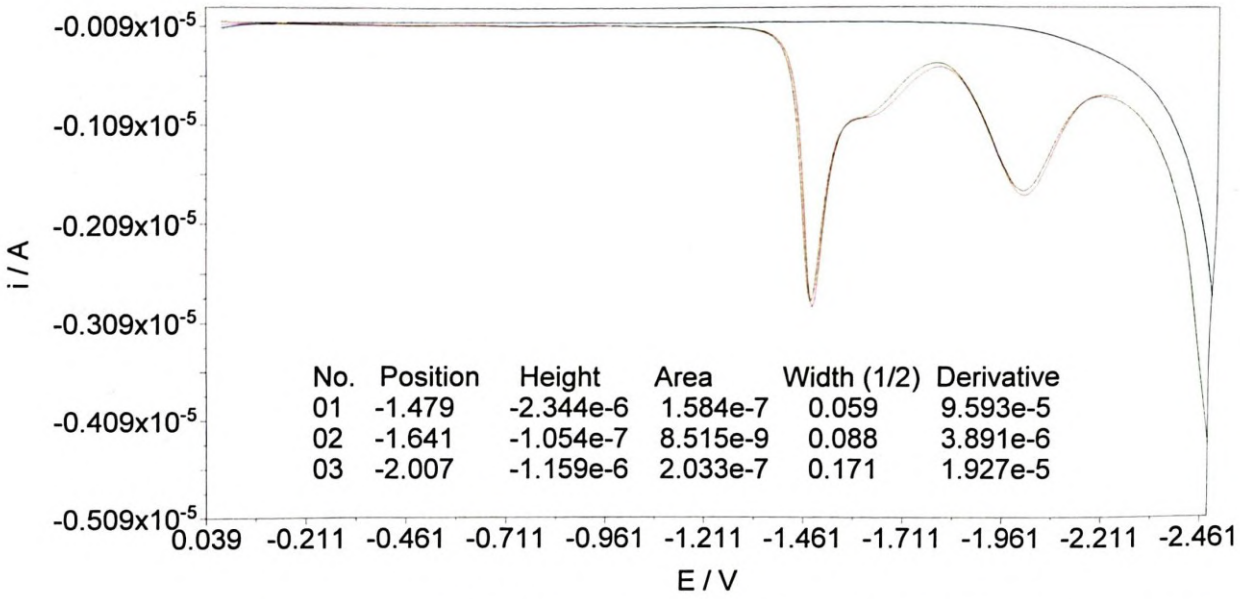

No.	Position	Height	Area	Width (1/2)	Derivative
01	-1.479	-2.344e-6	1.584e-7	0.059	9.593e-5
02	-1.641	-1.054e-7	8.515e-9	0.088	3.891e-6
03	-2.007	-1.159e-6	2.033e-7	0.171	1.927e-5

C:\DOCUME~1\Electro\Bureau\data Pgstat 100 2024\eq M\24 04 15 VM\d130 DCM TBAPF6 Pt sqw 20 20 5 red3.iew

verlay legends:
anc dcm tbapf6 pt 200 01 sc2 (Line-blue)
_ps dcm tbapf6 pt 200 01 sc1 (Line-green)

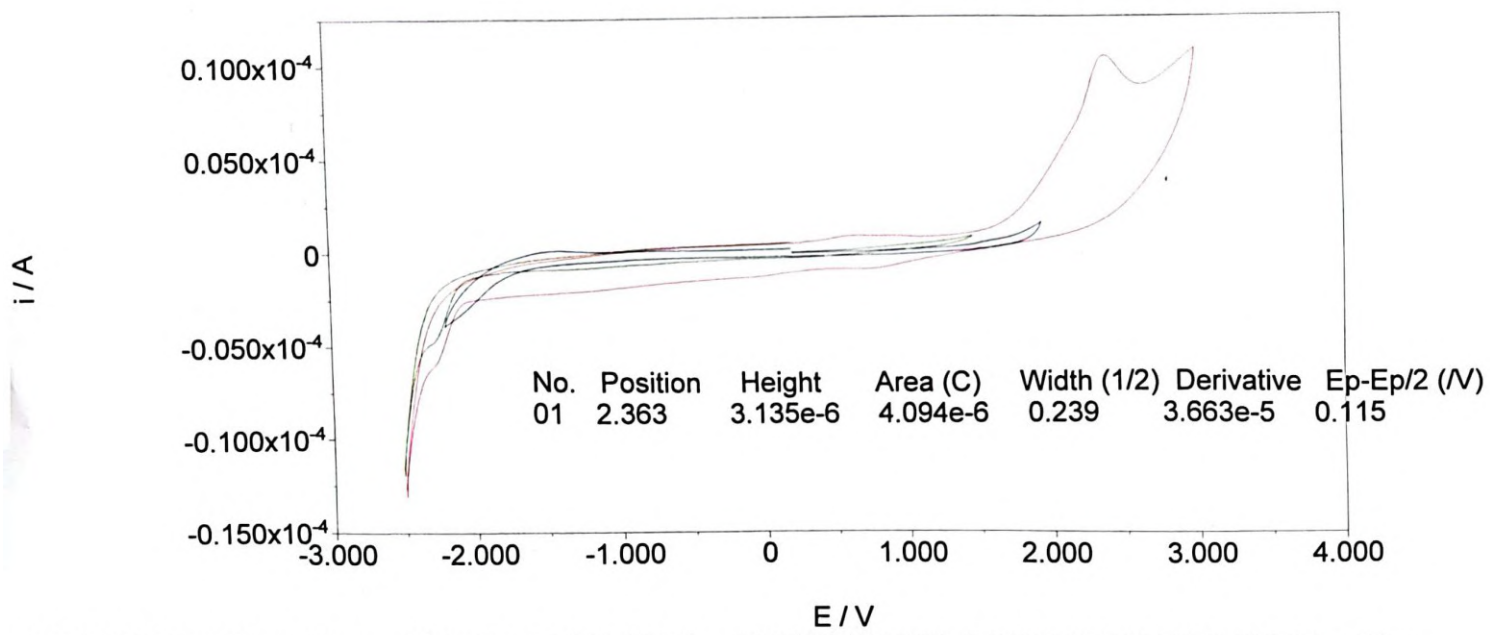

C:\DOCUME~1\Electro\Bureau\data Pgstat 100 2024\eq M\24 02 19 VM\2_PS DCM TBAPF6 Pt 200 01 sc2.icw

Electrochemistry Data of **46**

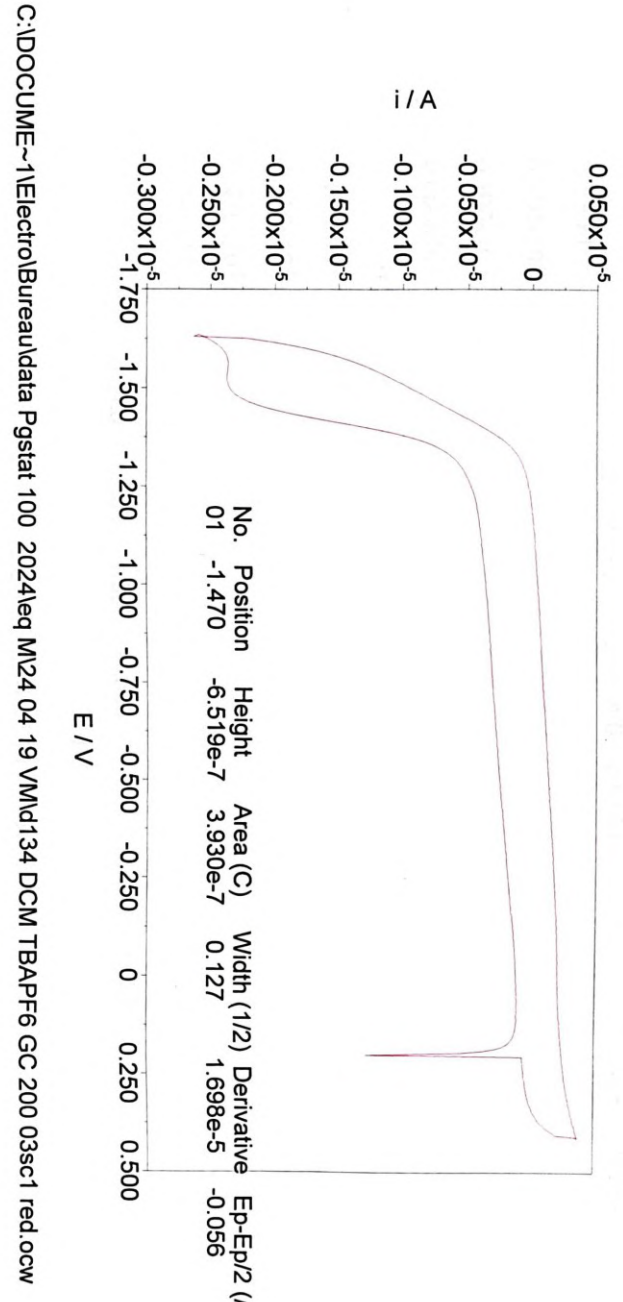

Overlay legends:
d134 dcm tbapf6 pt sqw 20 20 5 ox1 (Line-blue)
blanc dcm tbapf6 pt sqw 20 20 5 ox2 (Line-green)
blanc dcm tbapf6 pt sqw 20 20 5 ox2 (Line-blue)
d134 dcm tbapf6 pt sqw 20 20 5 ox1 (Line-green)

DCM + TBABF4

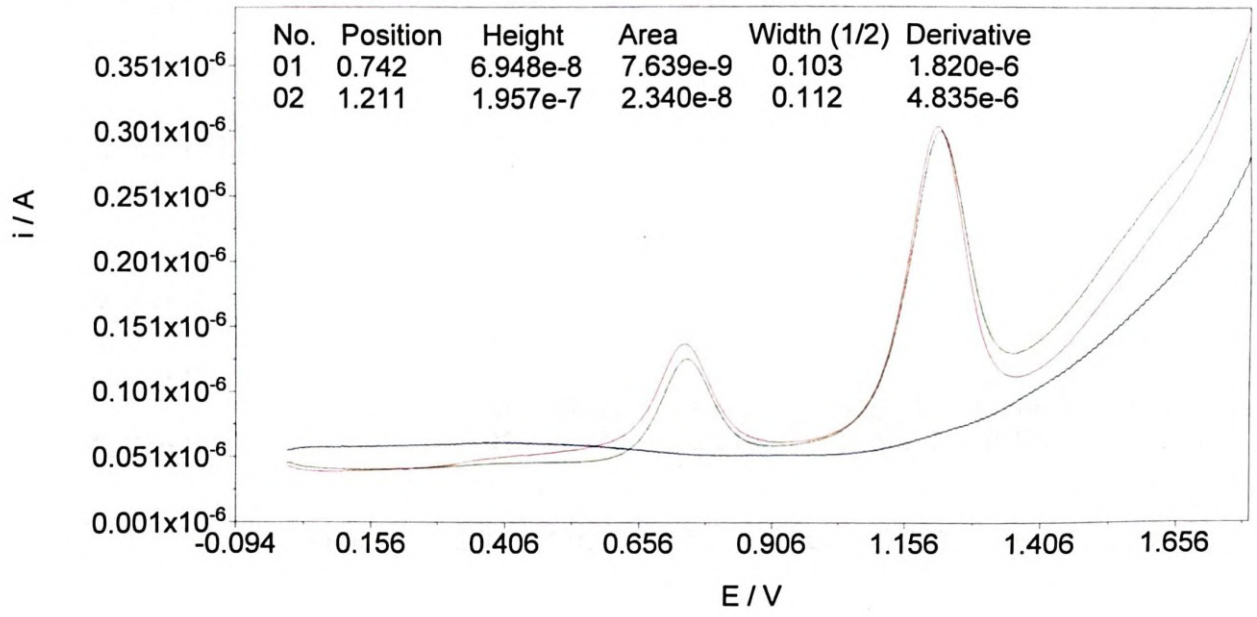

C:\DOCUME~1\Electro\Bureau\data Pgstat 100 2024\eq M\24 04 19 VM\d134 DCM TBAPF6 Pt sqw 20 20 5 ox1.oew

Overlay legends:
blanc dcm tbapf6 pt sqw 20 20 5 red1 (Line-blue)
d134 dcm tbapf6 pt sqw 20 20 5 red2 (Line-green)

DCM + TBABF4

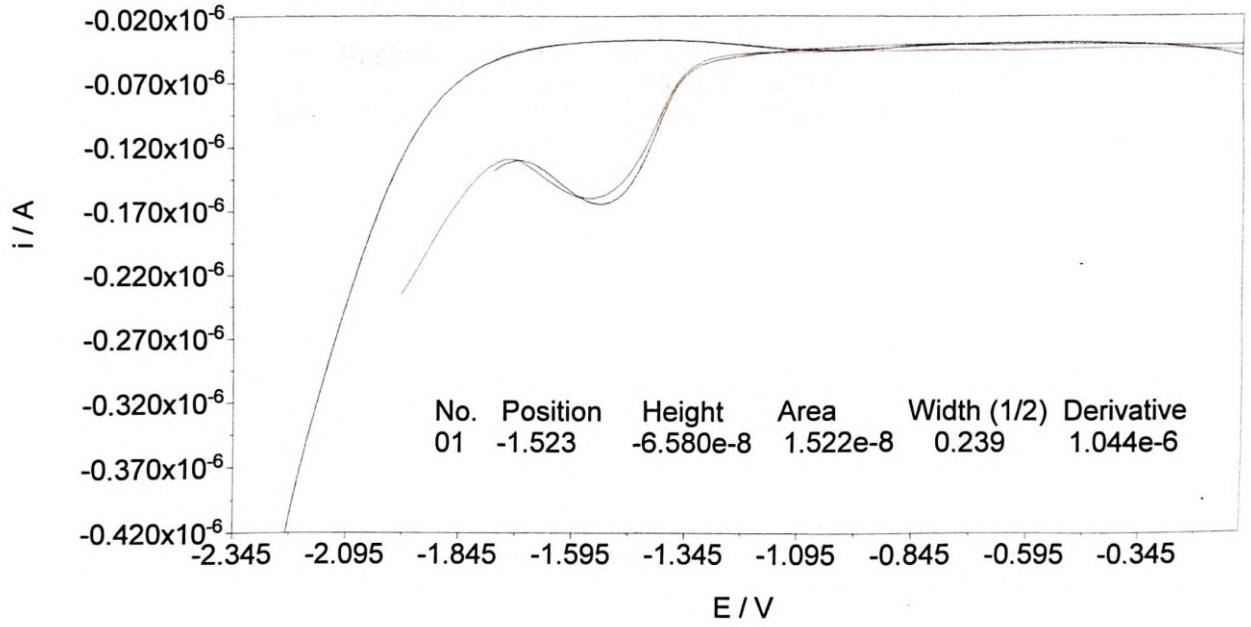

C:\DOCUME~1\Electro\Bureau\data Pgstat 100 2024\eq M\24 04 19 VM\d134 DCM TBAPF6 Pt sqw 20 20 5 red3.oew

No.	Position	Height	Area (C)	Width (1/2)	Derivative	Ep-Ep/2 (/V)
01	-0.298	6.014e-8	2.995e-8	0.098	1.727e-6	0.044
02	1.372	-2.528e-8	1.280e-8	0.098	7.136e-7	-0.043
03	0.239	1.668e-6	1.103e-6	0.127	3.705e-5	0.052
04	0.874	-1.433e-6	1.082e-6	0.137	2.952e-5	-0.054
05	-1.504	-3.017e-6	1.141e-6	0.073	1.150e-4	-0.030

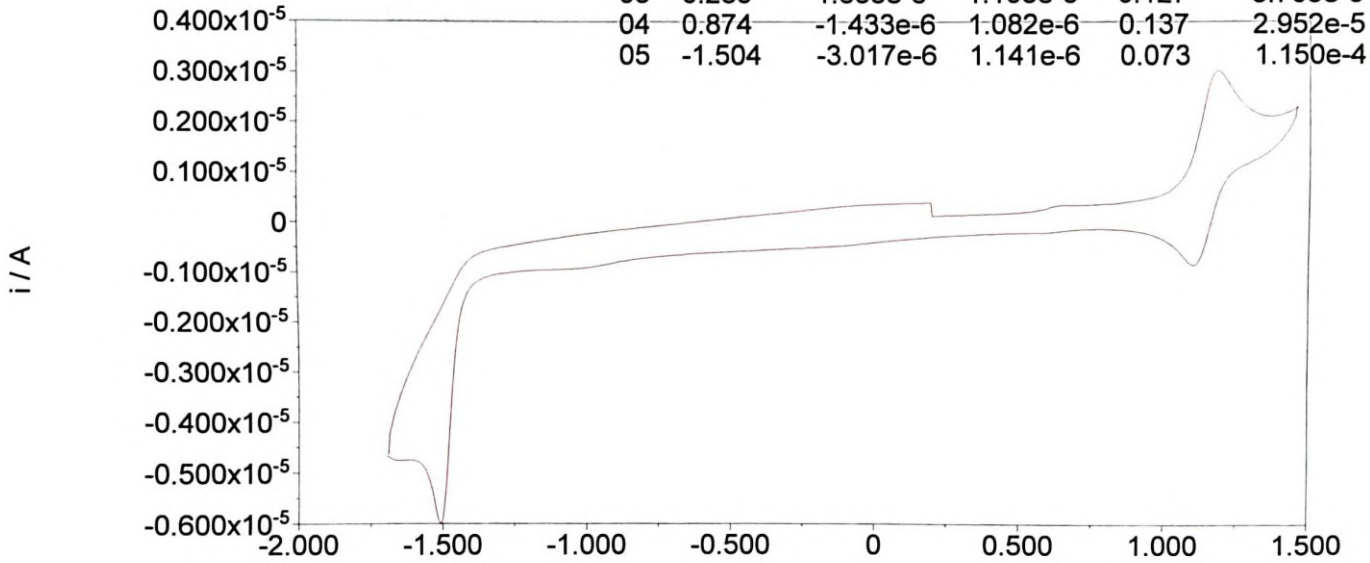

C:\DOCUME~1\Electro\Bureau\data Pgstat 100 2024\eq M\24 04 15 VM\d130 DCM TBAPF6 Pt 200 01 sc4.ocw

DFT calculations

Static DFT calculations were performed at the GGA level with the program Firefly v. 8.1.1, with the 6-31G(d,p) basis set for H, C, and P atoms.

Geometry optimizations were carried out under C_i, C_{2v} or D_3 symmetry constraint.

Total energies are given without zero-point correction.

• **Parent phosphinine**, symmetry = C_{2v}

NUCLEAR ENERGY = 253.2696848121
ELECTRONIC ENERGY = -788.0312519430
TOTAL ENERGY = -534.7615671309
COORDINATES OF ALL ATOMS ARE (ANGS)

ATOM	X	Y	Z
C	0.0000000000	0.0000000000	-1.7644655332
C	-1.2245647654	0.0000000000	-1.0955468691
C	1.2245647654	0.0000000000	-1.0955468691
C	-1.3347361132	0.0000000000	0.2905733559
C	1.3347361132	0.0000000000	0.2905733559
H	0.0000000000	0.0000000000	-2.8511552930
H	-2.1354004728	0.0000000000	-1.6918981650
H	2.1354004728	0.0000000000	-1.6918981650
H	-2.3330042304	0.0000000000	0.7243988195
H	2.3330042304	0.0000000000	0.7243988195
P	0.0000000000	0.0000000000	1.4088865436

• **Parent diphosphinine**, symmetry = C_i

NUCLEAR ENERGY = 310.4516298964
ELECTRONIC ENERGY = -1147.8029374553
TOTAL ENERGY = -837.3513075589
COORDINATES OF ALL ATOMS ARE (ANGS)

ATOM	X	Y	Z
C	-0.6930185649	-1.3610107708	0.0000000000
C	0.6930185649	-1.3610107708	0.0000000000
C	-0.6930185649	1.3610107708	0.0000000000
C	0.6930185649	1.3610107708	0.0000000000
H	-1.1900041415	-2.3321188028	0.0000000000
H	1.1900041415	-2.3321188028	0.0000000000
H	-1.1900041415	2.3321188028	0.0000000000
H	1.1900041415	2.3321188028	0.0000000000
P	1.7848957068	0.0000000000	0.0000000000
P	-1.7848957068	0.0000000000	0.0000000000

• ***carbo*-Phosphinine**, symmetry = C_{2v}

NUCLEAR ENERGY = 967.6093813471
ELECTRONIC ENERGY = -1959.0536545418
TOTAL ENERGY = -991.4442731946
COORDINATES OF ALL ATOMS ARE (ANGS)

ATOM	X	Y	Z
C	0.0000000000	0.0000000000	4.3700507698
C	-1.1989592969	0.0000000000	3.7098189823
C	1.1989592969	0.0000000000	3.7098189823
C	-2.2672811327	0.0000000000	3.0836765141
C	2.2672811327	0.0000000000	3.0836765141
C	-3.4359291948	0.0000000000	2.3705119304
C	3.4359291948	0.0000000000	2.3705119304
C	-3.4698205538	0.0000000000	1.0032218594
C	3.4698205538	0.0000000000	1.0032218594
C	-3.4860694365	0.0000000000	-0.2361114927
C	3.4860694365	0.0000000000	-0.2361114927
C	-3.4993507516	0.0000000000	-1.6024761430
C	3.4993507516	0.0000000000	-1.6024761430
C	1.3187378742	0.0000000000	-3.0422230850
C	-1.3187378742	0.0000000000	-3.0422230850
C	2.3593474459	0.0000000000	-2.3653432808
C	-2.3593474459	0.0000000000	-2.3653432808
H	0.0000000000	0.0000000000	5.4605534784
H	4.3804710069	0.0000000000	2.9159882124
H	-4.3804710069	0.0000000000	2.9159882124
H	4.4630129003	0.0000000000	-2.1140378094
H	-4.4630129003	0.0000000000	-2.1140378094
P	0.0000000000	0.0000000000	-4.1257456233

• ***carbo*-Diphosphinine**, symmetry = C_i

NUCLEAR ENERGY = 1057.4320255181
ELECTRONIC ENERGY = -2351.4851180270
TOTAL ENERGY = -1294.0530925089
COORDINATES OF ALL ATOMS ARE (ANGS)

ATOM	X	Y	Z
C	-0.6201151874	-3.4955788916	0.0000000000
C	0.6201151874	-3.4955788916	0.0000000000
C	-0.6201151874	3.4955788916	0.0000000000
C	0.6201151874	3.4955788916	0.0000000000
C	-1.9852367544	-3.4998580808	0.0000000000
C	1.9852367544	-3.4998580808	0.0000000000

C	-1.9852367544	3.4998580808	0.0000000000
C	1.9852367544	3.4998580808	0.0000000000
C	-3.4224367550	1.3174208970	0.0000000000
C	3.4224367550	1.3174208970	0.0000000000
C	-3.4224367550	-1.3174208970	0.0000000000
C	3.4224367550	-1.3174208970	0.0000000000
C	-2.7442918825	2.3566968887	0.0000000000
C	2.7442918825	2.3566968887	0.0000000000
C	-2.7442918825	-2.3566968887	0.0000000000
C	2.7442918825	-2.3566968887	0.0000000000
H	-2.5021269889	4.4607739818	0.0000000000
H	2.5021269889	4.4607739818	0.0000000000
H	-2.5021269889	-4.4607739818	0.0000000000
H	2.5021269889	-4.4607739818	0.0000000000
P	-4.5079325015	0.0000000000	0.0000000000
P	4.5079325015	0.0000000000	0.0000000000

• **Hexaphenyl-*carbo*-1,4-dithio-1,4-dihydro-1,4-diphosphinine**, symmetry = C_i

NUCLEAR ENERGY = 3081.3665616877
ELECTRONIC ENERGY = -5634.8692812258
TOTAL ENERGY = -2553.5027195381
COORDINATES OF ALL ATOMS ARE (ANGS)

ATOM	X	Y	Z
C	-0.7296563230	-3.4751670290	0.2598208163
C	0.7296563230	3.4751670290	-0.2598208163
C	0.5275223328	-3.5097410290	0.2381566373
C	-0.5275223328	3.5097410290	-0.2381566373
C	-2.0652974756	-3.4548006866	0.2818027059
C	2.0652974756	3.4548006866	-0.2818027059
C	1.8622655548	-3.5606051557	0.2158251581
C	-1.8622655548	3.5606051557	-0.2158251581
C	-3.4324228296	1.4618457278	-0.0271984699
C	3.4324228296	-1.4618457278	0.0271984699
C	3.5248914765	1.2735861545	-0.1440189492
C	-3.5248914765	-1.2735861545	0.1440189492
C	-2.6861509333	2.4245964294	-0.1093923706
C	2.6861509333	-2.4245964294	0.1093923706
C	2.8294822326	2.2747161989	-0.2142950575
C	-2.8294822326	-2.2747161989	0.2142950575
H	-2.3588222715	4.5298168069	-0.2792734723
H	2.3588222715	-4.5298168069	0.2792734723
H	2.6108579753	4.3962193253	-0.3590962164
H	-2.6108579753	-4.3962193253	0.3590962164

P	-4.5704079066	0.1401274967	0.2058338838
P	4.5704079066	-0.1401274967	-0.2058338838
C	-6.9400144115	0.0346385929	-3.7442392745
C	6.9400144115	-0.0346385929	3.7442392745
C	-7.6043175674	0.2296986153	-2.5351881505
C	7.6043175674	-0.2296986153	2.5351881505
C	-6.8883621397	0.2530972590	-1.3395300591
C	6.8883621397	-0.2530972590	1.3395300591
C	-5.5038266924	0.0800788852	-1.3623697393
C	5.5038266924	-0.0800788852	1.3623697393
C	-4.8336215235	-0.1192220768	-2.5756814207
C	4.8336215235	0.1192220768	2.5756814207
C	-5.5554780166	-0.1412509667	-3.7645791877
C	5.5554780166	0.1412509667	3.7645791877
H	-7.5009346818	0.0182456678	-4.6745373686
H	7.5009346818	-0.0182456678	4.6745373686
H	-8.6818692733	0.3640256233	-2.5203899665
H	8.6818692733	-0.3640256233	2.5203899665
H	-7.3901639498	0.4018848893	-0.3870906561
H	1.0 7.3901639498	-0.4018848893	0.3870906561
H	1.0 -3.7558060099	-0.2577496175	-2.5909473688
H	1.0 3.7558060099	0.2577496175	2.5909473688
H	1.0 -5.0383404967	-0.2959939797	-4.7070209097
H	1.0 5.0383404967	0.2959939797	4.7070209097
S	16.0 -5.6458976164	0.2817343734	1.8299849496
S	16.0 5.6458976164	-0.2817343734	-1.8299849496

• **Hexaphenyl-*carbo*-di(thiophospha)barrelene**, symmetry = D_3

NUCLEAR ENERGY = 8541.8967633992

ELECTRONIC ENERGY = -12323.8395929419

TOTAL ENERGY = -3781.9428295426

COORDINATES OF ALL ATOMS ARE (ANGS)

ATOM	X	Y	Z
C	-2.0579401159	3.5466991370	-0.6256286874
C	-2.0425614942	-3.5555779883	-0.6256286874
C	4.1005016101	-0.0088788513	0.6256286874
C	-2.0425614942	3.5555779883	0.6256286874
C	-2.0579401159	-3.5466991370	0.6256286874
C	4.1005016101	0.0088788513	-0.6256286874
C	-2.0391892062	3.4735161546	-1.9758372785
C	-1.9885586272	-3.5027477330	-1.9758372785
C	4.0277478334	-0.0292315784	1.9758372785
C	-1.9885586272	3.5027477330	1.9758372785

C	-2.0391892062	-3.4735161546	1.9758372785
C	4.0277478334	0.0292315784	-1.9758372785
C	-0.8130242780	1.3662503841	-2.9869366350
C	-0.7766954015	-1.3872248706	-2.9869366350
C	1.5897196795	-0.0209744866	2.9869366350
C	-0.7766954015	1.3872248706	2.9869366350
C	-0.8130242780	-1.3662503841	2.9869366350
C	1.5897196795	0.0209744866	-2.9869366350
C	-1.3842676546	2.3423804200	-2.5291568856
C	-1.3364271217	-2.3700011645	-2.5291568856
C	2.7206947763	-0.0276207446	2.5291568856
C	-1.3364271217	2.3700011645	2.5291568856
C	-1.3842676546	-2.3423804200	2.5291568856
C	2.7206947763	0.0276207446	-2.5291568856
P	0.0000000000	0.0000000000	-3.7282814403
P	0.0000000000	0.0000000000	3.7282814403
C	-3.8057094259	6.3894835683	-4.5549279755
C	-3.6306003742	-6.4905828264	-4.5549279755
C	7.4363098001	-0.1010992582	4.5549279755
C	-3.6306003742	6.4905828264	4.5549279755
C	-3.8057094259	-6.3894835683	4.5549279755
C	7.4363098001	0.1010992582	-4.5549279755
C	-3.8504086073	6.5606413583	-3.1696652151
C	-3.7564777777	-6.6148723480	-3.1696652151
C	7.6068863850	-0.0542309897	3.1696652151
C	-3.7564777777	6.6148723480	3.1696652151
C	-3.8504086073	-6.5606413583	3.1696652151
C	7.6068863850	0.0542309897	-3.1696652151
C	-3.2763933621	5.6162556280	-2.3308028593
C	-3.2256233669	-5.6455676984	-2.3308028593
C	6.5020167290	-0.0293120704	2.3308028593
C	-3.2256233669	5.6455676984	2.3308028593
C	-3.2763933621	-5.6162556280	2.3308028593
C	6.5020167290	0.0293120704	-2.3308028593
C	-2.6450688377	4.4801489862	-2.8627505219
C	-2.5573884159	-4.5307713013	-2.8627505219
C	5.2024572536	-0.0506223151	2.8627505219
C	-2.5573884159	4.5307713013	2.8627505219
C	-2.6450688377	-4.4801489862	2.8627505219
C	5.2024572536	0.0506223151	-2.8627505219
C	-2.6027339049	4.3161364036	-4.2563929425
C	-2.4365168193	-4.4121018827	-4.2563929425
C	5.0392507242	-0.0959654791	4.2563929425
C	-2.4365168193	4.4121018827	4.2563929425
C	-2.6027339049	-4.3161364036	4.2563929425

C	5.0392507242	0.0959654791	-4.2563929425
C	-3.1804372643	5.2655918055	-5.0922794261
C	-2.9699176374	-5.3871353688	-5.0922794261
C	6.1503549017	-0.1215435633	5.0922794261
C	-2.9699176374	5.3871353688	5.0922794261
C	-3.1804372643	-5.2655918055	5.0922794261
C	6.1503549017	0.1215435633	-5.0922794261
H	-4.2561427578	7.1295461622	-5.2099505428
H	-4.0462967150	-7.2507008314	-5.2099505428
H	8.3024394728	-0.1211546693	5.2099505428
H	-4.0462967150	7.2507008314	5.2099505428
H	-4.2561427578	-7.1295461622	5.2099505428
H	8.3024394728	0.1211546693	-5.2099505428
H	-4.3351122183	7.4345164203	-2.7440081405
H	-4.2709239757	-7.4715755194	-2.7440081405
H	8.6060361940	-0.0370590991	2.7440081405
H	-4.2709239757	7.4715755194	2.7440081405
H	-4.3351122183	-7.4345164203	2.7440081405
H	8.6060361940	0.0370590991	-2.7440081405
H	-3.3103700273	5.7502265430	-1.2540511986
H	-3.3246572501	-5.7419778111	-1.2540511986
H	6.6350272774	0.0082487319	1.2540511986
H	-3.3246572501	5.7419778111	1.2540511986
H	-3.3103700273	-5.7502265430	1.2540511986
H	6.6350272774	-0.0082487319	-1.2540511986
H	-2.1167618122	3.4420539373	-4.6792502086
H	-1.9225252448	-3.5541964718	-4.6792502086
H	4.0392870570	-0.1121425345	4.6792502086
H	-1.9225252448	3.5541964718	4.6792502086
H	-2.1167618122	-3.4420539373	4.6792502086
H	4.0392870570	0.1121425345	-4.6792502086
H	-3.1412046989	5.1252996417	-6.1683868352
H	-2.8680373423	-5.2830128886	-6.1683868352
H	6.0092420411	-0.1577132469	6.1683868352
H	-2.8680373423	5.2830128886	6.1683868352
H	-3.1412046989	-5.1252996417	6.1683868352
H	6.0092420411	0.1577132469	-6.1683868352
S	0.0000000000	0.0000000000	-5.6767816864
S	0.0000000000	0.0000000000	5.6767816864

• **Hexaphenyl-*carbo*-dihydroxybarrelene**, symmetry = C_2

NUCLEAR ENERGY = 7574.2162897285

ELECTRONIC ENERGY = -10104.9616929511

TOTAL ENERGY = -2530.7454032226

$VIB IVIB= 0
COORDINATES OF ALL ATOMS ARE (ANGS)

ATOM	X	Y	Z
O	0.3483336501	-4.9043218415	-0.0063138585
O	-0.3483336501	4.9043218415	-0.0063138585
C	0.2460750750	-3.4829585676	0.0073906758
C	-0.2460750750	3.4829585676	0.0073906758
C	-0.2237638556	2.9614931966	1.3925580570
C	0.2237638556	-2.9614931966	1.3925580570
C	0.9809142819	3.0268866266	-0.6829573000
C	-0.9809142819	-3.0268866266	-0.6829573000
C	1.4224495755	-2.9428794101	-0.6965459373
C	-1.4224495755	2.9428794101	-0.6965459373
C	-0.1856885752	2.5247776154	2.5253724856
C	0.1856885752	-2.5247776154	2.5253724856
C	1.9898502618	2.6441304495	-1.2407569716
C	-1.9898502618	-2.6441304495	-1.2407569716
C	2.3560248576	-2.4194866946	-1.2680342361
C	-2.3560248576	2.4194866946	-1.2680342361
C	-0.1279999643	1.9700295155	3.8336401188
C	0.1279999643	-1.9700295155	3.8336401188
C	3.1649355455	2.1635308128	-1.8817023725
C	-3.1649355455	-2.1635308128	-1.8817023725
C	3.4343464805	-1.7762975819	-1.9355297429
C	-3.4343464805	1.7762975819	-1.9355297429
C	-0.0360093006	0.6252301929	3.9132724052
C	0.0360093006	-0.6252301929	3.9132724052
C	3.3268613176	0.8235156841	-1.9262497755
C	-3.3268613176	-0.8235156841	-1.9262497755
C	3.4112314248	-0.4260088978	-1.9508739595
C	-3.4112314248	0.4260088978	-1.9508739595
C	-0.1733020410	2.8514343598	5.0128505346
C	0.1733020410	-2.8514343598	5.0128505346
C	4.1277729756	3.1161029046	-2.4616396253
C	-4.1277729756	-3.1161029046	-2.4616396253
C	4.4957984952	-2.5805543111	-2.5637491328
C	-4.4957984952	2.5805543111	-2.5637491328
C	0.0740498320	2.3459024270	6.2994603602
C	-0.0740498320	-2.3459024270	6.2994603602
C	5.3820756326	2.6821082011	-2.9200712363
C	-5.3820756326	-2.6821082011	-2.9200712363
C	5.5041733621	-1.9710533696	-3.3278690026
C	-5.5041733621	1.9710533696	-3.3278690026
C	-0.4667925691	4.2159061413	4.8676331243

C	0.4667925691	-4.2159061413	4.8676331243
C	3.8053523500	4.4779821420	-2.5648154890
C	-3.8053523500	-4.4779821420	-2.5648154890
C	4.5130627393	-3.9753594720	-2.4091622697
C	-4.5130627393	3.9753594720	-2.4091622697
C	0.0216897137	3.1810123948	7.4071938561
C	-0.0216897137	-3.1810123948	7.4071938561
C	6.2821558285	3.5833796368	-3.4721758020
C	-6.2821558285	-3.5833796368	-3.4721758020
C	6.5043706791	-2.7351662021	-3.9128934518
C	-6.5043706791	2.7351662021	-3.9128934518
C	-0.5195781583	5.0484013871	5.9804088164
C	0.5195781583	-5.0484013871	5.9804088164
C	4.7096795203	5.3771294759	-3.1197589110
C	-4.7096795203	-5.3771294759	-3.1197589110
C	5.5176913585	-4.7364239736	-2.9970543966
C	-5.5176913585	4.7364239736	-2.9970543966
C	-0.2765711504	4.5365148820	7.2538722517
C	0.2765711504	-4.5365148820	7.2538722517
C	5.9504630016	4.9356782066	-3.5762606266
C	-5.9504630016	-4.9356782066	-3.5762606266
C	6.5173396552	-4.1219513560	-3.7493250966
C	-6.5173396552	4.1219513560	-3.7493250966
H	0.2199262264	2.7758609006	8.3955072321
H	-0.2199262264	-2.7758609006	8.3955072321
H	7.2499018289	3.2320744512	-3.8187985889
H	-7.2499018289	-3.2320744512	-3.8187985889
H	7.2758606577	-2.2493867592	-4.5036614864
H	-7.2758606577	2.2493867592	-4.5036614864
H	0.3214763303	1.2950964306	6.4175416967
H	-0.3214763303	-1.2950964306	6.4175416967
H	5.6469680946	1.6333098310	-2.8245946833
H	-5.6469680946	-1.6333098310	-2.8245946833
H	5.4861586719	-0.8942190409	-3.4670608667
H	-5.4861586719	0.8942190409	-3.4670608667
H	-0.3156159573	5.1883779987	8.1218172064
H	0.3156159573	-5.1883779987	8.1218172064
H	6.6564958271	5.6393999446	-4.0075852357
H	-6.6564958271	-5.6393999446	-4.0075852357
H	7.3001896557	-4.7181665727	-4.2092694141
H	-7.3001896557	4.7181665727	-4.2092694141
H	-0.7533280886	6.1014725886	5.8518271064
H	0.7533280886	-6.1014725886	5.8518271064
H	4.4425567669	6.4272502459	-3.1974310631
H	-4.4425567669	-6.4272502459	-3.1974310631

H	5.5185048159	-5.8148293483	-2.8667365236
H	-5.5185048159	5.8148293483	-2.8667365236
H	-0.6628781754	4.6134134595	3.8763262232
H	0.6628781754	-4.6134134595	3.8763262232
H	2.8361918829	4.8212933797	-2.2155500370
H	-2.8361918829	-4.8212933797	-2.2155500370
H	3.7345214815	-4.4547788757	-1.8233992278
H	-3.7345214815	4.4547788757	-1.8233992278
H	-0.4350359878	-5.2357316732	0.4536841701
H	0.4350359878	5.2357316732	0.4536841701

• **Hexaphenyl-*carbo*-diphosphabarrelene**, symmetry = D_3

NUCLEAR ENERGY = 7446.6943091398

ELECTRONIC ENERGY = -10432.3248377843

TOTAL ENERGY = -2985.6305286444

COORDINATES OF ALL ATOMS ARE (ANGS)

ATOM	X	Y	Z
C	-2.0647227389	3.5582257318	-0.6259713808
C	-2.0491525067	-3.5672152095	-0.6259713808
C	4.1138752456	-0.0089894777	0.6259713808
C	-2.0491525067	3.5672152095	0.6259713808
C	-2.0647227389	-3.5582257318	0.6259713808
C	4.1138752456	0.0089894777	-0.6259713808
C	-2.0424048777	3.4787514100	-1.9758228305
C	-1.9914846557	-3.5081502139	-1.9758228305
C	4.0338895334	-0.0293988039	1.9758228305
C	-1.9914846557	3.5081502139	1.9758228305
C	-2.0424048777	-3.4787514100	1.9758228305
C	4.0338895334	0.0293988039	-1.9758228305
C	-0.8078142961	1.3578261911	-2.9504389637
C	-0.7720048274	-1.3785007975	-2.9504389637
C	1.5798191235	-0.0206746064	2.9504389637
C	-0.7720048274	1.3785007975	2.9504389637
C	-0.8078142961	-1.3578261911	2.9504389637
C	1.5798191235	0.0206746064	-2.9504389637
C	-1.3867945355	2.3463456885	-2.5289220282
C	-1.3385977046	-2.3741721418	-2.5289220282
C	2.7253922400	-0.0278264533	2.5289220282
C	-1.3385977046	2.3741721418	2.5289220282
C	-1.3867945355	-2.3463456885	2.5289220282
C	2.7253922400	0.0278264533	-2.5289220282
P	0.0000000000	0.0000000000	-3.7379713709
P	0.0000000000	0.0000000000	3.7379713709

C	-3.8107218452	6.3964064234	-4.5587017940
C	-3.6340895330	-6.4983851363	-4.5587017940
C	7.4448113781	-0.1019787130	4.5587017940
C	-3.6340895330	6.4983851363	4.5587017940
C	-3.8107218452	-6.3964064234	4.5587017940
C	7.4448113781	0.1019787130	-4.5587017940
C	-3.8558175754	6.5681037373	-3.1737002065
C	-3.7602359035	-6.6232878413	-3.1737002065
C	7.6160534789	-0.0551841040	3.1737002065
C	-3.7602359035	6.6232878413	3.1737002065
C	-3.8558175754	-6.5681037373	3.1737002065
C	7.6160534789	0.0551841040	-3.1737002065
C	-3.2818059073	5.6247374508	-2.3329800920
C	-3.2302625684	-5.6544960115	-2.3329800920
C	6.5120684757	-0.0297585606	2.3329800920
C	-3.2302625684	5.6544960115	2.3329800920
C	-3.2818059073	-5.6247374508	2.3329800920
C	6.5120684757	0.0297585606	-2.3329800920
C	-2.6496937268	4.4875768721	-2.8611206604
C	-2.5615087092	-4.5384905157	-2.8611206604
C	5.2112024361	-0.0509136436	2.8611206604
C	-2.5615087092	4.5384905157	2.8611206604
C	-2.6496937268	-4.4875768721	2.8611206604
C	5.2112024361	0.0509136436	-2.8611206604
C	-2.6079321546	4.3244390586	-4.2543241813
C	-2.4411080045	-4.4207550265	-4.2543241813
C	5.0490401591	-0.0963159680	4.2543241813
C	-2.4411080045	4.4207550265	4.2543241813
C	-2.6079321546	-4.3244390586	4.2543241813
C	5.0490401591	0.0963159680	-4.2543241813
C	-3.1844175126	5.2718716492	-5.0932500562
C	-2.9733660174	-5.3937222867	-5.0932500562
C	6.1577835300	-0.1218506375	5.0932500562
C	-2.9733660174	5.3937222867	5.0932500562
C	-3.1844175126	-5.2718716492	5.0932500562
C	6.1577835300	0.1218506375	-5.0932500562
H	-4.2611058728	7.1353227045	-5.2151590842
H	-4.0488177899	-7.2578872863	-5.2151590842
H	8.3099236627	-0.1225645818	5.2151590842
H	-4.0488177899	7.2578872863	5.2151590842
H	-4.2611058728	-7.1353227045	5.2151590842
H	8.3099236627	0.1225645818	-5.2151590842
H	-4.3408068903	7.4425170071	-2.7492531558
H	-4.2750053511	-7.4805075434	-2.7492531558
H	8.6158122414	-0.0379905363	2.7492531558

H	-4.2750053511	7.4805075434	2.7492531558
H	-4.3408068903	-7.4425170071	2.7492531558
H	8.6158122414	0.0379905363	-2.7492531558
H	-3.3157437807	5.7598472489	-1.2563368654
H	-3.3303021491	-5.7514419710	-1.2563368654
H	6.6460459299	0.0084052779	1.2563368654
H	-3.3303021491	5.7514419710	1.2563368654
H	-3.3157437807	-5.7598472489	1.2563368654
H	6.6460459299	-0.0084052779	-1.2563368654
H	-2.1210069253	3.4478855926	-4.6702880704
H	-1.9254530499	-3.5607886752	-4.6702880704
H	4.0464599752	-0.1129030826	4.6702880704
H	-1.9254530499	3.5607886752	4.6702880704
H	-2.1210069253	-3.4478855926	4.6702880704
H	4.0464599752	0.1129030826	-4.6702880704
H	-3.1444674894	5.1301172023	-6.1693740320
H	-2.8705780768	-5.2882473284	-6.1693740320
H	6.0150455663	-0.1581301261	6.1693740320
H	-2.8705780768	5.2882473284	6.1693740320
H	-3.1444674894	-5.1301172023	6.1693740320
H	6.0150455663	0.1581301261	-6.1693740320

Abstract

The manuscript describes the synthesis and study of ring *carbo*-mers of diphosphinines and diphosphabarrelene derivatives, and a preliminary study regarding their possible use as ligands towards metal centers. *Carbo*-diphosphinine and *carbo*-diphospha-barrelene derivatives were unknown experimentally before this work, and are attractive for their possible properties and applications. Indeed, the introduction of phosphorus atoms in *carbo*-meric molecules opens prospects in new areas such as catalysis and coordination chemistry, that have never been previously envisaged.

The first chapter of this thesis provides a description of the definition of '*carbo*-mer' and the different synthetic approaches to prepare them. Additionally, it presents an update on pericyclynes derivatives, including hydrocarbon and hetero-pericyclynes, as well as their construction by classical and "accelerated" synthetic methods. The synthesis of *carbo*-benzenes with various substituents is then described, followed by a comprehensive presentation of their properties and applications.

The personal work is presented in the following three chapters, and the experimental parts are attached at the end of each chapter.

In the second Chapter, a first example of *carbo*-1,4-dihydro-dithiodiphosphinine and related macrocyclic *carbo*-diphosphacyclohexane derivatives with different substituents and oxidation states are presented. Their preparation was achieved by a quite efficient and general method involving a tetracomponent [8+1+8+1] macrocyclization reaction with up to 67 % yield. After a final reductive elimination step with $SnCl_2$/HCl, the hexaphenyl-*carbo*-1,4-dihydro-dithiodiphosphinine was produced with 20 % yield and was fully characterized by NMR, HRMS, IR, UV, electrochemistry, single crystal X-ray diffraction.

In the third Chapter, the hexaphenyl-*carbo*-dithiodiphospha-barrelene and its *carbo*-dithiodiphospha-barrelane precursor are described. Their preparation was achieved by an overall pentacomponent [8+1+8+1+8] reaction with 5 % yield. After a final reductive elimination step with $SnCl_2$/HCl, the hexaphenyl-*carbo*-1,4-dihydro-dithiodiphospha-barrelene was produced with 20 % yield as a colored dark orange solid and partially characterized by NMR and UV-vis spectroscopy. These molecules are attractive for their possible applications, including cage behavior towards cations and enhanced single molecule conductance (SMC).

In the fourth Chapter, the reactivity and coordination chemistry of *carbo*-mers of phosphaheterocycles and model compounds thereof are studied. A first example of coordination complex, a *carbo*-diphosphacyclohexane di-ruthenium complex, was prepared as a stereoisomeric mixture through a two-step one-pot process using a method optimized on model compounds.

Key words: acetylenic phosphine, *carbo*-phospha benzene, *carbo*-mer, hetero-pericyclynes, *carbo*-phosphinine

Résumé

Le manuscrit décrit la synthèse et l'étude de *carbo*-mères de cycles de dérivés de diphosphinines et de diphosphabarrelène, ainsi qu'une étude préliminaire concernant leur utilisation possible en tant que ligands de centres métalliques. Les dérivés de *carbo*-diphosphinine et de *carbo*-diphospha-barrelène étaient inconnus expérimentalement avant ce travail, et sont attrayants pour leurs propriétés et applications possibles. En effet, l'introduction d'atomes de phosphore dans les molécules *carbo*-mères ouvre des perspectives dans de nouveaux domaines tels que la catalyse et la chimie de coordination, qui n'ont jamais été envisagés sous cet angle auparavant.

Le premier chapitre décrit la définition des *'carbo*-mères' et les différentes approches synthétiques pour les préparer. Il présente également les dérivés de type péricyclynes, à la fois hydrocarbures et hétéropéricyclynes, ainsi que leur préparation par les méthodes de synthèse classiques ou "accélérées". La préparation des *carbo*-benzènes portant divers substituants est ensuite décrite, suivie d'une présentation de leurs propriétés et de leurs applications.

Le travail personnel est présenté dans les trois chapitres suivants, et les parties expérimentales sont jointes à la fin de chaque chapitre.

Le deuxième chapitre présente la préparation d'un premier exemple de *carbo*-1,4-dihydro-dithiodiphosphinine et de dérivés macrocycliques de *carbo*-diphosphacyclohexane portant différents substituants et dont les atomes de phosphore sont à différents degrés d'oxydation. Leur préparation a été réalisée par une méthode assez efficace et générale impliquant une réaction de macrocyclisation à quatre composants [8+1+8+1] donnant jusqu'à 67 % de rendement. Après une étape finale d'élimination réductrice avec $SnCl_2$/HCl, l'hexaphényl-*carbo*-1,4-dihydrodithiodiphosphinine a été isolée avec un rendement de 20 % et a été entièrement caractérisée par RMN, HRMS, IR, UV, électrochimie et diffraction des rayons X sur monocristal.

Le troisième chapitre porte sur l'hexaphényl-*carbo*-dithiodiphospha-barrelène et son précurseur *carbo*-dithiodiphospha-barrelane. Leur préparation a été réalisée par une réaction à cinq composants [8+1+8+1+8] avec un rendement de 5 %. Après une étape finale d'élimination réductrice avec $SnCl_2$/HCl, l'hexaphényl-*carbo*-1,4-dihydrodithiodiphospha-barrelène a été obtenu avec un rendement de 20 % sous la forme d'un solide orange foncé qui a été partiellement caractérisé par RMN et spectroscopie UV-vis. Ces molécules sont intéressantes pour leurs applications potentielles, en particulier pour leur possible comportement de cage vis-à-vis de cations et leur conductance sur molécule unique (SMC) élevée.

Un premier exemple de complexe de coordination, un complexe dinucléaire de ruthénium du *carbo*-diphosphacyclohexane, a été préparé par un processus en deux étapes en utilisant la méthode optimisée sur des composés modèles et a été entièrement caractérisé.

Mots clés : phosphine acétylénique, *carbo*-phospha benzène, *carbo*-mer, hétéropéricyclynes, *carbo*-phosphinine.

Titre : Phosphanes acétyléniques et carbo-mères pour la chimie de coordination

Mots clés : phosphine acétylénique, carbo-phospha benzène, carbo-mer, hétéropéricyclynes, carbo-phosphinine

Résumé : Le manuscrit décrit la synthèse et l'étude de carbo-mères de cycles de dérivés de diphosphinines et de diphosphabarrelène, ainsi qu'une étude préliminaire concernant leur utilisation possible en tant que ligands de centres métalliques. Les dérivés de carbo-diphosphinine et de carbo-diphospha-barrelène étaient inconnus expérimentalement avant ce travail, et sont attrayants pour leurs propriétés et applications possibles. En effet, l'introduction d'atomes de phosphore dans les molécules carbo-mères ouvre des perspectives dans de nouveaux domaines tels que la catalyse et la chimie de coordination, qui n'ont jamais été envisagés sous cet angle auparavant.
Le premier chapitre décrit la définition des 'carbo-mères' et les différentes approches synthétiques pour les préparer. Il présente également les dérivés de type péricyclynes, à la fois hydrocarbures et hétéropéricyclynes, ainsi que leur préparation par les méthodes de synthèse classiques ou "accélérées". La préparation des carbo-benzènes portant divers substituants est ensuite décrite, suivie d'une présentation de leurs propriétés et de leurs applications.
Le travail personnel est présenté dans les trois chapitres suivants, et les parties expérimentales sont jointes à la fin de chaque chapitre.
Le deuxième chapitre présente la préparation d'un premier exemple de carbo-1,4-dihydro-dithiodiphosphinine et de dérivés macrocycliques de carbo-diphosphacyclohexane portant différents substituants et dont les atomes de phosphore sont à différents degrés d'oxydation. Leur préparation a été réalisée par une méthode assez efficace et générale impliquant une réaction de macrocyclisation à quatre composants [8+1+8+1] donnant jusqu'à 67 % de rendement. Après une étape finale d'élimination réductrice avec $SnCl_2$/HCl, l'hexaphényl-carbo-1,4-dihydrodithiodiphosphinine a été isolée avec un rendement de 20 % et a été entièrement caractérisée par RMN, HRMS, IR, UV, électrochimie et diffraction des rayons X sur monocristal.
Le troisième chapitre porte sur l'hexaphényl-carbo-dithiodiphospha-barrelène et son précurseur carbo-dithiodiphospha-barrelane. Leur préparation a été réalisée par une réaction à cinq composants [8+1+8+1+8] avec un rendement de 5 %. Après une étape finale d'élimination réductrice avec $SnCl_2$/HCl, l'hexaphényl-carbo-1,4-dihydrodithiodiphospha-barrelène a été obtenu avec un rendement de 20 % sous la forme d'un solide orange foncé qui a été partiellement caractérisé par RMN et spectroscopie UV-vis. Ces molécules sont intéressantes pour leurs applications potentielles, en particulier pour leur possible comportement de cage vis-à-vis de cations et leur conductance sur molécule unique (SMC) élevée.
Un premier exemple de complexe de coordination, un complexe dinucléaire de ruthénium du carbo-diphosphacyclohexane, a été préparé par un processus en deux étapes en utilisant la méthode optimisée sur des composés modèles et a été entièrement caractérisé.

Title: Acetylenic phosphanes and carbo-mers for coordination chemistry

Key words: acetylenic phosphine, carbo-phospha benzene, carbo-mer, hetero-pericyclynes, carbo-phosphinine

Abstract: The manuscript describes the synthesis and study of ring carbo-mers of diphosphinines and diphosphabarrelene derivatives, and a preliminary study regarding their possible use as ligands towards metal centers. Carbo-diphosphinine and carbo-diphospha-barrelene derivatives were unknown experimentally before this work, and are attractive for their possible properties and applications. Indeed, the introduction of phosphorus atoms in carbo-meric molecules opens prospects in new areas such as catalysis and coordination chemistry, that have never been previously envisaged.
The first chapter of this thesis provides a description of the definition of 'carbo-mer' and the different synthetic approaches to prepare them. Additionally, it presents an update on pericyclynes derivatives, including hydrocarbon and hetero-pericyclynes, as well as their construction by classical and "accelerated" synthetic methods. The synthesis of carbo-benzenes with various substituents is then described, followed by a comprehensive presentation of their properties and applications.
The personal work is presented in the following three chapters, and the experimental parts are attached at the end of each chapter.
In the second Chapter, a first example of carbo-1,4-dihydro-dithiodiphosphinine and related macrocyclic carbo-diphosphacyclohexane derivatives with different substituents and oxidation states are presented. Their preparation was achieved by a quite efficient and general method involving a tetracomponent [8+1+8+1] macrocyclization reaction with up to 67 % yield. After a final reductive elimination step with $SnCl_2$/HCl, the hexaphenyl-carbo-1,4-dihydro-dithiodiphosphinine was produced with 20 % yield and was fully characterized by NMR, HRMS, IR, UV, electrochemistry, single crystal X-ray diffraction.
In the third Chapter, the hexaphenyl-carbo-dithiodiphospha-barrelene and its carbo-dithiodiphospha-barrelane precursor are described. Their preparation was achieved by an overall pentacomponent [8+1+8+1+8] reaction with 5 % yield. After a final reductive elimination step with $SnCl_2$/HCl, the hexaphenyl-carbo-1,4-dihydro-dithiodiphospha-barrelene was produced with 20 % yield as a colored dark orange solid and partially characterized by NMR and UV-vis spectroscopy. These molecules are attractive for their possible applications, including cage behavior towards cations and enhanced single molecule conductance (SMC).
In the fourth Chapter, the reactivity and coordination chemistry of carbo-mers of phosphaheterocycles and model compounds thereof are studied. A first example of coordination complex, a carbo-diphosphacyclohexane di-ruthenium complex, was prepared as a stereoisomeric mixture through a two-step one-pot process using a method optimized on model compounds.